



NATO Science for Peace and Security Series - C:
Environmental Security

Uncertainties in Environmental Modelling and Consequences for Policy Making

Edited by
Philippe Baveye
Jaroslav Mysiak
Magdeline Laba



Springer



*This publication
is supported by:*

The NATO Science for Peace
and Security Programme

Uncertainties in Environmental Modelling and Consequences for Policy Making

NATO Science for Peace and Security Series

This Series presents the results of scientific meetings supported under the NATO Programme: Science for Peace and Security (SPS).

The NATO SPS Programme supports meetings in the following Key Priority areas: (1) Defence Against Terrorism; (2) Countering other Threats to Security and (3) NATO, Partner and Mediterranean Dialogue Country Priorities. The types of meeting supported are generally "Advanced Study Institutes" and "Advanced Research Workshops". The NATO SPS Series collects together the results of these meetings. The meetings are co-organized by scientists from NATO countries and scientists from NATO's "Partner" or "Mediterranean Dialogue" countries. The observations and recommendations made at the meetings, as well as the contents of the volumes in the Series, reflect those of participants and contributors only; they should not necessarily be regarded as reflecting NATO views or policy.

Advanced Study Institutes (ASI) are high-level tutorial courses intended to convey the latest developments in a subject to an advanced-level audience

Advanced Research Workshops (ARW) are expert meetings where an intense but informal exchange of views at the frontiers of a subject aims at identifying directions for future action

Following a transformation of the programme in 2006 the Series has been re-named and re-organised. Recent volumes on topics not related to security, which result from meetings supported under the programme earlier, may be found in the NATO Science Series.

The Series is published by IOS Press, Amsterdam, and Springer, Dordrecht, in conjunction with the NATO Public Diplomacy Division.

Sub-Series

A.	Chemistry and Biology	Springer
B.	Physics and Biophysics	Springer
C.	Environmental Security	Springer
D.	Information and Communication Security	IOS Press
E.	Human and Societal Dynamics	IOS Press

<http://www.nato.int/science>

<http://www.springer.com>

<http://www.iospress.nl>



Series C: Environmental Security

Uncertainties in Environmental Modelling and Consequences for Policy Making

edited by

Philippe C. Baveye

SIMBIOS Centre
Abertay University
Dundee, Scotland, U.K.

Magdeline Laba

School of Civil and Environmental Engineering
Cornell University
Ithaca, New York, U.S.A.

and

Jaroslav Mysiak

Foundation Eni Enrico Mattei
Venice, Italy



Springer

Published in cooperation with NATO Public Diplomacy Division

Proceedings of the NATO Advanced Study Institute on
Uncertainties in Environmental Modelling and Consequences for Policy Making
Vrsar, Croatia
30 September – 11 October 2007

Library of Congress Control Number: 2009926508

ISBN 978-90-481-2635-4 (PB)
ISBN 978-90-481-2634-7 (HB)
ISBN 978-90-481-2636-1 (e-book)

Published by Springer,
P.O. Box 17, 3300 AA Dordrecht, The Netherlands.

www.springer.com

Printed on acid-free paper

All Rights Reserved
© Springer Science + Business Media B.V. 2009
No part of this work may be reproduced, stored in a retrieval system, or transmitted
in any form or by any means, electronic, mechanical, photocopying, microfilming,
recording or otherwise, without written permission from the Publisher, with the exception
of any material supplied specifically for the purpose of being entered and executed on
a computer system, for exclusive use by the purchaser of the work.

Table of Contents

Preface	xi
Contributors.....	xvii
THEME I. MODEL CONCEPTUALIZATION.....	1
Spatially explicit versus lumped models in catchment hydrology – experiences from two case studies	3
<i>Helge Bormann, Lutz Breuer, Simone Giertz, Johan A. Huisman, and Neil R. Viney</i>	
Abstract.....	3
1. Introduction	4
2. General features of lumped and spatially explicit hydrological models	5
3. Case study I: The upper Ouémé catchment (Bénin)	6
4. Case study II: The Dill catchment (Germany)	16
5. Conclusions	23
References.....	24
Cellular automata modeling of environmental systems	27
<i>Salvatore Straface and Giuseppe Mendicino</i>	
Abstract.....	27
1. Introduction	27
2. Discrete formulation of flow in unsaturated soil	30
3. Discrete formulation of solute transport	33
4. Macroscopic cellular automata model	36
5. Subsurface flow modeling through CA.....	37
6. Cellular automata quantization	39
7. CA high-performance environment	41
8. Results	41
9. Cellular automata quantization effects.....	49
10. Conclusions	51
Appendix A. Direct discrete formulation of the Darcy equation	52
Appendix B. Convergence of discrete unsaturated flow equation.....	55
References	57

Agent-based modeling of socio-economic processes related to the environment: Example of land-use change.....	61
<i>J. Gary Polhill</i>	
Abstract.....	61
1. Introduction	61
2. Various motivations for agent-based modeling	62
3. Agent-based modeling in land-use change	69
4. Conclusion.....	73
References.....	73
THEME II. VERIFICATION OF MODELS.....	77
Interval analysis and verification of mathematical models.....	79
<i>Tibor Csendes</i>	
Abstract.....	79
1. Interval arithmetic	79
2. Tolerances in optimization and constraint satisfaction	82
3. Chaos verification in mathematical models of dynamical systems	93
References.....	99
Stochastic arithmetic and verification of mathematical models	101
<i>Jean-Marie Chesneauaux, Fabienne Jézéquel, and Jean-Luc Lamotte</i>	
Abstract.....	101
1. Introduction	101
2. Stochastic approach of rounding errors.....	103
3. Benefits of DSA in numerical programs	108
4. Dynamical control of approximation methods.....	116
5. Conclusion.....	124
References.....	124
THEME III. CALIBRATION AND SENSITIVITY ANALYSIS.....	127
Model calibration/parameter estimation techniques and conceptual model error	129
<i>Petros Gaganis</i>	
Abstract.....	129
1. Main sources of uncertainty in mathematical modeling	130
2. Simulation models, model calibration and prediction reliability	131
3. A simple synthetic example	132
4. Interrelation of parameter uncertainty and model error	134
5. Single-objective calibration and model conceptual errors.....	137
6. A per-datum approach to model calibration.....	144

7. Conclusions	152
References.....	153
User subjectivity in Monte Carlo modelling of pesticide exposure..... 155	
<i>Marco Trevisan</i>	
Abstract.....	155
1. Introduction	155
2. Rationale.....	156
3. Experimental framework.....	162
4. General conclusion	180
References.....	180
Recommended practices in global sensitivity analysis	
183	
<i>Andrea Saltelli, Daniele Vidoni, and Massimiliano Mascherini</i>	
Abstract.....	183
1. Introduction	183
2. Generalities about sensitivity analysis	184
3. The critique of models.....	185
4. Suggested requirements for a good sensitivity analysis	189
5. How to set up the analysis.....	190
6. Mathematical and numerical practices.....	194
7. Sensitivity analysis in regulatory documents.....	198
8. Avoiding traps and pitfalls. What can go wrong in a sensitivity analysis?	200
9. What can be obtained with sensitivity analysis?.....	200
References.....	201
THEME IV. EVALUATION OF MODELS.....203	
Predictive uncertainty assessment in real time flood forecasting	
205	
<i>Ezio Todini</i>	
Abstract.....	205
1. Introduction: definition of predictive uncertainty	205
2. Motivations for predictive uncertainty assessment.....	209
3. Difference between predictive uncertainty and model or parameter uncertainty	213
4. Using formal Bayesian inference instead of GLUE.....	214
5. The hydrological uncertainty processors	219
6. The incorporation of input forecasting uncertainty.....	225
7. Conclusions	226
References.....	227

THEME V. COMMUNICATING MODELLING RESULTS AND UNCERTAINTIES	229
Communicating uncertainty to policy makers	231
<i>Anthony Patt</i>	
Abstract.....	231
1. Introduction	231
2. Challenges for communication	233
3. Solutions.....	240
4. Conclusions	245
References.....	247
Communicating scientific uncertainty for decision making about CO ₂ storage.....	253
<i>Peter M. Haugan</i>	
Abstract.....	253
1. Introduction	253
2. Carbon storage: what is it?	255
3. Development of storage options and perceptions	257
4. Estimating environmental damage from leaky reservoirs.....	261
5. Environmental regulations and the use of models	261
6. Conclusions and outlook	263
References.....	264
THEME VI. DECISION MAKING ON THE BASIS OF MODEL PREDICTION.....	265
Approaches to handling uncertainty when setting environmental exposure standards	267
<i>Esben Budtz-Jørgensen, Niels Keiding, and Philippe Grandjean</i>	
Abstract.....	267
1. Introduction	267
2. The NOAEL approach.....	268
3. The benchmark approach	269
4. Benchmark analysis in structural equation models.....	274
5. Model uncertainty	275
6. Summary and discussion.....	279
References.....	280

CASE STUDY I. SOIL CARBON DYNAMICS	281
Sources of uncertainty in global modelling of future soil organic carbon storage	283
<i>Chris Jones and Pete Falloon</i>	
Abstract.....	283
1. Introduction	283
2. Model description and methodology	286
3. Impact of future climate uncertainty	289
4. Impact of vegetation litter uncertainty	292
5. Impact of carbon pool dynamics uncertainty	295
6. Impact of uncertainty in decomposition sensitivity to temperature.....	298
7. Impact of decomposition sensitivity to moisture uncertainty	302
8. Combined uncertainty	305
9. Conclusions	308
References.....	310
Uncertainties related to the temperature sensitivity of soil carbon decomposition.....	317
<i>Maria J.I. Briones</i>	
Abstract.....	317
1. Introduction	317
2. Soils as stores and sources of carbon	318
3. Soils as the most diverse habitats on earth	319
4. Enchytraeid worms: key stone group in organic soils	320
5. The link between climate, soil biology and the carbon cycle. Implications for climate change modeling.....	322
6. Conclusions	329
References.....	330
CASE STUDY II. GLOBAL CLIMATE CHANGE.....	337
Media representational practices in the Anthropocene Era.....	339
<i>Maxwell T. Boykoff</i>	
Abstract.....	339
1. Introduction	339
2. Media and climate risk: an abridged history	340
3. Factors that shape climate change media coverage	343
4. Continuing challenges at the climate science-media-policy/practice interface.....	346

5. The public space where climate science and practice interact	348
via mass media	
References.....	349
The stern review and the uncertainties in the economics of climate change 351	
<i>Vanessa Peña</i>	
Abstract.....	351
1. Introduction	351
2. Uncertainties in the SR's scientific projections	353
3. Uncertainties in the economic framework	362
4. The implications for policy and the uncertainties in the political framework.....	374
5. Conclusion.....	377
6. Appendix: Definition of symbols in Figure 7	378
References.....	379
CASE STUDY III. NATURAL ATTENUATION OF CONTAMINANTS AND RISK ASSESSMENT 383	
Phytotechnologies: how plants and bacteria work together..... 385	
<i>Stefan Shilev, Iordanka Kuzmanova, and Enrique Sancho</i>	
Abstract.....	385
1. Introduction	385
2. Phytoremediation technologies	386
3. Plant microbe-interactions in rhizosphere.....	389
4. Case study.....	391
5. Possibilities for biomass utilization	393
6. Further perspectives	395
References.....	395
Subject Index	399

Preface

Increasingly, as a result of accelerating environmental changes all over the globe and, in part, thanks to enormous advances in computing power in recent years, predictions made with mathematical models are used as a basis for the development of environmental policies, remedial actions and measures to prevent possible conflicts. Whether it be in relation to global warming, the contamination of soils and sediments, the prediction of catastrophic events (hurricanes, floods) or the pollution of shared groundwater resources, mathematical modelling has become an essential tool to try to foresee some of what lies ahead. On the basis of possible scenarios illustrated via simulation, policy makers now routinely attempt to take preventive measures.

This reliance on computer model predictions would not be an issue in itself if everyone, from the scientists to the policy makers and the public at large, had a clear understanding of the limitations of models, of the inherent uncertainties associated with their predictions, and of the approach most suitable to deal with these uncertainties in the development of environmental policies and regulations. Unfortunately, we are very far from that ideal at this point. Mathematical modelling is still not a required course at many of the engineering schools around the world, nor is it a regular part of most curricula in environmental sciences. As a result, many scientists and engineers, even when a large portion of their work revolves around developing computer models, have at best a fragmentary understanding of the multiple sources of uncertainty associated with the different phases of any modelling project. These uncertainties tend to be poorly reported in the scientific literature, and are only succinctly alluded to in reports on modelling predictions communicated to government and supranational agencies (e.g., the UN). Most accounts of scientific predictions that are published in the media, for example in relation to global climate change or possible massive emigrations from Africa resulting from desertification, consistently omit any mention, let alone discussion, of the oftentimes huge uncertainties afflicting these prognoses.

In this general context, a major, and urgent, effort is needed to educate everyone, from members of the scientific community upward to policy makers and the public at large, about the uncertainties associated with environmental models. There are undoubtedly several different venues to approach this education or communication task. Among them, NATO Advanced Study Institutes have the specific feature that they allow a bridge between Western and Eastern countries, which does not exist to any significant extent at this point. Computer modelling, to this date, has not been a very common activity among scientists in the former Eastern block countries, probably in part because of the lack of appropriate computer resources. All of this is rapidly changing, and researchers in those countries now have access to, and use increasingly, the same types of computers that are available in the west. In this context, in the Fall of 2006, a group of researchers came

up with the idea that, in parallel with other endeavours and to explicitly try to give a chance to scientists and policy makers in Eastern European countries to be part of the debate, it would be useful to propose a NATO Advanced Study Institute on the topic of “Uncertainties in environmental modelling and consequences for policy making”.

This NATO ASI was successfully held in Croatia in early October 2007. The present book is a direct outcome of this ASI. The various chapters contained in it have been peer-reviewed, revised and updated after the ASI, but their organisation follows closely the organisation of the ASI itself.

To structure the various talks during the ASI, use was made of a schematic diagram (Fig. 1) originally developed to clarify some of the terminology used to refer to various stages of the modelling process. While every environmental scientist and engineer recognizes now, some 17 years after Konikow and Bredehoeft wrote their celebrated article “Groundwater models cannot be validated”, that one should stay away from terms like “validation” of models, a consensus on a consistent terminology has yet to emerge. Practitioners routinely use terms like “confirmation” or “verification” of models in very different ways, and with conflicting meanings. Therefore, it seemed worthwhile, in preparation of the ASI, to come up with a nomenclature that would be unambiguous and sound. This gave rise to the schematic diagram of Fig. 1. But this diagram also provides a very nice way to organize discussions, and to identify sources of uncertainty in the modelling process, which are not always mentioned explicitly.

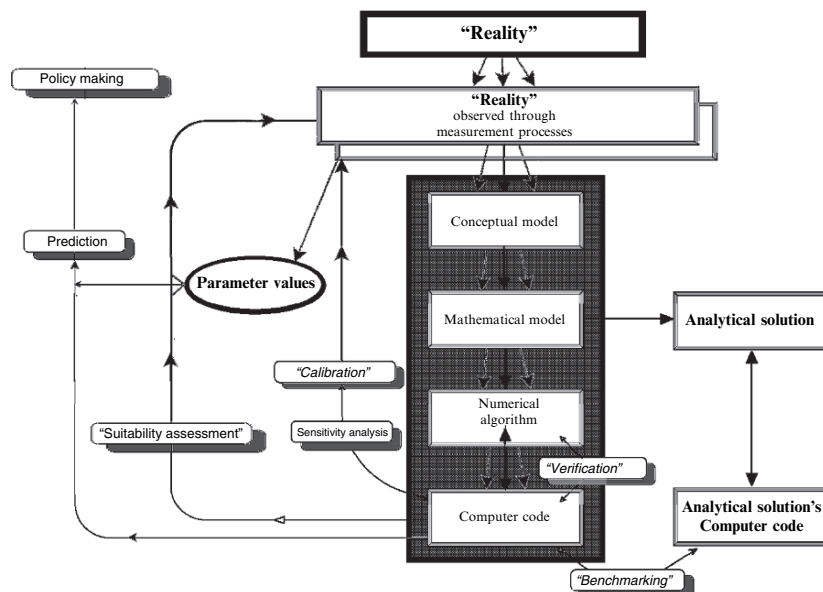


Fig. 1. Schematic illustration of the various steps involved in the modelling process.

Starting from the top, one finds the “reality” that is the focus of the modelling process. In most cases, and certainly in the overwhelming majority of situations related to the environment, this “reality” cannot be apprehended directly. It is only through the measurement process that this “reality” becomes quantifiable. Unfortunately, this measurement process is not unique. Different observers, if they use different measuring devices, may end up with different perceptions of reality. Perhaps the simplest example of this is the fact that images of a given object at different resolutions make the object appear differently. From these different perceived realities, different conceptual models can be developed, encompassing various levels of details of the reality to be described. Each of these conceptual models, in turn, can be translated using one of a number of different mathematical formalisms. For example, it used to be the case that the simple concept that water in soils moved in response to a gradient in matric potential led automatically to a partial differential equation (known as the Richards equation). However, in recent years, several researchers showed that a different type of mathematics (fractional calculus) could be used to represent the process mathematically, leading to a different form of partial differential equation, while other researchers demonstrated that very reliable simulations of the same process could be obtained without invoking partial differential equations at all, but by using another type of mathematics, related to Cellular Automata. These variety of ways by which a given perceived reality can be expressed mathematically is illustrated in this book by the 3 chapters under Theme I: “Model conceptualization”.

Once a model is conceptualized and formulated mathematically, it must be transformed into a numerical algorithm, which again can be done in a number of ways, and it must be ultimately implemented into a computer code, in one of a number of available higher-level languages and using one of a number of computing techniques (*e.g.*, object-oriented programming). Computer scientists have known for a long time that significant errors can creep in at this stage, making the outcome of running the computer code unlike anything that it should have produced. The culprit there is the inexact arithmetic performed by computers, and round-off errors that ensue. Fortunately, there is a number of techniques (described under Theme II in this book) that allow programmers to monitor the propagation of round-off errors, and suggest ways to re-write the code to avoid the most blatant computational errors. At this point, none of these techniques is commonly used by environmental scientists and engineers. One of the motivations for including detailed coverage of these techniques in a book like this one was precisely to show the environmental community that it is straightforward to make sure that computers really do what we think we ask them to do, and that the traditional comparison of computer code outputs with exact solutions of mathematical equations (a process known as benchmarking) is not the only option...

The next step in the modelling process, once a computer code has been produced and verified, is to attempt to determine how sensitive it is to input parameter values and to calibrate it, *i.e.*, obtain values for its parameters using available data. This calibration step is often referred to as “history matching” in some quarters

(petroleum engineering). Again, this can be done in a number of ways, leading to further uncertainty. The 3 chapters under Theme III (“Calibration and sensitivity analysis”) address some of the issues, and in particular, some of the subjectivity involved at this stage.

The next step is probably the one about which most of the writing on the modelling process has focussed. Some modellers have promoted for years the idea that if a calibrated model is able to “perform well” with one or more new sets of data, then the model (really the computer code one tests) should be considered “validated”, somehow. When the term “validation” became the object of heated debate, in the late 90s, some replaced it with the term “verification”, appropriating in the process a term used by computer scientists for something entirely different (see above). A term that seems better, in the sense that it does not claim more than what is actually attempted, is that of “suitability assessment”. All one does at this point is to determine if a computer code, produced for a specific purpose, within a sometimes narrow range of constraints, appears suitable for the task. That does not mean that the code, one of many that could have been developed to describe the given situation, is a true depiction of reality.

If a computer code is considered “suitable”, then one might perhaps consider using it to see what might happen in the future, if some sets of conditions are modified slightly from their current state, or if current trends continue unchanged. Issues involved in determining the overall predictive uncertainty one might expect under these conditions were dealt with in Theme IV during the ASI.

At this stage, the modelling process *per se* is completed, but some of the most significant problems remain. It is one thing for scientists and engineers to be aware of uncertainties that creep in the modelling process at various stages, but for this knowledge to be useful for those who use model predictions, it is crucial that these uncertainties be explained, and their extent described in detail. The problem there, in many cases, is that scientists shot themselves in the foot by claiming for centuries that science is about certainty and produces “truth” with a capital “T”. Now that scientists are dealing with horrendously complicated systems (environmental systems are undoubtedly among the most complicated that scientists have ever tried to describe), some back-pedalling is in order, and a new language about science needs to be invented, to provide the public and policy-makers with reliable information. The two chapters under Theme V (“Communicating modelling results and uncertainties”) deal with this occasionally very difficult process.

Environmental policy-making has traditionally relied on model predictions but the idea of taking modelling uncertainties into account still is in its infancy, in many contexts. This vital area, about which researchers and modellers should be far more knowledgeable than they generally tend to be, is addressed in the chapter under Theme VI (Decision making on the basis of model prediction).

Finally, three different sections, at the end of the book contain “Case study” chapters that were meant to illustrate some of the concepts and techniques described in earlier chapters. These case studies deal with the fate and dynamics of carbon in soils (Case study I), about which there are significant uncertainties in

models at this point, global climate change (Case study II), and the natural attenuation of contaminants and risk assessment (Case study III).

It is our hope that the material contained in this book will, like the NATO ASI from which it originates, serve a useful purpose of stimulating debate on a very important aspect of the use of models in support of environmental policy making. There are clear signs that this long-overdue debate is taking shape, that scientists are spending more time than in the past reflecting about the various steps involved in their modelling efforts, about the subjectivity they unavoidably introduce here and there, and about the uncertainties that result. At the same time, the users of model predictions are also becoming more keenly aware of the nature and limitations of the information they are getting. Undoubtedly, much more discussion will need to take place in the next few years in this area. We will be immensely pleased if, as a result of our efforts in editing this book, some of the material presented in the following pages is found helpful, and fosters further reflection.

The editors:

Philippe C. Baveye
Magdeline Laba
Jaroslav Mysiak

Contributors

Bormann, Helge

Junior professor für Hydrologie, Institut für Biologie und Umweltwissenschaften, Carl von Ossietzky Universität Oldenburg, Uhlhornsweg 84, D-26129, Oldenburg, Germany. Tel.: +49-441-798-4459. E-mail: helge.bormann@uni-oldenburg.de.

Boykoff, Maxwell T.

Environmental Change Institute, School of Geography and the Environment, South Parks Road, Oxford, OX1 3QY, United Kingdom. Phone: +44- 1865 285531 E-mail: maxwell.boykoff@eci.ox.ac.uk.

Breuer, Lutz

Institute for Landscape Ecology and Resources Management, Justus-Liebig-University Giessen, Heinrich-Buff-Ring 26, D-35392 Gießen, Germany, Phone: +49-641-9937395, Fax: +49-641-9937389, E-mail: lutz.breuer@agrar.uni-giessen.de.

Briones, Maria J.I.

Departamento de Ecología y Biología Animal, Universidad de Vigo, 36310 Vigo, Spain. Phone: +34 986 812594, Fax: +34 986 812556, E-mail: mbriones@uvigo.es.

Budtz-Jørgensen, Esben

Department of Biostatistics, Institute of Public Health, University of Copenhagen, Øster Farimagsgade 5B, 1014 København K, Denmark. E-mail: ejb@biostat.ku.dk.

Chesneau, Jean-Marie

Laboratoire d'Informatique de Paris 6, Université Pierre et Marie Curie - Paris 6, 4 place Jussieu, 75252 Paris cedex 05, France. Phone : +33 1 44 27 87 76. Fax : +33 1 44 27 53 53. E-mail: Jean-Marie. Chesneaux@lip6.fr.

Csendes, Tibor

Institute of Informatics, University of Szeged, Szeged, Hungary. Phone: +36 62 544 305. E-mail: csendes@inf.u-szeged.hu

Falloon, Pete

Met Office, Hadley Centre for Climate Prediction and Research, Fitzroy road, Exeter, EX1 3PB, United Kingdom. Phone: +44 0 1392 886336, Fax +44 0 1392 885681, E-mail: Pete.falloon@metoffice.com.

Gaganis, Petros

Department of the Environment, University of the Aegean, University Hill, Xenia Building, 81100 Mytilene, Greece. Phone: +30-22510-36293. E-mail: gaganis@aegean.gr.

Giertz, Simone

Geographical Institute, University Bonn, Meckenheimer Allee 166, D-53115 Bonn, Germany, Phone: +49-228-731635, Fax: +49-228-735393, E-mail: sgiertz@uni-bonn.de.

Grandjean, Philippe

Department of Environmental Medicine, Institute of Public Health, University of Southern Denmark, Winslowparken 17, DK-5000 Odense, Denmark. Telephone: +45 6550 1000 / 3769, Direct line: +45 6550 3769, Fax: +45 6591 1458, E-mail: pgrandjean@health.sdu.dk.

Haugan, Peter M.

Geophysical Institute, University of Bergen, Allegaten 70, N-5007 Bergen, Norway. Phone: +47 5558 2678. E-mail: Peter.Haugan@gfi.uib.no.

Huisman, Johan A.

ICG-4 Agrosphere, Forschungszentrum Jülich GmbH, D-52425 Jülich, Germany, Phone: 0049 2461 61 8607, Fax: 0049 2461 61 2518, E-mail: s.huisman@fzjuelich.de.

Jézéquel, Fabienne

Laboratoire d'Informatique de Paris 6, Université Pierre et Marie Curie - Paris 6, 4 place Jussieu, 75252 Paris cedex 05, France. E-mail: fabienne.Jezequel@lip6.fr.

Jones, Chris

Terrestrial Carbon Cycle Group, Met Office, Hadley Centre for Climate Prediction and Research, Fitzroy road, Exeter, EX1 3PB, United Kingdom. Tel: +44 (0)1392884514, Fax:+44 (0)1392 885681, E-mail: chris.d.jones@metoffice.gov.uk.

Keiding, Niels

Department of Biostatistics, Institute of Public Health, University of Copenhagen, Øster Farimagsgade 5B, 1014 København K, Denmark. E-mail: n.keiding@biostat.ku.dk.

Kuzmanova, Iordanka

Department of Microbiology and Environmental Biotechnologies, Agricultural University-Plovdiv, 12, Mendeleev Str., 4000-Plovdiv, Bulgaria. Cell phone: +359 4000 61 26. E-mail: iordanka.kuzmanova@au-plovdiv.bg.

Lamotte, Jean-Luc

Laboratoire d'Informatique de Paris 6, Université Pierre et Marie Curie - Paris 6, 4 place Jussieu, 75252 Paris cedex 05, France. E-mail: Jean-Luc.Lamotte@lip6.fr.

Mascherini, Massimiliano

The European Commission, Joint Research Centre, Institute for the Protection and Security of the Citizen (IPSC), TP 361, 21027 Ispra (VA), Italy. E-mail: Massimiliano.Mascherini@jrc.it.

Mendicino, Giuseppe

Dipartimento di Difesa del Suolo, Università della Calabria, Ponte Pietro Bucci, Cubo 41 b 87036, Arcavacata di Rende (CS), Italy. E-mail: menjoe@dds.unical.it.

Patt, Anthony

International Institute for Applied Systems Analysis, Schlossplatz 1, A-2361 Laxenburg, Austria, patt@iiasa.ac.at. Phone: +43 2236 807 306, Fax: +43 2236 807 466, Mobile: +43 664 438 9330. E-mail: patt@iiasa.ac.at.

Peña, Vanessa

London School of Economics, Department of Geography, London, United Kingdom. E-mail: v.pena@lse.ac.uk.

Polhill, J. Gary

Macaulay Institute, Craigiebuckler, Aberdeen. AB15 8QH, Scotland. E-mail: g.polhill@macaulay.ac.uk.

Saltelli, Andrea

The European Commission, Joint Research Centre, Institute for the Protection and Security of the Citizen (IPSC), TP 361, 21027 Ispra (VA), Italy. E-mail: andrea.saltelli@jrc.it.

Sancho, Enrique

Department of Microbiology, Edif. Severo Ochoa, Campus Rabanales, University of Córdoba, 14071, Córdoba, Spain. E-mail: edsancho@uco.es.

Shilev, Stefan

Department of Microbiology and Environmental Biotechnologies, Agricultural University-Plovdiv, 12, Mendeleev Str., 4000-Plovdiv, Bulgaria. Cell phone: +359 898 410991. E-mail: stefan.shilev@au-plovdiv.bg.

Straface, Salvatore

Dipartimento di Difesa del Suolo, Università della Calabria, Via P. Bucci, 42B, 87036, Rende, Italy. Phone: +39+0984+496572. E-mail: straface@dds.unical.it.

Todini, Ezio

Dipartimento di Scienze della Terra e Geologico-Ambientali, Piazza Di Porta S. Donato, 1 Bologna, Italy. Phone: +39 051 209 4537.
E-mail: todini@geomin.unibo.it.

Trevisan, Marco

Istituto di Chimica Agraria ed Ambientale, Facoltà di Agraria, Università Cattolica del Sacro Cuore, Piacenza, Italia. Phone: +39 0523599218. E-mail: marco.trevisan@unicatt.it

Vidoni, Daniele

The European Commission, Joint Research Centre, Institute for the Protection and Security of the Citizen (IPSC), TP 361, 21027 Ispra (VA), Italy. E-mail: daniele.vidoni@jrc.it.

Viney, Neil R.

CSIRO Land and Water, GPO Box 1666, Canberra, ACT 2600, Australia,
E-mail: neil.viney@csiro.au.

THEME I. MODEL CONCEPTUALIZATION

Spatially explicit versus lumped models in catchment hydrology – experiences from two case studies

Helge Bormann¹, Lutz Breuer², Simone Giertz³, Johan A. Huisman⁴,
Neil R. Viney⁵

¹ Department of Biology and Environmental Sciences, University of Oldenburg,
Uhthornsweg 84, D-26111 Oldenburg, Germany.

² Institute for Landscape Ecology and Resources Management, Justus-Liebig-University
Giessen, Heinrich-Buff-Ring 26, D-35392 Gießen, Germany.

³ Geographical Institute, University Bonn, Meckenheimer Allee 166, D-53115 Bonn,
Germany.

⁴ ICG-4 Agrosphere, Forschungszentrum Jülich GmbH, D-52425 Jülich, Germany.

⁵ CSIRO Land and Water, GPO Box 1666, Canberra, ACT 2600, Australia.

Abstract

This paper analyses the major features of spatially explicit and lumped hydrological models based on two case studies. For two different catchments in West Africa and Germany model intercomparison studies were performed to reveal the model structure and spatial resolution dependent advantages and disadvantages of the different model types. It can be shown that different model types (lumped versus distributed models and conceptual versus physically based models) have benefits and drawbacks. But all model predictions of different type models contain some valuable information when used for the simulation of catchment water fluxes. Using local scale data from intense field experiments, the sophisticated and spatially explicit models simulate stream flow of a West African catchment with the same performance obtained by lumped models that can be calibrated more efficiently. In addition, the spatially explicit models generate plausible spatial patterns of state variables and processes which can be validated by additional observations. Using regional scale available data to predict stream flow of a German catchment, the simpler models tend to perform better in both calibration and validation periods. But while all models tend to show improved performance during the less extreme validation period, this improvement is greatest for some of the more complex models. Applying the same models (of different model types) to three land use change scenarios, there is broad agreement among the models on the expected hydrological change. This suggests that we can predict with some confidence the direction and magnitude of stream flow changes associated with

land use change, especially by combining the predictions of different model types. As a short outlook, it is shown that a simple multi-model application offers a sound basis for multi-model ensembles that are based on a technique currently applied successfully in many atmospheric forecast and scenario studies.

Keywords: spatially explicit models, lumped models, model comparison, land use scenarios, scale, multi-model ensemble.

1. Introduction

Evaluating the impact of changing environmental conditions on water flows is an ongoing topic in hydrological research. For example climate and land use changes affect the water fluxes at the land surface. Hydrological modelling studies of such changes have been conducted since the 1970s (e.g., Binley *et al.*, 1991; Calder *et al.*, 1995; Onstad and Jamieson, 1970). One of the challenges in hydrological modelling is to account for environmental changes by altering at least some of the model parameters. Therefore, it is often assumed that spatially explicit and process based models are best suited to predict the effects of changing environmental conditions (Beven and Binley, 1992). As in many cases changes occur only in parts of a catchment, it is further argued that spatially explicit models depict these changes more precisely as compared to lumped model approaches (Beven, 2001). Following these assumptions, many complex models have been developed that are assumed to be capable of simulating environmental change. However, these spatially explicit and physically based model approaches are often criticised because the necessary a priori estimation of model parameters is difficult (Beven, 2001; Ewen and Parkin, 1996).

As an alternative, physically based, semi-distributed models with less complex spatial representation have been proposed. This group of models simulates all hydrological process within spatially non-explicit Hydrological Response Units (HRU). Results for each HRU can be lumped within subcatchments and routed downstream. HRUs can be defined based on soil units, land use or a combination of both. Although the impact of environmental change is not simulated with the same spatial resolution as in the spatially explicit approach, these semi-distributed models still require a considerable amount of parameters that might be difficult to obtain. A further simplification is achieved if hydrological fluxes are simulated with the subcatchment scale as the smallest spatial unit. Conceptual models such as HBV (Bergström, 1995) follow this concept. Depending on the size of these subcatchments, the spatial resolution of the simulations is rather coarse. At the lower end of complexity, fully lumped and mostly conceptual models can be found. These models are characterized by a simple model structure and a small number of conceptual model parameters. General catchment attributes, such as land use area and catchment area, can be used to regionalize model parameters.

It is argued that data limitations in many catchments limit the application of spatially explicit and physically based models, and that lumped or semi-distributed models provide a more appropriate alternative (Croke *et al.*, 2004).

Regardless of the model type chosen (conceptual versus physically based and lumped versus spatially explicit), extrapolations to future conditions are difficult to carry out (Refsgaard *et al.*, 2006). Despite increasing knowledge, a high degree of uncertainty remains in all model approaches. The origin of this uncertainty can be caused by measurement errors of model input and output data, determination of model parameters, and spatial as well as temporal heterogeneity. These different origins of uncertainty can be related to different model types, which is one issue to reveal in this paper. Furthermore, from two case studies presented, the general features of spatially explicit and lumped models will be discussed and shown to be closely related to hydrological process representation, scale and different sources of uncertainties.

2. General features of lumped and spatially explicit hydrological models

The citations mentioned in the introduction of this paper reveal that different modelling philosophies exist to represent the catchment water flows within catchments. A lot of modelling systems based on different model structures have been developed to analyse hydrological systems as well as changes in hydrological systems. And almost all of them have been proven successful in mimicing the behaviour of hydrological catchments. The authors of these models explain very well the advantages of the specific model type and justify why their model should be favoured in a specific case. However, it is evident that different concepts stand vis-à-vis, all of them featuring advantages as well as disadvantages. Therefore some of the general properties of lumped and spatially explicit (= spatially distributed) models will be mentioned in this section, partly derived from the literature mentioned in the introduction, partly based on modelling experience of the authors. A complete overview of the general features of the models is provided in Table 1.

From their definition, lumped models do not represent spatial structures, while spatially explicit models do. Therefore the effort to set up such models is relatively small for lumped models and considerably higher for spatially explicit ones. This context is enhanced by the fact that most lumped catchment models are conceptual (*e.g.*, storage based) while spatially explicit models can be conceptual or physically based. From the model structure it can be deduced that lumped models generate an integral response for the model space only. That limits the calibration against integral measurements but otherwise makes it very efficient. However, it also limits model validation in contrast to spatially explicit models, which can be parameterised and validated to spatially distributed observations (limited by the constraints of the scale triplet: scaling, support and extent; Blöschl, 1996). Thus,

Table 1. General features of different hydrological model types.

Model Features	Lumped Models	Spatially-Explicit Models
Effort for model setup	Low	High
Spatial structures	No	Yes
Model results	Integral response	Distributed water fluxes and integral response
Model parameterisation	Manual or automatical calibration	Mainly a priori estimation of parameters; calibration difficult (conceptual) or almost impossible (physically based)
Model validation	Only integral response	Integral response, distributed water flows and state variables
Main source of uncertainty	Concept, lumped	Input data, parameters (dependent on scale)
Suitability for scenarios	Limited	Yes

summarizing from this short discussion, it can be assumed that the main uncertainty source of lumped models is the simple model concept itself and the missing consideration of spatial structures. The latter is a concern if the particular application demands spatially explicit predictions or if non-linear interactions between different catchment characteristics can be assumed. On the other hand spatially explicit models take care of spatial structures and often describe the hydrological processes in a physical way although important processes can also be missed. But they are, as mentioned, more difficult to parameterise, as parameters (at least partly) have to be determined a priori. An efficient calibration of the models therefore is difficult due to the spatially distributed nature of those models. Due to the physical interpretability of parameters (in case of physically based models) and the consideration of spatial structures, most model users favour spatially explicit models for use in land use change scenario studies.

3. Case study I: The upper Ouémé catchment (Bénin)

Bénin is among the poorest countries worldwide. The majority of the population lives from rain-fed agriculture, performing self-supply or selling products on local markets. A few cash-crops are cultivated such as cotton and cashews, but the profit is limited due to low standard of techniques and the absence of fertilizers. Due to these boundary conditions the agricultural system is very vulnerable to changing environmental conditions such as climate change and land degradation.

The Upper Ouémé catchment (Figure 1) is located in the tropical, subhumid Guinea-zone which is characterized by a unimodal rainy season from May to October. The mean annual precipitation of the region is about 1100 mm. Most parts of the catchment are covered by degraded Savannah vegetation except agricultural

areas. Due to rapid increases in population, the area of agricultural land is increasing relatively fast, inducing a further degradation of the natural vegetation. The conversion of Savannah into agricultural fields also leads to severe soil degradation, because of the soil being compacted and less protected by vegetation when the rainy season starts. As most of the precipitation comes from squall lines causing short but highly intense rainfall events, soil erosion and therefore soil degradation are important issues.

Another important issue is the climate change in that region. During the 1970s and 1980s, the Guinea-zone – like the Sahel – was affected by many dry years with severe consequences for rain-fed agriculture and drinking water supply. Future regional climate scenarios predict decreasing rainfall amounts and/or a shorter rainy season which could have severe effects (Bormann, 2005a). Agriculture as well as drinking water supply systems could need to be reorganised to be able to account for the changing water availability. Based on these boundary conditions, modelling of the hydrological processes can help to understand and

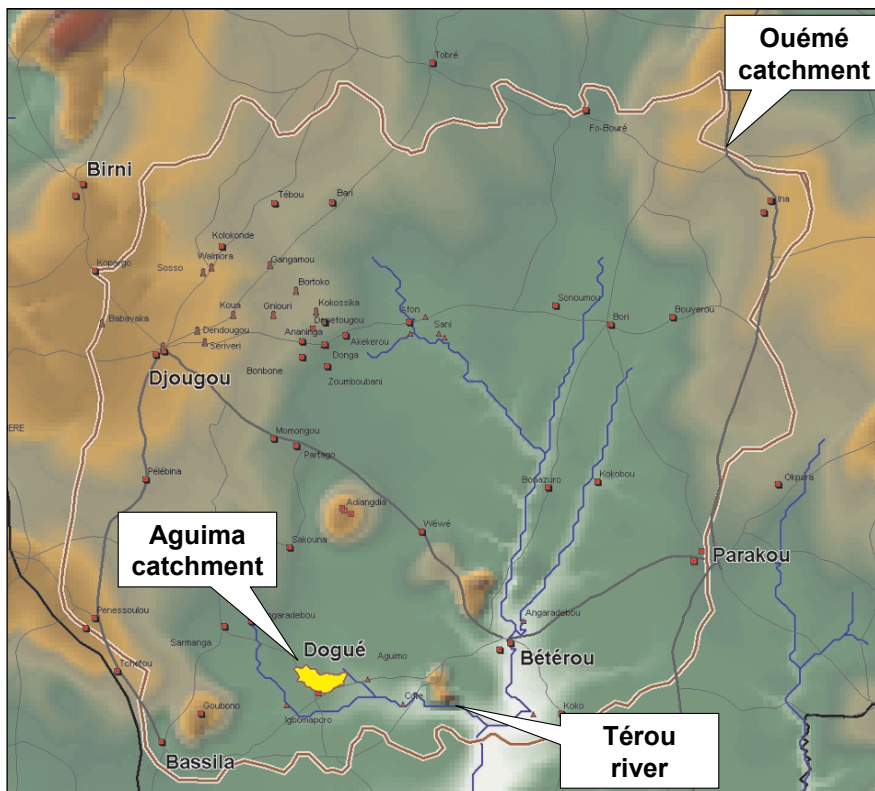


Fig. 1. Upper Ouémé (14,000 km²) and Aguima (30 km²) catchments in Bénin, West. Africa.

predict the effects of the changing environment in the upper Ouémé catchment on the hydrological processes. The results presented in this section were obtained in the framework of the IMPETUS project of the Universities of Cologne and Bonn (Germany) which is an interdisciplinary project focusing on an efficient management of water and soil in the subhumid tropics of Bénin (Impetus, 2008). At the local scale Aguima catchment (30 km^2), intensive field investigations were performed to understand the hydrological processes and to drive local scale hydrological models. On the regional scale, modelling activities are based on available maps and operational data bases.

3.1. *Hydrological catchment models*

Three hydrological models were applied at different scales in the Ouémé catchment: The fully distributed and spatially explicit TOPLATS model (Peters-Lidard *et al.*, 1997), the semi-distributed hillslope version of the physically based SIMULAT model (Diekkrüger and Arning, 1995), and the spatially lumped and conceptual UHP model (Bormann and Diekkrüger, 2004).

TOPLATS (TOPMODEL based land atmosphere transfer scheme; Peters-Lidard *et al.*, 1997) is a spatially explicit, grid based, time continuous and multi-scale model. It combines soil-atmosphere-transfer-scheme, calculating the local scale vertical water fluxes, with the TOPMODEL approach which laterally redistributes the water in the catchment. While the processes within the lower atmosphere are described in a physically based way, the soil water flow is simulated using an approximation of the Richards' equation for a limited number of soil layers. Interflow as well as a routing routine is not integrated into the model. Baseflow is calculated using a recession function based approach.

SIMULAT-H (Giertz *et al.*, 2006) is the hillslope version of the 1-dimensional SVAT-scheme SIMULAT. SIMULAT is physically based, calculating the soil water fluxes using the Richards' equation and evapotranspiration is based on the Penman-Monteith approach. Spatial variability of soil properties is accounted for by assuming for each soil a log-normal distributed saturated hydraulic conductivity and running ten different infiltration simulations. Parameter sampling is done based on the Latin Hypercube method and the average of the ten infiltration simulations finally infiltrates. In the hillslope version each slope is divided into a number of subunits. The surface runoff simulated upslope is considered as additional input into the downslope subunit. Baseflow is simulated using the conceptual, linear reservoir approach. Stream flow is simulated as simple superposition of the single runoff components of the riverine subunits.

The UHP model (Bormann and Diekkrüger, 2004) is a lumped and conceptual HBV type (Bergström, 1995) model. The model consists of four linear storages for interception, root zone, unsaturated zone and groundwater. Instead of the wetness-index of the HBV model the SCS curve number approach of the USGS is used (SCS, 1972). Percolation occurs if the soil water status exceeds field capacity.

Table 2. Models applied to the Aguima and upper Ouémé catchments: spatial resolution, model type and description of the main hydrological processes.

Model Characteristics	TOPLATS	SIMULAT-H	UHP
Model type	Distributed process based	Quasi distributed physically based	Lumped conceptual
Simulation units	Grid cells	Slopes	Catchments
Evapotranspiration	Penman-Monteith	Penman-Monteith	Priestley-Taylor
Surface runoff	Infiltration excess and saturation excess	Richards equation	SCS curve number
Soil moisture	Richards approximation	Richards equation	Bucket approach
Interflow	Not included	Darcy	Non-lin. storage
Base flow	TOPMODEL	Lin. storage	Lin. storage

Calculation of baseflow is based on a linear storage if the groundwater level exceeds a certain threshold. A summary of the main features of the models is provided in Table 2.

3.2. *Model application and comparison at the local scale*

For the parameterisation of the physically based model components, a comprehensive field survey was performed within the IMPETUS project. The following spatial data sets and time series were available for model application on the local scale (Aguima catchment): a digital elevation model, derived from topographic maps; a soil map (Junge, 2004); a vegetation classification based on Landsat data; data of three local climate stations and five stream gauges. Model parameters were based on field studies concerning soil hydrology (Giertz, 2004), vegetation (Orthmann, 2005) and agriculture (Mulindabigwi, 2005). Stream flow data of the years 2001–2003 were available to calibrate and to validate the models.

Therefore most model parameters of the TOPLATS and SIMULAT-H models were defined a priori. Only the groundwater components of those two models were calibrated. In contrast, all of the parameters of the UHP model had to be calibrated. The following model performance criteria were used: The coefficient of determination r^2 , the coefficient of model efficiency (me; equation 1; Nash and Sutcliffe, 1970) and the bias in annual stream flow which is defined as the relative difference between simulated (Q_{sim}) and observed (Q_{obs}) stream flow (equation 2):

$$me = 1 - \frac{\sum (Q_{sim} - Q_{obs})^2}{\sum (Q_{obs} - \bar{Q}_{obs})^2} \quad (1)$$

$$Bias = \frac{Q_{sim} - Q_{obs}}{Q_{obs}} \quad (2)$$

The TOPLATS model was manually calibrated for the year 2001 for the upper Aguima catchment (3.2 km^2). Only base flow parameters were adjusted, all other parameters were determined a priori. Total annual stream flow is simulated with high accuracy (Bormann *et al.*, 2005a). The comparison of simulated and observed stream flow hydrographs reveals that the model partly underestimates base flow (Figure 2). Peak flows are well simulated, except that the highest peak is simulated with 1-day delay as no routing is integrated in the model. Compared to the calibration period the validation of the model for the years 2002 and 2003 yields less satisfactory results. Stream flow is underestimated in the beginning of the rainy season and overestimated in the high rainy season and in the end of the rainy season. Model efficiency decreases significantly, and the bias in stream flow for single years is more than 100%. Furthermore, a recalibration of TOPLATS did not result in satisfactory simulation results (Giertz and Diekkrüger, 2006). Nevertheless, soil moisture patterns predicted by TOPLATS were plausible and in good agreement with observed soil moisture patterns in the field (Giertz, 2004).

The SIMULAT-H model was calibrated manually for 2002 against stream flow. Only parameters of the baseflow and the lateral saturated hydraulic conductivity were calibrated. Calibration resulted in high model efficiencies and acceptable simulation of the water balance (Giertz *et al.*, 2006). Observed and simulated

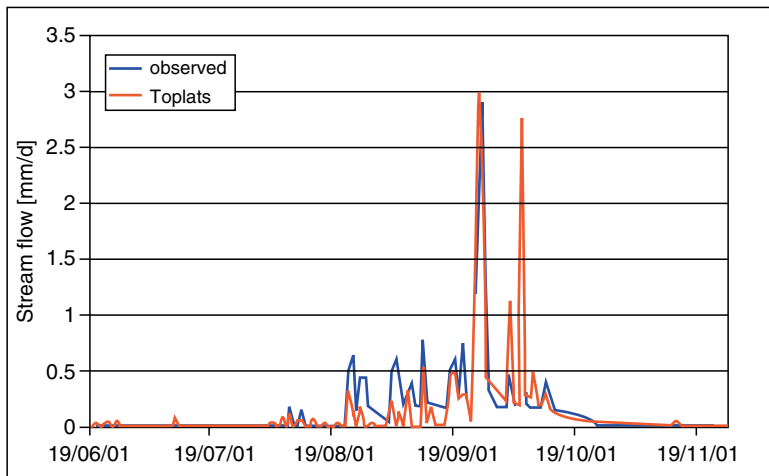


Fig. 2. Streamflow of the upper Aguima catchment (3.2 km^2), simulated by the TOPLATS model (calibration).

hydrographs show a good correlation (Figure 3). In addition, the split sample test (validation for the remaining years) as well as the proxy basin test (application of SIMULAT-H to the lower Aguima catchment for the remaining years 2001 and 2003) yielded satisfactory simulation results (Figure 4) and a model efficiency

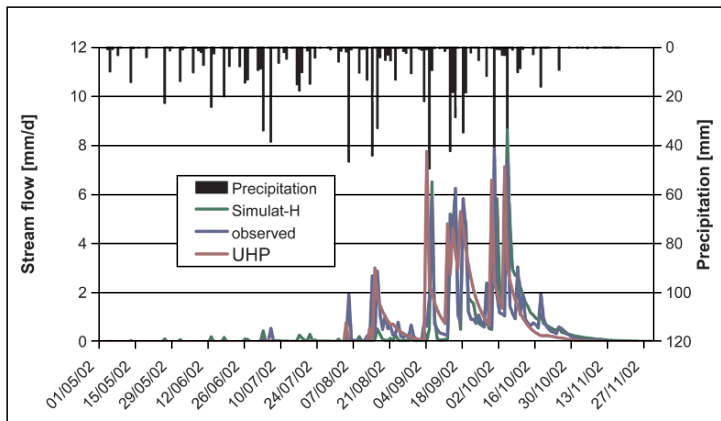


Fig. 3. Streamflow of the upper Aguima catchment (3.2 km^2), simulated by Simulat-H and UHP models (calibration).

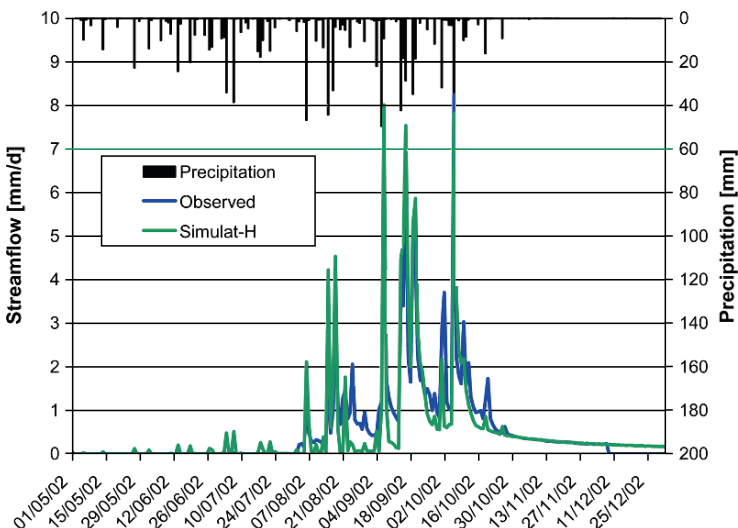


Fig. 4. Streamflow of the Aguima catchment (16 km^2), simulated by the Simulat-H mode (validation).

which for some years was even higher than for the calibration period. Furthermore, simulated soil moisture of two selected slopes could be compared to observed soil moisture at two soil moisture stations (Figure 5). Observed and simulated soil moistures revealed a good agreement in particular in the dynamics at the event scale as well as for the whole rainy season (Bormann *et al.*, 2005a).

The UHP model was calibrated for the year 2002. The performance of the lumped conceptual models was satisfactory (Figure 3). Stream flow dynamics as well as the peaks were well simulated. Annual stream flow was slightly overestimated. A validation for the upper Aguima for the years 2001 and 2003 revealed results with a decreasing but still satisfactory quality. A few stream flow events are highly overestimated. Nevertheless, the UHP model obtains satisfactory simulation results for all years (r^2 and model efficiency larger than 0.6). The model generally captures the stream flow dynamics well, overestimating the stream flow in the beginning of the rainy season and the declining discharge at the end of the rainy season (Giertz and Diekkrüger, 2006).

Comparing deviations between observed and simulated stream flow, a similar trend between SIMULAT-H and UHP models can be observed (Giertz and Diekkrüger, 2006). The lumped UHP model shows larger differences to observed values compared to the quasi-distributed SIMULAT-H model. The spatially explicit TOPLATS model shows different stream flow dynamics with respect to overestimation of specific events. This behaviour as well as the different quality of model results (performance criteria, see Table 3) can be explained by the model related uncertainties in the rainfall-runoff modelling process.

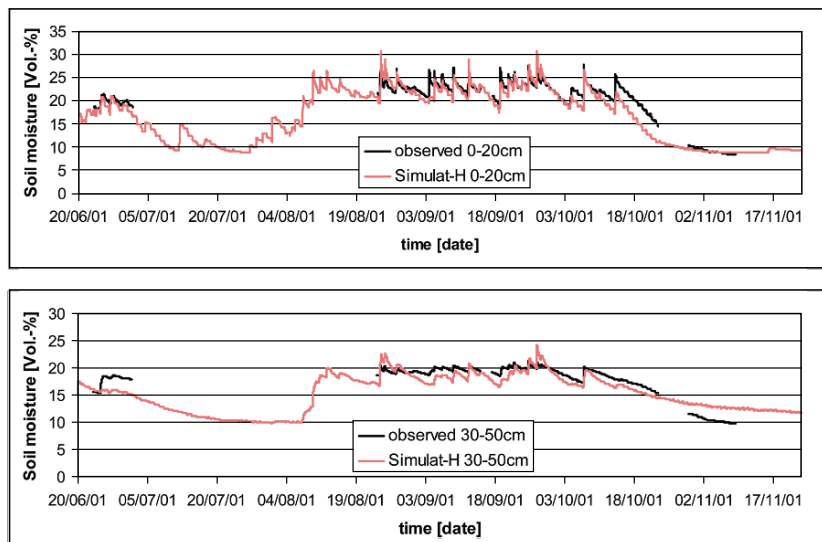


Fig. 5. Comparison of observed and simulated (Simulat-H) soil moisture at one soil moisture station in the upper Aguima catchment.

Table 3. Quality measures of different models applied at different scales within the upper Ouémé basin, Bénin (calibration). Time steps: days on local scale, weeks on regional scale.

Scale – Basin	TOPLATS	SIMULAT-H	UHP
Local – Upper Aguima (3.2 km ²)	$r^2 = 0.51$, $me = 0.62$ Bias = 7.4%	$r^2 = 0.78$, $me = 0.82$ Bias = 7.3%	$r^2 = 0.70$, $me = 0.69$ Bias = 11.5%
Local – Aguima (16 km ²)	$r^2 = 0.56$, $me = 0.38$ Bias = -3.5%	$r^2 = 0.87$, $me = 0.86$ Bias = -5.1%	$r^2 = 0.62$, $me = 0.61$ Bias = 6.6%
Regional – Térou (3,133 km ²)	$r^2 = 0.77$, $me = 0.50$ Bias = -13.9%	Not applicable	$r^2 = 0.81$, $me = 0.76$ Bias = 0.1%
Regional – Upper Ouémé (14,000 km ²)	Not applicable	Not applicable	$r^2 = 0.76$, $me = 0.74$ Bias = 5.3%

r^2 = coefficient of determination; me = model efficiency; Bias: see equation (1).

The UHP model cannot represent the spatial distribution of properties and processes due to its lumped character. However, lumped models, and conceptual models in general, can well represent the rainfall runoff process, as calibration is mostly very efficient. In addition, the SCS curve number approach (SCS, 1972) implemented in the UHP model partly considers the variability of land surface characteristics based on its statistical character. Thus, the good results for the representation of the rainfall-runoff process could be expected.

In contrast, the SIMULAT-H model is a physically based model and it is claimed that such models have less structural uncertainties with respect to process representation. As a very detailed data based is available, such a model concept can be successfully applied on the small scale. However, physically based models often have poor representations of macropore flow, for example. And even if they have, a sound parameterisation on the catchment scale is rather difficult. Another drawback of the model is the absence of a routing routine. Nevertheless, on the daily time scale where model results and observations were compared, the impact of this uncertainty can be expected to be small in a catchment of this size with a response time of 1–2 h. Compared to the fully distributed TOPLATS model, one disadvantage of SIMULAT-H is the limitation of spatial distribution of properties and processes to selected hillslopes. Only if a sufficient number of hillslopes are used to describe the catchment, and only if those hillslopes are representative, can SIMULAT-H be successfully applied to describe the catchment wide rainfall-runoff process.

Finally, the TOPLATS model is the only fully spatially explicit model. From this point of view it should be suited best to describe spatially distributed hydrological processes. But one important limitation of TOPLATS is the assumption that the concept of the topographic index (taken from TOPMODEL) is valid in the flat terrain of West Africa which is not the case as this study showed. In addition,

the lateral interaction between grid cells is limited to the redistribution of ground-water tables. Much more important would be the representation of the lateral interaction of fast flow processes on hillslopes as observed in the field (Giertz, 2004; Junge, 2004). These processes are not sufficiently represented by the TOPLATS model. Similarly, the representation of soil hydrological processes is limited, as TOPLATS considers only two different soil layers. Thus, vertical soil structures cannot be described in detail. Consequently, despite having the best spatial resolution and the most spatially explicit model structure, model results are significantly worse compared to the semi-distributed SIMULAT-H model and the lumped UHP model.

3.3. Model application and comparison at the regional scale

At the regional scale the applicability of the UHP and TOPLATS models was tested. The physically based SIMULAT-H model was not applied at the regional scale (upper Ouémé catchment) due to the high data requirements. The data availability of the upper Ouémé catchment was good compared to other West African countries but not sufficient for physically based hydrological model applications. Available maps have a scale of 1:200,000: a soil map and a topographic map from which a digital elevation model was derived. In addition, a Landsat based land use classification was available. However, data content of the maps was not comparable to the information provided by maps of the same scale in central Europe. For example, the soil maps did not contain the information on the soil physical properties (soil texture, porosity, thickness) required by the simulation models, as the soil maps originally were derived from geological maps. The time series available concerning rainfall and weather often included gaps of some weeks, months or even years. Thus it was difficult to compose a data set of homogenous quality.

TOPLATS was applied to a 3133 km² sized subcatchment of the Ouémé catchment, the Térou catchment (Bormann and Diekkrüger, 2003). Applying the TOPLATS model to the operationally available data base described above results in an unsatisfactory simulation of the discharge of the Térou river. Although the seasonality of the runoff was modelled in an acceptable way, the stream flow variability during the rainy season could only be poorly reproduced. The model efficiency (Nash–Sutcliffe-coefficient) during calibration for an individual rainy season (1996) reaches a value of only 0.46 for weekly stream flow, with a coefficient of determination r^2 of 0.77. It can be assumed that the main reasons for the poor correlation are the coarse spatial and temporal resolution of rainfall data, the unavailability of sufficient information on soil hydrological parameters and the impossibility of parameterising a spatially distributed and process based hydrological model in a reasonable way und the given conditions.

Applying the lumped and conceptual UHP model to the Térou basin, a considerably better correlation between observed and simulated discharge is achieved for the calibration period. In this case, the model efficiency reached a value of 0.91

for weekly stream flow and a coefficient of determination (r^2) of 0.95 for individual years (Bormann and Diekkrüger, 2003). For a seven-year time period (1993–1999), model efficiency and r^2 still reached values of 0.8 (Bormann *et al.*, 2005b) although the quality of rainfall data of individual years was poor. Due to the limited number of model parameters (altogether twelve parameters for storage volumes, constants and the SCS curve numbers) and the spatially lumped model type, an efficient calibration of the model was feasible. In this study a manual calibration was performed. The UHP model could also be successfully validated to additional data from the Térou catchment (year 2000) as well as to other sub-catchments of the upper Ouémé (Bormann, 2005b). For most of the catchments the model performance was comparable to the results of the Térou catchment without any further calibration. A model application to the entire upper Ouémé yielded a model efficiency of 0.75 for the years 1997–2000 (Figure 6). While in the early rainy season stream flow is underestimated, peak flows are slightly overestimated by the UHP model. The recession curve in the late rainy season is well reproduced as well as the annual water budget.

From the results presented for the regional scale catchments in Bénin it can be concluded that the applicability of process based models is very limited if only a poor standard data base is available. In particular in African countries, information content, resolution and completeness of data sets is very limited and mostly not sufficient to drive process based and spatially distributed models. Even if those models contain a more realistic process description, the uncertainty in the model parameters and input data is very high. We therefore tend to apply conceptual (storage based) models in regions that are characterised by poor databases. However, spatial patterns can (and mostly will) be very important also in those regions. Giertz *et al.* (2006) therefore suggest the application of spatially distributed versions of conceptual models to combine the advantages of simplification of process

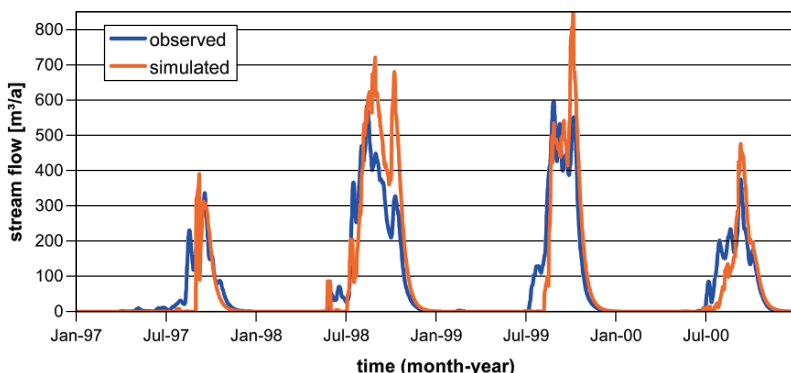


Fig. 6. Streamflow of the upper Ouémé catchment (14,000 km²), simulated by the UHP model (validation).

descriptions and robustness with information on the spatial distribution of properties and processes.

4. Case study II: The Dill catchment (Germany)

The Dill catchment in central Germany is a peripheral region dominated by forestry and extensive agriculture. Due to the traditional heritage system in the past, land was split between all children. Therefore, the pattern of land use across the catchment is highly fragmented, with an average field size of about 0.7 ha. Social, political and economic pressures are slowly transforming the land use. On the long-term, pastoralism and silviculture will likely increase because agriculture is not profitable anymore. In the framework of the Collaborative Research Center SFB 299 of the University of Gießen (Germany), strategies were investigated on how to make agriculture more profitable. One option was to think about a rearrangement of acreage by land reallocation. Based on a socioeconomic model, spatially explicit land use scenarios were developed. In the LUCHEM project, initiated by the working group on Resources Management of the University of Gießen, the effects of these land use scenarios on catchment hydrology were assessed by applying ten different hydrological catchment models to the Dill catchment.

The Dill river in central Germany is a tributary of the Lahn River, which ultimately flows into the Rhine River. The Dill River at Asslar has a catchment area of 693 km² (Figure 7). The topography of the catchment is characterised by low mountains and has an altitude range of 155–674 m. The mean annual precipitation

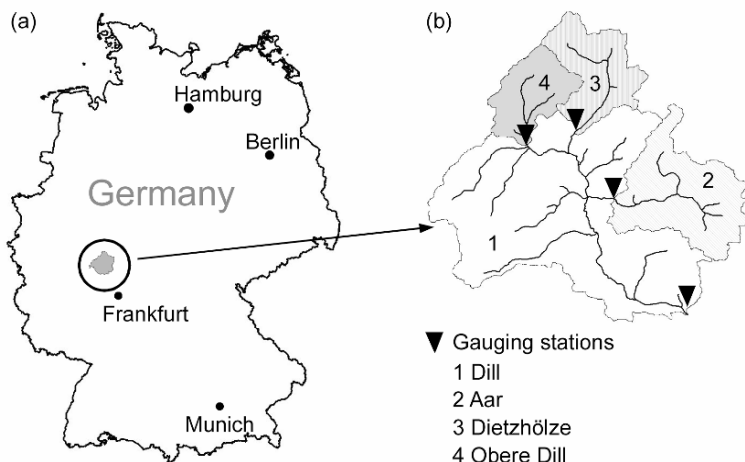


Fig. 7. Location of the Dill catchment, Germany.

of the Dill catchment varies from 700 mm in the south to more than 1100 mm in the higher elevation areas in the north. Just over half of the catchment is forested (with nearly even proportions of deciduous and coniferous species), while 21% is pasture, 9% is fallow, 6% is cropped (winter rape, winter barley, oats). The remaining 10% is almost entirely urban with a minor share of surface waters.

4.1. Hydrological catchment models

As mentioned above, ten models with the capability of predicting the impacts of land use change were applied to the Dill catchment. In approximately decreasing order of complexity (see Table 4), they were: DHSVM (Wigmsta *et al.*, 1994), MIKE-SHE (Refsgaard and Storm, 1995), TOPLATS (Peters-Lidard *et al.*, 1997), WASIM-ETH (Niehoff *et al.*, 2002), SWAT (Arnold *et al.*, 1998), PRMS (Leavesley and Stannard, 1995), SLURP (Kite, 1978), HBV (Bergström, 1995), LASCAM (Sivapalan *et al.*, 1996) and IHACRES (Jakeman *et al.*, 1990). In terms of their spatial resolution and the overall number of model parameters, the models represented a broad cross-section of complexity (Breuer *et al.*, 2009) ranging from fully distributed, physically-based models with explicit groundwater schemes (DHSVM, MIKE-SHE) to fully lumped, conceptual models (*e.g.*, IHACRES). Spatial computational areas were equivalent to pixels of the distributed models, Hydrological Response Units in the case of the semi-distributed models, and sub-catchments with respect to the more conceptual or even lumped models. The fully distributed models formed the group of the most complex models while the fully lumped models were most simple.

Table 4. Models applied to the Dill catchment, classified according to model parameters and computational units.

Model	Available Model Parameters	Number of Calibrated Parameters	Number of
Distributed			Pixels
DHSVM	>100	3	70.000
MIKE-SHE	>100	7	17.500
TOPLATS	>100	4	70.000
WASIM	>100	30	17.500
Semi-Distributed			HRU
SWAT	>100	6	795
PRMS	50	5	312
SLURP	36	8	252
HBV	10–20	10	100
LASCAM	24	24	29 sub catchments
Lumped			Simulation Units
IHACRES	6	5	1

In the LUCHEM project no common calibration procedure was applied as it was argued that the type and amount of model calibration is part of the model philosophy. The process based fully distributed models were generally calibrated manually while most of the more conceptual models were automatically calibrated using objective functions based on squared residual (e.g., root mean squared error or model efficiency after Nash and Sutcliffe, 1970). All models were calibrated using observed stream flow data for the period 1983–1989 and model predictions were developed for the validation period 1990–1998. A maximum of three years of additional weather data (1980–1982) was available for model spin-up (Breuer *et al.*, 2009).

In order to reduce the impact of model specific input data processing, a homogenous method for precipitation interpolation, a constant temperature lapse rate and common plant parameter sets were used. Such a homogenization of model input data improves the comparability of model structures and reduces the differences in model results due to data processing.

4.2. *Model application and comparison*

The models provided good predictions of the observed stream flow in terms of timing and magnitude of events (Figure 8). The envelope defined by the range of model predictions encompasses the observed stream flow on 96% of days, with little difference between calibration and validation periods. Model efficiency varied between 0.65 and 0.92 for the calibration period and between 0.61 and 0.92 for the validation period, with highest values simulated by the more conceptual and lumped to semi-distributed models such as LASCAM or HBV (Table 5).

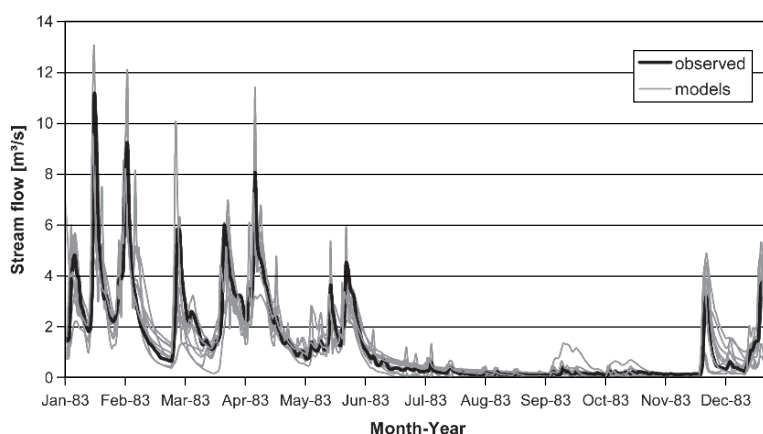
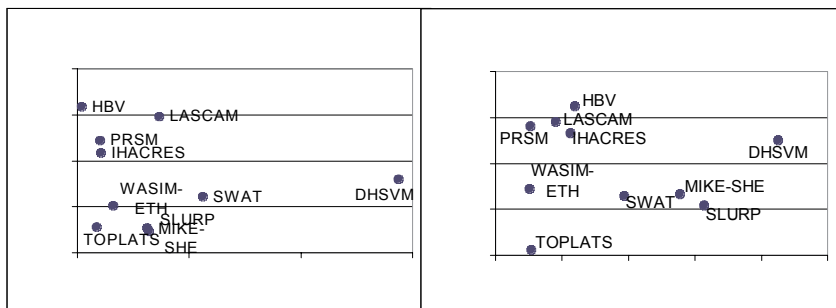


Fig. 8. Simulated stream flow of the Dill (gauge Asslar) for an exemplary year, using ten different catchment models.

Table 5. Model results of ten different models applied to the Dill catchment (calibration: 1983–1989; validation: 1990–1998).

Model	Calibration Period			Validation Period		
	RMSE	Absolute bias (%)	ME	RMSE	Absolute bias (%)	ME
SWAT	0.994	5.62	0.72	0.845	9.66	0.73
DHSVM	0.922	14.36	0.76	0.629	21.29	0.85
MIKE-SHE	1.118	3.21	0.65	0.839	13.86	0.73
HBV	0.540	0.18	0.92	0.444	5.96	0.92
TOPLATS	1.105	0.87	0.66	1.011	2.71	0.61
SLURP	1.106	3.11	0.65	0.876	15.67	0.71
IHACRES	0.806	1.04	0.82	0.595	5.65	0.87
LASCAM	0.606	3.67	0.90	0.538	4.52	0.89
PRMS	0.742	1.02	0.84	0.561	2.60	0.88
WASIM	1.026	1.60	0.70	0.821	2.53	0.74

Simulations under dry conditions scatter more as compared to under wet conditions. Some models overestimate discharge substantially as can be depicted in the bias for the entire simulation period for some models. Comparing observed and predicted peaks for the ten models, the fully distributed models such as TOPLATS, MIKE-SHE and WASIM tend to scatter more than the less complex models such as HBV or LASCAM. The better fit of peaks for the group of conceptual models can be partly explained by the fact that they were more effectively calibrated using automatic calibration techniques whereas the distributed physically based models were manually calibrated. It is obvious that most models that perform reasonably well in the calibration period also show acceptable model performance for the validation period. Scatter plots for two of the performance statistics (daily model efficiency and absolute bias) for each of the models are shown in Figure 9. Statistically, the best models are those with efficiencies approaching 1.0 and biases near 0%. For the calibration period, all but two of the models underpredict and

**Fig. 9.** Comparison of the model performance ten different hydrological catchment models applied to the Dill catchment: calibration versus validation.

have negative biases. However, no model has an absolute bias as high as 10%. The calibration efficiencies range from about 0.6–0.9, with the less complex models tending to have higher values. When the predictions in the validation period are assessed (Figure 9), the relative positions of the models remain largely unchanged. However, almost all models have increased biases, to the extent that they are all now overpredicting (Viney *et al.*, 2005). Most of the models also have increased efficiencies in the validation period despite increased biases.

The calibration statistics indicate that the semi-lumped conceptual models (especially HBV and LASCAM) tend to provide the best fits to the calibration period. This is possibly related to the generally larger numbers of optimisable parameters in this type of model as compared to the physically based models, which tend to have many parameters that must be prescribed *a priori*, but few optimisable parameters. The use of manual calibration for many of the physically based and spatially explicit models may also compromise their calibration efficiencies. However, in the validation period, the prediction efficiencies of some of the physically based and spatially explicit models (most notably DHSVM) tend to increase more than those of the semi-distributed conceptual models (Figure 9; Viney *et al.*, 2005), partly because they have greater scope for improvement. But, one of the physically based and distributed models also showed the largest decrease in efficiency.

4.3. Land use change scenarios

Physically based distributed models are based on universal physical principles. Since they cannot be easily calibrated, they are less able to mimic lumped observations. Even though it is widely assumed that these models are more suited to future predictions of environmental change, despite the problem of *a priori* parameterisation (Beven and Binley, 1992). On the other hand, lumped conceptual models mimic observations well, but are often assumed to be less able to predict the future behaviour of catchments because they are not based on physical principles (Beven, 2001). So although they mimic the past very well, most modellers are less confident about future predictions. Likewise, physically based distributed models are capable of incorporating readily available surface characteristic, whereas lumped conceptual models estimate these by calibration. Using transfer functions, distributed conceptual models can also incorporate readily available surface characteristics, without estimating them by calibration. For environmental change applications, the ability to use specific changing landscape characteristics is crucial. Particularly with regard to this requirement spatially explicit models have an advantage, whereas calibrated lumped models can mimic the past but modifying model parameters for future changes is based mainly on transfer functions or even on modelling experience (Breuer *et al.*, 2009).

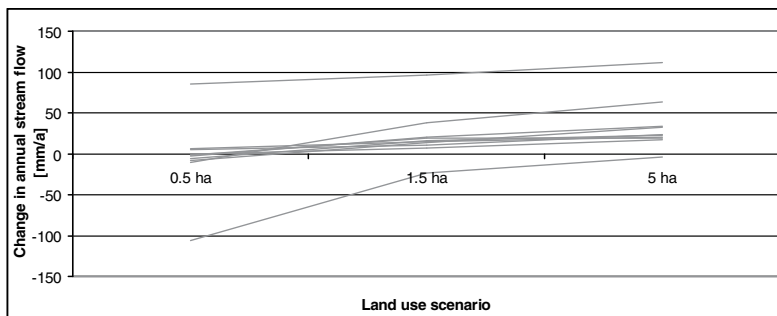


Fig. 10. Model specific effect of land use scenarios on simulated stream flow in the Dill catchment (1983–1998), compared to the current land use.

Three spatially distributed scenarios of land use change were considered which were based on land use simulations of the ProLand model (Weinmann *et al.*, 2006) involving different field sizes. The three scenarios reflected predicted land uses associated with target field sizes of 0.5 ha, 1.5 ha and 5.0 ha. In general, increasing field sizes were associated with intensified land use because the efficiency of the use of large machinery increases. Therefore areas of forested land decrease and areas of cropland increase. The impacts of land use change on stream flow are assessed by running all models which were calibrated for current land uses with the changed land use scenarios (Huisman *et al.*, 2009). Weather input from the period 1983–1998 and data sets on soils and topography are used. The resulting annual discharge predictions for the Dill catchment are presented in Figure 10. The slopes of the thin grey lines representing the ten individual models are quite similar. This indicates that all models predict a similar relative increase in stream flow if field size increases. However, three of the ten models show simulated discharges that are substantially offset either above or below the majority of models. Admittedly, two of these three outliers are spatially explicit models with the lowest efficiencies and therefore possibly the least reliable ones. It can be concluded that different well calibrated models which are applied by experienced modellers predict the same effects of land use change on stream flow regardless of the model type.

4.4. Reduction of structural uncertainty by multi-model ensembles

The results presented have shown that different model types have assets and drawbacks and contain substantial different major uncertainty sources when applied to simulate stream flow of example catchments. As a result, the different model types calculated different parts of the stream flow hydrographs better or worse than other models did. Therefore it can also be assumed that combining distributed (and physically based) models with lumped (and conceptual) models in an

ensemble approach can compensate for each other's weaknesses, and any predictions for future scenarios might benefit from this (Viney *et al.*, 2009). Ensemble predictions may be derived in a number of ways. Two simple ensembles are the arithmetic mean and the median of the every day's model predictions.

The prediction capabilities of the introduced simple ensembles compared to those of the single models are shown in Figure 11. For both, calibration and validation periods, the simple ensembles performed as well as or even better than the best single model. In the validation period, in particular, the median ensemble performed at least as well as ensembles composed by selected the best performing single models. Various additional ensembles were analysed by Viney *et al.* (2009) in detail. It can be concluded that the median ensemble is robust against outliers. The errors of the single models seem to be approximately equally distributed around the observations (e.g., Figure 8). This indicates that statistically the median of the simulations is at least as good as the best performing model. Ensembles composed by a limited number of selected best models do not show an advantage compared to the arithmetic mean of all models in the validation period. This indicates that large ensembles are more robust than small ensembles even if the small ensembles consist of the better performing models. These results are confirmed by application of two further quality measures (Figure 11; see also Bormann *et al.*, 2007).

This experiment showed that statistically simple ensembles such as the median of daily simulated stream flow outperformed the best single models in terms of different objective functions. In the ensemble, the deficiencies in one model may be masked by the strengths in others or even by a compensating weakness in another model. We assume that predictive uncertainty is reduced by sampling models with a range of structural uncertainties, and plausibility of the model predictions is increased by ensemble calculation (Viney *et al.*, 2005).

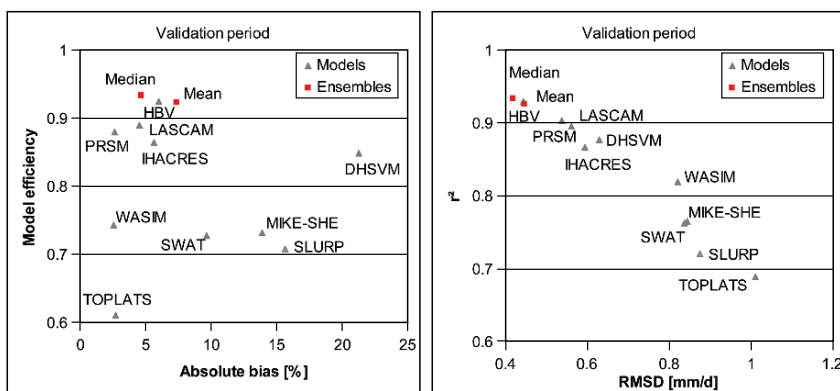


Fig. 11. Comparison of the performance of simple multi-model ensembles compared to ten different individual catchment models applied to the Dill catchment (1983–1998).

5. Conclusions

Different models and different model types have been applied to two catchments in different environments and on different scales to predict (at least) stream flow within two case studies. The general model performance of most models based on different model concepts and spatial catchment discretisations was satisfactory during both calibration and validation periods.

At the regional scale, with standard data sets available, the lumped and semi-distributed models performed better compared to spatially explicit ones during calibration and validation periods, but did not improve their fits during the validation period as much as some of the spatially explicit models did that do not require as much calibration. At the local scale, assuming high data quality and resolution, both model types predicted stream flow similarly well while the spatially explicit models were able to additionally predict spatially distributed variables and hydrological fluxes. This enables the modeller to better validate this type of model against spatially explicit observations of hydrological state variables (*e.g.*, soil moisture) or fluxes (*e.g.*, evapotranspiration). If a model can be validated sufficiently to a suite of observations, then the probability that a model predicts the right water fluxes for the right reason can be considerably increased. However, it has been demonstrated that model structure is often correlated to the spatial discretisation of the models. Therefore, not only spatial discretisation determines the quality of the simulation results but also the model structure in terms of process representation.

The general capabilities of lumped and spatially explicit models derived from literature statements and modelling experience could be proven by the two case studies which were carried out, while some of the features as shown by the case studies discussed in this paper were dependent on scale and data availability. In summary, both model types, spatially explicit and lumped models, doubtlessly are suitable tools for the simulation of catchment processes as they show advantages for different applications depending on data availability, scale and boundary conditions. And to a large extent, the choice of model is dictated by the modelling purpose. Where only flow at the catchment outlet is required, perhaps a lumped model is the best choice. But where spatially explicit predictions or land use change predictions are required a (semi-)distributed model would be more appropriate. Finally it could be shown that bringing together the results of different models to a combined approach (multi-model ensemble) reduces the uncertainty in the predictions and improves the performance of the simulations, providing a promising approach for future model applications.

References

Arnold, J.G., Srinivasan, R., Muttiah, R.S., and Williams, J.R., 1998, Large area hydrologic modelling and assessment. Part I: Model development, *Journal of the American Water Resources Association*, 34:73–88.

Bergström, S., 1995, The HBV model, In: Singh, V.P. (ed.), *Computer Models of Watershed Hydrology*, Highland Ranch, CO, Water Resources Publications, 443–476.

Beven, K.J., 2001, *Rainfall-Runoff Modelling, The Primer*, Chichester, Wiley.

Beven, K. and Binley, A., 1992, The future of distributed models: Model calibration and uncertainty prediction, *Hydrological Processes*, 6:279–298.

Binley, A.M., Beven, K.J., Calver, A., and Watts, L.G., 1991, Changing responses in hydrology: Assessing the uncertainty in physically based model predictions, *Water Resources Research*, 27:1253–1261.

Blöschl, G., 1996, *Scale and Scaling in Hydrology*, Habilitation, Wiener Mitteilungen Wasser, Abwasser, Gewässer, 132 p.

Bormann, H., 2005a, Regional hydrological modelling in Benin (West Africa): Uncertainty issues versus scenarios of expected future environmental change, *Physics and Chemistry of the Earth*, 30/8–10:472–484.

Bormann, H., 2005b, Evaluation of hydrological models for scenario analyses: Signal-to-noise-ratio between scenario effects and model uncertainty, *Advances in Geosciences*, 5:43–48.

Bormann, H. and Diekkrüger, B., 2003, Possibilities and limitations of regional hydrological models applied within an environmental change study in Benin (West Africa), *Physics and Chemistry of the Earth*, 28/33–36:1323–1332.

Bormann, H. and Diekkrüger, B., 2004 A conceptual hydrological model for Benin (West Africa): Validation, uncertainty assessment and assessment of applicability for environmental change analyses, *Physics and Chemistry of the Earth*, 29/11–12:759–768.

Bormann, H., Faß, T., Giertz, S., Junge, B., Diekkrüger, B., Reichert, B., and Skowronek, A., 2005a, From local hydrological process analysis to regional hydrological model application in Bénin: Concept, results and perspectives, *Physics and Chemistry of the Earth*, 30/6–7:347–356.

Bormann, H., Giertz, S., and Diekkrüger, B., 2005b, Hydrological catchment models between process representation, data availability and applicability for water management – Case study for Bénin, IAHS Publication, 295:86–93.

Bormann, H., Breuer, L., Croke, B., Gräff, T., Hubrechts, L., Huisman, J.A., Kite, G.W., Lanini, J., Leavesley, G., Lindström, G., Seibert, J., Viney, N.R., and Willems, P., 2007, Reduction of predictive uncertainty by ensemble hydrological modelling of catchment processes and land use change effects. Proceedings of the 11th Conference of the Euromediterranean Network of Experimental and Representative Basins (ERB), Luxembourg, 20–22 September 2006, IHP-VI/Technical Documents in Hydrology, 81:133–139.

Breuer, L., Huisman, J.A., Willems, P., Bormann, H., Bronstert, A., Croke, B.F.W., Frede, H-G., Gräff, T., Hubrechts, L., Jakeman, A.J., Kite, G., Leavesley, G., Lanini, J., Lettenmaier, D.P., Lindström, G., Seibert, J., Sivapalan, M., and Viney, N.R., 2009, Assessing the impact of land use change on hydrology by ensemble modeling (LUCHEM) I: Model intercomparison of current land use, *Advances in Water Resources*, doi:10.1016/j.advwatres.2008.10.003.

Calder, I.R., Hall, R.L., Bastable, H.G., Gunston, H.M., Sheila, O., and Chirwa, A., 1995, The impact of land use change on water resources in sub-Saharan Africa: A modelling study of Lake Malawi, *Journal of Hydrology*, 170:123–135.

Croke, B.F.W., Merritt, W.S., and Jakeman, A.J., 2004, A dynamic model for predicting hydrologic response to land cover changes in gauged and ungauged catchments, *Journal of Hydrology*, 291:115–131.

Diekkrüger, B. and Arning, M., 1995, Simulation of water fluxes using different methods for estimating soil parameters, *Ecological Modelling*, 81/1–3:83–95.

Ewen, J. and Parkin, G., 1996, Validation of catchment models for prediction land use and climate change impact. 1. Method, *Journal of Hydrology*, 175:583–594.

Giertz, S., 2004, Analyse der hydrologischen Prozesse in den sub-humiden Tropen Westafrikas unter besonderer Berücksichtigung der Landnutzung des Aguima-Einzugsgebietes in Bénin, Dissertation, University of Bonn, 249 p.

Giertz, S. and Diekkrüger, B., 2006, Evaluation of three different model concepts to simulate the rainfall-runoff process in a tropical headwater catchment in West Africa, *Geoöko*, 27:117–147.

Giertz, S., Diekkrüger, B., and Steup, G., 2006, Physically-based modelling of hydrological processes in a tropical headwater catchment in Bénin (West Africa) – Process representation and multi-criteria validation, *Hydrology and Earth System Sciences*, 10:829–847.

Huisman, J.A., Breuer, L., Bormann, H., Bronstert, A., Croke, B.F.W., Frede, H., Gräff, T., Hubrechts, L., Jakeman, A.J., Kite, G.W., Lanini, J., Leavesley, G., Lettenmaier, D.P., Lindström, G., Seibert, J., Sivapalan, M., Viney, N.R., and Willems P., 2009, Assessing the impact of land use change on hydrology by ensemble modelling (LUCHEM) III: Scenario analysis, *Advances in Water Resources*, doi:10.1016/j.advwatres.2008.06.009.

Impetus, 2008, IMPETUS – An integrated approach to the efficient management of scarce water resources in West Africa, <http://www.impetus.uni-koeln.de/> (date of access: 15.11.08).

Jakeman, A.J., Littlewood, I.G., and Whitehead, P.G., 1990, Computation of the instantaneous unit hydrograph and identifiable component flows with application to two small upland catchments, *Journal of Hydrology*, 117:275–300.

Junge, B., 2004, Die Böden im oberen Ouémé-Einzugsgebiet: Pedogenese, Klassifikation, Nutzung und Degradierung, Dissertation, University of Bonn, Germany, 217 p.

Kite, G.W., 1978, Development of a hydrological model for a Canadian watershed, *Canadian Journal of Civil Engineering*, 5:126–134.

Leavesley, G.H. and Stannard, L.G., 1995, The precipitation runoff modeling system – PRMS, In: V.P. Singh (ed.), *Computer Models of Watershed Hydrology*, Water Resources Publications, Highland Ranch, CO, 281–310.

Mulindabigwi, V., 2005, Influence des système agraires sur l'utilisation des terroirs, la séquestration du carbone et la sécurité alimentaire dans le bassin versant de l'Ouémé supérieur au Bénin, Dissertation, University of Bonn, Germany, 227 p.

Nash, J.E. and Sutcliffe, J.V., 1970, River flow forecasting through conceptual models. Part 1 – A discussion of principles, *Journal of Hydrology*, 10:282–290.

Niehoff, D., Fritsch, U., and Bronstert, A., 2002, Landuse impacts on storm-runoff generation: Scenarios of land-use change and simulation of hydrological response in a meso-scale catchment in SW-Germany, *Journal of Hydrology*, 267:80–93.

Onstad, C.A. and Jamieson, D.G., 1970, Modelling the effect of land use modifications on runoff, *Water Resources Research*, 65:287–1295.

Orthmann, B., 2005, Vegetation ecology of a woodland-savannah mosaic in central Benin (West-Africa): Ecosystem analysis with a focus on the impact of selected logging, Dissertation, University of Rostock, Germany, 115 p.

Peters-Lidard, C.D., Zion, M.S., and Wood, E.F., 1997, A soil-vegetation-atmosphere transfer scheme for modeling spatially variable water and energy balance processes, *Journal of Geophysical Research*, 102:4303–4324.

Refsgaard, J.C., van der Sluijs, J., Brown, J., and van der Keur, P., 2006, A framework for dealing with uncertainty due to model structure error, *Advances in Water Resources*, 29:1586–1597.

Refsgaard, J.C. and Storm B., 1995, MIKE SHE, In: V.P. Singh (ed.), *Computer Models of Watershed Hydrology*, Water Resources Publications, Highland Ranch, CO, 809–846.

SCS, 1972, Estimation of direct runoff from storm rainfall, *National Engineering Handbook*, Section 4 – Hydrology, USDA, Washington, D.C., U.S.A., 10.1–10.24.

Sivapalan, M., Ruprecht, J.K., and Viney, N.R., 1996, Water and salt balance modelling to predict the effects of land-use changes in forested catchments. 1. Small catchment water balance model, *Hydrological Processes*, 10:393–411.

Viney, N.R., Croke, B.F.W., Breuer, L., Bormann, H., Bronstert, A., Frede, H., Gräff, T., Hubrechts, L., Huisman, J.A., Jakeman, A.J., Kite, G.W., Lanini, J., Leavesley, G., Lettenmaier, D.P., Lindström, G., Seibert, J., Sivapalan M., and Willems, P., 2005, Ensemble modelling of the hydrological impacts of land use change, In Zerger, A. and Argent, R.M. (eds.), *MODSIM 2005 International Congress on Modelling and Simulation*, Modelling and Simulation Society of Australia and New Zealand, December 2005, 2967–2973.

Viney, N.R., Bormann, H., Breuer, L., Bronstert, A., Croke, B.F.W., Frede, H.-G., Gräff, T., Hubrechts, L., Huisman, J.A., Jakeman, A.J., Kite, G., Leavesley, G., Lanini, J., Lettenmaier, D.P., Lindström, G., Seibert, J., Sivapalan, M., and Willems, P., 2009, Assessing the impact of land use change on hydrology by ensemble modelling (LUCHEM) II: Ensemble combinations and predictions, *Advances in Water Resources*, doi:10.1016/j.advwatres.2008.05.006.

Weinmann, B., Schroers, J.O., and Sheridan, P., 2006, Simulating the effects of decoupled transfer payments using the land use model ProLand, *Agrarwirtschaft*, 55:248–256.

Wigmsta, M.S., Vail, L.W., and Lettenmaier, D.P., 1994, A distributed hydrology-vegetation model for complex terrain, *Water Resources Research*, 30:1665–1679.

Cellular automata modeling of environmental systems

Salvatore Straface, Giuseppe Mendicino

Dipartimento di Difesa del Suolo, Università della Calabria, Ponte Pietro Bucci, Cubo 41 b 87036, Arcavacata di Rende (CS), Italy.

Abstract

Flow and transport processes in unsaturated soil are analyzed through a simulation environment based on cellular automata (CA). The modeling proposed in this chapter represents an extension of the original computational paradigm of cellular automata, because it uses a macroscopic CA approach where local laws with a clear physical meaning govern interactions among automata. This CA structure, aimed at simulating a large-scale system, is based on functionalities capable of increasing its computational capacity, both in terms of working environment and in terms of the optimal number of processors available for parallel computing. Specifically, the performance of a three-dimensional unsaturated flow model has been verified comparing the results with reference multidimensional solutions taken from benchmarks in literature, showing a good agreement even in the cases where non-linearity is very marked. Furthermore, some analyses have been carried out considering quantization techniques aimed at transforming the CA model into an asynchronous structure. The use of these techniques in a three-dimensional benchmark allowed a considerable reduction in the number of local interactions among adjacent automata without changing the efficiency of the model, especially when simulations are characterized by scarce mass exchanges.

Keywords: flow and transport model, macroscopic cellular automata, parallel simulation, discrete approach, quantization techniques, model validation, environment.

1. Introduction

The capability of understanding and modeling hydrological processes at different spatial scales together with the need for a more detailed knowledge of mechanisms regulating soil interaction between surface and subsurface, has led experts to investigate and develop different forms of modeling.

In many cases, the models using fully-coupled system equations to describe the hydrological cycle of a basin completely have shown computational limitations, mainly due to both the reduced dimension of sampling-grids (or mesh), involving a narrow space domain, and smaller time steps which are essential to prevent eventual numerical instability.

These problems become even more evident during the simulation of soil dynamics because of the fast responses of this zone to atmospheric forcing, which limit us to a modeling characterized by very reduced space-time steps (Orlandini, 1999).

It becomes increasingly necessary to find alternative numerical solutions that, always under the aegis of describing physical phenomena, allow us to increase the spatial and temporal domain of simulations with acceptable computational requirements.

Modeling based on cellular automata (CA) represents a valid alternative to analytical-deductive methods based on the analysis of physical equations describing a particular phenomenon and their subsequent resolution carried out through numerical methods (Toffoli and Margolus, 1987; von Neumann, 1966; Wolfram, 1986, 1994). In complex physical phenomena, this modeling allows us to capture the fundamental characteristics of systems whose global behavior is derived from the collective effect of numerous simple components interacting locally. Many CA applications in fluid-dynamics exist, most of these based on microscopic approaches: lattice gas automata models were introduced to describe the motion and collision of particles interacting according to appropriate laws on a lattice space (Frisch *et al.*, 1987). These models can simulate the dynamic properties of fluids (Di Pietro *et al.*, 1994; Pot *et al.*, 1996) and their continuum limit leads to the Navier-Stokes equations (Rothman and Zaleski, 1997). Lattice gas models, due to the simplicity of both fluid particles and their interactions allow simulations of a large number of particles, but do not allow to express the velocity in explicit form, because an amount of fluid moves from one cell to another one in a CA step, which is defined as a constant time, involving a constant “velocity” in the CA context of discrete space-time. However, velocities can be achieved through the analysis of the global behavior of the system: in the space by considering clusters of cells; and in time by taking into account the average velocity of the advancing flow front in a sequence of CA steps.

Surface and subsurface flow modeling represent complex macroscopic fluid dynamical phenomena. Subsurface solute transport has been traditionally described by a deterministic advection-dispersion equation based on analogy to Fick's laws of diffusion. According to this analogy, the spread of a nonreactive contaminant in a hydrogeologic environment is controlled by a constant directional medium property called dispersivity which, when multiplied by absolute velocity, yields a directional dispersion coefficient. Flow and transport modeling seem difficult to model in these CA frames, because they occur on a large space scale and need, practically, a macroscopic level of description that involves the management of a large amount of data.

Lattice gas models are only capable of reproducing the birth of macroscopic flow patterns. The drawbacks of the lattice gas models have been overcome by the Lattice Boltzmann Method (LBM), where the state variables can take continuous values (instead of integer variables), as they are supposed to represent the density of fluid particles endowed with certain properties located in each cell (McNamara and Zanetti, 1988; Succi *et al.*, 1991; Chopard and Luthi, 1999). In the LBM space and time are discrete and they represent a very powerful approach which combines numerical efficiency with the advantage of having a model whose microscopic components are intuitive. Also for the Boltzmann models the equivalence with the Navier-Stokes equations for incompressible fluids has been demonstrated (Higuera and Jimenez, 1989; Qian *et al.*, 1992; Chen *et al.*, 1992; He and Luo, 1997).

LBM has been used to model flow in porous media, but the applications so far developed usually take a more microscopic approach and aim at describing phenomena which take place at the pore level (Martis and Chen, 1996; Zhang *et al.*, 2000; Knutson *et al.*, 2001; Zhang *et al.*, 2005). Some extensions to porous media and scaling up have been also proposed (Soll *et al.*, 1993; Soll and Birdsell, 1998; Sukop and Or, 2004; Chau *et al.*, 2005), as well as LBM has been used for macroscopic plots modeling (Deng *et al.*, 2001; Zhang *et al.*, 2002a,b; Ginzburg, 2005), but quantities such as density, velocity and concentration are obtained by taking the moments of the distribution function (Deng *et al.*, 2001).

Empirical CA methods were developed on the macroscopic scale in order to directly deal with the macroscopic variables associated to the representative elementary volume of the physical system under consideration (Di Gregorio and Serra, 1999; Di Gregorio *et al.*, 1999). In these methods an almost unlimited number of states are allowed and, each state is described by a Cartesian product of sub-states, each one describing a specific feature of the space portion related to its own cell. Furthermore, the transition function is split in different parts, each corresponding to an elementary process of the macroscopic phenomenon. When an amount of fluid is computed to pass from one cell to another, this particular characteristic of the transition function allows fluid to be added to the cell and, at the same step, to change all the sub-states involved, specifying the evolution of the main quantities of the macroscopic system such as velocity explicitly (Avolio *et al.*, 2003).

But, these empirical CA methods make use of some local laws where automata interactions are based on parameters whose physical meaning is not clear and, as a consequence, heavy calibration phases are necessary to estimate suitable values of the same parameters. The computational effort which results is partially justified by the possibility of making cellular automata directly compatible with parallel programming (Toffoli and Margolus, 1987; Crutchfield *et al.*, 2002).

In this chapter the same extended notion for *macroscopic* cellular automata has been considered to develop a three-dimensional model which simulates water flux in unsaturated soils, but the local laws governing the automata interactions are based on physically-based rules.

The model, developed in a problem solving CA environment called CAMELOT (Dattilo and Spezzano, 2003) has been used for different multidimensional schemes

and provides results similar to those of other approaches described in Paniconi *et al.* (1991), Paniconi and Putti (1994) and Huyakorn *et al.* (1986).

Moreover, in the second part of the chapter a particular aspect regarding the use of theory of quantized systems (Ziegler, 1998) applied to the proposed CA model has been investigated. This concerns the computational benefits derived from the application of some quantization techniques aimed at decreasing the number of local interactions by neglecting scarce mass exchanges occurring between neighboring automata. Through these techniques CA act as an asynchronous system, where according to a common quantum size rule a given automaton evolves or is kept at rest depending on its state and on those of the adjacent cells.

Following this approach, starting from the technique suggested by Muzy *et al.* (2002), dynamic quantization which makes CA structure both asynchronous and non-uniform is developed. In particular, the quantum size rule conditioning the transition function is varied locally according to the sub-state describing the degree of saturation of the soil, and this produces a considerable reduction in the local transitions without adversely affecting the performance of the model.

2. Discrete formulation of flow in unsaturated soil

All existing numerical methods for the solution of field equations have a differential formulation as their starting point. A discrete formulation is then obtained by means of one of the many discretization methods, such as Finite Difference Method (FDM), Finite Element Method (FEM) or, in general, a weighted residual or weak solution method. Even Boundary Element Method (BEM) and Finite Volume Method (FVM), which use an integral formulation, have a differential formulation as their substratum (Tonti, 2001). The formation of densities and rates and then the passage to the limit to form the field functions, that is typical of field and continuum theories, deprive physical variables of their geometrical content (for this reason any discretization process restored from the differential formulation is not based on geometrical but only on numerical considerations).

So, it follows that to obtain a discrete formulation of the fundamental equation of a physical theory, it is not necessary to go down to the differential form and then go up again to the discrete form. It is enough to apply the elementary physical laws to small regions where the uniformity of the field is attained to a sufficient degree, this being linked to the degree of accuracy of data input and to the observation scale of the physical phenomenon. In this way, we obtain a direct discrete formulation of the field equation.

If we consider a discrete cell system, in which the cells have smaller dimensions where the departure from uniformity is larger, we may use the same constitutive law used in the differential context, as an approximation.

In this section our aim is to obtain a direct discrete formulation of the unsaturated flow, the equation that we use in CA model. This equation, whose solution

provides the variables configuring the phenomenon, is the final result of the composition of the mass-balance equation and the constitutive equation (Darcy's law). The discrete mass-balance equation is the following (Straface *et al.*, 2006):

$$\sum_{\alpha} \Phi_{\alpha}^c + \frac{1}{\rho_c} \frac{\Delta m_c}{\Delta t} = S_c \quad (1)$$

where c is the cell where the water mass balance is performed, α is the generic direction obtained linking the center of the mass of cell c with that adjacent (see Figure 1a, for a two-dimensional case), Φ_{α}^c is the mass flux [$L^3 T^{-1}$], ρ_c is the fluid density [ML^{-3}], m_c is the mass inside the single cell c [M], Δt is the time step [T], $\frac{\Delta m_c}{\Delta t}$ [MT^{-1}] is the mass-time variation in the cell, and S_c is the mass source term [$L^3 T^{-1}$]. Equation (1) is valid both for internal nodes of the discrete domain and for boundary nodes, avoiding the typical differential approach where differential equations and boundary conditions are separated. The mass flux is given by Darcy's equation, which in discrete terms for a cubic regular mesh becomes:

$$\Phi_{\alpha}^c = -\bar{K}_{c\alpha} \left(\frac{h_{\alpha} - h_c}{l_{\alpha}} \right) A_{\alpha} = -\bar{K}_{c\alpha} g_{\alpha} A_{\alpha} \quad (2)$$

where $\bar{K}_{c\alpha}$ is the hydraulic conductivity averaged between cell c and that adjacent along the direction α (e.g., cell i in Figure 1), obtained assuming the energy dissipated between two adjacent cells equivalent to the energy dissipated in a fictitious cell containing them (Indelman and Dagan, 1993). Then, if we consider the hydraulic conductivity averaged between cell c and i (Figure 1b), we assume:

$$\bar{K}_{ci} = \frac{\frac{V_c + V_i}{V_c} \frac{V_i}{K_{i\alpha}}}{\frac{V_c}{K_{c\alpha}} + \frac{V_i}{K_{i\alpha}}} \quad (3)$$

where V_c and V_i [L^3] are the volumes of the cells, while $K_{c\alpha}$ and $K_{i\alpha}$ are the elements on the diagonal of the hydraulic conductivity tensor corresponding to the direction α in the cells c and i , assuming that the xyz Cartesian system is colinear with the principal anisotropy directions.

The remaining terms of equation (2) are the total heads h_c and h_{α} [L], the cell dimension l_{α} [L], the hydraulic gradient g_{α} [-] and the surface area A_{α} [L^2] where the flux Φ_{α}^c passes through (Figure 1b). Equation (2) is a particular form of a more general direct discrete formulation of the unsaturated flow equation. For more details see Appendix A.

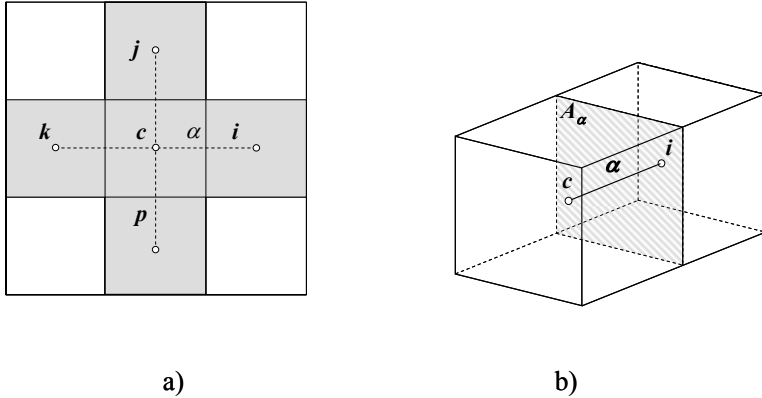


Fig. 1. (a) Scheme of a squared two-dimensional cells complex; (b) Representation of the flux through the face of two adjacent cells.

The time variation of mass content changes according to the flow type considered. For unsaturated flow, assuming the fluid is incompressible and density-independent, the mass time-variation becomes:

$$\frac{\Delta m_c}{\Delta t} = V_c \rho_c \frac{\Delta \theta_c}{\Delta t} \quad (4)$$

If the ratio between capillary pressure p_c [$ML^{-1}T^{-2}$] and specific weight of liquid γ_w [$ML^{-2}T^{-2}$] represents the pressure head ψ_c [L] and the specific retention capacity $C_c(\psi)$ [L^{-1}] is considered (Bear, 1972), then applying the chain rule to equation (4) the following equation is achieved:

$$\frac{\Delta \theta_c}{\Delta t} = \frac{\Delta \theta_c}{\Delta h_c} \frac{\Delta h_c}{\Delta t} = C_c \frac{\Delta h_c}{\Delta t} \quad (5)$$

from which the complete form of the unsaturated soil flux equation is obtained:

$$\sum_\alpha \bar{K}_{c\alpha} \left(\frac{h_\alpha - h_c}{l_\alpha} \right) A_\alpha + V_c C_c \frac{\Delta h_c}{\Delta t} = S_c \quad (6)$$

The discrete unsaturated flow equation (6) is applied to each cell of the domain, with h_c the only unknown term to be estimated. The gravitational effects are taken into account considering that is $h = \psi + z$, and consequently $h_\alpha - h_c = \psi_\alpha - \psi_c + (z_\alpha - z_c)$.

For the solution of unsaturated flow it is necessary to specify the non-linear dependencies among the assumed independent variable, total head h_c , and terms

characterizing the hydraulic properties of soil represented by water content θ_c , specific retention capacity C_c and hydraulic conductivity $K_c = K(\psi_c)$. Such relationships can be expressed in tabular form or more usually through empirical equations fitting experimental data using theoretical models (Mualem, 1974, van Genuchten and Nielsen, 1985).

In the discrete formulation that we present the hydraulic head is assumed to be continuous and need not to be differentiable. Each cell may have different constitutive properties: this allows composite porous or fractured media to be dealt with. The boundary conditions are of two kinds: on some parts of the boundary the hydraulic head h_c can be assigned, while on the remaining parts, the flow rate Φ_α^c can be assigned. The sources can be continuous (drainage trench or superficial recharge) and also may be concentrated (wells or sinks), by means of the mass source term S_c of equation (1). Our purpose is to find the hydraulic head of all cell nodes (barycenters) where it is not assigned: these can be internal as well as boundary nodes. Equation (6) is valid for interior or boundary cells: in this way, we can avoid the unnatural separation of the differential equations and the boundary conditions, which is typical of a differential formulation.

The discrete formulation of physical phenomena gives several computational advantages, such as discussed in Appendix A. This approach proves to be particularly suitable to the use of a macroscopic cellular automata environment and to be developed in a parallel computing system.

3. Discrete formulation of solute transport

The discrete form of the mass solute equation may be written as follows (Straface, 1998):

$$\sum_{c \in I(h)} \Phi_s^c + \frac{1}{\rho_s^c} \frac{\Delta m_s^c}{\Delta t} = 0 \quad (7)$$

where Φ_s^c is the solute mass flux and Δm_s^c is the cell mass change. This equation indicates that, the amount produced in the volume during a time interval is equal to the sum of the outgoing solute flow of the same quantity across the boundary of the volume during the time interval, and of the quantity stored inside the volume in the same interval. The equation is valid either for the internal nodes or for the lateral nodes. The mass time-variation becomes:

$$\frac{\Delta m_s^c}{\Delta t} = n_c \cdot V^c \cdot \frac{\Delta C^c}{\Delta t} \quad (8)$$

where C^c is the solute mass concentration in cell c .

The mass transport phenomenon in an aquifer is subdivided into three separated mechanisms: (1) convection, (2) molecular diffusion and (3) cinematic dispersion.

Convection is the phenomenon where dissolved substances are carried along by the movement of fluid displacement. In this case we assume:

$$\Phi_s^{conv} = \Phi_s^c \cdot C^c \cdot \frac{1}{\rho_s^c} \quad (9)$$

Molecular diffusion is a physical phenomenon linked to the molecular agitation. In a fluid at rest the Brownian motion projects particles in all directions of space. If the concentration of the solution is not uniform in space the point with the highest concentration sends out, on the average, more particles in all directions than the point with a lower concentration. The result of this molecular agitation is then that particles are transferred from zones of high concentration to those of low concentration (de Marsily, 1986).

Fick has found that the mass flux of particles in a fluid at rest is proportionate to the concentration gradient:

$$\Phi_s^{diff} = -A^c \cdot \frac{1}{\rho_s^c} \cdot n_c \cdot d_0 \cdot g^c \quad (10)$$

The coefficient d_0 , known as the molecular diffusion coefficient, is isotropic and can be expressed by the following equation:

$$d_0 = \frac{RT}{N} \frac{1}{6\pi\mu r}$$

where R is the constant of perfect gases, N the Avogadro's number, T absolute temperature, μ fluid viscosity and r the mean radius of diffusing molecular aggregates.

In fine, kinematic dispersion is a mixing phenomenon linked mainly to the heterogeneity of the microscopic velocities inside the porous medium on whatever scale they are observed:

- Inside a pore the velocities in mobile fraction are not uniformly distributed.
- The differences of aperture and travel distance from one pore to another create a difference in mean velocities.
- A stratification or any features of large scale heterogeneity.

The suggested mathematical formula adopts a transport law through dispersion similar to the Fick's law which accounts for the phenomena of mixing applied to the whole section of the medium, like the Darcy velocity, but with a dispersion coefficient \underline{D} :

$$\Phi_{s_h}^{disp} = -A^c \cdot \frac{1}{\rho_s^c} D \cdot g^c \quad (11)$$

Here, in explicit form, the balance equation becomes:

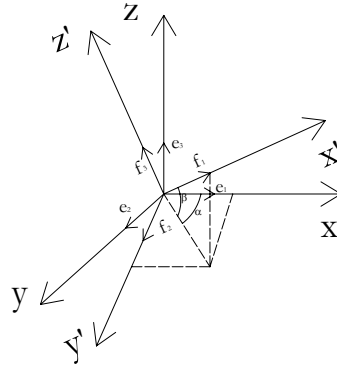
$$\sum_{c \in I(h)} \frac{1}{\rho_s^c} [\Phi_s^c \cdot C^c - (n^c \cdot d_0 + \underline{D}_c) \cdot A^c g^c] = \frac{1}{\rho_s^c} \frac{\Delta m_s^c}{\Delta t} \quad (12)$$

The function g_c is the concentration gradient, whose formulation depends on type of the used interpolation. Employing a linear interpolation it can be expressed by:

$$C(x, y, z) = a + g_x x + g_y y + g_z z$$

According to the analysis showed in Appendix A for the head gradient, we can write

$$g_c = \frac{1}{3V^c} A^c C^c$$



If we use a cubic cell, the reference system XYZ is co-linear with cubic faces and so the dispersion tensor \underline{D}^c assumes the form:

$$\underline{D}^c = \begin{bmatrix} D_L & 0 & 0 \\ 0 & D_T & 0 \\ 0 & 0 & D_T \end{bmatrix}$$

Because of more general flow directions, we have to express dispersion tensor on a new reference system $X'Y'Z'$, where X' is the flow direction, Y' and Z' his orthogonal. The change of the basis must be effected:

$$\underline{D}_f^c = \underline{T}^{-1} \underline{D}^c$$

where f indicates the new reference basis, where \underline{D} tensor will assume the form:

$$\underline{D}_f^c = \begin{bmatrix} D_{x'x'} & D_{x'y'} & D_{x'z'} \\ D_{y'x'} & D_{y'y'} & D_{y'z'} \\ D_{z'x'} & D_{z'y'} & D_{z'z'} \end{bmatrix}$$

4. Macroscopic cellular automata model

Cellular automata (CA) are a dynamic system where space, time and states are hypothesized as being discrete. They are based on a division of space in regular cells, each one having an identical computational device embedded in it: the finite automaton (fa). The physical quantities (or fa state) take only a finite set of values. The fa input is given by the states of the neighboring cells, including the cell which contains the fa .

The fa states vary according to a local rule (*transition function*); *i.e.*, in a given time step a fa state depends on its state and on those of neighboring cells at the previous time step. Finite automata have identical transition functions, which are simultaneously applied to each cell (*synchronous CA*). At the beginning all the fa are in arbitrary states representing the initial conditions of the system. Then the CA evolve by changing the state of all fa simultaneously at discrete time steps according to the fa transition function. Finally, the global evolution of the CA system is derived from the evolution of all the cells.

Since every cell has the same neighborhood structure, even the cell at the boundary of a physical domain has neighboring cells that are outside the domain. Conventionally, border cells are assumed to be connected to the cells on the opposite boundary like neighbors forming a closed domain. For example, for a two-dimensional rectangular domain, a site on the left border has the site in the same row on the right border as its left neighbor. With the same update rule applied to all the cells, this yields what is called a periodic boundary condition which is representative of an infinite system. Certainly, the type of the boundary condition to be used in a simulation depends on the physical application under consideration. Other types of boundary conditions may be modeled using preset values of the cell for the boundary nodes or writing suitable update rules for the cells at the boundary.

The previous definition is not sufficient for modeling spatially extended natural macroscopic phenomena such as soil infiltration. More detailed conditions need to permit a correspondence between the system with its evolution in the physical space-time and the model with the simulations in the cellular space-time. Thus, for many cases the complexity of macroscopic natural phenomena requires an extension of the original CA computational paradigm.

Firstly, the dimension of the cell and the time correspondence to a CA step must be fixed. These are defined as *global parameters*, as their values are equal for all the cellular space. They represent the set P together with other global parameters, which are frequently necessary for the simulation of complex phenomena involving time and/or space heterogeneity.

The state of the cell must account for all the characteristics (referring to the amount of space represented by the same cell), which are assumed to be relevant to the evolution of the system. Each characteristic corresponds to a sub-state, where the permitted values for a sub-state have to form a finite set. The set Q of possible states of a cell is given by the Cartesian product of the sets of the values of sub-states: $Q = Q_1 \times Q_2 \times \dots \times Q_n$. When a characteristic representing a physical quantity is expressed in terms of a continuous variable referring to a space point, then the cell size chosen must be small enough so that the approximation of considering a single value for the whole cell extension may be adequate to the features of the phenomenon. Actually, the continuity of the variable is not a problem because a finite, but adequate, number of significant digits are utilized, so that the set of values allowed is extremely large but finite. Furthermore, the cell size must be large enough to describe a macroscopic approach, even though it must be capable of catching the smallest variations in the sub-states, so that they can be hypothesized as constant within each cell.

As well as the state of the cell that can be partitioned in sub-states, the transition function σ may also be split into p *elementary* processes, defined by the functions $\sigma_1, \sigma_2, \dots, \sigma_p$. Elementary processes are applied sequentially according to a defined order compatible with the phenomenon under consideration. Different elementary processes may involve diverse neighborhoods, each one given by the union of all the neighborhoods associated to each process. If the neighborhood of an elementary process is limited to a single cell, such a process is defined as an *internal transformation*.

Specifically, according to the empirical approach suggested by Di Gregorio and Serra (1999), an elementary process is given by $\sigma: Q_n^m \rightarrow Q_c$, where Q_n and Q_c are Cartesian products of the elements of sub-sets of Q , m is the number of cells of the neighborhood, involved in the elementary process, Q_n describes the sub-states in the neighborhood that effect the change in the sub-state value and Q_c identifies the cell sub-states that change their value.

5. Subsurface flow modeling through CA

Using the same extended notion for macroscopic CA, the three-dimensional model simulating water flux in unsaturated soils consists of a three-dimensional domain, regularly subdivided into cubic cells described by the following functional structure (Mendicino *et al.*, 2006):

$$A = (E^d, X, Q, P, \sigma) \quad (13)$$

where $E^d = \{(x, y, z) | x, y, z \in N, 0 \leq x \leq l_x, 0 \leq y \leq l_y, 0 \leq z \leq l_z\}$ is the set of cells identified by points with integer co-ordinates in the finite region, where the phenomenon evolves; N is the set of natural numbers; l_x, l_y and l_z represent the limits of the region;

$$X = \{(0, 0, 0), (-1, 0, 0), (0, 1, 0), (0, 0, -1), (0, 0, 1), (0, -1, 0), (1, 0, 0)\}$$

identifies the von Neumann neighborhood, which influences the change in the state of the central cell; Q is the finite set of the *fa* states, given by the Cartesian product of the following sub-states:

$$Q = Q_h \times Q_\psi \times Q_\theta \times Q_k \times Q_\Delta$$

where Q_h is the sub-state describing the total head of the cell, Q_ψ is the sub-state describing the pressure head, Q_θ is the sub-state describing the water content (therefore, it may indicate the value of moisture content in volume θ or, according to the characteristic equation adopted, the water saturation S_w or the effective saturation S_e), Q_k describes the hydraulic conductivity sub-state (if the medium is anisotropic, this sub-state is further subdivided according to the principal anisotropic directions) and, for transient condition analyses Q_Δ indicates the sub-state corresponding to a parameter value necessary to guarantee the convergence of the system;

P is the finite set of CA global parameters which affects the transition function and is made up of some parameters associated with the characteristic equations, the saturated hydraulic conductivity, the automaton dimension and, the time step. Specifically, we have the residual water content θ_r , the saturation water content θ_s , the capillary air entry pressure ψ_a , the pore-dimension distribution index n , a continuity parameter for pressure head ψ_0 , the specific storage S_s , the saturated hydraulic conductivity K_s , the cell dimension l_α and the time step Δt .

$\sigma: Q_n^7 \rightarrow Q_c$ is the deterministic transition function. Once the initial conditions (total head, pressure head, conductivity and water content values) and the boundary conditions are fixed, it is based on two elementary steps, σ_1 and σ_2 :

1. The elementary process σ_1 consists in the update of the hydraulic characteristics of the soil (*i.e.*, the hydraulic conductivity K_c , the water content θ_c and the specific retention capacity C_c), depending on the pressure head through the characteristic equations. Many theoretical models for the constitutive equations $\theta = \theta(\psi)$ and $K_r = K_r(\psi)$ are available in literature. Those suggested by van Genuchten and Nielsen (1985) are commonly expressed as follows:

$$\begin{aligned}\theta(\psi) &= \theta_r + (\theta_s - \theta_r)[1 + \beta]^{-m} & \psi < 0 \\ \theta(\psi) &= \theta_s & \psi \geq 0\end{aligned}\quad (14)$$

$$\begin{aligned}K_r(\psi) &= (1 + \beta)^{-5m/2} \left[(1 + \beta)^m - \beta^m \right]^2 & \psi < 0 \\ K_r(\psi) &= 1 & \psi \geq 0\end{aligned}\quad (15)$$

where $\beta = (\psi/\psi_a)^n$, m is a parameter given by $m = 1 - 1/n$, and $K_r(\psi)[-]$ is the relative hydraulic conductivity (so that $K(\psi) = K_s K_r(\psi)$, with $K_s [LT^{-1}]$ saturated conductivity);

2. The elementary process σ_2 is the application of the unsaturated soil flux equation (6), to update the values of the total head h_c and the pressure head ψ_c of the cell.

Starting the simulation, the sub-states condition depend on the initial values assigned to the total head h_c , while the boundary conditions can be assigned either in terms of mass flow coming in (infiltration) or out (exfiltration) from the system (Neumann conditions), or fixing the total or pressure head values on some cells of the system (Dirichlet conditions).

6. Cellular automata quantization

Different conditions affect the nature of the CA. Among these the one based on quantized systems theory (Ziegler, 1998) was applied to the proposed model in order to reduce the state update transmission process. Such a process, called *quantization*, starting from the discretization of the states of a continuous process, fixes their evolution only through multiples of a specific value, called *quantum size*. Specifically, in a CA system the local interactions within the neighborhood, carried out through the transition function, involve each *fa* in temporal changes of the state: if during a time step the application of the transition function does not allow the cell to evolve from state D at least to state $D \pm 1$ (where the difference between two states is given by the quantum size), it maintains its current state, and does not exchange information with the neighborhood. The quantization makes cellular automata asynchronous, because for each iteration every *fa* decides, with respect to the value of its state and those of adjacent cells, whether to be updated or to remain *frozen* in its state during the previous time step.

For the proposed model the quantization procedure has been applied in a different way to the original approach. In Ziegler (1998) the cell evolves through fixed values from state D to states $D \pm 1, D \pm 2, D \pm 3$, etc. (like a step function). Instead we assume that the automaton state evolution, depending on a set of local interactions of the transition function, is only admitted if a fixed threshold is

exceeded. The local interactions of the transition function are conditioned by the difference between the values of a chosen sub-state of the cell (the *driving* sub-state) before and after a single time step; if this difference is greater than a fixed threshold value then interactions are allowed and the automaton state can assume any numerical value in the field of real numbers. Obviously, when all local interactions are not significant (all the differences are smaller than the fixed threshold) then the automaton is assumed to be at rest.

In the unsaturated flow problems, the mass exchanges among the cells are due to the differences (in the space) among the total heads. Mass exchanges can be considered as not significant when they lead to a total head variation (in time) in the analyzed cell lower than a fixed threshold. Exceeding the threshold has to be checked for every neighbor with the aim of allowing the interaction along the generic α direction. Therefore rewriting equation (6) it should be verified that (Mendicino *et al.*, 2006):

$$|\Delta h_{\alpha}| = \left| \frac{\Delta t}{V_c C_c} \left[S_c + \bar{K}_{c\alpha} \left(\frac{h_{\alpha} - h_c}{l_{\alpha}} \right) A_{\alpha} \right] \right| > quantum_h \quad (16)$$

where the term $quantum_h$ is the threshold, representing the minimum admissible total head variation in the time step Δt . This $quantum_h$ determines a constant threshold within the CA domain.

On the CA domain a different threshold can also be hypothesized based on variations in time of water content, defined as $quantum_{\theta}$. This $quantum_{\theta}$, according to equation (16) has different effects on each cell of the automata, depending on the water content value of the same cell at the beginning of the time step and on the characteristic equation $\psi(\theta)$ adopted.

Specifically, given the water content θ_c for the cell analyzed at the beginning of the time step, it is:

$$\begin{aligned} quantum_h &= \psi(\theta_c) - \psi(\theta_c - quantum_{\theta}) && \text{exfiltration} \\ quantum_h &= \psi(\theta_c + quantum_{\theta}) - \psi(\theta_c) && \text{infiltration} \end{aligned} \quad (17)$$

In this way, the CA system becomes both asynchronous and non-uniform: the transition function changes in each fa , because in each automaton the threshold depends on a local factor represented by the degree of saturation at the beginning of the time step.

For both thresholds depending on total head and water content, increasing values produce two opposite effects: on the one hand the number of interactions decreases and on the other the model is less accurate. Then, a suitable compromise has to be reached, such as that shown in the next section.

7. CA high-performance environment

The three-dimensional unsaturated flow model has been developed using a high-performance environment called CAMELOT, specifically developed for *macroscopic* cellular automata simulations (Dattilo and Spezzano, 2003; Folino *et al.*, 2006). In CAMELOT each transition function uses the same local rule, even though it is possible to define some cells characterized by different transient functions (heterogeneous CA). In contrast to the classical cellular approaches which make reference to the basic model, where the state of each *fa* is defined as a single bit or a set of bits, in this case the *fa* state is defined like a set of typed sub-states. This increases the range of applications which can be simulated through cellular algorithms. Furthermore, in CAMELOT a logical neighborhood representing a wide range of different neighborhoods within the same radius, which can also be time dependent, has been introduced.

The CAMELOT components also include load balancing procedures based on a scatter-type decomposition technique which allows the computation to be equally distributed among processors of the parallel computing system. This is carried out using the standard *Message Passing Interface* (MPI) library, which allows CAMELOT to run on different hardware platforms for all communications. More specifically, the working environment is capable of determining the best number of nodes to be used in parallel grid computing for a given CA system, making the overheads due to the remote communications among the single processors very small. Such a process, which identifies the *computational scalability* of the CA system, becomes more efficient as the spatial dimension of the problem to be analyzed increases. Therefore, the up-scaling from micro to meso-scale occurs without changing the local rule of the CA and, at the same time, the computational efficiency is improved by the working environment.

8. Results

The CA model was validated considering a wide range of benchmarks proposed in literature. Regarding the flow model, results were compared with numerical simulations of one-dimensional cases (benchmarks 1D1 and 1D2), a two-dimensional case (benchmarks 2D) and a three-dimensional case (benchmark 3D), while for the transport model a contaminant transport problem has been solved, starting from field data based on a real site where experimental measurements were available.

8.1. One-dimensional benchmarks

Two one-dimensional benchmarks were considered along two different soil columns (Paniconi *et al.*, 1991): the former refers to an infiltration problem and the

latter to an evaporation one. Both the cases are based on the unmodified Richards' equation which does not allow general closed form exact solutions. Then, for the estimate of errors produced by the CA model some reference numerical solutions were considered, assuming a very dense grid and small time step (Mendicino *et al.*, 2006).

The characteristic equations taken into account for these simulations are the (14) and (15), with a modified retention curve $\Theta(\psi)$ in a form like this (Paniconi *et al.*, 1991):

$$\begin{aligned}\theta(\psi) &= \theta_r + (\theta_s - \theta_r)[1 + \beta]^{-m} & \psi < \psi_0 \\ \theta(\psi) &= \theta_r + (\theta_s - \theta_r)[1 + \beta_0]^{-m} + S_s(\psi - \psi_0) & \psi \geq \psi_0\end{aligned}\quad (18)$$

where $\beta_0 = \beta(\psi_0) = (\psi_0/\psi_a)^n$, ψ_0 being a continuity parameter and S_s the specific storage. The general storage term of the Richards' equation in this case is given by $\eta(\psi) = d\theta/d\psi$. The variation in the original equations is necessary to avoid numerical problems, such as those indicated by Paniconi *et al.* (1991). The accuracy of the CA model was estimated by using both a first and a second order norm error:

$$\varepsilon 1(t) = \sum_{i=1}^n \frac{|\hat{\psi}(z_i, t) - \psi_{ref}(z_i, t)|}{n} \quad (19)$$

$$\varepsilon 2(t) = \sum_{i=1}^n \frac{[\hat{\psi}(z_i, t) - \psi_{ref}(z_i, t)]^2}{n} \quad (20)$$

where $\hat{\psi}$ and ψ_{ref} are the simulated and reference pressure head at time t respectively, for the $i=1..n$ soil profile points at level z_i .

Benchmark 1D1 consists of an infiltration and redistribution simulation into a soil column initially at hydrostatic equilibrium. The boundary condition at the surface is a time-varying specified Darcy flux q which increases linearly with time, while the boundary at the base is maintained at a fixed pressure head value of $\psi = 0$, allowing drainage of moisture through the water table. The space grid and time step have been chosen to guarantee the convergence of the system, following a criterion described in Appendix B (the same criterion has been applied for all simulations considered).

Figure 2 shows the comparison between CA simulations and reference numerical solutions: the differences are very small for all the times analyzed.

Benchmark 1D2 simulates evaporation from an initially wet soil with a fixed water table boundary condition at the base of the column. The boundary condition at the surface is a specified and constant Darcy flux, until the pressure head at the surface reaches its *air dry* value ψ_{min} , after which the surface becomes a fixed head boundary. The comparison between simulations and numerical reference solutions is shown in Figure 3.

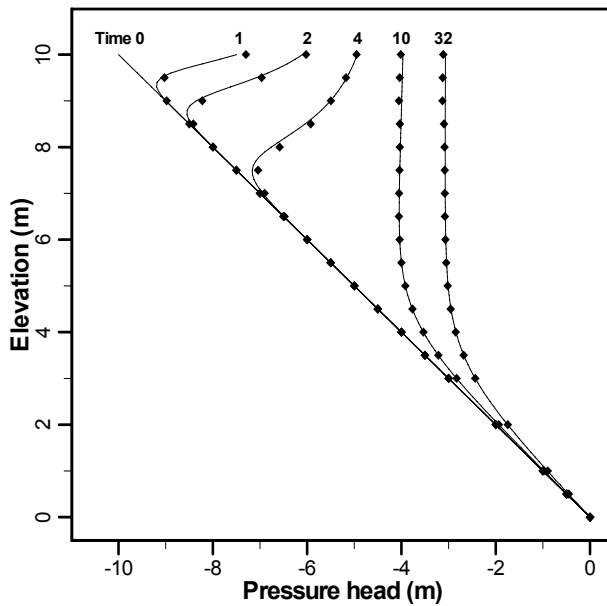


Fig. 2. Comparison between CA simulation (solid lines) and reference numerical solutions (points) for the bench-mark 1D1.

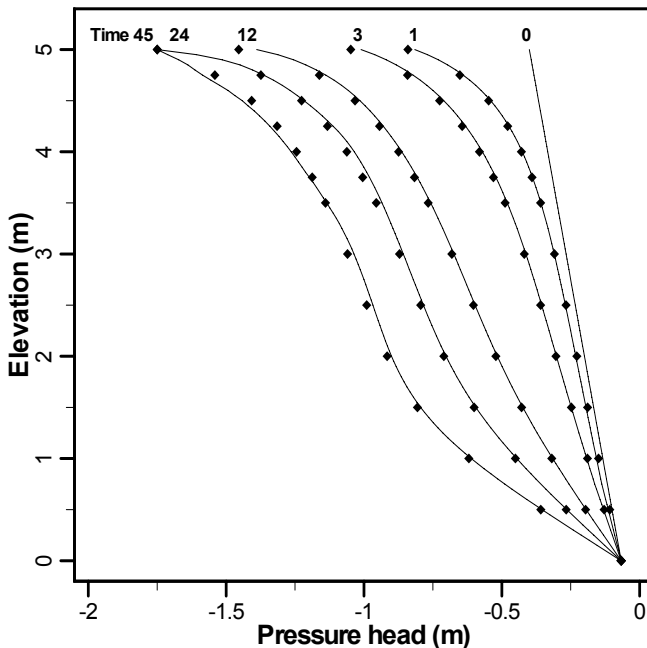


Fig. 3. Comparison between CA simulations (solid lines) and reference numerical solutions (points) for bench-mark 1D2.

The CA model shows a good agreement with the reference solutions, although small differences in pressure head at the soil surface were observed. This is mainly due to the constitutive equations in the conversion of surface boundary condition, which is expressed in terms of water content θ in the reference solution and in terms of total head h in the CA model.

8.2. Two-dimensional benchmarks

The 2D benchmark is partly based on textural, structural and hydraulic properties of Jornada Test Site soil at Las Cruces (New Mexico) which are described by Smyth *et al.* (1989). The test considers the transient phase of a 2D infiltration flow in a very-arid heterogeneous soil.

The test area consists of three soil layers with different characteristic properties. Within the bottom-layer, there is a very permeable small zone. The domain extends about 8.00 m horizontally and 6.50 m vertically. The experiment was carried out again numerically by Magnuson *et al.* (1990), utilizing FLASH (FEM) and PORFLOW (FDM) calculus codes, therefore the results (supplied by such codes) were assumed as standard numerical solutions for the comparison with the proposed AC model. Regarding the initial conditions, the soil piezometric head is uniform and equal to -7.34 m, corresponding to a saturation degree variable from 0.31 into the top-layer to 0.37 into the bottom-one. The boundary conditions are given by an infiltration zone of 0.02 m d^{-1} which extends on the area of 2.25 m starting from the left side of the domain. The remaining boundary is characterized by no flow conditions. Finally, soil properties are based on van Genuchten (1978) relationship according to the Mualem (1974) model.

The AC model which simulates soil moisture evolution consists of square cells with a 0.05 m side. The simulation time-step goes from a maximum value of 100 s to a minimum ones of about 28 s, according to the limits established by the following criterion of convergence (Mendicino *et al.*, 2006):

$$\Delta t \leq \frac{l^2 C_c}{4 K_c} \quad (21)$$

As shown in Figure 4 the saturation degree distribution along the analyzed plot is obtained through AC model after 30 days from the starting of the simulation, and compared with the results obtained by means of FLASH and PORFLOW codes (Figure 5). Thirty days step is enough to reach the conditions comparable with the steady ones. The effect of the high-saturation zone is clearly visible, because the curve indicating the saturation degree is strongly influenced by it. In particular, the AC model results shown a good agreement with PORFLOW ones, while the output of the FLASH code shows some differences (a greater horizontal extension of the curve at 0.4 saturation degree, and a less face along the vertical).

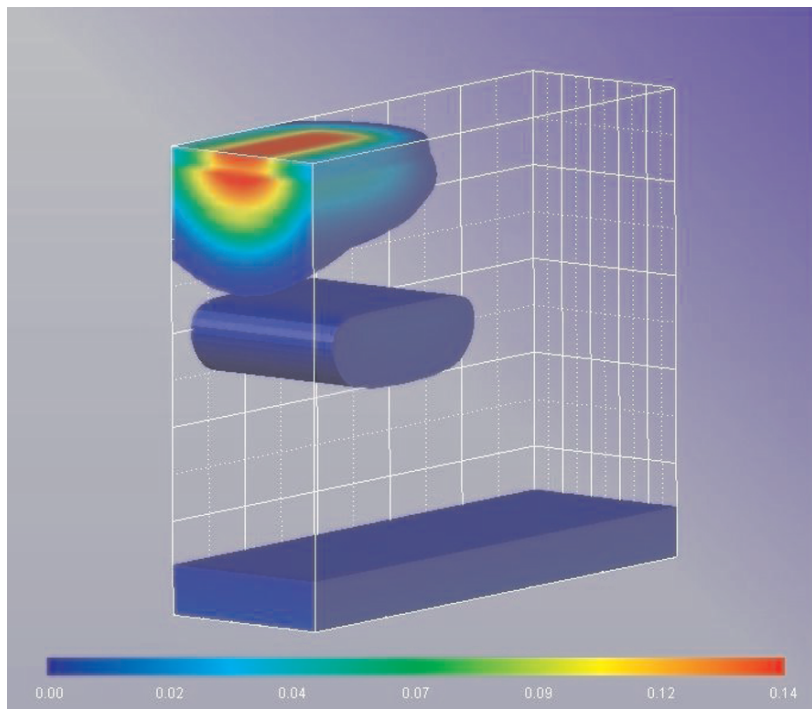


Fig. 4. Saturation degree change respect to the initial condition after 30 days. The saturation degree shown is greater than 0.0001.

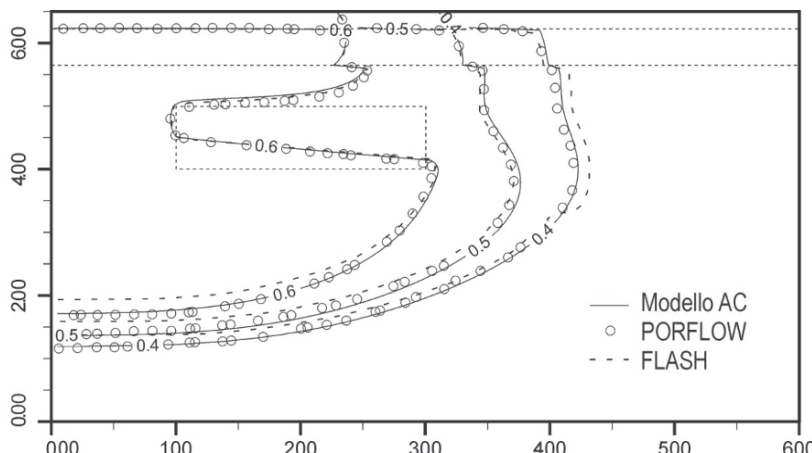


Fig. 5. Comparison between CA simulations and reference numerical solutions (PORFLOW and FLASH) for benchmark 2D after 30 days from the simulation start.

8.3. Three-dimensional benchmark

The benchmark 3D is taken from Huyakorn *et al.* (1986) and analyses a transient flow in a rectangular soil column of dimensions $0.50 \times 0.50 \times 2.00$ m subjected to infiltration and subsequent evaporation. The bottom and the top faces of this column correspond to the water table and the soil surface respectively. The initial pressure head was assumed to be zero at the water table, -0.90 m at the soil surface, and -0.97 m elsewhere. The soil column was first subjected to infiltration for 10 days and then subjected to evaporation for another 10 days; for both phenomena the maximum flux rate was assumed as equal to 0.05 m d^{-1} . The minimum allowable pressure head at the top of soil column is -0.90 m, saturated hydraulic conductivity K_s is equal to 0.1 m d^{-1} , porosity ϕ is 0.45, residual water saturation S_{wr} is 0.333 and air entry value ψ_a is equal to 0.0 m. The constitutive equations are given by the equation:

$$(\psi - \psi_a) / (-100 - \psi_a) = (1 - S_w) / (1 - S_{wr}) \quad (22)$$

$$K_r = (S_w - S_{wr}) / (1 - S_{wr}) \quad (23)$$

Simulations did not show particular convergence or stability problems because of the linearity of equations (22) and (23). The time step used for simulations was fixed as equal to 60 s while the automaton dimension was assumed as equal to 0.05 m. The results obtained with the CA model are compared with reference solutions in Figures 6a (infiltration) and 6b (evaporation).

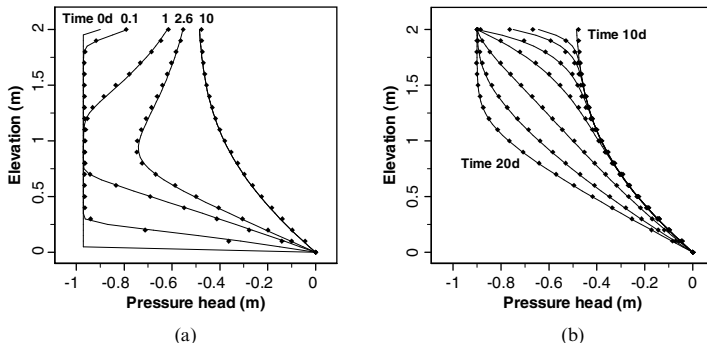


Fig. 6. Comparison between CA simulations (solid lines) and reference numerical solutions (points) for benchmark 3D, for infiltration (a) and evaporation (b).

8.4. Transport benchmark

In this section we report an example of a validation process using a two dimensional contaminant transport problem (Troisi *et al.*, 2000). The two PS sets have been defined starting from field data based on a real site where experimental measurements were available. The study area (Figure 7) is located near the town of Montalto Uffugo in Calabria, Southern Italy. It is a valley at the confluence of the Settimo River on the south, the Mavigliano River on the north and the Crati River on the east. The geology is formed by three layers: sand (0–7 m), clay (7–11 m), and silt (11 to about 40 m) (Troisi, 1995). A basal clay underlies the silty sand. A local perched water table is in the alluvium above the clay layer, and the silty sand layer constitutes a confined aquifer above the basal clay. Measurements of the hydraulic conductivity and its distribution have been made over the past few

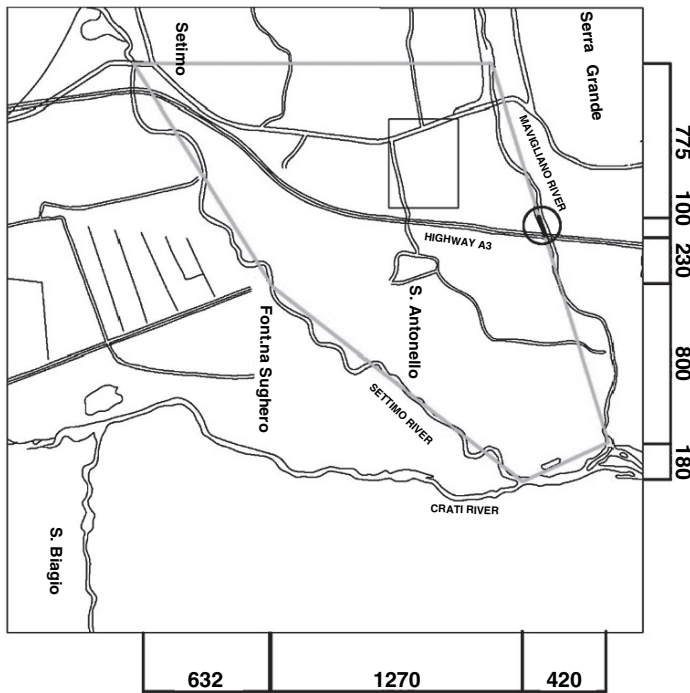


Fig. 7. Location of the study area used for the transport benchmark. The boundary of the numerical model is shown as a dotted line.

years using a kriging approach with external drift methodology applied to electrical-resistivity data (Troisi *et al.*, 2000). The domain for the flow and transport model application is defined as the area enclosed by the surface water system as shown in Figure 7. In the flow model a heterogeneous isotropic porous medium is assumed. Dirichlet boundary conditions are according to the water levels in the surface water system. Two permeability zones are assumed in the flow fields, and are indicated in Figure 7. Zone 1 is characterized by $K_{11} = K_{22} = 10^{-5}$, $S_s = 10^{-2}$ m while in zone 2, $K_{11} = K_{22} = 10^{-6}$, $S_s = 10^{-3}$ m. One extracting well, located at coordinates $X = 1640$ and $Y = 2525$ and pumping at a rate of $q_{out} = 0.003$ m, is coupled with an injecting well, located at $X = 114$ and $Y = 225$, where the head is kept constant at 138 m. In the transport test case we simulate a contaminant injection from the Mavigliano River, just east of Highway A3, where a contaminant source of 100 m of length is kept at constant concentration. A second contaminant point source is located at $X = 146$ and $Y = 241$. The parameters used in the simulations are: $n = 0.2$, $\alpha_L = 5$, and $\alpha_T = 1$.

The benchmark code for this test case has been run on a number of successively refined computational grids so that a reliable solution is obtained. The results for the test case at time $t = 2.3$ days are shown in Figure 8. The solutions obtained with the TRAN2D (Gambolati *et al.*, 1993) and CA models are not significantly different so that the CA model can be considered verified for this benchmark. However, more meaningful and objective comparison procedures need to be devised, as the contour plots give only a qualitative picture. Appropriate simulation quantities useful for these purposes could be, for example, mass balance measures (both local and global), stability measures (*e.g.*, negative concentrations in transport problems, existence of negative transmissivities in stiffness matrices), accuracy measures (*e.g.*, outgoing fluxes from zero Neumann boundaries), and so on.

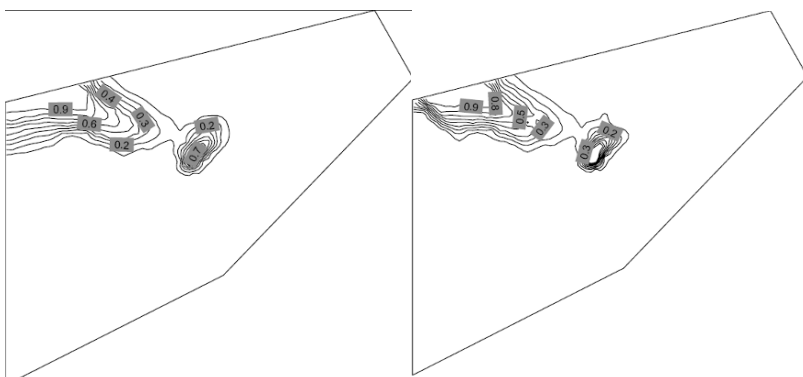


Fig. 8. Results of the transport problem at $t = 2.3$ days: benchmark solution (left), CA model solution (right).

9. Cellular automata quantization effects

The quantization effects considering both total head and water content thresholds were investigated using the benchmark 1D1 in a three-dimensional configuration. Figures 9a, 9b, 10a, 10b, 11a and 11b show the reduction in the number of automata interactions along a column of cells together with the corresponding norm error ε_1 values (assuming as reference values ψ_{ref} those obtained from the simulations without quantization), when the values of thresholds depending on total head ($quantum_h$) and water content ($quantum_\theta$) are changed, respectively at times of 4, 10 and 32 h. Obviously, messages exchanged for $quantum_h = quantum_\theta = 0$ are the same. For the particular structure of the 3D problem, it is clear that considering the whole automata instead of only a column leads to a number of exchanges equal to the values shown in the figures multiplied by the number of automata columns, not varying the ε_1 error values.

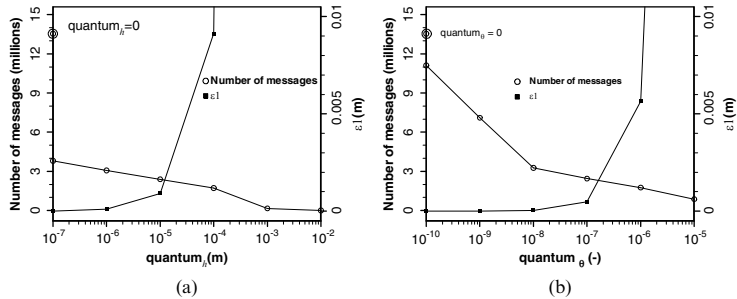


Fig. 9. Reduction in exchanged messages in a column of cells and variation of error norm ε_1 values at a time of 4 hours, varying (a) $quantum_h$ and (b) $quantum_\theta$ threshold values. Points drawn with two concentric circles represent the number of exchanged messages with $quantum_h = quantum_\theta = 0$.

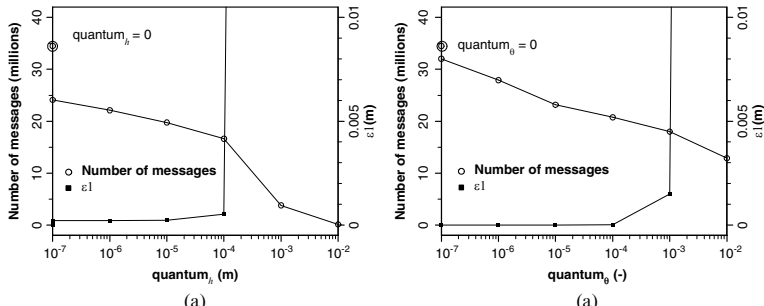


Fig. 10. Reduction in exchanged messages in a column of cells and variation of error norm ε_1 values at a time of 10 hours, varying (a) $quantum_h$ and (b) $quantum_\theta$ threshold values. Points drawn with two concentric circles represent the number of exchanged messages with $quantum_h = quantum_\theta = 0$.

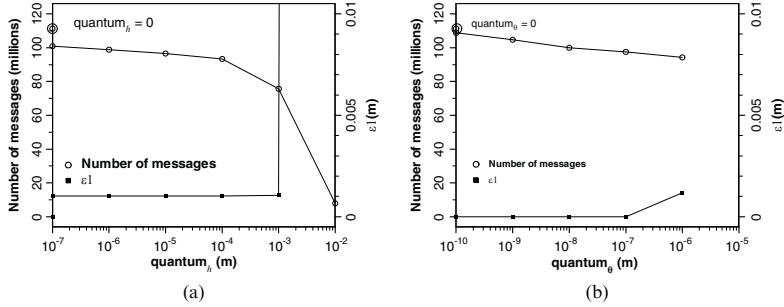


Fig. 11. Reduction in exchanged messages in a column of cells and variation of error norm ε values at a time of 32 hours, varying (a) $quantum_h$ and (b) $quantum_\theta$ threshold values. Points drawn with two concentric circles represent the number of exchanged messages with $quantum_h = quantum_\theta = 0$.

For all the times analyzed, starting from a very small threshold value ($quantum_h$ equal to 10^{-7} m and $quantum_\theta$ equal to 10^{-10}), an appreciable reduction in the number of automata interactions is obtained. This however appears less significant for increasing simulation times.

Once a certain threshold value is exceeded, for both kinds of thresholds the increase in the norm error is not tolerable, even if the reduction in exchanges still continues. Considering $quantum_h$ the critical threshold value seems to be between 10^{-5} and 10^{-4} m.

For $quantum_h$ equal to 10^{-5} m reductions in exchanged messages of 82.3% (with $\varepsilon_1 = 9.1 \times 10^{-4}$ m), 42.7% (with $\varepsilon_1 = 2.3 \times 10^{-4}$ m) and 13.3% (with $\varepsilon_1 = 1.0 \times 10^{-3}$ m) were obtained at times of 4, 10 and 32 hours respectively. Instead, for $quantum_h$ equal to 10^{-4} m reductions in exchanged messages of 87.3% (with $\varepsilon_1 = 9.1 \times 10^{-3}$ m), 51.8% (with $\varepsilon_1 = 5.2 \times 10^{-4}$ m) and 16.1% (with $\varepsilon_1 = 1.0 \times 10^{-3}$ m) were obtained at the same times respectively. For increasing simulation times it was observed that higher threshold values still provided acceptable results.

No essential differences were observed using $quantum_\theta$ threshold, even though for high values some numerical divergence problems occurred, especially for increasing simulation times.

For the same infiltration case 1D1, characterized by retention curves (18), the relationship between $quantum_h$ and $quantum_\theta$ is given by the following equation (Mendicino *et al.*, 2006):

$$quantum_h = \psi(\theta + quantum_\theta) - \psi(\theta) = \psi_a \left[\left(\frac{\theta + quantum_\theta - \theta_r}{\theta_s - \theta_r} \right)^{-1/m} - 1 \right]^{1/n} - \psi_a \left[\left(\frac{\theta - \theta_r}{\theta_s - \theta_r} \right)^{-1/m} - 1 \right]^{1/n} \quad (24)$$

Critical $quantum_\theta$ threshold values seem to vary between 10^{-7} and 10^{-6} . For $quantum_\theta$ equal to 10^{-7} reductions in exchanged messages of 82.0% (with $\varepsilon_1 = 4.8 \times 10^{-4}$ m), 39.8% (with $\varepsilon_1 = 7.0 \times 10^{-6}$ m) and 12.4% (with $\varepsilon_1 = 1.0 \times 10^{-6}$ m) were obtained at times of 4, 10 and 32 h respectively. Instead, for $quantum_\theta$ equal to 10^{-6} m reductions in exchanged messages of 87.0% (with $\varepsilon_1 = 5.6 \times 10^{-3}$ m), 47.9% (with $\varepsilon_1 = 1.5 \times 10^{-3}$ m) and 15.2% (with $\varepsilon_1 = 1.2 \times 10^{-3}$ m) were obtained at the same times respectively.

The reduction in exchanges varying the thresholds as well as specific effects produced by static ($quantum_h$) and dynamic ($quantum_\theta$) approaches should not be thought of as general results, but are associated with the problem analyzed. In fact, considering benchmark 1D1 we start from a top-perturbed initial condition and, consequently, the gradients between cells are initially very low and so even a small threshold significantly affects the behavior of the system.

10. Conclusions

Three-dimensional unsaturated flow and transport modeling has been developed by means of an extended notion for *macroscopic* cellular automata where local laws governing the automata interaction are based on physically-based rules. The modeling uses a CA structure based on functionalities capable of increasing its computational capacity, both in terms of working environment and in terms of the optimal number of processors available for parallel computing.

In terms of performance, the model has been verified considering multidimensional reference solutions taken from benchmarks in literature. The simulations carried out on one-, two- and three-dimensional benchmarks have shown results similar to the reference solutions, with first and second order norm error values never greater, respectively, than 0.028 m and 0.5 m². The AC characteristic equations are subjected to parameters which amplify the non-linearity of the phenomenon. Even if not explicitly shown in this chapter, the effects of non-linearity can be reduced using smaller dimension automata, which evolve with lower mass flow values, which better approximate the non-linearity condition.

Furthermore, in the three-dimensional configuration of the benchmark 1D1 the benefits of the use of quantization techniques to reduce the number of interactions occurring locally among adjacent automata have been observed. The CA structure working in an asynchronous and non-uniform manner, allowed a considerable reduction in the local transitions, which becomes very significant in the first steps of simulations characterized by scarce mass exchanges. In this case, in the first four hours of simulation a reduction greater than 80% in the messages exchanged among automata was achieved with negligible error values by considering both thresholds depending on total head and water content.

Therefore, at the end of this analysis, the modeling proposed appears to be: (1) innovative with respect to other macroscopic CA models, because its physically-based structure differs from the others commonly based on empirical methods

where local laws show some parameters whose physical meaning is not clear and, as a consequence, heavy calibration phases are necessary to estimate suitable values of the same parameters; (2) innovative with respect to other unsaturated flow models, because it solves the problem through a direct discrete approach; (3) reliable for all the simulations carried out with one-, two- and three-dimensional benchmarks; (4) faster than some other numerical approaches not based on quantization techniques aimed at reducing the local interactions among the elements of the discrete system.

The proposed discrete approach, coupled to the CA environment implementation, allows us to deal with heterogeneous and anisotropic soils and composite porous or fractured media, and with different (continuous or concentrated) sources in a quite simple way, by just varying the parameters of specific regions of the CA and not changing the transition function.

Finally, from a computational point of view the higher efficiency values shown by the model running on parallel machines increase the capability of the CA system also with respect to the fully-coupled modeling of complex macroscopic phenomena such as those represented in this chapter.

Appendix A. Direct discrete formulation of the Darcy equation

The aim of this appendix is to show that the direct discrete formulation of the unsaturated flow equation on three-dimensional cubic cells is a particular form of a more general direct discrete formulation of the Darcy equation.

Figure A1a shows the tetrahedral element c with a volume V_c whose vertices correspond to the barycenters of four tetrahedral cells belonging to a more complex cell system. Referring to this figure, we hypothesize that the variable H (total head) is given by the following equation:

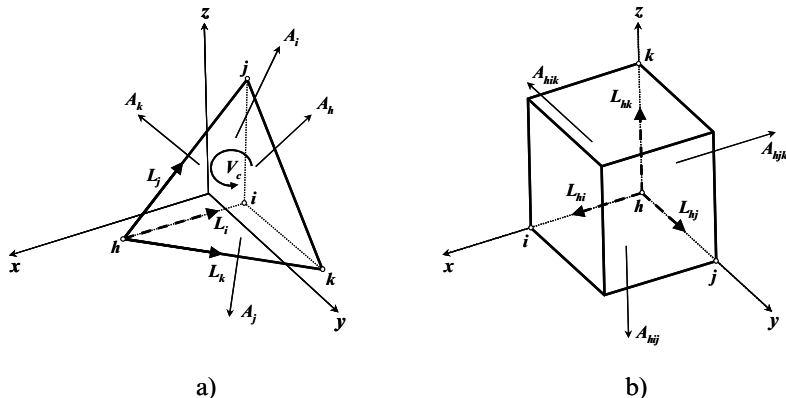


Fig. A1: (a) The elementary tetrahedron of a generic cell system; (b) The elementary cube of a three-dimensional cubic cell system.

$$H(x, y, z) = a + g_x x + g_y y + g_z z \quad (A.1)$$

where the coefficients g_x , g_y and g_z are the hydraulic gradient vector components, and a is a constant. Given h , i , j and k the tetrahedron vertices, with L_i , L_j and L_k the three sides starting from the vertex h , we can write:

$$\begin{cases} H_i - H_h = g_x(x_i - x_h) + g_y(y_i - y_h) + g_z(z_i - z_h) \\ H_j - H_h = g_x(x_j - x_h) + g_y(y_j - y_h) + g_z(z_j - z_h) \\ H_k - H_h = g_x(x_k - x_h) + g_y(y_k - y_h) + g_z(z_k - z_h) \end{cases} \quad (A.2)$$

or in matrix form:

$$\begin{bmatrix} L_{ix} & L_{iy} & L_{iz} \\ L_{jx} & L_{jy} & L_{jz} \\ L_{kx} & L_{ky} & L_{kz} \end{bmatrix}_c \begin{bmatrix} g_x \\ g_y \\ g_z \end{bmatrix}_c = \begin{bmatrix} H_i - H_h \\ H_j - H_h \\ H_k - H_h \end{bmatrix}_c \quad (A.3)$$

where the matrix of L terms contains the projections of the sides L_i , L_j and L_k on the x , y , z axes. The solution of the system, obtained by Cramer's rule, is the following:

$$\begin{bmatrix} g_x \\ g_y \\ g_z \end{bmatrix}_c = \frac{1}{3V_c} \begin{bmatrix} A_{hx} & A_{ix} & A_{jx} & A_{kx} \\ A_{hy} & A_{iy} & A_{jy} & A_{ky} \\ A_{hz} & A_{iz} & A_{jz} & A_{kz} \end{bmatrix}_c \begin{bmatrix} H_h \\ H_i \\ H_j \\ H_k \end{bmatrix}_c \quad (A.4)$$

where the matrix of A terms contains the projections of the oriented areas A_h , A_i , A_j and A_k of the tetrahedron on the x , y , z axes. System (A.4) can also be written in the following way:

$$\{g\}_c = \frac{1}{3V_c} [A]_c \{H\}_c \quad (A.5)$$

The Darcy equation links the mass flux Φ to the hydraulic gradient g through the following system:

$$\begin{bmatrix} \Phi_x(x, y, z) \\ \Phi_y(x, y, z) \\ \Phi_z(x, y, z) \end{bmatrix}_c = - \begin{bmatrix} k_{xx} & k_{xy} & k_{xz} \\ k_{yx} & k_{yy} & k_{yz} \\ k_{zx} & k_{zy} & k_{zz} \end{bmatrix}_c \begin{bmatrix} g_x(x, y, z) \\ g_y(x, y, z) \\ g_z(x, y, z) \end{bmatrix}_c \quad (A.6)$$

that is:

$$\{\Phi\}_c = -[k]_c \{g\}_c \quad (A.7)$$

If a cubic cell is considered (Figure A1b), the off-diagonal terms of the system (A.2) are null. In matrix form results:

$$\begin{bmatrix} L_{hi} & 0 & 0 \\ 0 & L_{hj} & 0 \\ 0 & 0 & L_{hk} \end{bmatrix}_c \begin{Bmatrix} g_x \\ g_y \\ g_z \end{Bmatrix}_c = \begin{Bmatrix} H_i - H_h \\ H_j - H_h \\ H_k - H_h \end{Bmatrix}_c \quad (A.8)$$

and the solution of the system is given by:

$$\begin{cases} g_x = (H_i - H_h)/L_{hi} \\ g_y = (H_j - H_h)/L_{hj} \\ g_z = (H_k - H_h)/L_{hk} \end{cases} \quad (A.9)$$

then, assuming that the xyz Cartesian system is colinear with the principal anisotropy directions, the Darcy equation becomes:

$$\begin{cases} \Phi_x = -k_x (H_i - H_h)/L_{hi} \\ \Phi_y = -k_y (H_j - H_h)/L_{hj} \\ \Phi_z = -k_z (H_k - H_h)/L_{hk} \end{cases} \quad (A.10)$$

The equations of the system (A.10) are equivalent to equation (2), showing that the direct discrete formulation of the unsaturated flow equation on three-dimensional cubic cells is a particular form of a more general direct discrete formulation of the Darcy equation.

The three-dimensional cubic cell system is a particular case of a Delaunay tessellation. With this kind of tessellation the discrete governing equation system is similar to the one achieved using Finite Difference or Finite Volume Method schemes (Mattiussi, 1997, Manzini and Ferraris, 2004). If we do not use a Delaunay tessellation (as in the case of an irregular mesh), we obtain a discrete governing equation system by means of an interpolation of the hydraulic head on the cells. It has been shown that, for linear interpolation the discrete governing equation system coincides with the one of the Finite Element Method (Tonti, 2001). However, for quadratic interpolation the discrete equation system, which is asymmetric, differs from the FEM scheme, achieving a convergence of the fourth order, greater than the one obtained with FEM using the same interpolation (Tonti, 2001).

When we use a method with a differential or integral formulation, the choice of the cell or the tessellation type depends on the method selected (FEM, FDM, FVM...). In contrast, if we use a direct discrete formulation, the cell or the tessellation type and the time interval can be chosen considering the physical laws governing the problem, the spatial and temporal scale of the phenomenon and, if the cells are considered as finite automata of a CA, the macroscopic CA environment can be chosen, with the opportunity, for example, of using different shapes (*e.g.*, squares and hexagons) for the single elements.

Appendix B. Convergence of discrete unsaturated flow equation

The problem of convergence, in a finite difference method, consists of finding the conditions under which the difference $U(i,j,k,t) - u(i,j,k,t)$ between the theoretical solutions of the differential (U) and difference (u) equations at a fixed point (i,j,k,t) tends to zero uniformly, as the net is refined in such a way that $\Delta x, \Delta y, \Delta z, \Delta t \rightarrow 0$, and $m_1, m_2, m_3, n \rightarrow \infty$, with $m_1 \Delta x (= i)$, $m_2 \Delta y (= j)$, $m_3 \Delta z (= k)$ and $n \Delta t (= t)$ remains fixed, and m_1, m_2, m_3, n being integers, with $m_1 = m_2 = m_3 = n = 0$ the origin.

The fixed point (i,j,k,t) is anywhere within the region under consideration, and it is sometimes necessary in the convergence analysis to assume that $\Delta x, \Delta y, \Delta z, \Delta t$ do not tend to zero independently but according to some relationship (Mitchell and Griffiths, 1980).

If we consider a discrete cell system directly, of course we can assume that a difference exists between the ‘exact’ infinitesimal (differential) solution and the discrete solution. Since the independent variable in the unsaturated soil flux equation (6) is the total head h , we can introduce the error e :

$$e_{i,j,k}^t = H_{i,j,k}^t - h_{i,j,k}^t \quad (B.1)$$

that is the difference between the exact solution H and the discrete solution h at the grid point i,j,k,t .

Rearranging equation (6) considering $\Delta x = \Delta y = \Delta z = 1$, we obtain:

$$\frac{\Delta h_c}{\Delta t} = \frac{1}{C_c l^3} S_c + \frac{1}{C_c l^2} \sum_{\alpha} \overline{K_{c\alpha}} (h_{\alpha} - h_c) \quad (B.2)$$

Expanding the terms and considering the introduced error term, we have with respect to the grid point i,j,k,t (*i.e.*, the cell c becomes the grid point i,j,k,t):

$$\begin{aligned}
& \frac{H_{i,j,k}^{t+\Delta t} - e_{i,j,k}^{t+\Delta t} - H_{i,j,k}^t + e_{i,j,k}^t}{\Delta t} = \\
& \frac{1}{C_{i,j,k}^t l^3} S_c + \frac{1}{C_{i,j,k}^t l^2} [\overline{K_{i-1,j,k}^t} (H_{i-1,j,k}^t - e_{i-1,j,k}^t) + \overline{K_{i+1,j,k}^t} (H_{i+1,j,k}^t - e_{i+1,j,k}^t) + \\
& + \overline{K_{i,j-1,k}^t} (H_{i,j-1,k}^t - e_{i,j-1,k}^t) + \overline{K_{i,j+1,k}^t} (H_{i,j+1,k}^t - e_{i,j+1,k}^t) + \\
& + \overline{K_{i,j,k-1}^t} (H_{i,j,k-1}^t - e_{i,j,k-1}^t) + \overline{K_{i,j,k+1}^t} (H_{i,j,k+1}^t - e_{i,j,k+1}^t) - \overline{K_{i\pm 1,j\pm 1,k\pm 1}^t} (H_{i,j,k}^t - e_{i,j,k}^t)] \\
& \quad (B.3)
\end{aligned}$$

where $\overline{K_{i\pm 1,j\pm 1,k\pm 1}^t} = \overline{K_{i-1,j,k}^t} + \overline{K_{i+1,j,k}^t} + \overline{K_{i,j-1,k}^t} + \overline{K_{i,j+1,k}^t} + \overline{K_{i,j,k-1}^t} + \overline{K_{i,j,k+1}^t}$ is the sum of the hydraulic conductivities averaged between the grid point i,j,k,t and the adjacent points $i \pm 1, j \pm 1, k \pm 1, t$, obtained considering in equation (3) the elements on the diagonal of the hydraulic conductivity tensor corresponding to the linking directions.

Isolating the error term in the time step $t + \Delta t$, we get

$$\begin{aligned}
e_{i,j,k}^{t+\Delta t} = & \left[1 - \overline{K_{i\pm 1,j\pm 1,k\pm 1}^t} \frac{\Delta t}{l^2 C_{i,j,k}^t} \right] e_{i,j,k}^t + \\
& + \frac{\Delta t}{l^2 C_{i,j,k}^t} (\overline{K_{i-1,j,k}^t} e_{i-1,j,k}^t + \overline{K_{i+1,j,k}^t} e_{i+1,j,k}^t + \overline{K_{i,j-1,k}^t} e_{i,j-1,k}^t + \overline{K_{i,j+1,k}^t} e_{i,j+1,k}^t + \\
& + \overline{K_{i,j,k-1}^t} e_{i,j,k-1}^t + \overline{K_{i,j,k+1}^t} e_{i,j,k+1}^t) - \frac{\Delta t}{C_{i,j,k}^t l^3} S_c + f(H, K) \\
& \quad (B.4)
\end{aligned}$$

where $f(H, K)$ is a function of permeability K and of the exact solution H :

$$\begin{aligned}
f(H, K) = & \\
& H_{i,j,k}^{t+\Delta t} - \left[1 - \overline{K_{i\pm 1,j\pm 1,k\pm 1}^t} \frac{\Delta t}{l^2 C_{i,j,k}^t} \right] H_{i,j,k}^t + \\
& - \frac{\Delta t}{l^2 C_{i,j,k}^t} (\overline{K_{i-1,j,k}^t} H_{i-1,j,k}^t + \overline{K_{i+1,j,k}^t} H_{i+1,j,k}^t + \overline{K_{i,j-1,k}^t} H_{i,j-1,k}^t \\
& + \overline{K_{i,j+1,k}^t} H_{i,j+1,k}^t + \overline{K_{i,j,k-1}^t} H_{i,j,k-1}^t + \overline{K_{i,j,k+1}^t} H_{i,j,k+1}^t) \\
& \quad (B.5)
\end{aligned}$$

From now on, for the sake of simplicity, we will not consider the source term S_c .

Let $E'_{i,j,k}$ denote the maximum value of $|e_{i,j,k}^t|$ at time t and M the maximum modulus of $f(H, K)$ for all i, j, k, t . When the term in the square brackets in equation (B.4) is equal or greater than zero, all the coefficients of e in the equation are positive or zero. The term in the square brackets is equal to or greater than zero when:

$$\Delta t \leq \frac{l^2 C_{i,j,k}^t}{K_{i\pm 1,j\pm 1,k\pm 1}^t} \quad (B.6)$$

and, working on equation (B.4), we have:

$$|e_{i,j,k}^{t+\Delta t}| \leq E_{i,j,k}^t + M$$

As this is true for all values of i,j,k it is true for $\max_{i,j,k} |e_{i,j,k}^{t+\Delta t}| \leq E_{i,j,k}^{t+\Delta t} + M$. Hence:

$$E_{i,j,k}^{t+\Delta t} \leq E_{i,j,k}^t + M \leq (E_{i,j,k}^{t-\Delta t} + M) + M = E_{i,j,k}^{t-\Delta t} + 2M$$

etc., from which it follows that:

$$E_{i,j,k} \leq E_{i,j,k} + n \cdot M = n \cdot M$$

because the initial values for h and H are the same, *i.e.*, $E_{i,j,k}^0 = 0$. When $\Delta x, \Delta y, \Delta z \rightarrow 0, 1 \rightarrow 0$ and, for the equation (B.6), also $\Delta t \rightarrow 0$, then the retention capacity tends to the general storage term of the Richards' equation ($C \equiv d\theta/dH$) and M tends to be a solution of the Richards' equation in a form like this:

$$\left(\frac{d\theta}{dH} \frac{\partial H}{\partial t} - \frac{\partial K_x(\psi)}{\partial x} \frac{\partial H}{\partial x} - K_x(\psi) \frac{\partial^2 H}{\partial x^2} - \frac{\partial K_y(\psi)}{\partial y} \frac{\partial H}{\partial y} - K_y(\psi) \frac{\partial^2 H}{\partial y^2} - \frac{\partial K_z(\psi)}{\partial z} \frac{\partial H}{\partial z} - K_z(\psi) \frac{\partial^2 H}{\partial z^2} \right)_{i,j,k}^t$$

As $|H_{i,j,k}^t - h_{i,j,k}^t| \leq E_{i,j,k}^t$, this proves that h converges to the exact solution H and that H is the solution of the Richards' equation, as $\Delta x, \Delta y, \Delta z \rightarrow 0$, when the condition expressed in equation (B.6) is respected and t is finite.

References

Avolio, M.V., Crisci, G.M., D'Ambrosio, D., Di Gregorio, S., Iovine, G., Rongo, R., Spataro, W., An extended notion of Cellular Automata for surface flows modelling, WSEAS Transactions on Computers, 2, 1080–1085, 2003.

Bear, J., Dynamics of Fluid in Porous Media, American Elsevier, New York, 1972.

Chau, J.F., Or, D., Sukop, M.C., Simulation of gaseous diffusion in partially saturated porous media under variable gravity with lattice Boltzmann methods, Water Resources Research, 41, W08410, 2005.

Chen, H., Chen, S., Matthaeus, W.H., Recovery of Navier-Stokes equations using lattice-gas Boltzmann method, *Physical Review A*, 45, 5339–5342, 1992.

Chopard, B., Luthi, P.O., Lattice Boltzmann computations and application to physics, *Theoretical Computer Science*, 217, 115–130, 1999.

Crutchfield, J.P., Mitchell, M., Das, R., The evolutionary design of collective computation in cellular automata, in Crutchfield, J.P. and Schuster, P.K., editors, *Evolutionary Dynamics-Exploring the Interplay of Selection, Neutrality, Accident, and Function*, Oxford University Press, New York, 2002.

Dattilo, G., Spezzano, G., Simulation of a cellular landslide model with CAMELOT on high performance computers, *Parallel Computing*, North Holland, 29(10), 1403–1418, 2003.

de Marsily, G., *Quantitative Hydrogeology: Groundwater Hydrology for Engineers*, Academic, San Diego, USA, 1986.

Deng, J.Q., Ghidaoui, M.S., Gray, W.G., Xu, K., A Boltzmann-based mesoscopic model for contaminant transport in flow systems, *Advances in Water Resources*, 24, 531–550, 2001.

Di Gregorio, S., Serra, R., An empirical method for modelling and simulating some complex macroscopic phenomena by cellular automata, *Future Generation Computer System*, 16, 259–271, 1999.

Di Gregorio, S., Serra, R., Villani, M., Applying cellular automata to complex environmental problems: the simulation of the bioremediation of contaminated soils, *Theoretical Computer Science*, 217, 131–156, 1999.

Di Pietro, L.B., Melayah, A., Zaleski, S., Modeling water infiltration in unsaturated porous media by interacting lattice gas-cellular automata, *Water Resources Research*, 30(10), 2785–2792, 1994.

Folino, G., Mendicino, G., Senatore, A., Spezzano, G., Straface, S., A model based on cellular automata for the parallel simulation of 3D unsaturated flow, *Parallel Computing*, 32, 357–376, 2006.

Frisch, U., d'Humieres, D., Hasslacher, B., Lallemand, P., Pomeau, Y., Rivet, J.P., Lattice gas hydrodynamics in two and three dimensions, *Complex Systems*, 1, 649–707, 1987.

Gambolati, G., Paniconi, C., Putti, M., Petruzzelli, D., Helfferich, F.G., Numerical modeling of contaminant transport in groundwater, *Migration and Fate of Pollutants in Soils and Subsoils*, NATO ASI Series G: Ecological Sciences, 32, 381–410, 1993.

Ginzburg, I., Equilibrium-type and link-type lattice Boltzmann models for generic advection and anisotropic-dispersion equation, *Advances in Water Resources*, 28, 1171–1195, 2005.

He, X., Luo, L.S., Lattice Boltzmann model for the incompressible Navier-Stokes equation, *Journal of Statistical Physics*, 88, 927–945, 1997.

Higuera, F.J., Jimenez, J., Boltzmann approach to lattice gas simulations, *Europhysics Letters*, 9, 663–668, 1989.

Huyakorn, P.S., Springer, E.P., Guvanasen, V., Wadsworth, T.D., A three-dimensional finite element model for simulating water flow in variably saturated porous media, *Water Resources Research*, 22(12), 1790–1808, 1986.

Indelman, P., Dagan, G., Upscaling of permeability of anisotropic heterogeneous formations, 1. The general framework, *Water Resources Research*, 29(4), 917–923, 1993.

Knutson, C.E., Werth, C.J., Valocchi, A.J., Pore-scale modeling of dissolution from variably distributed nonaqueous phase liquid blobs, *Water Resources Research*, 37, 2951–2963, 2001.

Magnuson, S.O., Baca, R.G., Sondrup, A.J., Independent verification and benchmark testing of the porflo-3 computer code, version 1.0, Technical Report EGG-BG-9175, Idaho National Engineering Laboratory, Idaho Falls, ID, 1990.

Manzini, G., Ferraris, E., Mass-conservative finite volume methods on 2-D unstructured grids for the Richards equation, *Advances in Water Resources*, 27, 1199–1215, 2004.

Marty, N.S., Chen, H., Simulation of multicomponent fluids in complex three-dimensional geometries by the lattice Boltzmann method, *Physical Review E*, 53, 743–750, 1996.

Mattiussi, C., An analysis of Finite Volume, Finite Element, and Finite Difference Methods using some concepts for algebraic topology, *Journal of Computational Physics*, 133, 289–309, 1997.

McNamara, G.R., Zanetti, G., Use of the Boltzmann equation to simulate lattice-gas automata, *Physical Review Letters*, 61, 2332–2335, 1988.

Mendicino, G., Senatore, A., Spezzano, G., Straface, S., Three-dimensional unsaturated flow modeling using cellular automata. *Water Resources Research*, 2006, 42, W1141, W1–W18.

Mendicino, G., Senatore, A., Spezzano, G., Straface, S., Automi cellulari macroscopici per la simulazione del moto tridimensionale in mezzi porosi non saturi. Proceedings of “XXX Convegno Idraulica e Costruzioni Idrauliche”, Rome, 2006.

Mitchell, A.R., Griffiths, D.F., *The Finite Difference Method in Partial Differential Equations*, J. Wiley & Sons, Chichester, 1980.

Mualem, Y., A conceptual model of hysteresis, *Water Resources Research*, 10, 514–520, 1974.

Muzy, A., Wainer, G., Innocenti, E., Aiello A., Santucci J.F., Cell-DEVS Quantization techniques in a fire spreading application, *Proceedings of the Winter Simulation Conference 2002 – Exploring new frontiers*, San Diego, USA, 2002.

Orlandini, S., Two-layer model of near-surface soil drying for time-continuous hydrologic simulations, *Journal of Hydrologic Engineering*, 4(2), 91–99, 1999.

Paniconi, C., Aldama, A.A., Wood, E.F., Numerical evaluation of iterative and noniterative methods for the solution of the nonlinear Richards equation, *Water Resources Research*, 27(6), 1147–1163, 1991.

Paniconi, C., Putti, M., A comparison of Picard and Newton iteration in the numerical solution of multidimensional variably saturated flow problems, *Water Resources Research*, 30(12), 3357–3374, 1994.

Pot, V., Appert, C., Melayah, A., Rothman, D.H., Zaleski, S., Interacting lattice gas automaton study of liquid–gas properties in porous media, *Journal de Physique II*, 6, 1517–1534, 1996.

Qian, Y., d’Humières, D., Lallemand, P., Lattice BGK models for Navier-Stokes equation, *Europhysics Letters*, 17, 479–484, 1992.

Rothman, D.H., Zaleski, S., *Lattice–Gas Cellular Automata: Simple Models of Complex Hydrodynamics*, Cambridge University Press, Cambridge, UK, 1997.

Smyth, J.D., Yabusaki, S.B., Gee, G.W., Infiltration evaluation methodology – letter report 3: Selected tests of infiltration using two dimensional numerical models, Technical Report, Pacific Northwest Laboratory, Richland, WA, 1989.

Soll, W.E., Celia, M.A., Wilson, J.L., Micromodel studies of three-fluid porous media systems: pore-scale processes relating to capillary pressure-saturation relationships, *Water Resources Research*, 29(9), 2963–2974, 1993.

Soll, W.E., Birdsell, K., The influence of coatings and fills on flow in fractured, unsaturated tuff porous media systems, *Water Resources Research*, 34(2), 193–202, 1998.

Straface S., A flow and transport numerical model based on the method of cells. PhD (in Italian), University of Calabria, Cosenza, Italy, 1998.

Straface, S., Troisi, S., Gagliardi, V., Application of the cell method to the simulation of unsaturated flow. *Computers, Materials, & Continua*, 3(3), 155–165, 2006.

Succi, S., Benzi, R., Higuera, F., The lattice Boltzmann equation: a new tool for computational fluid dynamics, *Physica*, 47 (D), 219–230, 1991.

Sukop, M.C., Or, D., Lattice Boltzmann method for modeling liquid–vapor interface configurations in porous media, *Water Resources Research*, 40, W01509, 2004.

Toffoli, T., Margolus, N., *Cellular Automata Machines*, MIT Press, Cambridge, MA, 1987.

Tonti, E., A discrete formulation of field laws: the cell method, *Computational Methods in Engineering and Science*, 1(1), 11, 2001.

Troisi, S., Problems of mathematical model validation in groundwater hydrology. *Excerpta*, 9199–236, 1995.

Troisi, S., Fallico, C., Straface, S., Migliari, E., Application of kriging with external drift to estimate hydraulic conductivity from electrical resistivity data in unconsolidated deposits near Montalto Uffugo, Italy, *Hydrogeology Journal*, 4, 356–367, 2000.

van Genuchten, M.Th., Calculating the unsaturated hydraulic conductivity with a new closed-form analytic model, *Water Resources Program Report 78-WR-08*, Department of Civil Engineering, Princeton University, Princeton, NJ, 1978.

van Genuchten, M.Th., Nielsen, D.R., On describing and predicting the hydraulic properties of unsaturated soils, *Annales Geophysicae*, 3(5), 615–628, 1985.

von Neumann, J., *Theory of Self-Reproducing Automata*, University of Illinois Press, Urbana, Illinois, 1966.

Wolfram, S., *Cellular Automata and Complexity*, Addison-Wesley, Reading, Mass, 1994.

Wolfram, S., *Theory and Application of Cellular Automata*, World Scientific, Singapore, 1986.

Zhang, D., Zhang, R., Chen, S., Soll, W.E., Pore scale study of flow in porous media: scale dependency, REV, and statistical REV, *Geophysical Research Letters*, 27, 1195–1198, 2000.

Zhang, X., Bengough, A.G., Crawford, J.W., Young, I.M., A lattice BGK model for advection and anisotropic dispersion equation, *Advances in Water Resources*, 25, 1–8, 2002a.

Zhang, X., Bengough, A.G., Deeks, L.K., Crawford, J.W., Young, I.M., A novel three-dimensional lattice Boltzmann model for solute transport in variably saturated porous media, *Water Resources Research*, 38, 1167–1177, 2002b.

Zhang, X., Deeks, L.K., Bengough, A.G., Crawford, J.W., Young, I.M., Determination of soil hydraulic conductivity with the lattice Boltzmann method and soil thin-section technique, *Journal of Hydrology*, 306, 59–70, 2005.

Ziegler, B.P., DEVS theory of quantized systems, Advanced simulation technology thrust DARPA contract, 1998.

Agent-based modeling of socio-economic processes related to the environment: Example of land-use change

J. Gary Polhill

Macaulay Institute, Craigiebuckler, Aberdeen AB15 8QH, UK.

Abstract

This chapter discusses some of the principles behind multi-agent modeling and shows through the examples from land-use change how they can be applied to deal with socio-economic aspects of environmental issues. An underlying theme is the divide between qualitative and quantitative approaches in the social sciences, though the chapter is also aimed at presenting agent-based modeling to those accustomed to mathematical modeling approaches.

Keywords: agent-based modeling, qualitative-quantitative debate, land-use change.

1. Introduction

Traditionally, there have been two options for describing and analyzing phenomena of interest. If sufficient measured data are available, then various mathematical techniques may be employed, essentially fitting a function (or functions) to the data describing the trajectory of the system. The resulting equations, and subsequent analysis conducted with them, particularly in a policy context, amount to a process of developing a narrative of the phenomena concerned. That is, the equations are not an end in themselves but a tool used as part of a supposedly rigorous process. The analytical techniques used to develop and assess the equations have ultimately derived from physics. It is a testament to their utility that such techniques have been applied beyond physics into other sciences, including ecology and the social sciences. In the social sciences (and arguably in ecology), however, the techniques may become somewhat strained and unwieldy in their application. The phenomena are, furthermore, so intricately interrelated, and individuals so varied, that doing justice to the complexity is often not possible with the language of mathematics. The only other language available has been natural language.

For hardened quantitative scientists, qualitative social science often poses something of a challenge. It seems difficult to accept that the elegant mathematics that has served so well in other scientific endeavors should prove so limited for studying societies. More difficult still to accept is the critique of the objectivity of science. Whilst there has been a tendency to overgeneralise, it should be acknowledged that when studying societies, it is difficult to honestly claim impartiality of observation, since modes of thought, norms of analysis and standards of practice are culturally and linguistically determined. Arguing for the superiority of one such set of modes, norms and standards over another can have awkward political connotations. Ultimately, however unpalatable these ideas may be to those familiar with the kinds of scientific certainties that allow us to land probes on Titan, at some level it must be accepted that at least some practitioners of social science, no less keen than natural scientists to rigorously study their domain of interest, have found that they cannot, in all integrity, pretend to the precision and objectivity that quantitative approaches seem to offer. Since societies are embedded within ecosystems, these issues may then extend into environmental studies. Political ecology is a discipline acknowledging that environmental issues are political issues: scientific evidence alone, however 'right' or 'true', is not sufficient to cause people to change those aspects of their lifestyles found to be harmful to the environment (Zimmerer and Bassett, 2003).

The choice of language is, however, not restricted to natural language or calculus. The modern computer is seen by some simply as a tool for performing calculations and derivations of numerical models that are impossible to undertake by hand. Yet programming languages, particularly object-oriented languages, can do much more than implement algorithms to crunch numbers. They offer a means to represent phenomena descriptively, not necessarily numerically, and yet still formally. Such representations can be more easily related to natural language than equations, and yet are founded in logics, offering greater precision than natural language. Though there are those on the qualitative side who would reject all formality, and those on the quantitative side who could not stand the loss of mathematical elegance and rigor, computer simulations offer those without such extreme views a third way to develop narratives of the phenomena they are interested in.

Agent-based modeling, closely related to ideas of individual-based modeling in ecology and sometimes referred to as social simulation or multi-agent simulation, forms a significant part of the effort to study social systems using representative forms derived from computer programming languages. This chapter provides some background on agent-based modeling and the issues it faces, and then offers some illustration of its use in the area of land-use change.

2. Various motivations for agent-based modeling

Agent-based modeling is an inherently multi- if not inter-disciplinary area, bringing together social scientists, computer scientists, and in some cases, the artificial

intelligence community. Some agent-based models are spatially explicit, bringing in geographers and, where environmental processes are also modeled, ecologists and the biophysical sciences become involved. There are deeper links with what is termed ‘individual-based modeling’ in ecology, the chief difference largely pertaining to what the individuals or agents in the models represent. Agents in agent-based models typically represent humans or human organizations, though they may also represent more abstract things such as human settlements or even areas of land. In individual-based models, agents may be non-human animals or plants.

Why the concern with representing individuals? If there is one principle underlying agent-based modeling, it is that agent heterogeneity matters. This is often held in contrast to neoclassical economics, where, for the sake of mathematical tractability, people are assumed to be the same (or at least, either sufficiently similar that their differences do not matter, or if not, then significant differences ‘cancel out’ (Weisskopf, 1955)).

It is not only the sameness of agents that is critiqued. Neoclassical economic analyses are portrayed as requiring ‘heroic assumptions’ (Johnson, 1998) about human cognitive capabilities that tend not to be supported by experimental evidence. Specifically, economists endow humans with unlimited information-processing powers, and knowledge of alternatives. The difference between this and observed patterns of human behavior has, at least in part, led to the term *‘Homo economicus’* being coined to denote the mythical species that neoclassical economists study (Persky, 1995).

In fact, in many agent-based models, the agents themselves do not differ other than in their location in time and space or connectedness in a social network (that is, their algorithms for decision-making are the same, but may produce different responses given different geographies, histories, and/or social embeddedness). This, however, is another area where more traditional mathematical modeling techniques struggle to represent phenomena, or can only do so in highly stylized ways (Chattoe, 1996). Some agent-based models may thus still use utility maximizing agents despite objections to them in other areas of the literature, the heterogeneity modeled pertaining to the context of the agent rather than their individual cognitive capabilities.

To read some of the agent-based modeling literature is to see neoclassical economics almost as a religion, ignoring empirical evidence found contrary to doctrine, obsessed with the Nirvana-like state of equilibrium and evangelizing a utilitarian morality of self-interest. Moss (1999), in his inaugural lecture at Manchester Metropolitan University, is blunt:

“Economics, as developed over the last half century and more, is not useful for the analysis and support of formal policy; it should simply be ignored by serious social scientists.”

The relationship between neoclassical economics and agent-based modeling need not, however, be so acrimonious. Whilst many in agent-based modeling reject neoclassical economics, others are less confrontational, and see ways in

which the two can be complementary. Axtell (2000) lists a number of cases where agent-based modeling could assist mathematical modeling in economics. Nevertheless, it is fair to say that most practitioners in agent-based modeling would see their work as distinct from neoclassical economics in emphasizing boundedly rational, heuristic, or cognitively plausible decision-making algorithms, and attaching rather less significance to the concept of equilibrium. To be fair to the economists, however, there are, at least in the former case, similar trends in the literature (e.g., Rabin, 2002).

The question of economic rationality in land-use decision-making is illustrated by a recent story in the *Guardian* newspaper pertaining to dairy farms (Lawrence, 2007). One farmer from the Cotswolds interviewed in the article was getting 19 p per liter of milk produced, whilst watering his cows from a spring that he could have bottled and sold for 80 p per liter. His response is revealing:

“We’re giving [the spring water] to cows and devaluing it by turning it into milk. Like all dairy farmers we could pack up tomorrow and do something better with our capital, but we do it because we have an emotional investment in the land and the animals.”

Whilst the dairy market in the UK has a complex history that is partly responsible for the tenuous situation dairy farmers found themselves in at the time the article was written, qualitative studies of British farmers by authors such as Burton (2004) highlight the importance of this emotional investment farmers have in their farm and their work. Further, Evans *et al.* (2006) have results from laboratory experiments comparing resource allocations of human subjects with those of utility-maximizing agents in an agent-based model. They conclude that these results “demonstrate the value of using non-maximizing agents in agent-based models of land-cover change” (p. 1034). Their results also highlight the need for representing agent heterogeneity (*ibid.*).

This debate can be seen as part of a much wider debate in science about formal versus narrative representations of reality – which in the social sciences manifests itself in the divide between qualitative and quantitative research. Agent-based modeling has been promulgated as a possible ‘third way’: both formal and descriptive in its representation of reality (Moss, 1999; Moss and Edmonds, 2005), addressing the lack of richness in mathematical representations used by quantitative researchers, and the perceived lack of rigor of qualitative approaches. Bridging this rift would be a significant contribution of agent-based modeling but there are no guarantees that this can be achieved. Depending on how entrenched the positions are (and how successful agent-based modeling is), agent-based modeling approaches could equally be rejected by both communities, perceived by the quantitative camp as lacking mathematical rigor, and by the qualitative camp as too formal. Even within the agent-based modeling community, there is something of a rift about the richness of representation that is appropriate in agent-based models that mirrors somewhat the wider debate over quantitative and qualitative descriptions. Various researchers (e.g., Johnson, 1998; Axtell, 2000) advocate the ‘KISS’ principle (Keep It Simple, Stupid), whilst others (e.g., Clarke, 2004; Edmonds and

Moss, 2005) question this ideology, Edmonds and Moss (2005) advocating ‘KIDS’ (Keep It Descriptive, Stupid) in its place. However, at least the debate is now couched in terms that can be more easily related to one another through the medium of the computer programs that implement the models. Further, the issue may simply derive from differences in the purposes for which the models are built. KISS tends to apply where theoretical issues are being explored, whilst KIDS is more often associated with policy-related work.

Why should agent heterogeneity matter? It may be argued that such heterogeneity can easily be captured in a distribution. Behavior can then be modeled at an aggregate level using this distribution as a basis. Even if it is accepted that behavior can be captured in a distribution, modeling at an aggregate level, however, would fail to capture the significance of interactions among the heterogeneous agents. Interactions among heterogeneous agents may produce unexpected behavior. Agent interactions, then, are a second significant underpinning to agent-based modeling practice.

If heterogeneity and interactions are key underpinnings of agent-based modeling, then it should come as little surprise that it draws on ‘complex adaptive systems’ literature. Though the term is widely used (Google Scholar returns over one million hits on it), its conceptualization is somewhat vague. It is linked to literature on complexity (itself a vague term), Manson (2001) describing complex systems as having ‘aggregative complexity’. Holland and Miller (1991, p. 365) define a complex system as a network of interacting agents that collectively manifest a dynamic emergent aggregate behavior, which can be described without a detailed knowledge of the individual behavior of the agents. They then say that such a system is adaptive if the agents’ actions take place in an environment that feeds back a value (*e.g.*, fitness, payoff, utility), which the agents increase over time. Arthur *et al.* (1997) also draw on the work of John Holland, listing six properties of economic systems presenting difficulties for traditional mathematical modeling techniques that are also properties of ‘adaptive nonlinear networks’: dispersed interaction of possibly heterogeneous agents, no global controller mediating the interactions, multiple levels of partially interacting structure, continual system adaptation, perpetual novelty, and out-of-equilibrium dynamics. Manson (2001) lists similar properties.

Of more interest may be the statistical signatures from observations of complex adaptive systems. Moss (2002), for example, finds leptokurtosis in distributions of weekly sales of shampoo, tea, shaving preparations and biscuits. Extreme events in such systems are thus more likely than in normally distributed phenomena, a point of possible interest to policy-makers (as well as vendors of domestic products and their shareholders). A further property that such systems may be found to have is heteroskedasticity (non-constant variance in samples). Both conditions would be observed in phenomena with power-law distributions (having power > 1), all of which have infinite variance, skew and kurtosis (*i.e.*, the sample statistic in question increases with sample size), and some of which have infinite mean. Power-law distributions are particularly interesting as they are scale-free. For critics

of complex systems (some of whom regard it as little more than a fad (Manson, 2001)), and specifically those in geography who regard complexity as a scale issue (essentially, something that will disappear with coarser grain), the existence of power-law distributed phenomena would thus pose a difficulty. Though there is some comfort for them in the fact that the finite planet bounds the extent to which phenomena can follow power-law distributions, such comfort would prove cold if the grain at which the complexity disappears were too coarse for meaningful analysis.

These statistical signatures pose a challenge to traditional mathematical modeling techniques. Though ARCH (Engle, 1982) and related techniques have been developed in the field of econometrics for analyzing heteroskedastic time series, such as those involving interspersed periods of rapid change and relative calm, Moss (2002, p. 7268) claims that for power law distributions with infinite mean, “No laws or theorems of classical statistics or econometrics are applicable.”

Agent-based modeling need not necessarily rely on complex adaptive systems theory (if theory it is). Axtell (2000) notes that simulation can be used to illustrate analytically derived results. Further, Gotts *et al.* (2003), covering the debate between Axelrod and Binmore on simulation versus mathematical theory in the study of the prisoner’s dilemma, point out that Binmore’s and subsequent analytical results were given impetus by Axelrod’s simulation studies. Chattoe (1996) highlights that simulations offer richer, more comprehensible, descriptions of systems than mathematical modeling, potentially making a model accessible even to non-specialists. Agent-based models may be preferred simply because they are more descriptively representative of the target phenomena than the equivalent (tractable) mathematical model. Parameters in agent-based models are more likely to relate directly to observed phenomena, as opposed to those in mathematical models, which serve only to make the functions contort to the shape that minimizes calibration error.

Furthermore, there is reason to question the value of mathematical modeling of aggregate phenomena emergent from interactions of heterogeneous adaptive individuals. It is all very well to fit a mathematical function to the time-series of the aggregate phenomenon, but this may provide little reliable indication of the future of that phenomenon, particularly beyond the short-term. The mathematical function does not descriptively capture the properties of the system it is modelling nor say anything interesting about its dynamics. Chattoe (1996, p. 101), contrasts the rewarding exercise of analyzing outputs from simulations with mathematical models thus: “the simplicity of mathematical systems reduces secondary analysis to the rather menial and potentially negative task of looking for errors”. Moss (2002, p. 7267) is more confrontational. Enquiring of the email discussion list of the Institute of International Forecasters whether there had been a single correct econometric forecast of an extreme event (e.g., a stock market crash), he found that, “No one was able to point to a correct forecast in real time”. It would not be unreasonable to pose the same question of agent-based modelers. Although the work of LeBaron *et al.* (1999) demonstrated that their agent-based model of a stock market

captured phenomena difficult to model mathematically such as weak forecastability and volatility persistence, one would in general find a more cautious community when it comes to prediction. An awareness of the complexity of the systems they are modeling yields a more circumspect attitude to prediction and, as a result, multiple possible trajectories would be expected from numbers of simulation runs. On the other hand, there are notable cases where agent-based models have made empirically verifiable predictions, a popularly cited example being that of Dean *et al.*'s (2000) work studying the Anasazi. Matthews *et al.* (2007), for example, describe Dean *et al.*'s model as being "able to simulate the temporal dynamics of [household numbers and settlement sizes] over most of the study period reasonably well", despite overestimating the values of these variables.

Agent-based modeling is not without its detractors. Indeed, most of its practitioners would acknowledge there are weaknesses with the approach. These issues can be summarized in the following main areas:

- *Validation.* The question of the validity of agent-based models is a thorny one, as discussed by Küppers and Lenhard (2005). To those used to mathematical modeling, validation is simply the process of evaluating the predictions of the model against some data not used during calibration to assess whether errors are within acceptable margins. Even for mathematical models, Oreskes *et al.* (1994) have raised pertinent questions about validation, verification and confirmation of models applied to the environment. For agent-based models, there is not only concern over the accuracy of the macro-level emergent outcomes but also over the accuracy of the micro-level representations that have been used to generate them. Indeed, arguably the latter are in some ways more important as they embody the assumptions from which the macro-level outcomes logically follow. Brown *et al.* (2005) make a similar distinction between checking the accuracy of the predictions of a model, and the accuracy of the processes by which the predictions are obtained. Part of the search, at least for some agent-based modelers, is for a minimum set of assumptions about individuals and their interactions required for a particular macro-level outcome to occur. There is thus not necessarily just one model to be validated and either accepted or rejected but a cyclic process of model building, assessment and incremental revision as the space of algorithms that might generate a particular narrative is explored. For models developed as part of a participatory process, validation may be a matter of deciding the acceptability of the models to the stakeholders concerned. Other agent-based models may be developed simply to explore a theory, with little or no appropriate empirical data available for validation. Boero and Squazzoni (2005) outline various classes of agent-based model, and how they may relate to empirical data. Windrum *et al.* (2007) consider emerging methodologies for validation in agent-based models.
- *Standardization.* There are a plethora of languages, libraries and platforms on which agent-based models are built (Gilbert and Banks, 2002). Many embarking on an agent-based modeling exercise may even start from scratch, rather

than using existing code, exposing the somewhat mythical status of one of the supposed advantages of object-oriented programming languages. Even within a given platform there may be several options for implementing or representing certain aspects of the target system. Though Kahn (2007) has developed an interesting approach based on 'microbehaviours' for the NetLogo modeling environment (Wilensky, 1999), standard methodologies, libraries and even algorithms have yet to emerge in agent-based modeling. This makes agent-based modeling a difficult area to start working in, as there is little scope to learn from the mistakes of others, and gives outsiders the impression that it lacks rigor. Efforts are under way to develop standard methodologies in social simulation, such as those outlined by Richiardi *et al.* (2006), whilst Janssen *et al.* (2008) report on the establishment of the Open Agent-Based Modeling Consortium (OABMC).

- *Communication.* One of the consequences of the lack of standardization is that agent-based models are difficult to communicate. This is exacerbated by the fact that, in contrast to numerical models, where a page or so of equations is sufficient to describe the action in a model, programs implementing agent-based models may run into tens of thousands of lines. Documenting the program in sufficient detail to enable replication of models (a pillar of the scientific endeavor) tends not to be possible within the confines of a typical journal article. For those who have attempted replication, even apparently minor details such as the difference between ' $>$ ' and ' \geq ' in a conditional expression can dramatically change the outcome of a model and the conclusions drawn from it (Edmonds and Hales, 2003). Failures to replicate are not uncommon. In a recent example, Will and Hegselmann (2008) report on a failure to replicate Macy and Sato's (2002) model relating trust and social mobility. Many authors attempting replication state that they need a significant degree of interaction with the original developers for their efforts to be successful. A contribution from the individual-based modeling community in ecology may help address this issue. Grimm *et al.*'s (2006) ODD protocol is a document structure designed to provide readable, complete accounts of individual and agent-based models in journal articles, and has been shown to be effective for describing agent-based models of land use change (Polhill *et al.*, 2008). However, even if ODD were more widely used, access to the source code of agent-based models should also be a more formally applied norm (perhaps even a condition of publication of an associated journal article). Informal requests for source code from the authors can, it seems, be misinterpreted (Macy and Sato, 2008). The OABMC's model archive¹ could be a useful contribution here, provided it becomes standard practice to use it. However, this is a contentious issue, as software has a more protective tradition of intellectual property rights. Polhill and Edmonds (2007) consider licensing issues associated with publishing scientific modeling software, stipulating licensing rights many would find too liberal, but without

¹ Link as at 25 November 2008: <http://www.openabm.org/site/models/browse>

which the scientific credentials of the work are impaired. Further efforts within the social simulation community to encourage replication include the Model-2-Model series of workshops (Hales *et al.*, 2003), the use of semantic grid technologies to allow access to social simulations, parameters and results (Polhill *et al.*, 2007) and the use of the forum of JASSS (*Journal of Artificial Societies and Social Simulation* – the main journal for social simulation) for communicating replication work.

Though agent-based modeling is not without its issues, it is also a relatively young discipline – if indeed ‘discipline’ is an appropriate word to describe such an eclectic, even anarchic, community. The power of computer programming languages and of computers themselves has perhaps given us rather too much freedom. That said, as more and more studies using agent-based modeling are conducted, lessons will be (and indeed are being) learned about how to undertake such work rigorously, and how to learn from each others’ work. Whatever the fate of the agent-based modeling community, its underlying tenets—that agent heterogeneity and interactions matter—are worth investigating, given that the technology is available to do so.

3. Agent-based modeling in land-use change

Various reviews of agent-based modeling in land-use change exist, and it would be pointless to repeat the exercise here. The interested reader is referred to articles such as Hare and Deadman (2004), Bousquet and Le Page (2004), Parker *et al.* (2003), and Matthews *et al.* (2007). Rather, I consider here an interesting example of agent-based modeling in land use, which has been used in a policy context, critiqued by the qualitative community, and independently reimplemented. This leads to a discussion of a more radically subjective approach to modeling.

One of the earliest examples of agent-based modeling in land use involving the interaction with policy-makers is the study of a rice irrigation system in Bali by Lansing and Kremer (1993), which took place in the context of the green revolution of the late 1970s and early 1980s. The irrigation system was heavily embedded in local religious practices, and there was considerable debate about whether these practices were detached from irrigation management or integral to them (Lansing, 1987). Lansing was able to demonstrate the effectiveness of the religion in coordinating rice paddy irrigation, and thus to persuade the authorities to cease in their opposition to irrigation management by water temple networks (Lansing, 2000).

In more detail, the rice growing system in Bali is based on the *subak*, a collective of rice growers who co-ordinate their planting of rice paddies to manage two constraints on rice yields with conflicting outcomes for scheduling plantings. The first constraint is the availability of water, which motivates farmers to plant at different times to minimize conflicts in demand for irrigation. The second constraint is the need to manage pest species, which spread from neighboring rice paddies.

Pests are controlled through having fallow periods, and the greater the area of contiguous fallow paddies, the more effective the control of the pests. This motivates farmers to plant at the same time. The water temple religion co-ordinates planting of rice among a group of subaks, though the process is so highly ritualized, its relevance was not immediately apparent.

Lansing and Kremer (1993) did two modeling exercises. Having implemented models of the hydrology, pest dynamics, and rice growth, in one exercise, they tried various different spatial scales of co-ordination for one year's rice planting, plotting yield against this scale. They found a maximum at approximately the scale corresponding to the temples. In the second exercise, they made a simple agent-based model by using an agent to represent each subak, giving them initially random planting schedules (which would mean too many pests due to lack of spatial contiguity of fallow periods). In each year thereafter, the agents imitated the planting strategy of their most successful (in terms of rice yield) neighbor. The consequence was a pattern of co-ordination of planting schedules that corresponded to temple scale co-ordination (see Figure 1).

Lansing was able to use the outcomes from his modeling work with Kremer to convince policy-makers of the significance of the water temple religion (Lansing, 2000), in the context of a view of a declining role for the temples in water management as a result of technological progress (Lansing and Kremer, 1993, p. 112). This is quite an achievement given that there was considerable pressure both on farmers and policy-makers to encourage the use of artificial fertilizers not needed

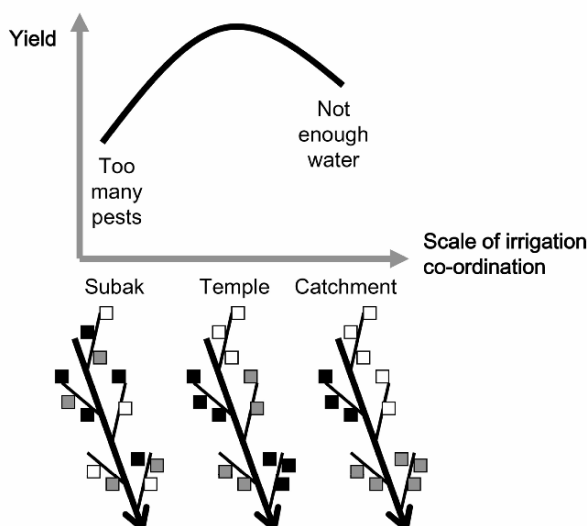


Fig. 1. Schematic of the Lansing-Kremer model. The top half shows a graph representing the yield obtained from a given scale of irrigation co-ordination, the bottom half shows the corresponding pattern of planting schedules. Here, each square represents a subak, shaded (black, white or grey) according to its planting schedule. The arrow represents flow of water.

by the traditional rice farming methods, the over-application of which threatened coastal ecosystems.

Lansing (2000, p. 316) points out that the models “proved to be more persuasive” in defense of traditional rice-farming practice in Bali than earlier letters he had written to the Asian Development Bank. Enthusiasm for the models is not universal. In an article revealing some of the struggle the agent-based modeling community may have in gaining acceptance of their work among some qualitative social scientists, Helmreich (1999) criticizes the Lansing-Kremer models for oversimplifying the political and historical context of Balinese rice farming (p. 260), and for romanticizing the integration of the traditional rice farmers in their ecosystem through couching the social phenomenon of co-operation in the naturalistic terminology of ‘fitness’ (p. 254).

To the modeling community, Helmreich’s comments may seem naive. After all, even if Lansing and Kremer could have included in their model at Helmreich’s behest, such things as Dutch imperialism, slavery, and the Indonesian struggle for independence, what difference would it have made to the appropriate scale at which to manage rice paddy irrigation? And if a term other than ‘fitness’ had been used to describe the comparative success of different planting schedules, would the model have changed its behavior? As modelers, we understand that there are limits to the narratives that any model can be used to explore: deciding the boundary is part of the modeling process, and there will always be more that could have been included. However, these issues highlight the difficulties associated with studying social systems. Ontological commitments in social simulations, whether made intentionally or otherwise, have political and cultural implications that should be acknowledged and open to discussion.

It is interesting to speculate on what might have happened had Lansing somehow devised an analytical rather than agent-based model of the Balinese rice farming system. Would the rift between qualitative and quantitative social scientists have meant that Helmreich would not have heard of the model? If he had, would he have bothered to critique it, since he would merely have been invoking well-rehearsed arguments? Or perhaps a mathematical model would have been more difficult to criticize because the underlying assumptions are not as clearly expressed as they are in an agent-based model? If agent-based models do make ontological commitments more explicit to non-modelers, even if this means potential exposure to greater criticism, such models are of benefit to the research and wider community as a whole.

Agent-based models are indeed used by some as a medium for discussion. Participatory agent-based social simulation is used by a number of groups and, in particular, researchers at CIRAD (Centre de coopération Internationale en Recherche Agronomique pour le Développement, France), who have developed what they call a ‘companion modeling’ approach (Barreteau *et al.*, 2003). This approach is developed out of an awareness of the uncertainty and complexity of decision-making in environmental resource management. It gathers together (possibly conflicting) information from multiple sources, scientific and non-scientific, empirical and

theoretical, using agent-based models and role-playing games to facilitate discussion among stakeholders. Decision-making becomes a continuous, evolving dialectic process of systematic revision to the models in the light of feedback from the stakeholders and the field. An overview of work conducted using companion modeling is provided by Bousquet *et al.* (2002).

The companion modeling approach is openly constructivist (Bousquet *et al.*, 2002, p. 249), and as such, will inevitably appall the committed positivist. Surely incorporating in a model the unscientific opinions and misperceptions of stakeholders untrained in the art of rationally processing observations will produce only nonsense as output? The problem is that, such is the uncertainty in these situations, there is insufficient high-quality indisputable information from the reality 'out there', to make a single, rational decision about the best way forward. Further, even if such a decision could be arrived at, the political and cultural context may prove too great an obstacle to the effective implementation of that decision. In the face of an impending environmental catastrophe (at least according to one domain of discourse), preserving a way of life may seem a foolish luxury: either the necessary changes are made or more people will suffer and die than need have been the case. Yet cherished lifestyles, traditions and beliefs tend not to be relinquished until there is rather more certainty than science may be able to offer. By involving stakeholders in the decisions, by giving them a voice in the models, it is possible to reflect back to people some of the consequences of their beliefs and give them a sense of ownership both in the model and in the evolving decision process. If the social construction of reality is too unpalatable, perhaps the social construction of virtual reality could be an acceptable compromise, at least if it oils the wheels of collective decision-making in situations of uncertainty towards more effective approaches to managing environmental resources.

Participatory agent-based social simulation is one of a suite of tools applied by the participatory integrated environmental assessment community (Hisschemöller *et al.*, 2001), with much the same motivations as those for companion modelling. Downing *et al.* (2000) have also used the approach in the area of climate change, noting the importance of models providing recognizable features that reflect the mental models of stakeholders, whilst still being validated against observed data (p. 206), suggesting that a constructivist outlook is not a necessary component of work in this area. Just as for Lansing and Kremer, the transparency of agent-based models and their more realistic representations are thus important parts of the contribution agent-based approaches offer. Becu *et al.* (2003), in the abstract of a paper describing work on water management with rice farmers in Thailand, also emphasize transparency. The integration of non-academic participants in interdisciplinary research is discussed in the literature on transdisciplinarity. (Lawrence and Després (2004) introduce a special issue of *Futures* on the subject.) Vandermeulen and Van Huylenbroeck (2008) report on a transdisciplinary research exercise on sustainable agricultural development in Belgium, arguing that such an approach is desirable because of the number of stakeholders involved and the complexity of the issue.

Lansing and Kremer's Bali model also offers the opportunity to demonstrate at least some scientific rigor in agent-based modeling. Janssen (2007) reimplemented their model. Though he confirmed Lansing and Kremer's results for the case study in Bali, he also found that there was sufficient sensitivity to pest dynamics that the results are not general. Thus, for different pest dynamics, the temple scale would not have been the most effective scale of co-ordination.

4. Conclusion

Agent-based modeling allows more transparent, descriptive representations of phenomena than traditional mathematical modeling, whilst still retaining the rigor of formal languages. Whilst this offers some hope of bridging the divide between qualitative and quantitative social science, in practical terms, this makes it ideal for incorporating social dynamics into environmental models, and for use in policy-making scenarios involving people from diverse, possibly non-scientific, backgrounds. It is not a panacea, and Gotts *et al.* (2003) suggest it should be seen as a complement to, rather than a replacement for, mathematical modeling and narrative descriptions. Computer science is, after all, another branch of mathematics. As a relatively young discipline, it is also not without its issues, in particular, a lack of established methodologies and standards of practice. However, these issues are gradually being addressed. By making full use of the facilities provided by modern computer programming languages, agent-based modeling allows scientists to gaze in wonder at the intricate complexity of the world around them, and ask questions other than "What's the underlying function?".

Acknowledgements

This work has been funded in part by the Scottish Government Rural and Environmental Research and Analysis Directorate.

References

Arthur, W. B., Durlauf, S., and Lane, D., 1997, Introduction, in Arthur, W. B., Durlauf, D., and Lane, S. (eds.) *The Economy as a Complex Evolving System II*. Reading, MA: Addison-Wesley. pp. 1–14.

Axtell, R., 2000, Why agents? On the varied motivations for agent computing in the social sciences, *The Brookings Institution, Center on Social and Economic Dynamics, Working Paper No. 17*. <http://www.brookings.edu/es/dynamics/papers/agents/agents.pdf>

Barreteau, O. and others, 2003, Our companion modelling approach, *Journal of Artificial Societies and Social Simulation*, 6(2):1. <http://jasss.soc.surrey.ac.uk/6/2/1.html>

Bechu, N., Perez, P., Walker, A., Barreteau, O., and Le Page, C., 2003, Agent based simulation of a small catchment water management in northern Thailand. Description of the CATCHSCAPE model, *Ecological Modelling*, **170**:319–331.

Boero, R. and Squazzoni, F., 2005, Does empirical embeddedness matter? Methodological issues on agent-based models for analytical social science, *Journal of Artificial Societies and Social Simulation*, **8**(4):6. <http://jasss.soc.surrey.ac.uk/8/4/6.html>

Bousquet, F., Barreteau, O., d'Aquino, P., Etienne, M., Boissau, S., Aubert, S., Le Page, C., Babin, D., and Castella, J.-C., 2002, Multi-agent systems and role games: Collective learning processes for ecosystem management, in Janssen, M. (ed.) *Complexity and Ecosystem Management: The Theory and Practice of Multi-Agent Systems*. Cheltenham, UK: Edward Elgar. pp. 248–285.

Bousquet, F. and Le Page, C., 2004, Multi-agent systems and ecosystem management: A review, *Ecological Modelling*, **176**:313–332.

Brown, D. G., Page, S., Riolo, R., Zellner, M., and Rand, W., 2005, Path dependence and the validation of agent-based spatial models of land use, *International Journal of Geographical Information Science*, **19**(2):153–174.

Burton, R. J. F., 2004, Seeing through the ‘good farmer’s’ eyes: Towards developing an understanding of the social symbolic value of ‘productivist’ behaviour, *Sociologia Ruralis*, **44**(2):195–215.

Chattoe, E., 1996, Why are we simulating anyway? Some answers from economics, in Troitzsch, K. G., Mueller, U., Gilbert, G. N. and Doran, J. E. (eds.) *Social Science Microsimulation*. Berlin: Springer-Verlag, pp. 78–104.

Clarke, K. C., 2004, The limits of simplicity: Toward geocomputational honesty in urban modeling, in Atkinson, P., Foody, G., Darby, S., and Wu, F. (eds.) *GeoDynamics*. Florida: CRC Press.

Dean, J. S., Gumerman, G. J., Epstein, J. M., Axtell, R., Swedlund, A. C., Parker, M. T., and McCarroll, S., 2000, Understanding Anasazi cultural change through agent-based modeling, in Gumerman, G. J. and Kohler, T. (eds.) *Dynamics in Human and Primate Societies: Agent-based Modeling of Social and Spatial Processes*. Oxford, UK: Oxford University Press. pp. 179–205.

Downing, T. E., Moss, S., and Pahl-Wostl, C., 2000, Understanding climate policy using participatory agent-based social simulation, in Moss, S. and Davidsson, P. (eds.) *MABS 2000. Lecture Notes in Artificial Intelligence*, **1979**:198–213.

Edmonds, B. and Hales, D., 2003, Replication, replication and replication: Some hard lessons from model alignment. *Journal of Artificial Societies and Social Simulation*, **6**(4):11. <http://jasss.soc.surrey.ac.uk/6/4/11.html>

Edmonds, B. and Moss, S., 2005, From KISS to KIDS – An ‘anti-simplistic’ modelling approach, in Davidsson, P., Logan, B. and Takadama, K. (eds.) *Multi-Agent and Multi-Agent-Based Simulation, Joint Workshop MABS 2004, New York, NY, July 19, 2004. Lecture Notes in Artificial Intelligence*, **3415**:130–144.

Engle, R. F., 1982, Autoregressive conditional heteroscedasticity with estimates of variance of United Kingdom inflation, *Econometrica*, **50**:987–1008.

Evans, T., Sun, W., and Kelley, H., 2006, Spatially explicit experiments for the exploration of land-use decision-making dynamics, *International Journal of Geographical Information Science*, **20**(9):1013–1037.

Gilbert, N. and Bankes, S., 2002, Platforms and methods for agent-based modelling, *Proceedings of the National Academy of Sciences*, **99**:7197–7198.

Gotts, N. M., Polhill, J. G., and Law, A. N. R., 2003, Agent-based simulation in the study of social dilemmas, *Artificial Intelligence Review*, **19**(1):3–92.

Grimm, V., Berger, U., Bastiansen, F., Eliassen, S., Ginot, V., Giske, J., Goss-Custard, J., Grand, T., Heinz, S. K., Huse, G., Huth, A., Jepsen, J. U., Jørgensen, C., Mooij, W. M., Müller, B., Pe'er, G., Piou, C., Railsback, S. F., Robbins, A. M., Robbins, M. M., Rossmanith, E., Rüger, N., Strand, E., Souissi, S., Stillman, R. A., Vabø, R., Visser, U., and DeAngelis, D. L., 2006, A standard protocol for describing individual-based and agent-based models, *Ecological Modelling*, **198**(1–2):115–126.

Hales, D., Rouchier, J., and Edmonds, B., 2003, Model-to-model analysis, *Journal of Artificial Societies and Social Simulation*, **6**(4):5. <http://jasss.soc.surrey.ac.uk/6/4/5.html>

Hare, M. and Deadman, P., 2004, Further towards a taxonomy of agent-based simulation models in environmental management, *Mathematics and Computers in Simulation*, **64**:25–40.

Helmreich, S., 1999, Digitizing ‘development’: Balinese water temples, complexity and the politics of simulation, *Critique of Anthropology*, **19**(3):249–265.

Hisschemöller, M., Tol, R. S. J., and Vellinga, P., 2001, The relevance of participatory approaches in integrated environmental assessment, *Integrated Assessment*, **2**:57–72.

Holland, J. H. and Miller, J. H., 1991, Artificial adaptive agents in economic theory, *The American Economic Review*, **81**(2):365–370.

Janssen, M. A., 2007, Coordination in irrigation systems: An analysis of the Lansing-Kremer model of Bali, *Agricultural Systems*, **93**:170–190.

Janssen, M. A., Na’ia Alessa, L., Barton, M., Bergin, S., and Lee, A., 2008, Towards a community framework for agent-based modelling, *Journal of Artificial Societies and Social Simulation*, **11**(2):6. <http://jasss.soc.surrey.ac.uk/11/2/6.html>

Johnson, P. E., 1998, Rational actors versus adaptive agents: Social science implications, *1998 Annual Meeting of the American Political Science Association, Boston*.

Kahn, K., 2007, Comparing multi-agent models composed from micro-behaviours, *M2M2007: Third Model-to-Model Workshop, Marseille, France, 15–16 March 2007*. <http://m2m2007.macaulay.ac.uk/M2M2007-Kahn.pdf>

Küppers, G. and Lenhard, J., 2005, Validation of simulation: Patterns in the social and natural sciences, *Journal of Artificial Societies and Social Simulation*, **8**(4):3. <http://jasss.soc.surrey.ac.uk/8/4/3.html>

Lansing, J. S., 1987, Balinese “water temples” and the management of irrigation, *American Anthropologist*, **89**:326–341.

Lansing, J. S., 2000, Foucault and the water temples: A reply to Heimrich, *Critique of Anthropology*, **20**(3):309–318.

Lansing, J. S. and Kremer, J. N., 1993, Emergent properties of Balinese water temple networks: Coadaptation on a rugged fitness landscape, *American Anthropologist*, **95**(1):97–114.

Lawrence, F., 2007, Rising prices, failing farms. The strange story of milk, *The Guardian*, Tuesday 24 April 2007.

Lawrence, R. J. and Després, C., 2004, Futures of transdisciplinarity, *Futures*, **36**(4):397–405.

LeBaron, B., Arthur, W. B., and Palmer, R., 1999, The time-series properties of an artificial stock market, *Journal of Economic Dynamics and Control*, **23**:1487–1516.

Macy, M. W. and Sato, Y., 2002, Trust, cooperation and market formation in the U.S. and Japan. *Proceedings of the National Academy of Sciences* **99** (Suppl. 3):7214–7220.

Macy, M. and Sato, Y., 2008, Reply to Will and Hegselmann, *Journal of Artificial Societies and Social Simulation*, **11**(4):11. <http://jasss.soc.surrey.ac.uk/11/4/11.html>

Manson, S. M., 2001, Simplifying complexity: A review of complexity theory, *Geoforum*, **32**:405–414.

Matthews, R. B., Gilbert, N. G., Roach, A., Polhill, J. G., and Gotts, N. M., 2007, Agent-based land-use models: A review of applications, *Landscape Ecology*, **22**(10):1447–1459.

Moss, S., 1999, Relevance, realism and rigour: A third way for social and economic research, *Manchester Metropolitan University, Centre for Policy Modelling Report No. 99–56*. <http://cfpm.org/cpmrep56.html>

Moss, S., 2002, Policy analysis from first principles, *Proceedings of the National Academy of Sciences*, **99**:7267–7274

Moss, S. and Edmonds, B., 2005, Towards good social science, *Journal of Artificial Societies and Social Simulation*, **8**(4):13. <http://jasss.soc.surrey.ac.uk/8/4/13.html>

Oreskes, N., Shrader-Frechette, K., and Belitz, K., 1994, Verification, validation and confirmation of numerical models in the earth sciences, *Science*, **263**(5147):641–646.

Parker, D. C., Manson, S. M., Janssen, M. A., Hoffmann, M. J., and Deadman, P., 2003, Multi-agent system models for the simulation of land-use and land-cover change: A review, *Annals of the Association of American Geographers*, **93**(2):314–337.

Persky, J., 1995, Retrospectives: The ethology of Homo economicus, *Journal of Economic Perspectives*, **9**(2):221–231.

Polhill, J. G. and Edmonds, B., 2007, Open access for social simulation, *Journal of Artificial Societies and Social Simulation*, **10**(3):10. <http://jasss.soc.surrey.ac.uk/10/3/10.html>

Polhill, J. G., Parker, D., Brown, D., and Grimm, V., 2008, Using the ODD protocol for describing three agent-based social simulation models of land-use change, *Journal of Artificial Societies and Social Simulation*, **11**(2):3. <http://jasss.soc.surrey.ac.uk/11/2/3.html>

Polhill, J. G., Pignotti, E., Gotts, N. M., Edwards, P., and Preece, A., 2007, A semantic grid service for experimentation with an agent-based model of land-use change, *Journal of Artificial Societies and Social Simulation*, **10**(2):2. <http://jasss.soc.surrey.ac.uk/10/2/2.html>

Rabin, M., 2002, A perspective on psychology and economics, *European Economic Review*, **46**:657–685.

Richiardi, M., Leombruni, R., Saam, N., and Sonnessa, M., 2006, A common protocol for agent-based social simulation, *Journal of Artificial Societies and Social Simulation*, **9**(1):15. <http://jasss.soc.surrey.ac.uk/9/1/15.html>

Vandermeulen, V. and Van Huylenbroeck, G., 2008, Designing trans-disciplinary research to support policy formulation for sustainable agricultural development, *Ecological Economics*, **67**(3):352–361.

Weisskopf, W. A., 1955, *The Psychology of Economics*. University of Chicago Press, Chicago, Illinois, USA.

Wilensky, U., 1999, NetLogo. <http://ccl.northwestern.edu/netlogo/>. Center for Connected Learning and Computer-Based Modeling, Northwestern University, Evanston, IL.

Will, O. and Hegselmann, R., 2008, A replication that failed: On the computational model in ‘Michael W. Macy and Yoshimichi Sato: Trust, cooperation and market formation in the U.S. and Japan. Proceedings of the National Academy of Sciences, May 2002’, *Journal of Artificial Societies and Social Simulation*, **11**(3):3. <http://jasss.soc.surrey.ac.uk/11/3/3.html>

Windrum, P., Fagiolo, G., and Moneta, A., 2007, Empirical validation of agent-based models: Alternatives and prospects, *Journal of Artificial Societies and Social Simulation*, **10**(2):8. <http://jasss.soc.surrey.ac.uk/10/2/8.html>

Zimmerer, K. S. and Bassett, T. J., 2003, Approaching political ecology: Society, nature, and scale in human-environment studies, in Zimmerer, K. S. and Bassett, T. J. (eds.) *Political Ecology: An Integrative Approach to Geography and Environment-Development Studies*. New York: Guilford Press, pp. 1–25.

THEME II. VERIFICATION OF MODELS

Interval analysis and verification of mathematical models

Tibor Csendes

Institute of Informatics, University of Szeged, Szeged, Hungary.

Abstract

This chapter provides an introduction to interval arithmetic-based techniques for the verification of mathematical models. Illustrative examples are described from the fields of circle packing, chaotic behaviour dynamical systems, and process network synthesis.

Keywords: model verification, interval methods, reliable numerical algorithm.

1. Interval arithmetic

Model verification, optimization, and especially global optimization are sensitive on the reliability of the numerical computations. There exist practical problems where good approximative solutions are more or less accepted as the true solutions. Still there remain important application fields where the guaranteed reliability of the provided solution is of ample importance. The uncertainties are mostly caused by the rounding errors. These are necessarily part of the calculations when the algorithms are coded with floating point arithmetic – which allows quick computation. To provide a remedy for these problems, we shall apply interval arithmetic based inclusion functions (Alefeld and Herzberger, 1983; Ratschek and Rokne, 1984). These offer a theoretically reliable and computationally tractable means of locating a feasible suboptimal interval.

Denote the real numbers by x, y, \dots , the set of compact intervals by $I := \{ [a, b] \mid a \leq b, a, b \in \mathbb{R} \}$, and the set of n -dimensional intervals (also called simply intervals or boxes) by I^n . Capital letters will be used for intervals. For real vectors and interval vectors the notations

$$x = (x_i), \quad x_i \in \mathbb{R}, \quad \text{and} \quad X = (X_i), \quad X_i \in I$$

are applied, respectively.

- **Definition 1.** A function $F: I^n$ to I is an *inclusion function* of the real function f if for all $Y \in I^n$ and for all $y \in Y$ $f(y) \in F(Y)$.

In other words, $f(Y)$ is a subset of (or equal to) $F(Y)$ where $f(Y)$ is the range of f over Y . We assume that f is continuous, then $f(Y)$ is an interval. The lower and upper bounds of an interval $Y \in I^n$ are denoted by $\min Y$ and $\max Y$, respectively, and the inclusion function of the gradient of $f(x)$ by $F'(X)$. The width of an interval is $w(Y) = \max Y - \min Y$, and $w(Y) = \max_i (\max Y_i - \min Y_i)$ if $Y \in I^n$ is an n -dimensional interval vector (also called a box). The midpoint of the interval X is defined by $m(X) = (\min X + \max X)/2$ if $X \in I$, and $m(X) = (m(X_i))$, if $X \in I^n$. $I(X)$ stands for all intervals in X . Three important possible properties of inclusion functions are:

- **Definition 2.** F is said to be an *isotone inclusion function* over X , which is a subset or equal to

R^n if for all $Y, Z \in I(X)$, Y is a subset or equal to Z implies $F(Y)$ is a subset or equal to $F(Z)$.

- **Definition 3.** We call the inclusion function F an α -convergent inclusion function over X if for all $Y \in I(X)$: $w(F(Y)) - w(f(Y)) \leq C w^\alpha(Y)$ holds, where α and C are positive constants.
- **Definition 4.** We say that the inclusion function F has the zero convergence property, if $w(F(Z_i)) \rightarrow 0$ holds for all the $\{Z_i\}$ interval sequences for which Z_i is a subset or equal to X for all $i=1,2,\dots$ and $w(Z_i) \rightarrow 0$.

An inclusion function obviously provides more information over an interval than could be conveyed with independent real function evaluations. The inclusion function gives upper and lower bounds on the objective function over the specified interval.

There are several ways to build an inclusion function (e.g., by using the Lipschitz constant, if it is known). Interval arithmetic (Alefeld and Herzberger, 1983; Hammer *et al.*, 1993; Hansen, 1992; Ratschek and Rokne, 1988) is a convenient tool for constructing the inclusion functions. This can be done for almost all functions that can be calculated by a finite algorithm (*i.e.*, not only for given expressions).

The idea of interval calculations is to extend the basic operations and the elementary functions from the real numbers to intervals. Finding the range for a function over an n -dimensional interval has in general the same complexity as an optimization problem, because we have to find the extreme values of the function over the interval. By using interval arithmetic it is possible to find bounds on the function values more efficiently. The interval operations can be carried out using only real operations. For the argument intervals $[a, b]$ and $[c, d]$ the following expressions hold:

$$\begin{aligned}
 [a, b] + [c, d] &= [a + c, b + d] \\
 [a, b] - [c, d] &= [a - d, b - c] \\
 [a, b] * [c, d] &= [\min\{ac, ad, bc, bd\}, \max\{ac, ad, bc, bd\}] \\
 [a, b] / [c, d] &= [a, b] * [1/d, 1/c] \quad \text{if } 0 \notin [c, d].
 \end{aligned}$$

As an example, consider the range of $x - x^2$: it is $[-2, 0.25]$ on the argument interval of $[0, 2]$. In contrast to that, the above interval arithmetic will provide the inclusion of $[-4, 2]$, which is much wider. This too conservative estimation can be improved at the cost of more computation with sophisticated numerical techniques.

If outwardly-directed rounding is also applied, then the interval calculated by a computer contains every real number that can be a result of the given function on real numbers inside the original intervals. The technique of producing an inclusion function by replacing the real variables and operations by their interval equivalent is called *natural interval extension* (Alefeld and Herzberger, 1983; Ratschek and Rokne, 1984).

Natural interval extension provides an isotone inclusion function, that is α -convergent with $\alpha = 1$, and hence it has also the zero convergence property. More sophisticated inclusion functions, such as the centered forms provide quadratic convergence as interval width approaches zero to tight bounds, but they are not necessarily isotone inclusion functions. The computational cost of the inclusions for higher derivatives, Taylor models, or slopes is certainly high, but this can pay off when solving difficult optimization problems. In the present work we apply natural interval extension, and inclusions of the gradient and the Hessian for the monotonicity and concavity tests, and also within the interval Newton step.

Applying automatic differentiation or differentiation arithmetic in connection with interval arithmetic (Hammer *et al.*, 1993), we are also able to compute the inclusion function for the gradient. Automatic differentiation combines the advantages of symbolic and numerical differentiation and handles numbers instead of symbolic formulas. The computation of the gradient is done automatically together with the computation of the function value. The main advantage of this process is that only the algorithm or formula for the function is required. No explicit formulas for the gradient are needed.

Many programming languages are now available that support interval datatypes and automatic differentiation with the corresponding operations and intrinsic functions (Bleher *et al.*, 1987; Jüllig, 1992; Klatte *et al.*, 1992, 1993). Matlab also has an interval extension package called Intlab (Rump, 1999). These programming environments provide a convenient access to inclusion functions (with automatic outward rounding), but one can also simulate interval operations and functions by subroutines in any algorithmic language. We used the natural interval extension to calculate the inclusion functions. For more information about inclusion functions and interval arithmetic, see (Alefeld and Herzberger, 1983; Ratschek and Rokne, 1984).

An often heard question is, how can we characterize the maximal size or difficulty of problems that still can be solved by interval inclusion function based methods. The short answer is that the dimension of a problem is a wrong measure, since low dimensional problems can be hopeless, and larger dimensional ones can be solved in a short time. For interval techniques the most dangerous is the large excess width, a bad estimation of the range of the related function on the studied intervals. It is most affected by the dependency problem, that is caused by multiple appearances of the same variable in a complex expression. According to this, the rule of thumb says that in case all involved variables appear only a few times in the expression of the objective and constraint functions, then the overestimation will be small, and the optimization algorithms can be successful even for larger dimensional problems (the number of variables can be up to 100).

A telling example for the capabilities of interval optimization methods is the results on circle packing problems (Figure 1). Markót (2004) and Markót and Csendes (2005) were able to solve the problem cases of $n = 28, 29$, and 30 , *i.e.*, to find the configuration of n congruent non-overlapping maximal circles fitting into the unit square. These problems were held before as hopeless, since the expected CPU time necessary for their solutions with the last available techniques were estimated to be around decades. The problems have 56, 58, and 60 variables, respectively, and hundreds of nonlinear constraints. The difficulty of the problems is highlighted by the facts that (due to obvious geometrical reasons) there are an astronomical number of equivalent, symmetric optimal solutions, and in the cases of $n = 28, 29$ there exist positive measure sets of global optimizer points.

Standard interval optimization algorithms could not solve the problems. A careful problem decomposition, and custom made built in acceleration devices based on the understanding of the problem structure enabled the successful solution. The running times were below 3 days, and ca. one million subintervals were stored during the solution process. The uncertainty in the position of the circles has been decreased by more than 700 orders of magnitude in each case. Due to the controlled outward rounding mode applied, the obtained results are reliable even in the sense of a rigorous mathematical theorem.

To demonstrate the capabilities of interval based computational methods, the following sections discuss example application in the fields of tolerance optimization and chaos verification for dynamic systems.

2. Tolerances in optimization and constraint satisfaction

Consider the nonlinear optimization problem (P)

$$\begin{aligned} & \text{minimize } f(x) \\ & \text{subject to } g_j(x) \leq 0 \quad j=1, 2, \dots, m, \end{aligned}$$

where $f: \mathbb{R}^n \rightarrow \mathbb{R}$ and the constraint functions $g_j(x): \mathbb{R}^n \rightarrow \mathbb{R}$ are continuous nonlinear functions, and n is the dimension of the problem. Let us denote the set

of feasible points by A , that is $A := \{x \in \mathbb{R}^n: g_j(x) \leq 0 \text{ for each } j = 1, 2, \dots, m\}$. Also let x^* be an optimal solution for problem (P) . Notice that we restrict now our investigations to continuous functions.

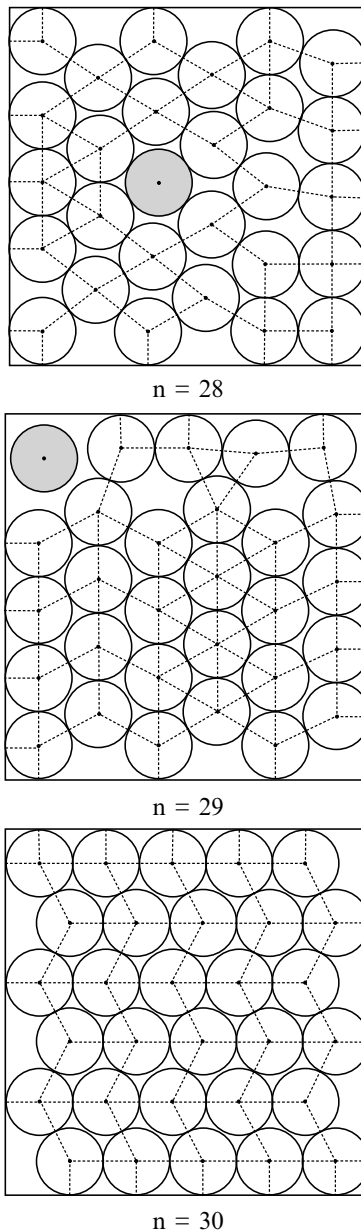


Fig. 1. The proven optimal circle packings into the unit square for 28, 29, and 30 circles.

It may happen that the optimal solution x^* , or an approximation of it, is known, yet this result is not suitable for practical use. For example, consider an engineering design problem which is formulated as a constrained global optimization problem, see for example those studied in Kovács *et al.* (1993) and Zabinsky *et al.*, (1992). It is possible that the optimal design cannot be reproduced exactly with current manufacturing processes, thus each variable has a specific manufacturing tolerance, $\delta > 0$.

Since the optimal solution x^* may be on one or more active constraints, then the n -dimensional interval $[x^*_{-i} - \delta, x^*_{-i} + \delta]$ for $i = 1, 2, \dots, n$ is not feasible. From a practical point of view, it is preferable to find a feasible suboptimal box instead of a single optimal point. Thus we seek a feasible n -dimensional interval X^* for which $g_j(x) \leq 0$, $j = 1, 2, \dots, m$, for all $x \in X^*$. It is also desirable to have this feasible box as close to the optimum as possible. Thus we also impose the constraint $f(x) \leq f(x^*) + \varepsilon$ for some $\varepsilon > 0$ for all $x \in X^*$. Such an interval would also reflect the sensitivity of the objective function (Fiacco, 1976) because the size of the feasible box may vary as ε varies.

We restate our problem: find an n -dimensional interval X^* such that for all $x \in X^*$

$$f(x) \leq f_\varepsilon = f(x^*) + \varepsilon, \text{ and} \quad (1)$$

$$g_j(x) \leq 0 \text{ for } j = 1, 2, \dots, m \quad (2)$$

Methods discussed in earlier papers (Csendes, 1989, 1990; Csendes and Pintér, 1993) study similar problems. In Csendes (1989, 1990), an interval method was introduced to find a bounding interval of the level set of an unconstrained nonlinear optimization problem. The algorithm converges to the smallest n -dimensional interval containing the specified level set. Another technique (Csendes and Pintér, 1993) locates the boundary of a level set in a given direction. Kearfott discussed an interval branch and bound method for bound constrained global optimization (Kearfott, 1992). In Ratschek and Rokne (1993), the solution of a difficult nonlinear optimization problem (in an alternate form) was reported by using a customized interval subdivision scheme. These methods provide a guaranteed reliable solution, although they are computationally tractable (Csendes, 1998). They are based on inclusion functions and interval arithmetic, which was briefly reviewed in the previous section.

2.1. The algorithm and its convergence

The suggested algorithm iteratively grows a box about a given seed point. A seed point x^{seed} , which lies interior to the region of feasibility and in the ε -level set must be provided to start the algorithm. Thus the seed point, x^{seed} , must satisfy the following conditions:

$$f(x^{seed}) < f_c \quad \text{and} \quad (3)$$

$$g_j(x^{seed}) < 0 \text{ for each } j = 1, 2, \dots, m \quad (4)$$

This will imply that there exists a feasible box with a positive volume containing the seed point. It is possible to construct nonlinear optimization problems for which no proper seed point exists which would satisfy the conditions (3) and (4) of our restated problem. In such cases the search for feasible suboptimal boxes makes no sense.

Seed points can be obtained in several ways. One is to find an approximation of x^* , and if it is interior to the feasible region, use it as x^{seed} . If it lies on an active constraint, search along the normal of the active constraint to generate x^{seed} . Another way is to sample randomly (a normal distribution may be appropriate) around the optimal point until a feasible interior point is found. This may also be used as x^{seed} . A slight variation would be to sample according to a uniform distribution in the interval hull of the feasible region intersected with the ε -level set. The first feasible point with objective function value less than f_c would then be used as x^{seed} .

We will call an interval X a *feasible interval around x^{seed}* , if $x^{seed} \in X$ and the equations (1) and (2) earlier in this section are satisfied for all $x \in X$. An interval will be called maximal regarding x^{seed} , if it is a feasible interval around x^{seed} , and there is no other feasible interval that contains it. Note that there may exist many maximal feasible boxes around a seed point. Also note that two different seed points may be contained in the same maximal feasible box.

It may appear disturbing that there is no one-to-one relationship between x^{seed} and a maximal feasible box around x^{seed} . For an example, suppose the set of feasible points with objective function values less than or equal to f_c is an ellipse. Suppose x^{seed} is interior to the ellipse. Then there is an infinite number of feasible boxes around x^{seed} which do not contain one another (see Figure 2). At some point, it

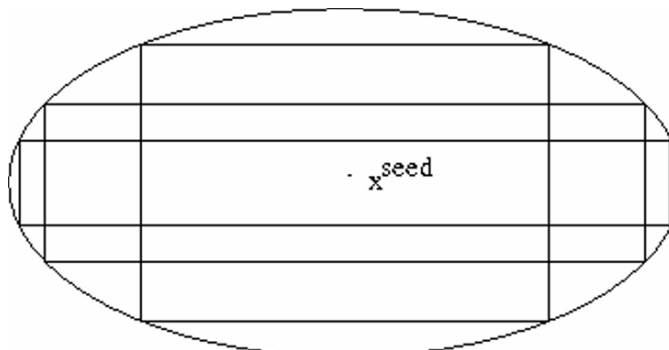


Fig. 2. Illustration of multiple maximal feasible boxes within the ε -level set (without constraints).

may be interesting to find the maximal feasible box around x^{seed} that has the largest volume. However at this point the algorithm does not find the largest volume box around a seed point, but simply a maximal feasible box. In our application to manufacturing tolerances this is not a disadvantage. It is more desirable to compare trade-offs between coordinate lengths of various maximal boxes, than it is to know the box with largest volume, as this has no direct meaning for the application.

We call an interval Y *strongly feasible*, if $f(y) < f_e$, and $g_j(y) < 0$ for all $y \in Y$ ($j = 1, 2, \dots, m$).

The Main algorithm is presented below. This uses parameters $d(i,1)$ and $d(i,2)$ for $i = 1, 2, \dots, n$ and η , which are set at the beginning to positive reals. To start, $d(i,1)$ and $d(i,2)$ must be larger than η . The stopping criterion indicates that the algorithm should stop increasing the size of the actual box X , when the change along each coordinate is less than the threshold $\eta \in$ all directions.

Main algorithm

1. Initialize interval vector $X_i = [x_{i,1}^{seed}, x_{i,2}^{seed}]$, and $d(i,j) \geq \eta > 0$ for all $i = 1, 2, \dots, n$ and $j = 1, 2$.
2. For $I = 1$ to n do:
3. Set $Y_j = X_j$ for $j = 1, 2, \dots, n; j \neq i$, and $Y_i = [\min X_i - d(i,1), \min X_i]$.
4. Use the checking routine to check whether $f(y) < f_e$ and $g_j(y) < 0$ ($j = 1, 2, \dots, m$) for each $y \in Y$. If the answer is yes, then set $X = X \cup Y$. Otherwise $d(i,1) = (\min X_i - \max Z_i)/2$, where Z is the interval passed back by the checking routine as not strongly feasible.
5. Set $Y_j = X_j$ for $j = 1, 2, \dots, n; j \neq i$, and $Y_i = [\max X_i, \max X_i + d(i,2)]$.
6. Use the checking routine to check whether $f(y) < f_e$ and $g_j(y) < 0$ ($j = 1, 2, \dots, m$) for each $y \in Y$. If the answer is yes, then set $X = X \cup Y$. Otherwise $d(i,2) = (\min Z_i - \max X_i)/2$, where Z is the interval passed back by the checking routine as not strongly feasible.
7. End of i-loop
8. Stopping criterion: if the number of inclusion function calls is less than 100,000, and there is an $i = 1, 2, \dots, n$ such that either $d(i,1) \geq \eta$ or $d(i,2) \geq \eta$ then go to Step 1.
9. Print X , and STOP.

The core of the algorithm is the checking procedure called in Steps 3 and 5 of the Main algorithm. This is a version of the interval subdivision method modified to check whether the actual box Y lies entirely in the region satisfying equations (1) and (2). The parameter θ is set to a small positive real value. It is better when the relation $d(i,j) \geq \theta$ holds (else the interval Y can be quickly rejected in Step 1 of the Checking routine. The checking procedure is defined in detail below.

Checking routine

1. Initialize the list L to be empty.
2. If the width of Y is less than θ , then go to Step 7.
3. Evaluate the inclusion functions $F(Y)$ and $G_j(Y)$ for each $j = 1, 2, \dots, m$.

4. If $\max F(Y) \geq f_\epsilon$ or $\max G_j(Y) \geq 0$ for any $j = 1, 2, \dots, m$, then go to Step 5.
5. If the list L is empty, then go to Step 6, else put the last item of the list L into Y, delete this item from the list, and go to Step 1.
6. Subdivide Y into subintervals U and V, set $Y = U$, put V into the list L as the last member, and go to Step 1. The subdivision should be made, such that the largest side of Y is halved.
7. RETURN that the checked interval was strongly feasible.
8. RETURN $Z = Y$, and the message that it could not be proved that the checked interval is strongly feasible.

If the checking routine indicates, that the checked interval is not strongly feasible, this means more precisely that a very small not strongly feasible subinterval was found. By properly setting θ , the place where the strong feasibility is violated can be located.

2.2. Convergence results

In this subsection the convergence properties of the algorithm introduced are characterized to provide theoretical background for the numerical implementations. The proofs of the statements can be found in Csendes *et al.* (1995) and Csendes (2007). First the checking routine is studied.

- **Lemma 1.**

1. If the checking routine accepts an interval Y as strongly feasible, then $f(x) < f_\epsilon$, and $g_j(x) < 0$ for each $x \in Y$, and $j = 1, 2, \dots, m$.
2. If the checking routine rejects an interval Y as not strongly feasible, then there exists a nested set of intervals, $Y = Y^1$ that contains Y^2 etc. generated by the routine, with the smallest interval having width less than θ , such that for each Y^i in the nested set of intervals one of the conditions $\max F(Y^i) < f_\epsilon$ or $\max G_j(Y^i) < 0$ was violated, where $i = 1, 2, \dots, p$ and $j = 1, 2, \dots, m$.

Only the inclusion property of F and G_j was utilized in the proof of Lemma 1, and no further requirement (like isotonicity or convergence order of the inclusion functions involved) was necessary.

- **Lemma 2.** Assume that

$$w(F(X)) \rightarrow 0 \text{ as } w(X) \rightarrow 0, \text{ and} \quad (5)$$

$$w(G_j(X)) \rightarrow 0 \text{ as } w(X) \rightarrow 0 \quad (6)$$

for all $j = 1, 2, \dots, m$, i.e., F and G_j are zero convergent. Then

1. If $f(x) < f_\epsilon$ and $g_j(x) < 0$ for every $x \in Y$ and $j = 1, 2, \dots, m$, then there exists a threshold value $\theta^T > 0$ such that for all $\theta: 0 < \theta < \theta^T$ the checking routine stops after a finite number of iteration steps and it states that Y is strongly feasible.
2. If $\theta > 0$ and there is a point $x \in Y$ such that $f(x) \geq f_\epsilon$ or $g_j(x) \geq 0$ for any $j = 1, 2, \dots, m$, then the checking routine will stop after a finite number of iteration steps and it states that Y is not strongly feasible.

Notice that Lemma 2 ensures that a not strongly feasible interval Y will always be detected in a finite number of steps. However, it is possible that a strongly feasible interval will be mistaken as not strongly feasible if θ is too large. Thus it is important that θ be chosen with care.

Consider, again, a fixed constrained nonlinear optimization problem (P) as given at the beginning of the present section. Denote the result box calculated with the algorithm parameters θ and $\dot{\eta}$ by $X_{\theta, \dot{\eta}}^*$, and the level set belonging to the function value f_ϵ by Sf_ϵ . Denote the vector of the G_j functions by G . The following theorems characterize the convergence properties of our main algorithm for the obvious case when the stopping criterion for the number of function calls is deleted.

- **Theorem 1.** If the set $Sf_\epsilon \cap A$ is bounded, the seed point x^{seed} fulfills the conditions (3) and (4), and the properties (5) and (6) hold for the inclusion functions $F(X)$ and $G(X)$, then there exist suitable $d(i, j) > 0$ ($i = 1, 2, \dots, n$; $j = 1, 2$) values and threshold values $\theta^T > 0$ and $\dot{\eta}^T > 0$ such that for all $\theta: 0 < \theta < \theta^T$ and $\dot{\eta}: 0 < \dot{\eta} < \dot{\eta}^T$.
 1. The algorithm stops after a finite number of steps.
 2. The result box $X_{\theta, \dot{\eta}}^*$ has a positive measure.
 3. The result interval $X_{\theta, \dot{\eta}}^*$ is strongly feasible, $X_{\theta, \dot{\eta}}^*$ is a subset of $Sf_\epsilon \cap A$.

The strong feasibility of the accepted intervals was utilized only in proving the positive volume of the result intervals. With the exception of this, the convergence results remain valid if the checking routine accepts feasible intervals.

Theorem 2 describes the limit of the result boxes when the algorithm parameters θ and $\dot{\eta}$ are equal and converge together to zero.

- **Theorem 2.** Let the $d(i, j)$ positive values be fixed. If the conditions of Theorem 1 are fulfilled, then each accumulation interval X^* of the interval sequence $\{X_{\theta, \dot{\eta}}^*\}$ when $\lim \theta \rightarrow 0$ is maximal in the sense that for every box X' the relations X^* is a subset or equal to X' and X' is a subset or equal to $Sf_\epsilon \cap A$ imply $X' = X^*$.

The limiting interval X^* is not necessarily strongly feasible. For example, if $Sf_\epsilon \cap A$ is an n -dimensional interval, then this not strongly feasible interval may be a limiting interval of a sequence of strongly feasible result intervals.

Theorem 1 suggests that for a problem satisfying its conditions, sufficiently small positive θ and $\dot{\eta}$ values ensure a positive measure result interval in a finite number of iteration steps, *i.e.*, after a finite number of objective and constraint function calls. Theorem 2 gives the basis that with θ and $\dot{\eta}$ values close to the

machine precision one may obtain a closely maximal result box. It has to be stressed that beyond the given algorithm many others can be given for the same problem, and that it is a very difficult problem to find a maximal volume feasible interval (equivalent to a global optimization problem cf. Csendes (1990)). In general, the location of a maximal volume feasible interval can only be solved with a certain kind of backtracking.

2.3. Numerical testing and examples

Consider the following simple constrained quadratic problem to illustrate how the algorithm discussed above proceeds. Let

$$\begin{aligned} f(x) &= x_1^2 + x_2^2, \\ g_1(x) &= (3 - x_1)^2 + (3 - x_2)^2 - 18, \text{ and} \\ g_2(x) &= 1 - (2 - x_1)^2 - (2 - x_2)^2. \end{aligned}$$

The set of feasible points A is now the circle C_1 with center at $(3, 3)$ and with a radius of $3\sqrt{2}$ with the exceptions of the points of the circle C_2 with center $(2, 2)$, and radius 1. The only global optimal point is at the origin, and the optimal function value is $f^* = f(0,0) = 0$. The level sets S_{f_ϵ} are circles around the origin with radii of $\sqrt{f_\epsilon}$, respectively. The constraint $g_1(x) \leq 0$ is active at the global minimum, and its normal is parallel to the line $x_1 = x_2$. The problem is illustrated on Figure 3.

The inclusion functions are generated by natural interval extension:

$$\begin{aligned} F(X) &= X_1^2 + X_2^2, \\ G_1(X) &= (3 - X_1)^2 + (3 - X_2)^2 - 18, \text{ and} \\ G_2(X) &= 1 - (2 - X_1)^2 - (2 - X_2)^2. \end{aligned}$$

The capital letters denote again intervals with the subscript indicating coordinate direction. These inclusion functions are exact in the sense that the so-called *excess width* (defined by $w(F(X)) - w(f(X))$) is zero for every argument interval. It is unfortunately not typical for interval calculations, yet it makes the demonstration of the working of the algorithm more transparent.

Assuming exact arithmetic

Set the seed point to $x^{\text{seed}} = (0.5, 0.5)^T$. The conditions (3) and (4) are now fulfilled for each $f_\epsilon > 0.5$:

$$\begin{aligned} g_1(x^{\text{seed}}) &= -5.5 < 0, \\ g_2(x^{\text{seed}}) &= -3.5 < 0, \\ f(x^{\text{seed}}) &= 0.5 < f_\epsilon. \end{aligned}$$

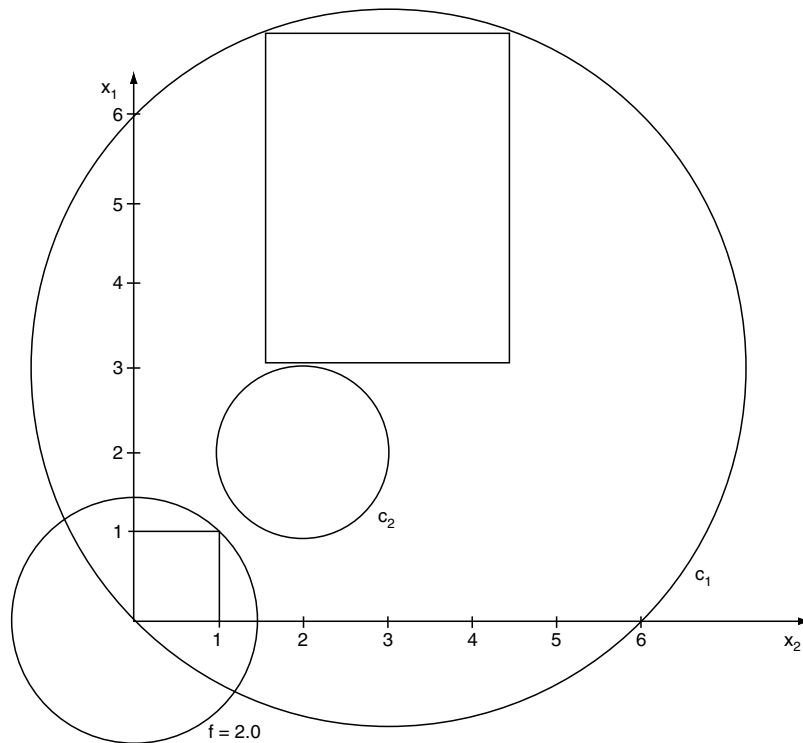


Fig. 3. Test problem and result intervals of the first and last lines of Table 1.

Choose the algorithm parameters $d(i,1) = d(i,2) = 0.1$ for $i = 1, 2$ and $\dot{\eta} = 0.01$. For $f_\epsilon = 2.0$ the intersection set of feasible points and the level set Sf_ϵ is the intersection of the circles with centres $(0, 0)$ and $(3, 3)$, and with radii $\sqrt{2}$ and $3\sqrt{2}$, respectively. It is a convex set, and the maximal volume inscribed box is $X_1^* = [0.0, 1.0]$, $X_2^* = [0.0, 1.0]$.

The starting interval is set to $X_1 = [0.5, 0.5]$ and $X_2 = [0.5, 0.5]$. The first check is made on the interval $Y_1 = [0.4, 0.5]$, $Y_2 = [0.5, 0.5]$. The corresponding inclusion function values are

$$\begin{aligned} F(Y) &= [0.4, 0.5]^2 + [0.5, 0.5]^2 = [0.16, 0.25] + [0.25, 0.25] = [0.41, 0.5], \\ G_1(Y) &= [6.25, 6.76] + [6.25, 6.25] - 18 = [-5.5, -4.99], \text{ and} \\ G_2(Y) &= 1 - [2.25, 2.56] - [2.25, 2.25] = [-3.81, -3.5]. \end{aligned}$$

The checking routine returns thus that Y is strongly feasible, and X is set in Step 3 of the main algorithm to $([0.4, 0.5], [0.5, 0.5])^\top$.

Table 1. The role of the seed point in locating maximal feasible boxes.

x^{seed}	X^{res}	vol. (X^{res})	NFE
$(0.50, 0.50)^T$	$([-0.000028, 1.046680], [0.000098, 0.951000])^T$	0.99532	1822
$(0.10, 0.10)^T$	$([-0.000056, 1.000066], [0.000069, 0.999902])^T$	0.99996	1945
$(0.01, 0.01)^T$	$([-0.003131, 1.034968], [0.003153, 0.963763])^T$	0.99721	2065
$(0.90, 0.90)^T$	$([-0.000028, 1.000160], [0.000098, 0.999805])^T$	0.99989	2118
$(0.10, 0.90)^T$	$([-0.400226, 0.556738], [0.462630, 1.300000])^T$	0.80133	1610
$(0.00, 1.00)^T$	$([-0.425529, 0.522607], [0.496856, 1.314084])^T$	0.77484	1669
$(-0.01, 0.10)^T$	$([-0.072507, 0.990052], [0.074328, 1.009826])^T$	0.99402	1996
$(4.0, 4.0)^T$	$([2.662546, 6.048340], [2.749031, 5.9508304])^T$	10.841	3015
$(5.0, 5.0)^T$	$([2.600000, 6.048340], [2.800000, 5.9508246])^T$	10.865	2677
$(3.0, 6.0)^T$	$([1.732192, 4.267773], [3.000000, 7.0487793])^T$	10.266	2801

The next check is then made in Step 5 on the interval $Y_1 = [0.5, 0.6]$, $Y_2 = [0.5, 0.5]$. The corresponding inclusion function values are $F(Y) = [0.5, 0.61]$, $G_1(Y) = [-5.99, -5.5]$ and $G_2(Y) = [-3.5, -3.21]$. The actual interval is then updated to $X_1 = [0.4, 0.6]$, $X_2 = [0.5, 0.5]$.

The actual interval is modified for $i = 2$ to $([0.4, 0.6], [0.4, 0.5])^T$, and then to $([0.4, 0.6], [0.4, 0.6])^T$. The sequence of subsequent actual intervals is as follows:

$$\begin{aligned} X &= ([0.3, 0.7], [0.3, 0.7])^T, \\ X &= ([0.2, 0.8], [0.2, 0.8])^T, \\ X &= ([0.1, 0.9], [0.1, 0.9])^T. \end{aligned}$$

The final interval X was obtained after 48 inclusion function evaluations. The calculation of inclusion functions involves on the average ca. two times more computation than the corresponding real functions do. Until this point was reached, the checking routine accepted all the extension intervals Y immediately, without subdivision. Thus the value of the algorithm parameter θ had no effect on this part of the result. In the next iteration the checked intervals and the inclusion function values $F(Y)$ are as follows:

$$\begin{aligned}
 Y &= ([0.0, 0.1], [0.1, 0.9])^T, \text{ and } F(Y) = [0.01, 0.82], \\
 Y &= ([0.9, 1.0], [0.1, 0.9])^T, \text{ and } F(Y) = [0.82, 1.81], \\
 Y &= ([0.0, 1.0], [0.0, 0.1])^T, \text{ and } F(Y) = [0.00, 1.01], \\
 Y &= ([0.0, 1.0], [0.9, 1.0])^T, \text{ and } F(Y) = [0.81, 2.00].
 \end{aligned}$$

The last interval is not strongly feasible, and a new $d(2,2) < 0.05$ is determined (depending on the value of θ). And in this way the next $X = ([0.0, 1.0], [0.0, 0.9])^T$.

With further calculations this actual interval may be refined to obtain a maximal box X^* . We have a computational proof that each point x of the result interval is feasible, and $f(x) < f_c$.

Computer implementation with outward rounding

The main difference between the results of the last subsection and those obtained by the computer program is that the latter is produced by operations with outward rounding. For example, $Y = ([0.0, 1.0], [0.9, 1.0])^T$ would be found feasible (but not strongly feasible) calculating with exact arithmetic (since then $\max F(Y) = 2.0$), while $\max F(Y) > 2.0$ if it is evaluated with outward rounding. This is the reason why the results in the first line of Table 1 may be slightly different from those discussed in the earlier subsection. It is worth mentioning that if the stopping condition would be based on the difference $(\min X_i - d(i,1)) - \min X_i$ then this value could also attain zero because of the computer representation of floating point numbers.

Table 1 contains details of the results on the numerical test that examines how the place of the seed point affects the result box constructed by the program. In the following, we use only one initial value for all $d(i,j)$ step sizes ($i = 1, 2$; $j = 1, 2$). All of the problem and algorithm parameters were constant during this test ($d(i,j) = 0.1$ for $i = 1, 2$ and $j = 1, 2$, $\dot{\eta} = 0.0001$ and $\theta = 0.0001$), only x^{seed} and f_c was changed. The latter was 2.0 for the first 7 lines and 72.0 for the last three. For the problem specified by $f_c = 2.0$, the maximal volume feasible box is $X^* = [0.0, 1.0]^2$. The result interval calculated by the program is denoted by X^{res} , and $\text{vol}(X^{\text{res}})$ is its volume. The latter is found close to one (it is, of course, not greater than $\text{vol}(X^*) = 1$). NFE stands for the number of function ($F(X)$ and $G_j(X)$ for $j = 1, 2, \dots, m$) evaluations.

The test results presented in Table 1 suggest that the seed point may be chosen close to the normal of the active constraint at x^* , even if it is outside of X^* . It is interesting that the center of the maximal volume inscribed box is not an optimal seed point. It is also worth mentioning that in the first 7 lines (where $S_{f_c} \cap A$ is symmetric for the $x_1 = x_2$ line) the first component of the result interval is always wider than the second one. The explanation for it is that the actual interval is always enlarged first along the first coordinate direction. Two result boxes are shown on Figure 4 together with the constraint functions and a corresponding levels.

The presented algorithm was also applied to a practical engineering design problem to construct manufacturing tolerances for an optimal design of composite materials (Zabinsky *et al.*, 1992) that motivated our study. The numerical experiences

on this composite laminate design problem are reported in the papers (Kristinsdottir *et al.*, 1993, 1996). The methodology was also applied in civil engineering, for providing optimal designs with manufacturing tolerances for building and construction problems (Csallner *et al.*, 2004). All these computational studies confirmed that the suggested algorithm is capable to provide applicable size suboptimal feasible tolerance intervals for a wide set of problems using an acceptable amount of computation.

In addition to our above mentioned applications, the related papers (Csendes *et al.*, 1995; Kristinsdottir *et al.*, 1993, 1996) were cited by several scientific publications reporting on the successful use of the introduced algorithms in several diverse application fields. The tolerance optimization approach was also used to describe the set of Hénon mapping parameters that allow chaotic behaviour (Bánhegyi *et al.*, 2007; Csendes *et al.*, 2006).

3. Chaos verification in mathematical models of dynamical systems

The last section is devoted to an optimization model and to the related algorithms to locate chaotic regions of dynamic systems (Csendes *et al.*, 2006). Computer-assisted proofs for the existence of chaos are important for the understanding of dynamic properties of the solutions of differential equations. These techniques have been intensively investigated recently (see *e.g.*, Galias and Zgliczynski, 2001; Neumaier and Rage, 1993; Rage *et al.*, 1994; Zgliczynski, 1997, 2003).

We study verified computational methods to check and locate regions the points of which fulfill the conditions of chaotic behaviour. The investigated Hénon mapping is $H(x,y) = (1 + y - Ax^2, Bx)$. Zgliczynski (1997) considered the $A = 1.4$ and $B = 0.3$ values and some regions of the two dimensional Euclidean space: $E = E_1 \cup E_2 = \{(x, y) \mid x \geq 0.4, y \geq 0.28\} \cup \{(x, y) \mid x \leq 0.64, |y| \leq 0.01\}$, $O_1 = \{(x, y) \mid x < 0.4, y > 0.01\}$, $O_2 = \{(x, y) \mid y < 0\}$.

According to Zgliczynski (1997), Theorem 3 below ensures the chaotic behaviour for the points of the parallelograms Q_0 and Q_1 with parallel sides with the x axis (for $y_0 = 0.01$ and $y_1 = 0.28$, respectively), with the common tangent of 2, and x coordinates of the lower vertices are $x_a = 0.460$, $x_b = 0.556$; and $x_c = 0.558$, $x_d = 0.620$, respectively. The mapping and the problem details (such as the transformed sides of the parallelograms, $H^7(a)$, $H^7(b)$, $H^7(c)$, and $H^7(d)$) are illustrated on Figure 4.

- **Theorem 3.** Assume that the following relations hold for the given particular Hénon mapping:

$$\begin{aligned} H^7(a \cup d) &\text{ is a subset of } O_2, \\ H^7(b \cup c) &\text{ is a subset of } O_1, \\ H^7(Q_0 \cup Q_1) &\text{ is a subset of } \mathbb{R}^2 \setminus E, \end{aligned}$$

then chaotic trajectories belong to the starting points of the regions Q_0 and Q_1 .

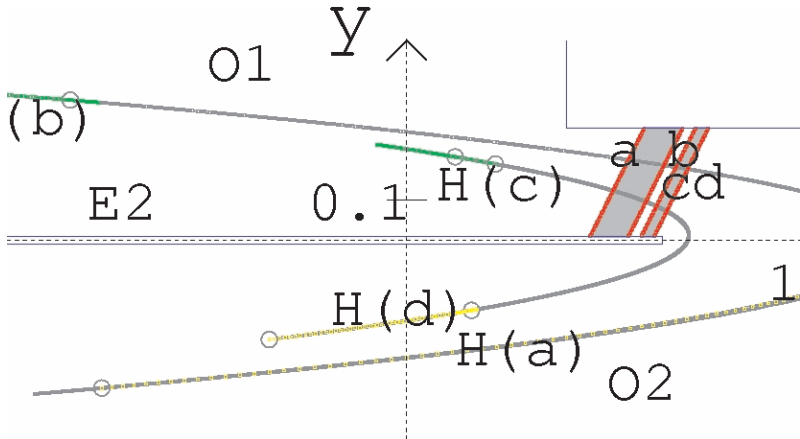


Fig. 4. Illustration of the H^7 transformation for the classic Hénon parameters $A = 1.4$ and $B = 0.3$ together with the chaotic region of two parallelograms. The a, b, c, and d sides of the parallelograms are depicted on the upper left picture of Figure 5.

The present section provides a method to verify chaos for certain mappings and regions. We discuss first how to check the set theoretical conditions of the above theorem in a reliable way by computer programs. Then we introduce optimization problems that provide a model to locate chaotic regions. We check the correctness of the earlier published chaotic region, the correctness of the underlying checking algorithms, and prove the optimization model. We also give new chaotic places located by the new technique. The articles by Bánhegyi *et al.* (2007) and Csendes *et al.* (2007) provide additional new chaotic regions located by the present method.

The main difficulty of checking the above conditions is that one has to prove these for a continuum of points. In Zgliczynski (1997), the author calculated the Lipschitz constant, gave an upper bound for the rounding error committed and thus reduced the whole task to investigating a finite number of points of a dense enough grid. This method works only with human interaction. To search chaotic regions an automated checking routine is more appropriate. The technique we applied combines interval arithmetic and adaptive branch-and-bound subdivision of the region of interest. It is basically a customized version of the technique introduced in section 2.

This algorithm first encloses the sets Q_0 and Q_1 in a 2-dimensional closed interval I , the starting interval. Then to prove subset relations an adaptive branch-and-bound technique generates such a subdivision of the starting interval that either:

- For all subintervals the given conditions of chaos hold – in case they contain points of the respective sets.
- It is shown that a small subinterval (of a user set size) exists that contains at least one point of the respective set, and it contradicts at least one of the relations.

Now the sets O_1 , O_2 , and $R^2 \setminus E$ in the conditions in Theorem 3 are all open sets, and the union of a finite number of closed sets is closed. It is why the algorithm should check whether the transformed subintervals are subsets of the respective sets.

Our algorithm is capable of recognizing that a region satisfies the conditions of chaos. We have proven the correctness of the procedure in Csendes *et al.* (2006).

3.1. *Global optimization model for locating chaotic regions*

Once we have a reliable computer procedure to check the conditions of chaotic behavior of a mapping it is straightforward to set up an optimization model that transforms the original chaos location problem to a global optimization problem.

The chaotic regions have several parameters that identify them. In the early phase of our investigation, where we have restricted the search to locate two parallelograms similar to that used in Zgliczynski (1997), we are allowed to change the vertical and horizontal positions and also the common tangent, but the parallelograms always had two sides parallel to the x axis. It is also possible to find fitting parameter values for the Hénon mapping, *i.e.*, for the mapping parameters A and B, and furthermore also for parameters of the aimed sets of the underlying theorem, *e.g.*, the border coordinates of the set E.

The search for a chaotic region was modeled as a constrained global optimization problem, subsequently the constraints were represented by a penalty function approach. The original objective function was constant, still the possibility exists to extend it to a more complex form that expresses further aims, *e.g.*, to locate a second chaotic region, different from the known one.

The key question for the successful application of a global optimization algorithm is how to compose the penalty functions. On the basis of earlier experiences collected solving similar constrained problems, we have decided to add a non-negative value proportional to how much the given condition was violated, plus a fixed penalty term in case at least one of the constraints was not satisfied.

As an example, consider the case when one of the conditions for the transformed region was hurt, *e.g.*, when the last condition of Theorem 3, *i.e.*, the relation $H^k(b \cup c)$ is a subset of O_1 does not hold for a given k-th iterate, and for a region of two parallelograms. For such a case the checking routine will provide a subinterval I that contains at least one point of the investigated region, and which contradicts the given condition. Then we have calculated the Hausdorff distance of the transformed subinterval $H^k(I)$ to the set O_1 of the right side of the condition,

$$\max \{z \in H^k(I)\} \inf_{y \in O_1} d(z, y)$$

where $d(z, y)$ is a given metric, a distance between two two-dimensional points.

Notice that the use of maximum in the expression is crucial, with minimization instead our optimization approach could provide (and has provided) result regions that do not fulfill the given conditions of chaotic behaviour. On the other hand, the minimal distance according to points of the aimed set (this time O_1) is satisfactory, since it enables the technique to push the search into proper directions. In cases when the checking routine answered that the investigated subinterval has fulfilled the given condition, we have not changed the objective function.

Summing it up, we have considered the following bound constrained problem for the T inclusion function of the mapping T:

$$\min_{x \text{ in } X} g(x)$$

where

$$g(x) = f(x) + p(\sum_{i=1}^m \max\{z \in T(I(x))\} \inf_{y \text{ in } S_i} d(z, y)),$$

X is the n-dimensional interval of admissible values for the parameters x to be optimized, $f(x)$ is the original, nonnegative objective function, and $p(y) = y + C$ if y is positive, and $p(y) = 0$ otherwise. C is a positive constant, larger than $f(x)$ for all the feasible x points, m is the number of conditions to be fulfilled, and S_i is the aimed set for the i -th condition. In this discussion $I(x)$ is the subinterval returned by the checking routine (or the empty set). The interval $I(x)$ depends implicitly on the parameter x to be optimized.

For more complicated cases the fixed sets given in Theorem 3 should also be changed subject to certain structural constraints, e.g., the x_a , x_b , x_c , and x_d coordinates of the parallelograms have to follow this order. These new conditions can also be represented in a similar way, following the penalty function approach defined in the previous paragraph.

We have proved that our optimization model fits the chaos location problem, and that the suggested global optimization method is capable to find chaotic places (Csendes *et al.*, 2006). The interval arithmetic based checking routine provides a computational proof for the existence of the chaos there.

3.2. Numerical results

For the computational experiments we have applied the C-XSC programming language (Klatte *et al.*, 1993) supporting interval arithmetic. The results were obtained both in Linux and in the Cygwin environment, on an average personal computer. In the present subsection we just provide some demonstrative examples for the functioning of the introduced technique. First we have checked the reported chaotic region (Zgliczynski, 1997) by our checking routine.

1. We have investigated the seventh iterate of the Hénon mapping with the classic parameters of $A = 1.4$ and $B = 0.3$. The checked region consists of two parallelograms with sides parallel to the x -axis, the first coordinates of the lower corner points were 0.460, 0.556, 0.588, and 0.620, while the second coordinates were the same, 0.01. The common y coordinate for the upper corner points was 0.28, and the tangent of the sides was 2. We have set the epsilon threshold value for the checking routine to be 10^{-10} .

First the algorithm determined the starting interval that contains the region to be checked:

$$[0.46000, 0.75500] \times [0.01000, 0.28000].$$

Then the three conditions were checked one after the other. All of these proved to be valid – as expected. The number of function evaluations (for the transformation, *i.e.*, for the seventh iterate of the Hénon mapping in each case) were 273, 523, and 1,613, respectively. The algorithm stores those subintervals for which it was impossible to prove directly whether the given condition holds; these required further subdivision to achieve a conclusion. The depth of the stack necessary for the checking was only 11, 13, and 14, respectively. The CPU time used was negligible, a few seconds.

The results are demonstrated in Figure 5 (together with the parallelograms). The density of the subintervals indicates that in the related subregion the given condition was just fulfilled, the overestimation involved in the interval calculations required much refinement.

Summarizing the results, we were able to prove with an acceptable amount of computation and human overhead that the published system is chaotic in the given, known regions. This confirms the result of Zgliczynski (2003).

2. As a second step, randomly chosen A and B values were checked close to the classical parameters. The following ones ensured chaos for the H^7 Hénon system with unchanged other region and algorithm parameters:

A	B
1.3555400848181643,	0.32668379383472889
1.3465721096594685,	0.32450555140362324
1.4403201855906845,	0.22585009468060412
1.4136297518450903,	0.26880306437090162
1.3702743902664050,	0.30756016043366862

Notice that without our automatic checking of the conditions for chaos it could have been very difficult when not even impossible to arrive at the above results, since the human interaction and insight necessary plus the required overhead could be prohibitive.

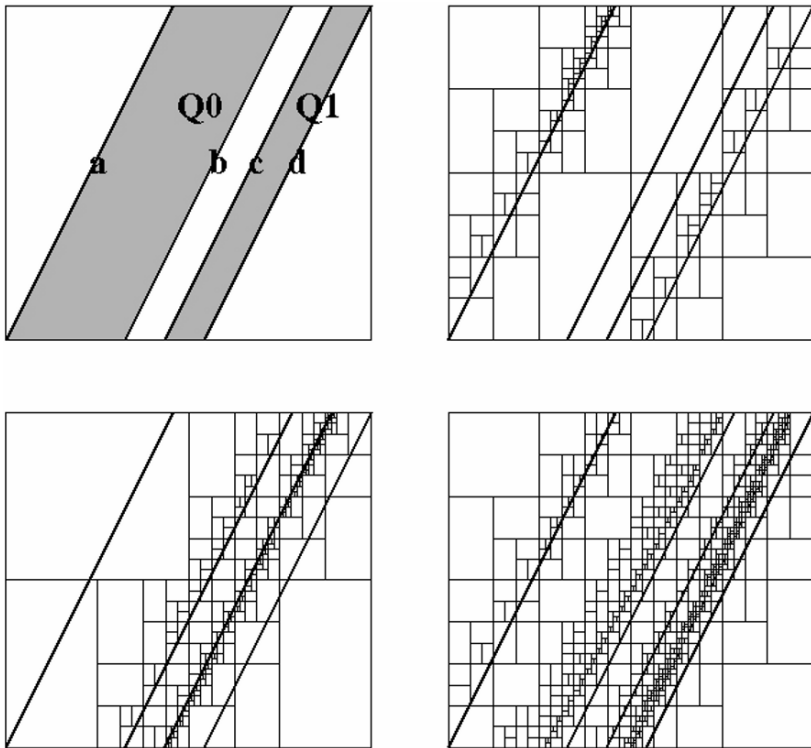


Fig. 5. The parallelograms and the starting interval covered by the verified subintervals for which the given condition holds (in the order of mentioning in Theorem 3).

3. As a third way of applying the checking routine, we have determined parameter intervals around $A = 1.4$ and $B = 0.3$ for which mapping H^7 still has chaos on the same pair of parallelograms. The obtained intervals were $A \in [1.377599, 1.401300]$ and $B \in [0.277700, 0.310301]$. Notice that these intervals do not contain all the A, B pairs given on the previous page.

The technique with which this result was obtained is the one discussed in Section 2. The key feature necessary for this algorithm is that the checking routine can accept interval valued parameters for the calculated mapping. More solved chaotic region location problems are reported with technical details in Bánhegyi *et al.* (2007) and Bánhegyi *et al.* (2008).

Acknowledgements

The presented work was supported by the Grants OTKA T 016413, T 017241, OMFB D-30/2000, OMFB E-24/2001, OTKA T 034350, T 048377, and T 046822.

References

Alefeld, G. and J. Herzberger, *Introduction to Interval Calculations*. Academic Press, New York (1983).

Bánhegyi, B., T. Csendes, and B.M. Garay, Optimization and the Miranda approach in detecting horseshoe-type chaos by computer. *International Journal of Bifurcation and Chaos*, 17, 735–748 (2007).

Bánhegyi, B., T. Csendes, B.M. Garay, and L. Hatvani, A computer-assisted proof for Sigma-3-chaos in the forced damped pendulum equation. *SIAM Journal on Applied Dynamical Systems*, 7, 843–867 (2008).

Bleher, J.H., S.M. Rump, U. Kulisch, M. Metzger, Ch. Ullrich, and W. Walter, FORTRAN-SC. A study of a FORTRAN extension for engineering/scientific computation with access to ACRITH, *Computing*, 39, 93–110 (1987).

Csallner, A.E., T. Csendes, and A.B. Kocsis, Reliable numerical computation in civil engineering. *Numerical Algorithms*, 37, 85–91 (2004).

Csendes, T., An interval method for bounding level sets of parameter estimation problems. *Computing*, 41, 75–86, (1989).

Csendes, T., Interval method for bounding level sets: revisited and tested with global optimization problems. *BIT*, 30, 650–657 (1990).

Csendes, T., Optimization methods for process network synthesis – a case study. In: C. Carlsson and I. Eriksson (eds.) *Global & Multiple Criteria Optimization and Information Systems Quality*. Abo Academy, Turku, 1998, pp. 113–132.

Csendes, T., Reliable optimization, methods and applications. DSc Dissertation, Hungarian Academy of Sciences, Budapest (2007).

Csendes, T. and J. Pintér, A new interval method for locating the boundary of level sets. *International Journal of Computer Mathematics*, 49, 53–59 (1993).

Csendes, T., B. Bánhegyi, and L. Hatvani, Towards a computer-assisted proof for chaos in a forced damped pendulum equation. *Journal of Computational and Applied Mathematics*, 199, 378–383 (2007).

Csendes, T., B.M. Garay, and B. Bánhegyi, A verified optimization technique to locate chaotic regions of a Hénon system. *Journal of Global Optimization*, 35, 145–160 (2006).

Csendes, T., Z.B. Zabinsky, and B.P. Kristinsdottir, Constructing large feasible suboptimal intervals for constrained nonlinear optimization. *Annals of Operations Research*, 58, 279–293 (1995).

Fiacco, A.V., Sensitivity analysis for nonlinear programming using penalty methods. *Mathematical Programming*, 12, 287–311 (1976).

Galias, Z., and P. Zgliczynski, Abundance of homoclinic and heteroclinic orbits and rigorous bounds for the topological entropy for the Hénon map. *Nonlinearity*, 14, 909–932 (2001).

Hammer, R., M. Hocks, U. Kulisch, and D. Ratz, *Numerical Toolbox for Verified Computing I*. Springer, Berlin (1993).

Hansen, E., *Global Optimization Using Interval Analysis*. Marcel Dekker, New York (1992).

Jüllig, H.P., BIBINS/2.0 – C++ Bibliotheken für Vektoren und Matrizen über beliebigem skalaren Datentyp unter Berücksichtigung spezieller spärlicher Strukturen sowie Intervall-datentypen. Bericht 92.6, Technical University of Hamburg-Harburg (1992).

Kearfott, R.B., An interval branch and bound algorithm for bound constrained optimization problems. *Journal of Global Optimization*, 2, 259–280 (1992).

Klatte, R., U. Kulisch, M. Neaga, D. Ratz, and Ch. Ullrich, *PASCAL-XSC – Language Reference with Examples*. Springer-Verlag, Berlin (1992).

Klatte, R., U. Kulisch, A. Wiethoff, C. Lawo, and M. Rauch, C-XSC – A C++ Class Library for Extended Scientific Computing. Springer, Heidelberg (1993).

Kovács, Z., F. Friedler, and L.T. Fan, Recycling in a separation process structure. *AICHE Journal*, 39, 1087–1089 (1993).

Kristinsdottir, B.P., Z.B. Zabinsky, T. Csendes, and M.E. Tuttle, Methodologies for tolerance intervals. *Interval Computations*, 3, 133–147 (1993).

Kristinsdottir, B.P., Z.B. Zabinsky, M.E. Tuttle, and T. Csendes, Incorporating manufacturing tolerances in optimal design of composite structures, *Engineering Optimization*, 26, 1–23 (1996).

Markót, M.C., Optimal packing of 28 equal circles in a unit square – the first reliable solution. *Numerical Algorithms*, 37, 253–261 (2004).

Markót, M.C. and T. Csendes, A new verified optimization technique for the “packing circles in a unit square” problems. *SIAM Journal on Optimization*, 16, 193–219 (2005).

Neumaier, A. and T. Rage, Rigorous chaos verification in discrete dynamical systems, *Physica D*, 67, 327–346 (1993).

Rage, T., A. Neumaier, and C. Schlier, Rigorous verification of chaos in a molecular model, *Physical Review E*, 50, 2682–2688 (1994).

Ratschek, H., and J. Rokne, Computer Methods for the Range of Functions, Ellis Horwood, Chichester (1984).

Ratschek, H. and J. Rokne, New Computer Methods for Global Optimization. Ellis Horwood, Chichester (1988).

Ratschek, H. and J. Rokne, Experiments using interval analysis for solving a circuit design problem. *Journal of Global Optimization*, 3, 501–518 (1993).

Rump, S.M., INTLAB – INTerval LABoratory. In: T. Csendes (ed.) *Developements in Reliable Computing*. Kluwer, Dordrecht, 1999, pp. 77–104.

Zgliczynski, P., Computer assisted proof of the horseshoe dynamics in the Hénon map. *Random & Computational Dynamics*, 5, 1–17 (1997).

Zgliczynski, P., On smooth dependence on initial conditions for dissipative PDEs, an ODE-type approach. *Journal of Differential Equations*, 195, 271–283 (2003).

Zabinsky, Z.B., D.L. Graesser, M.E. Tuttle, and G.I. Kim, Global optimization of composite laminates using improving hit-and-run, in: *Recent Advances in Global Optimization*. Princeton University Press, Princeton (1992), pp. 343–368.

Stochastic arithmetic and verification of mathematical models

Jean-Marie Chesneaux, Fabienne Jézéquel, Jean-Luc Lamotte

*Laboratoire d'Informatique de Paris 6, Université Pierre et Marie Curie (Paris 6),
4 Place Jussieu, 75252 Paris cedex 05, France.*

Abstract

Stochastic arithmetic enables one to estimate round-off error propagation using a probabilistic approach. With Stochastic arithmetic, the numerical quality of any simulation program can be controlled. Furthermore by detecting all the instabilities which may occur at run time, a numerical debugging of the user code can be performed. Stochastic arithmetic can be used to dynamically control approximation methods. Such methods provide a result which is affected by a truncation error inherent to the algorithm used and a round-off error due to the finite precision of the computer arithmetic. If the discretization step decreases, the truncation error also decreases, but the round-off error increases. Therefore it can be difficult to control these two errors simultaneously. In order to obtain with an approximation method a result for which the global error (consisting of both the truncation error and the round-off error) is minimal, a strategy, based on a converging sequence computation, has been proposed. Computation is carried out until the difference between two successive iterates has no exact significant digit. Then it is possible to determine which digits of the result obtained are in common with the exact solution. This strategy can apply to the computation of integrals using the trapezoidal rule, Simpson's rule, Romberg's method or the Gauss-Legendre method.

Keywords: approximation methods, CESTAC method, discrete stochastic arithmetic, Gauss-Legendre method, numerical validation, quadrature methods, Romberg method, rounding error, Simpson's rule, trapezoidal rule.

1. Introduction

To perform faster and faster numerical computations that are bigger and bigger is an old dream of human beings. Since four centuries, a lot of machines have been created for this aim and, 50 years ago, actual electronic computers were developed with the only goal of performing scientific computations. One of the first

mechanical calculating machine was the *Pascaline* (1642, France) followed by *Leibniz's machine* (1694, Germany). A first try of mechanical computer was the *analytical machine of Babbage* (1833, England) and a first mainframe computer was the *Z4 computer of K. Zuse* (1938, Germany). Until the beginning of the twentieth century, it only refers to computations on integer numbers. To perform efficient real numbers computations, we have to wait the birth of the famous BIT (*BI*nary *digi*T) which was introduced by C. Shannon (1937, USA) in his PhD thesis. The work of Shannon has imposed electronic for the building of computers and, then, the base 2 for coding integer or real numbers, although other bases have been tried. Nowadays, it is established that the base 2 is the most efficient base on computers for numerical computations, although the base 10 may be still used on pocket calculators.

For coding real numbers, we have also to determine the kind of coding we want to use. The decimal fixed-point notation was introduced at the end of the sixteenth century consecutively by S. Stévin (1582, France), J. Bürgi (1592, Switzerland) and G. Magini (1592, Italy). It is still the notation used in the whole world. If it is the most natural notation for human being, it is not very efficient for automatic computations. In fact, on this subject, one can say that nothing has changed since J. Napier's logarithm (1614, Scotland) and W. Oughtred's slide rule (1622, England). Logarithm was introduced by J. Napier to make multiplication easier (using logarithm, multiplication becomes addition). Three centuries later, the same idea was kept for the coding of real numbers on computers and led to the floating-point representation (see next section).

But whatever the representation is on computer, it is a finite representation, like for computations by hand. So, at each operation, because the result has to be truncated, an error may appear which is called the rounding error. It has been well-known by the scientists for four centuries. In the ninetieth century, when numerical computations were presented in an article, they were systematically followed by errors computations to justify the validity of the results. In 1950, in his famous article on eigen value computation with his new algorithm, C. Lanczos devoted 30% percent of his paper to error computation. Unfortunately, this use has completely disappeared since the beginning of the sixties because of the improvement of computers. When 8 billions floating-point operations are performed in 1 s on a processor, it seems to be impossible to quantify the rounding error even though neglecting rounding errors may lead to catastrophic consequences.

For instance, for real time applications, the discretization step may be $h = 10^{-1}$ s. One can compute the absolute time by performing $t_{abs} = t_{abs} + h$ at each step or performing $icount = icount + 1$; $t_{abs} = h * icount$ where *icount* is correctly initialized at the beginning of the process. Because the real number representation is finite on computers, only a finite number of them can be exactly coded. They are called floating-point numbers. The others are approximated by a floating-point number. Unfortunately, $h = 10^{-1}$ is not a floating-point number. Therefore, each operation $t_{abs} = t_{abs} + h$ generates a small but non-zero error. 100 h later, this error has grown around 0.34 s. It really happened during the first Gulf war (1991) in the

control programs of Patriot missiles to intercept Scud missiles (report of the General Accounting office, GAO/IMTEC-92-26). At 1600 km/h, 0.34 s corresponds to approximately 500 m, the interception failed and 28 persons were killed. With the second formulation, whatever the absolute time is, if no overflow occurs for *icount*, the relative rounding error remains below 10^{-15} using the IEEE double precision arithmetic. A good knowledge of floating-point arithmetic should be an obvious requirement for a computer scientist (Goldberg, 1991).

A goal of this chapter is to explain how it could be possible to give information and, sometimes, to answer the question in numerical computing “*What is the computing error due to floating-point arithmetic on the results produced by a program?*”

2. Stochastic approach of rounding errors

2.1. Preliminary definition

In this section, we present a probabilistic method that estimates in a computed result its number of exact significant digits, *i.e.*, the number of significant digits it has in common with the corresponding exact result. Therefore we need a theoretical definition for the number of significant digits common to two real numbers.

Definition 1. Let a and b be two real numbers, the number of significant digits that are common to a and b can be defined in \mathbb{R} by

1. For $a \neq b$, $C_{a,b} = \log_{10} \left| \frac{a+b}{2(a-b)} \right|$,
2. $\forall a \in \mathbb{R}$, $C_{a,a} = +\infty$.

Then $|a-b| = \left| \frac{a+b}{2} \right| 10^{-C_{a,b}}$. For instance, if $C_{a,b} = 3$, the relative difference between a and b is of the order of 10^{-3} , which means that a and b have three significant digits in common.

2.2. The CESTAC method

The CESTAC (Contrôle et Estimation Stochastique des Arrondis de Calculs) method, which has been developed by La Porte and Vignes (Vignes and La Porte, 1974; Vignes, 1990, 1993), enables one to estimate the number of exact significant digits of any computed result. This method is based on a probabilistic approach of rounding errors using a random rounding mode defined below.

Definition 2. Each real number x , which is not a floating-point number, is bounded by two consecutive floating-point numbers: X^- (rounded down) and X^+ (rounded up). The random rounding mode defines the floating-point number X representing x as being one of the two values X^- or X^+ with the probability 1/2.

With this random rounding mode, the same program run several times provides different results, due to different rounding errors.

It has been proved (Chesneaux, 1990) that a computed result R is modelled to the first order in 2^{-p} as:

$$R \approx Z = r + \sum_{i=1}^n g_i(d) 2^{-p} z_i \quad (1)$$

where r is the exact result, $g_i(d)$ are coefficients depending exclusively on the data and on the code, p is the number of bits in the mantissa and z_i are independent uniformly distributed random variables on $[-1, 1]$.

From equation (1), we deduce that:

1. The mean value of the random variable Z is the exact result r .
2. Under some assumptions, the distribution of Z is a quasi-Gaussian distribution.

Then by identifying R and Z , *i.e.*, by neglecting all the second order terms, Student's test can be used to determine the accuracy of R . Thus from N samples R_i , $i = 1, 2, \dots, N$, the number of decimal significant digits common to \bar{R} and r can be estimated with the following equation

$$C_{\bar{R}} = \log_{10} \left(\frac{\sqrt{N} |\bar{R}|}{\sigma \tau_{\beta}} \right), \quad (2)$$

where

$$\bar{R} = \frac{1}{N} \sum_{i=1}^N R_i \quad \text{and} \quad \sigma^2 = \frac{1}{N-1} \sum_{i=1}^N (R_i - \bar{R})^2 \quad (3)$$

τ_{β} is the value of Student's distribution for $N - 1$ degrees of freedom and a probability level $1 - \beta$.

Thus the implementation of the CESTAC method in a code providing a result R consists in:

- Performing N times this code with the random rounding mode, which is obtained by using randomly the rounding mode towards $-\infty$ or $+\infty$; we then obtain N samples R_i of R
- Choosing as the computed result the mean value \bar{R} of R_i , $i = 1, \dots, N$
- Estimating with equation (2) the number of exact decimal significant digits of \bar{R}

In practice $N = 3$ and $\beta = 0.05$. Note that for $N = 3$, then $\tau_\beta = 4.4303$.

Equations (1) and (2) hold if two main hypotheses are verified. These hypotheses are:

1. The rounding errors α_i are independent, centered uniformly distributed random variables.
2. The approximation to the first order in 2^{-p} is legitimate.

Concerning the first hypothesis, with the use of the random arithmetic, rounding errors α_i are random variables, however, in practice, they are not rigorously centered and in this case Student's test gives a biased estimation of the computed result. It has been proved (Chesneaux and Vignes, 1988) that, with a bias of a few σ , the error on the estimation of the number of exact significant digits of \bar{R} is less than one decimal digit. Therefore even if the first hypothesis is not rigorously satisfied, the reliability of the estimation obtained with equation (2) is not altered if it is considered as exact up to one digit.

Concerning the second hypothesis, the approximation to the first order only concerns multiplications and divisions. Indeed the rounding error generated by an addition or a subtraction does not contain any term of higher order. It has been shown (Chesneaux, 1990, 1995) that, if a computed result becomes insignificant, *i.e.*, if the rounding error it contains is of the same order of magnitude as the result itself, then the first order approximation may be not legitimate. In practice the validation of the CESTAC method requires a dynamic control of multiplications and divisions, during the execution of the code. This leads to the synchronous implementation of the method, *i.e.*, to the parallel computation of the N samples R_i , and also to the concept of computational zero, also named informational zero (Vignes, 1986).

Definition 3. *During the run of a code using the CESTAC method, an intermediate or a final result R is a computational zero, denoted by $@.0$, if one of the two following conditions holds:*

- $\forall i, R_i = 0$,
- $C_{\bar{R}} \leq 0$.

Any computed result R is a computational zero if either $R = 0$, R being significant, or R is insignificant. A computational zero is a value that cannot be differentiated from the mathematical zero because of its rounding error.

From the synchronous implementation of the CESTAC method and the concept of computational zero, stochastic arithmetic (Chesneaux and Vignes, 1992; Vignes, 1993; Chesneaux, 1995) has been defined. Two types of stochastic arithmetic actually exist; it can be either continuous or discrete.

2.3. Principles of stochastic arithmetic

2.3.1. Continuous stochastic arithmetic

Continuous stochastic arithmetic is a modelling of the synchronous implementation of the CESTAC method. By using this implementation, so that the N runs of a code take place in parallel, the N results of each arithmetical operation can be considered as realizations of a Gaussian random variable centered on the exact result. One can therefore define a new number, called *stochastic number*, and a new arithmetic, called *(continuous) stochastic arithmetic*, applied to these numbers. An equality concept and order relations, which take into account the number of exact significant digits of stochastic operands, have also been defined.

A stochastic number X is denoted by (m, σ^2) , where m is the mean value of X and σ its standard deviation. Stochastic arithmetical operations ($s+$, $s-$, $s\times$, $s/$) correspond to terms to the first order in σ/m of operations between two independent Gaussian random variables.

Definition 4. Let $X_1 = (m_1, \sigma_1^2)$ and $X_2 = (m_2, \sigma_2^2)$. Stochastic arithmetical operations on X_1 and X_2 are defined as:

$$X_1 s + X_2 = (m_1 + m_2, \sigma_1^2 + \sigma_2^2) \quad (4)$$

$$X_1 s - X_2 = (m_1 - m_2, \sigma_1^2 + \sigma_2^2) \quad (5)$$

$$X_1 s \times X_2 = (m_1 \times m_2, m_2^2 \sigma_1^2 + m_1^2 \sigma_2^2) \quad (6)$$

$$X_1 s / X_2 = \left(m_1 / m_2, \left(\frac{\sigma_1}{m_2} \right)^2 + \left(\frac{m_1 \sigma_2}{m_2^2} \right)^2 \right) \quad \text{with } m_2 \neq 0 \quad (7)$$

An accuracy can be associated to any stochastic number. If $X = (m, \sigma^2)$, λ_β exists (depending only on β) such that

$$P\left(X \in [m - \lambda_\beta \sigma, m + \lambda_\beta \sigma]\right) = 1 - \beta \quad (8)$$

$I_{\beta,X} = [m - \lambda_\beta \sigma, m + \lambda_\beta \sigma]$ is the confidence interval of m at $1 - \beta$. The number of decimal significant digits common to all the elements of $I_{\beta,X}$ and to m is lower bounded by

$$C_{\beta,X} = \log_{10} \left(\frac{|m|}{\lambda_\beta \sigma} \right) \quad (9)$$

The following definition is the modelling of the concept of computational zero, previously introduced.

Definition 5. A stochastic number X is a stochastic zero, denoted by $\underline{0}$, if and only if

$$C_{\beta,X} \leq 0 \quad \text{or} \quad X = (0, 0)$$

In accordance with the concept of stochastic zero, a new equality concept and new order relations have been defined.

Definition 6. Let $X_1 = (m_1, \sigma_1^2)$ and $X_2 = (m_2, \sigma_2^2)$ be two stochastic numbers.

- Stochastic equality, denoted by $s =$, is defined as: $X_1 \ s = X_2$ if and only if $X_1 - X_2 = \underline{0}$.
- Stochastic inequalities, denoted by $s >$ and $s \geq$ are defined as: $X_1 \ s > X_2$ if and only if $m_1 > m_2$ and $X_1 \ s \neq X_2$, $X_1 \ s \geq X_2$ if and only if $m_1 \geq m_2$ or $X_1 \ s = X_2$.

Continuous stochastic arithmetic is a modelling of the computer arithmetic, which takes into account rounding errors. The properties of continuous stochastic arithmetic (Chesneaux, 1994, 1995) have pointed out the theoretical differences between the approximative arithmetic of a computer and exact arithmetic.

2.3.2. Discrete stochastic arithmetic

Discrete Stochastic Arithmetic (DSA) has been defined from the synchronous implementation of the CESTAC method. With DSA, a real number becomes an N -dimensional set and any operation on these N -dimensional sets is performed element per element using the random rounding mode. The number of exact significant digits of such an N -dimensional set can be estimated from equation (2). From the concept of computational zero previously introduced, an equality concept and order relations have been defined for DSA.

Definition 7. Let X and Y be N -samples provided by the CESTAC method.

- Discrete stochastic equality denoted by $ds =$ is defined as: $X \ ds = Y$ if and only if $X - Y = @.0$.
- Discrete stochastic inequalities denoted by $ds >$ and $ds \geq$ are defined as: $X \ ds > Y$ if and only if $[\bar{X}] > [\bar{Y}]$ and $X \ ds \neq Y$, $X \ ds \geq Y$ if and only if $[\bar{X}] \geq [\bar{Y}]$ or $X \ ds = Y$.

Order relations in DSA are essential to control branching statements. Because of rounding errors, if A and B are two floating-point numbers and a and b the corresponding exact values, one can have

$$a > b \text{ and } A \leq B \quad \text{or} \quad A > B \text{ and } a \leq b.$$

Many problems in scientific computing are due to this dis-correlation: for example, unsatisfied stopping criteria or infinite loops in algorithmic geometry. Taking into account the numerical quality of the operands in order relations enables to partially solve these problems (Chesneaux, 1994).

Therefore DSA enables to estimate the impact of rounding errors on any result of a scientific code and also to check that no anomaly occurred during the run, especially in branching statements. DSA is implemented in the CADNA library.¹

The accuracy of a stochastic number can be related to the number of exact significant digits of an N -sample provided by the CESTAC method. Indeed, when N is a small value (2 or 3), which is the case in practice, the values obtained with equations (2) and (9) are very close. They represent in a computed result the number of significant digits which are not affected by rounding errors. So the two types of stochastic arithmetic are coherent. Properties established in the theoretical framework of continuous stochastic arithmetic can be applied on a computer via the practical use of DSA.

3. Benefits of DSA in numerical programs

With six examples, the behaviour and the benefits of DSA are illustrated. For each example, at first, results using the standard floating-point arithmetic are presented and, then, results using the CADNA library, which automatically implements the DSA, are also presented.

3.1. *Example 1: a rational fraction function of two variables*

In the following example (Rump, 1988), the rational fraction

$$F(x, y) = 333.75 y^6 + x^2(11 x^2 y^2 - y^6 - 121 y^4 - 2) + 5.5 y^8 + \frac{x}{2y}$$

is computed with $x = 77617$, $y = 33096$. The 15 first digits of the exact result are –0.827396059946821.

Using the IEEE double precision arithmetic with rounding to the nearest, one obtains:

res = 5.76460752303423E+17, and using CADNA in double precision, one obtains:

CADNA software-University P. et M. Curie---LIP6
 Self-validation detection: ON
 Mathematical instabilities detection: ON
 Branching instabilities detection: ON
 Intrinsic instabilities detection: ON
 Cancellation instabilities detection: ON

¹ URL address: <http://www.lip6.fr/cadna/>

```

Res = @.0
-----
CADNA software-University P. et M. Curie---LIP6
There is 1 numerical instability
0 UNSTABLE DIVISION(S)
0 UNSTABLE POWER FUNCTION(S)
0 UNSTABLE MULTIPLICATION(S)
0 UNSTABLE BRANCHING(S)
0 UNSTABLE MATHEMATICAL FUNCTION(S)
0 UNSTABLE INTRINSIC FUNCTION(S)
1 UNSTABLE CANCELLATION(S)

```

CADNA points out the complete loss of accuracy of the result.

3.2. Example 2: solving a second order equation

The roots of the following second order equation are computed:

$$0.3 x^2 - 2.1 x + 3.675 = 0$$

The exact values are: Discriminant $d = 0$, $x1 = x2 = 3.5$.

Using the IEEE single precision arithmetic with rounding to the nearest, one obtains:

```

D = -3.8146972E-06
There are two conjugate complex roots:
z1=0.3499999E+01 + i * 0.9765625E-03
z2=0.3499999E+01 + i * -.9765625E-03

```

and using CADNA in single precision, one obtains:

```

-----
CADNA software-University P. et M. Curie---LIP6
Self-validation detection: ON
Mathematical instabilities detection: ON
Branching instabilities detection: ON
Intrinsic instabilities detection: ON
Cancellation instabilities detection: ON
-----
```

```

D = @.0
Discriminant is zero.
The double solution is 0.349999E+01
-----
```

```

CADNA software-University P. et M. Curie---LIP6
There are 1 numerical instabilities
```

```

0 UNSTABLE DIVISION(S)
0 UNSTABLE POWER FUNCTION(S)
0 UNSTABLE MULTIPLICATION(S)
0 UNSTABLE BRANCHING(S)
0 UNSTABLE MATHEMATICAL FUNCTION(S)
0 UNSTABLE INTRINSIC FUNCTION(S)
1 UNSTABLE CANCELLATION(S)

```

The standard floating-point arithmetic cannot detect that $d = 0$. The wrong branching is performed and the result is false.

The CADNA software takes the accuracy of operands into account in the order relations or in the equality relation and, therefore, the good branching is performed and the exact result is obtained.

3.3. Example 3: computing a determinant

The determinant of Hilbert's matrix of size 11 is computed using Gaussian elimination without pivoting strategy. The determinant is the product of the different pivots. Hilbert's matrix is defined by: $a(i,j) = 1/(i + j - 1)$. All the pivots and the determinant are printed out.

The exact value of the determinant is $3.0190953344493 \cdot 10^{-65}$.

Using the IEEE double precision arithmetic with rounding to the nearest, one obtains:

```

Pivot number 1 = 0.1000000000000000D+01
Pivot number 2 = 0.833333333333331D-01
Pivot number 3 = 0.5555555555555522D-02
Pivot number 4 = 0.3571428571428736D-03
Pivot number 5 = 0.2267573696146732D-04
Pivot number 6 = 0.1431549050481817D-05
Pivot number 7 = 0.9009749236431395D-07
Pivot number 8 = 0.5659970607161749D-08
Pivot number 9 = 0.3551362553328898D-09
Pivot number 10 = 0.2226656943069665D-10
Pivot number 11 = 0.1398301799864147D-11
Determinant = 0.3026439382718219D-64

```

and using CADNA in double precision, one obtains:

```
-----
CADNA software-University P. et M. Curie---LIP6
Self-validation detection: ON
Mathematical instabilities detection : ON
Branching instabilities detection : ON
Intrinsic instabilities detection : ON
Cancellation instabilities detection : ON
-----
```

```

Pivot number 1 = 0.1000000000000000E+001
Pivot number 2 = 0.8333333333333333E-001
Pivot number 3 = 0.5555555555555555E-002
Pivot number 4 = 0.3571428571428E-003
Pivot number 5 = 0.22675736961E-004
Pivot number 6 = 0.1431549051E-005
Pivot number 7 = 0.90097493E-007
Pivot number 8 = 0.5659970E-008
Pivot number 9 = 0.35513E-009
Pivot number 10 = 0.2226E-010
Pivot number 11 = 0.14E-011
Determinant = 0.30E-064
-----
CADNA software-University P. et M.Curie---LIP6
No instability detected

```

The gradual loss of accuracy is pointed out by CADNA. One can see that the value of the determinant is significant even if it is very “small”. This shows how difficult it is to judge the numerical quality of a computed result by its magnitude.

3.4. Example 4: computing a second order recurrent sequence

This example was proposed by J.-M. Muller (Muller, 1989). The 25 first iterations of the following recurrent sequence are computed:

$$U_{n+1} = 111 - \frac{1130}{U_n} + \frac{3000}{U_n U_{n-1}}$$

with $U_0 = 5.5$ and $U_1 = [61/11]$. The exact value of the limit is 6.

Using the IEEE double precision arithmetic with rounding to the nearest, one obtains:

```

U( 3) = 0.5590163934426229D+01
U( 4) = 0.5633431085043980D+01
U( 5) = 0.5674648620510026D+01
U( 6) = 0.5713329052378341D+01
U( 7) = 0.5749120919664605D+01
U( 8) = 0.5781810919824309D+01
U( 9) = 0.5811314226859892D+01
U(10) = 0.5837656352257866D+01
U(11) = 0.5860948153832367D+01
U(12) = 0.5881319751541141D+01
U(13) = 0.5898177025615012D+01
U(14) = 0.5897965247556456D+01

```

```

U(15) = 0.5647011084038567D+01
U(16) = 0.9683399445297453D+00
U(17) =-0.5073216051624674D+03
U(18) = 0.1071206352328062D+03
U(19) = 0.1003959421894409D+03
U(20) = 0.1000235186060601D+03
U(21) = 0.1000014035745554D+03
U(22) = 0.1000000838527958D+03
U(23) = 0.1000000050131387D+03
U(24) = 0.1000000002998870D+03
U(25) = 0.1000000000179481D+03

```

and using CADNA in double precision, one obtains:

```

-----
CADNA software-University P. et M. Curie---LIP6
Self-validation detection: ON
Mathematical instabilities detection : ON
Branching instabilities detection : ON
Intrinsic instabilities detection : ON
Cancellation instabilities detection : ON

U( 3) = 0.55901639344262E+001
U( 4) = 0.5633431085044E+001
U( 5) = 0.56746486205E+001
U( 6) = 0.5713329052E+001
U( 7) = 0.574912092E+001
U( 8) = 0.57818109E+001
U( 9) = 0.581131E+001
U(10) = 0.58377E+001
U(11) = 0.5861E+001
U(12) = 0.588E+001
U(13) = 0.6E+001
U(14) =@.0
U(15) =@.0
U(16) =@.0
U(17) = 0.9E+002
U(18) = 0.999E+002
U(19) = 0.9999E+002
U(20) = 0.99999E+002
U(21) = 0.999999E+002
U(22) = 0.9999999E+002
U(23) = 0.999999999E+002
U(24) = 0.9999999999E+002
U(25) = 0.99999999999E+002

```

The exact limit is 6.

 CADNA software-University P. et M. Curie---LIP6
 CRITICAL WARNING: the self-validation detects major
 problem(s).

The results are NOT guaranteed

There are 9 numerical instabilities

7 UNSTABLE DIVISION(S)
 0 UNSTABLE POWER FUNCTION(S)
 2 UNSTABLE MULTIPLICATION(S)
 0 UNSTABLE BRANCHING(S)
 0 UNSTABLE MATHEMATICAL FUNCTION(S)
 0 UNSTABLE INTRINSIC FUNCTION(S)
 0 UNSTABLE CANCELLATION(S)

The traces UNSTABLE DIVISION(S) are generated by divisions where the denominator is a computational zero. Such operations make the computed trajectory turn off the exact trajectory and then, the estimation of accuracy is not possible any more. Even using the double precision, the computer cannot give any significant result after the iteration number 15.

3.5. Example 5: computing a root of a polynomial

This example deals with the improvement and optimization of an iterative algorithm by using new tools which are contained in CADNA. This program computes a root of the polynomial

$$f(x) = 1.47 x^3 + 1.19 x^2 - 1.83 x + 0.45$$

by Newton's method. The sequence is initialized with $x = 0.5$.

The iterative algorithm $x_{n+1} = x_n - \frac{f(x_n)}{f'(x_n)}$ is stopped with the criterion

$$|x_n - x_{n-1}| < 10^{-12}$$

Using the IEEE double precision arithmetic with rounding to the nearest, one obtains:

$$\begin{aligned} x(29) &= 0.428571431755150 \\ x(30) &= 0.428571431755150 \end{aligned}$$

and using CADNA in double precision, one obtains:

 CADNA software --- University P. et M. Curie --- LIP6
 Self-validation detection: ON

```

Mathematical instabilities detection : ON
Branching instabilities detection : ON
Intrinsic instabilities detection : ON
Cancellation instabilities detection : ON
-----
x( 24 ) = 0.42857143E+000
x( 25 ) = 0.42857143E+000
-----
CADNA software --- University P. et M. Curie --- LIP6
CRITICAL WARNING: the self-
validation detects major problem(s) .
The results are NOT guaranteed
There are 56 numerical instabilities
 1 UNSTABLE DIVISION(S)
 0 UNSTABLE POWER FUNCTION(S)
 0 UNSTABLE MULTIPLICATION(S)
 1 UNSTABLE BRANCHING(S)
 0 UNSTABLE MATHEMATICAL FUNCTION(S)
 2 UNSTABLE INTRINSIC FUNCTION(S)
 52 UNSTABLE CANCELLATION(S)

```

With CADNA, one can see that seven significant digits were lost (despite the apparent stability). By using a symbolic debugger, one can see that, at the last iteration, the denominator is a non-significant value (a computational zero) and that the last answer to the stopping criterion is not reliable. CADNA allows one to stop the algorithm when the subtraction $x_n - x_{n-1}$ is non-significant (there is no more information to compute at the next iteration). In Newton's method, a division by a computational zero may suggest a double root. One can simplify the fraction. When these two transformations are done, the code is stabilized and the results are obtained with the best accuracy of the computer. The exact value of the root is $x_{sol} = 3/7 = 0.428571428571428571\dots$ Now, we obtain:

```

-----
CADNA software --- University P. et M. Curie --- LIP6
Self-validation detection: ON
Mathematical instabilities detection : ON
Branching instabilities detection : ON
Intrinsic instabilities detection : ON
Cancellation instabilities detection : ON
-----
x( 48 ) = 0.428571428571429E+000
x( 49 ) = 0.428571428571429E+000
-----
CADNA software --- University P. et M. Curie --- LIP6
No instability detected

```

3.6. Example 6: solving a linear system

In this example, CADNA is able to provide correct results which were impossible to be obtained with the standard floating-point arithmetic. The following linear system is solved using Gaussian elimination with partial pivoting. The system is

$$\begin{pmatrix} 21 & 130 & 0 & 2.1 \\ 13 & 80 & 4.74 \cdot 10^8 & 752 \\ 0 & -0.4 & 3.9816 \cdot 10^8 & 4.2 \\ 0 & 0 & 1.7 & 9 \cdot 10^{-9} \end{pmatrix} \cdot X = \begin{pmatrix} 153.1 \\ 849.74 \\ 7.7816 \\ 2.6 \cdot 10^{-8} \end{pmatrix}$$

The exact solution is $x_{sol}' = (1, 1, 10^{-8}, 1)$. Using the IEEE single precision arithmetic with rounding to the nearest, one obtains:

```
x_sol(1) = 0.6261987E+02
x_sol(2) = -0.8953979E+01
x_sol(3) = 0.0000000E+00
x_sol(4) = 0.9999999E+00
```

and using CADNA in single precision, one obtains:

```
-----
CADNA software --- University P. et M. Curie --- LIP6
Self-validation detection: ON
Mathematical instabilities detection : ON
Branching instabilities detection : ON
Intrinsic instabilities detection : ON
Cancellation instabilities detection : ON
-----
x_sol(1) = 0.999E+00
x_sol(2) = 0.1000E+01
x_sol(3) = 0.999999E-08
x_sol(4) = 0.1000000E+01
-----
CADNA software --- University P. et M. Curie --- LIP6
There are 3 numerical instabilities
0 UNSTABLE DIVISION(S)
0 UNSTABLE POWER FUNCTION(S)
0 UNSTABLE MULTIPLICATION(S)
1 UNSTABLE BRANCHING(S)
0 UNSTABLE MATHEMATICAL FUNCTION(S)
1 UNSTABLE INTRINSIC FUNCTION(S)
1 UNSTABLE CANCELLATION(S)
```

During the reduction of the third column, the matrix element $A(3,3)$ is equal to 4864. But the exact value of $A(3,3)$ is zero. The standard floating-point arithmetic cannot detect that $A(3,3)$ is non-significant. This value is chosen as pivot. That leads to erroneous results. CADNA detects the non-significant value of $A(3,3)$. This value is eliminated as pivot. That leads to satisfactory results.

4. Dynamical control of approximation methods

DSA, which has been presented in section 2.3.2, enables one to estimate in a computed result which digits are affected by rounding errors. Furthermore, with DSA, the numerical quality of operands in an order relation is taken into account. For instance, a test for equality is satisfied if the operands have the same value, up to rounding errors. Therefore new algorithms, specific to DSA, can be proposed. This section is devoted to the use of approximation methods, such as quadrature methods, in DSA.

An approximation method, based on a discretization step, provides a numerical result affected by a global error, which consists of both a truncation error and a rounding error. If the discretization step decreases, the truncation error also decreases, but the rounding error usually increases. The optimal step size, for which the global error is minimal, can be computed dynamically (Vignes, 1996). In this section, we show how to determine in the corresponding result which digits are affected neither by the truncation error, nor by the rounding error.

4.1. On approximation methods of order p

A numerical method which uses a discretization step h enables one to approximate an exact value L by a value $L(h)$ such that $\lim_{h \rightarrow 0} L(h) = L$. The technique of “step halving” consists in computing a sequence of approximations based on several successive divisions of the step by 2. Theorem 1 enables one to determine the number of significant digits in common between two successive approximations and the exact result L .

Theorem 1. *Let us consider a numerical method which provides an approximation $L(h)$ of order p to an exact value L , i.e., $L(h) - L = K h^p + O(h^q)$ with $1 \leq p < q$, $K \in \mathbb{R}$. If L_n is the approximation computed with the step $\lceil (h_0)/(2^n) \rceil$, then*

$$C_{L_n, L_{n+1}} = C_{L_n, L} + \log_{10} \left(\frac{2^p}{2^p - 1} \right) + O(2^{n(p-q)})$$

Proof The truncation error on L_n is

$$L_n - L = K \left(\frac{h_0}{2^n} \right)^p + O \left(\frac{1}{2^{qn}} \right) \quad (10)$$

Using the same formula for L_{n+1} , one obtains

$$L_n - L_{n+1} = K \left(\frac{2^p - 1}{2^p} \right) \left(\frac{h_0}{2^n} \right)^p + O \left(\frac{1}{2^{qn}} \right) \quad (11)$$

From equation (10), we deduce

$$\frac{L_n}{L_n - L} = \frac{L_n}{K \left(\frac{h_0}{2^n} \right)^p} \left(1 + O \left(2^{n(p-q)} \right) \right) \quad (12)$$

$$\frac{L_n}{L_n - L} = \frac{L_n}{K \left(\frac{h_0}{2^n} \right)^p \left(1 + O \left(2^{n(p-q)} \right) \right)} \quad (13)$$

Therefore

$$\frac{L_n}{L_n - L} = \frac{L_n}{K \left(\frac{h_0}{2^n} \right)^p} + O \left(2^{n(2p-q)} \right) \quad (14)$$

Then

$$\frac{L_n + L}{2(L_n - L)} = \frac{L_n}{L_n - L} - \frac{1}{2} = \frac{L_n}{K \left(\frac{h_0}{2^n} \right)^p} + O \left(2^{n(2p-q)} \right) \quad (15)$$

Similarly, from equation (11), we deduce

$$\frac{L_n + L_{n+1}}{2(L_n - L_{n+1})} = \frac{L_n}{L_n - L_{n+1}} - \frac{1}{2} = \left(\frac{L_n}{K \left(\frac{h_0}{2^n} \right)^p} \right) \left(\frac{2^p}{2^p - 1} \right) + O \left(2^{n(2p-q)} \right) \quad (16)$$

From definition 1 and equation (15), we deduce

$$C_{L_n, L} = \log_{10} \left| \frac{L_n}{K \left(\frac{h_0}{2^n} \right)^p} \left(1 + O \left(2^{n(p-q)} \right) \right) \right| \quad (17)$$

$$C_{L_n, L} = \log_{10} \left| \frac{L_n}{K \left(\frac{h_0}{2^n} \right)^p} \right| + \log_{10} \left| \left(1 + O \left(2^{n(p-q)} \right) \right) \right| \quad (18)$$

Therefore

$$C_{L_n, L} = \log_{10} \left| \frac{L_n}{K \left(\frac{h_0}{2^n} \right)^p} \right| + O(2^{n(p-q)}) \quad (19)$$

Similarly, from definition 1 and equation (16), we deduce

$$C_{L_n, L_{n+1}} = \log_{10} \left| \left(\frac{L_n}{K \left(\frac{h_0}{2^n} \right)^p} \right) \left(\frac{2^p}{2^p - 1} \right) \right| + O(2^{n(p-q)}) \quad (20)$$

Finally

$$C_{L_n, L_{n+1}} = C_{L_n, L} + \log_{10} \left(\frac{2^p}{2^p - 1} \right) + O(2^{n(p-q)}) \quad (21)$$

If the convergence zone is reached, *i.e.*, if the term $O(2^{n(p-q)})$ becomes negligible, the significant digits common to two successive approximations L_n and L_{n+1} are also in common with the exact result L , up to one bit. Indeed the term $\log_{10}((2^p)/(2^p - 1))$ decreases as p increases and it corresponds to one bit for methods of order 1.

Remark 1. *This assertion can be related to previous works carried out on converging sequences (Jézéquel, 2004, 2005). The sequence (L_n) generated by the technique of “step having” converges linearly to the exact result L . Indeed it satisfies $L_n - L = K \alpha^n + o(\alpha^n)$ with $K \in \mathbb{R}$ and $0 < |\alpha| < 1$. In Jézéquel (2004, 2005), it has been pointed out that if $0 < \alpha \leq 1/2$ (which is the case here), then in the convergence zone, the significant bits common to two successive iterates are also in common with L , up to one.*

4.2. On Newton–Cotes methods

Theorem 1 can apply to Newton–Cotes quadrature rules.

Let $I(h)$ be the approximation to $I = \int_a^b f(x) dx$ by the trapezoidal rule with step h . If $f \in C^4[a, b]$, the truncation error expansion on $I(h)$ up to order 4 is (Stoer and Bulirsch, 2002):

$$I(h) - I = \frac{h^2}{12} [f'(b) - f'(a)] + O(h^4) \quad (22)$$

Let $I(h)$ be the approximation to $I = \int_a^b f(x)dx$ by Simpson's rule with step h . If $f \in C^6[a,b]$, the truncation error expansion on $I(h)$ up to order 6 is (Stoer and Bulirsch, 2002):

$$I(h) - I = \frac{h^4}{180} [f^{(3)}(b) - f^{(3)}(a)] + O(h^6) \quad (23)$$

Equations (22) and (23) are similar to equation (10), which characterizes approximation methods, with $p = 2$ and $q = 4$ for the trapezoidal rule; $p = 4$ and $q = 6$ for Simpson's rule. Therefore the following theoretical results, which had been given in Chesneau and Jézéquel (1998) with specific proofs, could have been established from theorem 1.

Corollary 1. *Let I_n be the approximation to $I = \int_a^b f(x)dx$ by the trapezoidal rule with step $h = [(b-a)/(2^n)]$. If $f \in C^4[a,b]$ and $f'(b) \neq f'(a)$, then*

$$C_{I_n, I_{n+1}} = C_{I_n, I} + \log_{10} \left(\frac{4}{3} \right) + O \left(\frac{1}{4^n} \right) \quad (24)$$

Corollary 2. *Let I_n be the approximation to $I = \int_a^b f(x)dx$ by Simpson's rule with step $h = [(b-a)/(2^n)]$. If $f \in C^6[a,b]$ and $f^{(3)}(b) \neq f^{(3)}(a)$, then*

$$C_{I_n, I_{n+1}} = C_{I_n, I} + \log_{10} \left(\frac{16}{15} \right) + O \left(\frac{1}{4^n} \right) \quad (25)$$

Let $I(h)$ be the approximation to $I = \int_a^b f(x)dx$ by the composite closed Newton–Cotes quadrature rule with v points and step h . Let $p = v + 1$ if v is odd and $p = v$ if v is even. If $f \in C^{p+2}[a,b]$, by applying the Euler–MacLaurin summation formula, we get

$$I(h) - I = K_v h^p [f^{(p-1)}(b) - f^{(p-1)}(a)] + O \left(\frac{1}{4^n} \right) \quad (26)$$

where K_v is a constant which depends on v .

Corollary 3 can be established from theorem 1 and equation (26).

Corollary 3. *Let I_N be the approximation to $I = \int_a^b f(x)dx$ by a composite closed Newton–Cotes quadrature rule of order p with step $h = [(b-a)/N]$. If $f \in C^{p+2}[a,b]$ and $f^{(p-1)}(b) \neq f^{(p-1)}(a)$, then*

$$C_{I_N, I_{2N}} = C_{I_N, I} + \log_{10} \left(\frac{2^p}{2^p - 1} \right) + O \left(\frac{1}{N^2} \right) \quad (27)$$

Assuming $N = 2^n$, corollary 3 is in perfect agreement with corollary 1 (specific to the trapezoidal rule) and with corollary 2 (specific to Simpson's rule).

4.3. On the Gauss–Legendre method

Theorem 1 can also apply to the Gauss–Legendre method. First let us briefly recall the principles of this quadrature method. The approximation to $\int_{-1}^1 f(x)dx$ by the Gauss–Legendre method with v points (Conte and de Boor, 1980; Engels, 1980) is $\sum_{i=1}^v C_i f(x_i)$, where for $i = 1, \dots, v$, $\{x_i\}$ are the roots of the v -degree Legendre polynomial P_v and

$$C_i = \frac{2}{(1 - x_i^2)(P'_v(x_i))^2} \quad (28)$$

For the computation of an integral on another interval such as $I = \int_a^b g(t)dt$, the following change of variable is required.

$$I = \int_a^b g(t)dt = \frac{b-a}{2} \int_{-1}^1 f(x)dx \quad (29)$$

with

$$\forall x \in [-1, 1], f(x) = g\left(\frac{(b-a)x + b + a}{2}\right) \quad (30)$$

The Gauss–Legendre method with v points is of order $2v$: it is exact if the integrand is a polynomial of degree r with $r \leq 2v - 1$.

Let us assume that the integration domain is partitioned into 2^n subintervals and that the integral on each subinterval is evaluated using the Gauss–Legendre method with v points. Theorem 2 presents the truncation error on I_n , the sum of the 2^n approximations obtained.

Theorem 2. Let $i = \int_a^b g(t)dt$ and for $i = 1, \dots, v$, let $\{x_i\}$ be the roots of the v -degree Legendre polynomial and $\{C_i\}$ the corresponding weights. Let us assume that the integral on each subinterval $[\alpha_{k-1}, \alpha_k]$ with $\alpha_k = a + k[(b-a)/(2^n)]$, for $k = 1, \dots, 2^n$, is evaluated using the Gauss–Legendre method with v points. Let I_n be the sum of the 2^n approximations obtained. If $g \in C^{2v+1}[a, b]$, then

$$I_n - I = \frac{K_v}{4^{nv}} + O\left(\frac{1}{2^{n(2v+1)}}\right)$$

with

$$K_v = \frac{(b-a)^{2v}}{2^{2v+1}(2v)!} \left(\sum_{i=1}^v C_i x_i^{2v} - \frac{2}{2v+1} \right) [g^{(2v-1)}(b) - g^{(2v-1)}(a)].$$

In Jéséquel *et al.* (2006), a more general form of theorem 2, where the integration interval is partitioned into q subintervals, is given with its proof.

Corollary 4 can be established from theorems 1 and 2. The same notations and assumptions as in theorem 2 are used.

Corollary 4.

$$C_{I_n, I_{n+1}} = C_{I_n, I} + \log_{10} \left(\frac{4^v}{4^v - 1} \right) + O\left(\frac{1}{2^n}\right)$$

Therefore if the convergence zone is reached, *i.e.*, if the term $O([1/(2^n)])$ becomes negligible, the significant digits common to two successive approximations are also in common with the exact value of the integral, up to one bit.

4.4. A strategy for a dynamical control of approximation methods

DSA enables one to estimate the number of exact significant digits of any computed result, *i.e.*, its significant digits which are not affected by rounding error propagation. Adopting the same notations as in 4.1, let (L_n) be a sequence computed in DSA with an approximation method using the step value $[(h_0)/(2^n)]$. And let us assume that the convergence zone is reached. If discrete stochastic equality is achieved for two successive iterates, *i.e.*, $L_n - L_{n+1} = @.0$, the difference between L_n and L_{n+1} is only due to rounding errors and further iterations are useless. The optimal iterate L_{n+1} can therefore be dynamically determined at run time. Furthermore, from theorem 1, the exact significant bits of L_{n+1} are in common with the exact result L , up to one.

Therefore one can dynamically determine the optimal approximation by performing computations until the difference $L_n - L_{n+1}$ has no exact significant digit. If the convergence zone has been reached, then the exact significant bits of the last approximation are in common with L , up to one.

4.5. Dynamical control of Romberg's method

Romberg's method (Bauer *et al.*, 1963; Burden and Faires, 2001; Stoer and Bulirsch, 2002), is based on Richardson's extrapolation on results of the trapezoidal rule. For the approximation of $I = \int_a^b f(x)dx$, Romberg's method consists in computing the following triangular table, with $h = [(b - a)/M]$ ($M \geq 1$).

$$\begin{array}{cccccc}
 T_1(h) & T_1\left(\frac{h}{2}\right) & \cdots & T_1\left(\frac{h}{2^{n-3}}\right) & T_1\left(\frac{h}{2^{n-2}}\right) & T_1\left(\frac{h}{2^{n-1}}\right) \\
 T_2(h) & T_2\left(\frac{h}{2}\right) & \cdots & T_2\left(\frac{h}{2^{n-3}}\right) & T_2\left(\frac{h}{2^{n-2}}\right) & \\
 T_3(h) & T_3\left(\frac{h}{2}\right) & \cdots & T_3\left(\frac{h}{2^{n-3}}\right) & & \\
 \vdots & \vdots & & & & \\
 T_{n-1}(h) & T_{n-1}\left(\frac{h}{2}\right) & & & & \\
 T_n(h) & & & & &
 \end{array}$$

The first row of the table represents approximations of I computed using the trapezoidal rule with step $[h/(2^j)]$ ($j = 0, \dots, n-1$). Rows 2 to n are computed using the following formula.

For $r = 2, \dots, n$ and $j = 0, \dots, n-r$,

$$T_r\left(\frac{h}{2^j}\right) = \frac{1}{4^{r-1}-1} \left(4^{r-1} T_{r-1}\left(\frac{h}{2^{j+1}}\right) - T_{r-1}\left(\frac{h}{2^j}\right) \right)$$

The sequence of approximations with Romberg's method $T_1(h), \dots, T_n(h)$ converges exponentially to I .

The following theorem enables one to determine from two successive approximations, $T_n(h)$ and $T_{n+1}(h)$, the first digits of the exact value of the integral.

Theorem 3. *We assume that f is a real function which is C^k over $[a, b]$ where $k \geq 2n+1$ and that $f^{(2n-1)}(a) \neq f^{(2n-1)}(b)$. Let $T_n(h)$ be the approximation of $I = \int_a^b f(x)dx$ computed with n iterations of Romberg's method using the initial step $h = [(b-a)/M]$ ($M \geq 1$). Then*

$$C_{T_n(h), T_{n+1}(h)} = C_{T_n(h), I} + O\left(\frac{1}{n^2}\right)$$

The proof of this theorem can be consulted in (Jézéquel and Chesneaux, 2004).

If the convergence zone is reached, *i.e.*, if $O(1/n^2) \ll 1$, the significant digits common to two successive approximations, $T_n(h)$ and $T_{n+1}(h)$, are also in common with the exact value of the integral.

If computations are performed until, in the convergence zone, the difference between two successive approximations has no exact significant digit, then the significant digits of the last approximation which are not affected by rounding errors are in common with the exact value of the integral.

The equation given in theorem 3 is different from the one in theorem 1, established for approximation methods. Indeed Romberg's method is not an approximation method with an order known beforehand. The approximation $T_n(h)$ obtained with n iterations of Romberg's method is exact if the integrand is a polynomial of

degree r with $r \leq 2n - 1$. Moreover the dynamical control of Romberg's method is not based on successive divisions of an integration step. This dynamical control consists in comparing two successive approximations, $T_n(h)$ and $T_{n+1}(h)$, and not $T_n(h)$ and $T_n([h/2])$.

4.6. Numerical experiment

Let us consider the integral

$$I = \int_0^1 \frac{\arctan(\sqrt{2+t^2})}{(1+t^2)\sqrt{2+t^2}} dt$$

The evaluation of this integral is a problem that has been posed by Ahmed (2002). Bailey and Li (2003) have indicated its exact value: $I = (5\pi^2)/96$. Therefore, its 16 first exact digits are: $I \approx 0.5140418958900708$.

This integral has been evaluated using the different strategies previously described. Let I_n be the approximation to I computed:

- Using the composite trapezoidal rule or the composite Simpson's rule with the step $1/(2^n)$.
- By partitioning the interval $[0,1]$ into 2^n subintervals on which the Gauss-Legendre method with 12 points is applied.
- Or by performing n iterations of Romberg's method with the initial step $h = 1$.

Approximations I_n have been computed in DSA, using the CADNA library, until the difference $I_n - I_{n+1}$ has no exact significant digit. From the theoretical results previously presented, the exact significant bits (*i.e.*, not affected by rounding errors) of the last approximation I_N are in common with I , up to one.

Table 1 presents the approximations to I obtained in single and in double precision. In every sequence, only the exact significant digits of the last iterate, estimated using DSA, are reported.

Table 1. Approximations to $I \approx 0.5140418958900708$.

Method	In Single Precision	In Double Precision
Trapezoidal	$I_8 = 0.51404E+000$	$I_{19} = 0.5140418958899E+000$
Simpson	$I_8 = 0.514041E+000$	$I_{10} = 0.51404189589007E+000$
Gauss-Legendre	$I_1 = 0.5140419E+000$	$I_1 = 0.514041895890070E+000$
Romberg	$I_8 = 0.514041E+000$	$I_8 = 0.514041895890070E+000$

It is noticeable that the exact significant digits of each approximation I_N obtained are in common with I , up to one. The error $I_N - I$ is always a computational zero. Because of rounding errors, the computer cannot distinguish the approximation obtained from the exact value of the integral.

The number of iterations required for the stopping criterion to be satisfied may depend on the precision chosen, but also on the quadrature method used. Indeed the convergence speed of the computed sequence and the numerical quality of the result obtained vary according to the quadrature method. Starting from I_0 (the approximation obtained with no partition of the integration interval), the sequence generated by the Gauss–Legendre method with 12 points converges particularly quickly: in two iterations, a result with an excellent numerical quality is obtained whatever the precision chosen is.

5. Conclusion

Discrete Stochastic Arithmetic (DSA) is an automatic method for rounding error analysis, which uses a random rounding mode. DSA has been implemented in the CADNA library, which enables one to estimate rounding error propagation in any scientific code. Furthermore CADNA can detect any numerical instability which may occur at run time.

In order to obtain with an approximation method a result for which the global error (consisting of both the truncation error and the rounding error) is minimal, a strategy, based on a converging sequence computation, has been proposed. Computation is carried out until the difference between two successive iterates has no exact significant digit. Then it is possible to determine which digits of the result obtained are in common with the exact solution. This strategy can apply to the computation of integrals using the trapezoidal rule, Simpson’s rule, Romberg’s method or the Gauss–Legendre method.

Improvements in automatic methods for rounding error analysis are required because of the performances, always higher, of computers. In order to enable an estimation of rounding errors at a moderate computing cost, one has to take into account the evolution of the architectures, the compilers and the processors.

References

Ahmed, Z. Definitely an integral. *American Mathematical Monthly*, 109(7):670–671, 2002.

Bailey, D.H. and X.S. Li. A comparison of three high-precision quadrature schemes. In *Proceedings of the 5th Real Numbers and Computers Conference*, pages 81–95, Lyon, France, September 2003.

Bauer, F.L., H. Rutishauser, and E. Stiefel. New aspects in numerical quadrature. In *Proceedings of the Symposia Applied Mathematics*, volume XV, pages 199–218, American Mathematical Society, Providence, R.I., 1963.

Burden, R.L. and J.D. Faires. *Numerical analysis*. Brooks-Cole Publishing, 7th edition, Pacific Grove, CA, USA, 2001.

Chesneaux, J.-M. Study of the computing accuracy by using probabilistic approach. In C. Ullrich, editor, *Contribution to Computer Arithmetic and Self-Validating Numerical Methods*, pages 19–30, IMACS, New Brunswick, New Jersey, USA, 1990.

Chesneaux, J.-M. The quality relations in scientific computing. *Numerical Algorithms*, 7:129–143, 1994.

Chesneaux, J.-M. *L'arithmétique stochastique et le logiciel CADNA*. Habilitation à diriger des recherches, Université Pierre et Marie Curie, Paris, November 1995.

Chesneaux, J.-M. and F. Jézéquel. Dynamical control of computations using the trapezoidal and Simpson's rules. *Journal of Universal Computer Science*, 4(1):2–10, 1998.

Chesneaux, J.-M. and J. Vignes. Sur la robustesse de la méthode CESTAC. *Comptes rendus de l'Académie des sciences, Paris, Série I, Mathématiques*, 307:855–860, 1988.

Chesneaux, J.M. and J. Vignes. Les fondements de l'arithmétique stochastique. *Comptes Rendus de l'Académie des Sciences de Paris, Série I. Mathématiques*, 315:1435–1440, 1992.

Conte, S.D. and C. de Boor. *Elementary numerical analysis*. McGraw-Hill, International Student edition, 1980.

Engels, H. *Numerical quadrature and cubature*. Academic Press, London, UK, 1980.

Goldberg, D. What every computer scientist should know about floating-point arithmetic. *ACM Computing Surveys*, 23(1):5–48, 1991.

Jézéquel, F. Dynamical control of converging sequences computation. *Applied Numerical Mathematics*, 50(2):147–164, 2004.

Jézéquel, F. *Contrôle dynamique de méthodes d'approximation*. Habilitation à diriger des recherches, Université Pierre et Marie Curie, Paris, February 2005.

Jézéquel, F. and J.-M. Chesneaux. Computation of an infinite integral using Romberg's method. *Numerical Algorithms*, 36(3):265–283, July 2004.

Jézéquel, F., F. Rico, J.-M. Chesneaux, and M. Charikhi. Reliable computation of a multiple integral involved in the neutron star theory. *Mathematics and computers in simulation*, 71(1):44–61, 2006.

Muller, J.-M. *Arithmétique des ordinateurs*. Masson, Paris, France, 1989.

Rump, S.M. *Reliability in computing. The role of interval methods in scientific computing*. Academic Press, London, UK, 1988.

Stoer, J. and R. Bulirsch. *Introduction to numerical analysis*, volume 12 of *Texts in applied mathematics*. Springer, 3rd edition, 2002.

Vignes, J. Zéro mathématique et zéro informatique. *Comptes rendus de l'Académie des sciences, Paris, Série I, Mathématiques*, 303:997–1000, 1986. also: *La Vie des Sciences*, 4 (1):1–13, 1987.

Vignes, J. Estimation de la précision des résultats de logiciels numériques. *La Vie des Sciences*, 7(2):93–145, 1990.

Vignes, J. A stochastic arithmetic for reliable scientific computation. *Mathematics and Computers in Simulation*, 35:233–261, 1993.

Vignes, J. A stochastic approach to the analysis of round-off error propagation. A survey of the CESTAC method. In *Proceedings of the 2nd Real Numbers and Computers conference*, pages 233–251, Marseille, France, 1996.

Vignes, J. and M. La Porte. Error analysis in computing. In *Information Processing 1974*, pages 610–614. North-Holland, 1974.

**THEME III. CALIBRATION
AND SENSITIVITY ANALYSIS**

Model calibration/parameter estimation techniques and conceptual model error

Petros Gaganis

Department of Environment, University of the Aegean, University Hill, Xenia Building, 81100 Mytilene, Greece.

Abstract

In a modeling exercise, errors in the model structure cannot be avoided because they arise from our limited capability to exactly describe mathematically the complexity of a physical system. The effect of model error on model predictions is not random but systematic, therefore, it does not necessarily have any probabilistic properties that can be easily exploited in the construction of a model performance criterion. The effect of model error varies in both space and time. It is also different for the flow and the solute transport components of a groundwater model and may have a significant impact on parameter estimation, uncertainty analyses and risk assessments. Structural errors may result in a misleading evaluation of prediction uncertainty associated with parameter error because model sensitivity to uncertain parameters may be quite different than that of the correct model. A substantial model error may significantly degrade the usefulness of model calibration and the reliability of model predictions because parameter estimates are forced to compensate for the existing structural errors. Incorrect uncertainty analyses and estimated parameters that have little value in predictive modeling could potentially lead to an engineering design failure or to a selection of a management strategy that involves unnecessary expenditures. A complementary to classical inverse methods model calibration procedure is presented for assessing the uncertainty in parameter estimates associated with model error. This procedure is based on the concept of a per-datum calibration for capturing the spatial and temporal behavior of model error. A set of per-datum parameter estimates obtained by this new method defines a posterior parameter space that may be translated into a probabilistic description of model predictions. The resulted prediction uncertainty represents a reflection on model predictions of available information regarding the dependent variables and measures the level of confidence in model performance.

Keywords: model calibration, parameter estimation, conceptual error, model error, inverse method, uncertainty, groundwater modeling.

1. Main sources of uncertainty in mathematical modeling

Computer models that simulate groundwater flow and contaminant transport are invaluable tools that can be used to aid in assessment of risks and management decisions. Unfortunately, there is typically considerable uncertainty in the predictions from a computer model. The error associated with mathematical modeling can be categorized into two main types: (1) model error which results from the use of an inadequate model with the true set of parameter values (the correct parameters for a perfect model), and (2) parameter error which assumes the use of a perfect model with parameters subject to uncertainty. When modeling natural hydrogeologic systems, these two types of error exist simultaneously.

In modeling groundwater flow and contaminant transport, parameter error is mainly produced from uncertainties in the values of the hydraulic parameters. In groundwater problems, such parameters are, for example, hydraulic conductivity, sorption coefficient or porosity. These medium properties can be measured in the field or on lab samples, independent from the model itself. Parameter measurements always carry a degree of uncertainty. Furthermore, additional uncertainty is introduced from the usually small number of available measurements and the differences between the scale of the parameter measurements and appropriate parameter value at the model grid scale (Beckie, 1996).

There are at least three important sources of model error. First, mathematical and modeling limitations result in all models being simplifications and approximations of reality (Sun *et al.*, 1998). This source of model error is related to such issues as the use of one-dimensional or two-dimensional models to describe three-dimensional processes, the assumption of isothermal conditions or steady-state flow, the use of the Fickian model to quantify the dispersive flux, and the use of a finite domain. Second, the representation of multiple processes as a single process when there is little information on their mathematical description will also lead to uncertainty in model prediction. The mathematical definition of such processes is often empirical and speculative. The release function of contaminants into a flow system can be cited as an example. The source concentration and its temporal and spatial distribution can be the result of complex serial or parallel processes. Such processes may involve mechanical and chemical weathering, biochemical and biological influences on the form of each component, infiltration and dissolution rates, and flow and transport through the unsaturated zone. Detailed modeling of all these processes is practically impossible. Third, our inability to predict how physical or chemical characteristics of the hydrogeological system might change in the future will give rise to additional uncertainty. In the common practice of extrapolating from the past to the future, there is not only uncertainty from the imperfect description of the past, but also uncertainty about how much the future will be like the past (Morgan *et al.*, 1990). Model error arising from sources one and two can be reduced with further research and more detailed modeling. However, the third source of model error should be distinguished from the other two as being

irreducible even in principle. Accounting for this source of error when modeling physical systems involves a great deal of subjective judgment defines the limits of prediction reliability.

2. Simulation models, model calibration and prediction reliability

The development of a simulation model to aid in the solution of a groundwater problem can be broadly viewed as a procedure that includes four sequential steps: (1) model construction, (2) model calibration, (3) model selection from among alternative calibrated models, which in a sense is equivalent to model validation, and (4) model prediction of system behavior under changed conditions or in the future. Step 1 begins with the formulation of an appropriate conceptual model, which is then translated into a mathematical model. In step 2 and step 3, the appropriate conceptual model and parameter values are selected by minimizing the model misfit to field data through an iterative (inverse) exercise. There are several criteria suggested during the last three decades for selecting among alternative conceptual models (e.g., Schwarz, 1978; Cooley *et al.*, 1986; Carrera and Neuman, 1986; Luis and McLaughlin, 1992; Poeter and Hill, 1997) or combinations of several model structures and parameters sets (Beven and Binley, 1992; Beven and Freer, 2001; Neuman, 2003, Ye *et al.*, 2004). More detail on the main model selection methodologies as well as their strengths and limitations can be found in (Gaganis and Smith, 2001). For a review and comparison of the most important approaches to model calibration the reader is referred to McLaughlin and Townley (1996), Zimmerman *et al.* (1998), Carrera *et al.* (2005) and Hill and Tiedeman (2007). Typically, the goodness of fit between model output and field data is used as a measure for judging not only the performance of model calibration and model selection but also the effectiveness of the selected model as a predictive tool (step 4). However, the primary goal of a groundwater modeling exercise is to obtain reliable model predictions, ideally in the form of a probability distribution for the dependent variables such as hydraulic head and/or solute concentration to be used, for example, in a decision process.

The incomplete knowledge of a hydrogeologic setting leads to a subjective model structure that depends on the modeler's interpretation of the available data. Although criteria suggested for selecting among alternative conceptual models (*i.e.*, Carrera and Neuman, 1986; Poeter and Hill, 1997) may assist in selecting the most likely model, more than one conceptual model is usually possible (Beven and Freer, 2001). A successful model calibration may be achieved with erroneous or inadequate models because of the non-uniqueness of parameter estimates, limited calibration data, limited prior information, as well as the subjectivity in defining a "good match" to observed data. Among the set of competing models, uncertain parameters can be adjusted to achieve an acceptable fit between model output and the corresponding field observations. The long-term predictions

obtained by these models, even though calibrated to the same set of observations, may be quite different and, in some cases, may be misleading. Therefore, as illustrated with several case histories in Konikow and Bredehoeft (1992), a “successful” application of model calibration methodologies does not necessarily justify high confidence in the predictive capability of a groundwater model.

Hydrogeological decision models provide a framework to take explicit account of the uncertainty in model predictions during the evaluation of different management alternatives (e.g., Freeze *et al.*, 1990; Smith and Gaganis, 1998). Typically, the smaller the standard deviation of the probability distribution for the dependent variable (*i.e.*, the model prediction), the more likely it is that a clear and unequivocal determination of the preferred management alternative will be achieved. A reduction in prediction uncertainty is usually addressed by reducing the parameter uncertainty through a combination of model calibration and collection of additional field data on parameters and/or the dependent variables. However, a substantial model error may significantly degrade the usefulness of model calibration and the reliability of model predictions because parameter estimates are forced to compensate for structural errors. As studies on aggregation error (a form of model error) by Warwick (1989) have shown, an emphasis on decreasing parameter uncertainty and ignoring the uncertainty in the model structure might not result in increased model predictive capability. Reliable predictions require all sources of error to be taken into account. The reliability of model predictions increases as the magnitude of model error decreases. Selecting an appropriate model structure is an important issue that may lead to more informative predictions, but evaluating the “goodness” of this model structure, that is quantifying the effect of model error, may be a critical step for assessing and increasing the reliability of model predictions.

This chapter is concerned with two main issues: (i) to demonstrate the effect of model error on the single-objective inversion problem for hydraulic head and contaminant concentration data, and (ii) to describe a general inverse methodology, which may complement the standard inverse procedures, to extract useful information on errors in model structure from the data and to project their effect onto model predictions and calibration process. This methodology may represent a useful tool for evaluating the performance of classical single-objective calibration in terms of the predictive capability of the model, testing the validity of assumptions regarding error statistical distributions underlying the estimation of parameters and their confidence interval in classical single-objective calibration, and evaluating alternative conceptual models in terms of the correctness of the model structure.

3. A simple synthetic example

In order to illustrate the main points and concepts that follow, a simple model of a two-dimensional synthetic flow system is used here. This flow problem was originally modified from Weiss and Smith (1998) and was also used in Gaganis and Smith (2001, 2006). The dimensions of the flow system is 600 m by 600 m and

contains two homogeneous and isotropic transmissivity zones, one zone of enhanced recharge and two specified head boundaries (Figure 1). The rest of the model boundaries are no flow boundaries. The flow system is assumed to be at steady state. For the contaminant transport problem, solute is introduced at the source area along the upstream constant head boundary. Hydraulic heads and solute concentrations are measured at 15 sampling locations equally distributed throughout the flow domain. Observed (free of measurement error) values of hydraulic heads and solute concentrations are simulated by running a forward deterministic simulation using the true parameter values shown in Table 1, and calculating them at the 15 sampling locations (see Figure 1). The true contaminant

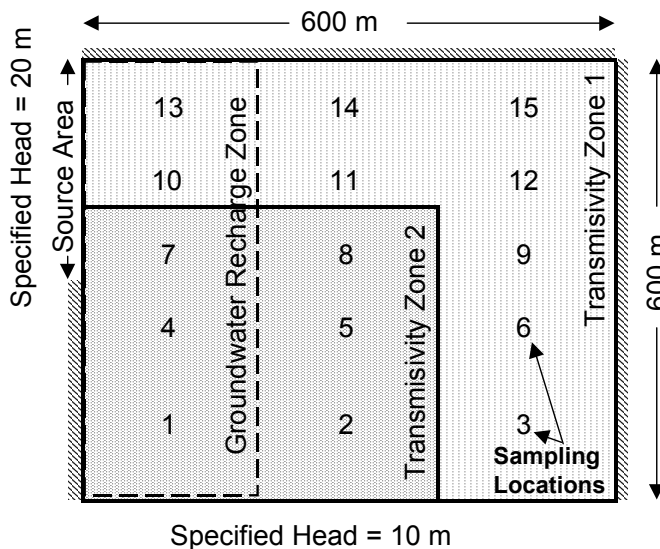


Fig. 1. Synthetic flow model. “True” geometry and boundary conditions.

Table 1. True parameter values in deterministic simulation of synthetic model.

Parameter	Value
Recharge (m/day)	0.0004
Porosity	
Zone 1	0.2
Zone 2	0.2
<i>Transmissivity (m²/day)</i>	
Zone 1	20
Zone 2	2
<i>Dispersivity (both zones) (m)</i>	
Longitudinal	10
Transverse	1

Table 2. Prior distributions assigned to uncertain parameters of synthetic model.

Parameter	Distribution	Lower Bound	Mean	Upper Bound
Transmissivity (m^2/day)				
zone 1	Uniform	10	20	30
zone 2	Uniform	1	2	3

release function used in this simulation is assumed to be a linear function of time with a normalized concentration value equal to 1 at time zero and 0 at 500 days. Adding Gaussian errors to the simulated true observations with a standard deviation of 10 cm for the hydraulic head and 5.0% of the concentration values generated the observed data values, subject to measurement error.

Two other models are constructed by introducing model error to the true model described above. Model 1 assumes a uniform contaminant source release function. The source duration is designed to introduce the same solute mass into the system as that of the true linear function. Only the solution of the transport problem of model 1 is influenced by the model error, the flow problem is not. In model 2, the recharge area is expanded in the horizontal direction from 200 m to 300 m. This increase in recharge will affect both the flow and the solute transport parts of the problem. The true linear source function is used in model 2. For all models, only the two transmissivities are considered uncertain and are estimated.

Prior information on the effective values of the two transmissivity zones is incorporated into our analysis by defining a range of feasible parameter values (prior parameter space) within the parameter space of the model (Table 2). For the given example problem, our analysis is not sensitive to the adoption of a greater prior parameter space. Therefore, a relatively small parameter range is assigned to the uncertain parameters to reduce the computational cost. For demonstration reasons, the prior parameter distributions are assumed uniform.

4. Interrelation of parameter uncertainty and model error

Let us denote by f^* and θ^* the forward operator of the perfect model and the true parameter vector, respectively. The n -dimensional space Θ represents the prior parameter space and contains all the feasible combinations of parameter values θ , where n is the number of model parameters. It is assumed that $\theta^* \in \Theta$. Given an error free set of observations d^* of the dependent variable, it follows that $f^*(\theta^*) = d^*$. The actual observations of the dependent variable are defined as $d = d^* + e_o$, where e_o represents the variability of observations about the true value and is referred to as *measurement error*. Measurement error arises from random error in direct measurement of a quantity and imperfections in the instruments and techniques used.

Let f be the forward operator of a model M that describes the same system but is subject to model error. Following the definitions given earlier, parameter error is the deviation of $f^*(\theta)$ from $f^*(\theta^*)$, and model error (of M) is the amount that $f(\theta^*)$ differs from $f^*(\theta^*)$. Both parameter error and model error are measured relative to the prediction of the dependent variable (*i.e.*, hydraulic head, solute concentration). On one hand, we see that parameter error is not model dependent (it does not depend on f) and its quantification requires knowledge of f^* , $f^*(\theta^*)$ and θ . The true forward estimator f^* is naturally unknown since it represents the absolute truth. Even the most complete characterization of a hydrogeologic system will not make the construction of a perfect model possible. This fact raises questions regarding the accuracy of any parameter error evaluation, especially in the absence of any information regarding model error. On the other hand, in quantifying model error we have to know θ^* and $f^*(\theta^*)$. These values for θ^* and $f^*(\theta^*) = d^*$ are properties of the true model and can be estimated from measurements in the field or on lab samples, independent from the model M . Prior information about the parameters and observations on the dependent variables impose constraints on θ^* and d^* in the form of probability distributions. Generally, d^* can be evaluated with acceptable accuracy. On the contrary, the estimation of θ^* is commonly highly uncertain due to inherent heterogeneity, scaling issues and limited project budgets. Prior information in most cases is sparse (if it exists), since the number of measurements required for “proper” characterization of θ^* involves considerable cost. These problems cause the evaluation of model error directly from its definition as $[f(\theta^*) - f^*(\theta^*)]$ to be subject to large uncertainties and of little use in practice.

Although the importance of model error is generally recognized, it has attracted relatively little research. There is still no general methodology for quantifying the impact of model error on model predictions, nor for assessing its importance relative to parameter error. The quantification and propagation of parameter uncertainty has been studied extensively in the past three decades (see Dagan, 1989; Gerhar, 1993) leading to the development of various stochastic methods for assessing the impact of input parameter uncertainty on model predictions. Parameter error is typically evaluated as the observed uncertainty in a model output obtained by propagating input parameter uncertainty through the model. Its effect on model predictions is approximated as $G[f(\theta) - f(\hat{\theta})]$. The function G allows for different measures of the distance between the two quantities, and $\hat{\theta}$ is the maximum likelihood parameter vector θ estimated as $f(\hat{\theta}) \approx d$. The appropriateness of parameter uncertainty analysis is typically justified with the argument that the contribution of parameter uncertainty on prediction uncertainty is far more important than that of the uncertainty about the form and structure of the model:

$$G[f^*(\theta) - f^*(\theta^*)] \gg G[f(\theta^*) - f^*(\theta^*)]$$

While the assumption of the relative unimportance of model error probably holds in stochastic modeling when parameter uncertainty is large and obscures the

impact of model error, this does not imply that $f \approx f^*$, nor that $\hat{\theta} \approx \theta^*$. Furthermore, no conclusions can be drawn regarding the accuracy of the estimated parameter error. Parameter error estimated as $G[f(\theta) - f(\hat{\theta})]$ may not be close to the true parameter error $G[f^*(\theta) - f^*(\theta^*)]$, since it is conditional to model M and therefore “contaminated” with model error, in addition to measurement error which enters the analysis through $\hat{\theta}$. Parameter sensitivities for model M may be quite different from the true sensitivities, resulting in a misleading evaluation of the uncertainty of model predictions. This point is illustrated in Figure 2. This figure shows the prediction uncertainty, regarding the transport solution at 500 days of the synthetic example presented in the previous section, associated with the input parameter uncertainty shown in Table 2 for the true model (solid lines) and model 2 (dotted lines). The prediction uncertainty is presented as upper and lower bounds of probable concentration values at the 12 out of 15 sampling locations that have reached by the contaminant. It can be seen that using model 2 (incorrect model structure) for assessing the impact of input parameter uncertainty on model predictions may result in overestimating the prediction uncertainty, in most sampling locations, by several orders of magnitude. In some cases, for example at sampling location 8, the effect of model error on such an assessment may be a possible cause of failure, let say, of an engineering design.

From the above discussion, it is apparent that model and parameter errors are interrelated. The minimization of model error is a prerequisite for a meaningful parameter uncertainty analysis. On the other hand, however, parameter uncertainty may obscure and “cover up” the impact of model error on model predictions. The effect of model error on model results can be only “seen” when its magnitude is

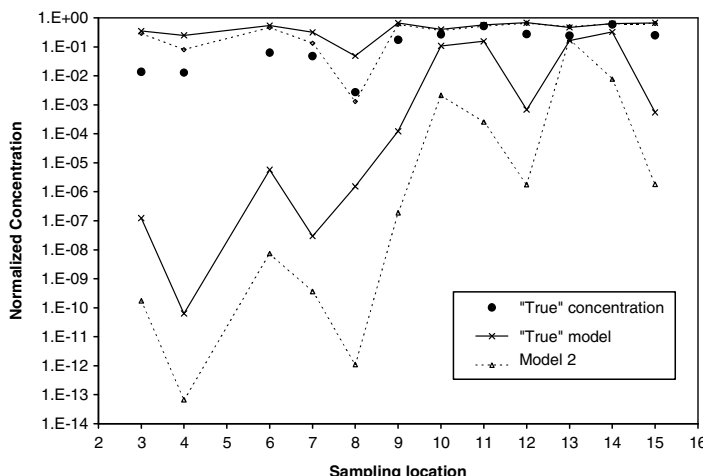


Fig. 2. Prediction uncertainty, associated with the parameter uncertainty in Table 2, regarding concentrations at 500 days for the true model (solid lines) and model 2 (dotted lines).

equivalent to or greater than the error imposed by the level of parameter uncertainty. It follows that if parameter uncertainty is reduced further than a certain level, model error will become dominant, and may result in model prediction uncertainty bounds that do not contain the “true” depended variables. The reduction of parameter uncertainty is typically achieved by model calibration, which brings in all the information on the parameters that is embedded in a set of measurements of the dependent variables. However, when accounting for model error in an inverse procedure, the degree to which parameter uncertainty may be reduced by model calibration, and the resulting level of model prediction uncertainty, should depend on the magnitude of model error present. This level of prediction uncertainty may also be an appropriate criterion for assessing the performance and comparing the different inverse approaches.

5. Single-objective calibration and model conceptual errors

5.1. Single objective inversion

The forward problem that describes the relation between the values of a dependent variable observed in the field and model predictions may be represented with an equation in the following form:

$$d = f(\theta) + e \quad (1)$$

where d and θ are the vectors of observations and model parameters respectively, f is the forward equation representing the mathematical model and the vector e is a residual which describes the deviation between measured and predicted values of the dependent variables. Thus, e accounts for measurement error in the observations e_o as well as for model imperfections ($e = e_o + e_m$), where e_m is the model error. In groundwater hydrology the forward equation is typically the groundwater flow or/and advection-dispersion equations, subject to initial and boundary conditions. Uncertainty in the parameters θ degrades the usefulness of the model $f(\theta)$ as a predictive tool. This is where an inverse problem arises. Inverse procedures define an inverse estimator \hat{f} that connects the observations d to “good” estimates $\hat{\theta}$ of the parameters of interest:

$$\hat{\theta} = \hat{f}^{-1}[f(\theta) + e] \quad (2)$$

There are a number of methods proposed for solving the inverse problem. An excellent review and comparison of these methods is presented in McLaughlin and Townley (1996). A solution is typically obtained by minimizing the residual e . Such an approach is the classical (weighted) least square method. In least squares fitting, the parameters $\hat{\theta}$ are selected by minimizing the sum of squared differences between measured values and the corresponding predictions:

$$\min_{\theta} \sum [d - f(\theta)]^2 \quad (3a)$$

or,

$$\min_{\theta} (d - f(\theta))^T V^{-1} (d - f(\theta)) \quad (3b)$$

where the superscript T denotes a matrix transpose, V is an $n \times n$ positive definite variance-covariance matrix and n is the number of parameters to be estimated.

When measurement error and errors in model structure are present, driving (3a) to zero or equivalently driving the residual e to zero is not achievable and obviously incorrect. In justifying (3a) as a solution of (2), we have to make some assumptions regarding the statistical distribution of e . In most applications the probability distribution for measurement error e_o is assumed to be Gaussian with mean zero and variance σ^2 . Apart from reasons of mathematical convenience, this probabilistic description of measurement error e_o appears reasonable. In contrast, describing model error e_m with a probability distribution may not be appropriate. Model error is not random but systematic. For example, the error introduced by overestimating the strength of the contaminant source in a solute transport model will not be random. The estimated solute concentrations by this model will be systematically higher than the observations, and the risk of contamination will be consistently overestimated. Therefore, e_m has to be assumed equal to zero or at least much smaller than e_o in order to have a minimal influence on the statistical behavior of e . The residual e and measurement error e_m are then expected to be statistically similar.

Given that the probability density for measurement error is Gaussian, criterion (3a) can be written as (3b). One of the most important limitations of the above approach in model calibration is the difficulty in locating a unique parameter set. The minimization (3b) may yield a number of plausible solutions that provide no means for the selection of a unique “best” parameter estimate. For dealing with this problem of non-uniqueness, Neuman (1973) proposed a second objective, that of physical plausibility. Inverse methods in groundwater hydrology have gradually evolved to include prior information with respect to model parameters. This was achieved by adding to the term that penalizes deviations of predictions from observations a second term that penalizes deviations of estimated parameter values from prior parameter estimates (e.g., Gavalas *et al.*, 1976; Cooley, 1982, 1983; Kitanidis and Vorvoris, 1983; Carrera and Neuman, 1986). These inverse algorithms adopted either a blocked (e.g., Carrera and Neuman, 1986) or a geostatistical approach (e.g., Kitanidis and Vorvoris, 1983) for describing spatial variability of the hydrogeologic properties.

The majority of available methods (linear or non-linear) that incorporate prior information are equivalent or minor variants of the Maximum a posteriori approach, given that the prior parameter distributions and measurement error probability densities are assumed to be Gaussian (McLaughlin and Townley, 1996). This approach, which is based on a Bayesian interpretation of parameter

uncertainty, uses Bayes' rule to identify the maximum likelihood parameter values. For single-objective parameter estimation using hydraulic heads, solute concentrations and prior information on the parameters, the general form of the objective function to be minimized is:

$$\begin{aligned}\Phi(\theta) = & w_h (d_h - f_h(\theta))^T V_h^{-1} (d_h - f_h(\theta)) \\ & + w_c (d_c - f_c(\theta))^T V_c^{-1} (d_c - f_c(\theta)) \\ & + (\theta_p - \theta)^T V_p^{-1} (\theta_p - \theta)\end{aligned}\quad (4)$$

where the subscripts h and c denote those terms relating to hydraulic head data and solute concentration data respectively, and the p subscript denotes the terms relating to prior information. The weights w_h and w_c represent the accuracy or importance of one data set relative to another. Matrices V_h and V_c define the covariances among the hydraulic head and concentration data respectively, and the matrix V_p represents the accuracy of prior information and weights the third term against the two first. Prior information usually enters the calculations in the form of parameter bounds or as an interpolation algorithm through the use of kriging (McLaughlin and Townley, 1996).

This formulation of the inverse problem assumes the forward equation f to be known perfectly. This assumption can be questioned in practical applications where the initial and boundary conditions and forcing terms are usually uncertain. As Gupta *et al.* (1998) suggested, the magnitude of model error for some regions of model predictions in space or time may be comparable to, if not much larger than measurement error. This suggestion is consistent with observations in most applications of the inverse procedures, where measurement errors are not large enough to explain the magnitude of the calculated residual e (McLaughlin and Townley, 1996). Model calibration can be thought as a process of forcing a model structure to fit the data. In the case of substantial model error, it results in incorrect parameter estimates forced to compensate for errors in model structure that are not taken into account (Beck, 1987). Therefore, model calibration does not necessarily lead to an estimation of $\hat{\theta}$ close to θ^* , and to a predictive tool $f(\hat{\theta})$ equivalent to $f^*(\theta^*)$. A simple example given in McLaughlin and Townley (1996) illustrates this point: when groundwater recharge is neglected (or incorrectly specified), the estimates of hydraulic conductivity generated by the inverse algorithms are unrealistic. The greater the error in specifying the recharge rate is, the greater the deviation of the estimated values from the true values. These conductivities may give a good match to observations but they have little value for predictive modeling.

It is clear that the parameter values estimated by an inverse procedure contain information regarding the magnitude of model error present. This fact suggests that model error could be evaluated in the parameter space \mathcal{O} . Gupta *et al.* (1998) proposed a formulation to parameter estimation that deals with the uncertainty in defining a "statistically correct" objective function for determining the best fit of model predictions to observations. With this formulation, the solution to the

inverse problem consists of a set of equally probable parameter vectors rather than a single parameter set. Given the existence of model error in addition to measurement error, such a solution to the inverse problem (in a form of such probability distributions for the parameter vectors) may better reflect the state of available information and provide more information on the strengths and limitations of a model. However, one may argue that the effect of model error on parameter estimates is often greater than the uncertainty associated with the existence of multiple ways in which the best fit of a model to the data can be defined. A more informative probability distribution of parameter estimates may be obtained through an evaluation of the total effect of model error on model calibration.

5.2. *Single-objective calibration and model error evaluation*

If we try to isolate the effect of errors in the model structure on parameter estimates obtained by equation (4), we will face the following four problems:

1. Model error is not random, and therefore does not necessarily have any probabilistic properties (Gupta *et al.*, 1998). Model error varies with location and time. The spatial and temporal distribution of model error for model 1 and model 2 regarding solute concentrations is shown in Figures 3 and 4, respectively. The spatial distribution of model error for the steady state flow solution of model 2 is presented in Figure 5. Model error is calculated by comparing the output of a deterministic simulation, using each model and the true parameter set, to the error-free data. It is presented as the percentage difference from the true dependent variable at a specific time and location. From these figures it is clear that an assumption of a probability distribution for model error is not justified. Furthermore, the effect of model error is also different for the flow and the solute transport components of the model. As can be seen by comparing Figure 4 with Figure 5, the effect of model error on the transport solutions of model 2 is different from its effect on flow solution regarding the magnitude, as well as, the spatial distribution. These characteristics of model error can not be captured by an objective function like equation (4), which is based on the normality assumption for error statistical distributions. The effect of model error in equation (4) appears in both the parameters estimates and the residual quantity. Even if we were able to isolate and evaluate the effect of model error on the parameters estimated by the equation (4), this would not be informative since it would represent an average measure of the effect of model error for both flow and transport components of the model in space and time. Such an evaluation of model error may not be correct because it will lead us to either overestimated or underestimated confidence levels to model predictions at different locations.

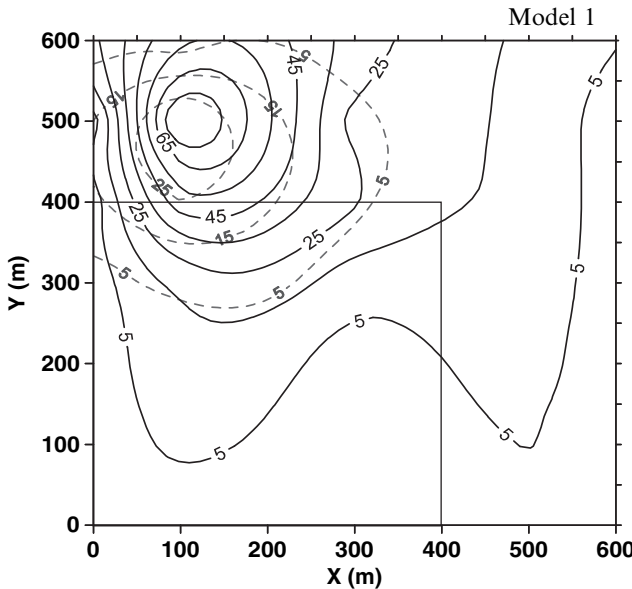


Fig. 3. Spatial and temporal distribution of model error for Model 1. The dashed and the solid lines represent model error contours at time 250 days and 500 days respectively. Model error is measured as the percent difference of model predictions with the true parameter values, from the true concentrations (prediction of the true model) at each location and time.

2. The inclusion of prior information in (4), even though it decreases the ill-posedness of the inverse problem, may not solve the problem of non-uniqueness of the parameter estimates (Carrera and Neuman, 1986). It is suggested that multiple minima in the objective function may also arise from errors in model structure. Let us define a high-likelihood region A as the region within Θ that corresponds to all parameter values that provide an acceptable fit to the data given the magnitude of measurement error (e.g., a joint confidence interval that correspond to one standard deviation about the parameter estimates). A unique high-likelihood region then exists for each data value used to calibrate a model. Assume we calibrate a model at each data point d_i , $i = 1, \dots, m$ separately (per-datum calibration). If the model is correct (exactly describes the true system), the true parameter vector will be contained in each one of the high-likelihood regions $A_1, A_2, \dots, A_m \in \Theta$. Then, the intersection $A_1 \cap A_2 \cap \dots \cap A_m = B$ of these high-likelihood regions, that consists of the parameter vectors contained in all A_1, A_2, \dots, A_m , will be different than zero and will contain the true parameter values. By definition, B also represents the solution to the single objective parameter estimation problem. Therefore, a correct model structure will result in a unique solution to the single-objective parameter estimation problem. This point is demonstrated in Figure 6 for the case where the number of unknowns and the number of observations are equal. Concentration data at only two

sampling locations (locations 7 and 13 at 500 days) are used in parameter estimation. These concentration data are corrupted with measurement error. For this example, no hydraulic head data are incorporated in the inversion. The response surfaces (plots of the objective function into the parameter space) of the true model and model 1 are shown in Figure 6a and 6b respectively. In these figures, the parameter values in both axes are scaled to their respective true values to better represent the relative uncertainties in the parameter estimates. Because of the scaling, the true parameter set coincides with the point in the normalized parameter space $T_1 = T_2 = 1$. In model 1, the different magnitude of model error at sampling locations 7 and 13 result in the development of two local minima in the solution of the objective function. The true model structure, on the other hand, produces a unique minimum. When hydraulic head and concentration data at all 15 sampling locations are used, the algebraically over-determined inverse problem yields the same unique solution for the true model and a unique, but different solution for model 1.

3. Different inverse approaches may result in large differences in parameter estimates due to linearizations and various assumptions regarding statistical distributions (see Zimmerman *et al.*, 1998). The model error resulting from these approximations is impossible to quantify in a practical sense.

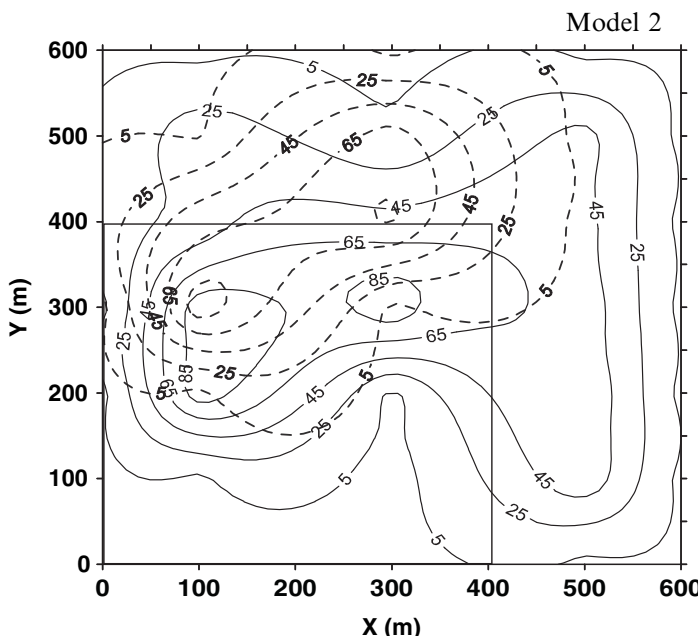


Fig. 4. Spatial and temporal distribution of model error for Model 2. The dashed and the solid lines represent model error contours at time 250 days and 500 days respectively. Model error is measured as the percent difference of model predictions with the true parameter values, from the true concentrations (prediction of the true model) at each location and time.

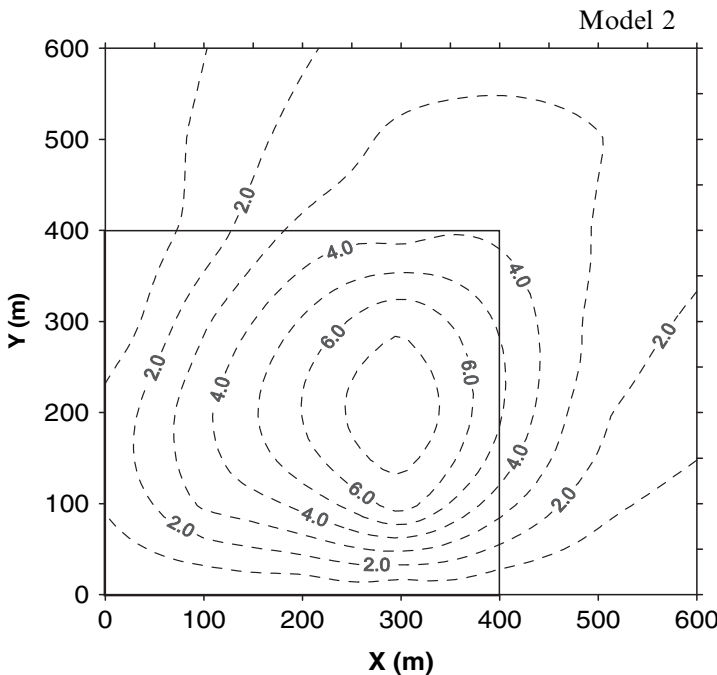


Fig. 5. Spatial and temporal distribution of model error for Model 2 regarding the steady state hydraulic heads. Model error is measured as the percent difference of model predictions with the true parameter values, from the true flow solution (prediction of the true model) at each location.

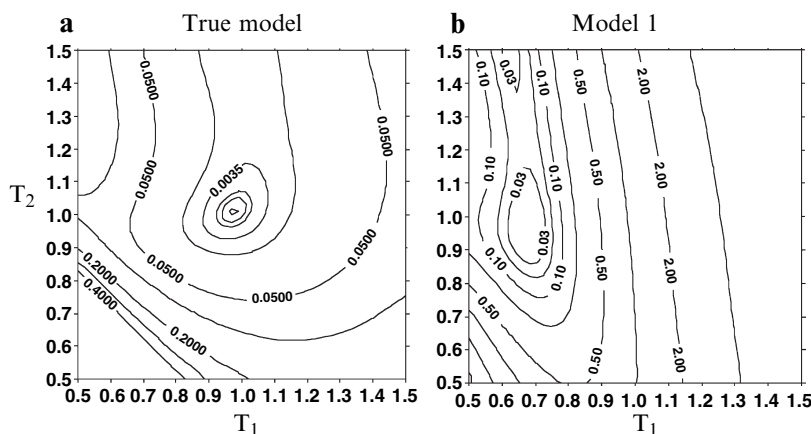


Fig. 6. Response surfaces for parameters using concentration data at sampling locations 7 and 13 (a) true model, (b) model 1 (Gaganis and Smith, 2006).

4. Each data set can be fitted in different ways. For example, a parameter set can match the early time data better than another parameter set that provides better predictions at late times. The criterion used for selecting the weights w_h and w_c in (4) may also result in significantly different parameter estimates (Weiss and Smith, 1998). Furthermore, the “optimum” parameter set will also be different when a different performance criterion is adopted (Gupta *et al.*, 1998).

These four limitations indicate that using equation (4) as the basis for evaluation of model error may offer only an approximate average measure of model error that is also subject to uncertainties related to the choice of a particular inverse procedure, weighting, and performance criteria. The reliability of model predictions strongly depends on the magnitude of model error. Because model error varies in space and time and does not have any inherent probabilistic properties, the reliability of a model will also exhibit the same behavior. One way to overcome the above limitations is to evaluate model reliability in terms of each model prediction of a dependent variable at each specific location and time, which is equivalent to evaluating the effect of model error at each data point. This idea forms the basis of the formulation of the inverse problem presented in the next section.

6. A per-datum approach to model calibration

6.1. Theoretical development

To capture the spatial and temporal characteristics of model error, the inverse problem (2) can be solved at each data point $d_{(v,l,t)}$, where v specifies the dependent variable (hydraulic head or solute concentration), l specifies the location and t the time of each available measurement. The maximum likelihood per-datum parameter vectors $\hat{\theta}_{(v,l,t)}$ may then be obtained by driving to zero an objective function of the following form:

$$\Phi(\theta_{(v,l,t)}) = G[d_{(v,l,t)} - f(\theta_{(v,l,t)})] \approx 0 \quad (5)$$

where $\Phi(\theta_{(v,l,t)})$ is the per-datum objective function and G is a performance criterion that measures the deviation of model response from the observed dependent variable. Since both measurement errors and model errors are present ($e_o + e_m > 0$), driving (5) to zero, at each measurement point of the dependent variable, offers the advantage of including all information regarding e_o and e_m within the parameter estimates $\hat{\theta}_{(v,l,t)}$. The effect of model error could then be taken into account and evaluated through an analysis of the distribution of those estimates in the parameter space \mathcal{O} .

If we include prior information on the parameters, for example in a form of specified bounds of acceptable values, equation (5) becomes (Gaganis and Smith, 2006):

$$\Phi(\theta_{(v,l,t)}) = G[d_{(v,l,t)} - f(\theta_{(v,l,t)})] - \ln p_\theta(\theta) \approx 0 \quad (6)$$

where $p_\theta(\theta)$ is the (uniform) prior probability density of θ . $p_\theta(\theta)$ is equal to 1 when $\hat{\theta}_{(v,l,t)}$ lies within the bounds and 0 when it lies outside. The second term on the right-hand side enforces the constraints imposed by prior information on the parameters by assigning an infinite penalty on estimates lying outside the feasible range \mathcal{O} . It follows that equation (6) may not have a solution within \mathcal{O} . This property of (6) offers a first test regarding the magnitude of model error. Given the correctness of \mathcal{O} , when a solution $\hat{\theta}_{(v,l,t)}$ does not exist within \mathcal{O} , it indicates that the model fails to meet the requirement of physical plausibility, or equivalently, that the degree of model error at that specific location and time is unacceptable and restructuring the model must be considered. Another important aspect of equation (6) is that it is independent of any weighting criterion. No weights have to be assigned. Furthermore, the same results will be obtained for any performance criterion G (*i.e.*, the square difference or the absolute difference or the difference of the logarithms of the predicted and measured values).

The per-datum formulation (6) to the inverse problem is always algebraically underdetermined, therefore, it does not have a unique minimum. Let us define the posterior parameter space \mathcal{Op} as the sub-region of \mathcal{O} that contains at least one solution $\hat{\theta}_{(v,l,t)}$ of (6) associated with each data point. Then, a unique per-datum solution to the inverse problem (6) can be selected through the minimization of the posterior parameter space of acceptable values \mathcal{Op} . Therefore, the bounds and size of \mathcal{Op} are determined by the location of $\hat{\theta}_{(v,l,t)}$ in the parameter space, which in turn is related to the magnitude of measurement and model errors. In order for model predictions to be informative, prediction uncertainty, or equivalently, the posterior parameter space \mathcal{Op} should be as small as it is allowed to be by the presence of errors. The minimization of \mathcal{Op} may be approximated by the following criterion applied at each measurement point in addition to equation (6) (Gaganis and Smith, 2006):

$$\min_{\hat{\theta}_{(v,l,t)}} G[\hat{\theta}_{(v,l,t)} - \hat{\theta}] \quad (7)$$

Criterion (7) minimizes \mathcal{Op} , by minimizing the spreading of $\hat{\theta}_{(v,l,t)}$ around a parameter vector $\hat{\theta}$ estimated with classical calibration using an objective function of the form of criterion (4). It solves the problem of non-uniqueness of equation (6) by providing the means for selecting a unique $\hat{\theta}_{(v,l,t)}^*$ from all possible solutions $\hat{\theta}_{(v,l,t)}$ at each data point. There are several other criteria that could be used for the

minimization of \mathcal{O}_p . The above criterion (7) is selected here in order to explore the usefulness of the presented method in assessing the performance of the classical single objective calibration procedures. A conceptual diagram that graphically describes our formulation of the inverse problem (per-datum calibration) in a two-dimensional parameter space for three data points is shown in Figure 7. The crosses and x's represent the non-unique solution to criterion (6). The three highlighted values are the three unique per-datum parameter estimates selected by criterion (7) by minimizing the distance R between each per-datum parameter estimate and the solution to classical calibration. The vector e_2 represents the deviation of the per datum parameter estimates derived for measurement 2 from the true parameter values; it reflects the cumulative influence of both model error and measurement error. The dashed-line rectangle represents an approximation of the posterior parameter space \mathcal{O}_p . The number of the estimated parameter vectors using (6) and (7) is equal to the number of measurements of the depended variable available. For example, 10 measurements of solute concentration at two different times will result in 20 sets of parameter estimates. These parameter vectors are contained in the smallest possible region \mathcal{O}_p allowed by the magnitude of both measurement and model errors. It follows that the uncertainty in model predictions associated with \mathcal{O}_p also represents the minimum expected range of values of model output, given the existence of model error in addition to measurement error.

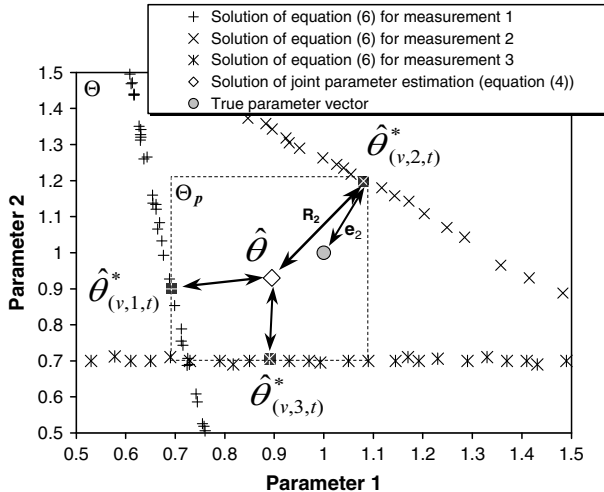


Fig. 7. Conceptual diagram of per-datum calibration for three measurements of the dependent variable.

6.2. Demonstration

To demonstrate the concepts above, the objective function (4) is used for solving the single-objective parameter estimation problem for model 1 and 2 of the synthetic problem (Figure 1) to obtain the most likely parameter values $\hat{\theta}$. To establish approximately equal weights for the hydraulic head and concentration data sets, the logarithm of the concentration values is used instead of the actual values, which vary by orders of magnitude. Concentration measurements at both 250 and 500 days are used in the single-objective inversion. Models 1 and 2 are then “calibrated” at each of the 15 data points using the criteria (6) and (7) to estimate the “best” values $\hat{\theta}_{(v,l,t)}^*$ for the two transmissivity zones. Monte Carlo sampling of the prior parameter space Θ is used to obtain the solution to the inverse problem. The estimated parameter values $\hat{\theta}_{(v,l,t)}^*$ and $\hat{\theta}$ for model 2 are shown in Figure 8. The dashed rectangle in this figure, which contains all per-datum parameter estimates, defines the posterior space of acceptable parameter values Θ_p .

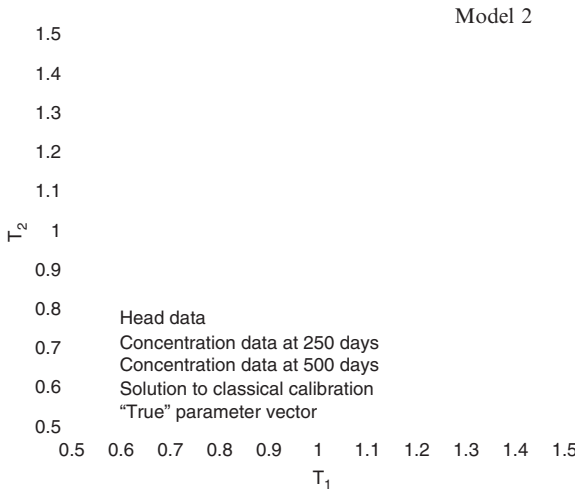


Fig. 8. Parameter estimates obtained by per-datum calibration (equation (6) and (7)) for model 2 (Gaganis and Smith, 2006).

A model calibrated using the joint data set (criterion (4)) provides a closer match to field measurements in some regions in the model domain than others. The residual e (see equation (1)) at each specific location and transport time of the single-objective inversion can be measured in the parameter space by measuring the deviation of each $\hat{\theta}_{(v,l,t)}^*$ from $\hat{\theta}$ (Figure 8). The location of $\hat{\theta}_{(v,l,t)}^*$ within the parameter space relative to $\hat{\theta}$ accounts for the information regarding model and measurement errors contained in the residual of (4). In the case of small model error, $\hat{\theta}$ will be close to the true parameter vector and the “true” confidence intervals

will be equivalent to those obtained by an analysis of the residual of (4) (e.g., Poeter and Hill, 1997). However, the true parameter vector and $\hat{\theta}$ may not coincide because of a substantial non-Gaussian model error (e.g., Figure 8). Then, the deviation of each $\hat{\theta}_{(v,l,t)}^*$ from $\hat{\theta}$ (vector R) is not equal to the sum of measurement and model error (vector e), which is the distance of the per-datum parameter estimates from the true parameter values (Figure 7), and assigning confidence intervals on model predictions based on the spread of $\hat{\theta}_{(v,l,t)}^*$ around $\hat{\theta}$ may be unrepresentative of the real situation.

With the residual driven to zero, the per-datum parameter estimates are forced to fully compensate for the error in model structure and measurement error at each data point (equation 5). In the presence of model error, the estimated values of the most sensitive parameters are forced to adjust to the greatest degree during the calibration. The relation between the location in Θ of these parameters, expressed as their deviation from the true parameter value in the normalized parameter space, and model error is shown in Figure 9. The influence of model error is measured the percent difference between the predicted concentration values (using the true parameter values in models 1 and 2), and the error-free observations at each sampling location, derived from the true model. Only those measurement locations that are reached by the plume at 250 days or 500 days are included in the plot. The effect of model error on $\hat{\theta}_{(v,l,t)}^*$ is apparent in the observed positive

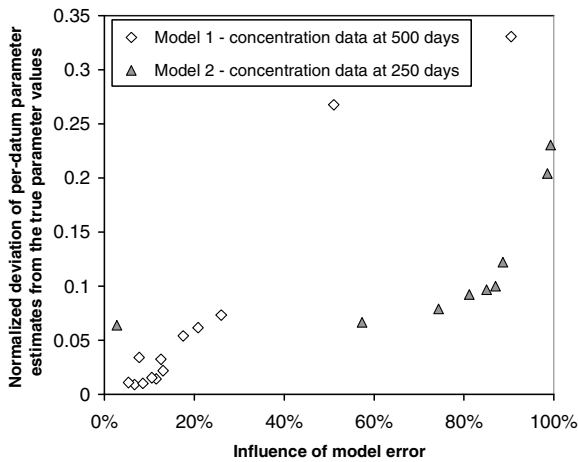


Fig. 9. Relation between model error and location of unique per-datum parameter estimates for model 1 using concentration data at 500 days and model 2 using concentration data at 250 days. Model error is measured as the percent difference between model predictions with the true parameter values at each sampling location, from the true concentrations at the same locations and time (Gaganis and Smith, 2006).

correlation between the magnitude of the difference between the predicted concentrations and the error-free observations, and the distance of each $\hat{\theta}_{(v,l,t)}^*$ from the true parameter values.

Since the spreading of $\hat{\theta}_{(v,l,t)}^*$ within the parameter space is dictated by the magnitude of model and measurement errors, the size of the posterior parameter space \mathcal{O}_p that contains all per-datum parameter vectors will represent the uncertainty due to these errors. Therefore, it can be suggested that the size of \mathcal{O}_p is inversely proportional to the correctness of the model structure and represents the level of uncertainty in the parameters imposed primarily by the magnitude of model error. In our example, \mathcal{O}_p is larger for model 2 than model 1 indicating that model 2 is subject to greater model error than model 1. A comparison of the magnitude of the calculated true model error (Figures 3 and 4) for models 1 and 2 demonstrates this statement. This relation between the size of \mathcal{O}_p and model error may provide a useful tool for evaluating alternative conceptual models (model discrimination). The size of the posterior parameter space \mathcal{O}_p may also offer a reasonable basis for selecting a “best” solution of the minimization problem of classical single objective calibration in the case that (4) does not have a unique minimum. Each of these possible solutions can be used in criterion (7) to select the unique per-datum parameter estimates. The resulting volume of the posterior parameter spaces can then be compared to determine the preferred solution of (4).

The rectangular \mathcal{O}_p shown in Figure 8 is a crude approximation of the posterior parameter space. A more informative probabilistic description of \mathcal{O}_p can be obtained by a statistical analysis of the locations of $\hat{\theta}_{(v,l,t)}^*$ in \mathcal{O} . The statistical distributions of the per-datum parameter estimates for model 2 are shown in Figure 10. These parameter distributions when compared to the prior parameter distributions (Figure 10) show the limit imposed by the model conceptual error in parameter uncertainty reduction through a calibration process. Since the per-datum inverse methodology does not require any assumptions to be made regarding the probabilistic properties of the error, these distributions may be used in testing the validity of the normality assumption and the performance of the single-objective parameter estimation. The parameter estimates from classical calibration (shown as arrows in Figure 10) are the weighted average of all $\hat{\theta}_{(v,l,t)}^*$. This figure demonstrates the influence of the weights assigned to different data in classical calibration. Assigning higher weights to the hydraulic head data will result in greater values of parameter estimates. The parameter estimates will be smaller if concentration data are weighted more than the hydraulic head data. Figure 10 also suggests that the problem of non-uniqueness of the single-objective inverse procedures may be a result of error in the model structure. As can be seen in this figure (see distribution of T_1), certain weights assigned to measurements of the dependent variables may result in two local minima in the objective function of the classical calibration. The location of these local minima in the parameter space will coincide with the

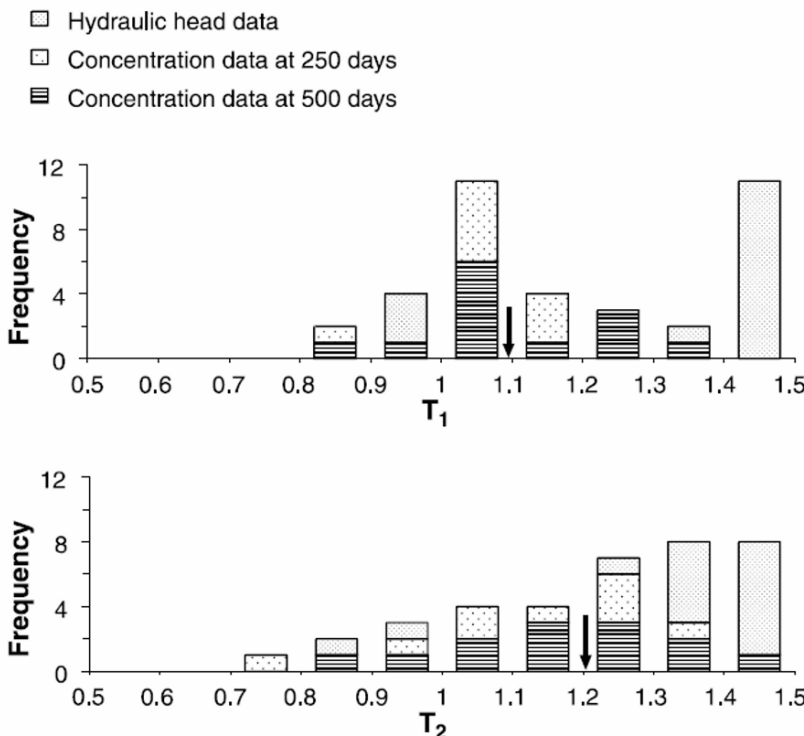


Fig. 10. Statistical distributions of the per-datum estimates of Transmissivity 1 and 2 for model 2. The arrows show the location of the solution of the classical single-objective calibration (equation 4) and the dashed line the prior parameter distribution.

two peaks in the distribution of the per-datum parameter estimates for T_1 . When the model structure is correct (for example the flow solution of model 1), the posterior parameter space is normally distributed around the true parameter values since it is subject only to measurement error (Figure 11).

Because model error is spatially distributed, location-specific uncertainty levels on the parameters would be more appropriate. A posterior feasible parameter space is estimated for each sampling location based on the range of the per-datum estimates $\hat{\theta}_{(v,l,t)}^*$ associated with this location. For example, the posterior parameter space associated with sampling location 15 is estimated as the region in the parameter space that contains the three per-datum estimates that correspond to the measurements of steady state hydraulic head and concentration at times of 250 and 500 days at this location. From these three values, upper and lower bounds are identified for T_1 and T_2 . The location-specific parameter uncertainty is then propagated through the model using these values to identify upper and lower bounds on the (location-specific) model predictions. These bounds are shown in Figure 12 for model 2. This figure does not include the sampling locations 2 and 5

because no concentration data were available at these locations as they were not reached by the contaminant within the time frame of 500 days used for model calibration. Although the parameter vector $\hat{\theta}$ is used for the estimation of $\hat{\theta}_{(v,l,t)}$, it is not taken into account in evaluating the posterior parameter space assigned to each location. As a result, the predictions of the models calibrated using the joint data set (equation 4) are not necessarily included within the estimated range of concentration values at 750 days (e.g., Figure 12 – locations 1, 8 and 14). These are the locations that contribute the most in the residual of the minimization problem (4). Model predictions presented here as a range of equally probable values (Figure 12) are based on information on model error for the calibration time frame. In other words, our predictions of probable future responses of the true system are based on an analysis of model error using past data. However, the ability of the model structure to describe the physical system may deteriorate with time. This behavior may result in prediction bounds that may not bracket the true values (Figure 12 – locations 9, 12 and 15). This is because the effect of errors in model structure for model 2 on concentrations predicted at 750 days is greater than their effect during the calibration period that was evaluated (temporal variation of model error). Updating the analysis as new data become available may (even partially) resolve this problem. Uninformative (highly uncertain to unacceptable levels) predictions indicate the need for model structure refinement. Refining the model structure will result in a smaller posterior parameter space and lead to a reduction of the prediction uncertainty. A real-world application of the above method can be found in Gaganis and Smith (2008).

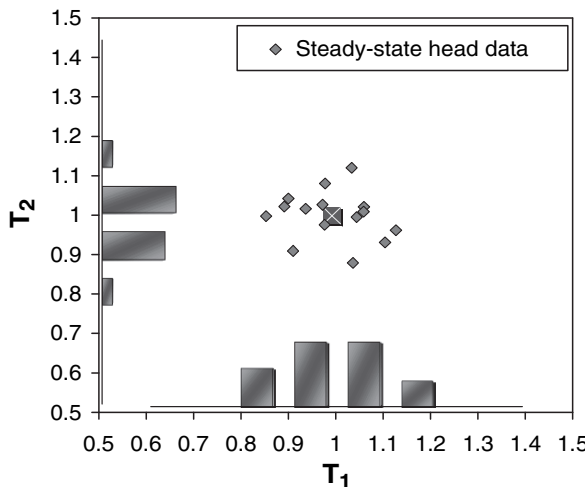


Fig. 11. Statistical distributions and location in the parameter space of the per-datum parameter estimates of Transmissivity 1 and 2 for model1 when only the hydraulic head data are used (subject to measurement error only).

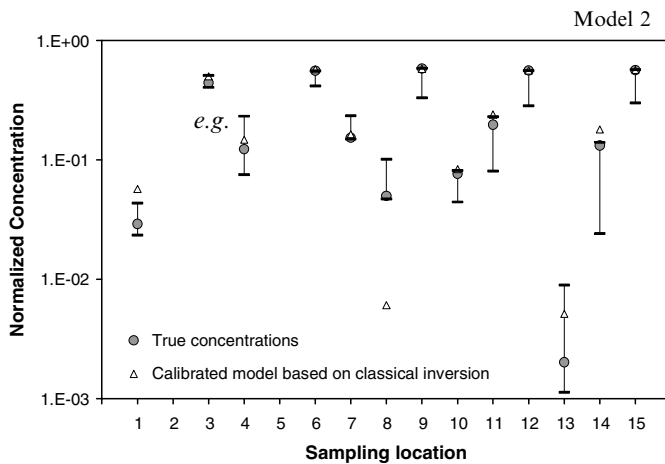


Fig. 12. Concentration estimates for model 2 at time 750 days. The error bars show the range of prediction uncertainty associated with accounting for model and measurement errors using the per-datum inverse method. Sampling locations are shown in Figure 1.

7. Conclusions

In a modeling exercise, errors in the model structure cannot be avoided because they arise from our limited capability to exactly describe mathematically the complexity of a physical system. The effect of model error on model predictions is not random but systematic, therefore, it does not necessarily have any probabilistic properties that can be easily exploited in the construction of a model performance criterion. The effect of model error varies in both space and time. It is also different for the flow and the solute transport components of a groundwater model. Model error cannot be ignored because it may have a significant impact on parameter estimation, uncertainty analyses and risk assessments. Structural errors may result in a misleading evaluation of prediction uncertainty associated with parameter error because model sensitivity to uncertain parameters may be quite different than that of the correct model. A substantial model error may significantly degrade the usefulness of model calibration and the reliability of model predictions because parameter estimates are forced to compensate for the existing structural errors. Incorrect uncertainty analyses and estimated parameters that have little value in predictive modeling could potentially lead to an engineering design failure or to a selection of a management strategy that involves unnecessary expenditures. The evaluation of model error and accounting for the associated uncertainty is a necessary next step in groundwater modeling applications.

A complementary to classical inverse methods model calibration procedure has been presented in this chapter for assessing the uncertainty in parameter estimates associated with model error. This procedure is based on the concept of a per-datum calibration for capturing the spatial and temporal behavior of model error. A set of per-datum parameter estimates obtained by this new method defines a posterior parameter space that may be translated into a probabilistic description of model predictions. The resulted prediction uncertainty represents an accurate reflection on model predictions of available information regarding the dependent variables and measures the level of confidence in model performance evaluated in terms of each model prediction. Potential applications of this method may include: (i) evaluating the performance of classical calibration in terms of the predictive capability of the model, (ii) testing the validity of assumptions regarding error statistical distributions underlying the estimation of parameters and their confidence interval in classical single-objective calibration, (iii) selecting the best solution of the minimization problem of classical calibration in the case that it does not have a unique solution, and (iv) evaluating alternative conceptual models in terms of the correctness of the model structure.

References

Beck, M.B., 1987, Water quality modeling: A review of the analysis of uncertainty, *Water Resources Research*, 23: 1393–1442.

Beckie, R., 1996, Measurement scale, network sampling scale, and ground water model parameters, *Water Resources Research*, 32: 65–76.

Beven, K.J. and Binley, A.M., 1992, The future of distributed models: Model calibration and uncertainty prediction, *Hydrological Processes*, 6: 279–298.

Beven, K.J. and Freer, J., 2001, Equifinality, data assimilation, and uncertainty estimation in mechanistic modelling of complex environmental systems using the GLUE methodology, *Journal of Hydrology*, 249: 11–29.

Carrera, J. and Neuman, S.P., 1986, Estimation of aquifer parameters under transient and steady state conditions: 1. Maximum likelihood method incorporating prior information, *Water Resources Research*, 22: 199–210.

Carrera, J., Alcolea, A., Medina, A., Hidalgo, J., and Slooten, L.J., 2005, Inverse problem in hydrogeology, *Hydrogeology Journal*, 13: 206–222.

Cooley, R.L., 1982, Incorporation of prior information on parameters into nonlinear regression groundwater models, 1, Theory, *Water Resources Research*, 18: 965–976.

Cooley, R.L., 1983, Incorporation of prior information on parameters into nonlinear regression groundwater models, 2, Applications, *Water Resources Research*, 19: 662–676.

Cooley, R.L., Konikow, L.F., and Naff, R.L., 1986, Nonlinear-regression groundwater flow modeling of a deep regional aquifer system, *Water Resources Research*, 22: 1759–1778.

Dagan, G., 1989, *Flow and Transport in Porous Formations*, Springer-Verlag, New York.

Freeze, R.A., Massmann, J., Smith, L., Sperling, T., and James, B., 1990, Hydrological decision analysis: 1. A framework, *Ground Water*, 28: 738–766.

Gaganis, P. and Smith, L., 2001, A Bayesian approach to the quantification of the effect of model error on the predictions of groundwater models, *Water Resources Research*, 37: 2309–2322.

Gaganis, P. and Smith, L., 2006, Evaluation of the uncertainty of groundwater model predictions associated with conceptual errors: A per-datum approach to model calibration, *Advances in Water Resources*, 29: 503–514.

Gaganis, P. and Smith, L., 2008, Accounting for model error in risk assessments: Alternatives to adopting a bias towards conservative risk estimates in decision models, *Advances in Water Resources*, 31: 1074–1086.

Gavalas, G.R., Shah, P.C., and Seinfeld, J.H., 1976, Reservoir history matching by Bayesian estimation, *Society of Petroleum Engineers Journal*, 16: 337–350.

Gerhar, L.W., 1993, *Stochastic Subsurface Hydrogeology*, Prentice-Hall, Englewood Cliffs, NJ.

Gupta, H.V., Sorooshian, S., and Yapo, P.O., 1998, Toward improved calibration of hydrologic models: Multiple and noncommensurable measures of information, *Water Resources Research*, 34: 751–763.

Hill, M.C. and Tiedeman, C.R., 2007, *Effective Groundwater Model Calibration: With Analysis of Data, Sensitivities, Predictions, and Uncertainty*, Wiley-Interscience, London, UK.

Kitanidis, P.K. and Vorvoris, E.G., 1983, A geostatistical approach to the inverse problem in groundwater modeling (steady state) and one-dimensional simulations, *Water Resources Research*, 19: 677–690.

Konikow, L.F. and Bredehoeft, J.D., 1992, Ground-water models cannot be validated, *Advances in Water Resources*, 15: 75–83.

Luis, S.J. and McLaughlin, D., 1992, A stochastic approach to model validation, *Advances in Water Resources*, 15: 15–32.

McLaughlin, D. and Townley, L.R., 1996, A reassessment of the groundwater inverse problem, *Water Resources Research*, 32: 1131–1161.

Morgan, M.G., Henrion, M., and Small, M., 1990, *Uncertainty: A Guide to Dealing with Uncertainty in Quantitative Risk and Policy Analysis*, Cambridge University Press, Cambridge University Press.

Neuman, S.P., 1973, Calibration of distributed groundwater flow models viewed as a multiple-objective decision process under uncertainty, *Water Resources Research*, 9: 1006–1021.

Neuman, S.P., 2003, Maximum likelihood Bayesian averaging of uncertain model predictions, *Stochastic Environmental Research and Risk Assessment*, 17: 291–305.

Poeter, E.P. and Hill, M.C., 1997, Inverse models: A necessary next step in ground-water modeling, *Ground Water*, 35: 250–260.

Schwarz, G., 1978, Estimating the dimension of a model, *Annals of Statistics*, 6: 461–465.

Smith, L. and Gaganis, P., 1998, Strontium-90 migration to water wells at the Chernobyl nuclear power plant: Re-evaluation of a decision model, *Environmental and Engineering Geoscience*, IV: 161–174.

Sun, N.-Z., Yang, S.-L., and Yeh, W.W.-G., 1998, A proposed stepwise regression method for model structure identification, *Water Resources Research*, 34: 2561–2572.

Ye, M., Neuman, S.P., and Meyer, P.D., 2004, Maximum likelihood Bayesian averaging of spatial variability models in unsaturated fractured tuff, *Water Resources Research*, 40: W05113.

Warwick, J.J., 1989, Interplay between parameter uncertainty and model aggregation error, *Water Resources Bulletin*, 25: 275–283.

Weiss, W. and Smith, L., 1998, Parameter space methods in Joint parameter estimation for groundwater models, *Water Resources Research*, 24: 647–661.

Zimmerman, D.A., de Marsily, G., Gotway, C.A., Marietta, M.G., Axness, C.L., Beauheim, R.L., Bras, R.L., Carrera, J., Dagan, G., Davies, P.B., Gallegos, D.P., Galli, A., Gomez- Hernandez, J., Grindrod, P., Gutjahr, A.L., Kitanidis, P.K., Lavenue, A.M., McLaughlin, D., Neuman, S.P., RamaRao, B.S., Ravenne, C., and Rubin, Y., 1998, A comparison of seven geostatistical based inverse approaches to estimate transmissivities for modeling advective transport by groundwater flow, *Water Resources Research*, 34: 1373–1413.

User subjectivity in Monte Carlo modelling of pesticide exposure

Marco Trevisan

Istituto di Chimica Agraria ed Ambientale, Facoltà di Agraria, Università Cattolica del Sacro Cuore, Via Emilia Parmense 84, 24100, Piacenza, Italia.

Abstract

Monte Carlo techniques are increasingly used in pesticide exposure modelling to evaluate the uncertainty in predictions arising from uncertainty in input parameters and to estimate the confidence that should be assigned to modelling results. The approach typically involves running a deterministic model repeatedly for a large number of input values sampled from statistical distributions. The present chapter summarizes the results of three different projects demonstrating that subjective choices made in Monte Carlo modelling introduce variability into probabilistic modelling of pesticide leaching, and that the results need to be interpreted with care.

Keywords: Monte Carlo; user subjectivity; pesticide exposure modelling; degradation; sorption.

1. Introduction

This chapter is based on three previous papers, already published. The first is a paper related with reproducibility in Monte Carlo modeling with a pesticide leaching model by Dubus and Janssen (2003). The second one is a paper on assessment of uncertainty associated with the simulation of pesticide leaching models by Trevisan and Vischetti (2005) and the later is a paper related to the user-subjectivity in Monte Carlo modeling of pesticide exposure by Beulke *et al.* (2006). In this chapter many figures are from these papers and also procedure, results and conclusion are already reported previously. The goal of this paper is to organize organically the work made previously and to point out the importance of the definition of harmonized procedure in the probabilistic risk assessment and so the necessity to define a protocol to reduce the user subjectivity.

2. Rationale

2.1. *Pesticide fate*

A pesticide applied on field may be sprayed on the bare or crop-covered field. When sprayed, some of the chemical will drift outside the target area, and if there is vegetation on the field, a part of it will settle on the canopy instead of soil surface. On crop canopy, the chemical may be volatilized, transformed, penetrate into the plant, or be washed off to the ground by precipitation or irrigation. On soil surface, the chemical may likewise be volatilized or transformed. When intensive rainfall generates runoff and erosion of soil from the field, which is particularly significant on fields situated on slopes, chemicals from the soil surface and topsoil are lost as solutes and with eroded soil particles (sediment). All these processes affect the amount of pesticide that actually enters the soil system. Pesticides enter the soil system together with infiltrating water, which is the most important medium that transports chemicals in the soil. Chemicals are constantly partitioned between the gas, liquid and solid (particle) phases of the soil according to their own, physical-chemical properties as well as the soil conditions. While dissolved in the liquid phase, chemicals may be transported in the soil in all directions, mainly sideways (with drainage) and downwards (with percolate as leaching) to the groundwater. Diffusion and dispersion also spread the chemicals in both phases. Sorption to soil particles takes several different forms: rapid and reversible equilibrium sorption, only partially reversible slow sorption and practically irreversible very slow sorption, which operates on a time scale from weeks to years. Chemicals are transformed in soil by chemical, photochemical and microbial processes, and important daughter compounds may be formed in the process. In the root zone, pesticides are taken up by plant roots both together with water and through sorption to roots surfaces and dissolution to root fats. Both sorption and transformation are affected by, *e.g.*, the temperature, moisture and pH of the environment (Figure 1).

The main controlling factors of pesticide fate are

- Compound properties (*e.g.*, degradation, sorption, volatilisation)
- Soil properties (texture, structure, organic matter)
- Weather conditions
- Crop (canopy architecture, root density and length)
- Agronomic practices (time of application, dose, method of application)
- Water body (depth to groundwater, surface topography, connections to surface water)

The mobility of a chemical in soil is largely determined by its solubility in water and partitioning between lipids and water (K_{ow}) as well as between soil particles and water (K_d). K_d , the coefficient of the sorption of the pesticide to soil, is a

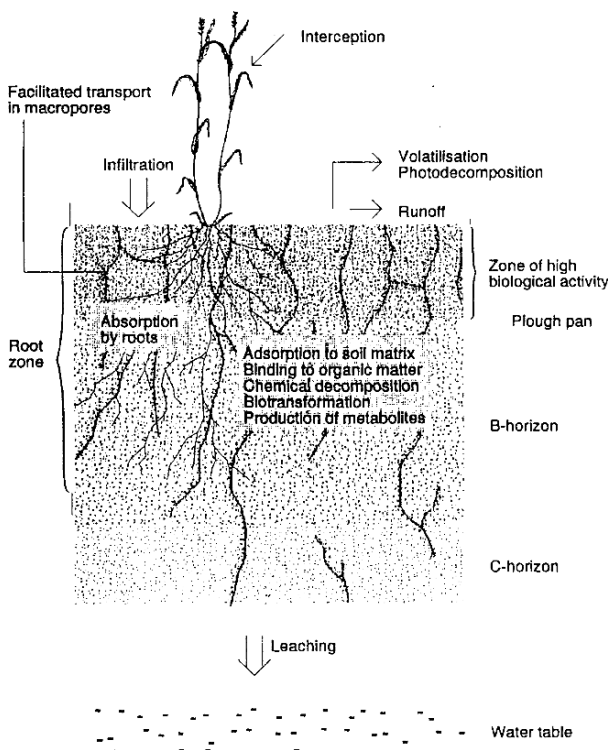


Fig. 1. Pesticide fate in soil.

soil-specific indicator of the degree of the tendency the compound has to adsorb to soil particles. There is usually a good correlation between sorption and the organic matter content of the soil, and K_{oc} , the coefficient of sorption to organic carbon, is considered a more universal property of a chemical. The transformation of a pesticide in the soil layers is commonly described by first-order degradation kinetics, characterized by the experimentally discovered half-life ($t_{1/2}$ or DT50) of the pesticide in soil. This description is assumed to cover both the chemical and the microbial transformation of the compound in the soil. The effect of temperature, moisture or depth in soil on the experimentally derived rate of transformation can be considered.

2.2. Model

A mathematical model able to simulate the behaviour of a pesticide applied on the field is normally one-dimensional and the computed rates of change are either per unit of volume or per unit of horizontal surface area (mainly above soil). The

simulated soil column is divided into horizontal computational layers, characterized according to the known properties of actual physical soil horizons. The computational layers are usually relatively thin at the top of the column and grow thicker as the column goes deeper into the soil. The soil-fate calculations are made separately for each layer. The model consists of at least two sub models: the soil hydrology model and the pesticide-fate model. The descriptions of above-soil processes often also form their own submodel that defines the actual flux of water and pesticide into the soil column and may also calculate pesticide losses outside the field with run-off or drift in order to quantify surface-water loads.

The time step of model simulations is a compromise between data requirements and accuracy needs and also affects the duration of the simulation and the quantity of output. The time scales of the relevant pesticide-fate processes vary from seconds to years. The most common time step currently selected is one day, but a shorter one would actually be needed in order to use good mechanistic descriptions of several processes (spray drift, run-off, volatilisation) which take place within a short time scale (minutes-hours) or fluctuate with the time of day.

The model may either demand the parameters it needs for the simulation as direct input from the user or include procedures, *e.g.*, pedo-transfer functions, for deriving these parameters from information that is more easily available for a non-expert user. Models are also commonly linked with databases and, *e.g.*, climate data generators in order to make running a simulation a much quicker and easier process.

The mathematical models to assess the fate and transport of pesticides at different scale have been used over the past 25 years and now are significantly increased to investigate and assess virtually every type of pesticide problem (Cheng, 1990; van der Werf, 1996; Klepper *et al.*, 1999; Bobba *et al.*, 2000; Vanclooster *et al.*, 2000). These models are useful tools for determining pesticide concentrations in the environment and for helping in environment management.

Mathematical models are used in the registration process due to their inexpensiveness and rapidity as compared to extensive field studies. As the assessment of environmental fate needs to cover, at least in theory, the entire variety of relevant combinations of crops, agricultural practices and environmental conditions, modeling can be practically the only way to come even close to meeting the requirements. However, it is not possible for models to describe reality with complete accuracy, and simulation results should never be the sole basis of regulatory decisions. Instead, modelling should be used as a registration tool together with laboratory and field studies. Models can be used for interpreting results of these studies, recognizing the areas where additional studies are needed, evaluating proposed study designs, comparing between chemicals and application procedures, and generally integrating and making best possible use of gathered data. Models can also produce conservative predicted environmental concentrations (PECs) for first-tier screening purposes.

Pesticide leaching models are usually originally designed as research tools, which means that their intended purpose is to explain real data instead of predicting it. In research use, models are typically calibrated against field data, and their resulting accuracy is much higher than it can be when no comparison with real data is possible, as is usually the case in regulatory use. One of the consequences is that these models can often predict quite accurately the transport of the main bulk of a chemical downwards through the soil column, but predictions of specific time-and-space concentrations in soil layers or the groundwater tend to be poor. It should also be remembered that even if a model accurately describes all significant and relevant pesticide-fate processes, the quality of the output of the model can only be as good as that of the input information, and even when the same model is used to simulate the same set-up, the results can vary widely according to parameterisation choices made by individual modelers. In order to minimize subjectivity and to guarantee some degree of consistency and reliability in the use of these models in the pesticide registration process, the models and the procedures for their use need to be standardized. Registration models also need to be extensively validated for their intended use in order to improve general confidence in them.

Current environmental risk assessments for pesticide registration in Europe rely on a comparison between a calculated exposure and an ecotoxicological endpoint (surface water) or a legal threshold concentration (groundwater). Mathematical models as PELMO, PRZM2, PEARL and MACRO are used to calculate exposure concentrations. Traditionally, deterministic approaches have been applied where a single combination of model input parameters is used to calculate a single set of predicted environmental concentrations. The parameter combination is often selected so as to be protective of the actual range of use conditions. Such deterministic 'realistic worst-case' approaches are useful at the lower tiers of the regulatory assessment process because they are relatively quick to deploy and act as a screening step. Obviously, such model predictions are uncertain because it is uncertain whether: the model structure is valid, mathematical equations describing each process are correct, the model parameters are correctly chosen and the input data is error free (Lei and Schilling, 1996).

2.3. Uncertainty

The uncertainty linked to deterministic simulations with 1D spatialised models is high, difficult to assess and somewhat unknown (Figure 2). The uncertainty in model structure and mathematical equations are usually referred to as conceptual errors and the uncertainty in model output is referred to as model predictive uncertainty (Lei and Schilling, 1996). The rainfall event was showed as most critical parameter (Fontaine *et al.*, 1992) in pesticide models sensitivity analysis. The weather conditions are indicate as the most important parameters affecting the runoff events (Wolt *et al.*, 2002). It is evident that the variability of natural event,

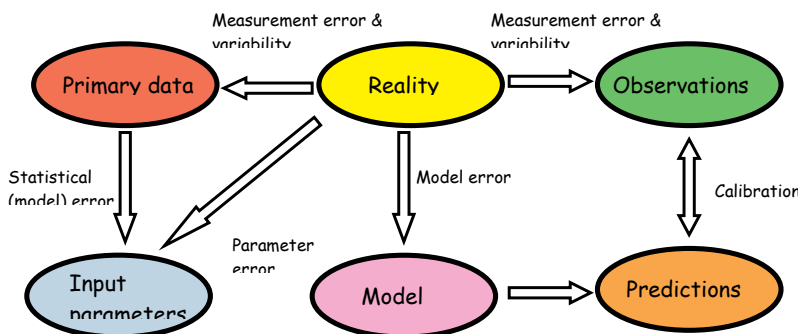


Fig. 2. The uncertainty linked to deterministic simulations with models.

as rainfall and temperature, can affect model simulations. Weather variability is at the same time temporal, during the year, and spatial, in the studied area. The causes of model uncertainty related to the input parameters can be: measurement errors in parameters estimation; spatial, site-specific, and temporal natural variability; extrapolation from controlled laboratory measurement conditions to uncontrolled environmental conditions; methods to estimate the numerical values of the input parameters; use of input parameters from available data sources or using pedo-transfer function (Souter and Musy, 1998; Bobba *et al.*, 2000; Dubus *et al.*, 2003).

The sources of uncertainty could be grouped into three categories: (i) errors resulting from the conceptual scheme of the world: model error; (ii) stochasticity of the real world, (f.i., temporal and spatial variability): natural variability; and (iii) uncertainty of the model parameters: input parameter error (Trevisan and Vischetti, 2005).

The importance of incorporating uncertainty analysis into fate models has been emphasized by many authors (Trevisan and Vischetti, 2005). Ignorance of the uncertainty associated with model predictions may result in misleading interpretations when the model is compared with field measurement and used for risk assessment by the decision-maker, who may draw a completely wrong conclusion from a single model prediction (Trevisan and Vischetti, 2005). It suggested that the inclusion of uncertainty analysis in modelling activities can be interpreted as the truthful representation of model limitation, and that uncertainties must be estimated and included in modelling activities. As reported in Dubus *et al.* (2003) terminology related to uncertainty within the context of contaminant modelling includes: variation, variability, ambiguity, heterogeneity, approximation, inexactness, vagueness, inaccuracy, subjectivity, imprecision, misclassification, misinterpretation, error, faults, mistakes and artefacts. In this chapter, the term uncertainty represents the combination of factors of various origins leading to a lack of confidence with regard to the description of the system under study. The terminology used encompasses both stochastic variability and incertitude (Dubus *et al.*, 2003).

The main characteristic of pesticide fate model was that they are 1D models, *i.e.*, able to make point simulations which were accepted everywhere as representations of reality at point and/or field scale (FOCUS, 2000). Several attempts have been made in the last years to extent the possibility to simulate with pesticide fate model at largest scale (catchment, region) but, their deterministic nature clashed with a probabilistic approach to get a real understanding of the actual environmental contamination risk by pesticides.

Probabilistic risk assessment is an approach to risk assessment which integrates uncertainty considerations and probability distributions to characterise risk. In contrast to point estimate risk assessment, the overall objective of the method is to avoid worst-case assumptions and come up with a more realistic assessment of risk.

Probabilistic modelling is related with an expression of the risk in terms of a probability of exceedance of a value (*i.e.*, $>0.1 \mu\text{g L}^{-1}$, legal limit for pesticide concentration in groundwater) or of an effects (*i.e.*, on algae as *Lemna*). Often it needs to carry out refinement from worst-case assumptions with strong interest for risk assessment activities. Two main angles of vision are present:

- Variability in environmental conditions across the landscape (GIS, mega-plot, spatially distributed)
- Uncertainty in the modelling

Probabilistic approaches to environmental risk assessment for pesticides are currently receiving a vast amount of interest to account for uncertainty in exposure assessment (ECOFRAM, 1999; EUPRA, 2001). Several protocols to account for uncertainty in these approaches have been proposed (Dubus and Brown, 2002; Warren-Hicks *et al.*, 2002; Carbone *et al.*, 2002). In some cases software packages have been proposed to automatically incorporate uncertainty analysis into pesticide fate models (Janssen *et al.*, 1994; Wingle *et al.*, 1999).

2.4. Monte Carlo approach

The most widely used technique to account for this uncertainty in pesticide fate modeling is the Monte Carlo approach. Monte Carlo analysis involves the modification of values for selected input parameters at the same time using Monte Carlo sampling from predefined probability density functions. There are a number of reasons why Monte Carlo approach is often used for investigating the model uncertainty. First, it allows for the simultaneous variation of the values of all the input parameters; second, it is relatively simple to conduct when using appropriate software. Third, the use of an efficient sampling scheme (such as the Latin hypercube sampling) greatly decreases the number of runs required. Fourth, Monte Carlo approach may avoid the attribution of specific values to each parameter in a model, if parameters are varied within their uncertainty range, the Monte Carlo approach can provide an assessment of uncertainty.

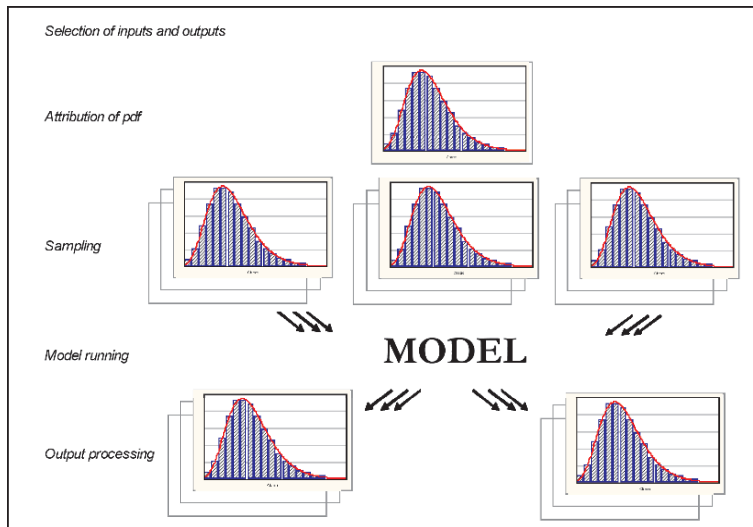


Fig. 3. Monte Carlo approach.

The Monte Carlo approach involves running a model iteratively for a large number of different input values or modeling scenarios followed by a statistical analysis of the model output. The parameter values are sampled from statistical distributions. A Monte Carlo analysis allows the user to evaluate the uncertainty in model predictions arising from uncertainty in the input parameters and to estimate the confidence that should be assigned to modeling results. Figure 3 shows how it is possible to carry out an uncertainty analysis using the Monte Carlo approach.

The main question arising with the Monte Carlo approach is how much confidence should we assign to Monte Carlo results? And related questions are

- Is the Monte Carlo approach reproducible?
- How uncertain are the results?
- Are the results useful for sound decision making?

To reply to these question an experimental framework was set up.

3. Experimental framework

3.1. Part 1

To reply these questions Dubus and Janssen (2003) planned a Monte Carlo framework exercise.

The PELMO model was selected for its speed and because it is a one-dimensional leaching model that describes water movement through the soil column using a capacitance approach. Solute transport is simulated using the convection-dispersion equation. Descriptions of pesticide sorption and degradation and of pesticide losses via runoff, soil erosion and volatilization are included in the model. The model output of interest was the average annual concentration in leachate at 1 m depth for the 20th year of the simulation period. This endpoint is normally compared with a threshold concentration of $0.1 \mu\text{g L}^{-1}$ within the context of pesticide registration in Europe (Figure 4). Simulated average annual concentrations in leachate tend to increase from one year of the simulation to the next until a plateau concentration is reached. A relatively long simulation period of 20 years was selected to ensure that the plateau concentration was reached by the end of the model run for all combinations of input parameters. Annual average concentrations in leachate for each of the 20 years were calculated from the simulated mass of pesticide in leachate and the volume of leachate. Monte Carlo approach adopted was standard and only two variables were modified (K_{oc} and DT50) considering a log-normal distribution; seed number sampling was performed using Latin Hypercube Sampling (LHS) and the target value was the exceeding probability of over-pass $0.1 \mu\text{g L}^{-1}$ and application rate was fixed to have at least an excedent around 5%.

The researches undertaken to establish the reproducibility of Monte Carlo approach were addressed on assessing the influence on Monte Carlo results of the random sample used (*i.e.*, the seed number used in the sampling); and, the number of model runs undertaken (*i.e.*, the size of the random sample). Twelve different sample sizes were considered (10, 50, 100, 150, 200, 250, 500, 750, 1000, 1500, 2500 model runs) and for each sample size, the Monte Carlo analysis was repeated 10 times by varying the seed number used in the sampling. Seed numbers were

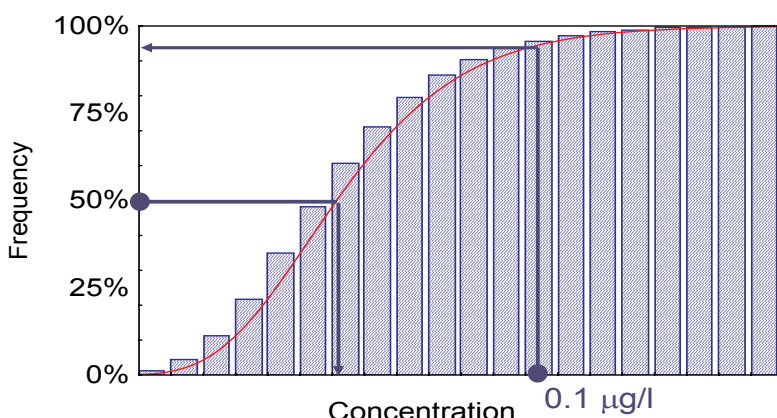


Fig. 4. Cumulative distribution and the threshold concentration of $0.1 \mu\text{g L}^{-1}$ within the context of pesticide registration in Europe.

generated randomly from a uniform distribution to avoid any bias in their selection and used in the generation of the Latin Hypercube samples. For each random sample, the probability of exceed a threshold concentration of $0.1 \mu\text{g L}^{-1}$ was calculated. A total of 315,200 PELMO runs were performed.

Figure 5 shows the results obtained, the minimum, average and maximum exceeding probabilities obtained for the 10 replicated random samples. Significant variability in the exceeding probability obtained for different seed numbers were found for all sample sizes. Coefficients of variation for the 10 probabilities were found to vary between 5.2% and 211%. The smallest CV was obtained for the largest number of model runs (5000 runs). The average exceeding probabilities for the 10 replicates was found to vary significantly with the number of model runs undertaken (from 2.0% to 4.6%). The range of exceeding probabilities predicted (*i.e.*, the difference between the minimum and maximum values) was also found to be relatively large. The inherent repeatability in the system was found to be scarce.

The second point investigated was the effect of the parameterisation of probability density functions (pdf's). It is well known that the type of random distribution assigned to input parameters (*e.g.*, normal, lognormal, uniform) influence Monte Carlo results but scarce information was available on the effects of the way of parameterisation of the pdf selected.

Five different assumptions for parameterising the log-normal distributions (Figure 6) which were assigned to K_{oc} and DT50 were used. Parameterisation was based on the absence/presence of truncation in the sampling and the amount of probability covered by the range $[M/2; M \cdot 2]$ where M is the initial value attributed to K_{oc} and DT50. Truncation in the sampling would reflect a belief of the modeller

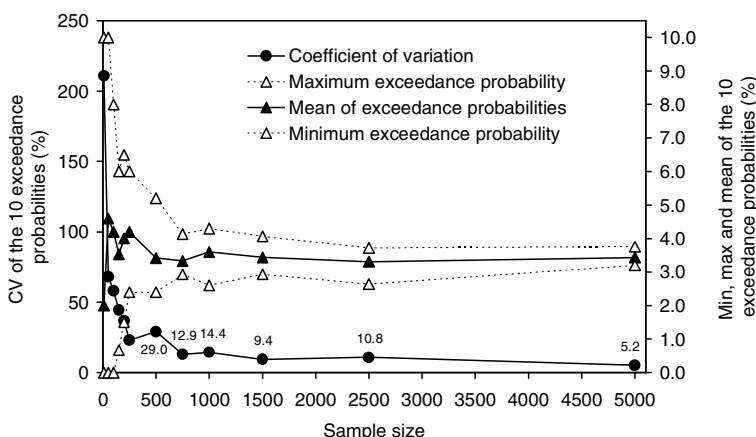


Fig. 5. The minimum, average and maximum exceeding probabilities obtained for the 10 replicated random samples and the coefficient of variation.

that an extremely small or large value for K_{oc} or DT50 as sampled from a log-normal distribution would not be realistic. The results on parameterisation are reported in Figure 7. The probability of exceeding a concentration of $0.1 \mu\text{g L}^{-1}$ ranged between 1.2% and 4.4%. The use of truncation in the sampling resulted in a decrease in the probability of exceeding (pdf 1 vs. pdf 2; pdf 4 vs. pdf 5) and the tighter the truncation applied, the smaller the exceeding probability (pdf 2 vs. pdf 3).

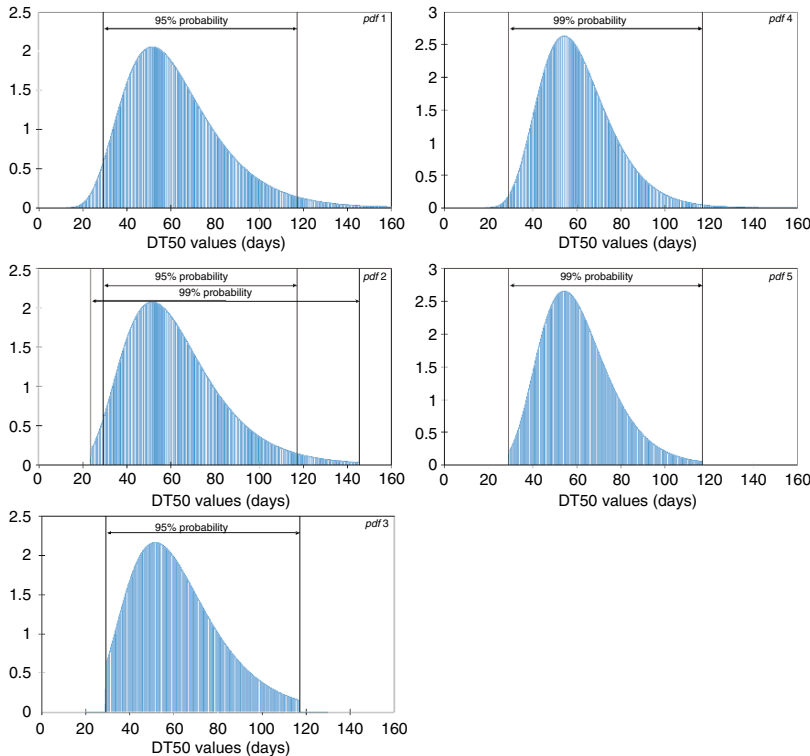


Fig. 6. Assumptions for parameterizing the log-normal distributions assigned to K_{oc} and DT50, where M is the initial value assigned to K_{oc} or DT50. pdf 1 It is assumed that 95% of values are within the range defined by $[M/2; M*2]$ and any value for K_{oc} and DT50 can be sampled through random sampling. pdf 2 It is assumed that 95% of values are within the range defined by $[M/2; M*2]$ and that no value can be sampled outside the 0.5th and 99.5th-percentiles of the log-normal distribution (truncation at the 99%-probability level). pdf 3 It is assumed that 95% of values are within the range defined by $[M/2; M*2]$ and that no value outside this range can be sampled (truncation at the 95%-probability level). pdf 4 It is assumed that 99% of values are within the range defined by $[M/2; M*2]$ and any value for K_{oc} and DT50 can be sampled through random sampling. pdf 5 It is assumed that 99% of values are within the range defined by $[M/2; M*2]$ and no value outside this range can be sampled (truncation at the 99%-probability level).

The impact of specifying positive correlations between K_{oc} and DT50 was investigated for parameterisation scenario 'pdf 1'. Correlations that were considered were $r = 0, 0.1, 0.2, 0.3, 0.4, 0.5, 0.6, 0.7, 0.8, 0.9$ and 1.0 (Figure 8). Results of Monte Carlo modelling obtained for these correlations were compared to

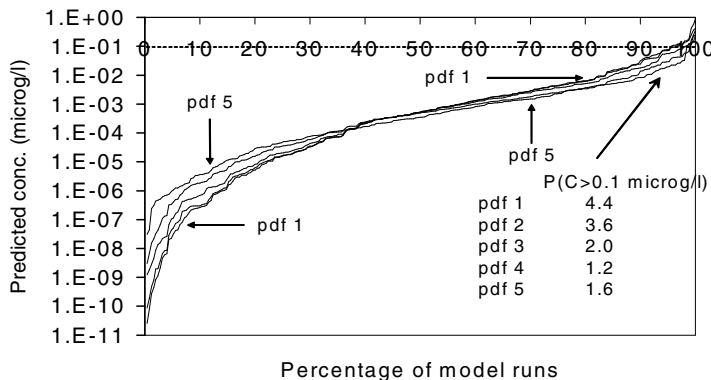


Fig. 7. Cumulative distribution charts displaying the probability of simulating a concentration below a given concentration. Each curve corresponds to a different parameterisation assumption.

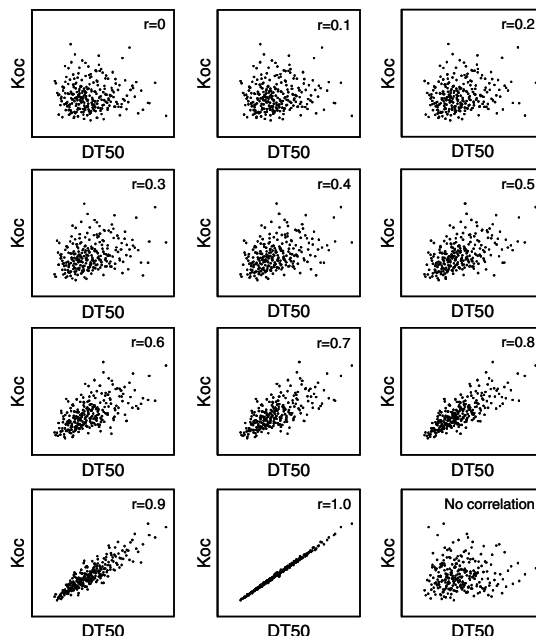


Fig. 8. Correlations between K_{oc} and DT50 for parameterisation scenario 'pdf 1'.

those obtained when no correlation was specified in the sampling (Figure 9). The specification of correlation between the two parameters was found to have a strong influence on the cumulative distribution chart. The increased flatness in the cumulative distribution curves with increasing correlation between K_{oc} and DT50 reflected the fact that sorption and degradation processes compensate for one another in the prediction of pesticide leaching. The stronger the correlation considered the smaller the exceeding probability.

In conclusion, Dubus and Janssen demonstrated that:

- Monte Carlo results may be strongly affected by the seed number used in the sampling and should be considered inherently uncertain.
- A number of subjective choices have to be made during MC modelling [e.g., (pdf selection), pdf parameterisation, attribution of correlations] and these will significantly affect MC results obtained.
- Results of Monte Carlo modelling should be interpreted with care.

Therefore,

- The subjective choices made during the implementation of this technique can influence the outcome of the analysis.
- These include choices of the type of statistical distribution attributed to model parameters.
- The upper and lower limits of the distribution within which samples are taken (truncation).
- Specification of dependencies and/or correlations between parameters.
- The tool and method used for sampling, and the number of samples generated from the distributions.

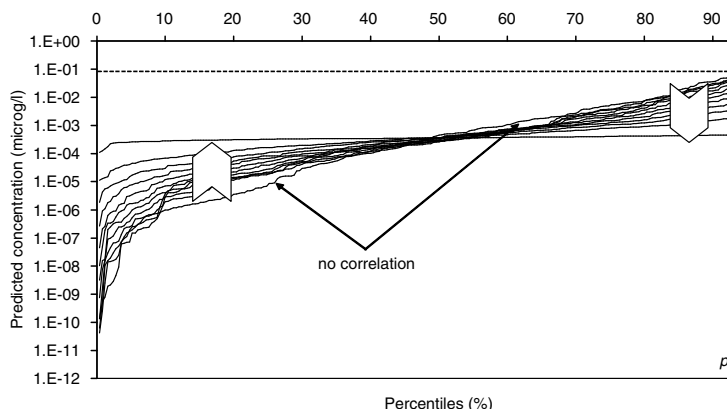


Fig. 9. Cumulative distribution charts obtained for random samples generated using different correlation coefficients between K_{oc} and DT50. The chevrons point towards curves obtained for the larger correlations.

3.2. Part 2

These consequences are the starting point of a new exercise carried out by six pesticide fate modelers with experience in the implementation of Monte Carlo approaches in the regulatory context (Beulke *et al.*, 2006). The staff involved in this study was composed of Sabine Beulke, Central Science Laboratory, Sand Hutton, York, UK coordinator of project; Colin D. Brown, Environment Department, University of York, UK; Igor G. Dubus, BRGM, Water Division, Orléans, France; Hector Galicia, Springborn Smithers Laboratories (Europe) AG, Horn, Switzerland; Nicholas Jarvis, Department of Soil Science, SLU, Uppsala, Sweden; Dieter Schaefer, Bayer CropScience, Metabolism and Environmental Fate, Monheim, Germany; Marco Trevisan, Istituto di Chimica Agraria ed Ambientale, Università Cattolica del Sacro Cuore, Piacenza, Italy.

They were provided with data on degradation and sorption of a pesticide measured in 18 soils. Each modeler was asked to analyze these data, assign statistical distributions and sample values from these distributions. A leaching assessment was then carried out using a harmonized scenario and modeling protocol (*e.g.*, simulation time, output generated) for each of the six sets of sampled degradation and sorption data.

The data on degradation and sorption of metamitron the pesticide chosen, are reported in Table 1. All modelers analyzed these data on metamitron sorption and degradation for correlations and selected statistical distributions. Correlation coefficients between degradation rate constants and K_f values (-0.35), degradation rate constants and K_{oc} values (-0.38), DT50 values and K_f values (0.20) and DT50 values and K_{oc} values (0.26) were not significant at the 10% probability level. Five of the six modelers evaluated the fit of different distributions and retained the normal or lognormal distribution, using Anderson Darling (AD), Kolmogoroff Smirnov (KS) indices and Shapiro-Wilk test (Figures 10, 11 and 12).

Table 1. Data on degradation and sorption of metamitron measured in laboratory studies with 18 soils with a range of properties.

	K _f (Lkg ⁻¹)	OC (%)	K _{oc} (Lkg ⁻¹)	k (d ⁻¹)	DT50 (d)
Min	0.77	0.6	71	0.0140	10.7
Max	7.6	2.4	380	0.0650	49.5
Mean	3.2	1.6	190	0.0267	30.2
Median	2.3	1.5	172	0.0260	26.7
s.d.	2.2	0.51	91	0.0122	11.1
CV (%)	69	32	48	46	37

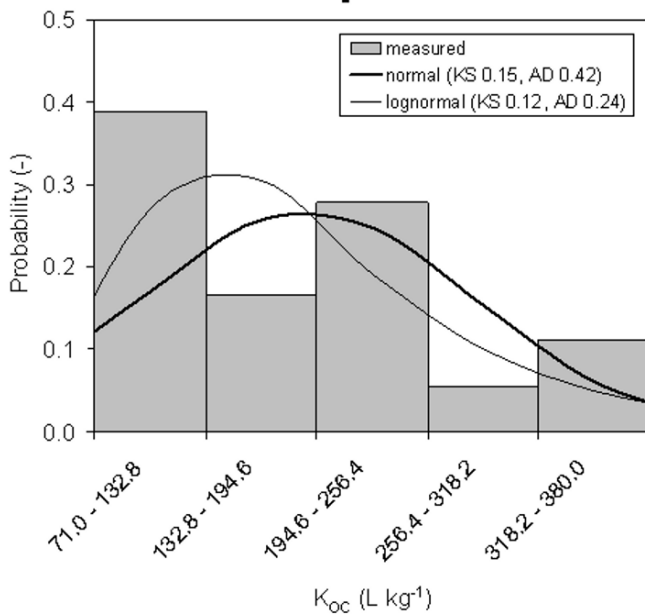


Fig. 10. The fit of K_{oc} values using Anderson Darling (AD), Kolmogoroff Smirnov (KS) indices.

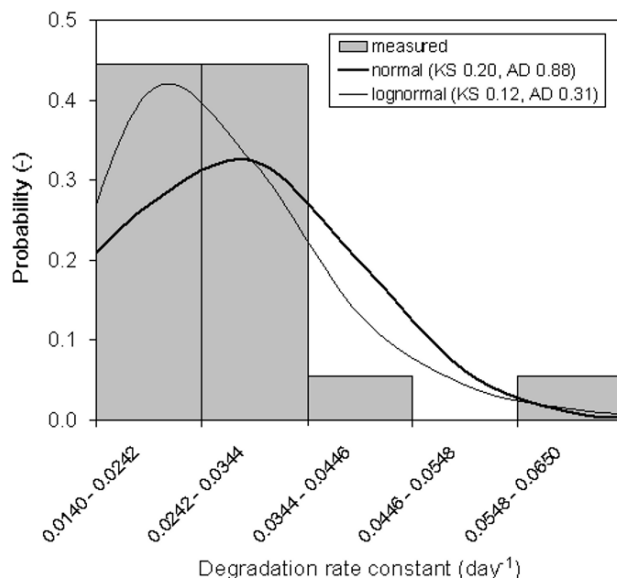


Fig. 11. The fit of degradation rate constant values using Anderson Darling (AD), Kolmogoroff Smirnov (KS) indices.

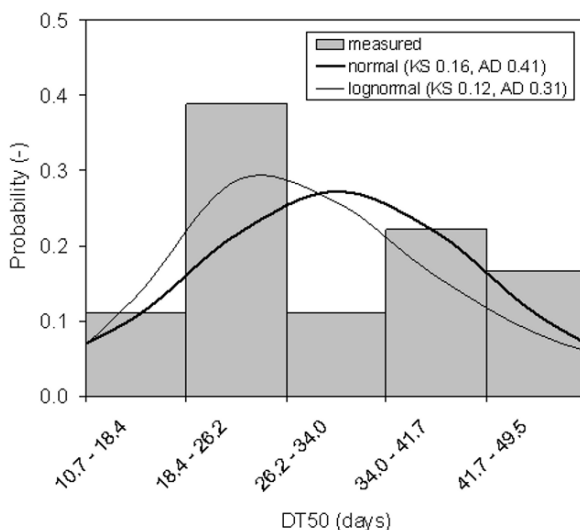


Fig. 12. The fit of DT50 values using Anderson Darling (AD), Kolmogoroff Smirnov (KS) indices.

3.3. Parametrisation

All modelers made a subjective decision on whether to truncate the distributions or not (*i.e.*, exclude values outside a certain range). Truncation is a means of avoiding the sampling of extreme values from the tails of the distribution. The modelers truncated the distribution if they considered the extreme values to be unrealistic. Six modelers made decisions on the type of statistical distribution assigned to degradation and sorption data for metamitron; the upper and lower limit of the distribution within which samples are taken (truncation); correlation between parameters; the tool and method used for sampling; the number of samples generated.

Based on the lack of a significant correlation between input parameters modeler 1 (Table 2) sampled sorption and degradation parameters of metamitron independently. The lognormal distributions gave a better fit and he calculated the log mean and log standard deviation of the lognormal distribution of the degradation rate constants and of K_{oc} . The distributions were not truncated. Combinations of degradation rate constants and K_{oc} values were then sampled from the lognormal distributions with the random number generator in Microsoft Excel 97. Sets of 100, 1,000, and 10,000 values were sampled from each distribution. The coefficient of variation of the 5th and the 95th percentiles of the sampled values between 10 consecutive samplings was approximately 10% for samples of 1000 values. For that 1000 model runs were considered sufficient for a robust leaching assessment.

Modeler 2 (Table 3) decided not to include correlation in the sampling. A log-normal distribution was chosen based on the Anderson Darling index for both parameters. The log mean and log standard deviation of the distribution of K_{oc} values and DT50 values were determined. The distribution was truncated at the 0.5th and 99.5th percentile. These percentiles were chosen such that the measured values were included in the sampling interval. A total number of 5000 combinations of K_{oc} values and DT50 values were sampled with Crystal Ball using Latin Hypercube Sampling. This method divides the distribution into intervals of equal probability and samples from each interval.

Table 2. Modelisation choice of modeler 1.

Modeler 1	
Variables considered	K_{OC} , k
Distributions assigned	Lognormal
Selection criterion/goodness of fit statistics	Kolmogorov-Smirnov
Original paper consulted	No
Correlation	No
Truncation	No
Sample size	1000
Software used	MS Excel
Sampling method	Random

Table 3. Modelisation choice of modeler 2.

Modeler 2	
Variables considered	K_{OC} , DT50
Distributions assigned	Lognormal
Selection criterion/goodness of fit statistics	Anderson-Darling
Original paper consulted	No
Correlation	No
Truncation	Yes
Sample size	5000
Software used	Crystal Ball
Sampling method	Latin Hypercube

Modeler 3 (Table 4) sampled 150 degradation rate constants and K_{oc} values from correlated lognormal distributions ($r = -0.39$) using a software package for sensitivity and uncertainty analysis (UNC SAM). The lognormal distribution was selected based on the Shapiro-Wilks test for normality of untransformed (test for normal distribution) and log-transformed (test for lognormal distribution) degradation rate constants and K_{oc} values. The parameters of the distributions were derived by fitting a normal distribution to log-transformed data. Modeler 3 truncated the distributions at the log mean $\pm 2.58 \times \log$ standard deviation (= 1st and 99th percentiles). Combinations of small K_{oc} values and long DT50 values were sampled less frequently by modeler 3 than by modelers 1 and 2.

Modeler 4 (Table 5) considered that none of the fits obtained were adequate from a statistical perspective. The modeler adopted an approach similar to those used in elicitation. The modeler assigned a triangular distribution with three parameters to the degradation rate constants (minimum = 0.008 d^{-1} , maximum = 0.074 d^{-1} , likeliest value = 0.026 d^{-1}) and K_{oc} values (minimum = 31.3 L kg^{-1} , maximum = 434.2 L kg^{-1} , likeliest value = 172.0 L kg^{-1}). The likeliest value of the triangular distribution (the mode) was set to the median of 18 measurements. The minimum and maximum of the distribution was selected so that the probability of sampling a value smaller than the measured minimum and maximum was 2.78%. The total probability of sampling a value outside the measured range was thus one divided by 18 with 18 being the number of measurements. Modeler 4 selected this approach of setting the minimum and maximum values of the triangular distribution according to the inverse of the number of data points available because it offers the advantage of being adapted to the size of datasets. If a small number of data points are available, then the probability of obtaining values outside the range defined by the minimum and maximum observed is considered to be large. Conversely, for large datasets, the probability of seeing a value outside the minimum-maximum values observed is considered to be small. A total of 5000 values of

Table 4. Modelisation choice of modeler 3.

	Modeler 3
Variables considered	K_{OC}, k
Distributions assigned	Lognormal
Selection criterion/goodness of fit statistics	Shapiro-Wilk test for normality of $\log K_{OC}$ and $\log k$
Original paper consulted	No
Correlation	Yes
Truncation	Yes
Sample size	150
Software used	UNC SAM
Sampling method	Latin Hypercube

Table 5. Modelisation choice of modeler 4.

	Modeler 4
Variables considered	K_{oc} , k
Distributions assigned	Triangular
Selection criterion/goodness of fit statistics	Statistical criteria, expert judgment
Original paper consulted	No
Correlation	No
Truncation	No
Sample size	5000
Software used	@RISK
Sampling method	Latin Hypercube

each parameter were sampled using the software @RISK. The number of runs was selected on the basis of literature information. The resulting distributions of sampled values were shifted towards shorter DT50 values and larger K_{oc} values compared with the measurements and with the values sampled by modelers 1, 2, and 3. This is due to the fact that the likeliest value was set to the median measured value. There was a significant discrepancy between the distribution of measured degradation rate constants and the triangular distribution specified by modeler 4 and a larger proportion of larger degradation rate constants were sampled by modeler 4 than by modelers 1, 2, 3 and 6.

In contrast to the other modelers and based on previous work with clay minerals, modeler 5 (Table 6) analyzed these data in the original publication and proposed a relationship between the DT50 values for metamitron, the K_{oc} values and the clay content of the soils tested:

$$DT50 = 3.677 + 0.897 \text{ Clay} + 0.0147 \text{ Koc}$$

with a multiple correlation coefficient $R = 0.6326$. An F-test indicated that there was a statistically significant dependence of the DT50 values on clay content and K_{oc} values at $p < 0.025$ with this model.

Modeler 5 assumed that the clay content of the soil for which the leaching assessment was undertaken was uncertain (*i.e.*, experimental and natural variability were considered by allowing the clay content in this soil to vary by $\pm 3\% =$ approximately 42% relative variation). The modeler sampled 1000 values for the clay content from a triangular distribution with a likeliest value of 7% and a minimum and maximum of 4% and 10%, respectively using Crystal Ball. Next, 1000 K_{oc} values were sampled from a truncated lognormal distribution. The DT50

Table 6. Modelisation choice of modeler 5. N/A = a linear regression was used to calculate DT50 values from Koc values and clay content.

	Modeler 5
Variables considered	K_{OC} , DT50
Distributions assigned	K_{OC} lognormal Clay content triangular DT50 from regression
Selection criterion/goodness of fit statistics	Anderson-Darling
Original paper consulted	Yes
Correlation	N/A
Truncation	Yes (K_{OC})
Sample size	1000
Software used	Crystal Ball
Sampling method	Latin Hypercube

value was then calculated for each run from the sampled clay content and K_{oc} value using the regression equation given above. The combinations of DT50 values and K_{oc} values generated by modeler 5 were much less scattered than those provided by the other modelers. The range of DT50 values (8.6–18.5 d) was smaller than the range of the values sampled by the other modelers. It was also smaller than the range of measured DT50 values. The reason for the relatively small range of sampled values may be that the unexplained error term in the regression was ignored. This will exaggerate the strength of the relationship between DT50, clay content and K_{oc} and reduce the randomness in the sampled DT50 values.

Modeler 6 (Table 7) assumed that sorption and degradation parameters of metamitron are independent based on correlation analysis and no correlation was included in the sampling. The modeler found that DT50 values and K_{oc} values were normally distributed based on the Shapiro-Wilks test (0.05 significance level). The distributions were not truncated. For each variable set for a given simulation, 400 values were generated by random sampling using a spreadsheet-based Monte Carlo approach (Microsoft Excel 2002). The modeler derived the sample size from the following equation:

$$n = 4 pq/L^2$$

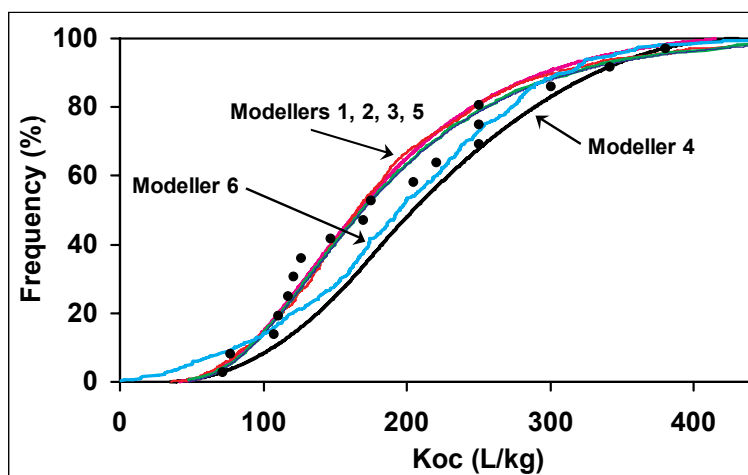
where n is the sample size, p is the event probability (here the probability of chemical leaching) and $q = 100 - p$, L is the accepted error ($= 100 - \text{confidence interval}$).

Table 7. Modelisation choice of modeler 6.

	Modeler 6
Variables considered	K_{OC} , DT50
Distributions assigned	Normal
Selection criterion/goodness of fit statistics	Shapiro-Wilk test for normality of K_{OC} and DT50
Original paper consulted	No
Correlation	No
Truncation	No
Sample size	400
Software used	MS Excel
Sampling method	Random

The number of samples calculated from this equation is largest when $p = q = 50$. For a confidence interval of 95%, the sample size was calculated to be 400 iterations.

Figures 13 and 14 show the cumulative frequency distribution of K_{OC} and DT50 values chosen by the six modelers. It is possible to see the different behavior due to the different choice made.

**Fig. 13.** The cumulative frequency distribution of K_{OC} values chosen by the six modelers.

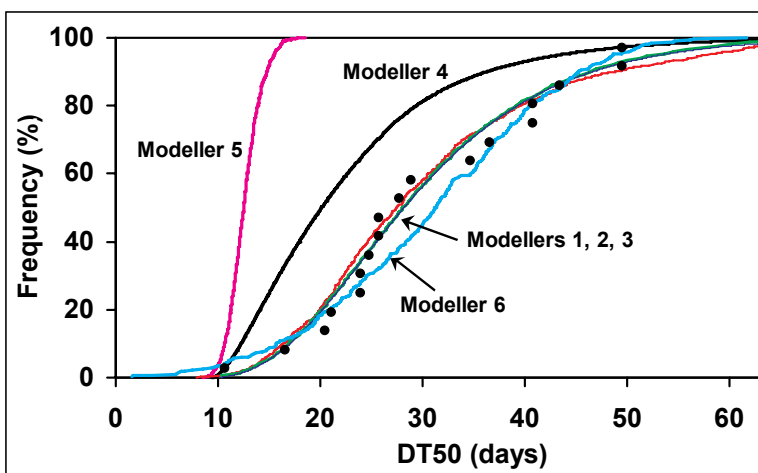


Fig. 14. The cumulative frequency distribution of DT50 values chosen by the six modelers.

3.4. Modelling

PELMO does not run in a probabilistic way and all input parameters must be sampled a priori outside the model. Correlation between the parameters or truncation was also included a priori in the sampling of the input values. Therefore PELMO was run deterministically every time.

Leaching of metamitron was simulated on the basis of a soil, weather and crop scenario that is commonly used within pesticide registration in Europe and are provided with the PELMO model.

These data for the single year were repeated to give a total simulation period of 20 years. Metamitron was assumed to be applied to a sugar beet crop on May 1st in each of the 20 years at a rate of 3 kg ha^{-1} . Routines for losses via runoff, erosion and volatilization were turned off in the model as the exercise concentrated on the simulation of leaching.

The model output of interest was the average annual concentration in leachate at 1 m depth for the 20th year of the simulation period. Annual average concentrations in leachate for each of the 20 years were calculated from the simulated mass of metamitron in leachate and the volume of leachate.

Comments on results shown in Figures 15, 16, and Table 8 are:

- Simulated concentrations based on data provided by modeler 5 were much smaller than for the remaining five sets of input data and did not exceed $0.001 \mu\text{g L}^{-1}$ for any of the 1000 model runs. Modeler 5 used a regression equation derived from the experimental data to calculate the K_{oc} and DT50 values. Since the error term from the regression was ignored, the resulting range of DT50 values (8.6–18.5 d) was much smaller than for the remaining sets of input parameters which were derived from sampled distributions.

- Concentrations at the upper percentiles calculated using data provided by modeler 4 were smaller than those for modelers 1, 2 and 6 and were also smaller than those for modeler 3 except for the upper 2% of values. This is due to the fact that the distributions of parameters sampled by modeler 4 were shifted towards shorter DT50 values and larger K_{oc} values due to triangular distribution adopted.

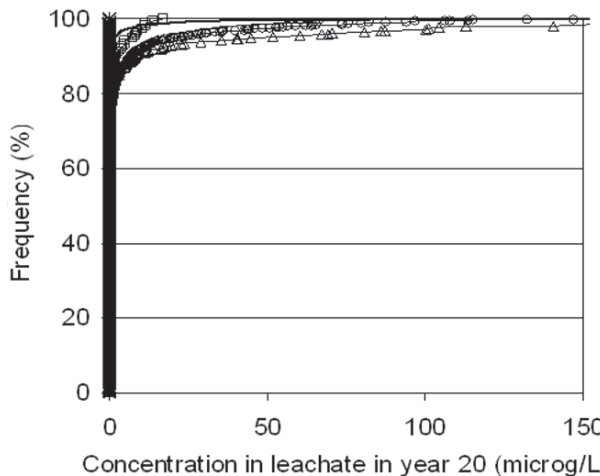


Fig. 15. Cumulative distribution curve of metamitrom concentration in leachate.

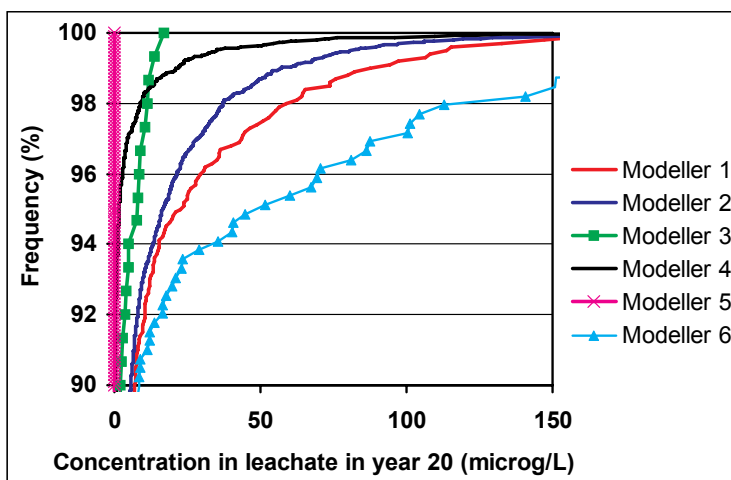


Fig. 16. The last 10% of cumulative distribution curve of metamitrom concentration in leachate.

Table 8. Percentiles and statistics of the cumulative frequency distributions for simulated maximum annual average concentrations in leachate at 1-m depth and probabilities of exceeding $0.1 \mu\text{g L}^{-1}$ generated from input data sampled by the modelers.

	Modeler 1	Modeler 2	Modeler 3	Modeler 4	Modeler 5	Modeler 6
50th Percentile	0.004	0.004	0.003	<0.001	<0.001	0.002
80th Percentile	1.2	0.88	0.39	0.009	<0.001	0.990
90th Percentile	7.0	5.6	2.0	0.25	<0.001	8.4
95th Percentile	22.8	16.5	7.8	1.7	<0.001	48.9
99th Percentile	87.8	57.2	12.7	21.7	<0.001	214.2
Exceedance probability (%)	35.7	33.2	27.0	12.8	0.0	29.4
Mean	4.2	3.0	0.92	0.83	<0.001	8.6
Standard deviation	16.3	12.2	2.7	6.6	0.004	36.0
CV (%)	390	408	297	803	1080	421

- Modeler 3 was the only participant in the ring test who included a correlation between the degradation and sorption parameters. As a result, combinations of small K_{oc} values and long DT50 values were sampled less frequently than by modelers 1, 2 and 6. The model simulated greater potential for the pesticide to leach to depth for these extreme combinations. Concentrations at the upper percentiles of the cumulative frequency curve were, thus, larger when the parameters were sampled from uncorrelated distributions. The 50th percentile concentration in leachate and the probability of exceeding $0.1 \mu\text{g L}^{-1}$ were similar with or without correlation. The correlation between K_{oc} and the degradation rate coefficient was only significant at $p = 0.12$, and might therefore be justifiably ignored. This illustrates one important subjective choice in probabilistic risk assessments for leaching.
- The 95th and 99th percentile concentration in leachate calculated from data provided by modeler 6 were much larger than those calculated for the remaining five sets of input parameters. This is because the parameters were sampled from untruncated normal distributions which generated a number of very small K_{oc} values. The upper percentiles of the output distribution were strongly influenced by truncation of the input distributions.
- Modelers 1 and 2 sampled K_{oc} values and DT50 values from almost identical lognormal distributions. This resulted in very similar combinations of sampled K_{oc} and DT50 values. However, modeler 1 sampled from untruncated distributions whereas modeler 2 used the 0.5th and 99.5th percentiles as cut-off values.

- A larger number of small K_{oc} values in combination with long DT50 values were, thus, sampled by modeler 1, giving somewhat larger simulated concentrations at the upper percentiles.
- Modeler 3 sampled 150 values from the distributions and modeler 2 5000. Both using Latin Hypercube method and same lognormal distributions. To test this effect, the probability of exceeding $0.1 \mu\text{g L}^{-1}$ and the 95th percentile concentration in leachate were calculated from 2, 3, 4... up to 5000 consecutive model runs to evaluate the influence of sample size on the model outcome. The exceeding probability changed considerably up to about 50 model runs. The changes in the exceeding probability were smaller from this point onwards. The 95th percentile concentration was almost constant from about 450 model runs. (Figure 17).
- It is difficult to objectively determine an adequate sample size. Modeler 6 selected the sample size using an equation which is based on statistical considerations. This equation can give an initial estimate. However, the sample size that is required for a robust assessment also depends on the number of combined parameters, the modeling scenario used, the model output of interest and the sampling method.
- Modelers 1 and 6 used conventional random sampling whereas modelers 2, 3, 4 and 5 used Latin Hypercube Sampling. The latter method divides the distribution into intervals of equal probability and samples from each interval. Latin Hypercube Sampling is more precise for producing random samples than conventional random sampling because the full range of the distribution is sampled in a more consistent manner. Thus, a smaller number of trials is required with Latin Hypercube Sampling to achieve the same accuracy.

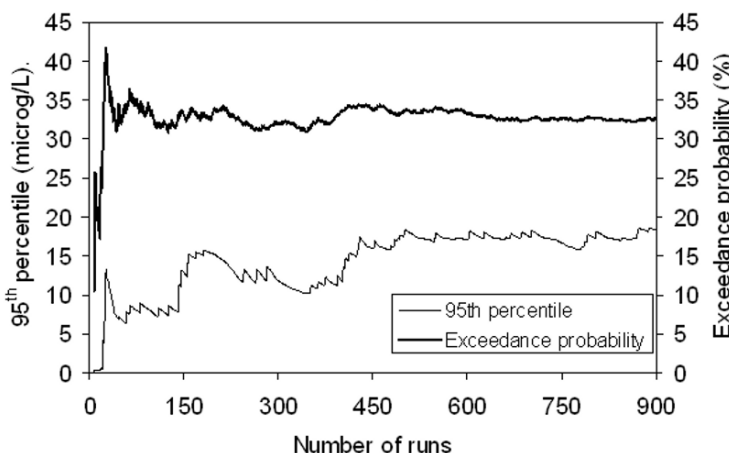


Fig. 17. The exceeding probability and the 95th percentile concentration in function of model runs numbers.

4. General Conclusion

User subjectivity can significantly influence the results of probabilistic exposure assessments, differences are greatest at the extremes of the distribution, which are normally the focus during regulatory decision-making. Standard protocols are required and all methodology should be documented to improve transparency and reproducibility. Guidance on how to report probabilistic exposure calculations must be adopted from regulatory point of view.

Uncertainty and decision-making are strictly related. As suggested by Jarvis (2007), prediction uncertainty depends strongly on the context of application, on the data available and on the training and level of expertise of the end-users (Figure 18). However, tools supporting regulatory decision-making should ensure that model error is weighted towards conservative estimates of risk (the precautionary principle), try at the outset to reach consensus among end-user and stakeholders on appropriate methodologies, make the uncertainty explicit.

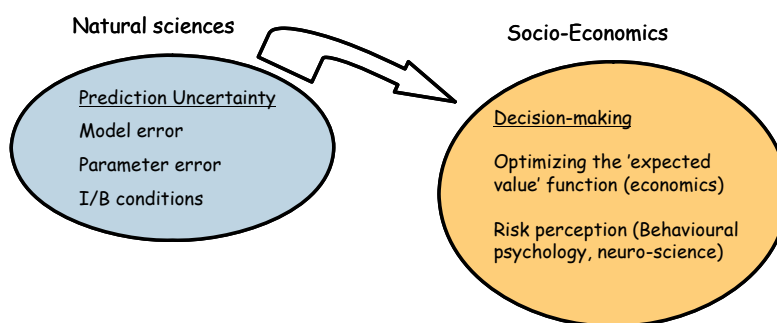


Fig. 18. Relationship between natural science and regulatory.

References

Beulke, S., Brown, C.D., Dubus, I.G., Galicia, H., Jarvis, N., Schaefer, D., and Trevisan, M. (2006) User-subjectivity in Monte Carlo modeling of pesticide exposure. *Environ. Toxicol. Chem.* 25:2227–2236.

Bobba, A.G., Singh, V.P., and L. Bengtsson. (2000) Application of environmental models to different hydrological systems. *Ecol. Model.* 125:15–49.

Carbone, J.P., Havens, P.L., and Warren-Hicks, W. (2002) Validation of pesticide root zone models 3.12: employing uncertainty analysis. *Environ Contam. Chem.* 21:1578–1590.

Cheng, H.H. (eds.) (1990) *Pesticides in the Soil, Environment: Processes, Impacts, and Modelling*. Soil Science Society of America, Inc., Madison, WI.

Dubus, I.G. and Janssen, PHM. (2003) Issues of replicability in Monte Carlo modeling: a case study with a pesticide leaching model. *Environ Toxicol. Chem.* 22:3081–3087.

Dubus, I.G. and Brown, C.D. (2002) Sensitivity and first step uncertainty analyses for the preferential flow model MACRO. *J. Environ. Qual.* 31:227–240.

Dubus, I.G., Brown, C.D., and Beulke, S. (2003) Sources of uncertainty in pesticide fate modelling. *Sci. Tot. Environ.* 317:53–72.

ECOFRAM (1999) <http://www.epa.gov/oppefed1/ecorisk/>

EUPRA (2001) Probabilistic risk assessment for pesticides in Europe. Implementation and research needs. Report from the European Workshop on Probabilistic risk Assessment for the Environmental Impacts of Plant protection products, The Netherlands, June 2001.

FOCUS (2000) FOCUS groundwater scenarios in the EU plant protection product review process. Report of the FOCUS Groundwater Scenarios Workgroup, EC Document Reference Sanco/321/2000, 197 pp.

Fontaine, D.D., Havens, P.L., Blau, G.E., and Tillotson, P.M. (1992) The role of sensitivity analysis in groundwater risk modeling for pesticides. *Weed Technol.* 6:716–724.

Janssen, P.H.M., Heuberger, P., and Klepper, O. (1994) UNSCAM: a tool for automating sensitivity and uncertainty of analysis. *Environ. Software.* 9:1–11.

Jarvis, N.J. (2007) Review of non-equilibrium water flow and solute transport in soil macropores: principles, controlling factors and consequences for water quality, *European Journal of Soil Science* 58:523–546.

Klepper, O., and den Hollander, H.A. (1999) A comparison of spatially explicit and box models for the fate of chemicals in water, air and soil in Europe. *Ecol. Model.* 116:183–202.

Lei, J.H. and Schilling, W. (1996) Preliminary uncertainty analysis – a prerequisite for assessing the predictive uncertainty of hydrologic models. *Wat. Sci. Tech.* 33:79–90.

Soutter, M., and Musy, A. (1998) Coupling 1D Monte-Carlo simulations and geostatistics to assess groundwater vulnerability to pesticide contamination on a regional scale. *J. Contamin. Hydro.* 32:25–39.

Trevisan M. and Vischetti, C. (2005) Assessment of uncertainty associated with the extent of simulation processes from point to catchment: application to 1D-pesticide leaching models. In *Soil-Water-Solute Process Characterization: An Integrated Approach* (Alvarez-Benedi, J. and Munoz-Carpena, R, eds.), CRC Press, ISBN: 1-56670-657-2, pp. 673–692.

Van der Werf, H.M.G. (1996) Assessing the impact of pesticides on the environment. *Agric. Ecosyst. Environ.* 60:81–96.

Vanclooster, M., Boesten, J.J.T.I., Trevisan, M., Brown, C.D., Capri, E., Eklo, O.M., Gottesburen, B., Gouy, V., and van der Linden, A.M.A. (2000) A European test of pesticide leaching models: methodology and major recommendations. *Agr. Water Manage.* 44:1–19.

Warren-Hicks, W., Carbone, J.P., and Havens, P.L. (2002) Using Monte Carlo techniques to judge model prediction accuracy: validation of the Pesticide Root Zone Model 3.12. *Environ. Toxicol. Chem.* 21:1570–1577.

Wingle, W.L., Poeter, E.P., and McKenna, S.A. (1999) UNCERT: geostatistics, uncertainty analysis and visualization software applied to groundwater flow and contaminant transport modeling. *Comput. Geosci.* 25:365–376.

Wolt, J., Singh, P., Cryer, S., and Lin, J. (2002) Sensitivity analysis for validating expert opinion as to ideal data set criteria for transport modeling. *Environ. Toxicol. Chem.* 21:1558–1565.

Recommended practices in global sensitivity analysis

Andrea Saltelli, Daniele Vidoni, Massimiliano Mascherini

The European Commission, Joint Research Centre, Institute for the Protection and Security of the Citizen (IPSC), TP 361, 21027 Ispra (VA), Italy.

Abstract

Practices for global sensitivity analysis of model output are described in a recent textbook (Saltelli *et al.*, 2007). These include (i) variance based techniques for general use in modelling, (ii) the elementary effect method for factor screening for factors-rich models and (iii) Monte Carlo filtering. In the present work we try to put the practices into the context of their usage. We start by describing the present debate on the use of scientific models, and how uncertainty and sensitivity analysis can assist in testing model quality. We discuss Type I, II and III errors in the context of sensitivity analysis and what are the requirements for a good analysis. We also present sensitivity analysis in relation to post normal science (PNS) and model pedigrees.

Keywords: uncertainty analysis, sensitivity analysis, impact assessment, Monte Carlo, post normal science.

1. Introduction

When and how do we need sensitivity analysis? According to Pilkey and Pilkey-Jarvis (2007) quantitative mathematical models used by policy makers and government administrators to form environmental policies is seriously flawed. Pilkey's remark is the last in a series of stark reminders on the limits of quantitative mathematical modeling of natural or man-made systems (see Chapter 1 in Saltelli *et al.*, 2007 for a review). Michael Crichton, an author more likely found on our bedside table than our desk at work, goes as far as to say that model based prediction should bear a label, "WARNING: COMPUTER SIMULATION MAY BE ERRONEOUS and UNVERIFIABLE." Like on cigarettes, Crichton (2004) who is more of a novelist than an essayist, shows that the discourse about models seems to have pervaded society, and that – particularly when models form the basis of policy, or are otherwise used to suggest such a use, more stringent standards of

proof are called for. Note that the present crisis, if we want to call it this, has a long story (e.g., Oreskes *et al.*, 1994).

It might be observed that even when models are used within closed disciplinary boundaries and academic contexts, scientist should be careful in their description of the mapping of assumptions into inferences to avoid being falsified. Recommendations on how to use sensitivity analysis to this effect can be found in disciplinary textbooks (Kennedy, 2007).

In fact the link between the critique of models and global sensitivity analysis is that the latter can be seen as a useful ingredient of an upgraded model pedigree.

We have used the qualification “global” in relation to sensitivity analysis. One point we shall try to make in this work is that the main criterion to be followed in choosing a method for sensitivity analysis is that it be global.

By global we mean that the effect of an input factor (assumption) on the output (inference) should be possibly averaged over the entire space of the input factors.

By contrast, local methods look at the effect of changing one factor/assumptions at a given point in the space of the input factors while keeping all other factors constant.

In the following section we highlight some general requirements for a convincing and defensible sensitivity analysis.

2. Generalities about sensitivity analysis

Global sensitivity analysis can be defined as “The study of how the uncertainty in the output of a model (numerical or otherwise) can be apportioned to different sources of uncertainty in the model input”. Global is a necessary specification, due to the fact that most analysis met in the literature are local or one-factor-at-a-time.

Our preferences in SA are for variance based methods. The variance of the out-come is decomposed (ANOVA-like) according to factors effects and their interactions.

Computations can be done via Monte Carlo as described briefly in the following. If this is too computationally expensive, one could go for averages of elementary effects by moving each factor a step at a time, but do it over and over and take the average. Finally one can use Monte Carlo filtering when the question of interest concern higher or lower tails in the distribution of the output.

An engineer’s view of sensitivity analysis is in Figure 1.

One can see how different kinds of assumptions in the data, in the estimation procedure, and in the model construction are plugged into the analysis to generate an empirical distribution function of the output of interest (the inference). Finally, some characteristic of this distribution, for example, the variance; can be broken down into bits attributed to this or that group of factors(s). This figure is a crude simplification of the messy state of affairs met when an analyst tries to understand what is driving the uncertainty in his/her inference. Combining model uncertainty

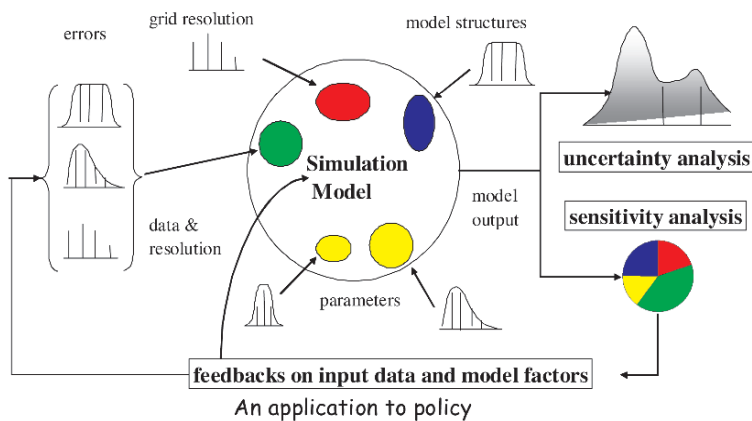


Fig. 1. Idealized scheme for sensitivity analysis.

with data uncertainty and estimation uncertainty is generally not as straightforward as one could imply from the scheme in Figure 1. Yet the point of this figure is that a careful sensitivity analysis should in principle include several layers of uncertainty not just those that are the easiest to assess. A common criticism of modeling is the so called 'Delusion of Uncertainty' (Taleb, 2007) whereby one carefully assesses those uncertainties which are the least influential but the most easy to handle. Van der Sluijs *et al.* (2005) argues that with present day uncertainty assessment practices the uncertainties that are more carefully scrutinized are usually those that are the least relevant (lamp-posting). The term lamp-posting comes from the old joke of the man searching for a lost key at night not in the garden before his house's door, where the key fell, but under the street lamp on the road as "it is dark over there in the garden".

3. The critique of models

As mentioned in the introduction, we may be witnessing a critique of models which, no longer confined to scientists and epistemologists, invests society at large, as shown by Crichton (2004). Have models fallen out of grace and is modeling just useless arithmetic as claimed by Pilkey and Pilkey-Jarvis (2007)? According to these authors quantitative mathematical models used by policy makers and government administrators to form environmental policies are seriously flawed. Yet this is not a radical book and the issue taken by the authors is not that modeling is useless, but rather that quantitative modeling should be used with caution in relation to environmental systems. One of the several interesting examples discussed in the book concerns the Yucca Mountain repository for radioactive waste disposal, where a very large model called TSPA (total system performance assessment) is used to guarantee the safe containment of the waste. TSPA is Composed

of 286 sub-models. TSPA (like any other model) relies on assumptions – a crucial one being the low permeability of the geological formation and hence the long time needed for the water to percolate from the desert surface to the level of the underground disposal. The confidence of the stakeholders in TSPA was not helped when evidence was produced which could lead to an upward revision of four orders of magnitude of this parameter. If the world of the ecologists is shaken by the Pilkey-Jarvis book, that of the financial mathematicians and modelers is the target of the attack of “The Black Swan” by Taleb (2007). We just can’t predict, concludes Taleb, and we are victims of the ludic fallacy, the illusion that game theories may help to model real-life financial system. Modeling is just another attempt to platonify reality, meaning: the attempt to force upon a messy state of affairs the simple and elegant structure of formal systems.

Taleb’s position (2007) on the ‘delusion of uncertainty’ is similar to the distinction between risk and uncertainty and between uncertainty and ignorance made by practitioners in post normal science.

Many will disagree with the works just cited as happened during the presentation at the NATO school in Vrsar on which the present contribution is based. Yet our point is that the cat is out of the bag already. Stakeholders and media alike will tend to expect or suspect instrumental use of computation models, amplification or dampening of uncertainty as a function of convenience, and so on.

The biologist Rosen (1990) had been among the first to draw attention to the fact that modeling is not a science but rather a craftsmanship (Figure 2). After Rosen, “World” (the natural system) and “Model” (the formal system) are internally entailed-driven by a causal structure. Nothing entails with one another “World” and “Model”; the association is hence the result of a craftsmanship. In fact most practitioners of modeling have come to live with the fact that more than one model may be compatible with the same set of data or evidence. Beven (2001), an hydrologist, calls this ‘equifinality’. Maybe none of this is particularly new or exciting. Since Galileo’s times scientists have had to deal with the limited capacity of the human mind to create useful maps of “World” into “Model”. The emergence of “laws” can be seen in this context as the painful process of simplification, separation, and identification which leads to a model of uncharacteristic simplicity and beauty.

“Groundwater models cannot be validated” was the provocative title of an article from Konikov and Bredehoeft (1992). Konikov and Bredehoeft’s work was reviewed on Science in “Verification, Validation, and Confirmation of numerical models in the earth sciences” (Oreskes *et al.*, 1994). Both papers focused on the impossibility of model validation. According to Oreskes, natural systems are never closed, and models put forward as description of these are never unique. Models can never be verified or ‘validated’, but only ‘confirmed’ or ‘corroborated’.

Van der Sluijs (2002) has written extensively on sciences crisis of credibility in model use, following the Netherlands media scandal of 1999. This is another instance in which the debate on the use of models has left the laboratories impact on the media and society. Titles such as “Environmental institute lies and deceits”;

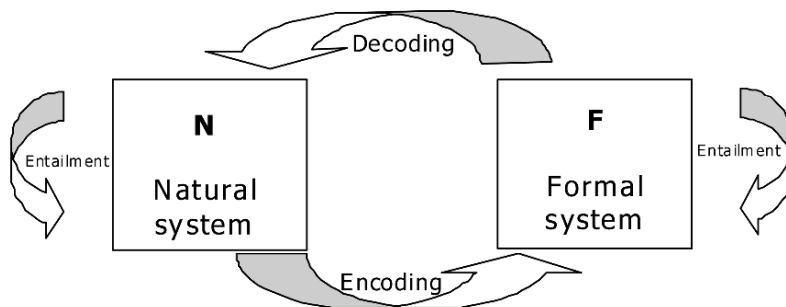


Fig. 2. The process of modeling, according to Rosen (1991).

“Fuss in parliament after criticism on environmental numbers”; “The bankruptcy of the environmental numbers”; “RIVM (Dutch acronym of the environmental institute focus of the scandal) over-exact prognoses based on virtual reality of computer models”, and so on are not what the average modeler would like to see in reference to his or her work.

Is the reference to virtual reality appearing on a Dutch tabloid an irreverence? Perhaps not according to the post-modern French thinker Baudrillard (1999) who presents “simulation models” as unverifiable artifacts which, used in the context of mass communication, produce a fictitious hyper reality that annihilates truth.

In short, this brief discussion of the critique of models (Saltelli *et al.*, 2007) serves the purpose to inform modelers of a present danger: that their inference might be called into question, that their motivation might be the subject of scrutiny, that in general, partial or instrumental use of models might be suspected by stakeholders whenever the inference offered by a model has a bearing on society.

Note that this is not a specific affliction of models but part of a wider debate on science’s legitimacy at the science-policy interface. Hindsight on the role of science in a post-modern world is offered by Post-Normal Science (Figure 3) (Funtowicz and Ravetz, 1993; Funtowicz *et al.*, 1996).

Post-Normal science suggests a taxonomy of the types of scientific production modes, depending on uncertainties and stakes.

- In “applied science”, when scientific theories are produced and consumed within a closed consortium of experts (peers). In the case of modelling, these could be chemists working on a chemical kinetics problem.
- In “consultancy” when the science is likely to be scrutinized, *e.g.*, a cost-benefit analysis for the construction of a new road or bridge that will affect a community; applied to modelling this could be the econometric analysis underpinning the cost-benefit study.

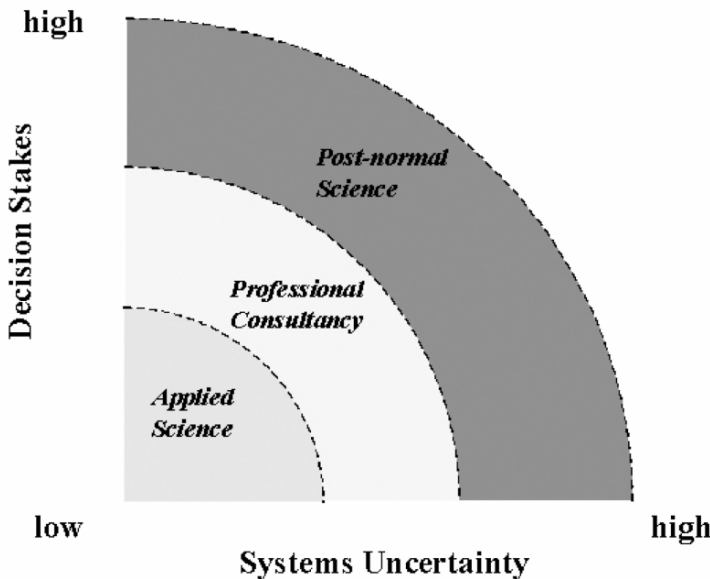


Fig. 3. Uncertainty/stakes diagram after Funtowicz and Ravetz (1990).

In Post-Normal Science, the issue is so uncertain and value-laden that conflicting theories are likely to be waived by opposing fields. In PNS parlance, PNS applies when “facts are uncertain, values in dispute, stakes high and decisions urgent” (Funtowicz and Ravetz, 1993). In modelling, computation of sea-level rise due to global change or the impact of nano-technology may fall in this category.

Distinctive elements of PNS are:

- Appropriate management of uncertainty quality and value-ladenness
- Plurality of commitments and perspectives
- Internal extension of peer community (involvement of other disciplines)
- External extension of peer community (involvement of stakeholders in environmental assessment & quality control)

Note also in Figure 3 that increasing the stakes of an issue will likely increase its uncertainty as well, as some of the parties, *e.g.*, producers of a potentially hazardous substance, may have an interest in amplifying uncertainty to prove that the assessment produced by regulators is of insufficient quality to modify an existing standard. The issue is brilliantly illustrated by Michaels (2005) in relation to fabricated uncertainty.

There is at present a hot debate in the US on whether the quality standard for risk analysis mandated by a recent publication of the Office for Budget Management (OMB, 2006) might be aimed at bogging the regulatory process in the name of transparency (Macilwain, 2006).

4. Suggested requirements for a good sensitivity analysis

Good practices in sensitivity analysis are suggested in several disciplines. Among econometricians Edward E. Leamer, says: "I have proposed a form of organized sensitivity analysis that I call 'global sensitivity analysis' in which a neighborhood of alternative assumptions is selected and the corresponding interval of inferences is identified. Conclusions are judged to be sturdy only if the neighborhood of assumptions is wide enough to be credible and the corresponding interval of inferences is narrow enough to be useful", (Leamer, 1990). The recommendation of Leamer seems more about uncertainty than sensitivity¹, but it is crucial. We should be careful to explore the uncertainty in the input realistically. If we find that the resulting uncertainty in the inference is too wide, and hence useless, we should not try to make it lower by arbitrarily restricting our range of exploration. Similar recommendations are made by Funtowicz and Ravetz, who talks about GIGO (garbage in garbage out) science, where uncertainties in inputs must be suppressed lest outputs become indeterminate (Funtowicz and Ravetz, 1990). Peter Kennedy, another econometrician, suggests anticipating criticism by applying sensitivity analysis. This is one of the ten commandments of applied econometrics according to this practitioner: "Thou shall confess in the presence of sensitivity. Corollary: Thou shall anticipate criticism" (Kennedy, 2007).

We would translate this into "Look at uncertainties before going public with findings".

Kennedy also suggests: "When reporting a sensitivity analysis, researchers should explain fully their specification search so that readers can judge for themselves how the results may have been affected."

Note that sensitivity analysis does not add to the quality of a model per se but to the quality of the model as applied to a well identified task. This is evident as different assumptions may be involved within a given model when applied to different questions. For this reason, we suggest to run the SA with respect to the top-most statement to be supported (or disproved) by the model. If the model investigates the feasibility of a practice, the output of interest is of the type yes or no. If the model computes the impact of a contaminant over a given region and time frame, perhaps an integrated cumulative measure of health effects is the output of interest. One should avoid distracting the user of the analysis with too much sensitivity details pertinent to specific model output.

Note that this requirement (stay with the focus of the analysis) might imply that the optimality of a model must be weighted with respect to the task. According to Beck *et al.* (1997), a model is relevant when it's input factors cause variation in the 'answer'. Hence rather than using systematically the same model we should

¹ As mentioned sensitivity analysis is the study of how uncertainty in the output of a model (numerical or otherwise) can be apportioned to different sources of uncertainty in the model input. Uncertainty analysis focuses instead on quantifying uncertainty in model output. Ideally, uncertainty and sensitivity analyses should be run in tandem, with uncertainty analysis preceding in current practice.

strive for essential (parsimonious) model representations where all active factors do have a bearing on the result being sought. In the context of an impact assessment study, this might imply that we must produce simplified model representations for the purpose of negotiation with stakeholders.

Another, more down to earth technical requirement for a good sensitivity analysis is to allow for a multidimensional averaging in the space of the input factors. In a sensitivity analysis all known sources of uncertainty should be explored simultaneously, to ensure that the space of the input uncertainties is thoroughly explored and that possible interactions are captured by the analysis.

Also the analyst should define unambiguously what he/she mean by importance in relation to input factors. We shall come back to these concepts when discussing the methods.

Finally, it is important that when feasible the sensitivity analysis method be a quantitative one. In most cases there are few important factors which capture – say – 90% of the variance of the output, and many factors who account at most for 10% of it. Just ranking the factors by importance (first, second...) would miss this salient feature of the problem.

5. How to set up the analysis

Here are a few possibilities on how to set up the ensemble of numerical experiments for a sensitivity analysis.

- **Parametric Bootstrap.** In this widely practiced approach one estimates first the model parameters (*e.g.*, kinetic constants), by comparing the selected model (a chemical reaction model) with available evidence (*e.g.*, yield rates for the end-products of the reaction at defined boundary and operating conditions). The estimation procedure yields a set of distributions for the model parameters. Note that these distributions will not be independent in general. The analysts can then draw samples from the distribution of the parameters to do a Monte Carlo type analysis of uncertainties and sensitivities of the yield rates. One shortcoming of this approach is that it does not include model uncertainty and the model is assumed true (if a different chemical process is at play a type III error may ensue – see later).
- **Bootstrapping of the modelling process.** In this approach we sample from the available data and identify a model based on the sample (*e.g.*, we use a subset of yield rate to identify a possible chemical reaction pathway). We then estimate the model parameters with the same sample or a different one (for a discussion see Chatfield, 1993), and iterate the process by drawing a new sample from the data, identifying a possibly different (or same) model, then estimate the parameters and so on. In this way, as more than one model structure may be identified in the process, some measure of model uncertainty is also propagated through the analysis (Chatfield, 1993).

- **Bayesian Model Averaging.** In this approach we start with prior belief about the probability of different model formulations and parameter values, and update these against the available information (e.g., we have more than one possible reaction mechanism, with prior beliefs attached to it, then update these beliefs in view of the available evidence). This way posterior model probabilities and parameter distribution functions are produced from which an uncertainty and sensitivity analysis can be run. This classical Bayesian approach (Hoeting *et al.*, 1999) is reviewed in (Saltelli *et al.*, 2004).

The schematic alternatives offered above should not be taken as unique or prescriptive; there may be several ways to set up an analysis and what is meaningful is clearly context dependent. A legitimate question is hence the following: “what are the implications of selecting an approach versus another for model quality?”.

A first remark is that what constitutes an input for the analysis depends upon how the analysis is set up. As shown above one might include or exclude uncertainty on the model specification, or in the uncertainty in the original data, or in the estimation and so on. Clearly the analysis will be instructive with respect to those elements of uncertainty which have been included; at the same time a modeller will remain ignorant of the importance of those variables which have been excluded or kept fixed in the analysis.

This may lead to type III errors, such as estimating the wrong model. A definition of type III error is: “Assessing the wrong problem by incorrectly accepting the false meta-hypothesis that there is no difference between the boundaries of a problem, as defined by the analyst, and the actual boundaries of the problem” (Dunn, 1997).

Type III is typically a framing error, or “answering the wrong question”. One of the commandments of econometrics of the work of Kennedy (2007) is “Thou shall answer the right question”.

Perhaps the best-known statement of a type III problem is due to the former US secretary of state Donald Rumsfeld. In a celebrated interview he stated: “Reports that say that something hasn’t happened are always interesting to me, because as we know, there are known knowns; there are things we know we know. We also know there are known unknowns; that is to say we know there are some things we do not know. But there are also unknown unknowns – the ones we don’t know we don’t know.” Surprisingly Mr. Rumsfeld was vilified in the press for this statement, which is instead – in the opinion of the authors – a fairly reasonable one.²

Note that in sensitivity analysis as well we have the more usual type I and type II errors. Specifically in sensitivity analysis type I error is “Assessing as important a non important factor”. Type II is “Assessing as non important an important factor.”

Note that in sensitivity analysis specifying a grossly inadequate range of uncertainty for an unknown input can also be classed as a type III error. In the case of

² Nassim Taleb wrote an entire book on type III errors (36), where he also notes that the militaries are normally more aware of type III events (the unexpected and at times fatal Black Swan) than – say – financial analysts.

the Yucca Mountain repository for radioactive waste disposal and TSPA (total system performance assessment) model, a range of 0.02–1 millimeter per year was used for water percolation or flux rate, from the surface down to the repository level. Applying sensitivity analysis to TSPA could or could not identify this as a crucial factor, but this would be of scarce use if the value of the percolation flux were later found to be of the order of 3,000 millimeters per year. This was in fact found to be the case, due to Chlorine 36 (a marker of the Bikini islands era nuclear test of the 70s) being found at the repository level (Pilkey and Pilkey-Jarvis, 2007).

Going back to our questions of the quality implications of running an uncertainty and sensitivity analysis, we would also like to note that high uncertainty in a model based assessment is not the same as low quality. More specifically, we believe that sensitivity analysis can help the analyst to ascertain whether uncertainty in the model based assessment hinders or not the capacity of the analyst to sort policy options outcomes, *i.e.*, to say something useful on whether policy options are distinguishable from one another given the uncertainties.

An example is offered in Figures 4–6. As explained in Figure 4, we are trying to calculate whether it is more convenient to bury or to burn urban waste at a given time and location (Saltelli *et al.*, 2000). In Figure 6, we see that the choice is quite uncertain as we have as many “bury” as we have “burn” in our output. The analyst’s message here should be: “Don’t know”. If the analysis had given us instead something like Figure 5, one would still be uncertain, but overall a landfill seems better than an incinerator. Sorting out whether policy options are distinguishable is possibly one of the most powerful uses for sensitivity analysis.

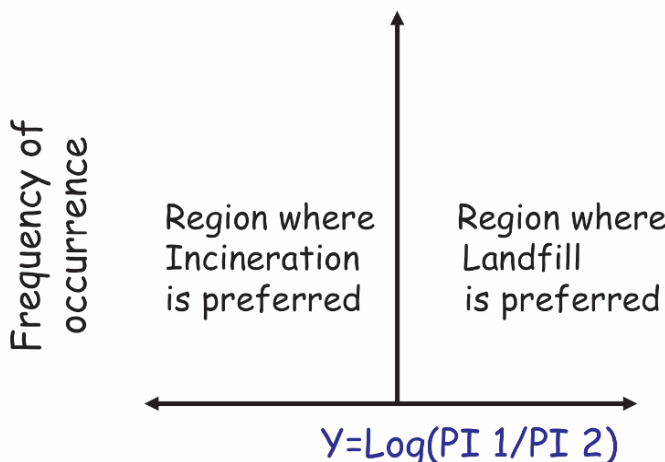


Fig. 4. Set up of the analysis: incineration or landfill? The abscissa is the logarithm of the ration of two pressure-to-decision indices, one pointing to landfill and the other to incineration.

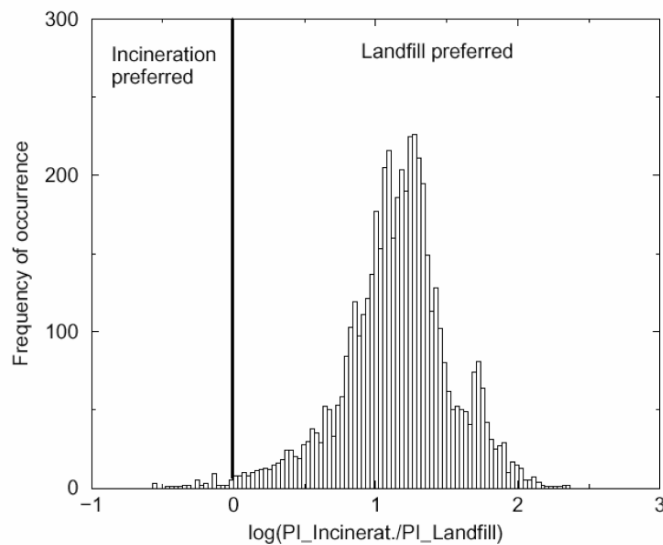


Fig. 5. A decision is possible in spite of the uncertainties; landfill is to be preferred.

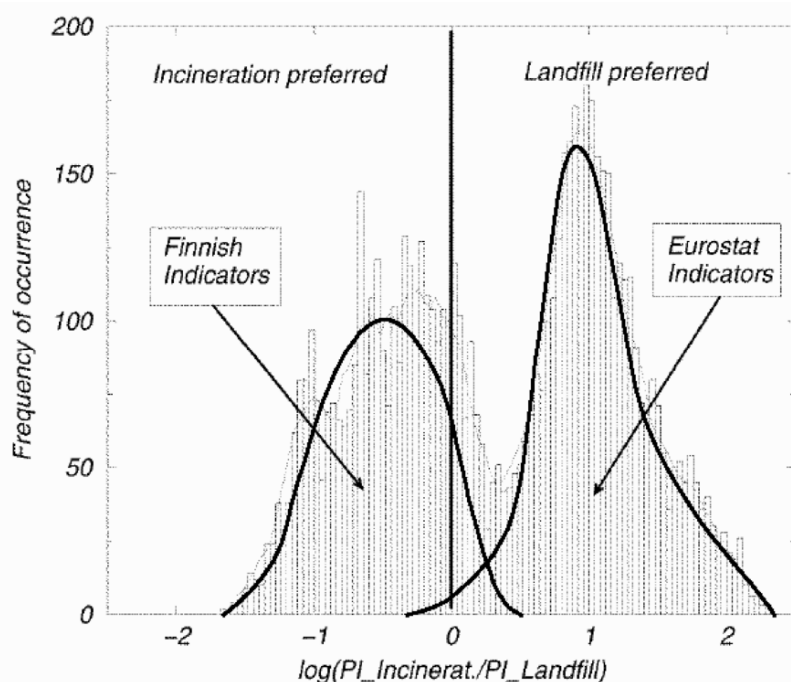


Fig. 6. Uncertainties do not allow a decision to be reached, given the available information and the model adopted.

6. Mathematical and numerical practices

6.1. Scatter-plots and variance based methods

The four scatter-plots in Figure 7 can be taken as a sensitivity analysis of sort. The represent input output maps whereby the output variable Y is plotted against each of the four input variables X_i , with $i = 1, \dots, 4$. All plots have the same vertical scale and all plots have the same ordinates values: the set of model outputs y_j , with $j = 1, \dots, N$. N is the sample size for this numerical simulation and corresponds to the number of time the model has been executed or “run”. N is also referred to as the cost of the analysis, *i.e.*, in sensitivity analysis the cost corresponds to the number of times the model has been executed, with the assumption that computer time needed for the sensitivity analysis itself (*e.g.*, the drawing of the four scatter-plots in this case) is negligible by comparison. The model in this case is a mathematical function of the type $Y = f(X_1, X_2, X_3, X_4)$, but in real case applications it will be a computer program describing a model – typically including a differential equation solver or optimization algorithm or other. The scatter-plot is generated via a Monte Carlo simulation, whereby the four input variables are

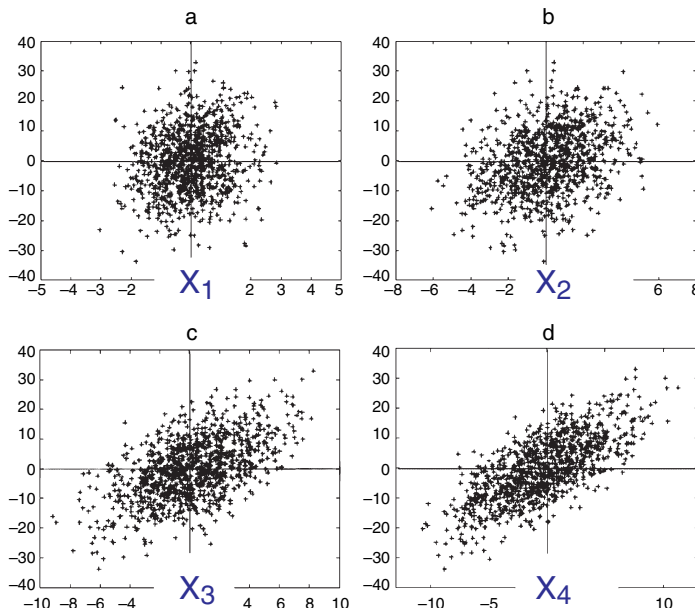


Fig. 7. Scatterplots of Y versus X_1, \dots, X_4 . Which is the most influential factor? One can compare occupancy of quadrants I and III versus that of II and IV to decide where the positive linear relationship is stronger.

sampled from their respective distributions for a total of N times the N row vectors $x_{1j}, x_{2j}, x_{3j}, x_{4j}$ are fed into the model to compute the corresponding vector of model outputs y_j , with $j = 1, \dots, N$. As mentioned all four plots in Figure 7 have the same ordinates (the y_j 's) while the abscissas are different in the four plots and correspond to the sampled values for the four variables. Each abscissa plots the sampled set from the marginal distribution of the corresponding factor. Note that the scales for the abscissas are different from one another as the input factors have different ranges of variation. In this case the factors are assumed independent. Which factor in the set X_1, X_2, X_3, X_4 is the most influent? To a practitioner's eye – and hopefully to our reader after a moment of reflection – it should be clear that the factor commanding more shape is also the one with the highest influence. While X_1 leaves the y_j coordinates as a rather shapeless cloud, X_4 seems capable of forcing the y_j 's along a roughly linear increasing pattern. Overall one would say, looking at the plot that the factors have increasing influence on the output moving from X_1 , the least influent, to X_4 , the most influent.

Thus scatter-plots can indeed serve as tool for sensitivity analysis. Yet in case of models with many input factors a comparison of several scatter-plots might become cumbersome and impractical. For this reason one would like to be able to translate the idea of "shape" or "pattern" into a more convenient mathematical representation. In Figure 8 the scatter-plots of Figure 7 have been cut into slices, with the care of keeping a constant number of points in each slices for the sake of comparison. We could at this point operationalize our concept of shape by saying if values of y_j change between one slice and the next, then the factor can drive variation in Y and is hence influent. This can be made quantitative by saying that the more the mean of Y changes from one slice to the next, the more the factor is influent. We can call the mean in the slice as $E(Y|X_i = x_{ij})$, meaning with this the mean of Y when factor X_i is fixed to the value x_{ij} . The concept of variation across slices could be captured by the variance of this, *i.e.*, by $V(E(Y|X_i = x_{ij}))$. This equation can be simplified by removing the conditioning argument within the mean operator as the variance operator removes overall the influence of the formula by a specific point x_{ij} , so that the formula can be written more simply as $V(E(Y|X_i))$. A more verbose version of this notation would be $V_{X_i}(E_{X_{\setminus i}}(Y|X_i))$ to remind that the variance is taken over the abscissa, *i.e.*, over X_i , while the mean is taken in the slice, *i.e.*, over all factors but X_i , which is fixed. What we have just derived is a so-called variance based sensitivity measure of the first order. The sensitivity measure used in practice is the above normalized by the total (unconditional) variance, *i.e.*,

$$S_i = \frac{V_{X_i}(E_{X_{\setminus i}}(Y|X_i))}{V(Y)} = \frac{V(E(Y|X_i))}{V(Y)}$$

where both the verbose and simplified notations have been used. S_i is known as Sobol's first order sensitivity index and is a very popular model free measure of

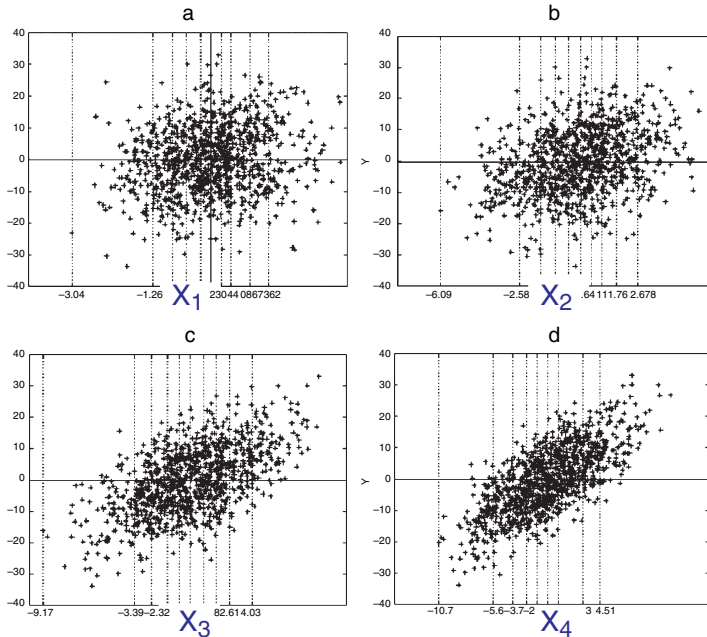


Fig. 8. Cutting the scatterplots into slices.

sensitivity. Model free means that this measure does not lose efficacy if the model is non linear or non additive, although for a full description of non additive models higher order sensitivity terms are needed which we do not describe here (Saltelli *et al.*, 2007). For additive models:

- The first order terms provide a full description of the sensitivity pattern of a model.
- The S_i 's add up to one, which is the same as to say that by adding up the terms $V(E(Y|X_i))$ for all factors, one re-obtains the total variance.

In summary, variance-based methods aim to decompose the variance of the output according to pieces which can be ascribed to individual factors (in the case of additive models) or to factors and combination of factors for the case of non-additive models.

6.2. Method of elementary effects

In the previous section we have not offered a recipe to compute the S_i terms. Efficient strategies are given in detail (Saltelli *et al.*, 2007). We anticipate here that the

cost of the analysis depends from the number of factors and is of the order of hundreds or runs even with the best strategy. When this is not affordable because the model is expensive to run cheaper, less descriptive measures are available. We describe next the elementary effect method.

The elementary effects method is straightforward to understand and to implement. Instead of running a full Monte Carlo experiment on the model $Y = f(X_1, X_2, X_3, \dots, X_k)$ one starts from a points in the space of the input and moves one step into one of the directions. One elementary effect is thus computed as

$$EE(X_{ij}) = \frac{f(X_{1j}, X_{2j}, \dots, X_{ij} + \Delta(X_i), \dots, X_{kj}) - f(X_{1j}, X_{2j}, \dots, X_{kj})}{\Delta(X_i)}$$

One continues the procedure by moving one more step into a different direction X_m of a step $\Delta(X_m)$ without replacement, *e.g.*, until all dimensions have been explored once and a trajectory composed of $k + 1$ points has been created. One trajectory gives k effects $EE(X_i)$ with $i = 1, 2, \dots, k$. One then randomly selects another point in the space of the input and draws another trajectory in the same fashion. Once a small number (n) of trajectories has been generated (say in the range of $n = 2$ to $n = 10$ to give an order of magnitude), the effect of a given factor is computed as the average of the effects of that given factor over the n trajectories:

$$\mu(X_i) = \sum_{j=1}^n EE(X_{ij})$$

Expedients to make this measure more effective are:

- Take the average of the modulus differences rather than the sample differences, *i.e.*, replace $EE(X_{ij})$ with $EE'(X_{ij})$ as follows:

$$EE'(X_{ij}) = \frac{|f(X_{1j}, X_{2j}, \dots, X_{ij} + \Delta(X_i), \dots, X_{kj}) - f(X_{1j}, X_{2j}, \dots, X_{kj})|}{\Delta(X_i)}$$

and

$$\mu'(X_i) = \sum_{j=1}^n EE'(X_{ij})$$

In this way one avoid that effects of opposite order cancel one another.

- Optimize the choice of the trajectories as to make them as far apart as possible in the space of the input factors.

The measure μ is more qualitative than the S_i discussed above, especially when used at low sample size (*e.g.*, two or three trajectories). It identifies those factors that do have an effect and is particularly resilient to both type I and type II errors. For this reason it can be used for screening: if a factor has zero modulus effect $EE'(X_{ij})$ at different points in the space of the input is most likely that it has no

influence on the output and can thus be fixed in subsequent analyses. When the number of trajectories is higher (say five to ten) the ordering of importance is also quantitative and similar to that provided by variance-based methods (Saltelli *et al.*, 2007).

6.3. Monte Carlo filtering

This method is appropriate to situations in which we are especially concerned with a particular portion of the empirical distribution of output Y . An example is when we are interested in the output Y being above or below a given threshold, as in impact assessment studies where Y is a contaminant and we are interested in Y being above a regulatory limit, or when Y is a financial loss and we are interested in characterizing those situations where the loss exceed a given maximum admissible level.

In these settings we are interested in how frequently these realizations occur. A related question is which factors and combinations of factors are responsible for the occurrences.

A way of analyzing this is by diving the possible outputs (Y) as obtained from a Monte Carlo experiment into ‘good’ and ‘bad’ (Monte Carlo Filtering, MCF, Saltelli *et al.*, 2004). MCF is a particular type of Monte Carlo experiment where realizations of the output of interest are compared against one or more thresholds and divided as a result in two subsets: that of the ‘good’ and that of the ‘bad’.

The same is done with the marginal distributions of each of the input factors. For each factor we will have a ‘good’ subset (all those sampled values x_{ij} which correspond to the y_j ’s in the ‘good’ subset), as well as a ‘bad’ subset (all other x_{ij} values). If the two subsets are called X_i^b and X_i^g the union of these two set will give back the original sample X ; different partitions of this original sample are of course generated by each of the input factors.

It is intuitive that if X_i is not an influential factor in moving Y across the ‘good’–‘bad’ divide, then the two sub-samples X_i^b and X_i^g though not identical will look like samples from the same distributions. If instead these two sub-samples are statistically different from one another, than factor X_i is an influential one.

7. Sensitivity analysis in regulatory documents

Prescriptions have been issued for sensitivity analysis of models when these used for policy analysis. In Europe, the European Commission recommends sensitivity analysis in the context of the extended impact assessment guidelines, a handbook

(European Commission SEC, 2005). Sensitivity analysis is recommended there as a good practice to handle uncertainty in impact assessment studies. More detailed prescriptions for sensitivity analysis can be found in the United States EPAs 2004 guidelines on modelling (EPA, 2003), where one reads: “methods should preferably be able to

- (a) Deal with a model regardless of assumptions about a models linearity and additivity.
- (b) Consider interaction effects among input uncertainties.
- (c) Cope with differences in the scale and shape of input probability density functions.
- (d) Cope with differences in input spatial and temporal dimensions.
- (e) Evaluate the effect of an input while all other inputs are allowed to vary as well [...].

While the EPA prescriptions seem modern from a practitioner viewpoint, those of the Intergovernmental Panel on Climate Change are rather conservative. The IPCC mentions the existence of “ ... sophisticated computational techniques for determining the sensitivity of a model output to input quantities...”, while in fact recommending merely local (derivative based) methods (see Saltelli *et al.*, 2004 for a discussion).

In the USA, the Office of Management and Budget (OMB) in its controversial “Proposed Risk Assessment Bulletin” mentioned previously also puts forward prescription for sensitivity analysis. Under section 4, “Standard for Characterizing Uncertainty”, one reads:

“Influential risk assessments should characterize uncertainty with a sensitivity analysis and, where feasible, through use of a numeric distribution. [...] Sensitivity analysis is particularly useful in pinpointing which assumptions are appropriate candidates for additional data collection to narrow the degree of uncertainty in the results. Sensitivity analysis is generally considered a minimum, necessary component of a quality risk assessment report.”

These consideration are evidently reasonable. Elsewhere (OMB, 2002), the same OMB makes a remark on sensitivity analysis, which we consider worth discussing:

“The primary benefit of public transparency is not necessarily that errors in analytic results will be detected, although error correction is clearly valuable. The more important benefit of transparency is that the public will be able to assess how much an agency’s analytic result hinges on the specific analytic choices made by the agency. Concreteness about analytic choices allows, for example, the implications of alternative technical choices to be readily assessed. This type of sensitivity analysis is widely regarded as an essential feature of high-quality analysis, yet sensitivity analysis can not be undertaken by outside parties unless a high degree of transparency is achieved. The OMB guidelines do not compel such sensitivity analysis as a necessary dimension of quality, but the transparency achieved by reproducibility will allow the public to undertake sensitivity studies of interest.”

In summary, the OMB invites the regulatory agencies to offer so many details to the regulated as to allow the latter to replicate the analysis possibly (and likely!) changing its assumptions. While this seems very positive in the name of transparency, it is clear that it amounts to stripping the regulator of any authority whatsoever to use tools of some sophistication. The authority and legitimacy of the regulator is thus denied and the regulated can have a fairly easy game to invalidate the agencies' studies by running their own sensitivity analysis.

8. Avoiding traps and pitfalls. What can go wrong in a sensitivity analysis?

What can go wrong in a sensitivity analysis? We will try to make a short summary for the reader based for the discussion so far.

- One way in which a SA can go wrong is because its purpose is left unspecified or vague (find the most important factors). One throws different statistical tests and measures to the problem and obtains different factors rankings. How to choose among the different rankings? Models can be audited and settings for sensitivity analysis can be audited as well. As a result, importance must be defined beforehand. We shall offer an example later in this contribution.
- Another malpractice best avoided is to present an analysis with too many outputs of interest. The output analysed should be the one relevant to the question addressed by the model.
- Also non advisable is to perform a piecewise sensitivity, taking one sub-model, or one factor at a time. Not only would this conflict with the multidimensional averaging requirement cited before, but could lead to an incomplete exploration of the uncertainties. Interactions could further be overlooked if I explore the space of the input moving one factor at a time. Note that overlooking interactions is a particular instance of Type II error.
- Once a model based analysis has been produced, its revision via sensitivity analysis by a third party is not something most modellers will willingly submit to. To avoid this danger a modeller should use sensitivity analysis in the process of model development, prior and within model use in analysis “Thou shall anticipate criticism”, in the words of Kennedy (2007). On the opposite, “Scientific mathematical modelling should involve constant efforts to falsify the model” (Pilkey and Pilkey-Jarvis, 2007).

9. What can be obtained with sensitivity analysis?

The classic use of sensitivity analysis is for model quality. A sensitivity analysis can identify errors, help to select optimal model gridding, and prepare the model for a calibration analysis (Saltelli *et al.*, 2004; Saltelli *et al.*, 2007).

Sensitivity analysis can also help to obtain minimal model representation, thus fulfilling the objective of parsimony in analysis.

Still on the quality dimension, sensitivity analysis can contribute to the pedigree of the assessment, in the sense discussed by Van der Sluijs *et al.* (2005).

As discussed above an important use of sensitivity analysis is that of checking if policy options are distinguishable, and prepare the analysts to defend his/her work, especially in view of controversy, *e.g.*, in case the assessment supported by the model should go to a stakeholders consultation with adversarial opinion.

References

Baudrillard, J., 1999, *Revenge of the Crystal*, Pluto Press, London, UK, p. 92.

Beck, M. B., Ravetz, J. R., Mulkey, L. A., and Barnwell, T. O., 1997, Stochastic Hydrology and Hydraulics, 11, 229–254.

Beven, K. J., 2001, *Rainfall-Runoff Modelling: The Primer*. John Wiley and Sons, Ltd, Chichester. See also (31), pp. 151–192, 2004.

Chatfield, C., 1993, Model uncertainty, data mining and statistical inference, *Journal of the Royal Statistical Society A*, 158(3), 419–466.

Crichton, M., 2004, *State of Fear*, Harper Collins, New York, New York.

Dunn, W. N., 1997, *Cognitive Impairment and Social Problem Solving: Some Tests for Type III Errors in Policy Analysis*, Graduate School of Public and International Affairs, University of Pittsburgh, Pittsburgh.

European Commission SEC, 2005, 791 IMPACT ASSESSMENT GUIDELINES, 15 June 2005, http://ec.europa.eu/governance/docs/index_en.htm

Environmental Protection Agency, Models Guidance Draft – November 2003 Draft Guidance on the Development, Evaluation, and Application of Regulatory Environmental Models Prepared by: The Council for Regulatory Environmental Modeling, <http://cfpub.epa.gov/crem/cremlib.cfm>.

Funtowicz, S. O. and Ravetz, J. R., 1990, *Uncertainty and Quality in Science for Policy*, Kluwer Academic, Dordrecht, NL.

Funtowicz, S. O. and Ravetz, J. R., 1993, Science for the post-normal age. *Futures*, 25, 735–755.

Funtowicz, S., O'Connor, M., Faucheur, S., Froger, G., and Munda, G., 1996, Emergent complexity and procedural rationality: post-normal science for sustainability, In: Costanza R, Segura O, Martinez-Alier J, editors. *Getting down to earth: practical applications of ecological economics*. Washington (D.C.): Island Press, 1996:223–48.

Hoeting, J. A., Madigan, D., Raftery A. E., and Volinsky C. T., 1999, Bayesian model averaging: a tutorial, *Statistical Science*, 14(4), 382–417.

Kennedy, P., 2007, *A Guide to Econometrics*, Fifth edition, Blackwell, Oxford, UK.

Konikov, L. F. and Bredehoeft, J. D., 1992, Groundwater models cannot be validated, *Advances in Water Resources*, 15(1), 75–83.

Leamer, E. E., 1990, “Let’s take the con out of econometrics” and “sensitivity analysis would help”, in *Modelling Economic Series* (ed. Granger, C. W. J.), Clarendon, Oxford.

Macilwain, C., 2006, Safe and sound? *Nature*, 442, 242–243 (20 July 2006).

Michaels, D., 2005, Doubt is their product, *Scientific American*, 292(6), 96–101.

Office of Management and Budget (OMB), 2002, Guidelines for Ensuring and Maximizing the Quality, Objectivity, Utility, and Integrity of Information Disseminated by Federal Agencies; Notice; Republication, <http://www.whitehouse.gov/omb/inforeg/>, February 22, 2002.

Office of Management and Budget (OMB), 2006, Proposed Risk Assessment Bulletin (January 9, 2006), <http://www.whitehouse.gov/omb/inforeg/>

Oreskes, N., Shrader-Frechette, K., and Belitz, K., 1994, Verification, validation, and confirmation of numerical models in the Earth sciences, *Science*, 263, 641–646.

Pilkey, O. and Pilkey-Jarvis, L., 2007, *Useless Arithmetic: Why Environmental Scientists Can't Predict the Future*, Columbia University Press, Irvington, New York.

Rosen, R., 1991, *Life Itself – A Comprehensive Inquiry into Nature, Origin, and Fabrication of Life*, Columbia University Press, Irvington, New York.

Saltelli, A., Andres, T., Campolongo, F., Cariboni J., Gatelli D., Ratto, M., Saisana, M., and Tarantola, S., 2007, *Sensitivity Analysis of Scientific Models*, John Wiley and Sons, to appear in winter 2007. (forthcoming)

Saltelli, K., Chan, A., and Scott, M., Editors, 2000, *Sensitivity Analysis, Probability and Statistics series*, John Wiley and Sons. (forthcoming)

Saltelli, A., Tarantola, S., Campolongo, F., and Ratto, M., 2004, *Sensitivity Analysis in Practice. A Guide to Assessing Scientific Models*, John Wiley and Sons, Chichester, New York.

Taleb, N., 2007, *The Black Swan*, Penguin, London.

Van der Sluijs, J. P., 2002, A way out of the credibility crisis of models used in integrated environmental assessment, *Futures*, 34, 133–146.

Van der Sluijs, J. P., Craye, M., Funtowicz, S., Kloprogge, P., Ravetz, J., and Risbey, J., 2005, Combining quantitative and qualitative measures of uncertainty in model-based environmental assessment: the NUSAP system, *Risk Analysis*, 25(2), 481–492.

THEME IV. EVALUATION OF MODELS

Predictive uncertainty assessment in real time flood forecasting

Ezio Todini

*Department of Earth and Geo-Environmental Sciences, University of Bologna,
Via Zamboni, 67, 40126, Bologna, Italy.*

Abstract

Scope of the present paper is to provide an assessment of the state of the art of predictive uncertainty in flood forecasting. After defining what is meant by predictive uncertainty, the role and the importance of estimating predictive uncertainty within the context of flood management and in particular flood emergency management, is here discussed. Furthermore, the role of model and parameter uncertainty is presented together with alternative approaches aimed at taking them into account in the estimation of predictive uncertainty. In terms of operational tools, the paper also describes three of the recently developed Hydrological Uncertainty Processors. Finally, given the increased interest in meteorological ensemble precipitation forecasts, the paper discusses possible approaches aimed at incorporating input forecasting uncertainty in predictive uncertainty.

Keyword: forecasting.

1. Introduction: definition of predictive uncertainty

Following Rougier (2007), a simple question may help at clarifying the predictive uncertainty concept:

What is the probability that the river dykes will be overtapped in the next 24 hours?

This seems to be a well-posed question, and certainly a topical one. It is the kind of question a flood emergency manager might ask to his technical staff.

There are two aspects of this question that ought to be highlighted. First, the question asks explicitly for a probability; second, it asks about the behaviour of the future flood levels.

So it is necessary to establish exactly what is meant by ‘probability’ in this context, and it is also necessary to understand that answers which only focus on the response of this or that flood forecasting model are inadequate. In order to satisfy the flood emergency manager, the forecasts of this or that flood forecasting model

must be linked to the real river behaviour, that their predictive statements about quantities such as future water levels address the needs of the flood manager, and, moreover, must also be capable of being compared with those obtained with other models.

There is also another point to be taken into account. Quoting Rougier (2007):

“The first thing to understand about probability in this context is that there is no such thing as ‘the’ probability. To ask for ‘the’ probability is to make a mistake. A probability is a numerical summary of a person’s state of knowledge about a proposition: it is inherently subjective (i.e., it relates to the mind of a subject). Therefore probability takes the possessive article, not the definite one: better to say your probability. Inference based on a subjective interpretation of probability is termed Bayesian Statistics.”

As a matter of fact, our state of knowledge is a mixture of “what we know”, or better “what we believe we know”, in the sense that we may be wrong, which is a “subjective state of mind” and what we learn from observations (which includes data and models), which can be seen as “objective”. Therefore, a definition of predictive uncertainty can be the following:

Predictive uncertainty is the expression of our assessment of the probability of occurrence a future (real) event conditional upon all the knowledge available up to the present and the information we were able to acquire through a learning inferential process.

Please note that the presently available knowledge may not necessarily be the truth, but rather what we presently subjectively believe to be the truth.

In terms of information to complement our prior belief, Krzysztofowicz (1999), points out that

“Rational decision making (for flood warning, navigation, or reservoir systems) requires that the total uncertainty about a hydrologic predictand (such as river stage, discharge, or runoff volume) be quantified in terms of a probability distribution, conditional on all available information and knowledge.” and that “Hydrologic knowledge is typically embodied in a deterministic catchment model.”

These statements underline two aspects usually not fully and clearly understood by hydrologists. The first is that, as previously mentioned, the objective of forecasting is the assessment of the uncertainty that at a future time the values of water stage, discharge, runoff volume, etc. that will occur will be smaller or equal to a given value (generally a threshold value, such as for instance the elevation of the dykes), rather than the uncertainty of predictions generated by the hydrological forecasting models.

The second aspect is that this uncertainty, generally expressed in terms of a probability density (or probability distribution) function, must be “conditional” upon the hydrological forecasting model prediction, which is now seen as the available, although uncertain, extension of observations into the future. In other words, the forecasting model prediction is now a way to complement the prior belief of the decision maker in order to reduce “his” prior uncertainty within the frame of the decision making process and not the provider of deterministic (and therefore “certain”) future levels, flows, etc.

To clarify these issues, let us consider the problem of issuing a flood warning at a given time t_0 . In general this is based on the water level overtopping a threshold value. Measurement errors on water levels are quite small (generally the standard error of measurement is ± 1 cm, which is irrelevant in the decision making process). Therefore, if, for the sake of clarity we disregard the measurement errors, all the predictand (water level) observed values have probability equal to 1 of occurrence, while their future value, for $t > t_0$ is unknown. In order to gain information into the future, at time t_0 , we run a model, which will generate a prediction of the future value of our predictand. If we consider it as a possible realization of the future value, it is obvious that the forecast is uncertain. It obviously reflects all the model+input+parameters+etc. uncertainties. Nonetheless, we can take another point of view; we can use the forecasted value in order to estimate the conditional probability of the future value at time t given this model forecast issued at time t_0 . In other words, we may consider this predicted variable, the model forecast, as “known” at time t_0 with probability equal to 1. This implies that, preliminary, we must have developed the distribution of observations conditional on the predicted ones, by simulating the forecasts over a historical period, as it will be described in the sequel. If the predicted value at time t_0 is “coherent” with this conditional distribution, then (in the sense that no substantial changes have occurred in the model performances) we can enter this value as the conditioning value and determine the probability of the predictand conditional on the forecast. Please note that this does not mean that the model forecast is taken as deterministic, but rather as an uncertain quantity a realisation of which is known at time t_0 .

Following Todini (2007) let us introduce the concept of the joint probability distribution of the real quantity of interest, the predictand (namely the discharge, the water level at a specific cross section, etc.) y , and the model forecast \hat{y} .

What is depicted in Figure 1 looks similar to a linear regression model, where y , the observations are the dependent variables and \hat{y} , the model forecasts, are the independent ones. Please note that the scope here is prediction not to build a model of y given \hat{y} .

As it happens for any regression, unless the model is exceptionally accurate, thus perfectly matching the observations, a scatter will always be observed in the y - \hat{y} plane as in Figure 1. This scatter is a representation of the joint sample frequency of y and \hat{y} that can be used to estimate the joint probability density.

For any $t > t_0$, where t_0 is the present time the model forecast \hat{y}_t is known (which means that the probability of \hat{y}_t is equal to 1). What is unknown, and therefore uncertain, is what will actually occur (namely y_t). Thus it is possible to

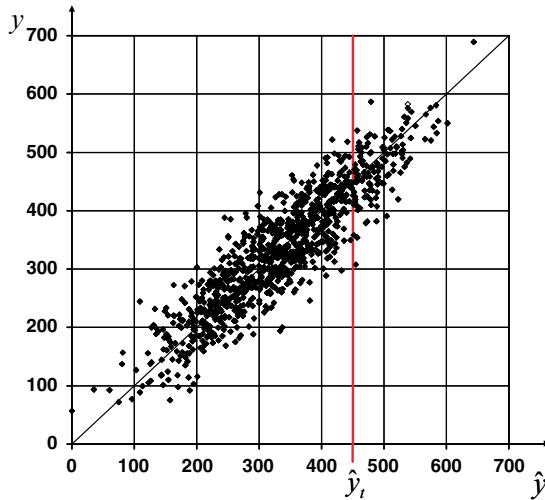


Fig. 1. Joint $y - \hat{y}$ sample frequency from which a joint probability density can be estimated. The conditional density of y given \hat{y} is then obtained by cutting the joint density for the given a value of \hat{y} , namely \hat{y}_t (redrawn from Liu *et al.*, 2005).

derive the probability density of what will occur, conditional upon the knowledge of the model forecast \hat{y}_t , as:

$$f(y_t | \hat{y}_t) = \frac{f(y_t, \hat{y}_t)}{\int_0^{+\infty} f(y_t, \hat{y}_t) dy_t} \quad (1)$$

This expression represents the simplest predictive uncertainty definition, when the decision maker prior knowledge is considered not informative and is not taken into account. It represents a sort of “dictionary” which translates the language of our model forecasts into the language of reality. Please note that the model forecast \hat{y}_t is here considered known at time t . Therefore, independently to all the model, parameter, etc. uncertainty, once \hat{y}_t is known, then equation 1 is perfectly valid to represent predictive uncertainty. Problems occur when \hat{y}_t is no-more coherent with the “dictionary” developed using the historical data. For instance, a rainfall runoff model used to forecast is no more run using the “observed” rainfall as input, but rather a quantitative precipitation forecast. This will produce a new quantity \hat{y}' which is not coherent with $f(y_t | \hat{y}_t)$, which was developed using historically measured rainfall. In this case there are only two possibilities. Either one directly develops the conditional distribution $f(y_t | \hat{y}')$ linking the observations of reality to the forecasts produced by using the forecasted rainfall or, even better, by

using the conditional density $f(y_t | \hat{y}_t, \hat{y}'_t)$, which conditions the real value to both the model forecast obtained using the observed rainfall and the model forecast obtained using the forecasted rainfall.

The same loss of coherence may occur for non-stationarities in model performances that may be due for instance to loss of model validity or changes in its parameter values. This problem will be further discussed in section 3.

2. Motivations for predictive uncertainty assessment

When dealing with flood emergency management, operational decisions may lead to dramatic consequences (economical losses, casualties, etc.), nonetheless, emergency managers are supposed to take decisions under uncertainty about the evolution of future events. Decision theory (Raiffa and Schlaifer, 1961; De Groot, 1970) addresses this problem and provides a solution for improving the soundness of decisions under uncertainty (in terms of maximum number of successful decisions and minimum number of wrong ones), by minimizing the expected value of a utility function $U(y)$ describing the manager's perception of losses, which is a function of the future unknown (therefore uncertain) value of the predictand y (water stage, discharge, etc.). This expected value can be computed if the probability density of a future value of the predictand is known and the decision whether or not to issue an alert will then descend from choosing the “less expensive” of the two “expected” damages obtained by integrating the product of each cost function times the predictand pdf over all its possible values as in equation 2:

$$\begin{aligned} E\{U_{NoAlert}\} &= \int_0^{\infty} U_{NoAlert}(y)f(y) dy \\ E\{U_{Alert}\} &= \int_0^{\infty} U_{Alert}(y)f(y) dy \end{aligned} \quad (2)$$

where $f(y)$ represents the probability density of the predictand.

Unfortunately, when dealing with a decision based on a future unknown quantity $y_{t>t_0}$, where t_0 is the present time, $f(y_t)$, which describes our knowledge on the future value, is generally quite flat (which means that we know very little of what will happen). For instance, we could assume $f(y_t) = f_c(y)$ where $f_c(y)$ is the climatological pdf estimated on the basis of the large number of available observations, which is unconditional on the present time and possible future events. This is why, by assuming $f(y_t)$ as the a priori knowledge, one tries to learn from additional information and to produce a sharper posterior pdf, conditional on the available information, namely $f(y_t | I_{t_0})$, where I_{t_0} represents all the

information available up to time t_0 , including the available measurements, as well as model forecast \hat{y}_t .

If a model forecast \hat{y}_t is available then equation 2 can be rewritten as:

$$\begin{aligned} E\{U_{NoAlert}\} &= \int_0^{\infty} U_{NoAlert}(y)f(y|\hat{y}) dy; \\ E\{U_{Alert}\} &= \int_0^{\infty} U_{Alert}(y)f(y|\hat{y}) dy \end{aligned} \quad (3)$$

because one expects that $f(y|\hat{y})$ will be less dispersed than $f(y)$ given that the uncertainty will be reduced by the additional information produced by the model.

By using the expected value of the utility function instead of the utility function computed in the model forecast taken as “deterministic” one vastly reduces the probability of false alarms as well as of missed alarms. In addition the peakier the predictive density, the more reliable the decision will result. Therefore improvements in forecasting, rather than looking for a better “deterministic” prediction, must essentially aim at reducing predictive uncertainty.

One of the issues that presently enriches the debate about uncertainty among hydrologists is how to show the benefits arising from the operational use of predictive uncertainty, a corollary of which is how to communicate uncertainty to the end-users, namely the decision makers. Indeed, the end-users such as water managers, emergency managers, etc. have a certain difficulty in perceiving the benefits arising from the operational use of predictive uncertainty. What is certain is that hydrologists must not make statements such as: “the probability of flooding in the next 12 h is 67.5 %”. This is meaningless to an end-user. What he/she would like to hear is the answer to the basic question: “what are the expected benefits and drawbacks of issuing a flood alert for the next 12 h?” Therefore, hydrologists must define, in dialogue with end-users, subjective utility functions, which can be used to compute the expected benefits or the expected damages contingent on the predictive density of the quantity of interest. The resulting operating rule inevitably depends on the subjective preferences of the decision maker embedded in the utility function. The resulting operating rules must then be assessed by simulating, over the past record, alternative choices of the utility function until the decision maker is satisfied and the decision rule meets his desired mental scheme.

A schematic example of such utility functions is shown in Figure 2, redrawn from Martina *et al.* (2006), for the case of a flood alert (please note that in this simple schematic example casualties are not taken into account). The dashed line represents the end-user perception of damage (not necessarily the real one) that will occur if the dykes are overtapped, namely $Q > Q^*$ where Q^* is the maximum discharge that may safely flow in the river. The solid line represents the perception of cost plus damages when an alert has been issued. As can be seen from Figure 2, if an alert is issued a cost must be inevitably incurred for mobilizing Civil Protection agents, alerting the population, laying sandbags, etc., but the damage in that

case will be smaller than in the previous case due to the raised awareness of the incoming flood. The decision on whether or not to issue an alert will then descend from the comparison of the "expected damage" for the two options, obtained by integrating the product of the cost function times the predictive uncertainty pdf over all possible values of future discharge. By using the expected value of damages instead of the "model forecast", the probability of false alarms as well as of missed alarms should be much reduced, as the uncertainty about the future discharge is taken into account. In addition, the peakier the predictive density is, the more reliable will the resulting decision be, so that improvements in forecasting, rather than looking for a better "deterministic" forecast, must essentially aim at reducing predictive uncertainty by whatever means is available.

To show how one can use predictive uncertainty in operation, the Lake Como real-time management decision support system is considered here as one of the few successful examples of the operational use of forecast uncertainty (Todini, 1999). Lake Como is a natural lake in Northern Italy closed at its exit and managed as a multi-purpose lake for flood control, irrigation and electric power production. Using a stochastic dynamic programming approach, a standard operating rule was developed on a ten day basis to optimise long term irrigation and energy production. However, when a flood is forecast, the reservoir manager would like to modify the standard operating rule to deal with the incoming flood. To achieve this goal, a utility function describing the damage perception of the manager was developed that penalizes too low and increasingly higher lake levels; every morning

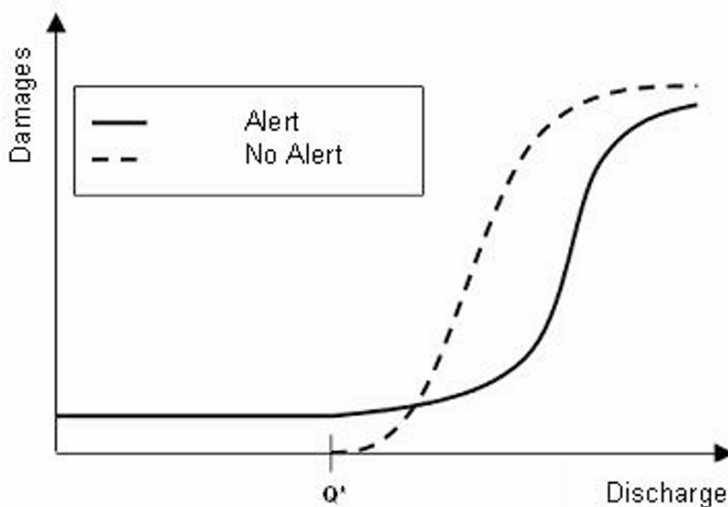


Fig. 2. The utility functions deriving from a flood alert problem (redrawn from Martina *et al.*, 2006). Solid line represents perceived cost and damage if an alert is issued; dashed line represents perceived damage if alert is not issued.

an incoming flood forecast, together with its predictive uncertainty, is issued and an optimal release, computed by minimising the expected damage, using the inflow predictive uncertainty, is then proposed. Note that all this process is totally hidden from the water manager who is aware only of the suggested optimal release and of its expected consequences as in Figure 3.

The performance of the system was assessed on the basis of a hindcast simulation for the 15 years period January 1st, 1981 to December 31st, 1995; the results are presented in Table 1. When applying the optimised rule, the lake level never falls below the lower acceptable limit of -0.40 m, while historically this was observed on 214 days. In terms of Como flooding, over the 15 years, the lake level was historically recorded to be above the lower flood limit of 1.20 m on 133 days, whereas the optimised rule reduced it to 75 days. A noticeable reduction also appears at higher lake levels: at 1.40 m, when the traffic must stop in the main square of Como, the reduction is from 71 to 52 days and at 1.73 , the legal definition of "normal flood" when people can claim compensation for their damage, the reduction is from 35 to 34 days. At the same time, the irrigation water deficit decreases by an average of more than $100 \text{ } 10^6 \text{ m}^3 \text{ year}^{-1}$. This result is exceptional, given that meeting irrigation demand implies higher lake levels, an objective conflicting with the need to reduce the frequency of flooding.

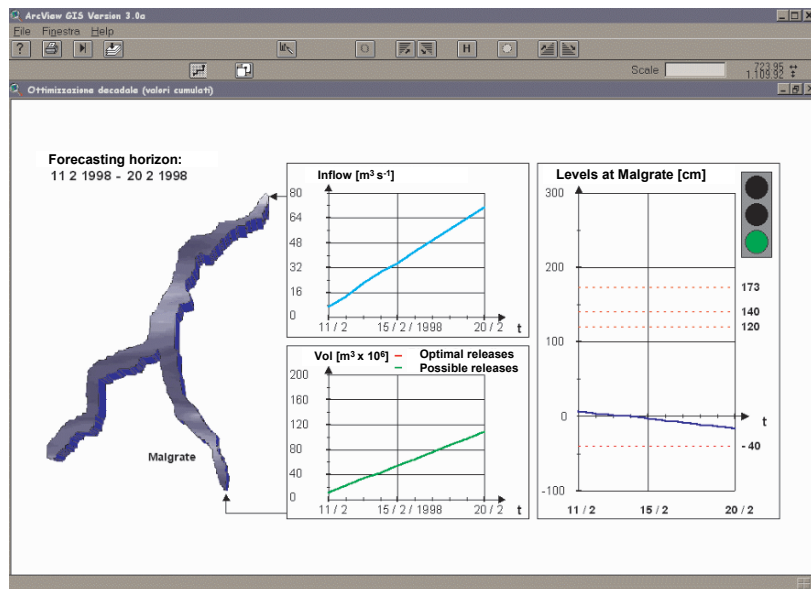


Fig. 3. The Lake Como operational decision support system. The system, on the basis of the expected value of inflows to the lake (light blue line) and its uncertainty (not shown on the screen, but used in the process) suggests to the water manager the optimal release (green line) which minimises the expected damage and shows the consequent expected lake level (blue line) for the following 10 days.

Table 1. Summary of results. A comparison between recorded water level occurrences and water deficits (Historical) and the results of the operation rule based on the forecasting uncertainty (Optimised) for the period January 1st, 1981 to December 31st, 1995.

Water Level	Number of Days	
	Historical	Optimized
≤ 40 cm	214	0
≥ 120 cm	133	75
≥ 140 cm	71	52
≥ 173 cm	35	34
Water Deficit	$890.27 \ 10^6 \text{ m}^3$	$788.59 \ 10^6 \text{ m}^3$

Since 1997, the system has been in operation and used successfully; it has produced not only a reduction in the number, frequency and magnitude of Como flooding events, but also a 3% increase in energy production and a large volume of extra water for irrigation.

3. Difference between predictive uncertainty and model or parameter uncertainty

As previously discussed, in section 1, the assessment of predictive uncertainty is mainly focussed at translating our prior knowledge and the model(s) forecast(s) into reality, which is done by computing the conditional density given by equation 1.

As explained at the end of section 1, if our model forecasts are coherent with the historical ones used to develop the conditional density, then the probability of the model forecast can be taken equal to 1, since the value is now known, and through equation 1 one can then estimate the conditional density of the real, albeit unknown, value of the predictand that may occur at a future time. Please note that the fact that the probability of model forecast is 1 does not mean that this value is the “real” value that will occur, but uniquely that the conditioning variable, namely the model forecast, which is coherent with the developed conditional density (the “dictionary”) has now been observed.

If instead of a unique model, several forecasting models are available, then one is supposed to develop the multi-variate joint probability distribution of the predictand and the ensemble of model forecasts in order to construct the probability distribution of the predictand conditional upon all the model forecasts, as in the Model Conditional Processor (Todini, 2008). Alternatively, one can develop a set of densities for the predictand conditional on each single model and successively marginalise the effect of the different models. This is achieved by taking the expected value of all the developed conditional densities by weighting them using the posterior probability of the different models, derived either through a Bayesian inferential approach or by means of the Bayesian Model Averaging (Raftery, 1993) technique.

Frequently, the variability of a model and of the model parameters randomly occurs in time without a real pattern (in the sense that one cannot isolate different periods with different behaviours). If this variability strongly affects the forecasts, following a Bayesian approach, one can still use the same underlying hydrological model, but must place all the uncertainty into the parameter values, which are now taken as uncertain quantities. In the classical Bayesian approach, the parameters of a model do not necessarily represent physically meaningful quantities which have true (albeit unknown) values, but rather temporary “dummy”, “convenient” or “nuisance” quantities of uncertain nature, over which all uncertainty in the model, observations, boundary conditions, etc. is projected, to be marginalised out by their “posterior probability density”, obtained from observations via the Bayesian inference process (de Finetti, 1975, Chapters 11 and 12).

If the objective of our work is “parameter estimation”, implicitly it is assumed, that the parameters have a real, albeit unknown, value to be found. Note that in this case the scope is not the estimation of the parameters posterior pdf successively used to determine the expected value of the probability of the predictand conditional on the forecast, but rather to estimate the true, physically meaningful parameter values. In this case, if the identifiability conditions are met and if all the uncertainties in the model, the input, the output, etc. are fully and correctly described in an appropriate likelihood function (which is not easy), then, and only then, it will be possible to estimate (for instance as an expected value, or using a ML approach or some other Bayesian or non Bayesian estimation) the physically meaningful parameter values after deriving the posterior parameter probability density function (which coincides with the likelihood function if one takes a uniform non informative distribution as the prior on the parameters). This is an extremely complex problem that in real cases can rarely be solved to produce unbiased estimates of physically meaningful parameter values.

On the other hand, the “prediction” problem is a less complex and more feasible one, because, if one follows for instance the Bayesian approach, the estimation of the “true” parameter values is not required; what must be found is their entire “posterior probability density”, which expresses their uncertainty after sampling the observations. This posterior density may not be the one associated with the “true” value of the parameters, since in Bayesian inference the parameters become “convenient” quantities, used to absorb and reflect all the sources of uncertainty, to be marginalised out at the end of the process.

4. Using formal Bayesian inference instead of GLUE

There are many situations where it is not necessary to account for the model-structure and parameter uncertainty in flood forecasting. This happens, for instance, when dealing with water level prediction based on flood routing models (Todini, 2008) on hydrological forecasting (Liu *et al.*, 2005).

On the contrary, when the level of model, parameters, observations, etc. uncertainty is high, one assumes uncertainty on the model parameters and tries to estimate a posterior parameter density following the Bayesian inference approach. At the outset of this Bayesian inference process, if one does not have prior information, all the models (one per parameter sample) are generally taken as equivalent. This is what one could define as “equi-initiality”, a better term than “equifinality” introduced by von Bertalanffy (1968), the founder of general systems theory and used by Beven and Freer (2001) within the framework of GLUE, because it gives the idea that at the beginning of the inference process all the models may be equivalent, but the learning process must inevitably lead to identifying the more likely models via a denser posterior probability (Mantovan and Todini, 2006).

Please note that, as previously mentioned, the main objective is not the estimation of an optimal sample of parameters and a “unique most likely” predictive density, but rather the identification of the “posterior parameter density” which will successively allow for the estimation of the expected value of all the conditional predictive densities over the parameter posterior pdf.

This is because, due to the generally high non-linearity of the models, one MUST NOT compute the model forecast using the expected (or more in general an “optimal”) value of parameters, but rather use all the parameter posterior density to estimate the “expected predictive density”, which is the usual statistical way of “marginalizing” (namely “eliminating”) the parameter (which in this case embed parameter, model, etc.) uncertainty. As it is well known that $E\{g(\theta)\} = g(E\{\theta\})$ holds with the equality sign only if $g(\bullet)$ is a linear function or if it is affine to the pdf of θ .

This rather important aspect of the problem has not been understood by several authors who use “model uncertainty”, directly derived from the posterior parameter density, instead of the “expected predictive probability”, estimated as the mean of all the predictive densities, each of which relevant to a specific value assumed for the parameters.

Therefore, in order correctly to assess and eliminate the model, parameter, data, etc., uncertainty by computing the expected predictive uncertainty, the following steps must be followed:

- (i) Select a model M .
- (ii) Select a prior pdf on the parameters $f_0(\theta)$.
- (iii) Assume a likelihood (possibly on sound statistical grounds) and derive, using one of the available Bayesian inference techniques (Qian *et al.*, 2003), the posterior parameter probability density $f_n(\theta|D_n) = L(\theta|D_n)f_0(\theta)$, with D_n an ensemble of historical observations record of length n , and estimate the probability associated with each parameter sample $p_n(\theta_i|D_n)$ by discretizing the posterior density.

- (iv) Generate a large ensemble samples $\Theta \equiv (\vartheta_1, \vartheta_2, \dots, \vartheta_m)$, with m the number of generated samples; this can be done either by generating the sample from the prior pdf, as in the Bayesian Monte Carlo approach or preferentially from the posterior, as in the Markov Chain Monte Carlo approach (Qian *et al.*, 2003).
- (v) For each parameter sample ϑ_i estimate the model prediction $\hat{y}_{t|t_0}(\vartheta_i)$ as a function of D_{t_0} , the ensemble of all the data used up to time t_0 , and $M(\vartheta_i)$, the model when the parameter values are set equal to ϑ_i ;
- (vi) For each parameter sample ϑ_i estimate predictive probability density $f_{\hat{y}_{t|t_0}}(y_t | \hat{y}_{t|t_0}(\vartheta_i))$. **Please note that the predictive densities to be developed are one per each parameter sample.**
- (vii) Compute the predictive probability by marginalizing the effect of parameters. This is done by computing the expected value of the predictive densities $f_{\hat{y}_{t|t_0}}(y_t | \hat{y}_{t|t_0}(\vartheta_i))$, each function of a parameter sample, weighted by the posterior probability $p_n(\vartheta_i | D_n)$ associated with the i^{th} parameter sample.

This leads to the following equation, which is nothing else than the expected value of the predictive densities, weighted using the posterior parameter density instead of the prior:

$$f_{\hat{y}_{t|t_0}}(y_t | D_n, \hat{y}_{t|t_0}) = \sum_{i=1}^n f_{\hat{y}_{t|t_0}}(y_t | \hat{y}_{t|t_0}(\vartheta_i)) p_n(\vartheta_i | D_n) \quad (4)$$

Equation 4 gives the “predictive probability density” in the case where a high level of uncertainty is affecting the model forecasts. Once again equation 6 puts in evidence that the parameter posterior distribution $p_n(\vartheta_i | D_n)$ must not be confused, as can be found in many papers, with the predictive probability but is only used to marginalize the effect of parameters uncertainty by weighting the predictive probabilities in the estimation of their expected value. This can be considered analogous to conventional Bayesian minimum risk estimation with conditional density in place of the loss function.

As can be easily noticed, this definition is totally different from the formal definition of “prediction quantiles” in GLUE (Beven and Binley, 1992) can be found in Beven and Freer (2001): “Given a large enough sample of Monte Carlo simulations, the range of likelihood weighted predictions may be evaluated to obtain prediction quantiles at any time step. This is most easily done if the likelihood values are renormalized such as $\sum_{i=1}^B L[M(\Theta_i)] = 1$, where $M(\Theta_i)$ now indicates the i^{th} behavioural Monte Carlo sample, so that at any time step t

$$P(\hat{Z}_t < z) = \sum_{i=1}^B L \left[M(\Theta_i) \middle| \hat{Z}_{t,i} < z \right] \quad (5)$$

where $\hat{Z}_{t,i}$ is the value of variable z at time t by model $M(\Theta_i)$.” (B is the total number of behavioural samples).

There are two aspects to be underlined. The first one is that the actual shape of the posterior density on parameters has a relatively limited effect on the final result, because what really matters is the shape of the individual conditional densities $f_{\hat{y}_{t|t_0}}(y_t | \hat{y}_{t|t_0}(\vartheta_i))$: the posterior parameter density $p_n(\vartheta_i | D_n)$ will only produce weights in the summation and even if these weights are not perfectly estimated they will produce a modest effect on the estimation of the expected value (a central moment) of the conditional densities. This is due to the fact that, even if the conditional densities are highly variable across the range of parameter samples, the more likely ones will be weighted more if the posterior parameters pdf is dense around the modal parameter values. Therefore, what is more important than the actual shape of the posterior parameter density is how dense it is around the mode: a denser posterior parameter density $p_n(\vartheta_i | D_n)$ will put more weight on the more likely models, thus improving the estimation of the expected value and reducing the predictive uncertainty from the initial expected value that can be estimated at the onset from the prior, namely

$$f_{\hat{y}_{t|t_0}}(y_t | \hat{y}_{t|t_0}) = \sum_{i=1}^n f_{\hat{y}_{t|t_0}}(y_t | \hat{y}_{t|t_0}(\vartheta_i)) p_0(\vartheta_i) \quad (6)$$

where $p_0(\vartheta_i) = 1/n$ derives from the multi-uniform distribution assumption for the prior on parameters generally used to generate the parameter samples.

To summarize, what really matters in assessing predictive uncertainty is (a) the assessment of the correct shape of the conditional distributions $f_{\hat{y}_{t|t_0}}(y_t | \hat{y}_{t|t_0}(\vartheta_i))$ (or at least the shape of the more likely ones), and (b) the peakiness of the posterior parameter density $p_n(\vartheta_i | D_n)$, around the more likely samples of parameters, which is usually granted by the learning capabilities of Bayesian inferential approaches (Qian *et al.*, 2003).

Figure 4 clearly shows the difference between the different approaches, together with the inconsistencies of the GLUE approach.

Figure 4a shows the expected value, the 0.05 and the 0.95 quantiles deriving from equation 6; this represents the prior predictive uncertainty before Bayes inference was applied to derive the posterior pdf of the parameters; Figure 4b displays the expected value, the 0.05 and the 0.95 quantiles obtained from equation 4 in discretised form using the posterior density of the parameters obtained via Bayesian inference; Figure 4c reproduces the 0.05, the 0.5 (not the expected value,

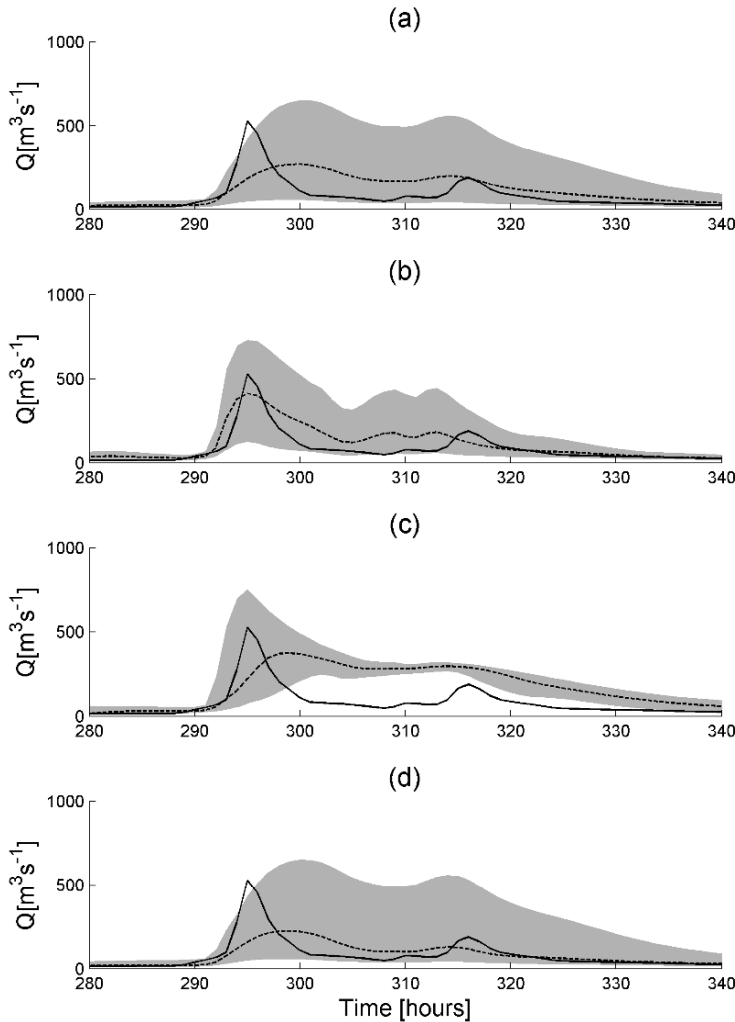


Fig. 4. Comparison of predictive uncertainty estimates. (a) expected value, 0.05 and 0.95 quantiles obtained using the prior parameter density by discretising equation 6; (b) expected value, 0.05 and 0.95 quantiles obtained using the posterior parameter density obtained via Bayesian inference by discretising equation 4; (c) 0.05, 0.50, 0.95 quantiles obtained using the GLUE approach of equation 5; (d) expected value, 0.05 and 0.95 quantiles obtained by discretising equation 4., where the posterior parameter density is obtained via GLUE.

since this is how GLUE results are typically shown) and the 0.95 quantiles obtained using the GLUE approach as for equation 5; Figure 4d displays the expected value, the 0.05 and the 0.95 quantiles obtained from equation 4 in discretised form

when using the posterior pdf of the parameters obtained with GLUE. It is interesting to see that, while the formal Bayesian inference approach, applied on the basis of the Normal Quantile Transform (Van der Waerden, 1952, 1953a,b), which does not require a formal assumption on the model errors likelihood (Mantovan *et al.*, 2007), largely reduces the prior predictive uncertainty, the predictive density obtained when using the posterior parameter pdf produced by GLUE (Figure 4d), is quite similar to the one produced by the prior, which confirms what was found by Mantovan and Todini (2006), namely that by use of less formal likelihoods, GLUE loses the coherence with the Bayesian learning process and is not capable of extracting information from the observations.

The result displayed in Figure 4c is also interesting because it shows how also the definition of the GLUE predictive quantiles given in equation 5 is not consistent with the observations. Between time steps 300 and 330 the “model” is less uncertain, namely all the parameter sets give more or less the same answer, therefore the quantiles are quite narrow, but this has nothing to do with the “predictive uncertainty”, namely the uncertainty of the observed flows given the model forecasts. And, as discussed in section 2, the latter is the measure of uncertainty which is of interest to a decision maker.

5. The hydrological uncertainty processors

As mentioned earlier, given that the focus is the description of predictive uncertainty, rather than model uncertainty, as well as for practical forecasting reasons, most of the hydrological processors available in the literature derive the conditional predictive density on the basis of one or more “calibrated” forecasting models, using fixed parameter values, which is the typical situation and availability of a flood forecasting centre. Three different approaches will be briefly illustrated in the sequel: the Hydrological Uncertainty Processor (Krzysztofowicz, 1999); The Bayesian Model Averaging (Raftery, 1993); and the Model Conditional Processor (Todini, 2008).

5.1. *The hydrological uncertainty processor*

Krzysztofowicz (1999) introduced a Bayesian processor, the Hydrological Uncertainty Processor (HUP) which aims at estimating the predictive uncertainty given a sample of historical observations and a hydrological model prediction. The HUP was developed around the idea of converting both observations and model predictions into a Normal space by means of the Normal Quantile Transform (NQT) (Van der Waerden, 1952, 1953a,b), in order to derive the joint distribution and the predictive conditional distribution from a treatable multivariate distribution.

The basic ideas of the Bayesian processor are here briefly synthesized.

- Step 1: from the real world to the Normal.

The first step is to convert both the n observations y and the corresponding model predicted values $\hat{y}^{(j)}$, using the quantiles associated to the order statistics, into the new variables standard Normal variables $\eta_i^{(j)}$ and $\hat{\eta}_i^{(j)}$, as previously described.

- Step 2: the a priori model.

The application of the Bayes theorem requires first of all the definition of an a priori estimate for the predictive probability. In HUP this is done by assuming a Markovian lag-one process for η the image of the observations in the Normal space. The a priori model can be formulated as $\eta_t = \rho\eta_{t-\Delta t} + \varepsilon_t$, where ε_t is a $N(0, 1 - \rho^2)$ independent process, and the parameter ρ can be estimated from the observations. In order to issue a forecast $k\Delta t$ in advance, this model can be extended by successive applications of the lag-1 model, leading to the following predictive model $\eta_t = \rho^k \eta_{t-k\Delta t} + \sum_{j=0}^k \rho^j \varepsilon_{t-j\Delta t}$. This model gives rise to a prior predictive probability $\Phi_k^0(\eta_t | \eta_{t-k\Delta t}) = N(\rho^k \eta_{t-k\Delta t}, \sqrt{1 - \rho^{2k}})$, which can be written, in terms of the probability density, as:

$$\varphi_k^0(\eta_t | \eta_{t-k\Delta t}) = \frac{e^{-\frac{1}{2} \frac{(\eta_t - \rho^k \eta_{t-k\Delta t})^2}{1 - \rho^{2k}}}}{\sqrt{2\pi} \sqrt{1 - \rho^{2k}}} \quad (7)$$

- Step 3: the likelihood function.

In the original Krzysztofowicz and Kelly's (2000) paper, the likelihood derivation is based upon a regression between the Normal space image of the observed and modelled variables η and $\hat{\eta}$:

$\hat{\eta}_t = a_k \eta_t + b_k \eta_{t-k\Delta t} + c_k + \xi_t$, where ξ_t is a $N(0, \sigma_k^2)$ independent process, where a_k, b_k, c_k and σ_k^2 are estimated from a linear regression in the Normal space.

This allows one to derive the likelihood function as:

$\Gamma_k(\hat{\eta}_t | \eta_t, \eta_{t-k\Delta t}) = N(a_k \eta_t + b_k \eta_{t-k\Delta t} + c_k, \sigma_k^2)$ or, in terms of the probability density, as:

$$\gamma_k(\hat{\eta}_t | \eta_t, \eta_{t-k\Delta t}) = \frac{e^{-\frac{1}{2} \frac{(\hat{\eta}_t - a_k \eta_t - b_k \eta_{t-k\Delta t} - c_k)^2}{\sigma_k^2}}}{\sqrt{2\pi} \sigma_k} \quad (8)$$

- Step 4: the posterior density function.

Following the Bayes theorem, the definition of the posterior density is:

$$\varphi_k(\eta_t | \hat{\eta}_t, \eta_{t-k\Delta t}) = \frac{\gamma_k(\hat{\eta}_t, \eta_t | \eta_{t-k\Delta t})}{\gamma_k(\hat{\eta}_t | \eta_{t-k\Delta t})} = \frac{\gamma_k(\hat{\eta}_t | \eta_t, \eta_{t-k\Delta t}) \varphi_k^0(\eta_t | \eta_{t-k\Delta t})}{\int_{-\infty}^{+\infty} \gamma_k(\hat{\eta}_t | \eta_t, \eta_{t-k\Delta t}) \varphi_k^0(\eta_t | \eta_{t-k\Delta t}) d\eta_t} \quad (9)$$

Given that both the prior density (equation 7) and the Likelihood function (equation 8), are normal, Krzysztofowicz and Kelly (2000) apply the theory of conjugate families of distributions (De Groot, 1970) to derive the posterior density, which becomes:

$$\varphi_k(\eta_t | \hat{\eta}_t, \eta_{t-k\Delta t}) = \frac{e^{-\frac{1}{2} \frac{(\eta_t - A_k \hat{\eta}_t - B_k \eta_{t-k\Delta t} - C_k)^2}{T_k^2}}}{\sqrt{2\pi} T_k} \quad (10)$$

with:

$$\begin{aligned} A_k &= \frac{a_k(1 - \rho_k^2)}{a_k^2(1 - \rho_k^2) + \sigma_k^2}; \quad B_k = \frac{\rho_k^2 \sigma_k^2 - a_k b_k (1 - \rho_k^2)}{a_k^2(1 - \rho_k^2) + \sigma_k^2} \\ C_k &= \frac{-a_k c_k (1 - \rho_k^2)}{a_k^2(1 - \rho_k^2) + \sigma_k^2}; \quad T_k = \frac{(1 - \rho_k^2) \sigma_k^2}{a_k^2(1 - \rho_k^2) + \sigma_k^2} \end{aligned}$$

- Step 5: the results are converted back into the real world from the Normal space as previously described.

5.2. The Bayesian model averaging

Introduced by Raftery (1993), Bayesian Model Averaging (BMA) has gained a certain popularity in the last few years.

The scope of Bayesian Model Averaging is correctly formulated in that it aims at assessing the unconditional mean and variance of any future value of the predictand on the basis of several model forecasts.

Raftery *et al.* (2003) developed the approach on the assumption that the predictand as well as the model forecasts were approximately Normally distributed, while Vrugt and Robinson (2007) relaxed this hypothesis and showed how to apply the BMA to Log-normal and Gamma distributed variables.

In practice the Bayesian Inference problem, namely the need for estimating a posterior density for the parameters, is overcome in the BMA by estimating a number of weights via a constrained optimization problem:

$$\begin{cases} \max_{w_j} \log L = \sum_{s=1}^S \sum_{t=1}^T \log \left(\sum_{j=1}^m w_j p_j(y_{st} | \hat{y}_{st}^{(j)}) \right) \\ s.t. \quad \sum_{j=1}^m w_j = 1 \end{cases} \quad (11)$$

where w_j are the weights to be estimated, $p_j(y_{st} | \hat{y}_{st}^{(j)})$ is the conditional probability of y_{st} , the predictand at site s and time t , given $\hat{y}_{st}^{(j)}$, model j unbiased prediction for y_{st} , with S the total number of observation sites, T the total number of observation time intervals and m the number of used models. Unfortunately, apart from the need for using a correct distribution in the evaluation of weights, the results of Bayesian Model Averaging were found to be not fully satisfactory by Vrugt and Robinson (2007). These authors showed that the assumption of Normal likelihood, on which the derivation of BMA is based, cannot be directly applied to hydrological forecasting where the probability distributions of errors are highly skewed. In addition, even when the data were transformed using appropriate distributions, such as the Log-Normal or the Gamma, the results in terms of width of the resulting uncertainty band could not meet the ones produced using an Ensemble Kalman Filter (Evensen, 2003).

It is worthwhile pointing out that the notation used by Raftery *et al.* (2003), and Vrugt and Robinson (2007), may lead to misunderstand the real scope of BMA. As previously stated, following the definition of predictive probability, here extended to the model structure, in addition to that due to the model parameters, BMA searches for an “unconditional” predictive probability, by marginalizing the effect of the different models using their posterior probability. Therefore, the following expression

$$p(y_t | \hat{y}_{t|t_0}^{(1)}, \hat{y}_{t|t_0}^{(2)}, \dots, \hat{y}_{t|t_0}^{(m)}) = \sum_{j=1}^m w_j p_j(y_t | \hat{y}_{t|t_0}^{(j)}) \quad (12)$$

given as equation 2 in Raftery *et al.* (2003) and more or less identically reported in equation 7 by Vrugt and Robinson (2007), may be misleading, since it might appear that BMA aims at finding the “conditional” predictive probability, which is the probability of observing the predictand y_t , given all the different model predictions $\hat{y}_{t|t_0}^{(1)}, \hat{y}_{t|t_0}^{(2)}, \dots, \hat{y}_{t|t_0}^{(m)}$.

A more convenient representation is that of Draper (1995):

$$p(y_t | D, M) = \sum_{j=1}^m w_j p_j(y_t | \hat{y}_{t|t_0}^{(j)}) \quad (13)$$

where D is the ensemble of historical observations and M represents the ensemble of models. This indicates that although the predictive density given in equation 13 represents the “model unconditional” predictive density, in reality it is still conditional on the “ensemble of models” chosen.

Once the weights w_j have been estimated, the BMA unconditional mean is given as:

$$E\{y_t|D, M\} = \sum_{j=1}^m w_j E\{y_t|\hat{y}_{t|t_0}^{(j)}\} \quad (14)$$

and an approximation of the unconditional variance results:

$$Var\{y_t|D, M\} \approx \sum_{j=1}^m w_j Var\{y_t|\hat{y}_{t|t_0}^{(j)}\} + \sum_{j=1}^m w_j \left(E\{y_t|\hat{y}_{t|t_0}^{(j)}\} - \sum_{j=1}^m w_j E\{y_t|\hat{y}_{t|t_0}^{(j)}\} \right)^2 \quad (15)$$

This is a correct approach, but as any Bayesian scientist know, to be reliable, the chosen ensemble of models M should be descriptive of all possible models, as was acknowledged by Draper (1995) when he talks of Cromwell’s rule (Lindley, 1968), and, possibly, should include the “real model”, if such utopia existed.

Unfortunately, in the real world only few models are generally available, frequently not fully representative of the entire variability of models, implicitly assumed in the BMA approach.

Therefore, as it will be clarified in the following section, the BMA must inevitably be considered a model “conditional” approach (as actually indicated by Raftery *et al.*, 2003). Nonetheless, it allows to make use of all the available, albeit not full, information derived from the different model forecasts, in the probabilistic characterization of the predictand.

Todini (2008) implemented BMA with the following modifications from the original Raftery (1993) proposal:

- Given that, as pointed out by Vrugt and Robinson (2007), the original assumption of approximately Normally distributed errors, is not appropriate for representing highly skewed quantities such as water discharges or water levels in rivers, the original data were converted in the Normal space using the Normal Quantile Transform. By doing this, the variables y_{st} and $\hat{y}_{st}^{(j)}$ were transformed into η_t and $\hat{\eta}_t^{(j)}$ which are marginally distributed according to standard Normal, $N(0,1)$, distributions. Note that, given that the approach was applied to one site only ($s = 1$), in the attempt of keeping some homogeneity with the formulation of the Bayesian processor (Krzysztofowicz, 1999) the index s was dropped.

- Given the unreliability of the “expectation-maximization” (EM) algorithm (Dempster *et al.*, 1977) proposed by Raftery *et al.* (2003), an alternative constrained optimisation techniques, was used to estimate the BMA parameters. Given the existence of an analytical expression for the first and second order derivatives of the objective function, it is was not deemed necessary to use sophisticated, complex optimization tools such as the SCEM-UA (Vrugt *et al.*, 2003) used by Vrugt and Robinson (2007). Therefore, a simple and original Newton-Raphson approach, which converges in a very limited number of iterations, was developed and used (Todini, 2008).

5.3. The model conditional processor

The analysis of the two previously described approaches, together with the convenient properties of the multivariate Normal distribution, generated the idea of generalizing the use of the NQT to derive what will be called the Model Conditional Processor (MCP), which allows to assess the density of the predictand conditional on all the model forecasts at the same time. For instance, in order to combine a lag-1 Markov model in the multi-Normal approach, the model is first defined in the real world (not in the NQT transformed space as proposed by Krzysztofowicz and Kelly, 2000), and the predictive distribution $f_{t|t_0}(y_t | Y_{t_0}, \hat{y}_{t|t_0}^{(1)}, \hat{y}_{t|t_0}^{(2)}, \dots, \hat{y}_{t|t_0}^{(m)})$,

will then be conditioned by the different model forecasts issued at time t_0 .

The conditional distribution can be found by converting, via the NQT as described at the beginning of the section, y_t and $\hat{y}_{t|t_0}^{(1)}, \hat{y}_{t|t_0}^{(2)}, \dots, \hat{y}_{t|t_0}^{(m)}$ into their corresponding Normal space images η_t and $\hat{\eta}_{t|t_0}^{(1)}, \hat{\eta}_{t|t_0}^{(2)}, \dots, \hat{\eta}_{t|t_0}^{(m)}$ and by building the joint distribution, which is assumed approximately multivariate Normal.

In this case, following Mardia *et al.* (1979), it is possible to define the joint distribution of $\eta^T = [\eta_t^{(1)}, \eta_t^{(2)}, \dots, \eta_t^{(r)}]$, a r -dimensional image of the predictand vector (obviously $r = 1$ when only one predictand is used, as in the case reported in this paper) in the normal space, and of $\hat{\eta}^T = [\hat{\eta}_{t|t_0}^{(1)}, \hat{\eta}_{t|t_0}^{(2)}, \dots, \hat{\eta}_{t|t_0}^{(m)}]$, the normal space image of all the used forecasts. If all these quantities have marginal Normal distributions and are linearly related, their joint distribution is the multivariate normal distribution:

$$\begin{bmatrix} \eta \\ \hat{\eta} \end{bmatrix} \approx N \left(\begin{bmatrix} \mu_\eta \\ \mu_{\hat{\eta}} \end{bmatrix}, \begin{bmatrix} \Sigma_{\eta\eta} & \Sigma_{\eta\hat{\eta}} \\ \Sigma_{\hat{\eta}\eta} & \Sigma_{\hat{\eta}\hat{\eta}} \end{bmatrix} \right) \quad (16)$$

Given the joint distribution one can then derive the distribution of each partition conditional on the other one. The distribution of the predictand normal image η conditional on $\hat{\eta}$, is the normal distribution $N(\mu_{\eta|\hat{\eta}}, \Sigma_{\eta\eta|\hat{\eta}})$ with mean

$$\mu_{\eta|\hat{\eta}} = \mu_\eta + \Sigma_{\eta\hat{\eta}} \Sigma_{\hat{\eta}\hat{\eta}}^{-1} (\hat{\eta} - \mu_{\hat{\eta}}) \quad (17)$$

and variance–covariance matrix

$$\Sigma_{\eta\eta|\hat{\eta}} = \Sigma_{\eta\eta} - \Sigma_{\eta\hat{\eta}} \Sigma_{\hat{\eta}\hat{\eta}}^{-1} \Sigma_{\hat{\eta}\eta} \quad (18)$$

In the case of η and $\hat{\eta}$ obtained by using the NQT, which implies that all the marginal distributions are zero mean and unit variances, equation 17 can also be simplified as:

$$\mu_{\eta|\hat{\eta}} = \Sigma_{\eta\hat{\eta}} \Sigma_{\hat{\eta}\hat{\eta}}^{-1} \hat{\eta} \quad (19)$$

where all the covariance matrices are now correlation matrices.

As one can see this result is fairly general and can be applied to one or more predictands (for instance the water stages in successive cross sections along a river) as well as conditioned to several forecasting models.

The degree of approximation in the assumption of multi Normality lies in the actual linearity of the statistical dependence among the variables and it is similar to the one used in the linear regression advocated by Krzysztofowicz and Kelly (2000) or by Raftery *et al.* (2005). In order to better understand the relation between MCP and BMA, it is not difficult to recognize that the following equation also holds for the MCP approach:

$$p(y_t|D, M) = p(y_t|D, \hat{y}_{t|t_0}^{(1)}, \hat{y}_{t|t_0}^{(2)}, \dots, \hat{y}_{t|t_0}^{(m)}) \quad (20)$$

showing that, if the BMA parameters are correctly estimated (namely that the likelihood in equation 11 is the right one), then the two approaches should lead to the same result. The basic difference is that in MCP the parameters are directly estimated in the Normal space from the covariance structure of models and observations, while BMA parameters must be obtained via constrained optimization.

With respect to HUP, the proposed MCP approach, similarly to BMA, may then lead to interesting generalizations. First of all it is no more limited to the choice of a lag-1 Markov process as in Krzysztofowicz and Kelly (2000), but can be extended to additional physically based models or other types of data driven or Artificial Neural Network models.

6. The incorporation of input forecasting uncertainty

A source of forecasting errors is the input forecast error. For instance, when a short or fast response river reach is modeled, the required forecasting horizon may be longer than the physically meaningful travel time of the flood wave, which implies the need for a forecast of the upstream inflows. A similar problem occurs when dealing with a small catchment or more in general when one needs to extend the forecasting horizon beyond the characteristic response time of the catchment. In this case statistical or meteorological quantitative precipitation forecasts are needed.

This error may significantly modify the properties of the model forecasts.

If the forecasting model, as well as the conditional predictive density, was developed using the measured upstream inflows or the measured precipitation, the forecasting error reflects the input measurement uncertainty on top of the model, parameters, initial and boundary conditions, etc. errors, but not the input “forecasting” uncertainty, which can be large. If one uses the obtained model forecast, this is no more coherent with the one used to develop the “dictionary”, namely the probability of the predictand conditional on the model forecast. Therefore its probability cannot anymore be assumed equal to 1.

To incorporate this information into the uncertainty processor one can either derive a conditional uncertainty processor of the measured input conditional on the forecasted one or directly use all the forecasted input(s) to derive the flood forecast uncertainty processor (similarly to what discussed in the previous Section). The derivation of an input uncertainty processor may be possible when dealing with upstream inflows, but unsatisfactory results have been obtained in terms of precipitation forecasts, due to the zero non-zero nature of rainfall.

When dealing with rainfall forecasts such as the ones produced by several meteorological offices (Buizza *et al.*, 1999), the best approach can be (1) use the deterministic run forecasted rainfall to derive the flood forecasting uncertainty processor, instead of the measured precipitation; or (2) use each member of the forecasted rainfall ensemble as a different model to be combined by the uncertainty processor (which is possible for the BMA and the MCP).

Nevertheless, these approaches have still to be thoroughly investigated and there is still the need in this area to assess the properties of the different alternatives.

7. Conclusions

This chapter aimed at describing the status of research in the domain of flood forecasting predictive uncertainty. A formal definition of predictive uncertainty was provided, which corresponds to the needs of flood emergency managers within the frame of operational real time flood forecasting. The possible incorporation of model and parameter uncertainty into the predictive uncertainty was also discussed, and it was shown how the focus on parameter uncertainty led several authors to confuse what can be defined as model uncertainty with predictive uncertainty, which is what decision makers actually need.

Three recently developed approaches to the assessment of predictive uncertainty, all based on a Normal Quantile Transform of data, have also been presented. Of the three approaches, the MCP (Todini, 2008), can be viewed as an extension and a generalization of the Krzysztofowicz and Kelly (2000) HUP processor, as well as an alternative and a more direct approach to BMA (Raftery, 1993). Similarly to BMA, the MCP approach is not necessarily limited to the inclusion of a priori lag-1 Markov models, as in HUP, but it opens interesting perspectives for

incorporating several alternative models in the derivation of the predictive probability. In MCP, “models” can in fact be either the model forecasts obtained using the individual members of an ensemble forecast or range from the physically based models to the data driven ones. This allows for the introduction and the marginalization of different types of uncertainties, and in particular of the input forecast uncertainty. This aspect becomes essential because in that case the estimated conditioning variable is no more coherent with the derived conditional forecasting uncertainty: this happens for instance when one derives the conditional forecasting uncertainty using model realisations based on observed rainfall and then assumes the value obtained using predicted rainfall to be coherent with the derived predictive density.

Extensive work is still required for the extension of these results to non stationary problems, the assessment of the benefits induced by the use of predictive uncertainty in the decision making process, and the communication of the results to the operational emergency managers.

References

Bertalanffy, L., General System Theory, George Braziller, New York, New York, 1968.

Beven, K.J. and Binley, A.M., 1992. The future of distributed models: model calibration and uncertainty prediction, *Hydrol. Processes*, 6, 279–298.

Beven, K.J. and Freer, J., 2001. Equifinality, data assimilation, and uncertainty estimation in mechanistic modelling of complex environmental systems, *J. Hydrol.*, 249, 11–29.

Buizza, R., Miller, M., and Palmer, T.N., 1999. Stochastic representation of model uncertainties in the ECMWF Ensemble Prediction System. *Quart. J. Roy. Meteorol. Soc.*, 125, 2887–2908.

de Finetti, B., 1975. Theory of Probability, vol. 2. Wiley, Chichester, UK.

De Groot, M.H., 1970. Optimal Statistical Decisions, McGraw-Hill, New York.

Dempster, A.P., Laird, N.M., and Rubin, D.B., 1977. Maximum likelihood from incomplete data via the EM algorithm. *J. Roy. Stat. Soc. Series B*, 39, 1–39.

Draper, D., 1995. Assessment and propagation of model uncertainty. *J. Roy. Stat. Soc. Series B (Methodological)*, 57(1), 45–97.

Evensen, G., 2003. The ensemble Kalman filter: theoretical formulation and practical implementation. *Ocean Dynamics*, 53, 343–367. DOI 10.1007/s10236-003-0036-9.

Krzysztofowicz, R., 1999. Bayesian theory of probabilistic forecasting via deterministic hydrologic model. *Water Resour. Res.*, 35, 2739–2750.

Krzysztofowicz, R. and Kelly, K.S., 2000. Hydrologic uncertainty processor for probabilistic river stage Forecasting. *Water Resour. Res.*, 36(11), 3265–3277.

Lindley, D.V., 1968. The choice of variables in multiple regression (with discussion). *J.R. Statist. Soc. B*, 30, 31–66.

Liu, Z., Martina, M.V.L., and Todini, E., 2005. Flood forecasting using a fully distributed model: application of the TOPKAPI model to the Upper Xixian Catchment. *Hydrol. Earth Syst. Sci.*, 9, 347–364.

Mantovan, P. and Todini, E., 2006. Hydrological forecasting uncertainty assessment: incoherence of the GLUE methodology. *J. Hydrol.*, 330, 368–381.

Mantovan, P., Todini, E., and Martina, M.V.L., 2007. Reply to comment by Keith Beven, Paul Smith and Jim Freer on “Hydrological forecasting uncertainty assessment: incoherence of the GLUE methodology”. *J. Hydrol.*, 338, 319–324.

Mardia, K.V., Kent, J.T., and Bibby, J.M., 1979. *Multivariate Analysis. Probability and Mathematical Statistics*. Academic Press, London.

Martina, M.L.V., Todini, E., and Libralon, A., 2006. A Bayesian decision approach to rainfall thresholds based flood warning. *Hydrol. Earth Syst. Sci.*, 10, 413–426.

Qian, S.S., Stow, C.A., and Borsuk, M.E., 2003. On Monte Carlo methods for Bayesian inference. *Ecological Modelling*, 159, 269–277.

Raftery, A.E., 1993. Bayesian model selection in structural equation models. In Bollen, K.A. and Long, J.S. (Eds.), *Testing Structural Equation Models*, pp. 163–180. Newbury Park, CA. Sage.

Raftery, A.E., Balabdaoui, F., Gneiting, T., and Polakowski, M., 2003. Using Bayesian model averaging to calibrate forecast ensembles, Tech. Rep., 440, Dep. of Stat., Univ. of Wash., Seattle.

Raftery, A.E., Gneiting, T., Balabdaoui, F., and Polakowski, M., 2005. Using Bayesian model averaging to calibrate forecast ensembles, *Mon. Weather Rev.*, 133, 1155–1174.

Raiffa, H. and Schlaifer, R., 1961. *Applied Statistical Decision Theory*. The MIT Press, Cambridge, MA.

Rougier, J., 2007. Probabilistic inference for future climate using an ensemble of climate model evaluations. *Climatic Change*, 81, 247–264.

Todini E., 1999. Using phase-space modeling for inferring forecasting uncertainty in non-linear stochastic decision schemes. *J. Hydroinformatics*, 01.2, 75–82.

Todini, E., 2007. Hydrological modelling: past, present and future. *Hydrol. Earth Syst. Sci.*, 11(1), 468–482

Todini, E., 2008. A model conditional processor to assess predictive uncertainty in flood forecasting, accepted JRBM, in press.

Van der Waerden, B.L., 1952. Order tests for two-sample problem and their power I. *Indagationes Mathematicae*, 14, 453–458.

Van der Waerden, B.L., 1953a. Order tests for two-sample problem and their power II. *Indagationes Mathematicae*, 15, 303–310.

Van der Waerden, B.L., 1953b. Order tests for two-sample problem and their power III. *Indagationes Mathematicae*, 15, 311–316.

Vrugt, J.A., Gupta, H.V., Bouten, W., and Sorooshian, S., 2003. A shuffled complex evolution metropolis algorithm for optimization and uncertainty assessment of hydrological model parameters. *Water Resour. Res.*, 39, 1201, doi: 10.1029/2002WR001642.

Vrugt, J.A. and Robinson, B.A., 2007. Treatment of uncertainty using ensemble methods: comparison of sequential data assimilation and Bayesian model averaging, *Water Resour. Res.*, 43, W01411, doi: 10.1029/2005WR004838.

**THEME V. COMMUNICATING
MODELLING RESULTS
AND UNCERTAINTIES**

Communicating uncertainty to policy makers

Anthony Patt

International Institute for Applied Systems Analysis, Schlossplatz 1, A-2361 Laxenburg, Austria.

Abstract

As the types of problems that policy-makers attempt to solve grow more complex, they increasingly are turning to scientists for specific advice. A critical challenge in communicating the results of scientific research arises when those results contain a great deal of uncertainty. Different academic disciplines offer diverging advice on how scientists should proceed, based in large part on differences in how the various disciplines view the process of decision-making process itself. In this chapter, the author links the strategies for communicating uncertainty to the decision-making models of economics, psychology, and sociology, respectively. He suggests that the relative strength of each strategy depends on the context within which the decision-maker is operating. To resolve this ambiguity about how best to communicate uncertainty, he offers first-best and second-best approaches. The first-best approach is rooted in a process of dialogue, with attention to two-way communication and the relationship between scientists and policy-makers. The second-best approach is rooted in the goal not of giving all decision-makers all of the information they need, but rather in providing them with just enough information to judge whether they need more. To assist in that latter task, the author suggests particular guidelines for the aspects of uncertainty that scientists need to communicate.

Keywords: uncertainty, policy-making, scientific assessment, decision-support systems.

1. Introduction

Describing uncertainty, either qualitatively or quantitatively, presents a major challenge to environmental modeling and assessment. Making decisions in cases where uncertainty is a defining feature of the problem likewise presents a major challenge to policy-makers and decision-makers. In between these two tasks lies the area of communication: characterizing uncertainty as scientists have described it in such a way as to assist decision-makers use the information in productive and consistent ways (Risbey and Kandlikar, 2007).

There is increasing consensus that it is important to communicate uncertainty. The United States National Research Council (2006), for example, recently suggested that it is vital for the National Weather Service to communicate the uncertainty associated with weather forecasts, and not just expected weather. The Intergovernmental Panel on Climate Change (IPCC), starting with preparation for its Third Assessment Report, recognized the importance of communicating uncertainty, as well as some of the challenges associated with doing so (Moss and Schneider, 2000).

There is less consensus, however, on the best practices for the process of communicating uncertainty, or even if a single set of best practices exists. There is a widespread recognition that most people working in both private and professional capacities can have major difficulties making important decisions when uncertainty is very high (Thaler, 1991). Breyer (1993), who later went on to become a member of the United States Supreme Court, suggested that regulatory policy faces major problems with issues of risk and uncertainty, leading to policies that actually increase the risks that people face, rather than decreasing them. He suggested special panels made up of experts, insulated from political forces, to make crucial regulatory decisions. Zeckhauser and Viscusi (1990) reached a similar conclusion, and then went on to suggest that issues of risk and uncertainty are a situation where some degree of government paternalism is required, to protect people from their own bad choices (Zeckhauser and Viscusi, 1996). One response has been to avoid communicating probabilities when it is felt that the audience does not have the skills to understand them. Indeed, this has been the approach that was taken for decades with information such as weather and climate forecasts, which reach a newspaper or television audience. Yet there is ample evidence that the divide between educated and non-educated people is not so great, and it would be a mistake to assume that just because an audience is not trained, it is incapable of comprehension. Gordon and Kammen (1996) found that in many cases trained analysts made the same mistakes at estimating probabilities that ordinary people make. Patt (2001) studied uneducated subsistence farmers in Africa, and found that they had essentially the same skills to interpret uncertainties, such as in a probabilistic rainfall forecast, as have been observed among the usual subjects of psychological tests, namely university students in the west. What the farmers, like the students, needed, was a little bit of time to familiarize themselves with the problem, and then their choices responded well to subtle changes in the assessed likelihoods of particular events.

Those who communicate uncertainty need to cope with these issues. In this chapter, I describe some of the suggestions for best practices, by tying these in to the problems that the communicator may be seeking to overcome. I start with this latter set of issues: what are the problems and difficulties associated with using information about uncertainty for decision-making, which communicators have to overcome? From there, I move on to some of the suggested solutions.

2. Challenges for communication

There is ample evidence that in some situations of decision-making under uncertainty, people make terrible judgments, both in terms of estimating likelihoods, and in making decisions that respond sensibly to those likelihoods. In one anecdote, a statistic teacher asks a student what the likelihood is that a six-sided die will land on the number 4. The student replies: "Fifty percent. Either it does, or it doesn't." The challenge for communicators is to provide people with information about uncertainty in a form that they will understand, remember, and use. Unfortunately, there is a lack of agreement about how to do so, stemming from a variety of models of how people actually make decisions. Depending on which model the communicator believes to be accurate, there are very different implications for when and how uncertainty ought to be communicated. In this section, I describe three general classes of models, showing how each carries different implications for communicators. I then pose the question of which model is correct.

2.1. Economic models

In arguing for more effective communication of uncertainty in the area of climate change, Webster (2003) proposed:

Uncertainty is not important merely for computing an expected value or 'best guess'. In fact, information on variability and on low-probability high-consequence events allows decision makers to account for society's risk-aversion in their choices. Furthermore, today's decision is not made once now, but will be continually revised in the future as our understanding evolves. The optimal decision today depends not only on current uncertainty, but our expectation of how it will change and how we will respond in the future. This adaptive decision process will be aided by carefully tracking how uncertainties change with new knowledge. Thus, carefully assessing the risks of future climate change impacts is a critical task as a component of scientific support for decision makers.

While this statement appears to simply reflect common sense, in fact it makes a number of assumptions about how people make decisions, all of which can be described as economic assumptions: people make optimal decisions, based on the information at hand; they change those decisions when new information suggests them to be sub-optimal; they are risk averse. The theory that captures all of these elements is *expected utility theory* (von Neumann and Morgenstern, 1944). According to this model, decision-makers derive utility from different patterns of consumption, and those patterns depend on the outcomes of their choices. Uncertainty implies that that each choice can lead to a range, or distribution, of future outcomes. Decision-makers decide among the choice options by selecting the option that will provide the greatest expected utility associated with its distribution of outcomes, *i.e.*, a weighted average of utility with the probabilities associated with each potential outcome acting as weights. To calculate the expected value

associated with each choice option, they need to integrate the utility function across the distribution of potential outcomes, and this means that they need to know, or make assumptions about, that distribution. It is commonly assumed that people are risk averse, which implies that the relationship between consumption and utility is not linear; if people gain decreasing marginal utility from increasing consumption, then the expected utility associated with a range of uncertain outcomes will be less than the single level of utility associated with the expected, or average outcome. Figure 1 shows an example of this. Since everybody knows – consciously or subconsciously – only their own utility function and their own degree of risk aversion, they need to calculate for themselves the utility associated with each possible outcome, and from that a level of expected utility. If people engage in these processes, again consciously or subconsciously, then it is essential only to provide them with estimates of the probability of different outcomes, and to let them make their own decisions with this information.

A growing number of economists have taken note of the fact that people often make decisions that are apparently inconsistent, such as simultaneously buying insurance (risk averse behavior) and playing the lottery (risk loving behavior).

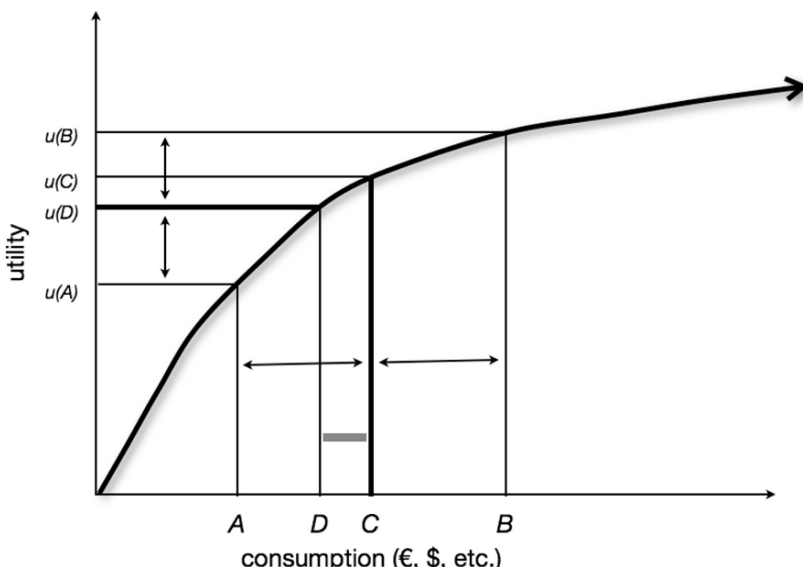


Fig. 1. Utility and risk aversion. The curve shows the relationship between consumption and utility for a person who is risk averse. Consumption levels A and B are the potential outcomes of a lottery, and if each is equally likely, then C is the expected value of that lottery. Because the utility function is concave, the expected utility of the lottery, $U(D)$, is less than the utility of the expected value of that lottery, $U(C)$. The consumption level D thus provides the same utility as the expected utility of the lottery, and the grey bar between D and C represents the amount of money that this person would be willing to pay for an insurance contract that would convert the lottery into a certain outcome.

Continuing to assume that people are trying to optimize their utility, two alternative explanations are that they get their math wrong working with probabilities, or that they have multiple utility functions. The field of behavioral economics straddles the line between economics and psychology, in that it uses both models and research methods associated with the field of psychology to examine both faulty math and multiple utility functions, while remaining true to economics in terms of still assuming some objective function (or set of objective functions) to be maximized.

Along the former line, behavioral economists have shown that people are often biased in the probability estimates, due to context-specific perceptions and mental shortcuts that they use (Kahneman and Tversky, 1979; Tversky and Kahneman, 1974). Where people are given precise probabilities of relatively abstract events occurring (e.g., the probabilities of winning different sums of money in a lottery), most people appear to over-react to especially small probabilities (close to 0), and under-react to especially large ones (close to 1) (Allais and Hagen, 1979; Kahneman and Tversky, 1979). Similarly, where there are two potential outcomes, the probability of each occurring are adjusted within most people's minds towards 0.5 (Bruine de Bruin *et al.*, 2000). In less abstract settings, most people's estimates are heavily influenced by a set of factors closely associated with the emotional impact of the event itself. Events that are more easily remembered are viewed as more likely than those that are not (Tversky and Kahneman, 1973), and events that generate strong emotional reactions of dread or a loss of control (e.g., a shark attack, a plane crash), not coincidentally because they are then more easily remembered, are also seen as more likely (Covello, 1990). Indeed, even when people are told the probabilities of different events occurring, most of them remember those probabilities differently depending on their emotional reaction to the events and how plausible those probabilities seem (Windschitl and Weber, 1999). The challenge for communicators, given these observed biases, is to provide information that helps people compare the probabilities of different events, to avoid using emotion-laden language that will trigger particular biases, and to help people use the information to calculate optimal strategies. The field of risk communication developed out of these efforts, and is based on the idea that the best way to assist decision-makers coping with risk and uncertainty is to give them information in such a way as to correct their mistaken beliefs (Leiss, 1996). In order to do so, the communicator needs to understand how the decision-maker is using information to form beliefs, and become a partner with the decision-maker in working with the new information to arrive at actual decisions (Fischhoff, 1995).

Along the latter line, economists have shown that the utility people anticipate receiving from the outcomes of choices depends on context-specific issues of perception: the perceived departure of outcomes from the status quo (Kahneman and Tversky, 1979; Munroe and Sugden, 2003; Patt and Zeckhauser, 2000; Samuelson and Zeckhauser, 1988); the agents perceived to be causing those changes (Ritov and Baron, 1992); the perceived fairness of the outcomes (Fehr and Schmidt, 1999; Kahneman *et al.*, 1986; Knetch, 1997); and a long list of other factors.

Often, there are consistent and predictable differences between the utility that people anticipate receiving from particular outcomes before they make a decision, and that which they do in fact experience once those outcomes actually occur. Framing is the inevitable act of describing a decision and the relevant background information to make it understandable and interesting to decision-makers (Kühberger, 1998). There are often many frames that are logically equivalent, but which can trigger different sets of values. For example, most people show different preferences for risk when decisions are framed as affecting either their gains relative to the status quo, or their losses (Kahneman and Tversky, 1979). The challenge for communicators is to be aware that they may be triggering counterproductive values when they frame uncertainty in particular ways. Either, they need to work with people to make sure that the people understand how their values may be influenced, at least temporarily, by the new information, so that they can then make decisions based on their “real” utility function, or the experts (who are presumably not influenced by emotions) need to figure out what the best decision is, and make it for them (Breyer, 1993; Zeckhauser and Viscusi, 1996).

2.2. *Psychological models*

Many prominent behavioral economists had their training in psychology, and there is substantial overlap between the psychological literature and the behavioral economics literature in the area of developing confidence judgments and estimating likelihoods. The point of departure is what people’s motivations while making decisions are, and hence how their beliefs actually influence their choices. The psychological models of people’s motivations are too numerous to discuss in detail here, but they share a common feature in that, unlike economic models, they do not assume that individuals make decisions in order to maximize the utility derived from consumption.

Bounded rationality, for example, suggests that people engage in a mental search of available options, and choose the first one that is satisfactory (Simon, 1956). This so-called *satisficing* is different from optimizing in that it involves comparing not the outcomes of different choice options, but of each choice option with a set of minimum criteria. Closely linked to bounded rationality is the concept of adaptive heuristics: people develop and use mental shortcuts to identify acceptable options quickly, with a minimal amount of necessary information (Payne *et al.*, 1993). One of the clearest examples is of a person trying to catch a ball hit into the sky, such as in a baseball game. A model based on optimization would have the person calculate where the ball will land, based on an estimation of the speed and direction at which the ball was hit, factoring in the effects of gravity and air resistance. To optimize the chances of catching ball, the person will run to that place as quickly as possible. Actual ball players, however, apparently doesn’t have time for such calculations, and instead rely on the “fast and frugal” *gaze heuristic*: they keep their eye on the ball and observe the angle at

which it appears above the horizon. When that angle appears to be decreasing, they accelerate towards the ball; when the angle is increasing, they accelerate away from the ball. If they can accelerate quickly enough, their path will always intercept that of the ball before it hits the ground, without their ever knowing where that point of interception will be (which is why they sometimes crash into walls while running) (Gigerenzer and Selten, 2001). People continually develop and improve upon such heuristics as they gain familiarity with a decision-domain; they use and refine the techniques that work.

Information can change people's beliefs and judgments of confidence, but as a result of not only the content of the information, but also its source (Weber *et al.*, 2000). Most people weight information gained from personal experience quite differently than they do information gained from third parties, and the form of the personal experience can also make a difference (Edgell *et al.*, 2004; Griffin and Tversky, 1992). People are more likely to trust expert opinion when they fully understand it, and when they perceive it coming from a source with an obligation to be honest, such as arising out of a previous social relationship (Birnbaum and Mellers, 1983; Birnbaum and Stegner, 1979; Birnbaum *et al.*, 1976; Darr and Kurtzberg, 2000; Patt *et al.*, 2006; Sniezak *et al.*, 2004). Indeed, many people modify their choices in response to new information not necessarily because they believe the information itself to be true, but rather in order to signal that they have accepted the help that was offered by the information provider (Harvey and Fischer, 1997). Perhaps most importantly, information can affect not only beliefs, but also the motivation to act on the basis of those beliefs. For example, information that ought to be most valuable from the perspective of belief updating—that which is quite different from their prior beliefs – often has little effect on people's actions, either because they reject it out of hand in order to preserve their own self-confidence (Petty and Cacioppo, 1986), or because accepting it reduces their self-confidence and motivation to take any action at all (Prentice-Dunn and Rogers, 1986). By contrast, offering people information that confirms their prior beliefs can provide additional motivation to act.

If people are not optimizing, then helping them to understand the precise probabilities associated with different possible outcomes of decisions is not a productive exercise. Rather, it is important for communicators to help them explore the consequences of their own actions on different future scenarios, and to see which decisions make them happiest given how their actions will change their future. Some types of information can lead them to withdraw from a decision, while other types of information can lead them to engage.

2.3. *Political models*

While both economic and psychological theories of decision-making explain people's actions in social settings, their focus is still on the individual. A separate set of models, which one can loosely label social (although they are rooted in a

number of disciplines, including sociology, anthropology, and geography), centers of the social context for decision-making and action. Historically, scholars in these fields have reached very different conclusions from economists and risk communicators about the role of scientific information in decision-making processes.

The role that scientific information plays in decision-making depends critically on the social processes through which that information is transmitted and processed (Jasanoff *et al.*, 2002), and Kasperson and Kasperson (1996) show how particular social institutions can amplify or attenuate the perception of risk. Proponents of the cultural theory of risk, for example, suggest that there are several distinct worldviews, or discourses, and that people interpret information in ways that are consistent with their own view (Douglas and Wildavsky, 1982; Thompson *et al.*, 1990). The same piece of information about a particular risk may to a *heirarchist* suggest great need for control, to an *egalitarian* greater need for caution, to an *individualist* greater need for individual autonomy, and to a *fatalist* greater cause for resignation. People can continue to believe that they are ignorant of a particular subject, even after having received a great deal of information about it, in order to maintain their social identity (Michael, 1996). People see their own type of knowledge as tied to their social identity, and often cannot communicate effectively with scientists, whose social identity is quite different (Wynne, 1996). The fault need not lie with the lay decision-makers, but with the scientists who assume that their own interpretation of evidence is more reliable.

Scientific uncertainty influences decision-making by altering political discourse. Policy-makers rely on scientific evidence to add legitimacy to their actions (Ezrahi, 1990). When the scientific community admits the it does not know the answer to policy relevant questions, it may bolster the credibility of scientists themselves (Shackley and Wynne, 1996), but at the same time it undercuts the legitimizing function that they provide, and becomes a publicly accepted justification for postponing action (Funtowicz and Ravetz, 1990, 1993). It is not surprising, then, that groups interested in maintaining the status quo in the climate change policy arena do not simply of deny the problem exists, but rather claim that the science is too uncertain to base any actions upon (Gelbspan, 1997). Conflict about issues of science does not necessarily have the same sedative effect (Dryzek, 1997; Lee, 1993). In highly contested issue areas, experts commonly line up on both sides of the political fence, each group playing a legitimizing role, with the media then highlighting these differences of scientific opinion (Boykoff and Boykoff, 2004). Conflict-based uncertainty may be a signal to the public that a particular issue is important and politically contested, and hence that policy actions may be necessary (Patt, 2007).

The observation that people will not take an action when the motivation for it is uncertain has led to the strategy of communicating the most likely outcome as relatively certain, rather than reveal uncertainty (Irwin and Wynne, 1996). But when events are uncertain, and scientists do not reveal them to be so, there is a chance that the scientists will appear to be wrong. This in turn can lead to a major loss of credibility. For example, in the early 1990s, the government of the state of

Ceará in Brazil began to warn farmers about upcoming droughts associated with El Niño, a pattern of warm water off the coast of South America. Farmers were happy to take the government's advice, and to plant drought tolerant crop varieties when they were warned of a bad year. But then 1 year the government warned of a bad year, and the rains turned out to be good. After that, the farmers were unwilling to follow the advice they were given (Orlove and Tosteson, 1999). Several years later, exactly the same story repeated itself in Zimbabwe (Glantz, 2000). Research has shown that the perception of error can destroy the credibility of some fragile mechanisms to generate trust in information, but has less of an effect when the decision-maker has good reason to believe that the communicator is being honest (Patt *et al.*, 2006).

2.4. Which model is correct?

One can argue that economic models offer a normatively correct model for making decisions, even if they do not accurately describe how people actually operate. One might suspect that well intentioned individuals, given enough time to consider all available information, and aware of the biases potentially inherent in psychology and politics, would adopt an economic approach. But this view is not universal. Gigerenzer (2000), for example, suggests that the heuristics associated with bounded rationality actually improve decision-making over what economic models can offer, given real constraints in information and processing ability. Supporting this view, a well-known story concerns a particular professor of economic decision-theory, who was faced with an especially life altering choice. His student asked him how he intended to make the decision, expecting him to say that he had assigned a value to all of the possible outcomes, considered the likelihoods of each, and calculated the expected utility associated with the two possible choices. The professor surprised him: "Normally I would do that, but this decision is important, so I need to follow my gut instinct."

Decision strategies are often context specific, and the strategies people adopt are the ones that can, in the relevant social context, provide a legitimate justification for their ultimate actions. When people are making individual decisions that touch their core values and that are laden with emotion, the psychological models likely do provide the best explanation of their behavior. In market situations, and when people are making decisions for an organization with prescribed rules, then the economic models may provide a more accurate description. When their decisions affect their social standing and power, then the political models may be more accurate. What is important for communicators is that each decision-making style responds to a different set of information concerning uncertainty. This suggests that there is no single best way to communicate uncertainty associated with a particular phenomenon to all decision-makers all the time.

3. Solutions

Ideally, communicators will understand their audience well enough to match their communication style to the relevant decision-making style. Research has identified features of good communication practice that make this possible, an indeed in some cases the conventional wisdom has evolved substantially. For example, it is now well accepted that uncertainty with respect to the weather ought to be communicated, whereas 20 years ago this was not the case. Advice for communication now centers on processes of communication, rather than exclusively on the information content.

3.1. *Processes of communication*

A constant theme in the recent literature is that it is essential for science communicators, especially when uncertainty plays a substantial role, to engage in practical and ongoing decision support (Cash *et al.*, 2003). Two factors help to promote this. First, it is essential that communication is participatory, flowing in both directions between scientists and decision-makers. Second, it is increasingly seen as important that trustworthy organizations fill the role of mediators.

Participation of stakeholders in assessment and decision-support processes is now recognized as the gold standard for efforts to bridge the gap between scientists and decision-makers (Cash *et al.*, 2003, 2006), drawing from findings concerning risk communication (Fischhoff, 1995) and social learning (Social Learning Group, 2001). This involves designing a forum in an assessment process where stakeholders can express both their concerns over outcome, and their own local knowledge, and be confident that the content of the assessment responds to both types of information. Participation serves several functions. First, scholars have argued that it is the means by which scientists and analysts discover what the concerns of their audience are and what information they will consider using (Cash, 2001; Michael, 1996; Moss *et al.*, 2002). It can allow the analysts to discover whether, in this particular context, economic, psychological, or political models better describe their audience, and within each of those classes what their goals for the decision are, and provide the type of information about uncertainty that is most relevant, which in turn is a function of the decision making model being used. Indeed, one would not enter into a stakeholder dialogue asking decision makers which model they use, but rather would explore, through the process of dialogue, the factors that are most relevant to them. Second, participation is the means for scientists to learn about locally relevant facts that could play a role in their analysis (Wynne, 1996). Often, scientists conduct their analysis at a coarse spatial scale, and participation is the means to obtain the local knowledge necessary to downscale their models. Third, through the participatory process of questions and answers, scientists can learn which parts of their message are difficult to understand, and

focus their communication on those points, correcting initial misperceptions and misunderstandings (Suarez and Patt, 2004). Fourth, participation is a way of developing an implicit connection between scientists and decision-makers that is necessary to improve trust in the information (Patt *et al.*, 2006).

Numerous case studies have suggested that participation increases the likelihood that decision-makers will use information containing uncertainty. A meta-analysis of studies looking at how uncertain climate information was communicated reached the conclusion that important decisions involving probabilistic information are only made when the decision-makers have the opportunity to talk with climate experts, who can answer their questions concerning the sources and other features of uncertainty (Patt *et al.*, 2007). One of the few controlled experiments involved subsistence farmers in Zimbabwe, who were being provided probabilistic seasonal climate forecasts, to which they could respond by changing particular planting decisions. The forecasts themselves were not locally specific, but required further analysis taking local conditions into account, such as historical variations in seasonal rainfall, soil types, and farmers' marketing opportunities. At the time of the study, the farmers had access to the forecasts over the radio, a non-participatory method of communication. The researchers invited a random selection of farmers from two communities to attend participatory workshops at the same time that the forecasts were being broadcast over the radio, shortly before planting decisions needed to be made. Several months later, after the harvest, the researchers interviewed a random sample of workshop attendees and non-attendees, asking them whether they had used the forecast information to make different decisions. The farmers who had attended the workshops were more than five times as likely as those who had received the same information, but via radio, to use the information for their farming (Patt *et al.*, 2005b).

It is also important for information to reach decision-makers through appropriate channels, ones that generate an appropriate amount of trust in the information. For example, consider a commercial farmer in North America or Europe, who wants to learn about whether climate change will have a significant impact on her business. She might use the Internet, and discover the report of the Intergovernmental Panel on Climate Change (IPCC), and even go so far as to read the relevant parts of it. The next day, however, she may see a program on television, or read an article in a magazine, that delivers a contradictory message. Which will she trust more? Probably the message from the source with which she is familiar, which is likely not the IPCC.

Social scientists have described organizations that facilitate the transfer of knowledge from the scientific community to the policy and decision-making communities "boundary organizations," because they span the boundary between science and action (Gieryn, 1995; Jasanoff, 1987). The most important feature of successful boundary organizations, ones that engender levels of trust that are appropriate for the information content, is that they have responsibility, or accountability, to both the science and action communities (Guston, 1999, 2001). A good example would be an agricultural extension service, which is located in a university setting,

but funded in part by an agricultural ministry, and which relies on the help of an agricultural member organization to reach out to farmers. Numerous case studies have shown that these types of organizations tend to communicate information that is relevant to their target audience, and which draws off of social connections and implicit obligations, in addition to a track record of success, for its reputation of trustworthiness (Cash, 2001; Cash and Buizer, 2005; Jasianoff *et al.*, 2002).

A study by Patt *et al.* (2006) examined whether the greater trust these organizations enjoy is rooted in their social connections, or in the fact that these organizations, partly because of their social connections, produce more relevant information. They conducted an experiment in which decision-makers could earn money by playing a probabilistic game two times. The game they used was the so-called Monty Hall Three Door Game, which is interesting because most people (about 80–90%) follow an intuitive decision-making strategy that generates the winning outcome one-third of the time, rather than the other decision-making strategy, which wins two-thirds of the time (Friedman, 1998; Granberg and Brown, 1995). In their experiment, the researchers randomly assigned participants to a control group, which played the game without advice, and to three experimental groups, all of which received advice from a third party, who was drawn from the same pool of people as the people participating as the decision-makers. The advice was always the same, namely that the counter-intuitive strategy would win with a much higher likelihood. In the first experimental group (“simple advice”), the experimenter did not reveal any information about the terms under which the advisor was participating, and indeed the advisor received no compensation for participating. In the second experimental group (“aligned incentives”), the advisor would be paid some money if and only if the decision-maker won the game. The experimenter described this to the decision-makers, and thus it was clear that the advisor had an obvious incentive to provide high quality advice. In the third experimental group (“purchased advice”), the advisor would participate only if the decision-maker paid him a small fee (a fraction of the money that everybody received for agreeing to participate in the first place). The results were interesting. There was no significant difference in decision-making strategy between the “control” group (no advice), and the “simple advice” group. Initially, only people in the “purchased advice” group were more likely to adopt the superior strategy. Over successive rounds, however, the “aligned incentives” group became more likely to adopt the correct strategy, and the “purchased advice” group settled back towards the “control” and “simple advice” groups. These results suggest that the relationship between the advisor and the decision-maker can make a large difference.

3.2. Information content and form

If one views participatory communication of uncertainty, involving trusted sources of information, as a prerequisite for decision-makers’ making difficult decisions wisely, then it becomes clear that one of the purposes of scientific assessment is to

stimulate that type of communication where it is appropriate. This is not a trivial point. Participatory communication is time consuming and expensive for all parties concerned. The goal of scientific assessment, when communicating uncertainty, ought not to give the right information to guide all decisions, but to provide enough background understanding of the nature of the uncertainty so as to stimulate those decision-makers whose decisions are particularly sensitive to the uncertainty to seek further help. There are a few features of the uncertainty that are, for most decision-makers, of central importance, and which can be communicated quickly and fairly easily. Some of these are statistical in nature, while others pertain more to the system being described. In this section I list some of these, and with them some guidelines about what form to provide the information in.

3.2.1. Shape of the distribution

From an economic standpoint, the most important piece of information to convey is the shape of the distribution, to the extent that this is, or can be, known. Some argue that for climate change, for example, it is not possible to attach any likelihood estimates on various possible future scenarios, and the best that can be done is to suggest a range over which uncertainty likely operates (Betz, 2007). Others, by contrast, argue that it is possible to describe some outcomes as more likely than others, even if it is not possible to describe a full probability density function (Risbey, 2007). These debates aside, it probably is relevant for decision-makers what the likely range of values that they might face actually is, and secondarily relevant what the distribution is within that range. If their decision is sensitive to the range of values within that distribution, then they will seek out more information about its precise shape.

People remember and use information about uncertainty differently, depending on whether they learn it through personal experience, or from a description (Weber, 2006). Thus, it may be relevant to use some example to describe the practical significance of this range, in such a way as to relate to people's personal experience. For example, the current range of climate sensitivity (amount of warming given a doubling of atmospheric CO₂ concentration) could be described as being between 0°C and 10°C. It is relatively obvious what the 0°C implies (*i.e.*, no change from the present), but could be worthwhile pointing out what a 10°C shift would mean, such as that the city of Boston would come to experience the climate now experienced in Houston.

To the extent possible, it is useful to convey information on the shape of the distribution, in the form of what ranges are more likely than others. Anecdotal evidence suggests that it can be dangerous to convey the mean value of a distribution, for people will place a great deal of emphasis on that, and in the process forget about the rest of the distribution, which might be more relevant. Statistics such as the variance or standard error are probably irrelevant for most people, who do not understand what they represent.

3.2.2. Likelihood of particular events

There are some singular events that people are very worried about, and their likelihood can be very relevant for decision-making. For example, if the West Antarctic Ice Sheet were to collapse quite quickly, this would be catastrophic for all coastal cities; the likelihood of this event alone should have an influence on climate policy (O'Neill and Oppenheimer, 2002). To the extent that it is possible to clarify this likelihood, it should be communicated.

In doing so, however, it is important to remember that people remember likelihoods in qualitative terms, rather than quantitative terms (Windschitl and Weber, 1999). The IPCC dealt with this issue by developing a confidence scale, which uses precise words matched to ranges of likelihood. While there are some problems with this approach (Patt and Dessai, 2005; Patt and Schrag, 2003), it has been praised almost uniformly (Risbey and Kandlikar, 2007).

3.2.3. When and if uncertainty will be resolved

The presence of uncertainty can be one of the strongest reasons for inaction (Funtowicz and Ravetz, 1993). If people believe that the uncertainty will be resolved in the foreseeable future, they will use that as a rationale for avoiding making a firm decision before then (Patt, 2007). This is consistent with the idea that maintaining freedom in the presence of uncertainty and the potential for learning has a real option value (Fleten *et al.*, 2007; Schatzki, 2003). Often it is assumed that uncertainty can and will be resolved fairly quickly. For example, in the climate change literature, there are many papers exploring what the optimal decision strategy is, given uncertainty about climate sensitivity that will be resolved within the next decade (Jones, 2000). But studies have suggested that such uncertainty is likely to be resolved very slowly (Andronova and Schlesinger, 2001), or potentially not at all (Roe and Baker, 2007). This in turns carries implications for the policy approach that is adopted (Allen and Frame, 2007; Lempert, 2002). Clearly, giving some indication of the pace at which uncertainty will be resolved is important.

3.2.4. Sources of uncertainty

Quite closely related is the issue of the sources of uncertainty. This is because while there may not be progress in eliminating the uncertainty, there may be major changes in the estimates of it in the near term, because one or more of the sources of uncertainty are resolved. An example of this was described by Suarez and Patt (2004). They were communicating probabilistic climate forecasts to forecasts, in a year where there was a great deal of uncertainty about the future development of El Niño, the most important predictor of seasonal climate. They were communicating the forecast, for the December to March rainy season, in September. The

uncertainty about El Niño would likely be resolved by October, which could substantially change the likelihood estimates. As they described, they found it useful to describe these two sources of uncertainty – uncertainty concerning the magnitude of El Niño, and uncertainty about the effect of El Niño on local rainfall – as a means to suggest to farmers that they should find out, in October, how the first of these uncertainty issues had been resolved. Moreover, they found it effective to explain this problem of joint probability using an analogy. They described the problem of betting on a football game, at a time when it was unclear whether the star player for one of the teams would be able to play, or would be injured. Clearly, the odds for the game would change after that player completed his medical check!

3.2.5. Characterizing the sensitivity of different decisions to uncertainty

Finally, it can be useful to provide general guidance for decision-makers on whether the particular decisions they face are sensitive to the range of uncertainty. Within the climate change issue, for example, there are two broad classes of decisions: mitigation, which is the reduction of emissions and of atmospheric CO₂ concentrations; and adaptation, which is the act of managing climate impacts in order to reduce their negative consequences, and to take advantage of opportunities (McCarthy *et al.*, 2001). Each type of action may be sensitive to different ranges and types of uncertainty. For example, the Stern Review (2007) made the somewhat controversial claims that the potential cost to society of failing to mitigate would be between 5% and 20% of global consumption, whereas the cost of mitigating to avoid most of those costs would be less than 2%. By offering ranges of uncertainty that do not overlap, the Stern Review thus suggests quite clearly that the decision to engage in at least this amount of mitigation is not sensitive to remaining uncertainties. By contrast, the types of decisions that can be made for adaptation are quite diverse, and many of them are very sensitive to uncertainties (Patt *et al.*, 2005a). It is important to tell climate change policy makers that they need more detailed information about uncertainty and adaptation than can fit in an assessment report, whereas for mitigation they do not.

4. Conclusions

Uncertainty needs to be communicated to policy makers, yet doing so in a way that the most important details are made salient is a task that can only be achieved through interactive dialog. There are several reasons for this.

First, different decision-makers, operating in different choice contexts, make decisions through very different sets of thought processes. The standard assumption in normative decision models is that people follow an economic model, which is based around the maximization of expected utility or value. In fact, people seldom do this. In most cases, they follow processes described by psychologists, or by

sociologists. When doing so, the types of information that might change their decisions, and the effects of that information, can be quite different. The process of dialog can identify which decision making pattern is in play, and in turn the information that is most salient.

Second, uncertainty has several dimensions, and it is difficult to communicate all of these quickly and easily in a one-way process. Some measure of the uncertainty is a result of ambiguity in existing theory, another part coming from measurement error, and a third from conflicting beliefs about what model is the more appropriate characterization. Moreover, people respond differently to the different dimensions, and often do so in ways that are counter productive. It is important to help people apply information to a salient choice problem, in order to guide them through the process of deciphering the uncertainty and identifying appropriate response strategies.

Third, the presence of uncertainty creates a large opportunity for the loss of credibility of the communicators of that information. If they identify a best response strategy to a problem that is sensitive to the uncertainty, that strategy will appear sub-optimal with some probability greater than zero. People need to participate in arriving at response strategies, taking some responsibility for their development, in order to see them as the best option given the conditions. Moreover, they are more likely to trust communicators who demonstrate that they have a real incentive to provide accurate information.

For all of these reasons, it has been observed that participatory communication is the *sine qua non* of effective decision-support and scientific assessment in the context of high uncertainty. Modelers need to be ready to be engaged by decision-makers, to help them arrive at good decisions. At the same time, however, modelers need to publish their results in non-participatory media, such as a published scientific assessment. What is the best way to do so? I have argued in this paper that the most important consideration is giving decision-makers enough information to know when they need to invest the time and resources to take part in a participatory process, and when they do not.

To do this, there are some basic pieces of information that need to be conveyed. First, the range of potential outcomes is of vital importance. Less important is the shape of that distribution, and even less importance still are the mean and variance. Second, qualitative verbal descriptions of the likelihoods of important outcomes are important. Third, it is essential to identify whether uncertainty can be expected to be resolved quickly. Fourth, it is often important to identify some of the sources of uncertainty, since these may influence whether uncertainty estimates will change over time. Fifth, it can be useful to offer guidance on specific classes of problems, and whether these are sensitive or not to the range of uncertainty.

References

Allais, M. and Hagen, O. (Editors), 1979. Expected utility hypotheses and the Allais Paradox. *Theory and Decision Library*. Kluwer, Dordrecht.

Allen, M.R. and Frame, D.J., 2007. ATMOSPHERE: call off the quest. *Science* %R 10.1126/science.1149988, 318(5850): 582–583.

Andronova, N.G. and Schlesinger, M.E., 2001. Objective estimation of the probability density function for climate sensitivity. *Journal of Geophysical Research-Atmospheres*, 106(D19): 22605–22611.

Betz, G., 2007. Probabilities in climate policy advice: a critical comment. *Climatic Change*, 85(1): 1.

Birnbaum, M.H. and Mellers, B.A., 1983. Bayesian inference: combining base rates with opinions of sources who vary in credibility. *Journal of Personality and Social Psychology*, 45(4): 792–804.

Birnbaum, M.H. and Stegner, S., 1979. Source credibility in social judgment: bias, expertise, and the judge's point of view. *Journal of Personality and Social Psychology*, 37: 48–74.

Birnbaum, M.H., Wong, R. and Wong, L.K., 1976. Combining information from sources that vary in credibility. *Memory and Cognition*, 4(3): 330–336.

Boykoff, M. and Boykoff, J., 2004. Balance as bias: global warming and the US prestige press. *Global Environmental Change*, 14: 125–136.

Breyer, S., 1993. *Breaking the Vicious Circle: Toward Effective Risk Regulation*. Harvard University Press, Cambridge, USA.

Bruine de Bruin, W., Fischhoff, B., Millstein, S., and Halpern-Felscher, B., 2000. Verbal and numerical expressions of probability: "It's a Fifty-Fifty Chance". *Organizational Behavior and Human Decision Processes*, 81(1): 115–131.

Cash, D., Borck, J., and Patt, A.G., 2006. Countering the 'loading dock' approach to linking science and decision making: a comparative analysis of ENSO forecasting systems. *Science, Technology, and Human Values*, 31: 465–494.

Cash, D. and Buizer, J., 2005. Knowledge-Action Systems for Seasonal to Interannual Climate Forecasting: Summary of a Workshop, National Academy of Sciences, Washington, DC.

Cash, D. *et al.*, 2003. Knowledge systems for sustainable development. *Proceedings of the National Academy of Sciences*, 100(14): 8086–8091.

Cash, D.W., 2001. 'In order to aid in diffusing useful and practical information': agricultural extension and boundary organizations. *Science, Technology, and Human Values*, 26(4): 431–453.

Covello, V., 1990. Risk comparisons in risk communication: issues and problems in comparing health and environmental risks. In: R. Kaspelson and D. Stallen (Editors), *Communicating Risks to the Public: International Perspectives*. Kluwer Academic Publishers, Dordrecht, pp. 79–124.

Darr, E. and Kurtzberg, T., 2000. An investigation of partner similarity dimensions on knowledge transfer. *Organizational Behavior and Human Decision Processes*, 82(1): 28–44.

Douglas, M. and Wildavsky, A.B., 1982. *Risk and Culture*. University of California Press, Berkeley.

Dryzek, J., 1997. *The Politics of the Earth: Environmental Discourses*. Oxford University Press, Oxford.

Edgell, S.E., Harbison, J.I., Neace, W.P., Nahinsky, I.D., and Lajoie, A.S., 2004. What is learned from experience in a probabilistic environment? *Journal of Behavioral Decision Making*, 17: 213–229.

Ezrahi, Y., 1990. *The Descent of Icarus: Science and the Transformation of Contemporary Democracy*. Harvard University Press, Cambridge, MA.

Fehr, E. and Schmidt, K., 1999. A theory of fairness, competition, and cooperation. *Quarterly Journal of Economics*, 114: 817–868.

Fischhoff, B., 1995. Risk communication and perception unplugged: twenty years of process. *Risk Analysis*, 15: 137–145.

Fleten, S.E., Maribu, K.M., and Wangensteen, I., 2007. Optimal investment strategies in decentralized renewable power generation under uncertainty. *Energy*, 32(5): 803.

Friedman, D., 1998. Monty Hall's three doors: construction and deconstruction of a choice anomaly. *American Economic Review*, 88(4): 933–946.

Funtowicz, S.O. and Ravetz, J.R., 1990. *Uncertainty and Quality in Science for Policy*. Kluwer, Dordrecht, the Netherlands.

Funtowicz, S.O. and Ravetz, J.R., 1993. Science for the post-normal age. *Futures*, 25(7): 739–755.

Gelbspan, R., 1997. *The Heat Is on: The High Stakes Battle over Earth's Threatened Climate*. Perseus, Cambridge.

Gieryn, T.F., 1995. Boundaries of science. In: S. Jasanoff *et al.* (Editors), *Handbook of Science and Technology Studies*. Sage Publications, Thousand Oaks, CA, 393–444.

Gigerenzer, G., 2000. *Adaptive Thinking: Rationality in the Real World*. Oxford University Press, Oxford, UK.

Gigerenzer, G. and Selten, R. (Editors), 2001. *Bounded Rationality: The Adaptive Tool-Box*. MIT Press, Cambridge, MA.

Glantz, M., 2000. Once burned, twice shy? Lessons learned from the 1997-98 El Niño. UNEP/NCAR/UNU/WMO/ISDR, Tokyo, Japan.

Gordon, D. and Kammen, D., 1996. Uncertainty and overconfidence in time-series forecasts: application to the Standard & Poor's 500 stock index. *Applied Financial Economics*, 6: 189–198.

Granberg, D. and Brown, T.A., 1995. The Monty Hall dilemma. *Personality and Social Psychology Bulletin*, 21(7): 711–723.

Griffin, D. and Tversky, A., 1992. The weighting of evidence and the determinants of confidence. *Cognitive Psychology*, 24: 411–435.

Guston, D.H., 1999. Stabilizing the boundary between politics and science: the role of the Office of Technology Transfer as a boundary organization. *Social Studies of Science*, 29(1): 87–112.

Guston, D.H., 2001. Boundary organizations in environmental policy and science: an introduction. *Science, Technology, and Human Values*, 26(4): 399–408.

Harvey, N. and Fischer, I., 1997. Taking advice: accepting help, improving judgment, and sharing responsibility. *Organizational Behavior and Human Decision Processes*, 70(2): 117–133.

Irwin, A. and Wynne, B. (Editors), 1996. *Misunderstanding Science? The Public Reconstruction of Science and Technology*. Cambridge University Press, Cambridge UK.

Jasanoff, S., Markle, G.E., Petersen, J.C., and Pinch, T. (Editors), 2002. *Handbook of Science and Technology Studies*. Sage Publications, Thousand Oaks, CA.

Jasanoff, S.S., 1987. Contested boundaries in policy-relevant science. *Social Studies of Science*, 17: 195–230.

Jones, R.N., 2000. Managing uncertainty in climate change projections: issues for impact analysis. *Climatic Change*, 45(3,4): 403–419.

Kahneman, D., Knetch, J., and Thaler, R., 1986. Fairness and the assumptions of economics. *Journal of Business*, 59: s285–s300.

Kahneman, D. and Tversky, A., 1979. Prospect theory: an analysis of decision under risk. *Econometrica*, 47: 263–291.

Kasperson, R.E. and Kasperson, J.X., 1996. The social amplification and attenuation of risk. *Annals of the American Academy of Political and Social Science*, 545: 95–105.

Knetch, J., 1997. Reference states, fairness, and the choice of measure to value environmental changes. In: M. Bazerman, D. Messick, A. Tenbrunsel and K. Wade-Benzoni (Editors), *Environment, Ethics, and Behavior*. New Lexington Press, San Francisco, pp. 13–32.

Kühberger, A., 1998. The influence of framing on risky decisions: a meta-analysis. *Organizational Behavior and Human Decision Processes*, 75(1): 23–55.

Lee, K., 1993. *Compass and Gyroscope: Integrating Science and Politics for the Environment*. Island Press, Washington, DC.

Leiss, W., 1996. Three phases in the evolution of risk communication practice. *Annals of the American Academy of Political and Social Science*, 545: 85–94.

Lempert, R., 2002. A new decision sciences for complex systems. *Proceedings of the National Academy of Sciences of the United States of America*, 99: 7309–7313.

McCarthy, J.J., Canziani, O.F., Leary, N.A., Dokken, D.J., and White, K.S. (Editors), 2001. *Climate Change 2001: Impacts, Adaptation, and Vulnerability*. Published for the Intergovernmental Panel on Climate Change. Cambridge University Press, Cambridge, 1032 pp.

Michael, M., 1996. Ignoring science: discourses of ignorance in the public understanding of science. In: A. Irwin and B. Wynne (Editors), *Misunderstanding Science? The Public Reconstruction of Science and Technology*. Cambridge University Press, Cambridge UK, pp. 107–125.

Moss, R. and Schneider, S., 2000. Uncertainties in the IPCC TAR: recommendations to lead authors for more consistent assessment and reporting. In: R. Pachauri, T. Taniguchi and K. Tanaka (Editors), *IPCC Supporting Material, Guidance Papers on the Corss Cutting Issues of the Third Assessment Report of the IPCC*. Cambridge University Press, Cambridge, pp. 33–51.

Moss, S., Downing, T., and Rouchier, J., 2002. Demonstrating the role of stakeholder participation: an agent based social simulation model of water demand policy and response, Centre for Policy Modelling Discussion Papers, Manchester. Available at <http://cfpm.org/~scott/water-demand/demand-pilot1.pdf> [last accessed: 15/04/2009].

Munroe, A. and Sugden, R., 2003. On the theory of reference-dependent preferences. *Journal of Economic Behavior and Organization*, 50: 407–428.

National Research Council, 2006. *Completing the Forecast: Characterizing and Communicating Uncertainty for Better Decisions Using Weather and Climate Forecasts*. The National Academies Press, Washington.

O'Neill, B.C. and Oppenheimer, M., 2002. Dangerous climate impacts and the Kyoto Protocol. *Science*, 296: 1971–1972.

Orlove, B. and Tosteson, J., 1999. The application of seasonal to interannual climate forecasts based on El Niño – Southern Oscillation (ENSO) events: lessons from Australia, Brazil, Ethiopia, Peru, and Zimbabwe. *Working Papers in Environmental Policy*, Institute of International Studies, University of California, Berkeley, Berkeley.

Patt, A.G., 2001. Understanding uncertainty: forecasting seasonal climate for farmers in Zimbabwe. *Risk Decision and Policy*, 6: 105–119.

Patt, A.G., 2007. Assessing model-based and conflict-based uncertainty. *Global Environmental Change*, 17: 37–46.

Patt, A.G., Bowles, H.R., and Cash, D., 2006. Mechanisms for enhancing the credibility of an advisor: prepayment and aligned incentives. *Journal of Behavioral Decision Making*, 19(4): 347–359.

Patt, A.G. and Dessai, S., 2005. Communicating uncertainty: lessons learned and suggestions for climate change assessment. *Comptes Rendus Geosciences*, 337: 425–441.

Patt, A.G., Klein, R., and de la Vega-Leinert, A., 2005a. Taking the uncertainties in climate change vulnerability assessment seriously. *Comptes Rendus Geosciences*, 337: 411–424.

Patt, A.G., Ogallo, L., and Hellmuth, M., 2007. Learning from 10 years of climate outlook forums in Africa. *Science*, 318: 49–50.

Patt, A.G. and Schrag, D., 2003. Using specific language to describe risk and probability. *Climatic Change*, 61: 17–30.

Patt, A.G., Suarez, P., and Gwata, C., 2005b. Effects of seasonal climate forecasts and participatory workshops among subsistence farmers in Zimbabwe. *Proceedings of the National Academy of Sciences of the United States of America*, 102: 12623–12628.

Patt, A.G. and Zeckhauser, R., 2000. Action bias and environmental decisions. *Journal of Risk and Uncertainty*, 21(1): 45–72.

Payne, J.W., Bettman, J.R., and Johnson, E.J., 1993. *The Adaptive Decision Maker*. Cambridge University Press, Cambridge.

Petty, R.E. and Cacioppo, J.T., 1986. The elaboration likelihood model of persuasion. In: L. Berkowitz (Editor), *Advances in Experimental Social Psychology*. Academic Press, New York, pp. 123–205.

Prentice-Dunn, S. and Rogers, R.W., 1986. Protection motivation theory and preventative health: beyond the health belief model. *Health Education Research*, 1: 153–161.

Risbey, J., 2007. Subjective elements in climate policy advice. *Climatic Change*, 85(1): 11.

Risbey, J. and Kandlikar, M., 2007. Expressions of likelihood and confidence in the IPCC uncertainty assessment process. *Climatic Change*, 85(1): 19.

Ritov, I. and Baron, J., 1992. Status quo and omission biases. *Journal of Risk and Uncertainty*, 5: 49–61.

Roe, G.H. and Baker, M.B., 2007. Why is climate sensitivity so unpredictable? *Science %R* 10.1126/science.1144735, 318(5850): 629–632.

Samuelson, W. and Zeckhauser, R., 1988. Status quo bias in decision making. *Journal of Risk and Uncertainty*, 1: 7–59.

Schatzki, T., 2003. Options, uncertainty, and sunk costs: an empirical analysis of land use change. *Journal of Environmental Economics and Management*, 46: 86–105.

Shackley, S. and Wynne, B., 1996. Representing uncertainty in global climate change science and policy: boundary-ordering devices and authority. *Science, Technology, and Human Values*, 21(3): 275–302.

Simon, H., 1956. Rational choice and the structure of the environment. *Psychological Review*, 63: 129–138.

Sniezek, J., Schrah, G.E., and Dalal, R., 2004. Improving judgment with prepaid expert advice. *Journal of Behavioral Decision Making*, 17: 173–190.

Social Learning Group, 2001. *Learning to Manage Global Environmental Risks – Volume 1*. MIT Press, Cambridge, MA.

Stern, N., 2007. *The Economics of Climate Change*. Cambridge University Press, Cambridge, UK, 712 pp.

Suarez, P. and Patt, A., 2004. Caution, cognition, and credibility: the risks of climate forecast application. *Risk Decision and Policy*, 9: 75–89.

Thaler, R. (Editor), 1991. *Quasi-Rational Economics*. Russel Sage Foundation, New York.

Thompson, M., Ellis, R., and Wildavsky, A.B., 1990. *Cultural Theory*. Westview Press, New York.

Tversky, A. and Kahneman, D., 1973. Availability: A Heuristic for Judging Frequency and Probability. *Cognitive Psychology*, 5: 207–232.

Tversky, A. and Kahneman, D., 1974. Judgment under uncertainty: heuristics and biases. *Science*, 211: 1124–1131.

von Neumann, J. and Morgenstern, O., 1944. *Theory of Games and Economic Behavior*. Princeton University Press, Princeton.

Weber, E., 2006. Experienced-based and description-based perceptions of long-term risk: why global warming does not scare us (yet). *Climatic Change*, 77: 103–120.

Weber, E., Bökenholt, U., Hilton, D., and Wallace, B., 2000. Confidence judgments as expressions of experienced decision conflict. *Risk Decision and Policy*, 5: 69–100.

Webster, M., 2003. Communicating climate change uncertainty to policy-makers and the public. *Climatic Change*, 61: 1–8.

Windschitl, P.D. and Weber, E., 1999. The interpretation of “likely” depends on the context, but “70%” is 70% – right? the influence of associative processes on perceived certainty. *Journal of Experimental Psychology: Learning, Memory, and Cognition*, 25(6): 1514–1533.

Wynne, B., 1996. Misunderstood misunderstandings: social identities and the public uptake of science. In: A. Irwin and B. Wynne (Editors), *Misunderstanding Science? The Public Reconstruction of Science and Technology*. Cambridge University Press, Cambridge UK, pp. 19–46.

Zeckhauser, R. and Viscusi, W.K., 1990. Risk within reason. *Science*, 248: 559–564.

Zeckhauser, R. and Viscusi, W.K., 1996. The risk management dilemma. *Annals of the American Academy of Political and Social Science*, 545: 144–155.

Communicating scientific uncertainty for decision making about CO₂ storage

Peter M. Haugan

Geophysical Institute, University of Bergen, Allegaten 70, N-5007 Bergen, Norway.

Abstract

As the severity of the global CO₂ problem gradually is becoming clear to everybody, decisions will have to be made concerning permitting of carbon storage projects. Fossil fuel based power plants can produce energy at competitive prices with other energy sources even if equipped with capture facilities. Thus, the fossil fuel industry is ready to implement carbon capture and storage (CCS) once a CO₂ tax regime or its equivalent is introduced. Questions associated with accounting for leaky storage reservoirs over millennial time scales in a carbon credit regime and estimating impacts of CO₂ on climate and ocean ecosystems will then have to be addressed in order to estimate the benefits and possible damage from any given storage project. Available environmental models for such questions have only limited validation data but are foreseen to play a key role, and acquisition of required site specific data may be costly. Experience from the past 15 years of research on CO₂ storage options and the associated science – policy interface suggests that uncertain models tend to be trusted too much by policy makers. In some cases, good intentions for environmental protection lead to a compartmentalized approach that is unsuitable for global problems where tradeoffs may be inevitable. In conclusion, the likelihood of poor environmental management decisions on carbon storage is large and the actual need for alternative solutions to the CO₂ problem is larger than proponents of CCS may like to think.

Keywords: climate change, carbon storage, carbon capture, oceans, energy, fossil fuels, CO₂ injection.

1. Introduction

The CO₂ problem may well be the most severe environmental challenge facing mankind. The amount of CO₂ that has already been emitted to the atmosphere will affect the earth system for thousands of years. The emissions are still rising and are very likely to do so for several decades. An option which has been proposed to curb the effective emissions is that of direct storage of CO₂, mostly from large

fossil fuel power plants, into geological reservoirs or the deep ocean. This raises several questions where environmental modeling has been used and will have to be used in decision making. One key question is whether the stored CO₂ can be expected to remain in place permanently or for long enough so that leakage to the atmosphere or ocean will not give significant climate change or ocean acidification effects for future generations. Carbon credits should only be given if this can be assured. Associated questions are what certainty is needed to make decisions, and whether it is acceptable to make trade-offs between impacts in different compartments of the earth system (ocean, atmosphere) and between impacts experience at different times (*e.g.*, this century and a thousand years later).

Modeling inevitably enters this arena primarily because of the long time scales involved and partly because of the complexity of the earth system response that needs to be understood when making globally significant perturbations to cycles of a key element like carbon. There is no way to make a global carbon emission and storage experiment like the present one with large emissions to the atmosphere and associated indirect storage in the ocean, and then afterwards decide on long term policy by learning from the measured response. There also seems to be no past event in earth history that is sufficiently similar to the present situation to be of much use. If there were, the observations of earth system response from that time would be indirect by proxies and very incomplete in spatial and temporal coverage. In effect there is no good way to test or validate the environmental models needed for present day decision making. For reasons that are somewhat obscure and probably go well beyond natural science, public trust in relevant modeling results may however be high.

Particularly for geological storage, the porous media in which CO₂ is planned to be stored are notably heterogeneous with relevant properties such as permeability varying by many orders of magnitude on centimeter scales. The lack of detailed data from any long term storage experiment in such a reservoir precludes model history matching, not to mention prediction for other reservoirs. Yet projects are being planned based on not much more data than those typically involved in exploring for oil and gas: seismic profiling from the surface supplemented by core data with rock and fluid properties from a single well cutting through the formation. When such data are used as a basis for field development decisions, the stakes are the money spent on exploration costs, and the potential revenues are those associated with the market value of the oil and/or gas. A 50% success rate is acceptable. When such data are used for decision making about CO₂ storage however, an annual leakage rate of 0.1% of the CO₂ stored in place can be shown to be unacceptable from a global climate perspective, *i.e.*, even without considering any local environmental impact. Can we have sufficient confidence in the models to make predictions at such accuracy for several millennia into the future?

CO₂ is not only a greenhouse gas, which alters the radiative balance in the atmosphere, but it also acidifies ocean waters after ocean uptake. Adding CO₂ to seawater leads to a shift in the balance between carbonate and bicarbonate ions with the indirect, but rather immediate effect that the availability of calcium carbonate

is reduced. Many marine organisms including both warm and cold water corals make their shells of calcium carbonate. Thus their growth rate is reduced and with increased CO₂ pressure they will even start to dissolve. For cold water corals at high latitudes where the effects happen faster and penetrate deeper into the water column than in warm water at lower latitudes, such dissolution is expected in the present century for almost all conceivable carbon emission scenarios. In case of direct deep ocean storage or leakage from subseabed geological storage, high carbon concentrations may also lead to additional acute effects in a range of organisms, but only on the local scale.

The present paper is intended to provide an introduction to carbon storage emphasising aspects relevant to environmental models and their use in decision making. The following section gives a short primer on carbon (dioxide capture and) storage. Thereafter comes a somewhat personal tour through 15 years of interaction with researchers and policymakers on development of direct carbon storage in oceans as well as in geological reservoirs. The problem of estimating and ultimately costing damage to the climate system from future leakage is addressed in section 4, followed by a critical discussion of the role of environmental modelling envisaged in present guidelines for permitting subseabed carbon storage. The windup in section 6 includes some prospects for development of carbon storage decisions in the near future.

2. Carbon storage: what is it?

The Kaya equation (named after Professor Yoichi Kaya, Japan) gives CO₂ emissions as:

$$CO_2 = N \times (GDP/N) \times (E/GDP) \times (CO_2/E), \quad (1)$$

showing that one or more of the four factors population (N), wealth (GDP = Gross Domestic Product), energy intensity (E/GDP where E is energy use) or carbon intensity (CO₂/E) has to be reduced in order to reduce total emissions (Kaya, 1995). Experience has shown that there is limited scope for reducing energy intensity as countries improve their standard of living. Historically there are only a few cases where it has been possible to reduce carbon intensity, notably in countries which have emphasized nuclear energy such as France. However, the abundance of cheaply available fossil fuel reserves has so far limited development of alternative energy sources. Coal is the most carbon intensive of the fossil fuels and available in such large quantities that it alone could supply the world energy for several centuries. The available amounts of oil are more limited also by political factors, but with the present oil prices (around 100 USD/barrel), it begins to become economically attractive to produce liquid fuels from other fossil sources. Natural gas is the least carbon intensive fossil fuel, abundantly available in many locations, although in smaller energy-equivalent quantities than coal. In addition there are potential huge reserves bound in methane hydrates.

About 40% of the global CO₂ emissions occur in the energy industry, mainly by burning coal in public electricity and heat generation plants. Transport is the second largest source, growing faster than the other sectors and now approaching 25% (IPCC, 2005). Other industries, manufacturing and construction, and other sectors including residential fuel use account for the rest. The IPCC Special Report on Carbon Dioxide Capture and Storage (IPCC, 2005) contains a wealth of reference and background material for sources, capture, transport and storage and cost estimates for these options as well as properties of CO₂, and may be consulted for information not given with specific reference information in the present text.

Technologies for CO₂ capture are mainly focussed on large stationary sources because of the economy of scale, the need to run complex chemical processes often at high pressures and the need for a receiving system for handling the CO₂. In order to decarbonize the transport sector, capture at each mobile unit is not considered feasible. Fuel switching *e.g.*, to hydrogen which may be produced from fossil fuels at large stationary plants is considered more realistic. Thus, if large scale capture and storage is to become a key part of future global energy supply, the capture will still take place at large power plants retrofitted or designed for capture. CO₂ captured at an industrial site would normally be pressurized and/or cooled to a liquid (or supercritical) phase suitable for transport by pipeline or ships. The two types of storage options which have volumetric capacities relevant for the scale of the global CO₂ problem are the deep ocean and underground geological storage.

Geological storage involves injection of liquid CO₂ at high enough pressures to displace the fluids which are naturally present in the geological formation, normally saline water (brine), but possibly also oil in which case enhanced oil recovery may result. The injectivity depends on porosity and permeability of the formation, typically sandstone. Low permeability reservoirs are less suitable because of the high injection pressures required and the possibility for formation damage. Because of the high temperatures encountered when drilling hundreds and thousands of meters below the surface, CO₂ will in almost all cases be less dense than the fluids in the formation and tend to penetrate upwards. Structural properties, such as availability of low permeability seals above the formation, and the properties of faults and fractures are therefore important for the fate of injected CO₂.

Direct ocean storage involves either injection of CO₂ droplets in the open water column with rapid dissolution and transport by ocean currents, or deposition on the deep sea floor. For depths of the order 3000 m and at the relatively cold temperatures of seawater, liquid CO₂ is denser than seawater and would tend to stay near the disposal site, particularly if confined in topographic depressions at the seafloor. Formation of CO₂ hydrate at the interface between CO₂ and water and interaction with sediments on the seafloor could further delay the dissolution into the water column above.

In addition to the economic costs of making and running facilities for carbon capture and storage (CCS), there is an energy penalty associated with the operation. Capture, compression and transport require energy input which in turn requires

more fossil fuel to be burnt, captured and stored. The penalty is highly dependent upon the type of power plant, suitable and available technology, transport distance etc. A typical assumed range is 5–20% energy penalty. This is the expected increase in total CO₂ produced in a facility with CCS compared to the CO₂ emitted if no CCS was implemented for the same production of electricity and heat.

3. Development of storage options and perceptions

Capture and storage of CO₂ (CCS) is often considered as a possible bridge from a fossil based energy sector towards carbon-free alternative energy sources. If sufficient economic incentives were provided, *e.g.*, by avoidance of a CO₂ tax which would otherwise apply, available technologies could be applied rapidly in some cases by adding capture facilities to existing power plants. More efficient, energy-saving and economically attractive technologies could be implemented in the design of new plants. However, the typical lifetime of heavy infrastructure in the energy sector is several decades and CO₂ emissions are growing rapidly also from other sectors. Even if the political incentives and technology were to develop favourably and the environmental aspects of CCS could be handled satisfactorily, there are therefore some inherent hard limitations on how fast CCS could handle a large fraction of present and future CO₂ emissions. A key question is whether environmental concerns should or will further limit its application, at least as a short term bridge. If so, the CO₂ problem is even harder and the need for alternative solutions even larger.

Modern studies of carbon capture and storage started with Cesare Marchettis proposal to inject CO₂ from European power plants in the Gibraltar outflow of saline dense water which would transport it deep into the Atlantic (Marchetti, 1977). During the past 30 years, a wide range of capture technologies have been developed although not yet applied to full size power plants due to lack of incentives. Transport of CO₂ in pipelines and by ship is mature technology already applied for enhanced oil recovery and industrial use of CO₂. The longest (since 1996) and largest (1 million tonnes of CO₂ per year) geological storage operation is that of StatoilHydro at the Sleipner gas field in the North Sea. The stored CO₂ in this case does not come from a power plant, but is naturally present in the produced natural gas from the field. The CO₂ is separated from the natural gas (mostly methane) at the offshore platform and injected into the highly permeable Utsira saline aquifer formation situated above the gas field but approximately 1000 m below the seafloor. The operation is motivated by purity requirements for the market value of the natural gas, making it necessary to separate much of the CO₂ anyway, in combination with a Norwegian carbon tax that would be applied to the CO₂ if emitted offshore. A similar operation is now coming onstream for the Snøhvit field in the Barents Sea north of Norway. Onshore storage occurs in several locations worldwide including the In Salah field in Africa and Weyburn in Canada. In the latter

case, injection occurs in oil bearing formations and prospects for enhanced oil recovery is a prime motivation.

Even if the ocean has been seriously considered since the 1970s as a primary possible storage reservoir for CO₂ and research on direct ocean storage was performed both experimentally and theoretically throughout the 1990s, the largest purposeful ocean disposal experiments that have been performed so far amount to less than one ton of CO₂ in total and time scales of hours to days for each individual experiment. This is if we exclude the largest CO₂ experiment of all, the release of CO₂ to the atmosphere, the subsequent uptake by gas exchange to the global ocean of between one third and one half of the cumulative emissions since the start of the industrial revolution and the expected final uptake of close to 90% over a time scale of millennia into the future. As mentioned in the introduction, the subsequent ocean acidification has potentially large detrimental effects on marine life. Public attention to this “second”, but not necessarily secondary, CO₂ problem has developed slowly and serious scientific efforts to elucidate the effects are only now beginning to be organized and widespread beyond a few pioneering research groups.

Against this background, the development over time of the scientific knowledge and public perceptions of different storage options may illuminate aspects of science-policy interaction. The following is not at all intended as a balanced history of carbon storage science being heavily biased towards references to work that the author has been involved in. Rather it is a collection of cases where interesting responses from the scientific and/or decision making community have been registered.

In 1992, my co-author Helge Drange and I published a paper entitled “Sequestration of CO₂ in the deep ocean by shallow injection” (Haugan and Drange, 1992). The paper dealt with fundamental physical and chemical properties and processes related to CO₂ in seawater. The implications of the study in effect transformed the Marchetti (1977) proposal of using the Mediterranean outflow into a technical option that could be applied anywhere with access to the deep ocean but with need for only shallow water facilities. The publication occurred shortly before the 1992 Rio meeting and created considerable attention. At the time, it had already been realized that simple release of single bubbles or droplets of CO₂ in the upper water column (upper 500 m) would not, except in special cases like Gibraltar, provide a conduit to the deep ocean. This was also before the development and demonstration of large and relatively cheap deep ocean pipelines, so deep ocean storage was considered by many to be prohibitively expensive. While we made important caveats about biological effects in the paper, such aspects received little attention. Technological optimism prevailed and many believed that if the climate problem became sufficiently serious, one could elaborate and roll out CCS as a fallback option. But strong action was not yet called for.

In 1996 we published a paper on “Effects of CO₂ on the ocean environment” (Haugan and Drange, 1996) contrasting the rapid anthropogenic pH reduction (acidification) in global ocean surface waters due to emissions with the localized effects of direct storage. Primarily we pointed out the global character of the largest of all CO₂ ocean storage experiments (via emissions to the atmosphere) and how

different and unique this is compared to all known glacial to interglacial environmental changes in the ocean. The paper was hardly noticed. Admittedly it was a short and relatively simple paper, published in a less visible journal, and our limited expertise made us stick to chemical environmental changes, their measurable amplitudes, spatial scales and rates. But even when skilled ocean biologists and ecologists started to publish alarming reports on measured effects of increased CO₂ on organisms, there was a very slow development of awareness.

Finally the Intergovernmental Commission (IOC) together with the non-governmental Scientific Committee on Oceanic Research (SCOR) hosted an important conference in Paris in 2004 on “The Ocean in a High CO₂ World”. Interestingly it was the appointed science committee which initiated a change in the focus for the conference from potential direct storage projects in international waters which was the prime concern of governments to acidification due to atmospheric emissions, which the scientists felt was a much more pressing issue. International science programs now have ocean acidification on the agenda and a followup conference was held in Monaco in 2008. The volume and topical breadth of research activity on ocean acidification is however still limited, indicated by the fact that 4 years is considered an appropriate time to develop sufficient amounts of research results to justify a new conference.

Government interest in ocean acidification due to emissions boosted temporarily in Norway in 2005/2006 when this second CO₂ effect was seen as another argument for allowing and stimulating subseabed geological storage projects (Haugan *et al.*, 2006, a commissioned report within the Oslo-Paris convention on protection of the North-East Atlantic, OSPAR). We will return to OSPAR in section 5, but for now just note that government interest in potential negative effects of CO₂ emissions on the oceanic environment has not yet had any measurable effect on stimulating any other technologies or options than CCS.

The ocean holds a special and sacred status for many people and many cultures throughout the world. It is a global commons and the precautionary principle has been used in many cases to limit or prohibit pollution and negative influences. From 1997 to 2002/2003 an international project (Japan, USA, Canada, Australia and Norway) on direct ocean storage of CO₂ was executed involving laboratory and field studies and modelling. The final culmination of the project was planned as an experiment releasing up to 5 ton of CO₂ at intermediate depths in the ocean (800 m; too shallow for long term storage but deep enough for hydrates to form and relevant lessons about spreading and dissolution to be learnt). First, public opposition prevented the planned experiment from taking place at the Kona coast of the Big Island of Hawaii. A combination of indigenous population religious concerns specifically about the planned experiment site, more general interests of international pressure groups, and complicated and time consuming US permitting procedures, forced the project to move the experiment elsewhere. Then just a few weeks before a re-designed experiment was to take place off the mid-Norwegian shelf, permits given by the Norwegian State Pollution Control Authority to run the experiment were overruled and withdrawn by the Norwegian minister of

Environment. Thus the project had no controlled experiment as basis for the models, but was left to make best possible use of measurements of existing natural seepages of liquid CO₂ through the seafloor which ironically do occur at large rates on the other side of the Big Island of Hawaii.

Returning to Norway, the reasoning presented by the minister is interesting. He stated that it is uncertain whether international law and regulations will permit large scale application of ocean storage of CO₂. Therefore it would not be appropriate to perform scientific experiments to learn more about this option and its potential impacts. While such decision is unfair and illogical, it was probably politically correct for a minister wishing to preserve an impression of protecting the ocean environment. (See Haugan, 2002, for further background and interpretation). Later it was confirmed that OSPAR, which was explicitly referred to by the minister, can not be applied to stop or prohibit scientific experiments. But by that time, the project had run out, the money was used up, and many scientists, both those directly involved in the project and others with interest in ocean storage, had turned away from the subject, realizing the extreme sensitivity of direct ocean storage in many influential decision making parties.

So, nobody takes the responsibility for the greatest ocean CO₂ storage experiment of all, that which has been going on for 200 years via emissions to the atmosphere. But being associated with small scale experiments in a localized site is considered to be so harmful for the public image of the responsible government that permission is not granted. In the present context, we note that the main objective of the experiment was to provide observations of phenomena (dissolving droplet plume dynamics, effect of hydrates and turbulence on dissolution, density effects on “peeling” etc.) which presently are represented in models with only theoretical parameters that cannot be determined in small scale laboratory tests. Thus, for estimating the efficiency and impacts of direct ocean storage we still have to rely on environmental models with untested process parameters.

At present, focus in Europe and mostly also in North America has turned to geological storage. Japan however which is plagued by high seismic activity and therefore hosts considerable public scepticism towards geological storage, maintains a substantial research programme on direct ocean storage. Interestingly this occurs in a country and culture with strong ties to the ocean and a genuine interest in preserving and utilizing the ocean environment. Key issues in geological storage in addition to capacity, efficiency and injectivity, are potential leakage pathways through abandoned wells, faults, fractures and imperfect seals as well as potential seismic events on time scales of millennia. Most of these issues require site specific data and future seismic activity is difficult to predict. In contrast ocean storage occurs in a medium of known properties and relatively uniform conditions at least in the deep sea. Thus, the challenge of developing credible process and prediction models for the fate of CO₂ disposed on the deep sea floor seems scientifically more tractable than developing similar models for any given geological reservoir. Both however, have to face the issue of leakage into the water column (if the geological site is subseabed) and into the combined atmosphere-ocean carbon repository.

4. Estimating environmental damage from leaky reservoirs

Haugan and Joos (2004) noted that there are several different metrics which may be used to estimate the damage of leaky reservoirs. Perhaps surprisingly, many of these metrics may be produced by global climate models which are reasonably well validated. This applies to ocean as well as geological storage. The main problem may be that it is hard to decide which metric to use and the choice may matter for estimating the value of any particular storage scheme.

5. Environmental regulations and the use of models

The IPCC Special Report (IPCC, 2005) gives an overview of relevant international law for both geological and ocean storage. Since then some important developments in the OSPAR Convention have taken place. A very similar process is ongoing with the global London Protocol. Due to space limitations, since the two conventions develop in so similar ways, and the first storage projects are expected to be in the OSPAR area, we here concentrate on OSPAR.

In 2007, OSPAR was amended at a ministerial meeting so that industrial scale subseabed geological storage in principle is allowed. Previously the “dumping” of any industrial waste except some materials explicitly included on a reverse list, in the water column or subseabed was prohibited. We note in passing that the CO₂ from the mentioned Sleipner and Snøhvit fields originates in the subseabed. Even if these storage projects have not been tried for OSPAR, they are likely to be formally acceptable. At least they are in principle quite different from any project involving CO₂ from a power plant or other industry. Thus it was clear that an amendment of OSPAR would be required in order to be able to offer geological storage facilities for industrially produced CO₂ in the subseabed in the OSPAR area regardless of whether the industrial CO₂ is produced onshore or offshore and whether it is to be transported by ship or pipeline.

The timing of this is crucial for the present political regime in Norway as several gas fired power plants are being built along the Norwegian coast and promises have been made that these shall shortly become CO₂ free, *i.e.*, with CCS implemented. As a short term solution a capture test facility which is being built at Mongstad close to Bergen on the west coast of Norway plans to deliver CO₂ for ship transport all the way to the Barents Sea in the north, capitalizing on the injection facility used for the Snøhvit field. In the meantime the Utsira formation and another formation closer to shore are being evaluated as possible storage sites for larger amounts of CO₂ to be transported by pipeline once the main power plants come on stream (Publicly available information from Gassnova SF, Norway, 2007; only in Norwegian).

So which procedures are envisaged to test whether these or any other subseabed storage project should be licensed by OSPAR? The political decision already made stipulates that a set of “Guidelines for Risk Assessment and Management of Storage of CO₂ Streams in Geological Formations” should be adopted and used against the individual projects. CO₂ streams from capture processes can be stored into a sub-soil geological formation if:

- The streams consist overwhelmingly of carbon dioxide.
- No wastes are added for the purpose of disposing.
- They are intended to be retained permanently and will not lead to significant adverse consequences for the marine environment.

The guidelines have not yet been formally adopted, but are likely to contain the following modeling-relevant elements taken from draft documents:

- From part 1, Problem formulation: Problem formulation is the scoping of a risk assessment and includes the collection of information that will be used to develop a site-specific conceptual model to direct a site-specific risk assessment.
- From part 2, Site selection: The site selection will typically include a reservoir simulation to assess a potential storage site, *e.g.*, by a three dimensional geological model.
- From part 3, Exposure assessment: The probabilities of the exposure processes, the amount of CO₂ and the spatial and temporal scale of fluxes may be assessed using appropriate numerical modelling tools.
- From part 6, Risk management: Predictive modelling of injection of CO₂ streams should include both flow (reservoir) simulation, prediction of fracturing and fracture propagation, *e.g.*, induced by CO₂ injection, and modelling of geochemical rock-fluid interaction. ... These will establish the transport and fate of the injected CO₂ stream and provide the operator with an integrated knowledge sufficient to manage the injection process in an environmentally protective manner. The modelling should provide predictions during the operational injection period and an assessment of the residual pressure fields during the period after shut-in of the injection well and prior to decommissioning. ... Modelling should be updated in the light of monitoring results.

An immediate comment to this is that there is an apparent confidence in models to be useful in assessment of the suitability of proposed storage sites and the movement of CO₂ as well as the general conditions in the subseabed. All models for geological storage will depend on site specific data, possibly history matching or 4D assimilation of flow data (*e.g.*, repeat seismic), *i.e.*, updating model parameters after project start. One may ask what level of certainty will be required to shut in an expensive storage operation once it has started, and how such decisions would be reflected back on the carbon credits given.

Papers on subsurface fluid migration, rock properties and interaction between reservoir rocks and fluids including CO₂ in the relevant geological storage chapter of IPCC report are mostly non-peer review oil and gas company reports. Data

requirements for site specific subsurface flow models are immense. However, site specific data can be costly to obtain, particularly offshore. Drilling wells also increases the number of potential leakage pathways, and decisions may be difficult.

The limited experience that exists from Sleipner-Utsira shows that reservoir description of this extremely favorable high permeability reservoir had to be updated after a few years since repeat seismic revealed that injected CO₂ penetrated surprisingly rapidly through what was considered impermeable shale layers. No account has so far been taken of effects of pressure buildup on fracturing or the possibility for enhanced release of shallow occurrences of natural gas, nor effects of natural seismic events on millennial time scales.

Present proponents of subseabed geological storage estimate a very low cost of monitoring compared to capture and transport. Capture is to be paid by the companies but storage costs have been accepted as a Norwegian government responsibility allegedly in order to stimulate the development of carbon free fossil fuel power. This cost sharing has yet to be accepted by the European Union and may be problematic to them since it can be seen to affect competition between different power suppliers.

This case illustrates the hurry with which storage projects are being brought forward and need to be brought forward if CCS is to play a significant role in the global CO₂ problem.

6. Conclusions and outlook

It would be easier if environmental impact assessment could be made more generic rather than site-specific. Thus if CCS is needed, storage in the ocean or in sediments just below the deep seafloor where CO₂ is negatively buoyant (House *et al.*, 2006) may be a better option than the geological options which presently seem to be favoured at least in Norway and Europe. Experimental data could be obtained, but legalities are uncertain and there are potential problems with public acceptance. Some other yet unexplored options such as injection into high salinity brine water in deep depressions, *e.g.*, the Red Sea, or injection into anoxic basins, *e.g.*, the Black Sea, could also play a role.

A CO₂ concentration in air of 1000 ppm is the legally determined maximum acceptable level in Norwegian primary school classrooms since higher levels give an unpleasant and ineffective learning environment. Present emissions would lead to similar levels in the global atmosphere before the end of this century. This is just one illustration of the severity of the CO₂ problem and the time scale over which we need to act. Ocean acidification and the multitude of climate changes expected are others.

In order to find ways out of this situation, public perception and its variation across cultures and conditions play significant role in decision making. It is to be hoped that there is also a role for the scientific method in making policy choices.

Burning of biofuels with CCS may be necessary to effectively pull CO₂ out of the atmosphere even if other energy sources are developed rapidly, but a significantly changed attitude towards stimulating and developing the necessary good science to underpin environmental models for carbon storage is required.

Acknowledgements

I would like to thank present members of the Bergen CO₂ storage and seafloor exchange modelling group Guttorm Alendal, Lars Inge Enstad, Kristin Rygg, previous contributors to this kind of work over the years including Ilker Fer, Sønke Maus, Reidun Gangstø, Eva Falck and Lars Henrik Smedsrød, others in Bergen involved in related studies including Helge Drange, Christoph Heinze, Richard Bellerby and Lars Golmen, and international partners and references including Peter Brewer, Ken Caldeira and Fortunat Joos. These and others have influenced my research and thinking about the subject but should share no blame for this write-up.

References

Haugan, P.M., 2002. On the production and use of scientific knowledge about ocean sequestration. Essay presented at the 6th International Conference on Greenhouse Gas Control Technologies, Kyoto, 2002. In J. Gale and Y. Kaya (Eds) Proceedings, Elsevier Science, Amsterdam.

Haugan, P.M. and F. Joos 2004. Metrics to assess the mitigation of global warming by carbon capture and storage in the ocean and in geological reservoirs. *Geophysical Research Letters* 31, L18202, doi:10.1029/2004GL020295.

Haugan, P.M. and H. Drange 1992. Sequestration of CO₂ in the deep ocean by shallow injection. *Nature* 357, 318–320.

Haugan, P.M. and H. Drange 1996. Effects of CO₂ on the ocean environment. *Energy Conservation and Management* 37(6–8), 1019–1022.

Haugan, P.M., C. Turley, and H.-O. Poertner 2006. Ocean acidification resulting from elevated levels of CO₂ in the atmosphere, DN-utredning 2006-1, 32 pp. Norwegian Directorate for Nature Management, Trondheim, Norway.

House, K.Z., D.P. Schrag, C.F. Harvey, and K.S. Lackner (2006). Permanent carbon dioxide storage in deep-sea sediments. *Proceedings of the National Academy of Sciences of the United States of America* 103(33), 12291–12295.

IPCC, 2005. IPCC Special Report on Carbon Dioxide Capture and Storage. Prepared by Working Group III of the Intergovernmental Panel on Climate Change [Metz, B., O. Davidson, H. C. de Coninck, M. Loos, and L. A. Meyer (eds.)]. Cambridge University Press, Cambridge, United Kingdom and New York, NY, USA, 442 pp. ISBN-13 978-0-521-86643-9.

Kaya, Y., 1995. The role of CO₂ removal and disposal. *Energy Conversion and Management* 36(6–9), 375–380.

Marchetti, C., 1977. On geoengineering and the CO₂ problem. *Climate Change* 1(1), 59–68.

**THEME VI. DECISION MAKING
ON THE BASIS OF MODEL
PREDICTION**

Approaches to handling uncertainty when setting environmental exposure standards

Esben Budtz-Jørgensen¹, Niels Keiding¹, Philippe Grandjean^{2,3}

¹ Department of Biostatistics, Institute of Public Health, University of Copenhagen, Øster Farimagsgade 5B, 1014 København K, Denmark.

² Department of Environmental Medicine, Institute of Public Health, University of Southern Denmark, Winslowparken 17, DK-5000 Odense, Denmark.

³ Department of Environmental Health, Harvard School of Public Health, Landmark 3-110E, 401 Park Drive, Boston, MA 02215, USA.

Abstract

The statistical properties of the two most widely used methods for setting environmental exposure standards are explored. The traditional NOAEL approach handles uncertainty in disagreement with the precautionary principle: a smaller and less sensitive study will tend to yield higher exposure limits. As an attractive alternative, the Benchmark dose approach estimates the exposure associated with a predefined risk increase above the background. Although advantageous in several respects, this method is sensitive to sources of uncertainty arising from measurement error and data dependent selection of the dose-response model as well the choice of critical endpoint. An improved Benchmark analysis can be conducted using structural equation models and Bayesian model averaging.

Keywords: benchmark dose, measurement error, multiple endpoints, model uncertainty, risk assessment, structural equations.

1. Introduction

A major aim in environmental risk assessment is to establish acceptable exposure levels in humans. The U.S. Environmental Protection Agency (USEPA) defines the Reference Dose (RfD) as an estimate of a daily exposure to the human population (including sensitive subgroups) that is likely to be without an appreciable risk of deleterious effects during a lifetime. FAO and WHO define the Acceptable Daily Intake in similar terms. Calculations of exposure limits are often based on experimental animal data, but when human epidemiological data are available these are generally preferred. The two most widely used methods for calculating exposure standards are the so-called NOAEL approach and the more recent

Benchmark approach. When one of these methods has been applied, the result is divided by so-called uncertainty factors (assessment factors) to obtain the RfD. Uncertainty factors are applied to take into account differences in sensitivity between the test animals and average humans as well as differences in sensitivity between humans.

This paper describes statistical methods for dealing with uncertainty in the process of setting environmental exposure standards. In this regard, the precautionary principle states that corrective action against a potentially serious hazard should not await definitive proof. Barnett and O'Hagan (1997) considered the consequence of this principle for handling uncertainty in the development of exposure standards. They concluded that a higher degree of uncertainty about the risk associated with an environmental agent should lead to a stricter standard. The aim of the paper is to explore whether the NOAEL and the Benchmark approach handle uncertainty in accordance with the precautionary principle. The two methods are based on different statistical principles. The NOAEL relies on traditional hypothesis testing, while the Benchmark approach uses an upper confidence limit for the risk. As we shall see, this leads to important differences and weaknesses in their treatment of uncertainty. We consider different sources of uncertainty affecting environmental dose-response data. A small sample will lead to uncertainty, but so will measurement error in study variables, and identification of the critical outcome and selection of the dose-response model may also be uncertain. Because we find the NOAEL to be simplistic and inferior, we focus mainly on the Benchmark approach which has the advantage of being applicable to epidemiological data. Our aim is to improve this method through the use of structural equation models and Bayesian model averaging.

2. The NOAEL approach

The most commonly used method for calculation of exposure standards is the so-called No Observed Adverse Effect Level (NOAEL). Calculations are typically based on experimental animal data where animals are divided in different dose groups including an unexposed control group. The NOAEL is defined as the exposure of the group that immediately precedes the first exposure group with a response level significantly (in the statistical sense) worse than the response level of the unexposed control group (EPA, 1997). Figure 1 gives a graphical illustration where d_1 is the NOAEL.

From a statistical point of view the NOAEL approach has some undesirable properties. In hypothesis testing lack of significance can be due either to genuine lack of effect or to data that are too noisy (often because there are too few of them) to enable any precise conclusion. The latter reason, known as the Type II error problem, is ignored in the NOAEL approach. Here lack of a significant result is interpreted as lack of an effect. As a consequence, an experiment conducted with few test animals will have weaker power and therefore tend to yield *higher*

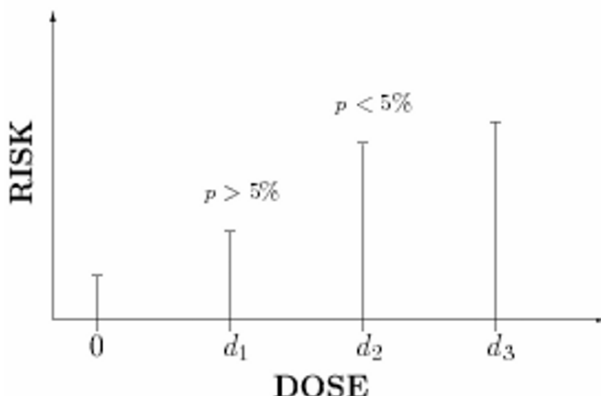


Fig. 1. Hypothetical result of an animal experiment illustrating the definition of the NOAEL. Here p denotes the p-value obtained by comparing the risk at a certain dose to the unexposed risk. The dose d_1 is the lowest associated with a significant increase in risk compared to the controls. Thus, in this example NOAEL = d_1 .

NOAELs than a well conducted experiment with better precision. This is contrary to the precautionary principle which led Keiding and Budtz-Jørgensen (2003) to describe the NOAEL as being anti-precautionary. As an alternative, Crump (1984) developed a procedure known as the Benchmark approach. This procedure has been adopted by USEPA and is now also being introduced by EU regulatory agencies.

3. The benchmark approach

This methodology was first developed for dichotomous (0/1) responses in experimental studies. The Benchmark dose (BMD) is the dose that leads to a specific increase in the risk of an abnormal event. In a dose-response model describing the risk as a function of dose d : $P(Y=1)=f(d)$, the BMD can be determined as the dose that increases the risk from P_o in un-exposed to $P_o + BMR$. Here the risk increase BMR is specified by the regulatory agency (typically between 1% and 10%). A higher BMR will lead to a higher BMD.

In the present paper we shall focus on quantitative responses. Thus, we let $Y(d)$ denote the response at exposure d and consider the model

$$Y(d) = f(d) + \varepsilon \quad (1)$$

where $\varepsilon \sim N(0, \sigma^2)$. Here the dose-response function $f(d)$ describes the dependence of the mean outcome on the exposure dose. Without loss of generality we will assume that larger response values are more adverse. Thus, f is expected to be increasing. In quantitative data, the BMD may be defined in various ways.

One possibility would be to estimate the dose which leads to a specific increase in the mean, *i.e.*, this BMD would solve the equation $f(\text{BMD}) - f(0) = \text{BMR}$. Another possibility would be to consider a relative increase in the mean compared to unexposed, *i.e.*, $[f(\text{BMD}) - f(0)]/f(0) = \text{BMR}$.

Alternatively, in the so-called hybrid approach all responses above a pre-specified limit t_0 are considered abnormal. According to the model (1), the risk of an abnormal response in an unexposed subject is $P_0 = P[Y(0) > t_0] = 1 - \Phi([t_0 - f(0)]/\sigma)$, where Φ is the standard normal cumulative distribution. As in dichotomous data, the BMD is now defined as the dose which increases the risk by BMR, *i.e.*, as the solution to the equation $P[Y(\text{BMD}) > t_0] = P_0 + \text{BMR}$. It is straightforward to see that the BMD satisfies the equation

$$\frac{f(\text{BMD}) - f(0)}{\sigma} = \Omega \quad (2)$$

where $\Omega = \Phi^{-1}(1 - P_0) - \Phi^{-1}(1 - P_0 - \text{BMR})$. Thus, in the hybrid approach, the BMD leads to a specific increase in the mean of the standardized response with variance one. In addition, Budtz-Jørgensen *et al.* (2001) showed how to take into account effects of confounding variables in this calculation.

The main result of the Benchmark analysis is the BMDL which is defined as a lower one-sided 95% confidence limit of the BMD. This means that the statistical uncertainty is taken into account. A poorer study with fewer subjects will have wider confidence limits and therefore produce lower exposure standards. Thus, in the Benchmark approach uncertainty from a limited sample size is treated in accordance with the precautionary principle. However, in environmental epidemiology, study results are affected by other sources of variability than uncertainty arising from a limited sample size. In the rest of this section, we will explore how the BMD depends on these sources of uncertainty.

3.1. Measurement error in study variables

Budtz-Jørgensen *et al.* (2004) showed that measurement error in the exposure variable will lead to a biased Benchmark analysis. In a simple regression model

$$Y(d) = \alpha + \beta d + \varepsilon, \quad (3)$$

the BMD is given by $\Omega\alpha/\beta$. If the exposure dose d has an additive measurement error, it is well known that if we ignore this error and simply replace the true exposure by the measured exposure in the regression analysis then the exposure

effect (β) is underestimated while the opposite is true for σ (Carroll *et al.*, 2006). Therefore, the BMD is overestimated. The BMDL also decreases as a function of β and increases as a function of σ (Budtz-Jørgensen *et al.*, 2001), so failure to adjust for measurement error in the exposure variable will lead to BMDLs that are biased toward higher and less safe exposure levels.

The outcome variable may also be affected by measurement error. This type of error will generally not lead to bias in the regression coefficient β , but the BMD analysis is sensitive also to this source of uncertainty. Assuming an additive error in the relationship between the true response (η) and the measured response (Y), *i.e.*, $(Y) = \eta + U$. The true BMD is $\Omega\sigma/\beta$, while the naive analysis estimates the larger value $\Omega\sqrt{\sigma^2 + \text{var}(U)}/\beta$. Thus, failure to adjust for errors in the response will lead to further overestimation of the BMD. Again a higher degree of imprecision will lead to a higher limit which according to the precautionary principle is an inappropriate way of dealing with uncertainty.

3.2. Multiplicity problems

Often the effect of the exposure is assessed via several endpoints. One such example is the study in the Faeroe Islands on possible cognitive effects of prenatal exposure to methylmercury (Grandjean *et al.*, 1997). Here prenatal mercury exposure was measured primarily by the mercury concentration in cord blood, while cognitive function was assessed using a number of different neurobehavioral test scores. Table 1 shows Benchmark results in seven verbal outcomes in this data. A high degree of variation is seen and it is debatable which of these results should be used when setting the exposure standard. In such a situation, the classical statistical-epidemiological advice is to exercise considerable caution towards possible spurious effects of the inevitable “fishing expeditions” in the search for statistically significant results. However, the precautionary principle would encourage focus on the “most sensitive” endpoint. This was indeed recommended in the practical implementation of the Faroese study by the National Research Council (2000) where the final exposure limit was based on the Boston Naming test that had resulted in the lowest BMDL result.

If the most sensitive endpoint is determined from a data-driven process, the risk assessment may be biased. We have illustrated this problem in a small simulation study shown in Tables 2 and 3. Here data sets were simulated with different numbers of endpoints and with different degrees of intercorrelation between outcomes. In Table 2 all outcomes were simulated from the estimated distribution of the Boston Naming test in the Faroese data set. So we are considering a situation where all

outcomes are equally sensitive with a common BMD of 84.9 $\mu\text{g/L}$. The simulations explore the statistical properties of basing the risk assessment on the outcome with the lowest BMDL. Thus, in each data set we identified this endpoint and stored its BMD and BMDL. Table 2 provides the median of these BMD estimates and the coverage probability of the BMDL, which can be estimated by the frequency of data sets where the BMDL was lower than 84.9 $\mu\text{g/L}$. We see that the estimated BMD is biased toward zero and that the coverage probability of the BMDL is higher than the nominal value of 95%. These tendencies become stronger when the number of endpoints is increased and the correlation between them is decreased. Thus, these results illustrate, that the lowest BMDL observed in a given data set will be lower than the BMD of the truly most sensitive outcome with a probability which is greater than 95%. In this sense, the procedure of selecting the seemingly most sensitive endpoint is biased.

Table 1. Benchmark results ($\mu\text{g/L}$) estimated from the relationship between the cord blood mercury concentration and the seven verbal outcomes in the Faroese data.

Response	BMD	BMDL
Wechsler Intelligence Scale		
Digit spans (DS)	222.5	99.9
Boston Naming Test		
No cues (BNT1)	101.7	64.9
With cues (BNT2)	84.9	57.6
California Verbal Learning Test		
Learning (CVLT1)	404.3	124.7
Short-term repro. (CVLT2)	219.2	99.1
Long-term repro. (CVLT3)	250.3	104.2
Recognition (CVLT4)	227.7	99.7

Table 2. 10,000 data sets were simulated with different numbers of endpoints with different degrees of correlation. All outcomes had a true BMD of 84.9. In each data set, the endpoint with the smallest BMDL was identified and its BMD and BMDL saved. The median of these BMDs is shown together with the coverage probability of the BMDL, which can be estimated by the frequency of data sets where the BMDL was lower than 84.9.

No. of End Points	Median BMD			Coverage Probability of BMDL		
	Corr. = 0	Corr. = 0.2	Corr. = 0.5	Corr. = 0	Corr. = 0.2	Corr. = 0.5
2	73.2	74.4	76.5	0.9984	0.9944	0.9864
5	64.1	65.6	68.9	1	1	0.9986
10	59.3	60.9	64.8	1	1	0.9997

Table 3. 10,000 data sets were simulated with ten endpoints with different degrees of correlation. The truly most sensitive outcome had a BMD of 84.9, while the nine others had a common higher BMD as indicated above. In each data set, the endpoint with the smallest BMDL was identified and its BMD and BMDL saved. The median of these BMDs is shown together with the coverage probability of the BMDL, which can be estimated by the frequency of data sets where the BMDL was lower than 84.9.

BMD	Common		Median BMD		Coverage Probability of BMDL		
	Corr. = 0	Corr. = 0.2	Corr. = 0.5	Corr. = 0	Corr. = 0.2	Corr. = 0.5	Corr. = 0.5
100	65.3	67.4	71.8	1	1	0.9974	
200	80.7	82.2	83.9	0.9991	0.9905	0.9653	
300	83.3	83.7	84.9	0.9923	0.9781	0.9547	

Table 2 describes the situation with the greatest potential for bias from selection of the seemingly most sensitive outcome: the case where all outcomes are equally sensitive. Instead Table 3 considers a situation where one outcome is more sensitive than the others. Thus, one outcome was simulated to have a distribution like the Boston Naming test, while nine other outcomes had a common higher BMD. We observe that when the BMD of the remaining endpoints is increased, the bias from selecting the seemingly most sensitive outcome decreases. The risk that another outcome by chance is deemed more sensitive becomes lower and therefore the multiple comparisons problem becomes less important.

In the Faroese data set, the strength of bias due to selection of the most sensitive endpoint was explored using bootstrap simulations. New data sets were sampled with replacement from the original data set and in each new data set the Benchmark results of the (seemingly) most sensitive outcome were retained. Rather than selecting the endpoint with the lowest BMDL, here we define the most sensitive outcome as the one associated with the most significant exposure regression coefficient, which is more in line with the approach of the NAS (2000). In the bootstrap setup, the original data plays the role of the truth. Therefore, we know that the true lowest BMD is given by 84.9 $\mu\text{g/L}$ of the Boston Naming test. The median of the bootstrap BMDs was 82.2. This similarity indicates that selection of the most sensitive outcome does not lead to an important amount of bias here. This was confirmed by the fact that the frequency of data sets where the BMDL was lower than 84.9 was 98%. Thus, the coverage probability is quite close to the nominal value 95%. Given the results of Table 2 and the fact that this data set contained seven endpoints, the small magnitude of this bias may seem surprising. However, in these data two outcomes (Boston Naming) had clearly the lowest BMDLs (Table 1). In addition, these two outcomes are highly correlated. As illustrated in Table 3, both of these characteristics decrease the potential for bias.

4. Benchmark analysis in structural equation models

The previous section illustrated that failure to allow for measurement error in the exposure or the outcome variable will lead to overestimation of the BMD and the BMDL. On the other hand a Benchmark analysis based on the seemingly most sensitive outcome may be biased in the opposite direction. Standard applications of the Benchmark approach ignore both problems, and therefore the direction of the overall bias is difficult to predict. As a potential solution to these problems, Budtz-Jørgensen *et al.* (2007) proposed to carry out the Benchmark calculation in structural equation models (Bollen, 1989; Sanchez *et al.*, 2005). These models typically consist of two parts: a measurement part and a structural part. In the measurement part, observed variables are considered to be manifestations of a limited number of underlying latent variables. The structural part of the model then describes causal relations between the latent variables.

Figure 2 illustrates a possible structural equation model for the Faroese data (Budtz-Jørgensen *et al.*, 2002). Mercury concentrations in cord blood and maternal hair were assumed to be linearly related to a common true exposure (η_1). Similarly, cognitive test scores on the Boston Naming Test (BNT), the Wechsler Intelligence Scale Digit Spans (DS) and the California Verbal Learning Test (CVLT) were considered manifestations of a latent verbal function (η_2). In addition, each of these variables is assumed to be affected by a random measurement error, as indicated by the ε -terms in Figure 2. The structural part of the model assumed that the true verbal level was affected by the true mercury exposure and possibly a set of confounding variables Z_1, \dots, Z_k

$$\eta_2 = \beta_0 + \beta_1 \eta_1 + \beta_2 z_1 + \dots + \beta_k z_k + \varepsilon_2, \quad (4)$$

where ε_2 is a normally distributed residual term. Although this equation involves latent variables it has the same basic structure as equation (3) and therefore the standard Benchmark methodology of Section 3 can be directly applied. Thus, the BMD is the dose which increases the risk of a latent response above the threshold form P_0 in an unexposed subject to $P_0 + \text{BMR}$.

The structural equation model allows for measurement error *both* in the exposure and in the response. In the structural part of the model the relation between true exposure and true response is estimated. Thus, BMD calculations based on this relationship avoid problems caused by measurement errors. In addition, multiple comparisons are not an issue as only one dose-response relationship is considered. Finally, the BMD is efficiently estimated as information from multiple exposure and outcome variables are pooled. Efficient estimation is of critical importance in the Benchmark approach because the exposure standard is determined from the lower confidence limit. Therefore inefficient estimation procedures may lead to exposure limits that are biased toward zero.

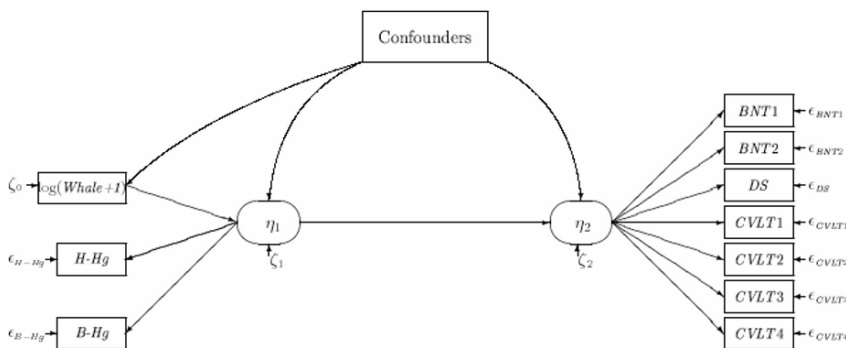


Fig. 2. Path diagram for the association between indicators of mercury exposure and childhood verbal function. Mercury concentration in cord blood and hair are assumed to depend on the true exposure and a random error. Similarly, seven neurobehavioral test scores are assumed to measure a common latent the verbal function. True prenatal mercury exposure and confounders affects the latent the verbal function.

For the Faroese data, the structural equation model yielded a BMD of 64.8 $\mu\text{g/L}$ with a BMDL of 44.1 $\mu\text{g/L}$. Interestingly, it is seen that the integrated structural equation result is lower than each of the individual regression results (Table 1). Thus, in this study, the standard procedure of selecting the BMDL of the seemingly most sensitive response is not overly protective. Failure to account for measurement error more than outweighed the effect of ignoring the multiple testing issue.

5. Model uncertainty

Risk assessment typically involves the selection of a statistical model for the dose-response data. One issue regards the selection of confounders while another regards the choice of the functional form of the dose response relationship. Different models may yield very different results. For instance, Budtz-Jørgensen *et al.* (2001) documented a considerable variability in Benchmark results when using a square root model, a logarithmic, and a K-power model for the relationship between mercury exposure and cognitive performance. In practice this problem is “solved” by restricting attention to the results of a single best fitting model. Furthermore, these results are reported as if there were no uncertainty about the choice of model. In fact, the estimation process is a two-step procedure consisting of first the model selection and then the effect estimation, but the first step is ignored when standard errors of estimators are calculated. This unfortunate procedure will also affect the Benchmark analysis because the confidence limits will take into account only one part of the estimation uncertainty. As a consequence the BMDL is likely to be biased toward higher and less safe levels.

The choice of model selection strategy for Benchmark analysis is another important problem. Traditional selection procedures optimize the fit of the model to the data. However, from the viewpoint of the Precautionary Principle one could possibly argue that the exposure-response model yielding the lowest reference dose should be preferred. A compromise may be to select the lowest BMDL among models with a reasonable fit. Still this “maximin” approach may be too extreme if the environmental standard is to be determined completely or mainly on epidemiological data which have been shown to provide highly model dependent BMD results (Budtz-Jørgensen *et al.*, 2001; Morales *et al.*, 2006).

In situations where the model selection procedure depends solely on the data, in principle, it becomes possible to take model selection uncertainty into account. However, because of the complex nature of the two-step selection estimators, no firm theory is currently available to perform such adjustments. Although Hjort and Claeskens (2003) presented some asymptotic results on bias and precision for estimators after model selection, results on the properties in finite samples have not been provided. Therefore, the bootstrap approach constitutes an obvious alternative. In the Faroese data, Budtz-Jørgensen *et al.* (2007) used this method to study the properties of conventional methods for selection of confounder variables. New data sets were developed by sampling with replacement from the original data. The model selection procedure was then applied to each of the data sets and the mercury regression coefficient of the final models was stored. Since the model selection process was repeated in each set of bootstrap data, the variability in the stored coefficients correctly reflects the uncertainty in the two-step estimation process. The same procedure could be used to allow for model selection uncertainty in the BMDL calculation.

Bayesian model averaging offers an interesting alternative. Here a single model is not selected, but the final result depends on all models.

5.1. Benchmark analysis after Bayesian model averaging

Here we briefly describe how a Benchmark analysis can be conducted based on Bayesian model averaging. For a general review of this method we refer to Hoeting *et al.* (1999). To explain the idea, we let Y denote the data. We consider K different models $M = 1, \dots, K$, where θ_j is the parameter in model j . Thus, the BMD in model j is a function of θ_j .

The first step is to specify the prior probability $P(M = j)$ that model j is “true”. Often models will be considered equally likely a priori corresponding to a uniform prior, *i.e.*, $P(M = j) = 1/K$. Next a prior distribution $P(\theta_j | M = j)$ must be defined for the parameters in model j . This distribution can be interpreted as the conditional distribution of the unknown parameters given that model j is

true. The likelihood function for model j is the distribution of the data given the model and the parameters: $P(Y|\theta_j, M = j)$. The likelihood function measures the ability of the model to explain the variation in data. In the Bayesian framework it is interpreted as the probability of the data given the model and the parameters. By applying Bayes theorem the probability of model j given the data is

$$P(M = j|Y) = P(M = j)P(Y|M = j)/P(Y), \quad (5)$$

where $P(Y|M = j) = \int P(Y|\theta_j, M = j)P(\theta_j|M = j)d\theta_j$. Here determination of $P(Y|M = j)$ may be computationally demanding, but feasible also in available software.

Based on the posterior model probabilities, the posterior distribution of the BMD given data has the following from

$$P(\text{BMD}|Y) = \sum_{j=1}^K P(\text{BMD}|M = j, Y)P(M = j|Y) \quad (6)$$

This distribution is a mixture of the posterior distributions $P(\text{BMD}|M = j, Y)$ of the BMD assuming each of the models. An obvious estimator of the BMD is given by the posterior mean

$$E(\text{BMD}|Y) = \sum_{j=1}^K E(\text{BMD}|M = j, Y)P(M = j|Y) \quad (7)$$

Thus, the overall BMD estimate is an average of the model specific estimates. The BMDs are averaged with respect to the posterior model probabilities, so that the better fitting models get up-weighted at the expense of more poorly fitting models. This is of course the reason why the approach is called model averaging. However, it is important to note that the BMDL is not obtained as a simple weighted average of BMDLs from different models. The BMDL is calculated as 5th percentile in the posterior distribution of the BMD. This number will typically be much smaller than the value obtained by weighing model specific BMDLs according to the model probabilities. We illustrate this important point in an example.

The two top curves in Figure 3 show posterior BMD distributions in a hypothetical situation with two models. In model 1, the posterior BMD distribution is normal with mean 10 and variance 1 [$P(\text{BMD}|M = 1, Y) = N(10, 1)$]. Model 2 holds a similar distribution except that the mean is 5, *i.e.*, [$P(\text{BMD}|M = 2, Y) = N(5, 1)$]. Thus, in model 1 the estimated BMD is 10, while the model 2 estimate is 5. BMDLs are determined as the 5th percentile in the BMD distribution. From the properties of the normal distribution, it is seen that these are 8.35 and 3.35 in model 1 and 2, respectively. If we assume that the

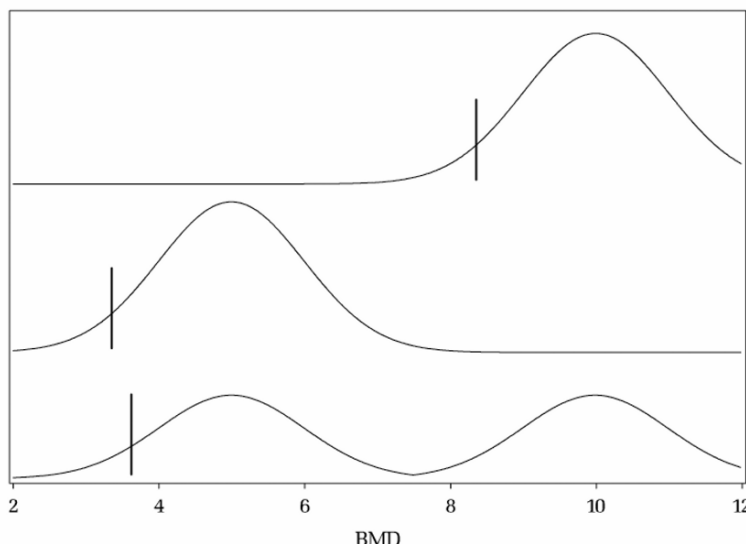


Fig. 3. The two top curves show the posterior BMD densities in two different models. BMDLs are given by the 5th percentile in each of the distributions and marked with a vertical bar. Assuming that the models posterior are equally likely, the bottom curve shows the model averaged BMD distribution. Note that the model averaged BMDL is much closer to the lower of the model specific BMDLs.

models are equally likely given the data $[P(M = j|Y) = 0.5, j = 1, 2]$, then the model averaged BMD distribution is given by the bipolar density shown as bottom curve in Figure 3. The model averaged BMD estimate is the mean in this distribution. By equation (7) this is obtained as the mean of the model specific BMDs: $0.5 \cdot 5 + 0.5 \cdot 10 = 7.5$. However, the BMDL is the 5th percentile in this bipolar distribution. This value is 3.62. Thus, the BMDL in model averaging is considerably lower than the mean BMDL value of 5.85 $[(3.35 + 8.35)/2]$. This example illustrates that, in situations with strong model uncertainty, *i.e.*, in situations where the models producing the smallest BMDLs have reasonable posterior support, the model averaged BMDL is likely to be closer to the lowest BMDL than to the mean value obtained by weighing model specific BMDLs according to the model probabilities.

Recently, Bayesian model averaging has been applied for Benchmark analysis of both experimental and epidemiological data. For instance, Morales *et al.* (2006) analyzed data on the effect of exposure to arsenic from drinking on the risk of lung cancer in Taiwan. Here a total of 18 different regression models were considered. Table 4 shows the Benchmark results for the six best fitting models. We observe a high degree of model uncertainty, with models producing BMDs between 4 and 111 $\mu\text{g/L}$ and BMDLs ranging from 2 to 98 $\mu\text{g/L}$. While the model averaged BMD is close to the arithmetic mean of the model specific BMDs, as a

Table 4. BMDs and BMDLs ($\mu\text{g/L}$) from the six best fitting models in the analysis of the effect of arsenic on the risk of lung cancer (from Morales *et al.*, 2006). The last column gives the posterior model probability, while the last row gives the benchmark results after model averaging.

Model	BMD	BMDL	$P(M Y)$
6	111	98	0.1
9	14	11	0.29
12	65	53	0.16
14	53	43	<0.1
15	52	43	0.34
18	4	2	0.20
Model averaging	50	3	—

result of the substantial model uncertainty the model average BMDL is very close to the lowest BMDL value. Also notice that the difference between the BMD and the BMDL is much smaller in the individual models than after model averaging, thereby illustrating the effect of taking the model uncertainty into account.

6. Summary and discussion

Identification of safe exposure limits is an important part of the risk assessment process. The statistical methodology has improved somewhat in recent years, but current methods are imperfect. The NOAEL is still the most widely used approach despite the fact that with this method a poorly performed study with a small sample size will tend to generate higher and less protective exposure limits. A main advantage of the Benchmark approach is that the uncertainty arising from sample size limitations is taken into account. However, as we have illustrated, other sources of uncertainty are not handled appropriately in the Benchmark approach. Measurement errors in study variables will lead to overestimation of the BMD and BMDLs, while a data dependent identification of the critical endpoint may have the opposite effect. We described how these problems can be handled in structural equation models. Here observed exposure and outcome variables are considered to be manifestations of underlying latent variables. The structural part of the model estimates the relationship between the true exposure and the true response. Not only are measurement errors taken into account, but problems with multiple comparisons are also avoided. In the Faroese data set, the integrated structural equation result was lower than each of the individual BMDLs obtained using standard regression techniques that ignored measurement error. This illustrates that the simple approach of selecting the BMDL of the (apparently) most sensitive outcome may not be protective if measurement errors are not taken into account.

The difficult challenge of incorporating model selection uncertainty into the risk assessment process was also considered. The standard procedure is to ignore

this uncertainty and rely completely on the results of the best fitting model. As a consequence, confidence intervals will be too narrow and BMDLs are likely to be biased toward higher levels. Bayesian model averaging was shown to provide an elegant framework for adjusted Benchmark calculations. Application of structural equation models will always involve selection between different models. Therefore an obvious future challenge would be to calculate model averaged BMDLs in structural equation models.

References

Barnett, V. and O'Hagan, A., 1997, Setting environmental standards: The statistical approach to handling uncertainty and variation. London: Chapman & Hall.

Bollen, K.A., 1989, Structural Equations with Latent Variables. John Wiley and Sons, Chichester, UK.

Budtz-Jørgensen, E., Keiding, N., and Grandjean, P., 2001, Benchmark dose calculation from epidemiological data, *Biometrics* **57**: 698–706.

Budtz-Jørgensen, E., Keiding, N., and Grandjean, P., 2004, Effects of exposure imprecision on estimation of the benchmark dose, *Risk Analysis* **24**: 1689–1696.

Budtz-Jørgensen, E., Keiding, N., Grandjean, P., and Weihe, P., 2002, Estimation of health effects of prenatal mercury exposure using structural equation models, *Environmental Health* **1**: 2.

Budtz-Jørgensen, E., Keiding, N., Grandjean, P., and Weihe, P., 2007, Confounder selection in environmental epidemiology: Assessment of health effects of prenatal mercury exposure, *Annals of Epidemiology* **17**: 27–35.

Carroll, R.J., Ruppert, D., Stefansky, L.A., and Crainiceanu, C., 2006, Measurement error in nonlinear models. New York: Chapman & Hall.

Crump, K., 1984, A new method for determining allowable daily intakes, *Fundamental and Applied Toxicology* **4**: 854–871.

Grandjean, P., Weihe, P., White, R.F., Debes, F., Araki, S., Yokoyama, K., Murata, K., Sørensen, N., Dahl, R., and Jørgensen, P.J., 1997, Cognitive deficit in 7-year-old children with prenatal exposure to methylmercury, *Neurotoxicology and Teratology* **19**: 417–428.

Hoeting, J.A., Madigan, D., and Raftery, A.E., 1999, Bayesian model averaging: A tutorial, *Statistical Science* **14**: 382–417.

Hjort, L.H. and Claeskens, G., 2003, Frequentist model average estimators, *Journal of the American Statistical Association* **98**: 879–900.

Keiding, N. and Budtz-Jørgensen, E., 2003, The precautionary principle and statistical approaches to uncertainty, *European Journal of Oncology Library* **2**: 185–191.

Morales, K.H., Ibrahim, J.G., Chen, C.J., and Ryan L., 2006, Bayesian model averaging with applications to Benchmark dose estimation for arsenic in drinking water, *Journal of the American Statistical Association* **101**: 9–17.

National Academy of Sciences (NAS), 2000, Toxicological effects of methylmercury. National Academy Press, Washington, D.C., USA.

Sanchez, B.N., Budtz-Jørgensen, E., Ryan, L., and Hu, H., 2005, Structural equation models. A review with applications to environmental epidemiology, *Journal of the American Statistical Association* **100**: 1443–1455.

CASE STUDY I. SOIL CARBON DYNAMICS

Sources of uncertainty in global modelling of future soil organic carbon storage

Chris Jones*, Pete Falloon

Met Office Hadley Centre, Exeter, EX1 3PB, United Kingdom.

Abstract

It is now widely accepted that the natural carbon cycle has a key role to play in determining future climate. As climate changes, this will affect the ability of the carbon cycle to take up and store anthropogenic carbon. However, great uncertainty surrounds the magnitude of this sensitivity to climate and how to represent this in Earth System models. Much of this uncertainty comes from the terrestrial biosphere and in particular the storage of carbon in soil organic material. Therefore it is vitally important to understand the factors which will determine future soil carbon storage and their inherent uncertainties. We show that significant uncertainty in future soil carbon storage comes from many sources, both external to the soil such as climate uncertainty or uncertainty in vegetation productivity and internal to the soil such as uncertainty in soil carbon structure and its sensitivity to changing temperature and moisture. Understanding and reducing this uncertainty is key to improving reliability of future climate projections and their utility for informing climate mitigation policy.

Keywords: global carbon cycle, soil carbon, climate change, earth system modeling.

1. Introduction

It is now widely accepted that the natural carbon cycle has a key role to play in determining future climate (Denman *et al.*, 2007; Meehl *et al.*, 2007). Currently about half of anthropogenic CO₂ emissions remain airborne (Denman *et al.*, 2007), with the rest being absorbed roughly equally between the ocean and terrestrial carbon cycle. This airborne fraction has remained remarkably constant for several decades now, partly due to the time history of anthropogenic emissions, but is predicted to increase in future (Cox *et al.*, 2000; Friedlingstein *et al.*, 2001; Zeng *et al.*, 2004). In fact Canadell *et al.* (2007) have already reported the first suggestion that there may be an upwards trend in the airborne fraction.

As climate changes, this will affect the ability of the carbon cycle to take up and store carbon. Consequently a greater proportion will remain in the atmosphere than in the absence of climate change (Denman *et al.*, 2007). For a given scenario of emissions, this feedback will result in higher atmospheric CO₂ concentrations than previously assumed and hence greater climate change (Cox *et al.*, 2000; Friedlingstein *et al.*, 2006). Alternatively, to achieve a given level of CO₂ stabilisation, reduced natural carbon uptake means that more stringent emissions reductions will be required (Matthews, 2005; Jones *et al.*, 2006a,b). It is now common for climate models to include a representation of the global carbon cycle in future projections – such models, which may also represent other aspects of biogeochemistry – are becoming known as Earth System Models (ESMs).

Unfortunately, although understanding carbon cycle behaviour is crucial to reliable projections of future climate, great uncertainty surrounds the magnitude of its sensitivity to climate (Friedlingstein *et al.*, 2006). In the Coupled Climate Carbon Cycle Model Intercomparison Project of Friedlingstein *et al.* (2006), commonly referred to as “C4MIP”, they compare 11 different coupled climate carbon cycle models and show differences of almost an order of magnitude in amplification of atmospheric CO₂ by 2100 following the SRES A2 emissions scenario (Nakicenovic *et al.*, 2000) – by between 20 and 200 ppmv. Booth *et al.* (submitted) have shown carbon cycle uncertainty is of similar magnitude to climate uncertainty in an experiment designed to explore uncertainty in a single ESM. Much of this uncertainty comes from the terrestrial biosphere and in particular the storage of carbon in soil organic matter (SOM).

Soil organic carbon (SOC) currently comprises about twice the amount of carbon stored in the atmosphere. Hence it is an important potential store of anthropogenic carbon and a potentially large contributor to carbon release under climate change. Future SOC change has become a leading order uncertainty in climate prediction and therefore it is vitally important to understand the factors which will determine future SOC storage and their inherent uncertainties. Here we present a review of the treatment of SOC in ESMs and the multiple sources of its uncertainty, both internal sensitivities of SOM and external drivers of change. We draw on existing modelling research and intercomparison studies, quantifying uncertainty in each element and identifying key areas for future research.

Figure 1 denotes schematically the main components of the Earth System commonly represented in global models, which drive future evolution of SOC. It shows external drivers of SOC such as organic carbon input from overlying vegetation and weather and climate conditions, and internal behaviour of SOC such as multi-pool dynamics and sensitivity to soil environmental conditions. The structure of the review is to discuss the different elements shown in Figure 1 in turn. First, section 2 will describe briefly how soil carbon is typically simulated in coupled climate-carbon cycle models both in terms of model structure and experimental design.

Sections 3 and 4 will discuss the external factors shown in Figure 1 – these are the “drivers” of future SOC change, being external to the soil system, but

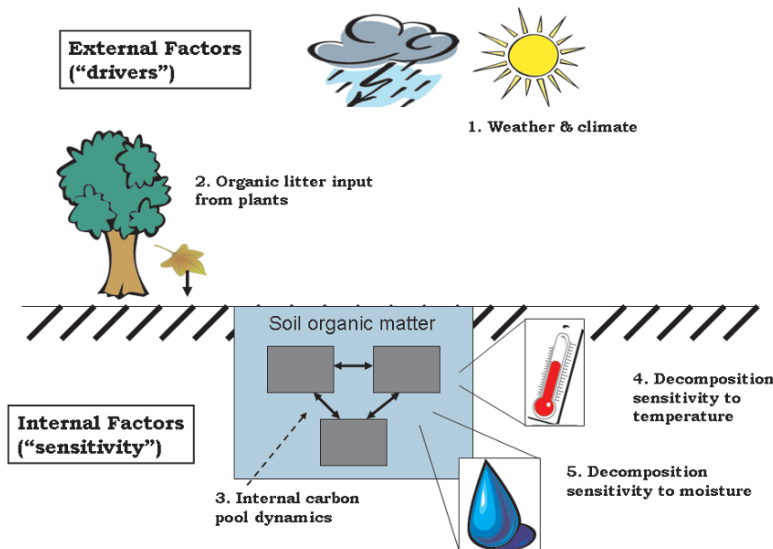


Fig. 1. Schematic diagram showing the key different elements determining future SOC behaviour in ESMs, divided into external “drivers” and internal “sensitivities”.

fundamental in determining future behaviour. Section 3 discusses future climate change and how its uncertainty affects projections of future soil carbon storage. Section 4 examines the role of organic carbon input to the soil from vegetation. There is of course a third important component of external driving of SOC changes – anthropogenic disturbance through agriculture (Smith *et al.*, 2007) and deforestation (Nabuurs *et al.*, 2007). Although this has undoubtedly been important in the past (Bondeau *et al.*, 2007) and will be in the future (Vuichard *et al.*, in press) we will not discuss it further here but will concentrate on the other, natural, aspects of the system. Anthropogenic disturbance is an area where further research is urgently needed to inform land-management practices and quantify their potential contribution to a portfolio of climate mitigation options (Smith *et al.*, 2007; Gullison *et al.*, 2007; Falloon *et al.*, 2008). Many modelling groups expect to include at least basic management and land-use change in future simulations but results are not yet widespread.

Then sections 5–7 will discuss the internal aspects of the SOC system and its sensitivity to environmental changes. Section 5 examines uncertainty in internal carbon pool dynamics: the number of different carbon pools, their characteristic turnover times, depth profiles and sensitivity to soil conditions. Sections 6 and 7 explore the relative uncertainty in soil decomposition sensitivity to temperature and moisture respectively. Section 8 then discusses interactions between these different sources of uncertainty and presents some SOC results from the C4MIP

project (Friedlingstein *et al.*, 2006) when all five factors in Figure 1 vary between 11 complex climate-carbon cycle models.

2. Model description and methodology

2.1. Model description

Typically, soil C is treated fairly simplistically in coupled climate models, although as its importance becomes more recognised the complexity is increasing. Early simulations of the Hadley Centre carbon cycle-climate model (HadCM3LC; Cox *et al.*, 2000) used just a single pool of SOC at each grid point. This pool received input from plant residue as a single litter flux without distinguishing the type of vegetation or above/below ground input. The SOC then decomposed with a characteristic turnover time modified by conditions in the top 10cm of soil by an exponential “Q10” function of temperature and a simple sensitivity to soil moisture based on McGuire *et al.* (1992).

Other models in the C4MIP study of Friedlingstein *et al.* (2006) have slightly greater levels of complexity *e.g.*, the UMD model (Zeng *et al.*, 2004) has three SOC pools with different sensitivities to temperature, and the IPSL model, ORCHIDEE, has three SOC pools in addition to four litter pools (Krinner *et al.*, 2005). An improved representation based on the RothC soil carbon model (Coleman and Jenkinson, 1999) has been implemented in the Met Office Hadley Centre GCM and this is expected to modify the transient sensitivity of SOC as shown by Jones *et al.* (2005) and discussed further here in section 5.

The models generally assume a characteristic turnover rate or residence time for each pool at a specified reference temperature and moisture and calculate “rate modifying factors” representing the sensitivity to moisture and temperature to calculate the *specific respiration rate* (the respiration rate per unit mass of soil carbon). The total respiration is then derived by multiplying by the soil carbon amount:

$$R_H = k C_S f_T(T) f_M(M) f_A \quad (1)$$

where R_H is the heterotrophic respiration, C_S is the soil carbon amount, k is a constant representing the turnover rate at the reference conditions, f_T and f_M are functions of temperature, T , and moisture, M , respectively, and f_A represents an optional additional rate modifying factor which some models use to represent further factors (for example RothC represents changes in respiration due to protection from crop cover or clay fraction of the soil). Given these rate modifying factors, the model can now simulate evolution of soil carbon amount by balancing input from fresh plant litter, L , and losses from decomposition:

$$\frac{dC_s}{dt} = L - R_H \quad (2)$$

Most models still have independent sensitivity to temperature and moisture (*i.e.*, two separate rate modifying factors which are simply multiplied together to give the joint sensitivity), whereas it is now seen as likely that these terms should interact (Davidson and Janssens, 2006). Reichstein *et al.* (2007) showed how the temperature sensitivity of total ecosystem respiration varies with changing moisture conditions at flux tower sites across Europe.

However, most of these models still rely on some very basic assumptions – *e.g.*, they generally do not account for depth structure within the SOC pool, nor above/below ground separation of plant litter input. They also often assume the same temperature and moisture dependence for each pool, although Zeng *et al.* (2004) discuss the possible implications of this. They show results when this is not the case and long lived carbon is less sensitive to temperature than the younger pools. It is possible however that the converse is true – the longer lived pools may be more sensitive to temperature (residence time and sensitivity are not the same thing of course). Some models also simulate a litter pool separately from the body of SOC.

Few of the coupled carbon cycle GCMs yet represent nutrient cycling and the impact of soil Nitrogen on soil Carbon or vegetation activity, although this is widely believed to be a potentially significant control of vegetation productivity (Gabrielle *et al.*, 2002; Magnani *et al.*, 2007) and may alter or even reverse the sign of the feedback between climate change and the carbon cycle (Sokolov *et al.*, 2008; Bonan, 2008). This is a priority area for future research and model development.

None of the C4MIP simulations included any representation of land management on soil C such as tillage or harvest. Falloon *et al.* (2008) discuss in some detail how agricultural disturbance may affect long term carbon storage and greenhouse gas emissions from cultivated soils and Vuichard *et al.* (2008) show how recovery of abandoned agricultural land may lead to significant soil carbon sinks. Another important mechanism missing in most of these models to date is decomposition of organic soils. With the rapid rate of climate change at high latitudes, the potential importance of permafrost melting (Zimov *et al.*, 2006) and wetlands drying (Smith *et al.*, 2005) is becoming clear. Models exist to simulate decomposition in organic soils (Bradbury *et al.*, 1993; Smith *et al.*, 1996; Chen and Twilley, 1999) and methane release from wetlands (Grant and Roulet, 2002; Gedney *et al.*, 2004), but as yet are not fully coupled in carbon cycle GCMs. Khvorostyanov *et al.* (2008) and Ise *et al.* (2008) discuss the possible importance of feedbacks between organic soils and soil temperature and hydrology as the high organic content directly affects the water table, and decomposition releases heat energy. These positive feedbacks can enhance peat formation under favourable conditions but can also destabilise it under unfavourable conditions. Large and

rapid release of organic carbon, as CO_2 or methane, is a possible dangerous climate change and further research is urgently required to better understand the risks involved.

2.2. *Experimental design*

Experimental design of carbon cycle GCM simulations often aim to assess whole “Earth System” behaviour rather than target any specific component. The goal of such experiments as C4MIP is to measure the overall impact of interactions between climate and the carbon cycle but due to the computational expense of running such models (typically many weeks or months of super computing time are required to simulate century scale changes) only a small number of experiments are possible. Hence it is not always easy to separate out the many contributing (and often conflicting) influences on a single component of the Earth System such as soil carbon.

For example, the C4MIP protocol consisted of two experiments, “coupled” and “uncoupled”. In the uncoupled experiment anthropogenic CO_2 emissions were input to the model which then simulated natural carbon uptake by terrestrial and marine carbon cycles and hence evolution of atmospheric CO_2 , but in this case the CO_2 was not coupled to the climate and so the experiment experienced no climate change. In the coupled experiment, as atmospheric CO_2 concentrations increased the models additionally simulated the radiative forcing of the extra CO_2 and hence the associated climate change which then affected the carbon cycle, leading to altered evolution of CO_2 . The difference between these two experiments, *e.g.*, in SOC behaviour, can thus be diagnosed and is termed the “climate-carbon cycle feedback” (Friedlingstein *et al.*, 2006, Gregory *et al.*, submitted). However, changes in individual components such as SOC may have been affected by any or all of changing soil temperature or moisture as temperature and precipitation changed, also changes in litter input from vegetation as plants responded to elevated CO_2 levels as well as changing climate. With this in mind and the fact that the C4MIP models differed in their internal representation of SOC behaviour, the C4MIP experiment spanned all of the internal and external drivers of SOC change shown in Figure 1. The implications of this are discussed in section 8.

Various experiments and modelling structures have been applied to isolate the impacts of, for example, different external drivers or different model structures/sensitivities. Approaches include running off-line simulations, holding some inputs fixed or varying individual model equations in isolation. These are discussed and explained in the following sections.

3. Impact of future climate uncertainty

Whilst it is now accepted with near certainty that anthropogenic activity has increased global mean temperatures over recent decades and will continue to do so throughout the twenty-first century, the magnitude of this warming, and in particular the details of local weather patterns are still subject to considerable uncertainty.

The climate sensitivity, the equilibrium global warming for a doubling of atmospheric CO₂ levels, is the metric most commonly used to characterise global scale climate change. The most recent IPCC assessment (IPCC, 2007) concluded it is likely to lie in the range 1.5–4.5 K, although many studies have shown a small but non-zero probability of even higher values. Attempts to constrain climate sensitivity from observed changes have been unable to completely rule out climate sensitivity greater than 5 K even up to 10 K (e.g., Gregory *et al.*, 2002; Forest *et al.*, 2002; Knutti *et al.*, 2002). Likewise, large ensembles of GCMs have been used, with many perturbations to their internal parameters, to estimate possible ranges and likelihoods of climate sensitivity (Murphy *et al.*, 2004, Stainforth *et al.*, 2005) and have also found a finite probability of similarly high values. Such high climate sensitivity would have significant consequences for the global carbon cycle (Andreae *et al.*, 2005).

Warming is predicted to be greatest over land and high northern latitudes (IPCC, 2007). However, there is much less agreement regarding which regions will experience increases or decreases in precipitation and soil moisture. Increases in the total annual amount of precipitation are predicted in high latitudes, while decreases of up to 20% by 2100 are predicted in most subtropical land regions. Changes in the seasonal pattern of precipitation are also likely. In Northern Hemisphere winter, precipitation increases of over 20% are predicted for Northern Hemisphere high latitudes and Eastern Africa, whilst decreases of over 20% are predicted for the Southern USA, North Africa and the Middle East. In Northern Hemisphere summer, precipitation increases of up to 20% by 2100 are predicted for Northern Hemisphere high latitudes, and decreases of up to 20% for Southern Europe, North Africa, South Africa, Brazil and Central America.

As well as these changes in annual totals and seasonal patterns, changes in the magnitude and frequency of extreme climate events are predicted, including warmer and fewer cold days and nights, warmer and more frequent hot days and nights, and an increased frequency of heat waves and heavy precipitation events. All these uncertainties lead to significant uncertainty in future SOC stocks even if all relevant soil processes were fully represented in carbon cycle models.

Jones *et al.* (2003b) performed simulations with the same model as Cox *et al.* (2000) but included additional drivers of climate: natural changes in solar output and volcanic aerosol, and anthropogenic sulphate aerosols. They found that these changes (mainly from the anthropogenic sulphate aerosols) lead to a cooling over industrialised land areas relative to Cox *et al.* (2000) and hence greater increases in SOC during the twentieth century (see Figure 4 of Jones *et al.*, 2003b). Globally,

this led to a greater present day terrestrial uptake, in agreement with observations, but ultimately a greater terrestrial release of carbon towards the end of the twenty-first century as more SOC was available for more rapid decomposition in the warmer future climate.

A much greater sampling of model uncertainty in future climate change was performed by the QUMP ensemble of Murphy *et al.* (2004; “Quantifying Uncertainty in Model Predictions”). They systematically varied many internal GCM parameters to explore a wide range of model climate sensitivities and behaviours, finding the most likely range of climate sensitivity from 2.4–5.4 K, in broad agreement with the IPCC findings, but with finite probability extending above 7 K.

Although these GCM experiments did not explicitly represent carbon cycle behaviour, vegetation dynamics or SOC directly, we have been able to use their results from some of the members of the ensemble to assess sensitivity of soil carbon to uncertainty in future climate. In experiments analogous to those of Jones *et al.* (2005) we ran the RothC soil carbon model offline forced by climate data from 4 members of the QUMP ensemble. The ensemble did simulate terrestrial NPP, so we used this as a proxy for plant litter input as vegetation uptake and turnover must balance in steady state.

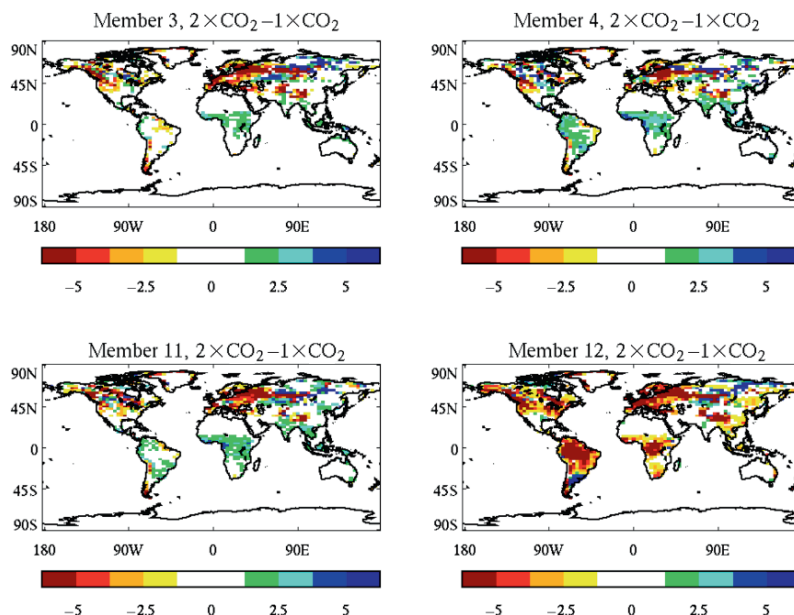


Fig. 2. Changes in global soil carbon stocks (kg C m^{-2}) driven by four ensemble members of the QUMP study (Murphy *et al.*, 2004). The difference is taken between simulations with $2 \times \text{CO}_2$ and $1 \times \text{CO}_2$.

Table 1. Summary of climate sensitivity and NPP changes in 4 QUMP ensemble members and the associated change in global soil carbon stocks simulated offline by RothC.

Experiment Number	Climate Sensitivity	Global Soil C Storage (Pg) $1 \times \text{CO}_2$	Global Soil C Storage (Pg) $2 \times \text{CO}_2$	Change in Global C Storage (Pg) $(2 \times \text{CO}_2) - (1 \times \text{CO}_2)$	Global NPP (GtC/year) $1 \times \text{CO}_2$	Global NPP (GtC/year) $2 \times \text{CO}_2$	Change in Global NPP (GtC/year) $(2 \times \text{CO}_2) - (1 \times \text{CO}_2)$
1	4.1	1012	943	-69	51.0	77.7	26.6
2	2.9	1115	1154	39	54.5	87.2	32.7
3	3.6	1103	1084	-19	54.8	86.9	32.1
4	7.0	1042	725	-317	54.4	55.9	1.4

Table 1 shows the initial level and changes in global SOC for the four members, and their respective climate sensitivity. It is clear that greater levels of climate change in the members with high climate sensitivity are associated with much greater loss of SOC. In fact, the member with lowest sensitivity showed a small increase in soil carbon storage due to strongly increased vegetation productivity. Typically, the offline simulations showed approximately 100 GtC extra loss of SOC for each extra 1 degree of climate change at double CO₂, although this change is not entirely due to the direct climate impact on soil, but also NPP changes. In experiments 2 and 3, NPP is very similar and shows a large increase. The greater climate change in experiment 3 (3.6 K globally) compared with experiment 2 (2.9 K) results in SOC loss rather than gain. In experiment 1 greater climate change (4.1 K) and smaller NPP increase lead to greater SOC loss. In experiment 4, where global average NPP is virtually unchanged, the climate signal alone is shown – the large warming (7.0 K) leads to large global loss of SOC of 317 GtC. Apart from uncertainty in global changes in SOC stock to uncertainty in global mean temperature change, regional changes are apparent also. Figure 2 shows maps of changes in soil carbon for the 4 QUMP ensemble members. While there seems to be some consensus on soil carbon losses in the north, especially in temperate latitudes, the responses in the tropics are very different due to uncertain climate change there. Both in Africa and South America, some members show loss, gain or no change in SOC.

4. Impact of vegetation litter uncertainty

This aspect has received little attention in the literature, probably because vegetation sensitivity in the future is largely controlled by climate and this response itself is highly uncertain. Researchers in vegetation modelling are rightly concentrating on understanding the link between climate change and vegetation productivity and functioning (e.g., Cox *et al.*, 2004; Scholze *et al.*, 2006; Sitch *et al.*, 2008), rather than specifically on the downstream impact of this uncertainty on future SOC behaviour.

However, the Net Primary Production (NPP) and input of plant-derived C to the soil are major driving variables of the soil C balance at scales from field to globe (Falloon, 2001) and are predicted to change, perhaps significantly, in future (Liu *et al.*, 2004). Hence, their accurate estimation is essential for predictive SOM modelling and terrestrial global change studies (Bolinder *et al.*, 1997). Indeed, as shown by both simulation modelling and experimental data, there is a direct relationship between SOC and C inputs to soil (Paustian *et al.*, 1997; Buyanovsky and Wagner, 1998). However, C inputs to soil are difficult to measure directly (Jenkinson *et al.*, 1992) and the lack of theory and data regarding soil C inputs make strict SOM model evaluation virtually impossible (Katterer and Andren, 1999).

The major inputs to the soil carbon system are the amount and quality of plant (and any additional) carbon input, which in croplands are controlled by NPP and

management of organic residues. Future changes in the amount and quality of plant C and N inputs returned to soils could play an important role in determining future SOC (Feng *et al.*, 2008). These changes depend on several factors including changes in large scale land use, crop suitability, vegetation productivity, and possible changes in future biodiversity.

However, we can see some clues to the impact of differences in future vegetation functioning on soil carbon storage from existing model simulations. We have looked at the soil carbon results from the intercomparison study of Sitch *et al.* (2008) which forced five dynamic global vegetation models (DGVMs) with the same patterns of climate change. The top panel of Figure 3 shows changes in the litter input to the soil throughout the twentieth and twenty-first centuries following emissions from the SRES A2 scenario (Nakicenovic *et al.*, 2000). There are clear differences between models, with litter input increasing by between 20 and 40 GtC year⁻¹. The middle panel shows changes in soil residence time (identifying the climate impact on decomposition), and the bottom panel changes in SOC in these same experiments. Note that for each model, changes in SOC amount are not the same as changes in turnover time – this is explained by the different changes in NPP. For example, the climate impact on soil residence time in the Sheffield DGVM, Orchidee and Triffid (pale blue, green and black lines) is to enhance decomposition by very similar amounts with residence times decreased to 75% in each case by 2100. However, these 3 models exhibit very different accumulations of SOC, ranging from 170 GtC in Sheffield to 70 GtC in Triffid, with Orchidee intermediate at 130 GtC. This is clearly driven by differences in litter input where SDGVM simulates a greater increase than Orchidee which in turn is greater than Triffid. Similarly, LPJ and Hyland simulate similar changes in residence time although Hyland has slightly greater enhancement of respiration under climate change. However, because Hyland simulates significantly greater increases in litter input than LPJ, it experiences less loss of SOC. In other words, different responses of vegetation productivity to climate in these models, and hence different future scenarios of organic carbon input to the soil, modify the future behaviour of soil carbon beyond just the direct climate impact.

Similarly, the offline RothC simulations driven by the QUMP ensemble members of Murphy *et al.* (2004) presented in section 3 also display different future NPP, and hence litter, response to climate which modifies the direct climate effect on soil decomposition.

Changes in litter input in response to climate change are extremely uncertain and probably contribute significantly to the large uncertainty found by Friedlingstein *et al.* (2006). Future changes in litter are driven in part by changes in vegetation productivity and mortality and in part also by changes in geographical coverage of vegetation. Sitch *et al.* (2008) discuss how high-latitude warming may lead to greening (as observed by Myneni *et al.*, 1997) and boreal forest expansion, whereas in the tropics (notably Amazonia) widespread loss of forest may occur (Cox *et al.*, 2004; Betts *et al.*, 2004; Scholze *et al.*, 2006). However, changes in litter composition could also be important since increasing atmospheric CO₂

concentration and changes in nitrogen cycling may change the root-to-shoot ratio of plant biomass allocation. Decomposability of litter residue may also change as would the depth profile of the organic carbon input to the soil. In turn, these factors could then affect the turnover time of SOC and hence the long-term storage.

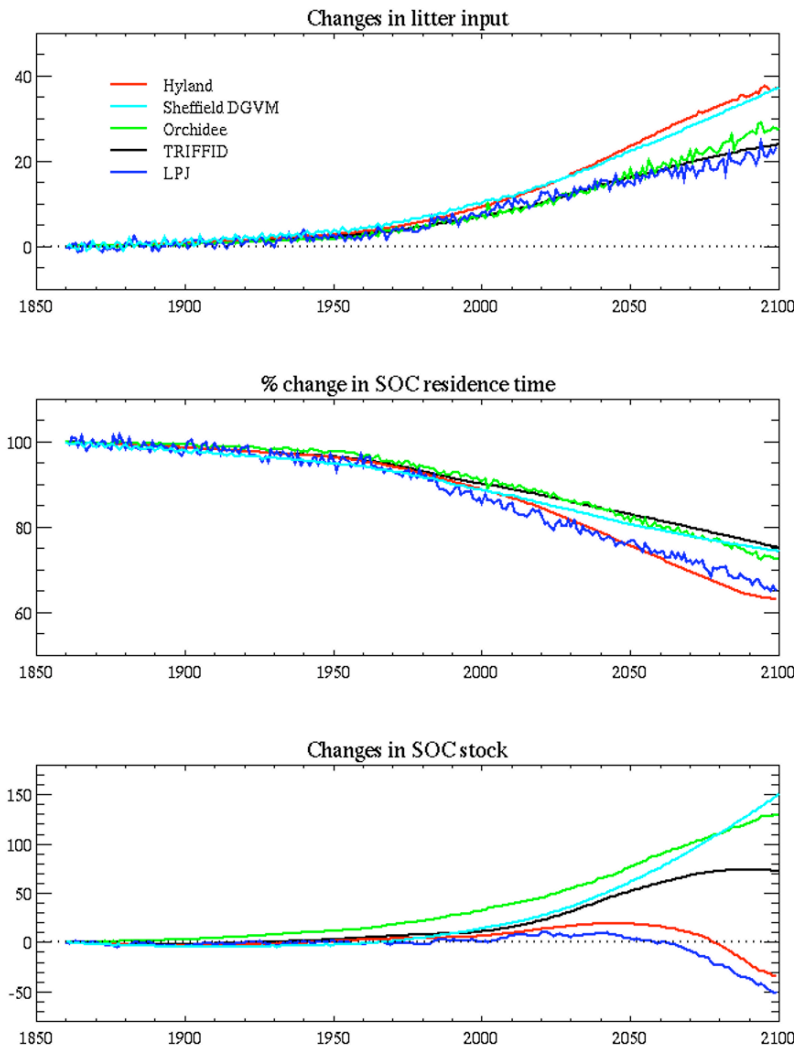


Fig. 3. Soil C results from the 5 DGVMs compared under similar climate forcing by Sitch *et al.* (2008). Top panel: changes since pre-industrial in global organic carbon inputs, diagnosed here as the difference between SOC changes and soil respiration. Middle panel: percentage changes in soil residence time defined as the total global SOC amount divided by global soil respiration rate. Bottom panel: changes in global total SOC amount.

5. Impact of carbon pool dynamics uncertainty

Soil organic carbon is not a single homogeneous mass of carbon, rather it consists of a continuum of different pools with different chemical and biological properties, sensitivities and turnover times (Trumbore and Czimezik, 2008). Some organic matter decomposes readily, some more slowly and some is virtually inert on the timescales of interest to coupled climate-carbon cycle modelling. These pools are formed by input of different plant organic matter, such as roots, branches or leaves, or, in the case of black carbon, are formed by incomplete combustion of organic matter (Lehmann *et al.*, 2008).

SOM is composed of a spectrum of compounds varying in chemical composition and turnover time, and soils contain traces of free sugars, amino acids, organic acids and lipids, as well as polymers, carbohydrate, and amino sugars (Jenkinson, 1988). The most active and youngest components of SOM are the plant residues and debris entering the soil, composed of largely unaltered (and usually cellulose dominated) plant material. Vegetative material has turnover times of the order of 0.5–3.0 year (Buyanovsky and Wagner, 1998). Most of this material is utilised as a substrate for the microbial community, the other relatively fast turnover component of the SOM system, although some may be highly resistant and may never decompose (Hyvonen *et al.*, 1998). The microbial biomass commonly has a turnover time of 1–10 year (Buyanovsky *et al.*, 1994). Upon decomposition, the plant residues give rise to more microbial biomass and metabolites, with an associated release of CO₂. These products are then substrates for a much slower phase of decomposition, which forms humified and more stable products with greater turnover times. For example, SOC in whole soil has a mean turnover time around 7 years, whilst SOC associated with the silt and clay fractions turns over between 400 years and 1000 years (Buyanovsky *et al.*, 1994). It has been difficult in the past to isolate the intrinsic temperature sensitivity of different pools, but new techniques in NMR allow determination of this at a molecular level (Feng *et al.*, 2008).

These pools are also broken down by different processes and different species of microbes, or even fungi. Because they form differently they exist at different horizons in the soil profile and therefore experience different environmental conditions, such as temperature, moisture and oxygen availability. The pools also interact. For example, fresh litter can be decomposed to produce humus – a different pool of soil organic matter which then decomposes in a different manner to release CO₂ back to the atmosphere (or under anaerobic conditions, methane).

Previous work has considered the use of multi-pool models of soil carbon (Schimel *et al.*, 1994; McGuire *et al.*, 1995; Post *et al.*, 1996; Trumbore, 2000; Telles *et al.*, 2003). All such studies agree on the importance of the inclusion of multiple pools in order to represent the heterogeneous nature of the different turnover times within the soil. They show that soil carbon stocks are largely determined by the slow turnover pools but the fluxes are determined by the fast turnover pools (Schimel *et al.*, 1994; Trumbore, 2000). Hence an attempt to simulate

transient soil carbon behaviour with a single pool and just one turnover rate is not possible – it will overestimate the rate of response because large changes to the total stock will require changes to the slow pool (Telles *et al.*, 2003). Single pool models can represent the same equilibrium changes (providing all the pools have the same temperature sensitivity), but not the transient response to them (Schimel *et al.*, 1994; Telles *et al.*, 2003). A study with RothC (Gu *et al.*, 2004) demonstrated that the inclusion of a fast turnover pool of soil carbon could dramatically alter the magnitude of observed respiration in response to seasonal temperature changes due to the seasonality of the organic carbon inputs, a result corroborated experimentally by Yuste *et al.* (2004). The determination of temperature sensitivity of large slow pools is therefore hampered as fluxes can be dominated by smaller but more active pools. Yet it is the slow pools which may dominate the future long-term behaviour of SOC in response to climate change.

In reality there are no hard distinctions between a finite number of pools, but rather a continuum of SOM with a range of different sensitivity and residence times. However, for the purposes of numerical modelling, a finite (and generally

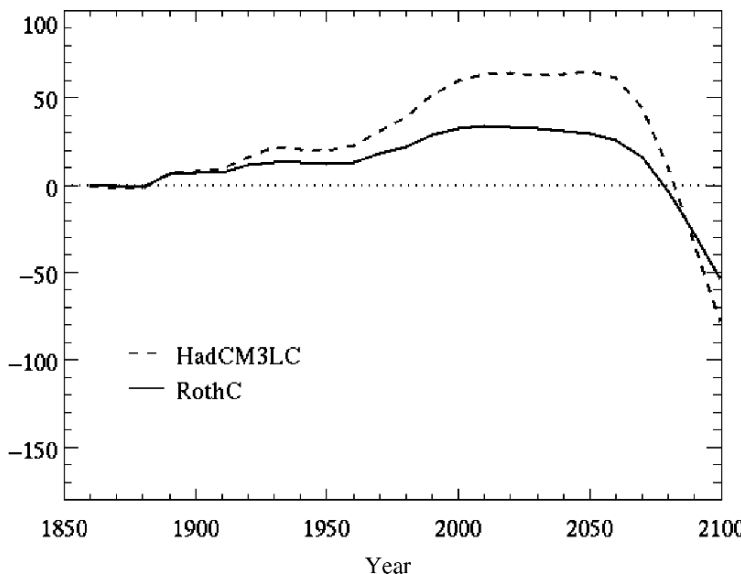


Fig. 4. Simulated changes in global soil carbon amount (GtC) for the offline runs of the single pool soil carbon component of HadCM3LC (dashed line) and the multi-pool model RothC (solid line).

small) number of distinct pools are represented. The soil carbon component of the coupled model used by Cox *et al.* (2000) had the simplest possible representation with a single pool of SOC fed by all the plant litter, and having spatially and temporally uniform sensitivity to temperature and moisture. Other models (such as RothC or Century) may split plant input into 2 or more pools of varying quality (*e.g.*, to reflect leaf or coarse woody debris litter) which decay at different rates. Further complexity can be included when these pools interact and decomposition of one feeds into the others.

This representation of internal carbon dynamics can significantly affect the evolution of total SOC storage. Jones *et al.* (2005) showed different global SOC evolution when two models (the single pool of HadCM3LC, and the multi-pool RothC model) were driven by identical climate and litter input for a transient climate change scenario. They found that the two models exhibited conceptually similar behaviour of carbon accumulation during the twentieth century as litter input increases followed by release towards the end of the twenty-first century as temperature enhances heterotrophic respiration (Figure 4). However, in agreement with Telles *et al.* (2003), the rate of both accumulation and release was slowed by the internal carbon pool dynamics of RothC. This is explained by Figure 5 where the single pool of carbon in HadCM3LC (*right*) exhibits the same turnover time for newly input litter and for well established soil carbon – it cannot differentiate these different pools. However RothC represents the behaviour of two more readily decomposable pools (Decomposable and Resistant Plant Material – DPM, RPM) fed by plant litter input. These pools then decompose to feed a biomass pool and the main body of longer-lived Humus soil carbons. Because the litter pools have a

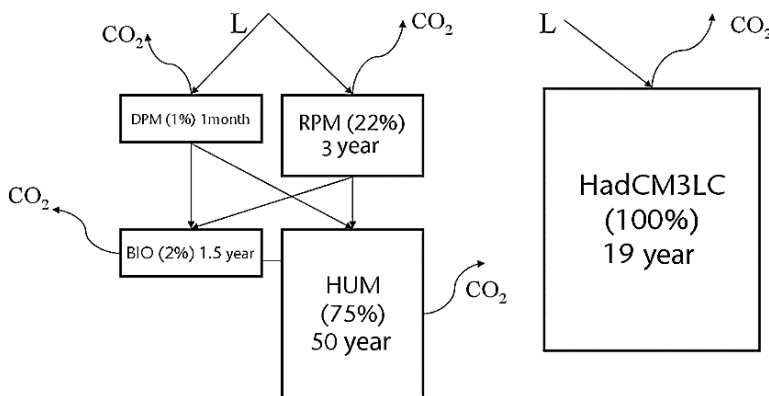


Fig. 5. Schematic representation of the flow of plant litter carbon, L, into soil carbon, and release of CO₂ from respiration out of soil carbon, for the HadCM3LC single pool (*right*) and multi-pool RothC (*left*). Numbers in brackets denote approximate proportions of total SOC in each in each model pool, the time scale shown denotes the characteristic turnover time of each pool under reference conditions.

lower residence time than the single pool of HadCM3LC, fresh litter can decompose more readily and less is accumulated into the soil carbon, leading to a slower rate of accumulation in RothC during the twentieth century.

Conversely, because the humus pool in RothC has a greater residence time than the single pool of HadCM3LC it decomposes more slowly in response to warming, slowing the release of SOC during the twenty-first century. Lehmann *et al.* (2008) show how inclusion of pools with very long residence time can affect the transient behaviour of the climate-carbon cycle feedback, as this damps the response to changing conditions. This could be important in regions, such as Australia, with significant black carbon content of SOC.

We note again, however, that this affect may be just transient. If the pools of carbon in RothC were to exhibit the same sensitivity to changes in temperature and moisture as in HadCM3LC then the ultimate steady state change of SOC would be the same (even for very long lived pools such as black carbon) – the internal carbon dynamics therefore affect the transient response but not necessarily the long term state of the amount of global SOC storage. On the other hand, if the different pools exhibit different sensitivity to temperature changes (*e.g.*, as in Zeng *et al.*, 2004) then this may not be true. There is, as yet, no consensus whether or not different pools exhibit different sensitivities. Although there is no first principle reason that they should do, this is often assumed as a modelling convenience and due to lack of comprehensive observational evidence to the contrary. Giardina and Ryan (2000) argue that long-lived pools would not respond to temperature, whilst Fang *et al.* (2005) found near constant sensitivity of SOM decomposition to warming across a range of soil C pools. Davidson and Janssens (2006) argued that due to reaction kinetics, resistant soil carbon pools may actually be *more* sensitive to temperature than labile pools.

6. Impact of uncertainty in decomposition sensitivity to temperature

This is possibly the most studied area of soil carbon modeling in the context of global scale carbon cycle research, and probably the first aspect people think about when talking about uncertainty in future soil carbon behaviour. It was postulated by Jenkinson *et al.* (1991) that increases in global temperature could release SOC through enhanced heterotrophic respiration, contributing to more atmospheric CO₂ and hence creating a positive feedback. The magnitude of response, though, is highly uncertain as discussed further by Schimel *et al.* (1994), and Kirschbaum (1995).

The potential implications were quantified in a fully coupled climate-carbon cycle model first by Cox *et al.* (2000) and subsequently by others (Friedlingstein *et al.*, 2001; Zeng *et al.*, 2004). Although these studies see a positive feedback coming from various aspects of the global carbon cycle – both terrestrial and marine (Friedlingstein *et al.*, 2006), there is an overwhelming consensus of a positive

feedback which is in no small part due to the response of SOC to warming. The magnitude, timing and even the sign of the feedback between climate and the carbon cycle will depend critically on the response of soil carbon to climate changes. There has been much discussion in the literature about the magnitude of soil decomposition sensitivity to temperature and over whether this response would be sustained over the coming decades or if it is a short-lived phenomenon. Giardina and Ryan (2000) argued that readily decomposable matter is mainly responsible for observed temperature sensitivity and as this would be rapidly depleted the long term sensitivity of SOC would be much smaller than typically modelled. They suggest, rather, that soil respiration is governed in the long-term by substrate availability and organic input quality. However, Davidson *et al.* (2000) have refuted the conclusions of Giardina and Ryan (2000) and argue that temperature sensitivity is just one of many uncertain factors and difficult to ascertain in isolation. Further, Knorr *et al.* (2005) suggest that these conflicting opinions are compatible with long-term temperature sensitivity of SOC turnover and may be explained by rapid depletion of labile SOC combined with the negligible response of non-labile SOC on experimental timescales. Since non-labile SOC may be more sensitive to temperature than labile SOC, the long-term positive feedback of soil decomposition could be even stronger than predicted by global models (Knorr *et al.*, 2005). Feng *et al.* (2008) use NMR spectroscopy techniques to examine the response of different components of plant litter to elevated soil temperature and find leaf lignin to decompose in response but not so for leaf cutin which they found to be surprisingly resistant to the warming.

The temperature sensitivity of heterotrophic respiration, R_H , is often referred to in terms of its “q10” value – q10 being the factor by which decomposition increases for a 10 K rise in temperature. For example, for q10 = 2, the decomposition rate doubles for each 10 K warming. Simple models of soil carbon often use a fixed q10 value (equation 3) for the temperature rate modifying factor, but there is no process based reason why this should be so.

$$f_T = q_{10}^{\left(\frac{T-T_0}{10}\right)} \quad (3)$$

where T_0 is the reference temperature at which the rate modifier equals 1, and q_{10} is a model parameter typically close to 2.0.

More complex models may use an Arrhenius type equation (equation 4) based on the activation energy required for decomposition to proceed. The review by Davidson and Janssens (2006) identified the need for decomposition to be seen as dependent on many factors simultaneously such as soil temperature, moisture, structure and litter quality. A process based analysis using activation energy and Michaelis-Menton kinetics led them to the conclusion that the more resistant soil carbon pools may be more sensitive to temperature than the faster decomposing labile pools.

$$f_T = ke^{\left(\frac{-E_a}{RT}\right)} \quad (4)$$

where E_a is an activation energy for the decomposition reaction, and R is the gas constant ($8.314 \text{ J K}^{-1} \text{ mol}^{-1}$).

Being more physically based the Arrhenius equation also allows models to represent the observed geographical variation of R_H sensitivity to temperature. Soil

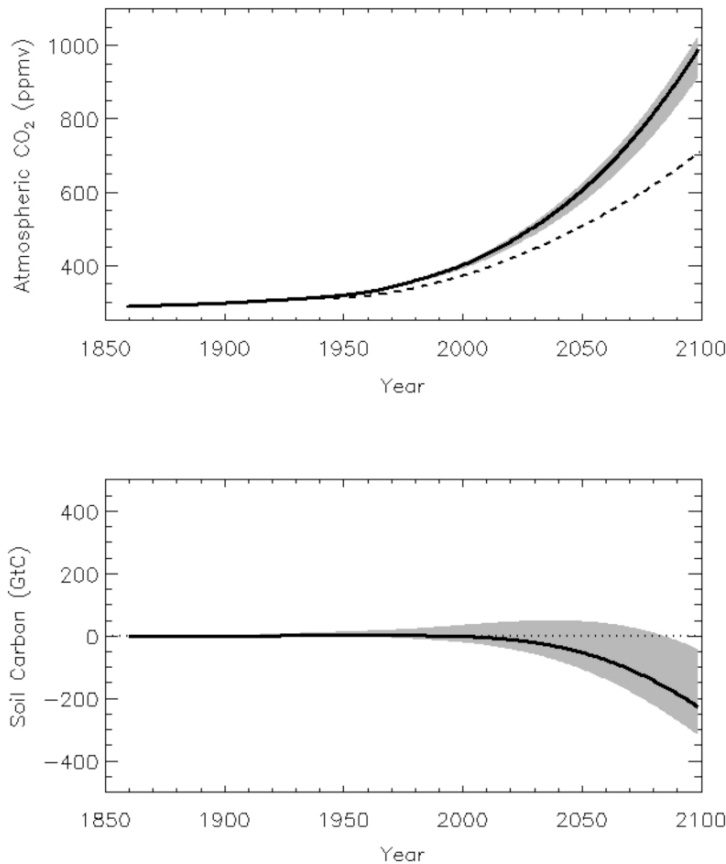


Fig. 6. Uncertainty bounds on future CO₂ levels (top panel) and soil carbon storage (bottom panel) for a range of soil decomposition sensitivity to temperature (q10 values from 1.5 to 2.3 as proposed by Jones *et al.*, 2003a,b). The central solid line shows coupled GCM results with q10 = 2 and the shaded region shows results for the range of q10 values consistent with observed CO₂ variability. The IS92a CO₂ concentration scenario is shown for comparison by the dashed line – even simulations with weakly sensitive soil decomposition provide a strong positive feedback and elevated CO₂ by 2100 due to other responses of the climate-carbon cycle system.

samples from different regions often show very marked heterogeneity making precise determination of q_{10} difficult, but a generally recognised feature is that cold regions exhibit higher sensitivity to warming than do hot regions.

It is, however, useful to be able to consider a large scale, bulk value for soil decomposition sensitivity, and in this case a Q_{10} relationship may be appropriate. To avoid the problems associated with very heterogeneous soil properties, large scale measurements of changes in atmospheric CO_2 in response to climate fluctuations can be used to infer aspects of soil decomposition behaviour. Jones and Cox (2001) used interannual variability of global climate and CO_2 concentration to constrain estimates of a global-mean value of q_{10} , and concluded that at a global scale, q_{10} was likely to fall in the range of 1.5–2.3 (2.1 ± 0.7 based on CO_2 variability related to the ENSO cycle, and 1.9 ± 0.4 constrained by the response to the Mount Pinatubo volcanic eruption in 1991). Rayner *et al.* (2005) and Scholze *et al.* (2007) use a much more sophisticated Carbon Cycle Data Assimilation System (CCDAS) to constrain many model parameters using long-term flask measurements of atmospheric CO_2 , and conclude a range of q_{10} of around 1.3–2.0 for slow or fast processes, in broad agreement with Jones and Cox (2001).

Therefore, although more complex models allow different regional responses to climate, at the global scale constraints exist on future, large-scale sensitivity of soil carbon decomposition to temperature. Jones *et al.* (2003a) explored the implications of this uncertainty to future projections of atmospheric CO_2 and climate–carbon cycle feedback, finding uncertainty of 120 ppm (910–1030 ppm) by 2100 following an SRES-A2 emissions scenario, as SOC loss varied from 50 to 300 GtC (Figure 6).

Unfortunately, isolating further large scale constraints from large scale climate and CO_2 observations is difficult. The twentieth century was characterised by simultaneous temperature and CO_2 increase which likely had conflicting impacts on the terrestrial carbon cycle (Harrison *et al.*, 2008). Whilst the moderate warming likely increased respiration rates slightly, the rising CO_2 concentration likely increased rates of photosynthesis (the so-called CO_2 fertilisation effect, Norby *et al.*, 2005). However, the exact sensitivity of either effect is not precisely known. Jones *et al.* (2006b) found that either strong fertilisation and strong enhancement of respiration, or weak fertilisation and weakly enhanced respiration could both fit the observed record of increasing temperature and CO_2 . In other words, the historical record can offer a joint constraint on CO_2 fertilisation and enhanced decomposition, but not on either individually. To reduce uncertainty further a 2-pronged approach is required. Firstly, more process-based observational studies are required, such as the FACE experiments (Free Air CO_2 Enrichment, Norby *et al.*, 2005) and large scale campaigns such as the analyses of CarboEurope flux towers which has yielded much important understanding of ecosystem functioning and carbon balance (e.g., Ciais *et al.*, 2005; Reichstein *et al.*, 2006).

Secondly, an increasing emphasis in ecosystem research is on the use of data assimilation techniques to constrain model behaviour. Also termed, “model-data fusion”, data assimilation allows a formally optimal combination of process

knowledge embedded within models with direct observations of the real world. Techniques including Monte Carlos (Knorr and Kattge, 2005), Kalman Filter (Williams *et al.*, 2005) and variational data assimilation (Kaminski *et al.*, 2002; Rayner *et al.*, 2005) offer very powerful potential to improve our ability to simulate natural carbon dynamics. In the coming era of observations of the carbon cycle from space, such techniques will allow greater use of satellite data, and greater understanding of global carbon cycle. This in turn means greater confidence in our ability to simulate changes in carbon cycling in the future under climate change conditions (Law *et al.*, 2003).

7. Impact of decomposition sensitivity to moisture uncertainty

We have already discussed how SOC response to future environmental changes will have a profound impact on global carbon stores. The focus in the literature is often on the temperature response (see section 6). Here we look at uncertainty due to soil moisture, arising from uncertainty in the relationship between soil moisture and heterotrophic respiration. In organic peat soils where a high water table slows decomposition due to anoxic conditions, moisture is clearly the dominant control on SOC storage (Ise *et al.*, 2008). But moisture is also an important environmental component in mineral soils. We investigate the response of 12 soil moisture-respiration functions driven by data from a coupled-climate carbon cycle GCM to investigate the impact of heterotrophic respiration dependence on soil moisture on the climate-carbon cycle feedback. It is found that global changes in soil moisture acted to oppose temperature-driven decreases in soil carbon, and hence tended to increase soil carbon storage. Climate change-driven soil moisture changes could therefore reduce the positive climate-carbon cycle feedback, but there remains considerable uncertainty in this response of soil respiration to moisture, warranting further research into this relationship. There may also be considerable uncertainty in the regional responses of soil carbon to soil moisture changes since climate model predictions of regional soil moisture changes are less coherent than temperature changes.

To isolate the moisture impact on decomposition, Falloon *et al.* (submitted) used the experimental set-up of Jones *et al.* (2005) where climate change output and changes in organic litter input are taken from a transient climate change simulation with the coupled climate carbon cycle model, HadCM3LC (Cox *et al.*, 2000). These are used to force the soil carbon model RothC (Coleman and Jenkinson, 1999) which simulates changes in global SOC stocks to 2100.

In a series of sensitivity experiments, simulations were performed with different equations for the moisture rate modifier – *i.e.*, with different functional forms of f_M in equation 1. The external drivers, temperature sensitivity and carbon pool dynamics are kept identical between experiments. There were two series of simulations: “All forcings” (AF) in which all of temperature, moisture and litter were taken from the climate change output, and “moisture only” (MO) where tempera-

ture and litter were held fixed at pre-industrial levels and only soil moisture forcing was varied during the course of the simulation.

The simulations showed a large spread of uncertainty in future global soil carbon totals. The AF simulations all showed an increase in global soil carbon stocks until around 2060 followed by a rapid loss of global soil carbon thereafter (Figure 7a), mainly caused by an increase in respiration due to higher temperatures. The relative sensitivity of each model to soil moisture differed between simulations with moisture change only or all forcings, showing a non-linear interaction

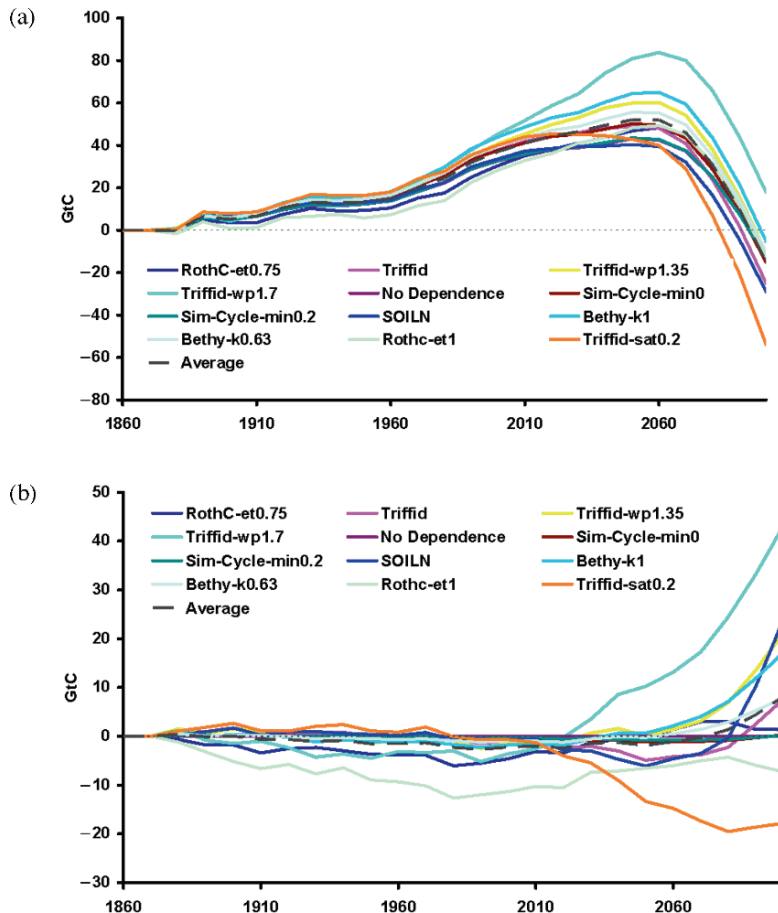


Fig. 7. Changes in global total soil carbon from 1860 values using the RothC model and different soil moisture-respiration functions driven by HadCM3LC outputs. Top panel shows results when all forcings (soil temperature, moisture and plant carbon inputs) are changing and bottom panel shows results when soil moisture only is changing.

between the controlling factors of soil carbon decomposition, perhaps due to changes in the initial soil C state of each model. Under the AF scenario, most of the members resulted in a net loss of soil carbon globally by 2100. Although one member showed a net gain of global soil carbon by 2100, even this model was still simulating a sharp decline by that stage. The range of global soil carbon changes from 1860 to 2100 was 72 GtC (−54 to 18 GtC), corresponding to an uncertainty of about 34 ppm in atmospheric CO₂. Relatively small global soil carbon changes under the MO simulations were found for each case until around 2010 (Figure 7b). Thereafter a large range of changes in global soil carbon stocks was found spanning both large negative and positive values (from −18 GtC to 43 GtC). Thus the impact of uncertainty in soil moisture response on uncertainty in the global soil carbon-climate feedback is large when considering both changes in soil moisture values only, and changes in all climate forcings.

Typically, these changes in SOC due to moisture changes are driven by the fact that drier soils experience reduced decomposition and hence increased SOC storage, whilst wetter soils experience enhanced decomposition and SOC losses. However, some models assume optimal soil moisture content for decomposition with reduced rates for saturated soils, representing inhibition of decomposition under anaerobic conditions. In some regions therefore, drying of soils could lead to increased respiration and soil carbon loss. This is particularly true in high latitude wetlands, where melting of permafrost may lead to changes in the water table depth and large scale drying (Smith *et al.*, 2005).

The relationship between soil moisture and heterotrophic respiration is generally poorly understood and represented in various ways in soil carbon cycle models. In contrast, the role of the relationship between soil temperature and soil carbon storage has been investigated in depth. The simulations of Fallon *et al.* (submitted) using different moisture functions found a wide range of changes in future global soil carbon stocks from large losses to small gains. Falloon *et al.* (2007) also found that regionally, precipitation controlled the sign of soil carbon changes with wetter conditions resulting in higher soil carbon stocks and drier conditions in lower soil carbon stocks, since increased NPP in wetter conditions could override any increase in respiration. However, globally, temperature seemed to control changes in total carbon, probably because whilst temperature increases were predicted everywhere, the nature of precipitation changes varied greatly between regions. This highlights considerable uncertainty in the magnitude and direction of the future soil carbon feedback attributable to differences in the moisture sensitivities currently used in carbon cycle models. A better understanding of the relationship between soil moisture and respiration is needed in order to reduce this uncertainty and improve our confidence in climate change predictions.

8. Combined uncertainty

We started this review by discussing sources of uncertainty in future SOC stocks, and characterising them into external “drivers” of SOC changes or internal “sensitivities” of SOC to environmental changes. This was summarised in Figure 1. Each individual component we identified there is an important contributor to uncertainty in future SOC storage, and we have examined each in turn. In this section we discuss the implications of the combined uncertainty of all these factors when they operate together.

The C4MIP simulations described by Friedlingstein *et al.* (2006) provide the perfect opportunity to see all these sources of uncertainty acting together in 11 different complex coupled climate carbon cycle models. Although forced by the same future scenario of anthropogenic carbon emissions, the 11 models simulate different CO₂ levels and degree of climate change (both globally and regionally). They also simulate different responses of vegetation productivity and hence litter input to the soil. These are the external drivers. Internally, the C4MIP models have different representations of SOC, with different numbers of carbon pools and carbon dynamics, and different sensitivities to temperature and moisture. These are the internal sensitivities.

It is worth here summarising again the C4MIP experimental design. The climate-carbon cycle feedback is diagnosed in this study by comparing two numerical simulations – one where the CO₂ effect on the carbon cycle is considered alone, in the absence of climate change (termed the “Uncoupled” experiment), the other where CO₂ and climate both change and affect natural carbon fluxes (the “Coupled” experiment). Figure 8 shows how global SOC stocks change in the two experiments. The top panel shows results from the uncoupled experiment. Apart from one outlier, all models show strong increases in global SOC stocks by 250–600 GtC. This is driven by increases in litter input in turn caused by enhanced terrestrial productivity in response to elevated CO₂ levels. The middle panel shows results from the coupled experiment when climate change additionally affects both soil and vegetation carbon fluxes. Most models still simulate significant amounts of carbon accumulation in soil, by up to 400 GtC, but by much less than in the uncoupled experiment. Some models see an initial accumulation of SOC followed by rapid loss later in the simulation. Two models simulate a net loss of SOC during the course of the simulation from 1860 to 2100.

The climate impact on SOC is shown in the bottom panel as the difference between coupled and uncoupled experiments. All models show a marked decrease in SOC due to climate change (by between 50 and 450 GtC reduction). Note, by this we don’t necessarily mean a loss of SOC relative to initial conditions in 1860 (only 2 of 11 models see this), but rather a loss relative to the case when no climate change occurs (all 11 models simulate this). It is also important to note that this climate impact on soil carbon storage is not entirely due to a climate impact

on soil carbon residence time, but could equally be caused by changes in organic litter input from vegetation.

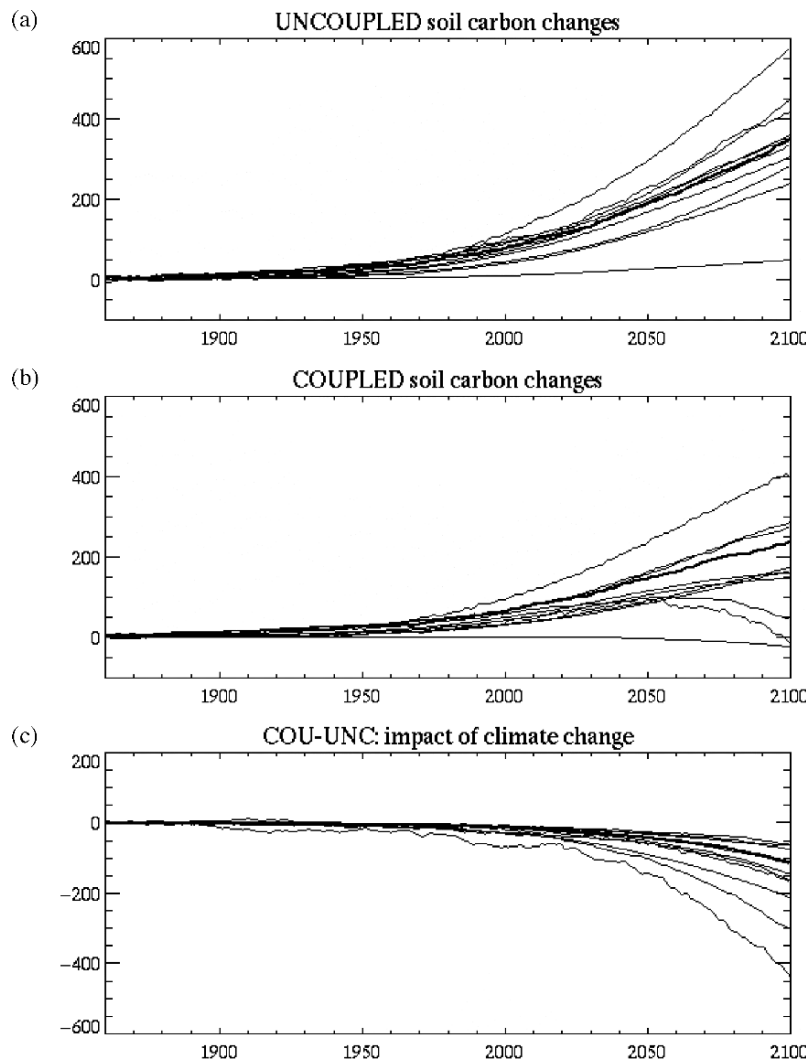


Fig. 8. Simulated changes in global soil carbon storage for the C4MIP experiment of Friedlingstein *et al.* (2006). Top panel, SOC changes in the “uncoupled” simulation when only rising CO₂ affects the natural carbon cycle; middle panel, SOC changes in the “coupled” experiment when both CO₂ and climate change affect the carbon cycle; bottom panel, difference between coupled and uncoupled experiments demonstrating the impact of climate change on SOC.

To demonstrate the importance of SOC changes and their uncertainty, we can look at what contribution soil carbon makes to the total sensitivity of the carbon cycle to climate change. Friedlingstein *et al.* (2006) define a measure of feedback, the gain, g . This is related to the ratio of increases in atmospheric CO₂ between the coupled and uncoupled simulations. The higher the gain, the stronger the feedback. All models simulate a positive value of g – *i.e.*, a positive feedback, implying that climate change causes an acceleration of CO₂ increase by reducing natural carbon uptake and storage. We find that the strength of the feedback is strongly related to the climate impact on SOC in these models. Figure 9 shows the SOC change at 2100 due to climate change (the values from Figure 8c) plotted against the feedback gain, g for each model. All models have negative changes in SOC due to climate change and all models have a positive feedback. The more SOC loss, the higher the gain. The model with greatest reduction of SOC storage shows the strongest feedback. It is clear that response of soil carbon storage to climate change is a very strong determinant of the strength of the global climate-carbon cycle feedback.

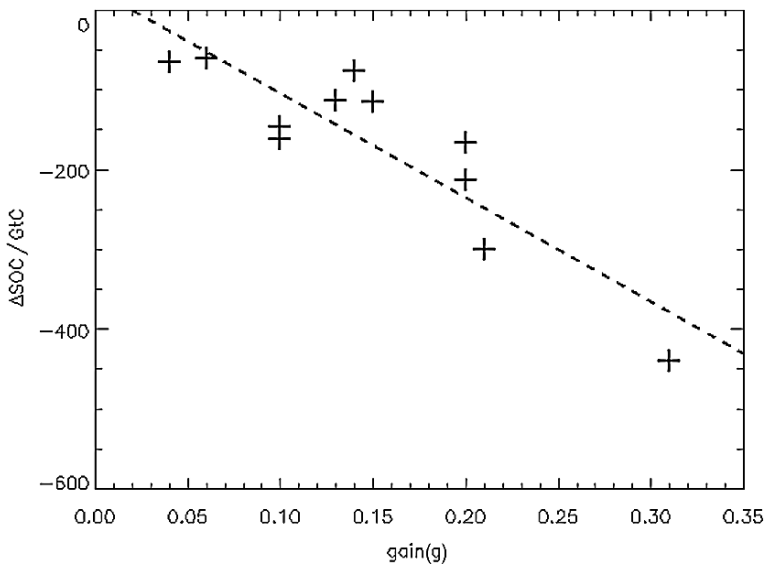


Fig. 9. Correlation of climate impact on SOC and total climate-carbon cycle feedback gain, g . ΔSOC is defined as the difference in SOC accumulation between coupled and uncoupled simulations of C4MIP (Friedlingstein *et al.*, 2006) as shown in Figure 8. Gain, g , denotes feedback strength: higher values of g indicate stronger positive climate-carbon cycle feedback.

9. Conclusions

We have shown that the natural carbon cycle has a pivotal role to play in determining future climate, either by determining atmospheric CO₂ levels in response to anthropogenic emissions, or by contributing to limits on emissions required to achieve CO₂ stabilisation targets. It is undeniable that storage of organic carbon in the world's soils is a very important (and possibly the most important) aspect of the global carbon cycle on the timescales of the next few decades or century.

We have also shown that the future of SOC is very uncertain. It is a crucial goal, now, for the research community to address this issue. Both field researchers and climate and ecosystem modellers must contribute to reducing this uncertainty. The first steps are to quantify and understand the sources of uncertainty, and this is what we have attempted to present in this review. To achieve this, we have broken the issue down into external driving factors and internal sensitivities of SOC. These are summarised below:

External drivers

- Uncertainty in future climate drives large uncertainty in future SOC. Future climate is uncertain in both global mean change and regional detail, and also in both annual mean changes and changes in the seasonal cycle or temporal distribution of extreme events. Typically greater degrees of climate change drive greater changes in SOC. Many such effects are driven by long-term gradual climate changes but carbon cycle vulnerability to extreme events (Ciais *et al.*, 2005) and climate variability (especially drought, Ise *et al.*, 2008) is also important and requires more study.
- Uncertainty in future inputs of organic carbon to the soil. We note that this has received less attention in the literature than some aspects, because vegetation modelling studies tend to focus on the impacts of climate change on the vegetation itself (in terms of productivity, carbon storage, vegetation coverage, ecosystem health, etc.) and less on the impact of these changes on soil carbon. Analysis of model results has shown that different changes in future litter inputs can modify and even outweigh the uncertainty due to climate change.
- Uncertainty in the response to future land-use change. Although few experiments exist to quantify this in full Earth System models, we know land-use change and land management affect soil carbon content (Soussanna *et al.*, 2004; Smith *et al.*, 2007; Bondeau *et al.*, 2007) and future management may contribute to climate mitigation efforts. Improving understanding and inclusion of this effect in models is a research priority.

Internal drivers

- Uncertainty in representation of internal carbon pool dynamics in SOC. It has been noted before that failure of models to simulate turnover of different carbon pools at different rates will lead to failure to be able to capture the transient response of SOC to environmental changes, especially if significant quantities of SOC exist in very long-lived components. We have shown how this manifests itself as carbon pool dynamics dampen the response to both litter and climate changes by a factor of about 2. Research is also needed into the different temperature sensitivity of different SOC pools.
- Uncertainty in sensitivity of decomposition to temperature. This is both one of the most studied aspects of SOC behaviour and one of the most important in the context of climate change. The overwhelming consensus in coupled climate carbon cycle models of a positive climate feedback on the carbon cycle is due partly to all such models predicting reduced global SOC storage and enhanced SOC turnover in response to climate change. The main mechanism to explain this is accelerated decomposition due to warmer conditions. Differences in temperature sensitivity of different SOC pools is an ongoing area of active research.
- Uncertainty in sensitivity of decomposition to moisture. This is a less well studied aspect of the system, and again has been shown to be potentially important, not just in organic peat soils, but in mineral soils also. The impact of future global changes in soil moisture typically oppose the reductions due to warming, as drier soils generally experience slowed decomposition. However, this response is spatially very variable and not strong enough to counter the warming-induced losses. There is much less process understanding of the moisture control on soil respiration and much less appreciation by modellers of its importance than is the case for temperature. Therefore, this is an important gap area for future research to fill.

In order for scientific research to be used, reliably, in any decision making process, the decision must be informed by both the scientific prediction, and the extent of uncertainty surrounding it. Only if decision makers are aware of uncertainty in scientific advice can they properly account for risks. A multitude of approaches exist to assess and quantify uncertainty. This review has presented many examples from the literature where discrete aspects of the modelling system have been isolated to study their contribution to uncertainty. Results from complex coupled models have also been analysed to assess the impact of combining multiple sources of uncertainty.

Our conclusion is thus that understanding future changes in soil organic carbon behaviour is crucial for understanding the role of the global carbon cycle in the Earth System, and in planning for environmental change. The world's soils are a

huge store of organic carbon and can have a very significant role to play in controlling future atmospheric CO₂ levels. Future research must concentrate on understanding the processes involved in determining future SOC and on both quantifying and reducing the uncertainty explored here. Only then can we make advances in providing reliable projections of future environmental conditions.

Acknowledgements

This work was supported by the Integrated Climate Programme, GA01101 (DECC) and CBC/2B/0417 Annex C5 (MoD).

References

Andreae, M. O., Jones, C. D., and Cox, P. M., 2005. Strong present-day aerosol cooling implies a hot future. *Nature*, **435**, 1187–1190.

Betts, R. A., Cox, P. M., Collins, M., Harris, P. P., Huntingford, C., and Jones, C. D., 2004. The role of ecosystem-atmosphere interactions in simulated Amazonian precipitation decrease and forest dieback under global climate warming. *Theoretical and Applied Climatology*, **78**, 157–175.

Bolinder, M. A., Angers, D. A., and Dubuc, J. P., 1997. Estimating shoot to root ratios and annual carbon inputs in soils from cereal crops. *Agriculture, Ecosystems & Environment*, **63**, 61–66.

Bondeau, A., Smith, P., Zehle, S., Schaphoff, S., Lucht, W., Cramer, W., Gerten, D., Lotze-Campen, H., Muller, C., Reichstein, M., and Smith, B., 2007. Modelling the role of agriculture for the 20th century global terrestrial carbon balance. *Global Change Biology*, **13**, 679–706.

Bonan, G., 2008. Carbon cycle: Fertilizing change. *Nature Geoscience*, **1**, 645–646, doi: 10.1038/ngeo328.

Booth, B., Jones, C., Collins, M., Totterdell, I., Cox, P., Sitch, S., Huntingford, C., and Betts, R., 2008. Global warming uncertainties due to carbon cycle feedbacks exceed those due to CO₂ emissions, *Nature*, submitted.

Bradbury, N. J., Whitmore, A. P., Hart, P. B. S., and Jenkinson, D. S., 1993. Modelling the fate of nitrogen in crop and soil in the years following application of ¹⁵N-labelled fertilizer to winter wheat. *Journal of Agricultural Science*, **121**, 363–379.

Buyanovsky, G. A., and Wagner, G. H., 1998. Changing role of cultivated land in the global carbon cycle. *Biology and Fertility of Soils*, **27**, 242–245.

Canadell, J. G., Le Quéré, C., and Raupach, M. R. *et al.*, 2007. Contributions to accelerating atmospheric CO₂ growth from economic activity, carbon intensity, and efficiency of natural sinks. *Proceedings of the National Academy of Sciences*, **104**, 18866–18870, doi:10.1073/pnas.0702737104.

Chen, R., and Twilley, R. R., 1999. A simulation model of organic matter and nutrient accumulation in mangrove wetland soils. *Biogeochemistry*, **44**, 93–118.

Ciais, P., Reichstein, M., and Viovy, N. *et al.*, 2005. Unprecedented Reduction in European Primary Productivity caused by Heat and Drought in 2003. *Nature*, **437**, 529–533.

Coleman, K., and Jenkinson, D. S., 1999. RothC-26.3, A model for the turnover of carbon in soil: Model description and User's guide. Lawes Agricultural Trust, Harpenden, UK, 30 pp.

Cox, P. M., Betts, R. A., Collins, M., Harris, P. P., Huntingford, C., and Jones, C. D., 2004. Amazonian forest dieback under climate-carbon cycle projections for the 21st Century. *Theoretical and Applied Climatology*, **78**, 137–156.

Cox, P. M., Betts, R. A., Jones, C. D., Spall, S. A., and Totterdell, I. J., 2000. Acceleration of global warming due to carbon-cycle feedbacks in a coupled climate model. *Nature*, **408**, 184–187.

Davidson, E., and Janssens, I., 2006. Temperature sensitivity of soil carbon decomposition and feedbacks to climate change. *Nature*, **440**, 165–173.

Davidson, E. A., Trumbore, S. E., and Amundson, R., 2000. Soil warming and organic carbon content, *Nature*, **408**, 789–790.

Denman, K. L., Brasseur, G., and Chidthaisong, A. *et al.*, 2007. Couplings between changes in the climate system and biogeochemistry. In: Climate Change 2007: The Physical Science Basis. Contribution of Working Group I to the Fourth Assessment Report of the Intergovernmental Panel on Climate Change [Solomon, S., Qin, D., Manning, M., Chen, Z., Marquis, M., Averyt, K. B., Tignor, M., and Miller, H. L. (eds.)]. Cambridge University Press, Cambridge, United Kingdom and New York, NY.

Falloon, P., 2001. Large scale spatial modelling of soil organic matter dynamics. PhD Thesis, School of Life and Environmental Sciences, University of Nottingham, UK.

Falloon, P., Jones, C. D., and Cerri, C. E. P. *et al.*, 2007. Climate change and its impact on soil and vegetation carbon storage in Kenya, Jordan, India and Brazil. *Agriculture, Ecosystems and Environment*, **122**, 114–124 doi:10.1016/j.agee.2007.01.013.

Falloon, P. D., Jones, C. D., Ades, M., and Paul, K. I., 2008a. Soil moisture controls of future global soil carbon changes; an unconsidered source of uncertainty. *Global Geochemical Cycles* (submitted).

Falloon, P., Smith, P., Betts, R., and Jones, C. D., 2008b. Carbon sequestration and greenhouse gas fluxes in cropland soils – climate opportunities and threats. In: Climate Change and Crops, [Singh, S. N. (ed.)]. (in press).

Fang, C., Smith, P., Moncrieff, J., and Smith, J. U., 2005. Similar response of labile and resistant soil organic matter pools to changes in temperature. *Nature*, **433**, 57–59.

Feng, X., Simpson, A. J., Wilson, K. P., Dudley Williams, D., and Simpson, M. J., 2008. Increased cuticular sequestration and lignin oxidation in response to soil warming. *Nature Geoscience*, **1**, 836–839.

Friedlingstein, P., Bopp, L., and Caias, P. *et al.*, 2001. Positive feedback between future climate change and the carbon cycle. *Geophysical Research Letters*, **28**, 1543–1546.

Friedlingstein, P., Cox, P., and Betts, R. *et al.*, 2006. Climate-carbon cycle feedback analysis, results from the C4MIP model inter-comparison. *Journal of Climate*, **19**, 3337–3353.

Forest, C. E., Stone, P. H., Sokolov, A. P., Allen, M. R., and Webster, M. D., 2002. Quantifying Uncertainties in Climate System Properties with the Use of Recent Climate Observations. *Science*, **295**, 113–117.

Gabrielle, B., Mary, B., Roche, R., Smith, P., and Gosse, G., 2002. Simulation of carbon and nitrogen dynamics in arable soils: a comparison of approaches. *European Journal of Agronomy*, **18**, 107–120.

Gedney, N., Cox, P. M., and Huntingford, C., 2004. Climate feedback from wetland methane emissions. *Geophysical Research Letters*, **31**, 10.1029/2004GL020919.

Giardina, C., and Ryan, M., 2000. Evidence that decomposition rates of organic carbon in mineral soil do not vary with temperature. *Nature*, **404**, 858–861.

Grant, R. F., and Roulet, N. T., 2002. Methane efflux from boreal wetlands: Theory and testing of the ecosystem model Ecosys with chamber and tower flux measurements. *Global Biogeochemical Cycles*, **16**(4), 1054.

Gregory, J. M., Stouffer, R. J., Raper, S. C. B., Stott, P. A., and Rayner, N. A., 2002. An observationally based estimate of the climate sensitivity. *Journal of Climate*, **15**, 3117–3121.

Gregory, J. M., Jones, C. D., Cadule, P., and Friedlingstein, P., 2008. Quantifying carbon cycle feedbacks. *Journal of Climate* (submitted).

Gu, L., Post, W. M., and King, A. W., 2004, Fast labile carbon turnover obscures sensitivity of heterotrophic respiration from soils to temperature: A model analysis. *Global Biogeochemical Cycles*, **18**, doi: 10.1029/2003GB002119.

Gullison, R. E., Frumhoff, P. C., and Canadell, J. G. *et al.*, 2007. Tropical forests and Climate policy. *Science*, **316**, 985–986, doi:10.1126/science.1136163.

Harrison, R., Jones, C. D., and Hughes, J., 2008. Competing roles of rising CO₂ and climate change in the contemporary European carbon balance. *Biogeosciences*, **5**, 1–10.

Hyvonen, R., Agren, G. I., and Bosatta, E., 1998. Predicting long-term soil carbon storage from short-term information. *Soil Science Society of America Journal*, **62**, 1000–1005.

IPCC, 2007. Summary for policymakers. In: Climate Change 2007: The Physical Science Basis. Contribution of Working Group I to the Fourth Assessment Report of the Intergovernmental Panel on Climate Change [Solomon, S., Qin, D., Manning, M., Chen, Z., Marquis, M., Avery, K. B., Tignor, M., and Miller, H. L. (eds.)]. Cambridge University Press, Cambridge, United Kingdom and New York, NY.

Ise, T., Dunn, A. L., Wofsy, S. C., and Moorcroft, P. R., 2008. High sensitivity of peat decomposition to climate change through water-table feedback. *Nature Geoscience*, **1**, 763–766.

Jenkinson, D.S., 1988. Soil organic matter and its dynamics. In: Russell's Soil Conditions and Plant Growth, 11th Edition, [Wild, A. (ed.)], pp. 504–607. Longman, London.

Jenkinson, D. S., Adams, D. E., and Wild, A., 1991. Model estimates of CO₂ emissions from soil in response to global warming. *Nature*, **351**, 304–306.

Jenkinson, D. S., Harkness, D. D., Vance, E. D., Adams, D. E., and Harrison, A. F., 1992. Calculating net primary production and annual input of organic-matter to soil from the amount and radiocarbon content of soil organic-matter. *Soil Biology and Biochemistry*, **24**, 295–308.

Jones, C. D., and Cox, P. M., 2001. Constraints on the temperature sensitivity of global soil respiration from the observed interannual variability in atmospheric CO₂. *Atmospheric Science Letters*, **2**, 166–172, doi:10.1006/asle.2000.0041.

Jones, C. D., Cox, P. M., and Huntingford, C., 2003a. Uncertainty in climate-carbon cycle projections associated with the sensitivity of soil respiration to temperature. *Tellus*, **55B**, 642–648.

Jones, C. D., Cox, P. M., Essery, R. L. H., Roberts, D. L., and Woodage, M. J., 2003b. Strong carbon cycle feedbacks in a climate model with interactive CO₂ and sulphate aerosols. *Geophysical Research Letters*, **30**, 10.1029/2003GL016867.

Jones, C. D., McConnell, C., Coleman, K. W., Cox, P., Falloon, P. D., Jenkinson, D., and Powlson, D., 2005. Global climate change and soil carbon stocks; predictions from two contrasting models for the turnover of organic carbon in soil. *Global Change Biology*, **11**, 154–166, doi: 10.1111/j.1365-2486.2004.00885.x.

Jones, C. D., Cox, P. M., and Huntingford, C., 2006a. Impact of climate-carbon cycle feedbacks on emission scenarios to achieve stabilisation. In: Avoiding Dangerous Climate Change [Schellnhuber, H. J., Cramer, W., Nakicenovic, N., Wigley, T., and Yohe, G. (eds.)]. Cambridge University Press.

Jones, C. D., Cox, P. M., and Huntingford, C., 2006b. Climate-carbon cycle feedbacks under stabilization. *Tellus*, **58B**, doi: 10.1111/j.1600-0889.2006.00217.x.

Kaminski, T., Knorr, W., Rayner, P. J., and Heimann, M., 2002. Assimilating atmospheric data into a terrestrial biosphere model: A case study of the seasonal cycle, *Global Biogeochemical Cycles*, **16**, 1066.

Katterer, T., and Andren, O., 1999. Long-term agricultural field experiments in Northern Europe: analysis of the influence of management on soil carbon stocks using the ICBM model. *Agriculture, Ecosystems and Environment*, **72**, 165–179.

Khvorostyanov, D., Ciais, P., Krinner, G., Zimov, S. A., Corradi, C., and Guggenberger, G., 2008. Vulnerability of permafrost carbon to global warming. Part II. Sensitivity of permafrost carbon stock to global warming. *Tellus*, doi:10.1111/j.1600-0889.2007.00336.x.

Kirschbaum, M. U. F., 1995. The temperature dependence of soil organic matter decomposition and the effect of global warming on soil organic carbon storage. *Soil Biology Biochemistry*, **27**, 753–760.

Knorr, W., and Kattge, J., 2005. Inversion of terrestrial ecosystem model parameter values against eddy covariance measurements by Monte Carlo sampling. *Global Change Biology*, **11**, 1333–1351.

Knorr, W., Prentice, I. C., House, J. C., Holland, E. A., 2005. Long-term sensitivity of soil carbon turnover to warming. *Nature*, **433**, 298–301.

Knutti, R., Stocker, T. F., Joos, F., and Plattner, G. K., 2002. Constraints on radiative forcing and future climate change from observations and climate model ensembles. *Nature*, **416**, 719–723.

Krinner, G., Viovy, N., deNoblet, N. *et al.*, 2005. A dynamic global vegetation model for studies of the coupled atmosphere-biosphere system. *Global Biogeochemical Cycles*, **19**, GB101510.1029/2003GB002199, 2005.

Law, R. M., Rayner, P. J., Steele, L. P., and Enting, I. G., 2003. Data and modelling requirements for CO₂ inversions using high-frequency data. *Tellus*, **55B**, 512–521.

Lehmann, J., Skjemstad, J., Sohi, S., Carter, J., Barson, M., Falloon, P., Coleman, K., Woodbury, P., and Krull, E., 2008. Australian climate-carbon cycle feedback reduced by soil black carbon. *Nature Geoscience*, **1**, 832–835.

Liu, C., Westman, C. J., Berg, B., Kutsch, W., Wang, G. Z., Man, R., and Ilvesniemi, H., 2004. Variation in litterfall-climate relationships between coniferous and broadleaf forests in Eurasia. *Global Ecology and Biogeography*, **13**, 105–114.

McGuire, A., Melillo, J., Joyce, L., Kicklighter, D., Grace, A., Moore, B., III, and Vose, C., 1992. Interactions between carbon and nitrogen dynamics in estimating net primary productivity for potential vegetation in North America. *Global Biogeochemical Cycles*, **6**, 101–124.

McGuire, A. D., Melillo, J. M., Kicklighter, D. W., and Joyce, L. A., 1995. Equilibrium responses of soil carbon to climate change: Empirical and process-based estimates. *Journal of Biogeography*, **22**, 785–796.

Matthews, H. D., 2005. Decrease of emissions required to stabilize atmospheric CO₂ due to positive carbon cycle-climate feedbacks. *Geophysical Research Letters*, **32**, 10.1029/10.1029/2005GL023435.

Magnani, F., Mencuccini, M., and Borghetti, M. *et al.*, 2007. The human footprint in the carbon cycle of temperate and boreal forests. *Nature*, **447**, 849–851.

Meehl, G. A., Stocker, T. F., and Collins, W. D. *et al.*, 2007. Global climate projections. In: Climate Change 2007: The Physical Science Basis. Contribution of Working Group I to the Fourth Assessment Report of the Intergovernmental Panel on Climate Change [Solomon, S., Qin, D., Manning, M., Chen, Z., Marquis, M., Averyt, K. B., Tignor, M., and Miller, H. L. (eds.)]. Cambridge University Press, Cambridge, United Kingdom and New York, NY.

Murphy, J. M., Sexton, D. M. H., Barnett, D. N., Jones, G. S., Webb, M. S., Collins, M., and Stainforth, D. A., 2004. Quantification of modelling uncertainties in a large ensemble of climate change simulations. *Nature*, **430**, 768–772.

Myneni, R. B., Keeling, C. D., Tucker, C. J., Asrar, G., Nemani, R. R., 1997. Increased plant growth in the northern latitudes from 1981 to 1991. *Nature*, **386**, 698–702.

Nabuurs, G. J. *et al.*, 2007. Forestry. In: Climate Change 2007: Mitigation. Contribution of Working Group III to the Fourth Assessment Report of the Intergovernmental Panel on Climate Change [Metz, B., Davidson, O. R., Bosch, P. R., Dave, R., and Meyer, L. A. (eds.)]. Cambridge University Press, Cambridge, UK and New York.

Nakicenovic, N., Alcamo, J., and Davis, G. *et al.*, 2000. IPCC Special Report on Emission Scenarios. Cambridge University Press, Cambridge, UK, pp. 599.

Norby, R. J., DeLucia, E. H., and Gielen, B. *et al.*, 2005. Forest response to elevated CO₂ is conserved across a broad range of productivity. *Proceedings of the National Academy of Sciences, USA*, **102**, 18052–18056.

Paustian, K., Elliott, E. T., and Killian, K., 1997. Modeling soil carbon in relation to management and climate change in some agroecosystems in central North America. In: Soil Processes and the Carbon Cycle [Lal, R., Kimble, J. M., Follett, R. F., and Stewart, B. A. (eds.)]. pp. 459–471. CRC Press, Boca Raton, FL.

Post, W. M., King, A. W., and Wullschleger, S. D., 1996. Soil organic matter models and global estimates of soil organic carbon. In: *Evaluation of Soil Organic Matter Models Using Existing Long-Term Datasets* [Powlson, D. S., Smith, P., and Smith, J. U. (eds.)]. Volume I38 of *NATO ASI*, pp. 201–224. Springer-Verlag, Berlin, Germany.

Rayner, P. J., Scholze, M., Knorr, W., Kaminski, T., Giering, R., and Widmann, H., 2005. Two decades of terrestrial carbon fluxes from a carbon cycle data assimilation system (CCDAS). *Global Biogeochemical Cycles*, **19**, GB2026, 10.1029/2004GB002254.

Reichstein, M., Ciais, P., and Papale, D. *et al.*, 2006. Reduction of ecosystem productivity and respiration during the European summer 2003 climate anomaly: a joint flux tower, remote sensing and modelling analysis. *Global Change Biology*, **13**, 634–651. doi: 10.1111/j.1365-2486.2006.01224.x.

Reichstein, M., Papale, D., Valentini, R., Aubinet, M., Bernhofer, C., Knohl, A., Laurila, T., Lindroth, A., Moors, E., Pilegaard, K., and Seufert, G., 2007. Determinants of terrestrial ecosystem carbon balance inferred from European eddy covariance sites. *Geophysical Research Letters*, **34**, L01402, doi:10.1029/2006GL027880.

Schimel, D. S., Braswell, B. H., and Holland, E. A. *et al.*, 1994. Climatic, edaphic and biotic controls over storage and turnover of carbon in soils. *Global Biogeochemical Cycles*, **8**, 279–293.

Scholze, M., Knorr, W., Arnell, N. W., and Prentice, I. C., 2006. A climate-change risk analysis for world ecosystems. *Proceedings of the National Academy of Sciences, USA*, **103**, 13116–13120.

Scholze, M., Kaminski, T., Rayner, P., Knorr, W., and Giering, R., 2007. Propagating uncertainty through prognostic carbon cycle data assimilation system simulations, *Journal of Geophysical Research*, **112**, D17305, doi:10.1029/2007JD008642.

Sitch, S., Huntingford, C., and Gedney, *et al.*, 2008. Evaluation of the terrestrial carbon cycle, future plant geography and climate-carbon cycle feedbacks using 5 Dynamic Global Vegetation Models (DGVMs). *Global Change Biology*, **14**, 2015–2039, doi:10.1111/j.1365-2486.2008.01626.x.

Smith, J. U., Bradbury, N. J., and Addiscott, T. M., 1996. SUNDIAL: A user-friendly, PC-based system for simulating nitrogen dynamics in arable land. *Agronomy Journal*, **88**, 38–43.

Smith, L. C., Sheng, Y., MacDonald, G. M., and Hinzman, L. D., 2005. Disappearing Arctic lakes, *Science*, **308**, 1429.

Smith, P., Martino, D., and Cai, Z. *et al.*, 2007. Chapter 8 agriculture. In: *Climate change 2007: Mitigation. Contribution of Working group III to the Fourth Assessment Report of the Intergovernmental Panel on Climate Change* [Metz, B., Davidson, O. R., Bosch, P. R., Dave, R., and Meyer, L. A. (eds.)]. Cambridge University Press, Cambridge, United Kingdom and New York, NY.

Sokolov, A. P., Kicklighter, D. W., Melillo, J. M., Felzer, B. S., Schlosser, C. A., and Cronin, T. W., 2008. Consequences of Considering Carbon-Nitrogen Interactions on the Feedbacks between Climate and the Terrestrial Carbon Cycle. *Journal of Climate*, **21**, 3776–3796, doi:10.1175/2008JCLI2038.1.

Soussana, J. -F., Loiseau, P., Vuichard, N., Ceschia, E., Balesdent, J., Chevallier, T., and Arrouays, D., 2004. Carbon cycling and sequestration opportunities in temperate grasslands. *Soil Use and Management*, **20**, 219–230, doi:10.1079/SUM2003234.

Stainforth, D. A., Aina, T., and Christensen, C. *et al.*, 2005. Uncertainty in predictions of the climate response to rising levels of greenhouse gases *Nature*, **433**, 403–406.

Telles, E. D. C., de Camargo, P. B., and Martinelli, L. A. *et al.*, 2003. Influence of soil texture on carbon dynamics and storage potential in tropical forest soils of Amazonia. *Global Biogeochemical Cycles*, **17**, doi:10.1029/2002GB001953.

Trumbore, S., 2000. Age of organic soil matter and soil respiration: Radiocarbon constraints on belowground C dynamics. *Ecological Applications*, **10**, 399–411.

Trumbore, S. E., and Czimczik, C. I., 2008. An Uncertain Future for Soil Carbon. *Science*, **321**, 1455–1456.

Vuichard, N., Ciais, P., Belelli, L., Smith, P., and Valentini, R., 2008. Carbon sequestration due to the abandonment of agriculture in the former USSR since 1990, *Global Biogeochemical Cycles*, doi:10.1029/2008GB003212, in press.

Williams, M., Schwarz, P. A., Law, B. E., Irvine, J., and Kurpius, M., 2005. An improved analysis of forest carbon dynamics using data assimilation. *Global Change Biology*, **11**, 89–105.

Yuste, J. C., Janssens, I. A., Carrara, A., and Ceulemans, R., 2004. Annual Q10 of soil respiration reflects plant phenological patterns as well as temperature sensitivity. *Global Change Biology*, **10**, doi:10.1111/j.1529-8817.2003.00727.x.

Zeng, N., Qian, H., Munoz, E., and Iacono, R., 2004. How strong is carbon cycle-climate feedback under global warming? *Geophysical Research Letters*, **31**, doi:10.1029/2004GL020904.

Zimov, S. A., Schuur, E. A. G., and Chapin III, F. S., 2006. Permafrost and the Global carbon budget, *Science*, **312**, 1612–1613.

microbial respiration (Thornley and Cannell, 2001). Consequently, an energetic barrier of more recalcitrant C will be buried below the fresh deposits which could reduce or cancel the current assumed responses of decomposition to warming (Fontaine *et al.*, 2004, 2007; Rinnan *et al.*, 2007). However, the decomposition of this deep resistant pool could be activated if, for example, as a result of land management practices, a deeper distribution of fresh C occurs (Fontaine *et al.*, 2007). Furthermore, other experimental data indicate that decomposition could be completely insensitive due to biological adaptation (Luo *et al.*, 2001) or to the influence of other factors such as nutrient availability (Kirschbaum, 2004; Eliasson *et al.*, 2005; Knorr *et al.*, 2005), moisture (Saleska *et al.*, 2003, 2007; Ciais *et al.*, 2005; Davidson and Janssens, 2006) as well as temperature. Each of these assumptions has important repercussions for current predictions of soil carbon turnover and any potential feedbacks from soils to climate.

2. Soils as stores and sources of carbon

Globally, soils contain approximately 1580 Gt of stored carbon, which represents more than twice the stock of carbon held within terrestrial vegetation, and more than twice that presently resident in the atmosphere (Schimel, 1995). A great proportion of the global carbon reservoir is present in organic soils which are estimated to store a third of all terrestrial carbon stocks (Gorham, 1991). In the European Community the quality and quantity of these particular ecosystems has significantly decreased, with surface area losses up to 90% in the majority of the states members. The environmental conditions in these organic rich soils (continuous high precipitation, more than 30 days per annum with risk of frost, frequent cloudiness) have a strong influence on the activities of their communities (plant and animals).

Atmospheric warming is expected to be most pronounced at higher latitudes so that Arctic and upland systems will be particularly influenced by this ecological driver (Sala *et al.*, 2000). Therefore, carbon stores are predicted to respond to climatic change as it has been proven that SOM decomposition rates respond to varying moisture and temperature regimes (Parton *et al.*, 1987; Schimel *et al.*, 1994; Alm *et al.*, 1999). For example, concomitant with a 1°C rise in temperature, soils globally are predicted to release between 10 and 30 Pg of carbon to the atmosphere (Schimel *et al.*, 1994). Furthermore, recent findings suggest that increased temperatures in the UK have been offsetting absorption of carbon by terrestrial sinks and are responsible for carbon losses of 0.6% y^{-1} (relative to the existing soil carbon content) over the past 25 years (Bellamy *et al.*, 2005). This high impact of warming on C fluxes in these particular systems is the result of the stimulation of organic matter mineralisation with associated release of CO₂ to the environment (e.g., Oechel *et al.*, 1993; Lloyd and Taylor, 1994; Trumbore *et al.*, 1996; Grace and Rayment, 2000; Fang and Moncrieff, 2001) and the leaching of

nutrients (dissolved organic carbon, DOC) by increasing temperatures (*e.g.*, Ineson *et al.*, 1998; Tipping *et al.*, 1999). Indeed, current concerns have focussed on the potential risk for these systems to become unstable, *i.e.*, changing its role from ‘sinks’ to ‘carbon sources’ in response to changes in climate and land use (*e.g.*, Gill *et al.*, 2002). In relation to this, ‘the coupling between climate and the terrestrial C cycle’ has been included in the Third and Fourth Reports of the Intergovernmental Panel on Climate Change (IPCC, 2001, 2007) to predict the future responses of terrestrial ecosystems to global change. However, our understanding of the biological mechanisms involved in the regulation of soil C remains limited. This information is central to the development of meaningful strategies in the future.

3. Soils as the most diverse habitats on earth

Environmental change scenarios suggest that the sensitivity of biomes to climate variations is a product of their diversity (Sala *et al.*, 2000). Soil is one of the most diverse habitats on earth and contains one of the most diverse assemblages of living organisms (Giller *et al.*, 1997; Hågvar, 1998). For example, a single gram of soil may contain millions of individuals and several thousand species of bacteria (Torsvik *et al.*, 1994). This is a consequence of the complex physical and chemical nature of the soil. Its porous structure, immense surface area, and extremely variable supply of organic materials, food, water and chemicals mean that various animal, plant and microbial worlds can co-exist simultaneously and find appropriate niches for their development.

Soil communities are so diverse in both size and numbers of species, yet they are still extremely poorly understood and in dire need of further assessment. The easiest and most widely used system for classifying soil organisms is by using body size (length or width) and dividing them into three main groups: macrofauna meso-fauna and micro-biota (Wallwork, 1970; Swift *et al.*, 1979). Unfortunately, the ranges that determine each size group are not exact for all members of each group, often leading to considerable confusion as to whether a particular organism should be considered macro or meso, and so on. More recently, ‘functional classifications’ have been launched for certain groups. They are based on the fact that soil biota are responsible, to a varying degree (depending on the system), for performing vital functions in the soil ecosystem. These functions, performed and often controlled by the myriad of organisms in soils, range from physical effects such as the regulation of soil structure and edaphic water regimes, to chemical and biological processes such as degradation of pollutants, decomposition, nutrient cycling, greenhouse gas emission, carbon sequestration, plant protection and growth enhancement or suppression. The division of soil biota into roots, ecosystem engineers, litter transformers, phytophages and parasites, micro-predators and microflora (Figure 1) is a good example (see Lavelle, 1996), because it also takes into account the potential top-down regulatory controls of larger organisms (*e.g.*, the ecosystem engineers) over smaller ones.



Fig. 1. Functional classification of soil fauna (drawn using information given by Lavelle 1996).

Functional classifications are important because it is the only way to understand the effects of global change on ecosystem functioning. And thus, acting through the diversity of soil organisms, the various climate and land use factors influence 5 main ecosystem functions (decomposition, trace gas flux, nutrient dynamics, soil physical structure, trophic structure). These in turn have both actual and potential feedback effects, through the vegetation and the above ground fauna, and through climate and land use (Heal, 1997).

4. Enchytraeid worms: key stone group in organic soils

Enchytraeid worms (Figure 2) are frequently the most abundant oligochaete invertebrates in carbon rich soils of peatlands and pastures. This group of invertebrates (individual 1–4 mm length) can comprise over 70% of the belowground faunal biomass and have a larger mass (on a live weight basis) than the sheep on a unit area (Coulson and Whittaker, 1978). In spite of the numerical abundance of Nematodes, Acarina and Collembola they never contributed more than 3% of the total biomass (Table 1).

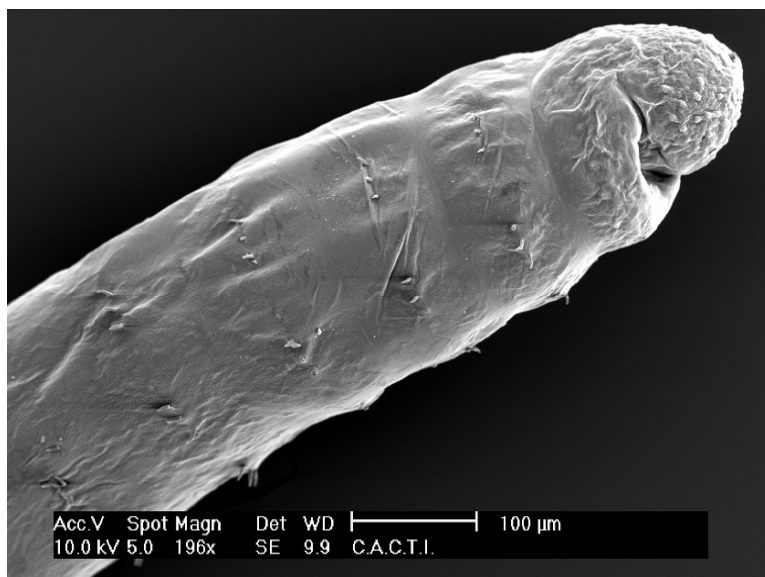


Fig. 2. Scanning electron micrograph (SEM) of *Cognettia sphagnetorum*, a dominant enchytraeid worm in carbon rich soils where it may constitute up to 95% of the total enchytraeid biomass.

Table 1. Population densities (numbers m^{-2} in summer) and biomass of animals on shallow peat soils at Moor House (*Juncus* grasslands) (from Coulson and Whittaker, 1978).

	Density (Numbers m^{-2})	Biomass (g m^{-2})
Enchytraeids	200,000	4.6
Tipulids	2,500	1.96
Nematodes	3,900,000	0.18
Collembola	23,000	0.05
Acari	45,000	0.32
Sheep	0.00013	3.2

These soil animals are distributed worldwide although a recent review study (Briones *et al.*, 2007a) showed that the greatest numbers of these organisms are found in moorlands and associated to pH values between 4 and 5 (Table 2). This comprehensive study also evidenced the strong relationship between climate and their population numbers, with temperature being the most critical factor controlling their geographical distribution. Indeed, enchytraeids have been found at sites with mean annual temperatures (MAT) in excess of 25°C but some genera (*e.g.*, *Bryodrilus*, *Mesenchytraeus*, *Cernosvitoviella*, *Stercucus*) and the species *Buchholzia fallax* have never been recorded at MAT > 12.5°C. Crucially, the usual dominant species in moorland systems (*Cognettia sphagnetorum*) has never been reported at MAT > 16°C and it is not present in sites with hot dry summers.

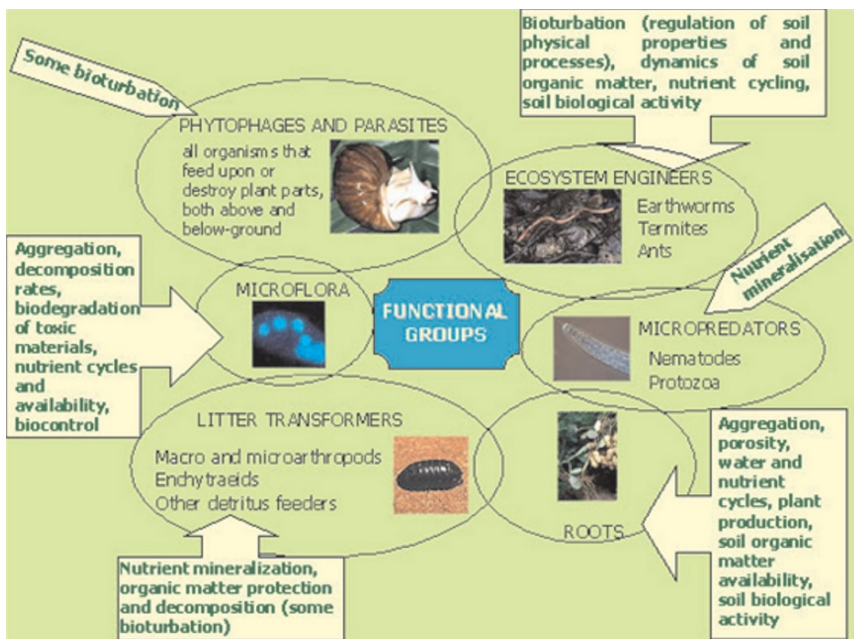


Fig. 1. Functional classification of soil fauna (drawn using information given by Lavelle 1996).

Functional classifications are important because it is the only way to understand the effects of global change on ecosystem functioning. And thus, acting through the diversity of soil organisms, the various climate and land use factors influence 5 main ecosystem functions (decomposition, trace gas flux, nutrient dynamics, soil physical structure, trophic structure). These in turn have both actual and potential feedback effects, through the vegetation and the above ground fauna, and through climate and land use (Heal, 1997).

4. Enchytraeid worms: key stone group in organic soils

Enchytraeid worms (Figure 2) are frequently the most abundant oligochaete invertebrates in carbon rich soils of peatlands and pastures. This group of invertebrates (individual 1–4 mm length) can comprise over 70% of the belowground faunal biomass and have a larger mass (on a live weight basis) than the sheep on a unit area (Coulson and Whittaker, 1978). In spite of the numerical abundance of Nematodes, Acarina and Collembola they never contributed more than 3% of the total biomass (Table 1).

Table 2. Results from meta-analysis and non-parametric ANOVA for enchytraeid abundance data of 44 published papers (from Briones *et al.* 2007a).

Higher Enchytraeid Densities	
Habitat	Mostly moorlands but also grasslands
Soil type	Moder, loamy, brown, calcareous and podzol
Soil pH	4–5
Climate regime	Main association is temperate rainy climates, moist all year with moderate or cold summers (<i>i.e.</i> , < 4 months with means >10°C)
Mean annual temperature (MAT)	0–16°C
Mean monthly rainfall (MMR)	No apparent relationship

Enchytraeids also exhibit an aggregated horizontal distribution, giving rise to a high spatial and temporal heterogeneity (Didden, 1993). It also seems to be a common feature that populations are concentrated in the top soil layers with significantly higher numbers being found in the first 4 cm of the soil profile and gradually decreasing with depth (Briones *et al.*, 2007a). Living in the surface horizons in this way makes the population vulnerable to the regnant conditions, and consequently, these key species could be lost if atmospheric temperatures increase, particularly at sites where the mean annual temperature crosses the temperature boundaries identified above, with important implications for those systems where these species are dominant (*e.g.*, moorlands and tundra biomes) (Briones *et al.*, 2007a).

In addition, field and controlled laboratory experiments showed that the potential effects of climate change on these organisms is highly specific, with warmer temperatures having a positive effect on the reproduction rates of the more tolerant species and a detrimental effect on the less resilient ones (Briones *et al.*, 1997). For certain species survival is attained by vertical migration (Springett *et al.*, 1970; Briones *et al.*, 1997), however readily available organic matter is concentrated in the first top 10 cm and could limits the extent to which downward faunal movements occur. Furthermore, migration to the deeper layers can also become an unsuitable strategy if the new conditions persist.

5. The link between climate, soil biology and the carbon cycle. Implications for climate change modeling

It is now accepted that the diversity, abundance and activity of soil organisms (bacteria, fungi, mesofauna and macrofauna) will be central to the capacity of soils to both sequester and respire carbon inputs derived from net primary producers

(Bradford *et al.*, 2002). However, they are often underestimated in carbon turnover predictions and uncertainties will remain until the interaction between soil animals and soil carbon stocks is better represented in soil carbon models. Some examples of how soil biology could challenge previous assumptions of the temperature responses of SOM decomposition are given below.

5.1. Dissolved organic carbon (DOC) release from soils

The observed rapid increase in the DOC concentrations in the rivers draining from peatland systems has drawn scientific attention as it is considered as an unequivocally sign of destabilization (Freeman *et al.*, 2001a; Tranvik and Jansson, 2002), with important implications for water quality (Worrall *et al.*, 2003). Nonetheless, the causes for the losses of this globally important source of carbon remain uncertain.

Field studies have shown that increasing temperatures have a major effect on DOC release, with maximum concentrations occurring during the summer (Tipping *et al.*, 1999). Furthermore, the reported increase in DOC concentrations in 11 English lakes during 1988–2000 and the parallel increment of phenolic compounds in peat soils in response to rising temperatures led Freeman *et al.* (2001a) to conclude that warmer conditions are responsible for the export of peatland carbon to the oceans. Additionally, the fact that the observed seasonal increases in DOC production mimic the peaks of solar radiation (Harrison *et al.*, 2008) confirms previous assumptions that DOC release is linked to primary production (Fitter *et al.*, 1999).

However, these increases are not fully explained by the direct effect of increasing temperatures alone (Pastor *et al.*, 2003). And for example, the observed reductions in sulphur emissions during the last 20 years in the UK has been identified as a key cause of rising DOC in north America and northern Europe (Evans *et al.*, 2006; Monteith *et al.*, 2007) due to decreased soil water acidity. Hydrology has been considered to be another contributing factor to increasing DOC concentrations and thus, the observed increases in the discharge capacity of the rivers (Forsberg, 1992) could be related to DOC release, although this relationship between DOC concentrations and discharge volume has not always been recorded (Evans *et al.*, 2002; Worrall *et al.*, 2003).

Other possible explanations for carbon losses in the soil solution are related to the iron mobility (Lundström, 1993), possibly as result of its role in the formation of organic matter complexes. Alternatively, the increase in the concentrations of greenhouse gasses, such as CO₂, in the atmosphere and their effects on plant structure (increasing dominance of vascular plants in detriment of mosses) and root exudation could also be responsible for these carbon exportations (Freeman *et al.*, 2004).

It is also possible that increased aerobic conditions during the summer months, as a result of lower water levels (Wetherald and Manabe, 1999), could remove the enzymatic constraints causing the accumulation of phenolic compounds in wetlands



Fig. 3. Dissolved organic carbon (DOC) release from microcosms containing soil from the 0–3 cm, 3–6 cm and 6–9 cm layers in the absence and presence of enchytraeids.

and peatlands (Freeman *et al.*, 2001b) and thus, promoting decomposition and the subsequent release of DOC. In relation to this, other biological changes such as the temperature induced increases of enchytraeid numbers in C rich soils have also been correlated with leaching of DOC (Figure 3), suggesting that warmer temperatures will result in an increase in the turnover of soil carbon and other nutrients (Briones *et al.*, 1998a,b; Cole *et al.*, 2000, 2002a,b). Therefore, a better understanding of the biological mechanisms responsible for the mobilization of this long-standing carbon is essential to develop more realistic predictions of the future carbon export rates from peatlands.

5.2. Carbon dioxide (CO_2) emissions from soils

Soil respiration is the second largest pathway in the global carbon cycle, producing an annual global flux of $68\text{--}100 \times 10^5 \text{ g C y}^{-1}$ (Musselman and Fox, 1991; Raich and Schlesinger, 1992). With such a significant flux, even small changes could be significant on global scale. Due to a large increase in anthropogenic CO_2 emissions into the carbon cycle, global surface temperature has been seen to increase in $0.74 \pm 0.18 \text{ }^{\circ}\text{C}$ over the period 1906–2005 (IPCC, 2007).

However, despite the importance of soil global carbon cycles, little is known about the way soil will respond to future climate predictions. Some studies suggest the terrestrial biosphere is gaining carbon at a rate of $2 \pm 1 \text{ Gt C y}^{-1}$ (Steffen *et al.*, 1998; Royal Society, 2001), but concerns also exist that, due to increases of heterotrophic respiration in a warming climate, soil will convert to a carbon source (positive feedback) accentuating the problem (Woodwell *et al.*, 1998; Cox *et al.*, 2000; Lenton, 2000; Sarmiento, 2000; Cramer *et al.*, 2001; Powlson, 2005; Heimann and Reichstein, 2008).

Cox *et al.*'s (2000) model incorporating the response of biota to warmer climates to predict future climate, contains large uncertainties with regard the respiration of organic matter in soils. In particular, the temperature sensitivity of soil carbon decomposition is identified as an important determinant of carbon driven climate change in the future (Trumbore *et al.*, 1996; Kätterer *et al.*, 1998; Grace and Rayment, 2000; Holland *et al.*, 2000; Fang and Moncrieff, 2001; Thornley

and Cannell, 2001; Sanderman *et al.*, 2003). However, this response of SOM decomposition to temperature is hotly debated and several answers to this question have been published in the recent literature:

(i) *Rising temperatures will result in a faster decomposition rate of SOM, releasing additional amounts of CO₂ and accelerating climate change.* This will be the consequence of the positive influence of temperature on microbial activities (e.g., Knorr *et al.*, 2005).

A conventional way to express the response of soil heterotrophic respiration to temperature increases is the soil respiratory quotient Q_{10} which has been widely used in several climate models (e.g., HadCM3LC). Within this framework it has been estimated that soil heterotrophic respiration and CO₂ production doubles with every 10°C increase in atmospheric temperature, *i.e.*, $Q_{10} = 2$ (Sarmiento, 2000). However, this simple exponential function is only true under specific conditions, *i.e.*, providing that soil substrate availability does not become limiting (Knorr *et al.*, 2005), and for reactants with an activation energy around 50 kJ mol⁻¹ incubated at temperatures between 273 K and 303 K (Davidson and Janssens, 2006). Other difficulties in their application derive from mathematical restrictions in its calculation (Tuomi *et al.*, 2008) and its natural variation with soil depth (Graf *et al.*, 2008).

Furthermore, when soil biology is taken into account significant increases in the Q_{10} value are observed. For example, under warmer conditions (>10°C) the interactions between mesofauna and microorganisms could increase the respiratory quotient over 3.4 (Briones *et al.*, 2004). This higher Q_{10} is closer to the upper limit forecast by previous models ($Q_{10} = 3.63$) (Lenton and Huntingford, 2003), and confirms stronger sensitivity of soil respiration to temperature in the presence of invertebrates. This has important implications for future climate predictions, and concomitant with temperature increases we will see an increase in the biomass of these soil invertebrates. Such animal increases have been observed in the field (Briones *et al.*, 1997; Cole *et al.*, 2002b) and have the potential to increase soil CO₂ production that could, in turn, contribute further to climate forcing. Indeed the results of a simple regression model between atmospheric temperature, enchytraeid biomass and total soil CO₂ for two organic soils suggest that soil warming could produce important increases in soil CO₂ release (Table 3). This model assumes that the role of enchytraeids in this process is biomass dependent and that soil temperature and moisture levels are maintained within a range suitable for the survival and reproduction of these organisms.

However, this observed soil respiration enhancement in response to warming could be a transient response and therefore, heterotrophic 'acclimatization' could be an important factor in reducing soil CO₂ release in the longer term (Luo *et al.*, 2001). From this study it is also anticipated that this process would be less important in ecosystems with high carbon content than in those with low carbon storage. However, evidence suggests that there is not thermal adaptation of microbial communities and consequently, the temperature sensitivity of the C mineralisation rate is not affected by the microflora structure (Vanhala *et al.*, 2008). Furthermore,

Table 3. Potential soil CO₂ production at current and elevated mean annual atmospheric temperatures at 60% soil moisture for Sourhope and Great Dun Fell soils. Sourhope mean annual temperature (1993–2003) was 7.38 ± 0.15°C and Great Dun Fell mean annual temperature (1993–2003) was 5.97 ± 0.12°C. Actual biomass is that measured from soil cores (0–10 cm) obtained from field sites. Calculations were performed based on results obtained in a previous microcosm experiment (Briones *et al.* 2004). Predicted biomass represents biomass calculated as a function of temperature, *i.e.*, (biomass = 0.05 × temperature) – 0.0591; R = 0.78, p < 0.04, n = 12. Total respiration was calculated as a function of biomass *i.e.*, 1 mg biomass = 77.0 ± 6.05 CO₂-C µg mg enchytraeid tissue⁻¹ day⁻¹. Total respiration = (62.802 × biomass) + 3.6508; R = 0.65, p < 0.05, n = 8. Estimates of potential soil respiration annotated with different letters were significantly different (ANOVA; p < 0.01).

Site	Temperature °C	Enchytraeid Biomass (g m ⁻²)	Potential Soil Respiration CO ₂ -C (mg m ⁻² day ⁻¹)
Sourhope grassland			
Actual biomass	Ambient	0.30 ± 0.04 ^a	18.60 ± 2.39 ^a
Predicted biomass	+2.6	0.39 ± 0.05 ^{ab}	29.88 ± 3.83 ^b
Predicted biomass	+5.0	0.46 ± 0.06 ^b	35.57 ± 4.56 ^c
Great Dun Fell moor			
Actual biomass	Ambient	5.17 ± 0.45 ^c	324.81 ± 28.31 ^d
Actual biomass*	+2.6	5.28 ± 0.99 ^{cd}	331.90 ± 61.90 ^d
Predicted biomass	+2.6	6.73 ± 0.59 ^{de}	422.25 ± 36.79 ^d
Predicted biomass	+5.0	8.07 ± 1.54 ^e	621.25 ± 118.35 ^e

Actual biomass* at ambient and +2.6°C in the Great Dun Fell moor soil were taken from Briones *et al.* (1997, 1998a). Actual biomass at ambient in the Sourhope grassland was taken from Briones *et al.* (2004).

our results in organic soils indicate that the impacts of soil warming on frequently large enchytraeid populations and their interactions with microbial activities will be determinant to the C sink/source function of these ecosystems and that the net effect of increasing atmospheric temperatures on soil carbon stocks will be determined by the interaction between short-term ‘ecological adaptation’ and longer term ‘acclimatization’ of soil respiration (Oechel *et al.*, 2000, Luo *et al.*, 2001).

(ii) *Temperature does not dominate the carbon balance.* After compiling decomposition data from 82 sites on five continents Giardina and Ryan (2000) found that decomposition rates are not controlled by temperature limitations to microbial activities and consequently, global warming will not result in a positive feedback from soil to climate.

However, other studies assume that although biological processes respond to temperature in an exponential way they are not affected by the atmospheric CO₂ concentrations (Kirschbaum, 2006; Davidson and Janssens, 2006) and consequently, led to the erroneous conclusion that positive feedbacks will not be observed until the temperature stimulating effect on soil respiration exceeds that of CO₂ fertilisation (Heimann and Reichstein, 2008).

There are other factors besides temperature which could alter SOM decomposition rates in response to climate change. Among them, nitrogen limitation can alter plant productivity (and hence the rate of uptake of CO₂ from the atmosphere), plant C allocation and enhance decomposition of lignin by fungi (Heimann and Reichstein, 2008). This has led to claim for the need of an Earth-system perspective of the nitrogen–carbon–climate interactions to reduce uncertainties in the climate change projections (Gruber and Galloway, 2008).

(iii) The temperature sensitivity of SOM decomposition varies with the different carbon pools existing in the soil. This conclusion has raised a new debate not only regarding the number of these hypothetical pools to be considered in the models, but also in relation to their dynamic behaviour in response to warming.

First attempts to obtain a more realistic simulation of SOM matter turnover included two pools: (i) a young, rapidly turned over labile pool and (ii) an older, longer lived non labile pool. The investigation of the responses of these two SOM pools to changes in temperature has resulted in opposite conclusions. One current opinion is that the decomposition of soil labile carbon is sensitive to temperature variation whereas resistant components are insensitive (Liski *et al.*, 1999; Giardina and Ryan, 2000; Thornley and Cannell, 2001). This is derived from the idea that most respired carbon dioxide is derived from recently deposited or ‘young’ labile SOM stocks (Trumbore, 2000). Consequently, as labile C pools become depleted, by increasing heterotrophic activity, a decrease in the rate of soil respiration will be observed (Kirschbaum, 2004; Eliasson *et al.*, 2005; Knorr *et al.*, 2005; Hartley *et al.*, 2007).

In contrast, other authors (*e.g.*, Fang *et al.*, 2005; Reichstein *et al.*, 2005; Connen *et al.*, 2006) claimed that both pools show the same temperature sensitivity, and resistant carbon responds equally to temperature variations as labile carbon pools. From this, the observed decline in soil basal respiration with incubation time is the result of the rapid degradation of the more labile substrates so that the resistant C component contributed in a greater proportion to soil respiration.

However, this conclusion was challenged by Knorr *et al.* (2005) who re-examined Giardina and Ryan data and used a model containing three carbon pools, *i.e.*, fast, intermediate and very slow. The outcome of this study shows that increasing temperatures accelerate SOM decomposition rates resulting in an even greater positive feedback to climate than previously thought. This is the consequence of the non-labile soil organic carbon being more sensitive to temperature than labile soil organic carbon. Accordingly, the temperature sensitivity of SOM decomposition increases with substrate recalcitrance and hence determining the magnitude of the feedback response to the climate system (Hartley and Ineson, 2008).

Multipool carbon models such as CENTURY (Parton *et al.*, 1987) and ROTH-C (Jenkinson, 1990) incorporate up to seven conceptual pools, although reliable measures of the decomposability of these various pools has been only partly successful (Davidson and Janssens, 2006). Further research using more powerful techniques

to better characterise the diversity of soil substrates found in soils is therefore needed to determine the stability of SOM to future temperature increases.

(iv) *The temperature sensitivity of SOM turnover is also determined by the temperature sensitivity of soil biology.* It has already been shown that microbial (Fontaine *et al.*, 2004) and certain key soil invertebrates are important regulators of soil carbon storage (Briones *et al.*, 1998b, 2004), with their activities being constrained by prevailing climatic conditions. Yet, despite considerable knowledge of soil invertebrate ecology and their role in nutrient cycling (e.g., Coleman *et al.*, 2004) their contribution to net terrestrial carbon balances has not yet been addressed (Fang *et al.*, 2005; Knorr *et al.*, 2005; Wall *et al.*, 2008). This omission is of particular concern when attempts are made to predict the effects of climate change on the decomposition and respiration of old non-labile carbon from organic soils.

For example, Fontaine *et al.* (2004, 2007) found that the addition of labile materials to the soil could stimulate the decomposition of 'old' carbon. Similarly, although studies indicate that enchytraeid worms assimilate carbon components which are predominantly of material that is ca. 5–10 years old (Briones and Ineson, 2002), recent findings suggest that warming induced changes in below-ground invertebrate populations increased the turnover of old non labile soil carbon (Briones *et al.*, 2007b). Therefore, feeding adaptation by soil organisms will increase the temperature sensitivity of non labile soil carbon to offset acclimatization of soil respiration (Oechel *et al.*, 2000; Luo *et al.*, 2001).

Organic soils such as peatlands and upland pastures represent a large global carbon reservoir with decomposition being constrained by low biological activity due to cold temperature regimes (Moorhead and Reynolds, 1993). Furthermore, molecular oxygen limitation on a single enzyme (phenol oxidase) prevents these systems from releasing 455 Gt of stored carbon into the atmosphere (Freeman *et al.*, 2001b). Increased aeration through, for example, enchytraeid burrowing and warmer temperatures would then have the potential to accelerate carbon losses.

Taken together it becomes clear that both the 'biological' and 'temperature' sensitivity of SOM decomposition are both critical for modelling changes in soil carbon stocks. It seems that increasing atmospheric temperatures will result in a rapid decomposition of labile SOM and, as the ordinarily exploited sources of food become limited, the 'biological feeding flexibility' of certain soil organisms (e.g., enchytraeids) will lead to increased forage of older organic substrates and hence a progressive respiration of old, previously unused soil carbon to the atmosphere. These findings clearly contradict the opinion that non labile soil carbon is insensitive to temperature increases (Liski *et al.*, 1999; Thornley and Cannell, 2001; Luo *et al.*, 2001), but do confirm that the mechanism for the release of these resistant C pools can be attributed to 'ecological adaptation' of soil biology.

6. Conclusions

The future of our terrestrial sink under warmer scenarios is highly controversial with no clear trends of decreasing soil carbon with increasing temperature regimes at least for certain parts of the world (e.g., Kirschbaum, 2000; Thornley and Cannell, 2001). Part of the problem is the lack of agreement in the direction of these responses, *i.e.*, top-down (e.g., climate variables (temperature, rainfall patterns), CO₂ concentrations in the atmosphere, plant growth, etc.) or bottom-up (e.g., nutrient availability, chemical reactions, substrate complexity and soil biology) regulation. Soils are very heterogeneous systems where a great number of complex interactions occur, not only between below-ground components but also between plants above and organisms and nutrients below and therefore, predicting decomposition rates in a future warmer scenario is not a simple task and requires a multi-disciplinary approach.

Another conflicting issue is that temperature dependencies in the carbon models are usually expressed using a fixed Q₁₀ value without taking into account the intrinsic characteristics of the soil (e.g., organic matter content, physical protection of soil aggregates, nutrient availability, enzymatic activities and the structure of the soil communities) and ecosystem processes (e.g., changes in net primary production and variations in the potential evapotranspiration:precipitation ratio across different biomes). Obviously, an understanding of soil respiration and its potential responses to climate is critical to predict future changes in the terrestrial carbon pools (van Hees *et al.*, 2005).

Importantly, the temperature sensitivity of different carbon pools has become an important source of uncertainty in current climate driven carbon models. From the published literature it is clear that using multipool soil carbon models provides a more realistic estimate of the fate of global carbon (see also Davidson and Janssens, 2006). And thus, re-examination of previous published data using three different carbon pools instead of one contradicted previous conclusions (Knorr *et al.*, 2005) and led to a greater appreciation of the importance of the different organic fractions in the soil responses to climate change (Powlson, 2005). Similar re-analyses of previous published data have been produced by Smith *et al.* (2007) who concluded that the predicted carbon losses for the England and Wales (Bellamy *et al.*, 2005) are only possible if an unrealistic Q₁₀ value of 13 is included in the model and consequently, only 10–20% of the overall losses reported are explained by climate change alone. However, for these calculations a single pool model and a fixed value of Q₁₀ of 2 was used which perhaps questions this new re-assessment. More research is needed to identify all the different pools which integrate SOM and to determine the influence of a great number of factors (including chemical protection, the effect of CO₂ fertilisation on primary productivity, N deposition, frequency of droughts, land use, etc.) which may affect the decomposition rates of the different soil C compounds.

Surprisingly, soil biology is usually underestimated in most models despite the fact that some keystone organisms (such as enchytraeids) do have the potential to exert a positive influence on C release from organic soils (e.g., Briones *et al.*, 1998a,b, 2004) and more importantly, to 'unlock' previously unused C sources (Briones *et al.*, 2007b), adding more information to the current debates on the temperature sensitivity of different carbon pools described above. Therefore, they could be used as measurable indices of biological sensitivity to climatic changes which should be monitored at selected 'vulnerable' ecosystems (such as those with the higher carbon densities, *i.e.*, wetlands, peatlands and permafrost soils) to detect any important changes in their carbon storage function.

In summary, to answer the question of how climate change under different changing land scenarios will alter the carbon balance in our terrestrial sink will require of more experimental work at the communities and processes level. Only with this type of information it would be possible to calculate more realistic Q_{10} values and to define more adequately the factors which need to be included in the models.

References

Alm, J., Schulman, L., Walden, J., Nykanen, H., Martikainen, P.J., and Silvola, J., 1999, Carbon balance of a boreal bog during a year with an exceptionally dry summer, *Ecology*, 80: 161–174.

Bellamy, P.H., Loveland, P.J., Bradley, R.I., Lark, R.M., and Kirk, G.J.D., 2005, Carbon losses from all soils across England and Wales 1978–2003, *Nature*, 437: 245–248.

Bradford, M.A., Jones, T.H., Bardgett, R.D., Black, H.I.J., Boag, B., Bonkowski, M., Cook, R., Eggers, T., Gange, A.C., Grayston, S.J., Kandeler, E., McCaig, A.E., Newington, J.E., Prosser, J.I., Setälä, H., Staddon, P.L., Tordoff, G.M., Tscherko, D., and Lawton, J.H., 2002, Impacts of soil faunal community composition on model grassland ecosystems, *Science*, 298: 615–618.

Briones, M.J.I. and Ineson, P., 2002, Use of ^{14}C carbon dating to determine feeding behaviour of enchytraeids, *Soil Biology and Biochemistry*, 34: 881–884.

Briones, M.J.I., Ineson, P., and Pearce, T.G., 1997, Effects of climate change on soil fauna; responses of enchytraeids, Diptera larvae and tardigrades in a transplant experiment, *Applied Soil Ecology*, 6: 117–134.

Briones, M.J.I., Carreira, J., and Ineson, P., 1998a, *Cognettia sphagnorum* (Enchytraeidae) and nutrient cycling in organic soils: a microcosm experiment, *Applied Soil Ecology*, 9: 289–294.

Briones, M.J.I., Ineson, P., and Poskitt, J., 1998b, Climate change and *Cognettia sphagnorum*: effects on carbon dynamics in organic soils, *Functional Ecology*, 12: 528–535.

Briones, M.J.I., Poskitt, J., and Ostle, N., 2004, Influence of warming and enchytraeid activities on soil CO_2 and CH_4 fluxes, *Soil Biology and Biochemistry*, 36: 1851–1859.

Briones, M.J.I., Ineson, P., and Heinemeyer, A., 2007a, Predicting potential impacts of climate change on the geographical distribution of enchytraeids: a meta-analysis approach, *Global Change Biology*, 13: 2252–2269.

Briones, M.J.I., Ostle, N., and Garnett, M.H., 2007b, Invertebrates increase the sensitivity of non-labile carbon to climate change, *Soil Biology and Biochemistry*, 39: 816–818.

Ciais, P., Reichstein, M., Viovy, N., Granier, A., Ogee, J., Allard, V., Aubinet, M., Buchmann, N., Bernhofer, C., Carrara, A., Chevallier, F., De Noblet, N., Friend, A.D., Friedlingstein, P., Grunwald, T., Heinesch, B., Keronen, P., Knohl, A., Krinner, G., Loustau, D., Manca, G., Matteucci, G., Miglietta, F., Ourcival, J.M., Papale, D., Pilegaard, K., Rambal, S., Seufert, G., Soussana, J.F., Sanz, M.J., Schulze, E.D., Vesala, T., and Valentini, R.E., 2005, Europe-wide reduction in primary productivity caused by the heat and drought in 2003, *Nature*, 437: 529–533.

Cole, L., Bardgett, R.D., and Ineson, P., 2000, Enchytraeid worms (Oligochaeta) enhance mineralisation of carbon in organic upland soils, *European Journal of Soil Science*, 51: 185–192.

Cole, L., Bardgett, R.D., Ineson, P., and Hobbs, P.J., 2002a, Enchytraeid worm (Oligochaeta) influences on microbial community structure, nutrient dynamics and plant growth in blanket peat subject to warming, *Soil Biology and Biochemistry*, 34: 83–92.

Cole, L., Bardgett, R.D., Ineson, P., and Adamson, J.K., 2002b, Relationships between enchytraeid worms (Oligochaeta), climate change and the release of dissolved organic carbon from blanket peat in northern England, *Soil Biology and Biochemistry*, 34: 599–607.

Coleman, D.C., Crossley, D.A. Jr., and Hendrix, P.F., 2004, *Fundamentals of Soil Ecology*, Second Edition, Elsevier Academic Press, Burlington.

Connen, F., Leifeld, J., Seth B., and Alewell, C., 2006, Warming mineralises young and old soil carbon equally, *Biogeosciences*, 3: 515–519.

Coulson, J.C. and Whittaker, J.B., 1978, Ecology of moorland animals. In: *Production Ecology of British Moors and Montane Grasslands*. (Eds. O.W. Heal and D.F. Perkins), pp. 52–93, Springer-Verlag, Berlin.

Cox, P.M., Betts, R.A., Jones, C.D., Spall, S.A., and Totterdell, I.J., 2000, Acceleration of global warming due to carbon-cycle feedbacks in a coupled climate model, *Nature*, 408: 184–187.

Cramer, W., Bondeau, A., Woodward, F.I., Prentice, I.C., Betts, R.A., Brovkin, V., Cox, P.M., Fisher, V., Foley, J., Friend, A.D., Kucharik, C., Lomas, M.R., Ramankutty, N., Sitch, S., Smith, B., White, A., and Young-Molling, C., 2001, Global responses of terrestrial ecosystem structure and function to CO₂ and climate change: results from six dynamic vegetation models, *Global Change Biology*, 4: 217–227.

Davidson, E.A., and Janssens, I.A., 2006, Temperature sensitivity of soil carbon decomposition and feedbacks to climate change, *Nature*, 440: 165–173.

Didden, W.A.M., 1993, Ecology of terrestrial Enchytraeidae, *Pedobiologia*, 37: 2–29.

Eliasson, P.E., McMurtrie, R.E., Pepper, D.A., Strömgren, M., Linder, S., and Ågren, G.I., 2005, The response of heterotrophic CO₂ flux to soil warming, *Global Change Biology*, 11: 167–181.

Evans, C.D., Freeman, C., Monteith, D.T., Reynolds, B., and Fenner, N., 2002, Climate change – terrestrial export of organic carbon – reply, *Nature*, 415: 862.

Evans, C.D., Chapman, P.J., Clark, J.M., Monteith, D.T., and Cresser, M.S., 2006, Alternative explanations for rising dissolved organic carbon export from organic soils, *Global Change Biology*, 12: 2044–2053.

Fang, C.M., and Moncrieff, J.B., 2001, The dependence of soil CO₂ efflux on temperature, *Soil Biology and Biochemistry*, 33: 155–165.

Fang, C.M., Smith, P., Moncrieff, J.B., and Smith, J.U., 2005, Similar response of labile and resistant soil organic matter pools to changes in temperature, *Nature*, 433: 57–59.

Fitter, A.H., Self, G.K., Brown, T.K., Bogie, D.S., Graves, J.D., Benham, D., and Ineson, P., 1999, Root production and turnover in an upland grassland suggested to artificial soil warming respond to radiation flux and nutrients, not temperature, *Oecologia*, 120: 575–581.

Fontaine, S., Bardoux, G., Abbadie, L., and Mariotti, A., 2004, Carbon input to soil may decrease soil carbon content, *Ecology Letters*, 7: 314–320.

Fontaine, S., Barot, S., Barre, P., Bdioui, N., Mary, B., and Rumpel, C., 2007, Stability of organic carbon in deeper soil layers controlled by fresh carbon supply, *Nature*, 450: 277–280.

Forsberg, C., 1992, Will an increased greenhouse impact in Fennoscandia give rise to more humic and coloured lakes? *Hydrobiologia*, 229: 51–58.

Freeman, C., Evans, C.D., Monteith, D.T., Reynolds, B., and Fenner, N., 2001a, Export of organic carbon from peat soils, *Nature*, 412: 785.

Freeman, C., Ostle, N., and Kang, H., 2001b, An enzymic latch on a global carbon store, *Nature*, 409: 149.

Freeman, C., Fenner, N., Ostle, N.J., Kang, H., Dowrick, D.J., Reynolds, B., Lock, M.A., Sleep, D., Hughes, S., and Hudson, J., 2004, Export of dissolved organic carbon from peatlands under elevated carbon dioxide levels, *Nature*, 430: 195–198.

Giardina, C.P., and Ryan, M.G., 2000, Evidence that the decomposition of carbon does not vary with temperature, *Nature*, 404: 858–861.

Gill, R.A., Polley, H.W., Johnson, H.B., Anderson, L.J., Maherli, H., and Jackson, R.B., 2002, Nonlinear grassland responses to past and future atmospheric CO₂, *Nature*, 417: 279–282.

Giller, K.E., Beare, M.H., Lavelle, P., Izac, A.M.N., and Swift, M.J., 1997, Agricultural intensification, soil biodiversity and agroecosystem function, *Applied Soil Ecology*, 6: 3–16.

Gorham, E., 1991, Northern peatlands – role in the carbon-cycle and probable responses to climatic warming, *Ecological Applications*, 1: 182–195.

Grace, J., and Rayment, M., 2000, Respiration in the balance, *Nature*, 404: 819–820.

Graf, A., Weihermüller, L., Huisman, J.A., Herbst, M., Bauer, J., and Vereecken, H., 2008, Measurement depth effects on the apparent temperature sensitivity of soil respiration in field studies, *Biogeosciences*, 5: 1175–1188.

Gruber, N., and Galloway, N., 2008, An Earth-system perspective of the global nitrogen cycle, *Nature*, 451: 293–296.

Hågvar, S., 1998, The relevance of the Rio-Convention on biodiversity to conserving the biodiversity of soils, *Applied Soil Ecology*, 9: 1–7.

Harrison, A.F., Taylor, K., Scott, A., Poskitt, J., Benham, D., Grace, J., Chaplow, J., and Rowland, P., 2008, Potential effects of climate change on DOC release from three different soil types on the Northern Pennines UK: examination using field manipulation experiments, *Global Change Biology*, 14: 687–702.

Hartley, I.P., Heinemeyer, A., and Ineson, P., 2007, Effects of three years of soil warming and shading on the rate of soil respiration: substrate availability and not thermal acclimation mediates observed response, *Global Change Biology*, 13: 1761–1770.

Hartley, I.P., and Ineson, P., 2008, Substrate quality and the temperature sensitivity of soil organic matter decomposition, *Soil Biology and Biochemistry*, 40: 1567–1574.

Heal, O.W., 1997, Effects of global change on diversity-function relationships in soil. In: *Functional Implications of Biodiversity in Soil* (Ed. V. Wolters), pp. 27–40, *Ecosystems Research Report No. 24*, European Commission, Belgium.

Heiman, M., and Reichstein, M., 2008, Terrestrial ecosystem carbon dynamics and climate feedbacks, *Nature*, 451: 289–292.

Holland, E.A., Neff, J.C., Townsend, A.R., and McKeown, B., 2000, Uncertainties in the temperature sensitivity of decomposition in tropical and subtropical ecosystems: implications for models, *Global Biogeochemical Cycles*, 14: 1137–1151.

Ineson, P., Taylor, K., Harrison, A.F., Poskitt, J., Benham, D.G., Tipping, E., and Woof, C., 1998, Effects of climate change on nitrogen dynamics in upland soils. 1. A transplant approach, *Global Change Biology*, 4: 143–152.

IPCC, 2001, In: *Climate Change 2001: The Scientific Basis* (Eds. J.T. Houghton, B.A. Callander, and S.K. Varney), pp. 1–896, Cambridge University Press896.

IPCC, 2007, In: *Climate Change 2007: The Physical Science Basis. Contribution of Working Group I to the Fourth Assessment Report of the Intergovernmental Panel on Climate Change* (Eds. S. Solomon, D. Qin, M. Manning, Z. Chen, M. Marquis, K.B. Averyt, M. Tignor, and H.L. Miller), Cambridge University Press.

Jenkinson, D.S., 1990, The turnover of organic carbon and nitrogen in soil, *Philosophical Transactions Royal Society B*, 329: 361–368.

Kätterer, T., Reichstein, M., Andrén, O., and Lomander, A., 1998, Temperature dependence of organic matter decomposition: a critical review using literature analyzed with different models, *Biology and Fertility of Soils*, 27: 258–262.

Kirschbaum, M.U.F., 2000, Will changes in soil organic carbon act as a positive or negative feedback on global warming, *Biogeochemistry*, 48: 21–51.

Kirschbaum, M.U.F., 2004, Soil respiration under prolonged soil warming: are rate reductions caused by acclimation or substrate loss? *Global Change Biology*, 10: 1870–1877.

Kirschbaum, M.U.F., 2006, The temperature dependence of organic-matter decomposition – still a topic of debate, *Soil Biology and Biochemistry* 38: 2510–2518.

Knorr, W., Prentice, I.C., House, J.I., and Holland, E.A., 2005, Long-term sensitivity of soil carbon turnover to warming, *Nature*, 433: 298–301.

Lavelle, P., 1996, Diversity of soil fauna and ecosystem function, *Biology International*, 33: 3–16.

Lenton, T.M., 2000, Land and ocean carbon cycle feedback effects on global warming in a simple Earth system model, *Tellus*, 52: 1159–1188.

Lenton, T.M., and Huntingford, C., 2003, Global terrestrial carbon storage and uncertainties in its temperature sensitivity examined with a simple model, *Global Change Biology*, 9: 1333–1352.

Liski, J., Ilvesniemi, H., Mäkelä, A., and Westman, C.J., 1999, CO₂ emissions from soil in response to climatic warming are overestimated-The decomposition of soil organic matter is tolerant of temperature, *Ambio*, 28: 171–174.

Luo, Y.Q., Wan, S.Q., Hui, D.F., and Wallace, L.L., 2001, Acclimatization of soil respiration to warming in a tall grass prairie, *Nature*, 413: 622–625.

Lloyd, J., and Taylor, J.A., 1994, On the temperature dependence of soil respiration, *Functional Ecology*, 8: 315–323.

Lundström, U.S., 1993, The role of organic acids in the soil solution chemistry of a podzolized soil, *Journal of Soil Science*, 44: 121–133.

Monteith, D.T., Stoddard J.L., Evans, C.D., de Wit, H.A., Forsius, M., Høgåsen, T., Wiklander, A., Skjelkvåle, B.L., Jeffries, D.S., Vuorenmaa, J., Keller, B., Kopácek, J., and Vesely, J., 2007, Dissolved organic carbon trends resulting from changes in atmospheric deposition chemistry, *Nature*, 450: 537–541.

Moorhead, D.L., and Reynolds, J.F., 1993, Effects of climate-change on decomposition in arctic tussock tundra – a modeling synthesis, *Artic Alpine Research*, 25: 403–412.

Musselman, R.C., and Fox, D.G., 1991, A review of role of temperate forests in the global CO₂ balance, *Journal of Air Waste Management Association*, 41: 798–807.

Oechel, W.C., Hastings, S.J., Vourlitis, G., Jenkins, M., Riechers, G., and Grulke, N., 1993, Recent change of arctic tundra ecosystems from a net carbon dioxide sink to a source, *Nature*, 361: 520–523.

Oechel, W.C., Vourlitis, G.L., Hastings, S.J., Zulueta, R.C., Hinzman, L., and Kane, D., 2000, Acclimation of ecosystem CO₂ exchange in Alaska Arctic response to decadal climate warming, *Nature*, 406: 978–981.

Parton, W.J., D.S. Schimel, C.V. Cole, and Ojima, D.S., 1987, Analysis of factors controlling soil organic matter levels in Great Plains grasslands, *Soil Science Society of America Journal*, 51: 1173–1179.

Pastor, J., Solin, J., Bridgman, S.D., Updegraff, K., Harth, C., Weishampel, P., Dewey, B., 2003, Global warming and the export of dissolved organic carbon from boreal peatlands, *Oikos*, 100: 380–386.

Powlson, D., 2005, Will soil amplify climate change? *Nature*, 433: 204–205.

Raich, J.W., and Schlesinger, W.H., 1992, The global carbon dioxide flux in soil respiration and its relationship to vegetation and climate, *Tellus*, 44: 81–99.

Reichstein, M., Kätterer, T., Andren, O., Ciais, P., Schulze, E.D., Cramer, W., Papale, D., and Valentini, R., 2005, Temperature sensitivity of decomposition in relation to soil organic matter pools: critique and outlook, *Biogeosciences*, 2: 317–321.

Rinnan, R., Michelsen, A., Bååth, E., and Jonasson, S., 2007, Mineralization and carbon turnover in subarctic heath soil as affected by warming and additional litter, *Soil Biology and Biochemistry*, 39: 3014–3023.

Royal Society, 2001, The role of land carbon links in mitigating global climate change, Policy Document 10/01, 9th July.

Sala, O.E., Chapin, F.S. III, Armesto, J.J., Berlow, E., Bloomfield, J., Dirzo, R., Huber-Sanwald, E., Huenneke, L.F., Jackson, R.B., Kinzig, A., Leemans, R., Lodge, D.M., Mooney, H.A., Oesterheld, M., Poff, N.L., Sykes, M.T., Walker, B.H., Walker, M., and Wall, D.H., 2000, Global biodiversity scenarios for year 2100, *Science*, 287: 1770–1774.

Saleska, S.R., Miller, S.D., Matross, D.M., Goulden, M.L., Wofsy, S.C., da Rocha, H.R., de Camargo, P.B., Crill, P., Daube, B.C., de Freitas, H.C., Hutyra, L., Keller, M., Kirchhoff, V., Menton, M., Munger, J.W., Pyle, E.H., Rice, A.H., and Silva, H., 2003, Carbon in Amazon forests: unexpected seasonal fluxes and disturbance-induced losses, *Science*, 302: 1554–1557.

Saleska, S.R., Didan, K., Huete, A.R., and da Rocha, H.R., 2007, Amazon forests green-up during 2005 drought, *Science*, 318: 612.

Sanderman, J., Amundson, R.G., and Baldocchi, D.D., 2003, Application of eddy covariance measurements to the temperature dependence of soil organic matter mean residence time, *Global Biogeochemical Cycles*, 17: 1061–1075.

Sarmiento, J., 2000, Global change: that sinking feeling, *Nature*, 408: 155–156.

Schimel, D.S., 1995, Terrestrial Ecosystems and the carbon cycle, *Global Change Biology*, 1: 77–91.

Schimel, D.S., Braswell, B.H., Holland, E.A., McKeown, R., Ojima, D.S., Painter, T.H., Parton, W.J., and Townsend, A.R., 1994, Climatic, edaphic, and biotic controls over storage and turnover of carbon in soils, *Global Biogeochemical Cycles*, 8: 279–293.

Smith, P., Chapman, S.J., Scott, W.A., Black, H.I.J., Wattenbach, M., Milne, R., Campbell, C.D., Lilli, A., Ostle, N., Levy, P.E., Lumsdon, D.G., Millard, P., Towers, W., Zaehle, S., and Smith, J.U., 2007, Climate change cannot be entirely responsible for soil carbon loss observed in England and Wales, 1978–2003, *Global Change Biology*, 13: 2605–2609.

Springett, J.A., Brittain, J.E., and Springett, B.P., 1970, Vertical movement of Enchytraeidae (Oligochaeta) in moorland soils, *Oikos*, 21: 16–21.

Steffen, W., Noble, I., Canadell, J., Apps, M., Schulze, E.D., Jarvis, P.G., Baldocchi, D., Ciais, P., Cramer, W., Ehleringer, J., Farquhar, G., Field, C.B., Ghazi, A., Gifford, R., Heimann, M., Houghton, R., Kabat, P., Körner, C., Lambin, E., Linder, S., Mooney, H.A., Murdiyarso, D., Post, W.M., Prentice, I.C., Raupach, M.R., Schimel, D.S., Shvidenko, A., and Valentini, R., 1998, The terrestrial carbon cycle: implications for the Kyoto protocol. *Science*, 280: 1393–1394.

Swift, M.J., Heal, O.W., and Anderson, J.M., 1979, *Decomposition in Terrestrial Ecosystems*, Blackwell Scientific Publications, Oxford.

Thornley, J.H.M., and Cannell, M.G.R., 2001, Soil carbon storage response to temperature: a hypothesis. *Annals of Botany*, 87: 591–598.

Tipping, E., Woof, C., Rigg, E., Harrison, A.F., Ineson, P., Taylor, K., Benham, D., Poskitt, J., Rowland, A.P., Bol, R., and Harkness, D.D., 1999, Climatic influences on the leaching of dissolved organic matter from upland UK moorland soils, investigated by a field manipulation experiment. *Environment International*, 25: 83–95.

Torsvik, V.L., Goksoyr, J., Daae, F.L., Sørheim, R., Michalsen, J., and Salte, K., 1994, Use of DNA analysis to determine the diversity of microbial communities. In: *Beyond the Biomass: Compositional and Functional Analysis of Soil Microbial Communities* (Eds. K. Ritz, J. Dighton, and K.E. Giller), pp. 39–48, John Wiley and Sons, New York.

Tranvik, L.J., and Jansson, M., 2002, Climate change – terrestrial export of organic carbon, *Nature*, 415: 861–862.

Trumbore, S., 2000, Age of soil organic matter and soil respiration: radiocarbon constraints on belowground C dynamics. *Ecological Applications*, 10: 399–411.

Trumbore, S.E., Chadwick, O.A., and Amundson, R., 1996, Rapid exchange between soil carbon and atmospheric carbon dioxide driven by temperature change, *Science*, 272: 393–396.

Tuomi, M., Vanhala, P., Karhu, K., Fritze, H., and Liski, J., 2008, Heterotrophic soil respiration – comparison of different models describing its temperature dependence, *Ecological Modelling*, 211: 182–190.

Vanhala, P., Karhu, K., Tuomi, M., Björklof, K., Fritze, H., and Liski, J., 2008, Temperature sensitivity of soil organic matter decomposition in southern and northern areas of the boreal forest zone, *Soil Biology and Biochemistry*, 40: 1758–1764.

van Hees, P.A.W., Jones, D.L., Finlay, R., Godbold, D.L., and Lundström, U.S., 2005, The carbon we do not see – the impact of low molecular weight compounds on carbon dynamics and respiration in forest soils: a review, *Soil Biology and Biochemistry*, 37: 1–13.

Wall, D.H., Bradford, M.A., John, M.G.S.T., Trofymow, J.A., Behan-Pelletier, V., Bignell, D.E., Dangerfield, J.M., Parton, W.J., Rusek, J., Voigt, W., Wolters, W., Gardel, H.Z., Ayuke, F.O., Bashford, R., Beljakova, O.I., Bohlen, P.J., Brauman, A., Flemming, S., Henschel, J.R., Johnson, D.L., Jones, T.H., Korakova, M., Kranabetter, J.M., Kutny, L., Lin, K., Maryati, M., Masse, D., Pokarzhevskii, A., Rahman, H., Sabará, M.G., Salamon, J., Swift, M.J., Varela, A., Vasconcelos, H.L., White, D. and Zou, X., 2008, Global decomposition experiment shows soil animal impacts on decomposition are climate-dependent, *Global Change Biology*, 14: 2661–2677.

Wallwork, J.A., 1970, *Ecology of soil animals*, McGraw-Hill, London.

Wetherald, R.T. and Manabe, S., 1999, Detectability of summer dryness caused by greenhouse warming, *Climate Change*, 43: 495–511.

Woodwell, G.M., Mackenzie, F.T., Houghton, R.A., Apps, M., Gorham, E., and Davidson, E., 1998, Biotic feedbacks in the warming of the Earth, *Climate Change*, 40: 495–518.

Worrall, F., Burt, T., and Shedden, R., 2003, Long-term records of riverine dissolved organic matter, *Biogeochemistry*, 64: 165–178.

CASE STUDY II. GLOBAL CLIMATE CHANGE

Media representational practices in the Anthropocene Era

Maxwell T. Boykoff

Environmental Change Institute, School of Geography and the Environment, South Parks Road, Oxford, OX1 3QY, UK.

Abstract

Media representational practices are vitally important to conceptions of challenges and possibilities for action to address the issue of anthropogenic climate change. They shape processes between science, policy and the public and thereby influence issues of governance and practices in our everyday lives and livelihoods in the twenty-first century. Many complex factors contribute to media representation practices: external (such as political economic challenges associated with corporate media consolidation) as well as internal influences (such as contributions from the deployment of journalistic norms). In this chapter, I touch on salient and swirling factors that contribute to how issues, events and information have often become climate ‘news’ about anthropogenic climate change. To the extent that these pressures have led to problematic representational practices, media coverage of climate change has contributed to misperceptions, misleading debates, and divergent understandings. Such practices are therefore detrimental to efforts that seek to enlarge rather than constrict the spectrum of possibility for appropriate responses to various environmental challenges.

Keywords: climate change, media, discourse, framing, representations, anthropogenic.

1. Introduction

How many reading this chapter start their day with a cup of coffee or tea and the latest peer-reviewed scientific journal article? Rather, how many turn more frequently to a media source, such as television or radio news, a newspaper or the internet for science news? I would suspect the responses favor the latter. Beyond readers here, studies have consistently found that the public garners much of its knowledge about science (and more specifically climate change) from the mass media (e.g., Nelkin, 1987; Wilson, 1995). Frequently and necessarily, global citizens rely on mass media to translate the ‘unruly complexities’ of climate science into digestible morsels of news and commentary.

When producing ‘news’, journalists and editors face an inevitable series of choices regarding how to portray aspects of the climate issue within a larger current of dynamic activities. In other words, they must consider how to ‘frame’ it. Framing is an inherent facet of cognition, contextualizing and organizing the dynamic swirl of issues, events and occurrences we encounter. Consequently, elements of discourse then privilege certain views and interpretations over others (Goffman, 1974). Over time, various actors – both individuals and collective – have sought to access and utilize mass media sources in order to shape perceptions of various aspects of the climate change issue (Nisbet and Mooney, 2007). In this high-stakes and heavily politicized ‘battlefield of knowledge’, mass media have proven to vitally contribute to shaping dynamic interactions between science, policy and the public. Influencing content, some have asserted that aspects of climate sciences have been overly hyped through the mass media, while others have considered coverage overly laden with inaccurate consternation of the science.

2. Media and climate risk: an abridged history

Concurrent with early studies of climate change during the 1700s and early 1800s – modern media had begun early stages of what was to become its rapid development. During that time, media growth faced constraints by a number of competing and contradictory factors, such as strong state-control over the public sphere, legacies of colonialism, low literacy rates and technological capacity challenges (Starr, 2004). However, in the mid-1800s, media communications expanded their reach and influence tremendously in North America and Europe. Media took shape primarily as mass-circulation print presses in urban centers, where daily newspaper production quadrupled in 40 years, and circulation grew from 0.34 papers per household in 1870 to 1.21 papers per household in 1910 (Starr, 2004). Thus, during this time, mass media outlets formed increasingly significant and powerful social, political, economic and cultural institutions (Starr, 2004).

Climate science and mass media first came together in coverage of climate change in the 1930s. In the *New York Times* it was written, “The earth must be inevitably changing its aspect and its climate. How the change is slowly taking place and what the result will be has been considered...” (*New York Times*, 1932, 4). Media coverage of human contributions to climate change appeared more clearly in the 1950s. For instance, the *Saturday Evening Post* published a story by Abarbanel and McClusky (1950), entitled ‘*Is the World Getting Warmer?*’, exploring links between atmospheric temperature change and agricultural shifts as well as sea level rise. In 1956, Kaempffert wrote for the *New York Times*, “Today more carbon dioxide is being generated by man’s technological processes than by volcanoes, geysers and hot springs. Every century man is increasing the carbon dioxide content of the atmosphere by 30% – that is, at the rate of 1.1°C in a century. It may be a chance coincidence that the average temperature of the world since 1900 has risen by about this rate. But the possibility that man had a hand in the rise cannot

be ignored.” (Kaempffert, 1956, 191). Then in 1957 – the International Geophysical Year – science reporter Robert C. Cowen wrote an article that appeared in the *Christian Science Monitor* called ‘Are Men Changing the Earth’s Weather?’ The article began:

Industrial activity is flooding the air with carbon dioxide gas. This gas acts like the glass in a greenhouse. It is changing the earth’s heat balance. It could bring anything from an ice age to a tropical epoch.... Every time you start a car, light a fire, or turn on a furnace you’re joining the greatest weather “experiment” men have ever launched. You are adding your bit to the tons of carbon dioxide sent constantly into the air as coal, oil and wood are burned at unprecedented rates (Cowen, 1957).

However, in the subsequent three decades, mass media coverage regarding climate change remained sparse. These pieces regarding human’s role in a changing climate served to be a rare instances of media coverage of climate science, as well as clarity regarding anthropogenic climate change. There was scant newspaper, radio and television news coverage on topics such as U.S. National Academy of Sciences reports in the 1960s and 1970s that made repeated reference to emergent climate science, and links to anthropogenic sources.

International and domestic climate policy began to take shape in the mid-1980s, primarily through activities of the International Council of Scientific Unions, the United Nations Environment Program and the World Meteorological Organization. In 1985, the Villach Conference convened in Austria to examine impacts of greenhouse gas emissions on the planet. Meanwhile, modern media communications were taking their present globalized form, marked prominently by increased corporate concentration, conglomeration and commercialism (McChesney, 1999). Media power continued to grow, as did conflicting pressures of corporate control and democratic principles (Graber, 2000; Doyle, 2002). The three media-science-policy spheres collided in the mid-1980s, when media coverage of climate change science and policy increased dramatically.¹ To illustrate, Figure 1 shows that the quantity of ‘climate change’ or ‘global warming’ coverage in forty of the most influential English-language world newspapers has risen over time, like increases in global atmospheric temperature. Increases have been noted during the times of the releases of the Intergovernmental Panel on Climate Change (IPCC) assessment reports in 1990, 1995 and 2001. There are also increases in coverage during the 1992 UN Framework Convention on Climate Change (UN FCCC) and the 1997 Kyoto Protocol. A large increase in coverage was evident in Australia, New Zealand, the Middle East, Asia, Eastern Europe and South Africa during the 1997 Kyoto Protocol. At the meetings in Kyoto, Japan, registrants included 3500 journalists from over 400 media organizations in 160 countries (Leggett, 2001).

¹ Various studies in different countries demonstrate an increase in media coverage beginning in 1988: in the United States (Boykoff and Boykoff 2004), Germany (Weingart *et al.* 2000) and United Kingdom (Carvalho and Burgess 2005).

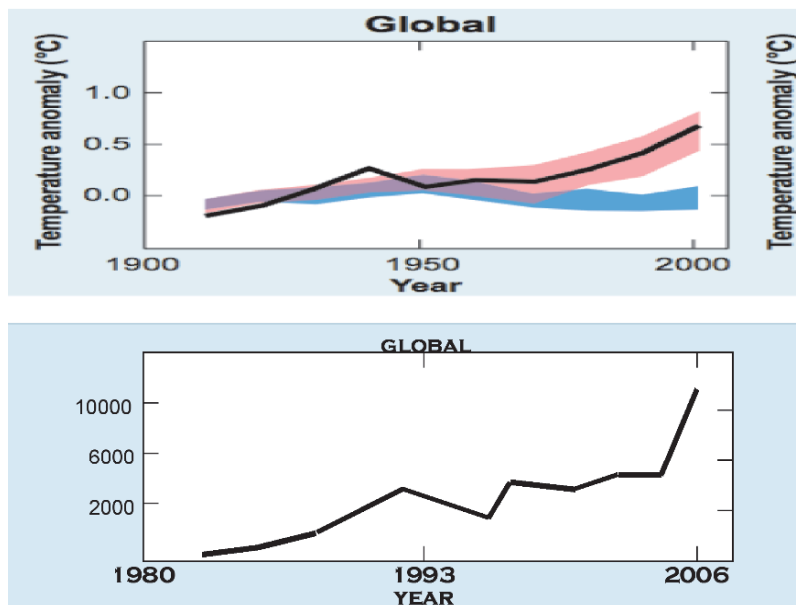


Fig. 1. The plot of global temperature anomaly over time (*top*) is from the Fourth Assessment Report Working Group I Summary for Policymakers from the Intergovernmental Panel on Climate Change (IPCC, 2007). The black line depicts decadal averages of observations relative to the corresponding temperature average for 1901–1950. The blue band shows the general range from simulation runs in climate models using only natural forcings due to volcanic and solar activity. The red band shows the range using both natural and anthropogenic forcings. The plot of number of newspaper articles over time (*bottom*) shows the general trends in the amount of coverage in forty of the most influential English-language newspapers, across seventeen countries and on five continents: the Sydney Morning Herald, The Age (Melbourne), the Courier-Mail (Brisbane), The Australian, the Daily Telegraph (Sydney), Globe and Mail (Toronto), the Toronto Star, the South China Morning Post (Hong Kong), the Prague Post, the Irish Times (Dublin), the Jerusalem Post, the Jerusalem Report, Yomiuri Shimbun (Tokyo), the Japan Times (Tokyo), Mainichi Shimbun (Tokyo), the Korea Herald, the Korea Times (Seoul), the New Straits Times (Wilayah Persekutuan), Het Financieele Dagblad (Eindhoven), the New Zealand Herald (Auckland), the Dominion Post (Wellington), The Press (Christchurch), the Moscow News, the Moscow Times, The Straits Times (Singapore), Business Day (Johannesburg), the Financial Mail (Johannesburg), the Sunday Times (Johannesburg), The Nation (Bangkok), the Guardian (London), the Observer (London), the Independent (and Sunday Independent) (London), the Times (and Sunday Times) (London), the Financial Times (London), The Herald (Glasgow), The Scotsman (and Scotland on Sunday) (Edinburgh), the Los Angeles Times, the *New York Times*, U.S.A Today (McLean, VA), the Wall Street Journal (New York), and the Washington Post. (This figure is adapted from Boykoff, 2008.)

Many factors contributed to the initial rise in coverage in 1988. Among them was NASA scientist James Hansen's testimony to the U.S. Congress that summer. Hansen testified that he was “99% certain” that warmer temperatures were caused by the burning of fossil fuels and not solely a result of natural variation (Shabecoff,

1988, A1). Moreover, this summer was one marked by extreme drought and high temperatures throughout North America. These concomitant events were thought to sensitize many in the climate science and policy communities, as well as the media and public, to the issue of climate change. Demeritt has asserted, “The 1988 heat wave and drought in North America were arguably as influential in fostering public concern as any of the more formal scientific advice” (Demeritt, 2001, 307). In the science and policy spheres, 1988 was also the year in which UNEP and WMO created the IPCC, and the WMO held a landmark international conference called ‘Our Changing Atmosphere’ (Gupta, 2001).² Overall, Ungar has written, “what rendered 1988 so extraordinary was concatenating physical impacts felt by the person in the street” (Ungar, 1992, 490). These climate change science and policy events and activities were pivotal in shaping media coverage from 1988 forward, during the time when multi-national media corporations underwent further and significant consolidation, through various mergers and acquisitions (Bagdikian, 2004).

Generally, increases in media coverage can be attributed to concatenate ecological/meteorological, cultural, scientific and political events and issues (Boykoff, 2007a,b). For instance, the powerful 2005 hurricane season, the 2006 drought in Australia and 2007 floods in the UK have fed into many media stories. Culturally-relevant events like the 2006 release of the film ‘An Inconvenient Truth’, and fluctuating oil and gas prices in 2006 and 2007 have contributed to surges in news reporting in Western Europe and North America. Increases have also been connected to scientific reports such as the 2006 ‘Stern Review’, and the three 2007 UN Intergovernmental Panel on Climate Change Working Group Reports. Moreover, political events such as the UN Twelfth Conference of Parties meeting to the Kyoto Protocol in Kenya and the June 2007 Group of Eight Summit in Germany have generated substantial climate change media coverage. These interrelated issues have provided abundant journalistic ‘news hooks’ to reporting on interwoven aspects of carbon-based industry and society. So if media coverage does matter, how does it matter?

3. Factors that shape climate change media coverage

Interactions unfolding today at the interface of science, policy and media are steeped in histories that include media institutions and asymmetrical power relationships buttressing journalistic practices therein (Bennett, 2002; Starr, 2004). It is clear that science and politics have influenced media coverage of climate change over time. Conversely, journalistic framings have shaped ongoing scientific and political considerations as well as policy decisions and activities. Moreover, much

² At this conference in Toronto, 300 scientists and policy-makers representing 46 countries convened, and from this meeting, participants called upon countries to reduce carbon dioxide emissions by 20% or more by 2005 (Gupta 2001).

as storylines are fueled within environmental politics, the mass media play an important role in framing understandings as an interpreter, translator and disseminator of information.

In this dynamic milieu, has the recent deluge of coverage signaled or prompted a flood of new awareness and motivation to address climate change? Is more coverage 'better' in this respect, or has this contributed to public saturation and despair? What actually is 'good' action based on 'good' information via mass media? In combination, answers to these questions are complex, and influencing elements as they relate to mass media are often subtle as well as contradictory. Nonetheless, here I assemble a mosaic of comments to describe four contingent and multi-scale factors that prominently shape how rising media coverage may (or may not) matter to enhancing public understanding and action.

3.1. Journalistic accuracy

Beyond the quantity of coverage is the obvious concern of accuracy. Media professionals – such as editors and journalists – operate within an often-competitive political, economic, institutional, social and cultural landscape. Therefore, the negotiated meanings and representations derive through combined structural and agential components of mass media. These processes take place simultaneously at multiple scales (Boykoff, 2007a,b). Large-scale social, political and economic factors (such as decision-making in a capitalist political economy) influence everyday individual journalistic decisions (such as how to focus or frame a story with limited time to press as well as finite number of column inches). These issues intersect with processes such as journalistic norms and values, such as 'objectivity' and 'balance' (Boykoff and Boykoff, 2004, 2007a,b). A number of polls have queried reader comprehension of climate change. For instance, research has found that more accurate information on climate change causes increases people's stated intentions to do something about it (Bord *et al.*, 2000). Further, research examining coverage of uncertainty in climate change found that greater contextualization within climate science stories helps to mitigate against controversy stirred up through uncertainty (Corbett and Durfee, 2004).

3.2. Issue salience

Various aspects of the climate change issue can become salient for a host of reasons. As an example linked to lives and livelihoods, displaced people and affected communities due to sea level rise make this a more prominent issue for them. Similarly, farmers facing new dangers of flooding or drought may consider climate change as an important driver, and thus, concern. However, a 2006 study found that beliefs about climate change were a function of three main factors: possible relevant personal experiences (e.g., exposure to weather disasters), perceived consequences

of climate change (e.g., relative vulnerability) and messages from informants (e.g., scientists via the mass media). Through this empirical research, the authors put forward a mechanism linking knowledge and action: “knowledge may have increased certainty, which in turn increased assessments of national seriousness, which in turn increased policy support...knowledge about an issue *per se* will not necessarily increase support for a relevant policy. It will do so only if existence beliefs, attitudes, and beliefs about human responsibility are in place to permit the necessary reasoning steps to unfold” (Krosnick *et al.*, 2006, 36, 37). Despite some of our best intentions, the reality often is that our behaviors may not match our concern if the issue does not significantly impact the functioning of our daily lives.

3.3. Geography

Related to issue salience, differences between humans and physical landscapes (and the processes that affect them) across space influence perceptions of climate change. Mass media is an important driver in these variegated perceptions (Boykoff, 2007a,b). Recent AC Nielsen polling captures these differences over time (Figure 2).

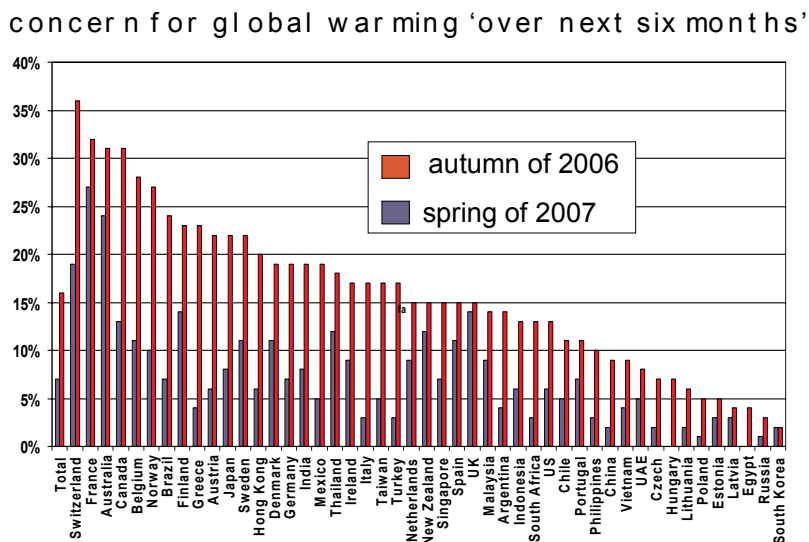


Fig. 2. This figure depicts the changing concern for climate change through an online 47-country survey between autumn 2006 (in red) and spring 2007 (in blue). To the question ‘what is your biggest and second biggest concern over the next six months, 16% of 26,486 respondents in Spring 2007 selected ‘global warming’, up from 7% in autumn 2006. Global warming moved past ‘terrorism’, ‘war’, ‘crime’ and ‘political stability’ into the fourth biggest concern after ‘economy’, ‘health’ and ‘job security’. This figure was initially assembled by Jonathan Banks, Business Insight Director at AC Nielsen. (AC Nielsen, 2007).

To the question ‘what is your biggest and second biggest concern over the next six months’, respondents selected global warming more than two times more frequently in spring 2007 than six months previously (AC Nielsen, 2007). However, within this general trend there are many geographic disparities. For instance, in UK the increase moved from 14% to 15% concern, while concern in the US jumped from 6% to 13%. Meanwhile, since 2003 reporting in daily print media has roughly quadrupled in the UK and tripled in the US (Boykoff and Rajan, 2007). On one hand, this shows that stated concern in the US remains lower than that in the UK. On another hand, this may indicate that despite dramatic increases in media reports, the UK may be saturated on this issue while it contributes to a rise in concern in the US. Clearly, there are many explanatory limits to these connections with online polling and national aggregates. It harkens to the Roberts Chambers classic intervention into ‘whose reality counts’ (Chambers, 1997). Nonetheless, such juxtapositions provide opportunities to explore these differences in human and physical geography, as situated in varied histories and political contexts.

3.4. Information and/or education

Studies have shown that without some kind of knowledge of science to help provide a foundation of understanding to follow ongoing issues, more journalism will not help (Miller, 1997). Moreover, attempts to agree on ‘appropriate’ action – such as in the case of purchasing carbon offsets for air travel – can prove to be highly contested. Ungar (2000, 309) has argued that through various mass media processes, “the public could very well be concerned but relatively ill informed”. So in this case more media coverage may not be helpful. Journalists and editors have consistently stated that their role as one of information dissemination rather than education. However, in practice, the distinction between these roles becomes blurred. Media representations, by their very nature, frame aspects of climate change, so such practices inevitably contribute to how people understand them. Turning to climate science education in schools and university, it generally has been slow to permeate curricula amid the growing instrumental approaches to educational practices. Furthermore, relying on the leaders of tomorrow through education to tackle what many consider a pressing contemporary issue may be deemed a form of inter-generational irresponsibility.

4. Continuing challenges at the climate science-media-policy/practice interface

When Smith (2000) assembled the valuable edited book *The Daily Globe: Environmental change, the public and the media* in 2000, the science-media-policy/practice landscape looked much different. At that time, Smith asserted that such

issues were ‘routinely underreported’, and connected this to problems in appropriate actions to address environmental degradation. However, now that climate change is often widely reported through mass media outlets, it remains an open question as to how this really may connect to multi-scale action, from individual to international mitigation and adaptation practices.

Nonetheless, mass media comprise a community where these issues can readily and potentially effectively be addressed, analyzed and discussed. This is a complex arena: mass media portrayals simply do not translate truths or truth-claims nor do they fill knowledge gaps for citizens and policy actors to make ‘the right choices’. If only things were that straightforward. In fact, increased media attention to the issue often unearths more questions to be answered and *greater* scientific understanding actually can contribute to a *greater* supply of knowledge from which to develop and argue varying interpretations of that science (Sarewitz, 2004). While this can vary depending on which aspect of climate change one is focused on – from anthropogenic signals and noise to what should be done about it – the interacting factors can simultaneously illuminate and obfuscate connections between media coverage and public engagement.

In theorizing interactions at the science-practice interface, researchers have considered three main ‘waves’ of engagement (Collins and Evans, 2002). The first wave of interactions was that of a ‘deficit model’ approach to understanding interaction. This perspective posited that poor choices and actions were attributed to ‘deficits’ of knowledge and information to make the ‘correct’ choice. The approach was associated with norms and ideals of science as open, universal and objective practices. However, this set of ideal interactions is much more complicated in practice. Since the 1950s, this view has been critiqued (mainly within the discipline of science studies) for being too simple a characterization of the dynamic interactions between science and policy/practice. However, in the policy and public spheres, there are residual impulses such as the stated reliance on ‘sound’ science in order to make decisions, as well as the stated pursuits to eliminate uncertainty as a precondition for action. The second wave of engagement is considered the wave of ‘democracy’. Ulrich Beck examined the democratization of the science-practice interface, particularly in his book ‘Risk Society’ (Beck, 1992). There he posited that there are common ‘bads’ in our risk society as well as common ‘goods’: techno-economic development itself could actually increase problems in practice rather than solve them. He called for more non-state actor/policy/public engagement and feedback into the processes of science (or ‘upstream engagement’) in order to more properly account for and deal with the contested spaces of (public and private) engagement with science. The third wave is called the ‘normative theory of expertise’. It is similar to the second wave in terms of the democratizing commitments, though it further maps institutional boundaries between formalized science-policy/politics and the lay public. This theoretical move seeks to delineate the variegated roles of generally legitimized and authorized ‘experts’ vis-à-vis specialist ‘experts’ in the field in question. In other words, in the case of

climate change, this modeling seeks to clarify which groups and institutions may be ‘authorized’ speakers on climate science, while others are not (Collins and Evans, 2002).

5. The public space where climate science and practice interact via mass media

Taken together, ‘awareness’ and ‘knowledge’, broadly construed, can prompt a range of responses in the public sphere. With and without access to accurate information on climate change science and policy/practices, people can often feel overwhelmed or paralyzed, and ‘switch off’ to possibilities for smaller-scale changes that can potentially aggregate to larger changes to address this global issue. For instance, media reporting on the *Live Earth* July 2007 concerts may inspire and motivate some people to strive for more low-carbon lifestyles. Meanwhile, media attention on the events might irk others, and cause them to surrender their carbon sacrifices as they learn of the high carbon-intensity lifestyles of some of the performers. Borrowing from David Foster Wallace, self-sacrifice in the face of such a diffuse problem could be deemed ‘supposedly good things I’ll never do again’.

While all humans are implicated to varying degrees in contributing to sources of greenhouse gas emissions – through household activities, engagement in industrial activities through consumption, transport – those experiencing concentrated impacts are much fewer. So while responsibility is diffuse, subsets of more vulnerable human groups feel the concentrated costs. This ‘depersonalization’ is also reflected in intersecting research on public trust and climate change action. Lorenzoni and Pidgeon (2006, 88) have found that, “successful action is only likely to take place if individuals feel they can and should make a difference, and if it is firmly based upon the trust placed in government and institutional capabilities for adequately managing risks and delivering the means to achieve change”. On a community level, public perceptions of trust are shaped by varied political contexts and histories often translated via mass media practices. Then on an individual level, conflicts between knowledge and behavior may also stir up anxiety (or cognitive dissonance) between what one knows what one *ought* to do, and what one actually does. Again, mass media coverage has proven to be a key contributor – among a number of factors – that have shaped and affected science and policy discourse as well as public understanding and action. Amid a number of open questions raised, it can be said with certainty that more media coverage of climate change – and fair and accurate coverage at that – will not ‘solve’ the problem. Moving forward, it is our perhaps diffuse yet shared responsibility to continue to consider the variegated role of mass media in improving public understanding of climate science and enhancing policy implementation.

References

Abarbanel, A. and T. McClusky (1950). Is the world getting warmer? *Saturday Evening Post* 22, 23, 57: 60–63.

AC Nielsen (2007). Global Omnibus Survey. Oxford, UK, AC Nielsen.

Bagdikian, B. (2004). *The Media Monopoly*. Boston, Beacon Press.

Beck, U. (1992). *Risk Society: Towards a New Modernity*. London, Sage.

Bennett, W. L. (2002). *News: The Politics of Illusion*. New York, Longman.

Bord, R. J., R. E. O'Connor, and A. Fisher (2000). In what sense does the public need to understand global climate change? *Public Understanding of Science* 9: 205–218.

Boykoff, M. T. (2007a). Flogging a dead norm? Newspaper coverage of anthropogenic climate change in the United States and United Kingdom from 2003–2006. *Area* 39(4): 470–481.

Boykoff, M. T. (2007b). From convergence to contention: United States mass media representations of anthropogenic climate change science. *Transactions of the Institute for British Geography* 32(4): 477–489.

Boykoff, M. T. (2008). The real swindle, *Nature Reports Climate Change* 2(2): 31–32.

Boykoff, M. T. and J. M. Boykoff (2004). Bias as balance: Global warming and the U.S. Prestige Press. *Global Environmental Change* 14(2): 125–136.

Boykoff, M. T. and J. M. Boykoff (2007). Climate change and journalistic norms: A case study of U.S. mass-media coverage. *Geoforum* 38(6): 1190–1204.

Boykoff, M. T. and S. R. Rajan (2007). Signals and noise: Mass-media coverage of climate change in the USA and the UK. *European Molecular Biology Organization Reports* 8(3): 1–5.

Carvalho, A. and J. Burgess (2005). Cultural circuits of climate change in UK broadsheet newspapers, 1985–2003. *Risk Analysis* 25(6): 1457–1469.

Chambers, R. (1997). *Whose Reality Counts? Putting the First Last*. London, ITDG Publishing.

Collins, H. M. and R. Evans (2002). The third wave of science studies: Studies of expertise and experience. *Social Studies of Science* 32(2): 235–296.

Corbett, J. B. and J. L. Durfee (2004). Testing public (un) certainty of science: Media representations of global warming. *Science Communication* 26(2): 129.

Cowen, R. (1957). Are Men Changing the Earth's Weather? *Christian Science Monitor*. Boston, Massachusetts, USA 13.

Demeritt, D. (2001). The construction of global warming and the politics of science. *Annals of the Association of American Geographers* 91(2): 307–337.

Doyle, G. (2002). *Media Ownership: The Economics and Politics of Convergence and Concentration in the UK and European Media*. London, Sage Publications.

Goffman, E. (1974). *Frame Analysis: An Essay on the Organization of Experience*. Harvard University Press, Cambridge, Massachusetts, USA.

Graber, D. (2000). *Media Power in Politics*. Washington D.C., CQ Press.

Gupta, J. (2001). *Our Simmering Planet: What to Do About Global Warming?* New York, NY, Zed Books.

IPCC (2007). *Climate Change 2007: The Physical Science Basis, Summary for Policymakers*. Cambridge University Press, Cambridge, UK.

Kaempfert, W. (1956). Science in review: Warmer climate on Earth may be due to more carbon dioxide in the air. *New York Times*. New York: 191.

Krosnick, J. A., A. L. Holbrook, L. Lowe, and P. S. Visser (2006). The origins and consequences of democratic citizens' policy agendas: A study of popular concern about global warming. *Climatic Change* 77(1): 7–43.

Leggett, J. K. (2001). The carbon war: Global warming and the end of the oil era. New York, Routledge.

Lorenzoni, I. and N. F. Pidgeon (2006). Public views on climate change: European and USA perspectives. *Climatic Change* 77(1): 73–95.

McChesney, R. W. (1999). Rich Media, Poor Democracy: Communication Politics in Dubious Times. Urbana and Chicago, University of Illinois Press.

Miller, B. (1997). Political action and the geography of defense investment: Geographical scale and the representation of the Massachusetts Miracle. *Political Geography* 16: 171–185.

Nelkin, D. (1987). Selling Science: How the Press Covers Science and Technology. New York, W.H. Freeman.

New York Times (1932). Next great deluge forecast by science. *New York Times*. New York: 4.

Nisbet, M. C. and C. Mooney (2007). Framing science. *Science* 316(6 April): 56.

Sarewitz, D. (2004). How science makes environmental controversies worse. *Environmental Science and Policy* 7: 385–403.

Shabecoff, P. (1988). Global warming has begun, expert tells senate. *New York Times*. New York: A1.

Smith, J., Ed. (2000). The Daily Globe: Environmental Change, the Public and the Media. London, Earthscan Publications Ltd.

Starr, P. (2004). The Creation of the Media: Political Origins of Modern Communications. New York, NY, Basic Books.

Ungar, S. (2000). Knowledge, ignorance and the popular culture: Climate change versus the ozone hole. *Public Understanding of Science* 9: 297–312.

Ungar, S. (1992). The rise and (relative) decline of global warming as a social problem. *The Sociological Quarterly* 33(4): 483–501.

Weingart, P., A. Engels, *et al.* (2000). Risks of communication: Discourses on climate change in science, politics, and the mass media. *Public Understanding of Science* 9: 261–283.

Wilson, K. M. (1995). Mass media as sources of global warming knowledge. *Mass Communications Review* 22(1&2): 75–89.

The stern review and the uncertainties in the economics of climate change

Vanessa Peña

*Department of Geography, The London School of Economics and Political Science,
Houghton Street, London WC2A 2AE, UK.*

*School of International and Public Affairs, Columbia University, 420 West 118th Street,
New York, NY 10027, USA.*

Abstract

The Stern Review of the Economics of Climate Change presented by Lord Nicholas Stern and his team has been touted as the most rigorous analysis at present regarding the risks associated with global climate change. The Stern Review presents the costs and benefits of reducing greenhouse gas emissions and comes to the stark conclusion that global inaction could result in even greater costs than the investment in immediate preventative action for long-term emission stabilization. However, even though the Stern Review addresses important aspects needed to establish an effective global policy on climate change, it is necessary to review the uncertainties associated with the Stern Review's conclusions and overall analysis. The uncertainties in the economics of climate change arise from three distinct realms: (i) the scientific uncertainties, (ii) the uncertainties in the economic framework, and (iii) the uncertainties in the implications for policy. This review addresses these individual aspects in brief in an attempt to give a general understanding of the critiques and debates regarding the Stern Review.

Keywords: the Stern Review, global climate change, climate model, scientific uncertainty, environmental economics, economic framework, technological diffusion, discount rate, environmental policy.

1. Introduction

The Stern Review of the Economics of Climate Change presented by Lord Nicholas Stern and his team has been touted as the most rigorous analysis at present regarding the risks associated with global climate change. The Stern Review (or SR as it will be referred to in the rest of this chapter) was published in 2006 when Nicholas Stern was Head of the Government Economic Service and Adviser to the Government on the economics of climate change and development. It is a 600 page

document that aims to provide answers, or at least a deeper understanding, of the following questions:

- “What are the economic and social implications for people in different countries and regions of a range of possible climate change outcomes, including in terms of incomes, lives and vulnerabilities?
- How should we tackle the problem of forecasting future emissions growth, and what is the range and likelihood of possibilities under different assumptions?
- How should policymakers understand and respond to the predicted increased risk of extreme events and major irreversible changes?
- What do we know about the possibilities for, and constraints to, adaptation to climate change?
- More generally, how can the world act in a coherent and collaborative way to tackle a problem that is global in its origins and effects?” (Stern, 2006c).

The first part of the SR presents the costs and benefits of reducing greenhouse gas (GHG) emissions and comes to the stark conclusion that global inaction could result in even greater costs than the investment in immediate preventative action for long-term emission stabilization. This section draws upon four central themes of the climate change problem: it is a global problem, it is long-term, it involves risks and uncertainties, and it has the potential to involve major and irreversible damage (Stern, 2006a). Hence, the SR acknowledges that the economic analysis must incorporate an international perspective, take consideration of the future generations, and include a greater scope than regular economic marginal analysis (Stern, 2006a).

In addition, the SR identifies key questions for the analysis of the costs and benefits of climate change as the following:

- “What is our understanding of the risks of the impacts of climate change, their costs, and on whom they fall?
- What are the options for reducing greenhouse-gas emissions, and what do they cost? What does this mean for the economics of the choice of paths to stabilization for the world? What are the economic opportunities generated by action on reducing emissions and adopting new technologies?
- For mitigation of climate change, what kind of incentive structures and policies will be most effective, efficient and equitable? What are the implications for the public finances?
- For adaptation, what approaches are appropriate and how should they be financed?
- How can approaches to both mitigation and adaptation work at an international level?” (Stern, 2006b)

In the SR, the proposed answers to these questions have significant implications for environmental policy, what actions should be undertaken, and on whom the responsibilities for action fall.

Overall, the SR establishes clear initiatives and guidelines to be followed by developed and developing countries in order to adequately mediate and minimize the risks of catastrophic climate events from ensuing. However, even though the SR addresses important aspects needed to establish an effective global policy on climate change, it is necessary to review the uncertainties associated with the SR's conclusions and overall analysis. The uncertainties in the economics of climate change arise from three distinct realms: (i) the scientific uncertainties, (ii) the uncertainties in the economic framework, and (iii) the uncertainties in the implications for policy. This chapter addresses these individual aspects in brief in an attempt to give a general understanding of the critiques and debates associated with the SR.

2. Uncertainties in the SR's scientific projections

2.1. *The scientific underpinnings of climate change*

The growth of scientific evidence indicating that global climate change is a serious and urgent issue has galvanized governmental action all over the world to avert a potentially disastrous environmental crisis. Studies have indicated that the Earth has warmed an average of 0.7°C since 1900 as shown in Figure 1 (Brohan *et al.*, 2006). In addition, the evidence of the role of humans in climate change is ever increasing. The anthropogenic effects of GHG production have produced an environment in which carbon dioxide (CO₂) concentrations have increased by over one-third from 280 parts per million (ppm) in pre-industrial times (1750s) to 380 ppm today (Stern, 2006b). Figure 2(a) (Butler, 2006) displays the rise of global atmospheric and anthropogenic CO₂ emissions. Additionally, the radiative forcing of the Kyoto GHGs¹, which include CO₂, methane, nitrous oxide, perfluorocarbon (PFC), hydrofluorocarbon (HFC) and sulfur hexafluoride (SF6), has increased the warming effect of these GHGs, and thus the temperature in our climate as shown in Figure 2(b) (Stern, 2006b).

The SR attempts to address climate scenarios and the range of outcomes which may span up to two centuries in the future. For example, Figure 3 (Stern, 2006b) demonstrates the three scenarios for emissions paths to stabilization proposed in the SR. These three scenarios represent the 'business-as-usual' scenario – emissions are allowed to grow as population and economies grow – the stabilization at 450 parts per million CO₂ equivalent (ppm CO₂e) scenario, and the stabilization at 550 ppm CO₂e scenario, each projected to 2100. The business-as-usual scenario involves an environment similar to stabilization at 550 ppm for near future (30–35 years). However, once this projection is extrapolated to the far future, emissions levels could reach beyond 850 ppm by the end of the twenty-first century (Stern,

¹ Kyoto greenhouse gases are the six main greenhouse gases covered by the targets set out in the Kyoto Protocol.

2006b). The observed peaks of the curve are of particular importance since the peaks indicate when the atmospheric emission concentrations will begin to decrease. Stabilization at 450 ppm will involve peaking in the next 5 years and at 550 ppm peaking in the next 10–20 years and falling by between 1% and 3% per year (Stern, 2006b). The small difference in the respective years of the 450 ppm or 500 ppm stabilization peaks and our current year gives an indication of how strong emission mitigation actions must be².

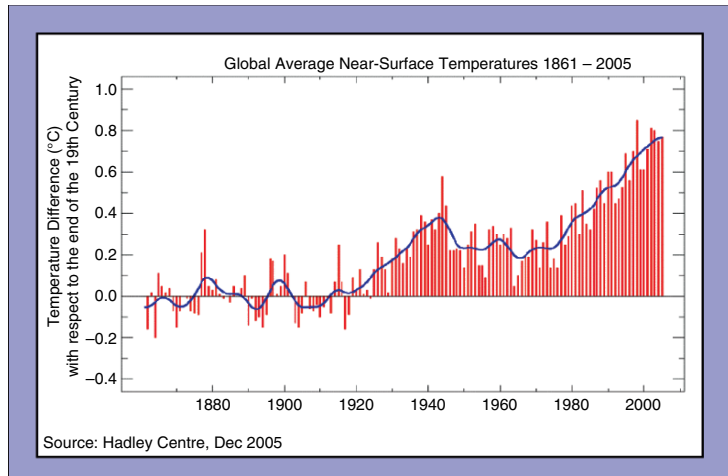


Fig. 1. Global average near surface temperature from 1861 to 2005. The blue line is the result of using a 21-year binomial filter to smooth the annual data. *Source: Brohan et al. (2006).*

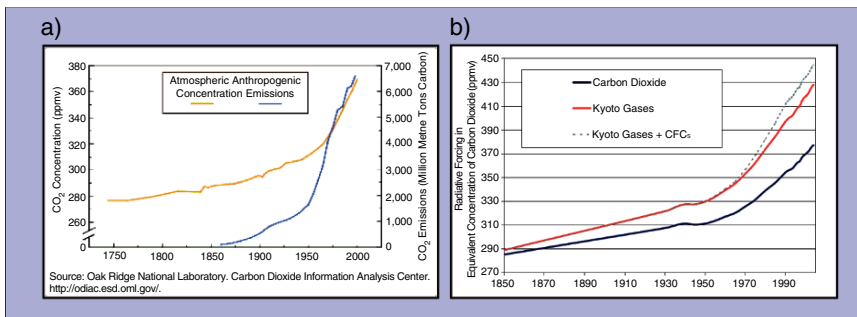


Fig. 2. (a) Global CO_2 concentrations with anthropogenic emissions, 1750–2000 *Source: Butler (2006)*, and (b) the warming effect of greenhouse gases (the ‘radiative forcing’) in terms of the equivalent concentration of CO_2 . *Source: Dr. L. Gohar and Prof. K. Shine, Department of Meteorology, University of Reading (from Stern 2006b).*¹

² The SR questions whether we may have missed the boat with reference to a possible stabilization at 450 ppm. However, despite the pessimism towards achieving stabilization at 450 ppm, the SR is optimistic in its claims that there is still feasible and sufficient time to invest in stabilization at 550 ppm.

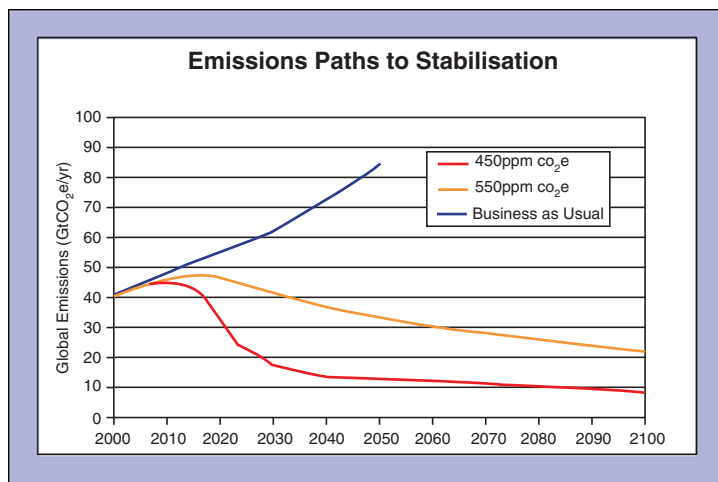


Fig. 3. Emission Paths to Stabilization. *Source: Stern, (2006b).*

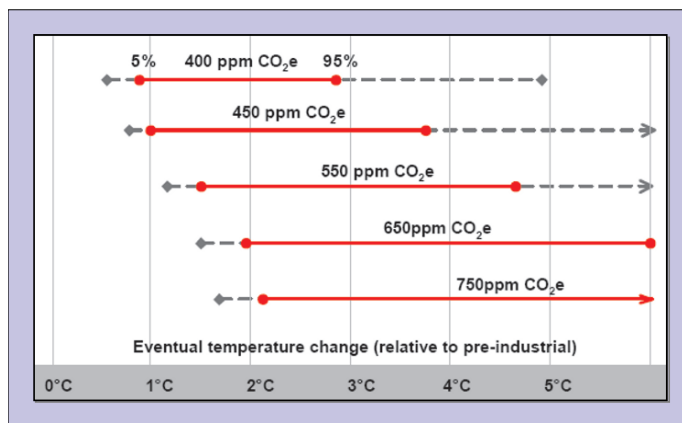


Fig. 4. Probabilistic link between emission concentrations and temperature change. The solid horizontal lines indicate the 5–95% range based on climate sensitivity estimates from the IPCC 2001 and a recent Hadley Centre ensemble study. The dashed lines show the 5–95% range based on eleven recent studies. *Source: Meinshausen(2006); from Stern (2006b).*

The business-as-usual scenario corresponds to a 4–5°C rise in temperature above pre-industrial levels in 100–150 years (Stern, 2006b). Melting glaciers, declining crop yields, ocean acidification, rising sea levels, malnutrition and heat stress, and the vulnerability of ecosystems are among the other impacts of global climate change which must be incorporated into the scientific and economic analyses. Moreover, at high levels of warming, less is known about how the climate will respond and there are higher risks from extreme events occurring.

There is also uncertainty in the direct linkage between emission levels and temperature change, it is generally accepted that as levels of GHGs increase the probable temperature also increases. The SR uses a range of temperature values provided by Meinshausen (2006), which uses climate sensitivity analyses from eleven recent climate studies. Temperatures projected at stabilization levels between 400 ppm and 750 ppm CO₂e and the corresponding temperature increases based on current scientific literature are shown in Figure 4 (Stern, 2006b).

2.2. Uncertainty of climate projections and models

Even though the consensus among the majority of scientists is that global temperature rise is occurring, there are serious limitations to temperature projections estimated from climate models. In addition, the use of a variety of models and varied assumptions between models affects the projection results, since different models have different representations of physical processes along with the strengths and weakness associated with the assumptions and initial conditions (Giorgi and Francisco, 2000). Because the science shapes the economics of climate change, principally the prices and social costs of carbon and marginal abatement costs, it is important to understand the climate model forecasts and the limitations of projections for global temperature change beyond the near future.

Because climate change models are dependent on physical and chemical parameters, some of which are highly uncertain, it is essential perform sensitivity analyses for the range of possible values associated with each uncertain parameter. The ‘goodness-of-fit’ test is one possible criteria for selecting values for uncertain parameters, however, other methods incorporate varying the value of the parameter to plot the probability distribution functions (PDFs) across the climate model (Stern, 2006c). The Hadley Centre addresses the uncertainty related to climate modeling by quantifying it in the form of probabilistic estimates (Hadley Centre, 2005). A variety of climate models are run with varying parameters for uncertain components³ of and stochastic perturbation of the feedback parameter on the climate system. The ensemble probability spread of reaching stabilization at a certain emission level can be plotted for a specific temperature target as shown by the blue line in Figure 5 (Hadley Centre, 2005) for an increase in 2°C above the present day temperature. Moreover, the values in the ensemble spread can be weighted based on the reliability of the estimates with observed data, as was done for the blue line spread with the weighted spread shown by the red line in Figure 5 (Hadley Centre, 2005).

³ These components include but are not limited to: Clouds, Land surface, Air temperature, Rainfall, Snowfall, River flow, Soil moisture and temperature, Wind speed and direction, Surface sunlight amount, Cloud amount, Ecosystem productivity, Sea-ice amount, and Ocean temperature and salinity.

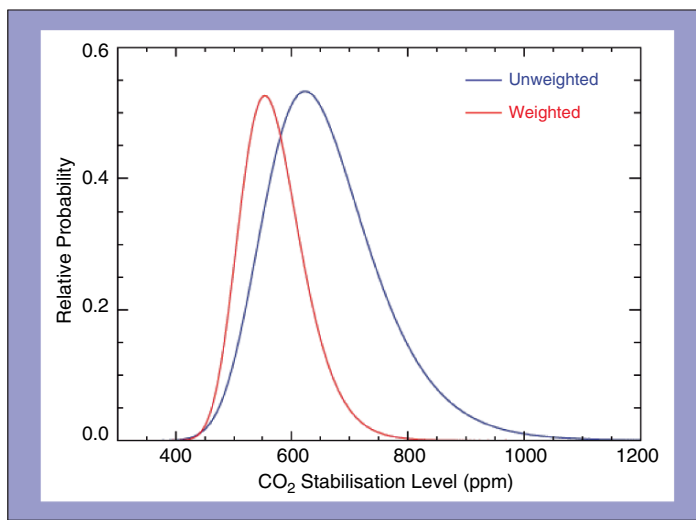


Fig. 5. Probability distributions of climate sensitivity (for weighted (red) and unweighted (blue) ensemble model probability estimates of a temperature rise by 2°C relative to present day). *Source: Hadley Centre (2005).*

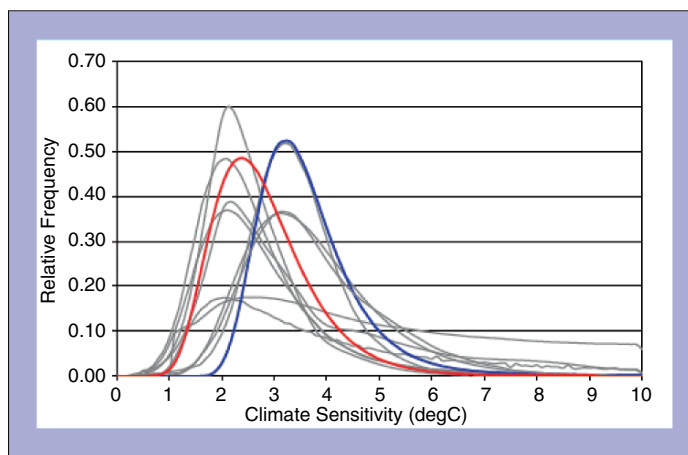


Fig. 6. Climate sensitivity results for eleven climate model studies. The red and blue lines represent the IPCC TAR (Wigley and Raper, 2001) and Hadley Centre ensemble work (Murphy *et al.*, 2004), respectively, which are shown to be distributed close to the center of all distributions. *Source: Meinshausen, (2006), from Stern, (2006b).*

However, the robustness of estimates for ensemble models will be enhanced by better estimates of model reliability, which will help produce a weighted probability distribution that is more representative of the current and future situation. In the example shown in Figure 5 from the Hadley Centre, 53 models were used in

order to address the full range of model projections in order to plot the probabilities and range of emission stabilization levels. In the SR's climate analysis, the SR supports the use of ensemble models, since they help to develop a further understanding of climate sensitivity by allowing for further comparison between climate models and the combination of datasets, statistical techniques, and methodologies.

However, the Review specifically utilizes a study of eleven climate model sensitivity distributions (see Figure 6; Meinshausen, 2006).

A comprehensive use of climate models would present a better estimate of model reliability, and the SR's use of Meinshausen's model sensitivity distributions presents concrete limitations to further analysis. The SR specifically notes that further analysis is conducted with greater weight being given to the Intergovernmental Panel on Climate Change (IPCC) Third Assessment Report (TAR) (Wigley and Raper, 2001) and Hadley Centre (Murphy *et al.*, 2004) models since these models are shown to be distributed close to the center of all climate sensitivity distributions. However, there exists a wide range of uncertainty between each model used. Figure 7 (IPCC, 2001) depicts a range of climate model projections through the year 2100 for seven different emission scenarios described in the IPCC special Report on Emission Scenarios (SRES) (IPCC, 2000). Emission scenario descriptions are described further on Figure 7 (IPCC, 2001) and all scenarios do not include additional climate policy above current ones. The blue shading represents uncertainty between the 35 models in total that were run within the seven scenarios. Each SRES has underlying assumptions regarding socioeconomic, demographic and technological change. The varied assumptions between each model may yield a dominant source of uncertainty in the simulation, which, in regional climate modeling, is principally due to inter-model variability with inter-scenario rather than internal model variability (Giorgi and Francisco, 2000). This presents a different perspective of uncertainty in the models, since, ideally, the models should represent the full spectrum of possibilities with no scenario receiving more weight than the other. However, this can lead to a greater source of uncertainty and inter-model variability, even though the results may exhibit a high level of precision among different scenarios.

In addition, because the SRES scenarios are dependent on relationships between emissions, abundances, and radiative forcing, ultimately the scenario results are dependent on the climate feedbacks on the carbon cycle and the given range of climate sensitivity which dictate the level of warming. Wigley and Raper describe the uncertainty associated with SRES assumptions for the carbon cycle model and the range of values for climate sensitivity (Wigley and Raper, 2001). For the TAR, the SRES scenarios are tuned such the climate sensitivity and climate feedbacks match those for other models used in the TAR, such (Jain *et al.*, 1996; Joos *et al.*, 1996). However, these values do not span the full range of possible sensitivities or address the possibility of dramatic changes to the carbon cycle. This leads to another argument on the limitations of climate sensitivity analysis, and the assumption that the model or SRES scenarios are assumed 'true' within each individual scenario and with respect to the entire realm of possibilities.

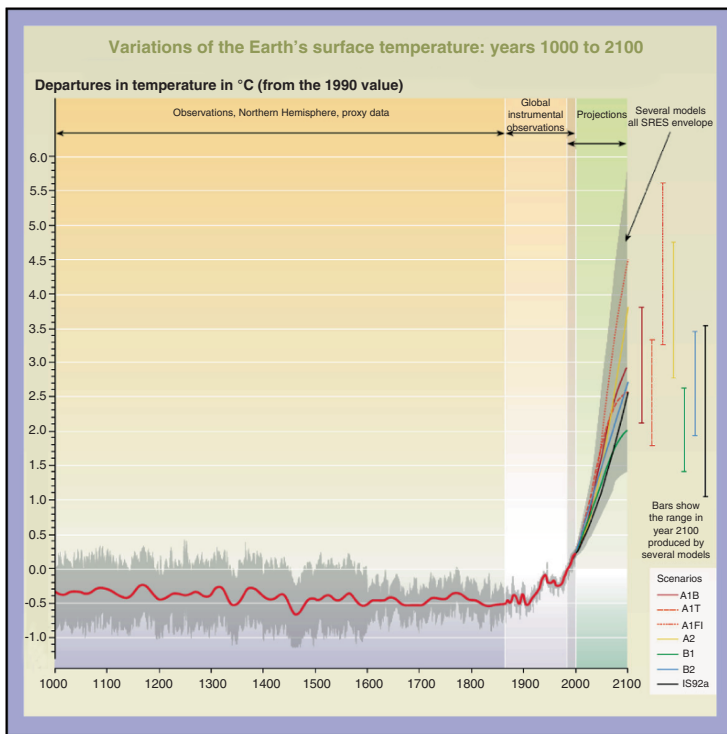


Fig. 7. Climate model predictions through 2100. The line shows the 50-year average, the grey region the 95% confidence limit in the annual data. From years 2000 to 2100 projections of globally averaged surface temperature are shown for the six illustrative SRES scenarios and IS92a using a model with average climate sensitivity. The grey region marked “several models all SRES envelope” shows the range of results from the full range of 35 SRES scenarios in addition to those from a range of models with different climate sensitivities. *Source: IPCC (2001). Special Report on Emissions Scenarios (SRES). Symbols are defined in the appendix (end of chapter).*

2.3. Climate model limitations and future prospects

One aspect that addresses the limitations of climate models being ‘true’ is in the ability to model the distributional pattern of temperature change across regions. Currently, climate models from the Hadley Centre include predictions for regional changes, however, a limitation includes the ability to simulate the North Atlantic Oscillation, and thus the particular effects this has on European weather and climate (Hadley Centre, 2005). In terms of expanding technological capability, the Hadley Centre acknowledges that the aim of the next generation computer model is to improve regional predictions while noting that future work must focus to

expand the range of outputs by incorporating the event of extreme temperature changes (Hadley Centre, 2005).

Additionally, the availability of technology and the advancement of scenarios, models, and methods are crucial factors to achieve greater reliability of climate change pathways. For example, in the 1980's there existed only a few distinct groups globally with the technology and ability to run and analyze model outputs, with limited opportunity to exchange model data. This situation led to the creation of the World Climate Research Programme (WCRP) in 1980, with specific aims to improve the understanding of climate and model projections (WCRP, 2007). This international partnership has helped pave the way forward for developments and improvements to climate models, in addition to analyzing uncertainty and errors within simulations. Previous limitations related to data transfer and storage impeded the collection, distribution, and analysis of climate model outputs. For example, authors of the IPCC TAR were only able to analyze a few fields from few models and experiments, which were analyzed by a limited climate science community (WCRP, 2007). For the IPCC Fourth Assessment Report (AR4), WCRP facilitated the collection, archiving, and access of model simulations and results in conjunction with the Working Group of Coupled Models (WGCM), established under WCRP, which leads the development as well as the identification of errors of coupled ocean, atmosphere, and land models used for climate studies on longer time-scales (WCRP, 2007). Other valuable efforts to advance climate modeling include the ability for researchers to compare between models and subsets of model data, which is also organized through WCRP.

Nonetheless, despite these efforts in progressing climate model projections, climate uncertainties are specifically vulnerable to concerns relating to magnitude, timing, persistence, reversibility, the potential for us adaptation, distributional aspects, and the weight of importance of the impacts (IPCC, 2007). As Article 2 of the UNFCCC states:

“The ultimate objective of this Convention and any related legal instruments that the Conference of the Parties may adopt is to achieve, in accordance with the relevant provisions of the Convention, stabilization of greenhouse gas concentrations in the atmosphere at a level that would prevent dangerous anthropogenic interference with the climate system. Such a level should be achieved within a time-frame sufficient to allow ecosystems to adapt naturally to climate change, to ensure that food production is not threatened and to enable economic development to proceed in a sustainable manner.” (UNFCCC, 2002, pg.2).

The terms dangerous and sufficient time-frame necessary to adapt to climate change identify the main cause for concern, since many of these aspects to mitigate interference with the climate system cannot be represented by climate models explicitly but must instead be decided by implicit societal values (which will be addressed in the section 3.0 Uncertainties in the Economic Framework). For example, IPCC has identified five areas for concern: (i) risks to unique and threatened systems, (ii) risks of extreme weather events, (iii) distribution of impacts and

vulnerabilities, (iv) aggregate impacts, and (v) risks of large scale singularities.⁴ Each of these concerns requires the placement of judgment in order to identify the extent to which the impacts from these scientific studies will be integrated into climate models. However, many of these aspects are limited the ability to observe their impacts on the climate system. It will be particularly important in the future to increase reliability of regional impact projections, which will enable better identification of particularly vulnerable systems, sectors and regions.

Because, as the SR acknowledges, the science shapes the economics of climate change, it is important to understand the limitations mentioned above with regards to the science and the uncertainties inherent within the various climate model predictions and the effect this has on further economic analysis which uses these climate models to identify the baseline for emission stabilization goals. Climate predictions are continuously being updated and economic models and climate change policy should be flexible and adaptable to incorporate new data and results arising from updated studies. For instance, the SR's analysis is based on projections from previous IPCC studies, while updated projections are available in the IPCC AR4 (IPCC, 2007). These studies include newer results that have emerged from methodological changes in probabilistic climate simulations, such as the inclusion of carbon cycle feedbacks in the Hadley Centre's model (Stern, 2006b). Furthermore, the Hadley Centre notes an important uncertainty lies in the many feedbacks in the current climate system and the possibility of the strength of those feedbacks changing in the future (Hadley Centre, 2005).

⁴ The five areas of concern identified by the IPCC AR4: Risks to unique and threatened systems. There is new and stronger evidence of observed impacts of climate change to unique and vulnerable systems (such as polar and high mountain communities and ecosystems). Risks of extreme weather events. Responses to some recent extreme climate events reveal higher levels of vulnerability in both developing and developed countries than was assessed in the TAR. There is now higher confidence in the projected increases in droughts, heat-waves, and floods as well as their adverse impacts. Increases in drought, heatwaves and floods are projected in many regions and would have mostly adverse impacts, including increased water stress and wild fire frequency, adverse effects on food production, adverse health effects, increased flood risk and extreme high sea level, and damage to infrastructure. Distribution of impacts and vulnerabilities. There are sharp differences across regions and societal groups with regards to susceptibility to climate-related damages. Aggregate impacts. Compared to the TAR, initial net market-based benefits from climate change are projected to peak at a lower magnitude and therefore sooner than was assessed in the TAR. It is likely that there will be higher damages for larger magnitudes of global temperature increase than estimated in the TAR and the net costs of impacts of increased warming are projected to increase over time. Risks of large scale singularities. During the current century, a large-scale abrupt change in the meridional overturning circulation (MOC) is very unlikely. The sea level rise contribution from thermal expansion is projected to be much larger than observed over the twentieth century. There is better understanding than in the TAR that the risk of additional contributions to sea level rise and possibly Antarctic ice sheets may be larger than projected by ice sheet models and could occur on century time scales. This is because ice dynamical processes seen in recent observations but not fully included in ice sheet models assessed in AR4 could increase the rate of ice loss. Complete deglaciation of the Greenland ice sheet would raise sea level by 7 m and could be irreversible (explanations quoted from IPCC, 2007).

2.4. Extreme events and final notes on scientific uncertainties

The SR acknowledges the following key messages regarding the science of climate change: (1) climate change threatens the basic elements of life for people around the world access to water, food, health, and use of land and the environment, and (2) the consequences of climate change will become disproportionately more damaging with increased warming.

Overall, the SR claims that the potential risk and the climate system's vulnerabilities to higher temperatures entering into "dangerous territory", which will have disproportional effects for global security of the basic elements of life, gives further justification for the inclusion of extreme events into the scientific and economic analysis (Stern, 2006b). However, as explained above, the ability to identify extreme events and their impacts are limited by their observation and technological capability in modeling. Thus, these analyses must be continuously reviewed as scientific research and climate models are expanded to achieve greater understanding of potential feedbacks, such as the effect of low versus high clouds on climate sensitivity and temperature change.

In addition, another aspect to mention but not to be delved into deeply is the criticisms surrounding the SR's scientific analysis lacking peer-review by others in the scientific community, since the SR was commissioned by the Chancellor of the Exchequer, Gordon Brown, in the United Kingdom (UK) and involved independent academics to take part only as consultants. This in itself has inherent biases, as the SR was mainly a product of a team of economists from the UK's HM Treasury.

Now that the uncertainties related to the science of climate change and modeling have been exposed, we can turn to the uncertainties associated with the SR's economic analysis.

3. Uncertainties in the economic framework

3.1. Estimating the costs of climate change and model uncertainties

The SR has focused the economic analysis based on stabilization of GHG concentrations in the range of 450–550 ppm CO₂e. This is based on scientific analysis and thus incorporates a range of uncertainties related to the climate models as explained in the previous section. Given technological advances in science and economic modeling, the risks and probabilities of climate change can be analyzed to give an estimate of the costs of the risks. There are several approaches that can be taken when estimating the costs of climate change: (1) evaluating the physical impacts on economic activity, on human life and on the environment, (2) taking a

technology based approach to costing fossil fuel emissions, and (3) using integrated assessment models to provide aggregate monetary estimates. I will focus on the last two approaches.

Earlier economic models have concluded that a rise in 2–3°C will produce a loss of 0–3% in global output, and a rise in excess of 2–3°C will produce a loss in the range of 5–10% (Stern, 2006b). The results for the high range of given by the latter scenario are justified since recent climate predictions indicate that global climate change has a possibility of reaching into the 5–6°C range within the next century. The SR attempts to include the impacts and the potential costs of large-scale climate events to a certain extent through economic analysis. However, it is stated that recent findings of stronger feedbacks and the possibility of reaching higher temperatures are not incorporated into the analysis, thus under-estimating the resulting costs.

3.2. Uncertainties in the role of technology

In evaluating the costs associated with reducing GHG emissions through abatement and conservation schemes, it is possible to categorize two distinct cost groups: (1) the costs associated with investments in research and development of new technologies – this will involve the development and deployment of low-emission and high-efficiency technologies, and (2) the costs involved at the consumer level – such as actions to switch from high-intensive to low-emission goods and services. A key component of this analysis involves the rate of diffusion of technology. In general, the cost of technologies tends to fall over time due to its learning curve and achievement of economies of scale. For example, the options for low-emission technologies to replace fossil-fuel based electricity generating technologies include wind power, hydro power, photovoltaics, fuel from biomass, geothermal, and various others. Figure 8 (Stern, 2006b) shows the cost evolution of selected technologies and their respective learning rates based on published learning-rate estimates. As shown in Figure 8 (Stern, 2006b), the learning rates span a range of 3% to over 35%. The incorporation of costs for these technologies will be highly dependent on the market dynamics, public investment, and political/financial mechanisms to support technological adoption. In addition, in computing the costs, selection bias occurs since the technologies that are not successful are dropped from the market and the economics analysis. To account for this, the SR attempts to embed the high risks associated within the market for low-emission technologies into the respective learning curves and overall cost assessment.

In addition to the uncertainties and risks of costs and development previously mentioned, a significant amount of uncertainty lies in the dynamics within the energy system as a whole, and to what extent the entire energy system can help mitigate the effect of emissions and global climate change. Certain technological advancements may be dependent on advancements of other types of technology, such as energy

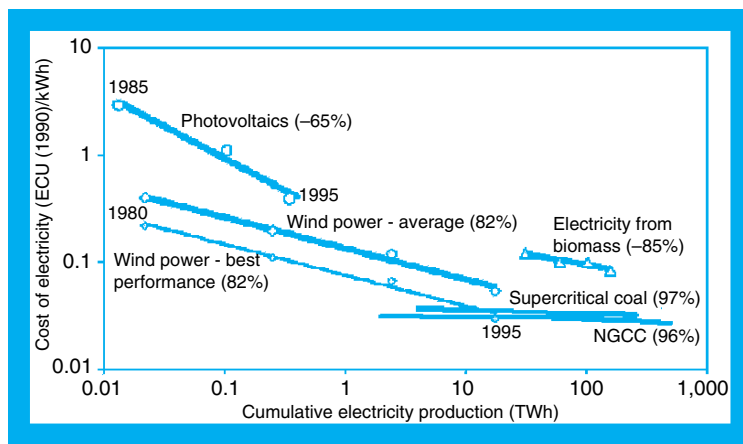


Fig. 8. Cost evolution of learning rates for selected technologies. The number in brackets indicates the speed of learning: For example, (97%) means that unit costs are 97% of their previous level after each doubling of installed capacity – meaning costs of a good are 3% cheaper than the previous level. *Source: IEA (2000); from Stern (2006b).*

storage techniques and the instantaneous generation of electricity or heat (Stern, 2006b). Moreover, the advancement of technologies face certain limitations within the energy system. No one technology can be depended on as the solution to the climate change problem, which adds an additional level of uncertainty since one cannot predict what technologies will become available in the future due to innovation. Thus, the SR emphasizes the importance of developing a portfolio of options to offset the limitations and uncertainties present in individual technologies. Figure 9 (Stern, 2006b) shows the associated costs pertaining to the investment needed for the development of innovative technologies, in this case a new technology for electricity production is used. The marginal costs of the technology are shown to decrease as time increases due to adoption and development, or learning-by-doing/learning-by-using and other effects.

However, there is an important and complex interplay between the effect of the rising social cost increasing the marginal cost of a new technology and the decrease in the average cost associated with innovation, learning, and experience. This is demonstrated in Figure 10 (Stern, 2006b). Thus, this dynamic must be accounted for in evaluating the total costs of technology over time. Overall, abatement costs are summarized in Figure 11 (Stern, 2006b), indicating the costs of abatement of fossil-fuel emissions to 18 gigatons CO₂e per year in 2050. The costs estimated are \$930 billion, or less than 1% \pm 2.5% of GDP in 2050 with an average abatement cost of \$22 per ton of CO₂ per year in 2050. These estimates consider the full range of possible costs for each technology, future oil prices specified as a probability distribution ranging from \$20 to \$80 per barrel, as similarly done for

gas prices, coal prices, and future energy demands. The SR states there are inescapable uncertainties inherent in the projections – as can be observed with the price of oil currently reaching \$100 per barrel, above the range given for the SR's

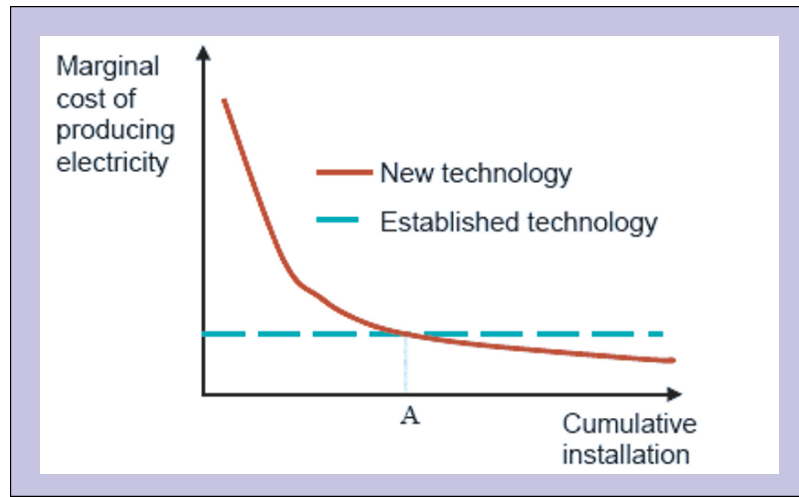


Fig. 9. Illustrative experience curve for a new technology showing the marginal cost of producing electricity and the significant investment needed for development of a new technology before it becomes cost-effective. *Source: Stern (2006b).*

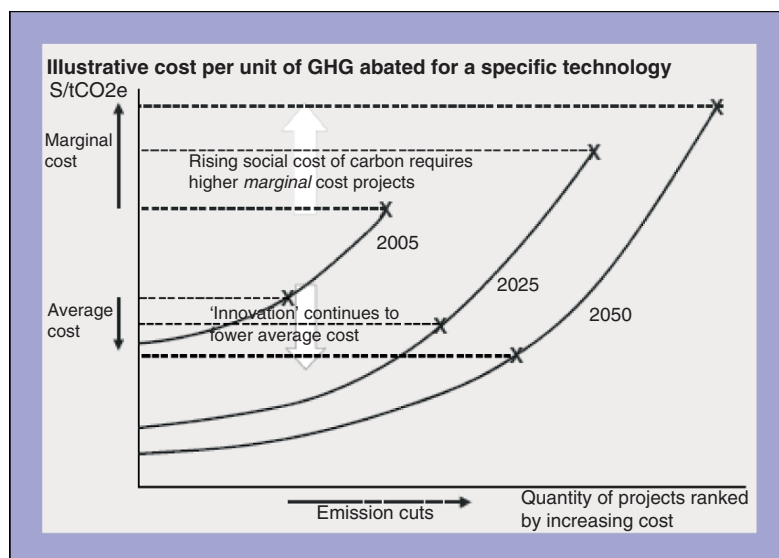


Fig. 10. Illustrative cost per unit of GHG abated for a specific technology. *Source: Stern (2006b).*

analysis. Figure 12 (Barker *et al.*, 2006) represents the effect of various components of the SR's economic model, including the effect of induced technology and backstop technology, on world gross domestic product (GDP) in 2030 for stabilization at 500–550 ppm CO₂e⁵. On average, these technological components compose a possible 2.5% difference in the global percentage costs of stabilization at this emission concentration in 2030, giving an indication of the impact that uncertainty can have on the overall outcome. To discuss these issues with uncertainty a bit further, we now turn to the economic model used in the SR.

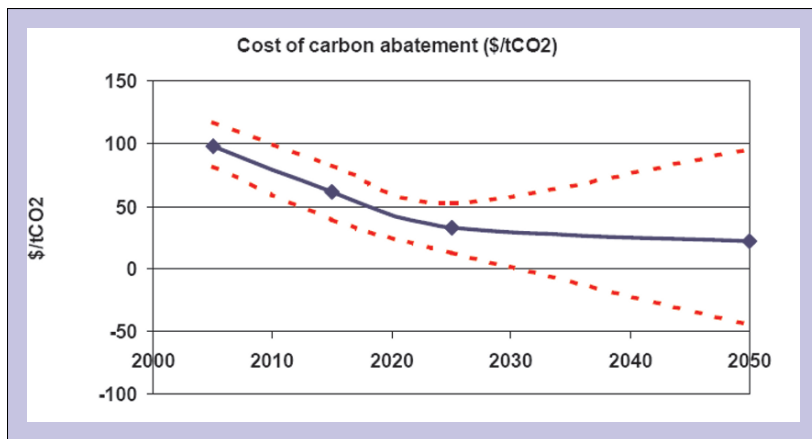


Fig. 11. Conclusions of the cost of carbon abatement. The red lines give uncertainty bounds around the central estimate using Monte Carlo analysis. *Source: Stern (2006b).*

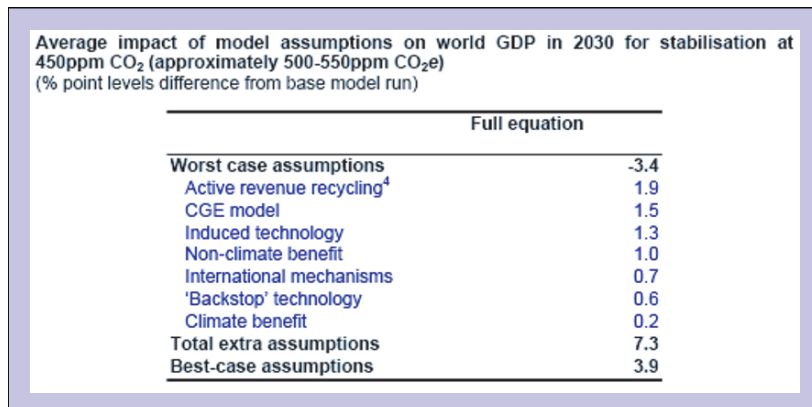


Fig. 12. Meta-analysis estimates, contributions to cost reduction. *Source Barker *et al.* (2006).*

⁵ Referring to the effect that technological progress due to backstop resources will support unlimited technological progress.

3.3. Basics of the economic model

On to the integrated modeling approach, which is used to aggregate the overall costs of climate change given the impacts of temperature increases, the economic model used in the SR is the Policy Analysis of the Greenhouse Effect 2002 (PAGE2002) Integrated Assessment Model (IAM) (Hope, 2003; Stern, 2006b). This model allows for direct modeling of the probabilities or risks of climate change and at small temperature changes obtains similar results to other models. However, two significant differences in comparison with other models is that it incorporates bigger risks described by the possibility of a 5–6°C change in temperature and it takes into consideration long-term future predictions (Stern, 2006b). The model involves aggregating costs and benefits both over time and across possible outcomes.

3.3.1. Aggregating over time and the discounting debate

The process of aggregating over time involves a principle assumption in discounting, or the rate in which the value of one unit of something decreases as each year or time period passes. Thus, the question of uncertainty essentially lies in how one should value the future and if it is justified to give more or less value to future periods of consumption. This is valued as the pure time discount rate. In general, the higher the discount rate equates to less weight being placed on future utility. A discount rate of unity in effect means that generations in the indefinite future are treated equal to the current generation. The SR uses a pure time discount rate of 0.1% per year, which is justified, as the SR frankly states, by the probability that there is a 10% chance of wiping out our generation in the next hundred years (Stern, 2006b). Normally, economists use discount rates of 3–5% (but can be anywhere from 0% to 20% (Portney and Weyant, 1999)) to value future damages and, thus, the SR's choice has been harshly criticized. The discount rate assumption is a valid cause for concern to judge the reliability of the SR's analysis and should be questioned as it defines a prescriptive discount rate rather than a descriptive one, on which will now be elaborated.

Thus, we enter the great discount rate debate. The choice of the discount rate has been as controversial in recent times as it was 40 years ago (Lind, 1982; Portney and Weyant, 1999). The value of the discount rate is generally an ethical question, however, various methodologies have been proposed. In one extreme, one could argue that the issue of discounting requires a subjective perspective of value and decisions being made for individuals in future generations and it should not be done.⁶ Furthermore, those who benefit in the future cannot compensate the 'losers' in the current generation. Thus, discounting would not be consistent with

⁶ For a historical lesson of the objections to discounting see positions by Mill (1848); Marshall (1890), and Pigou (1920).

our moral concerns (Broome, 1992). In a similar vein, Cobb and Daly note that discounting is beneficial only in dealing with our current portfolio of investments, and not justifiable to address responsibility to future generations (Cobb and Daly, 1989). The SR's view is much aligned with this school of thought. In fact, the SR's strategy has been supported by Nobel Prize recipient Kenneth Arrow:

"Critics of the Stern Review don't think serious action to limit CO₂ emissions is justified, because there remains substantial uncertainty about the extent of the costs of global climate change, and because these costs will be incurred far in the future. However, I believe that Stern's fundamental conclusion is justified: we are much better off reducing CO₂ emissions substantially than risking the consequences of failing to act, even if, unlike Stern, one heavily discounts uncertainty and the future." (Project Syndicate, 2007).

However, a morally justified approach for discounting is proposed by Koopmans (1965), who noted the reduction in current consumption is acceptable in the sense that it will bring future generations greater consumption with overall benefits which will far outweigh the current generation's sacrifices. Moreover, with respect to expected utility, it is justified to discount on the basis that we may not be around to enjoy future consumption (e.g., due to mortality or an extreme event causing annihilation) (Quiggin, 2006a). Additionally, because individuals facing uncertainty often put more weight on low-probability extreme outcomes (in this case extreme temperature increases) than would be implied by measures of expected utility, the use of a low discount rate is further supported (Kahneman and Tversky 1979). Solow (1994) echoes the opinion for placing a low discount rate for natural resources in order to support conservation and sustainability decisions.

Thus, we now turn to the options for choosing a discount rate. Portney and Weyant (1999) have described two approaches to the selection of the discount rate: (i) the prescriptive approach, and (ii) the descriptive approach. The prescriptive approach involves the selection of discount rate based on ethical guidelines that suggest how future generations should be considered. The descriptive approach involves choosing the discount rate based on observations of the rates of return to capital invested in a variety of assets. In general, Kenneth Arrow suggests that the prescriptive approach will yield a lower discount rate (Portney and Weyant, 1999). Thus, the SR's use of a pure time discount rate of 0.1% per year places an ethical judgment from the economists and analysts that costs of climate change future generations should be considered almost as equally as the present costs to our generation.

Other forms of discounting can be applied by substituting the private or market discount rate, or the rate of investment in capital markets; the social discount rate, or the rate set by the government to evaluate social projects which is usually lower than the market rate; the social opportunity cost rate, or the rate of return that investments earn in society; and finally the social rate of time preference, or the rate of interest that savings earn in society. Specifically, the SR uses the social rate of time preference (from now on referred to as SRTP) which is based on the Ramsey model of optimal growth theory and shown in equation (1) (Ramsey, 1928; Koopmans, 1965):

$$SRTP = p + m \times g \quad (1)$$

where p is the pure rate of time preference, g denotes the growth rate of per capita consumption, and m represents the elasticity of the marginal utility of consumption.

The discount rate mentioned previously in this discussion now refers to the pure rate of time preference, p , which is set to 0.1% per year. The values for g at a stable population and m are 1.3% per year and 1 respectively, which produces a SRTP of ~1.4% per year. Equation (1) dictates that the SRTP is composed of a growth rate parameter, which can be varied to depict various scenarios incorporating the extent of high climate, market impacts, risk of catastrophe, and non-market impacts – as shown in Figure 13. These three scenarios (four including the baseline business as usual scenario) are discussed in the SR and show the model results for the costs in per-capita GDP for global mean temperature and the estimates for costs associated with temperature increases of 2–5°C from the PAGE20002 model.

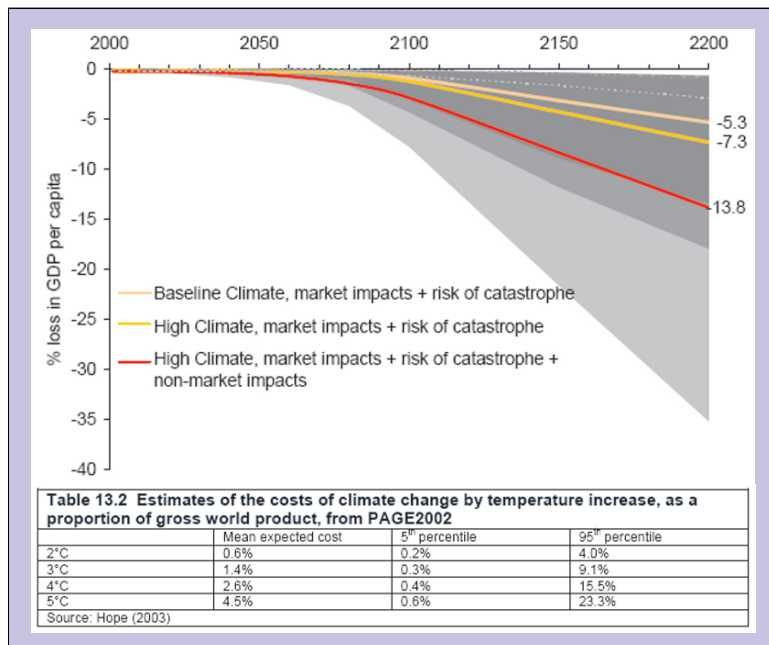


Fig. 13. Mean losses in income per capita from four scenarios of climate change and economic impacts, plotted against time. This figure traces losses in income per capita due to climate change over the next 200 years, according to three of the main scenarios of climate change and economic impacts. The mean loss is shown in a color matching the scenarios. The range of estimates from the 5th to the 95th percentile is shaded grey. It plots mean losses in per-capita GDP due to climate change as a function of increasing global mean temperature. *Source: Stern (2006b).* The bottom panel shows estimates of costs as a proportion of gross world product associated with a change in temperature, from the PAGE2002 model runs. *Source: Hope (2003).*

Nordhaus has criticized the mean losses as interpreted from the impact of near-zero discounting. Nordhaus states, with reference to Figure 13 (Stern, 2006b):

“Take as an example the high-climate scenario with catastrophic and non-market impacts. For this case, the mean losses are 0.4 percent of world output in 2060, 2.9 percent in 2100, and 13.8 percent in 2200.78 This is calculated as a loss in “current per capita consumption” of 14.4 percent...with near-zero discounting, the low damages in the next two centuries get overwhelmed by the long-term average over the many centuries that follow. In fact, using the Review’s methodology, more than half of the estimated damages “now and forever” occur after the year 2800. The damage puzzle is resolved. The large damages from global warming reflect large and speculative damages in the far-distant future magnified into a large current value by a near-zero time discount rate.” (Nordhaus, 2007, pg.156–157).

In addition, Nordhaus (2007) argues that the parameters for equation (1) depicting the optimized growth model must be chosen inter-dependently in order to design the model such that it simulated observable real interest rates or savings rates. The choice of the elasticity of marginal utility of consumption is not well justified throughout the SR. In order to reach a 4% interest rate with the assumed growth per capita of 1.3%, there would need to be a combination of high pure time discounting and high elasticity, which is not the case with the SR.⁷

Other notable suggestions for a discount rate framework are provided by Bradford and Lind. Bradford (1975) argues that the aggregate of benefits and costs does not reveal dynamics in the distribution of the benefits or costs. Thus it may not be possible to say if a policy is good or bad since it must weigh the gains to the gainers and the losses to the losers, which are overall difficult to identify. Bradford suggests using a declining social marginal utility of consumption and the market rate for long-term evaluations (Bradford, 1975). Lind argues that all future costs and benefits should be converted into changes in consumption for those who will experience them. The consumption measure of costs of public investment should be adjusted upward to reflect the marginal productivity of capital, and the adjusted streams of consumption equivalents should be discounted using the social rate of time preference. Lind explains that the discount rate should not be based on the utilitarian welfare function, in which we should aim to maximize the well-being of the poorest individual in society (for further discussion see Rawls, 1971).

Additionally, another area of recent research that should be addressed with regards to the pure time discount rate involves the concept that people do not behave as if their own discount rates are a constant. Specifically, Cropper *et al.* (1994) performed a survey of individual trade-offs over time which estimated a nominal rate of around 16.8% in valuing the present versus future risks. This finding strikes dissonance with the notion that the pure time discount rates follow a constant exponential rate through time. Other studies have found similar sugges-

⁷ Using the SR’s assumption for the economic growth rate, a near-zero pure time discount rate requires a consumption elasticity of 3 to produce a 4% rate of return per year. If we adopt the Stern consumption elasticity of 1, then we need a pure time discount rate of 2.7% per year to match observed rates of return. (Nordhaus, 2007).

tions that the discount equations are hyperbolic with discount rates that are likely to decline as time goes on (Weitzman, 1998, 1999; Gollier, 2002; Frederick *et al.*, 2002; Pearce *et al.*, 2006). In addition, Wietzman supports the use of a declining interest rate when evaluating projects in the long term and suggests revisiting the deep future discount rate every year.

Thus, the debate is far from concluded. Overall, there is most obviously an enormous amount of uncertainty when evaluating the future. These arguments and the fact that the discount rate can be chosen on ethical guidelines and the variety of approaches mentioned in choosing the discount rate fuels further uncertainty into the economic models used in the SR. However, the review sides with using a lower discount rate based on the justification that the probability of a catastrophic event no matter how small should be evaluated and included in the analysis. Essentially, the SR has chosen a pure time discount rate value based on practice that for shorter term projections (40 years or so) the discount rate should reflect the opportunity cost of capital and for longer term (over the span of centuries) it may be prudent to use a lower or near-zero pure time discount rate. This, in addition to the assumptions in equation (1) for optimal growth, enlists a wide range of criticism and uncertainty related to the SR's final cost scenarios and results.

3.3.2. Sensitivity calculations of the economic model

In order to dispel some of the concerns, the economic analysis includes a sensitivity analysis as shown in Figure 14 (Stern, 2006b). The model is sensitive to a variety of inputs, however only analyzed for changes in future prices of fossil fuels, assumptions of increased energy efficiency, and prices of low-carbon technologies (e.g., carbon capture and storage). This SR sensitivity analysis is limited at best. Figure 14 (Stern, 2006b) shows the cost estimates range from -1.0% to 3.5% of global GDP by 2050. In comparison to the costs of global GDP in the business as usual or other climate scenarios presented in Figure 13 (Stern, 2006b), the costs of mitigation are far less. However, this figure is in fact a lower estimate on the costs considering the assumptions given in the SR's analysis and the optimism of future technology and innovation.

Furthermore, the calculation of the damage from impacts stemming from climate change reflect high estimates due to the combination of the low discount rate and low elasticity of marginal consumption discussed earlier, as well as major assumptions on society's ability to properly adapt (e.g., probability for farmers to change crop to suit a change in temperature, probability of protecting against floods through building dams, etc.) and its costs (Stern, 2006b). Adaptation plays significant role in assessing the damage costs from climate change.

Nordhaus (2007), who has also conducted various studies on the economics of climate change, uses the Dynamic Integrated model of Climate and the Economy (DICE-2007) model to arrive at damage costs per output for 2100 shown

in Figure 15 (Nordhaus, 2007). The costs function is a function of the growth in total factor productivity (TFP), the rate of decarbonization, the temperature sensitivity coefficient, the intercept of damage function, the price of backstop technology, the asymptotic population, the fraction in carbon cycle, and the resource

Table 9.3 Sensitivity analysis of global costs of cutting fossil fuel emissions to 18 GtCO₂ in 2050 (costs expressed as % of world GDP)^a

Case	2015	2025	2050
(i) Central case	0.3	0.7	1.0
(ii) Pessimistic technology case	0.4	0.9	3.3
(iii) Optimistic technology case	0.2	0.2	-1.0
(iv) Low future oil and gas prices	0.4	1.1	2.4
(v) High future oil and gas prices	0.2	0.5	0.2
(vi) High costs of carbon capture and storage	0.3	0.8	1.9
(vii) A lower rate of growth of energy demand	0.3	0.5	0.7
(viii) A higher rate of growth of energy demand	0.3	0.6	1.0
(ix) Including incremental vehicle costs ^b			
• Means	0.4	0.8	1.4
• Ranges	0.3-0.5	0.5-1.1	-0.6- 3.5

Fig. 14. Sensitivity analysis. *Source: Stern (2006b).*

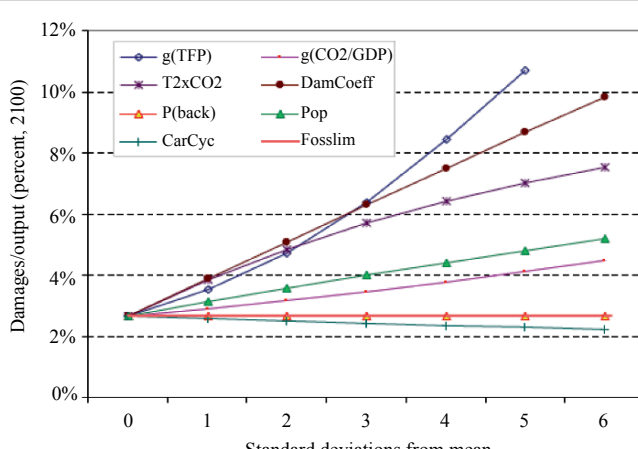


Fig. 15. Damage ratio as function of uncertain parameter. This figure shows the ratio of climate damage to output in 2100 for the mean value of each parameter and for the values at the given number of standard deviations shown on the horizontal axis. Variable key: g(TFP) = growth in total factor productivity; g(CO₂/GDP) = rate of decarbonization; T₂ × CO₂ = temperature sensitivity coefficient; DamCoeff = intercept of damage function; P(back) = price of backstop technology; Pop = asymptotic population; CarCyc = atmospheric fraction in carbon cycle; Fosslim = resource abundance of carbon fuels. *Source: Nordhaus (2007).*

abundance of carbon fuels. According to Figure 15 (Nordhaus, 2007), the growth in TFP is most affected by future uncertainty, with the damage coefficient and the rate of decarbonization also ranking high in uncertainty. This emphasizes the importance of future technology and output productivity (e.g., through energy efficiency) for future calculations on the costs of climate change, given the model's assumptions.

3.4. Cognitive limitations of economic models

One last point about uncertainty in the economic models includes cognitive capacity limitations and the notion that science does not have all the answers to future outcomes. As we mentioned, one of the main limitations of scientific and economic models is the inability to incorporate the entire set of outcomes possible in the future. Thus, the analysis is interpreted to the best of the analyst's own capacities. This bounded rationality hinders the ability to consider the optimal alternative (e.g., choosing the status quo BAU or mitigation efforts), and this is a major critique of cost–benefit analyses (Simon, 1991). Moreover, cognitive factors are particularly important when: (1) project benefits and costs vary simultaneously on many dimensions; (2) benefit cost functions are discontinuous or complex (interaction terms); or (3) there is uncertainty about the interactions or the functional forms (Simon, 1957). It can be argued that many of these cases apply to the SR's economic analysis, since the path of many scientific and economic parameters are uncertain through time and there are many climate system feedbacks and interactions related to economic and political factors that are not yet understood.

3.5. Final words

Overall, the SR's economic conclusions are measures that instigate action towards mitigating climate change (Quiggin, 2006b). In addition, Stern (2006b, pg. 145) acknowledges that economic models "...must make drastic, often heroic simplifications along all stages of the climate-change chain [but]...remain the best tool available for estimating aggregate quantitative global costs and risks of climate change." However, the case of uncertainty and the SR's cost analysis of a possible worst-case scenario brings into light that more demanding climate change goals are needed. Ultimately the extent of the costs incurred by society will depend on the design and application of current environmental policies (Stern, 2006b). The possible steps for action and the effect of uncertainty in long-term policies will be explained in the proceeding section.

4. The implications for policy and the uncertainties in the political framework

4.1. Options for climate policy: taxes and markets

To address the final chapter of the story, the SR addresses the implications of its results on policy. The SR emphasizes action to mitigate global climate change is necessary across all sectors and countries, since emissions are not limited to any one sector or border. In addition, the SR raises the issue of inequity in terms of impacts or burdens of climate change (developing countries) and the responsibility for paying for mitigation and influencing policy (developed countries).

There are various strands to the political framework that can be undertaken. The first is establishing a carbon price via a tax, which has already been implemented under various governments. A carbon tax provides the incentive to reduce emissions and accounts for externalities to provide a mandated representation of the true price of carbon. The second is to promote diffusion of technology through research and development. Investment can be promoted through proper deployment policy. Figure 16 (Grubb, 2004) illustrates a conceptual model of important factors in the innovation chain. Innovation can be fueled by the commitment for investments from the business and finance community as well as contribution through policy interventions from the government (Grubb, 2004). In this way, the creation and stabilization of markets is achieved to promote efficiency in climate change initiatives.

This last point is particularly important in light of the launch of the European Union Emission Trading Scheme (EU-ETS) in 2005. The cap and trade scheme was plagued by uncertainties and inefficiencies, which led to the eventual decline of the commodity price for carbon in May 2006. Even though the initiative indicated progress in climate change policy, the market was faced with inefficiencies

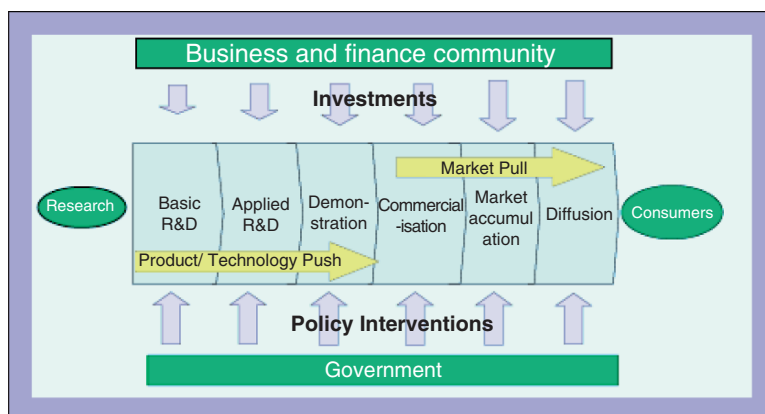


Fig. 16. The main steps in the innovation chain. Source: Grubb (2004).

from many perspectives including the limitations in the legal framework and its short time frame, the regulatory uncertainty, market disturbance and imperfection, the lack of political commitment and predictability, and ultimately the threat in retaining political support in years ahead, which are all serious concerns facing the implementation of environmental policy today.

In fact, many uncertainties and biases are inherent within the political framework that is chosen to battle climate change. A case in point is the decision over implementing a carbon market or a tax. Ideally, with perfect information, one would be able to plot the marginal costs or damage (MD) and marginal benefits or savings (MS) related to abatement strategies, such as shown in Figure 16 (Kolstad, 2000). The problem lies in the fact that there is a lack of data to identify the relationship between the MD and MS curves, thus, making it difficult to distinguish between the scenarios present in Figure 17(a) and 17(b) (Kolstad, 2000). Because it is the total stock of GHGs which drive global climate change, this suggests the MD curve is likely to be flat in the short-term, since the effect on the MD curve of emitting one more unit of carbon is likely to be constant over short periods of time (Lydon, 2002; Pizer, 2002). However, because of the uncertainty and the possibility of reaching a threshold above which GHG stock reaches critical levels, the MD curve has the potential to be strongly convex (Stern, 2006b). As shown in Figure 16 (Kolstad, 2000), the inefficiencies apparent for the carbon tax or market scenario depend on the slope of the MD curve, in which a steeper MD curve will signify higher efficiency losses from quantity control (light shaded areas) than from an emission fee (dark shaded areas).

Basically, prices or taxes are preferred where the benefits of pollution abatement change less with the level of pollution than do the costs of pollution abatement. Quantity controls or markets are preferred where the benefits of pollution abatement increase more with the level of pollution than do the costs of pollution

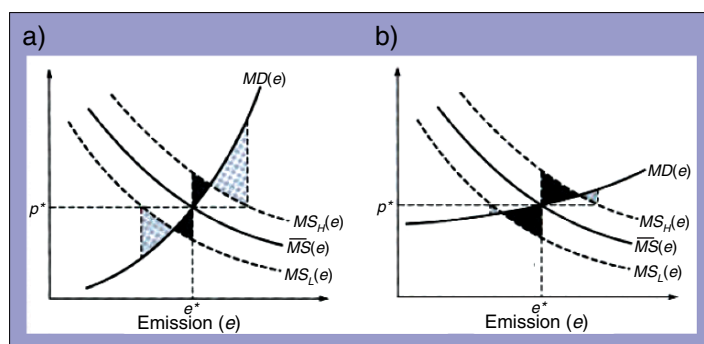


Fig. 17. (a) Welfare losses from price and (b) quantity control. $MD(e)$, marginal damage from emissions; $MS_H(e)$, $MS_L(e)$, marginal savings from emitting for high(H) and low(L)-cost firms; e^*, p^* , optimal quantity and price allocations; dark shaded area, inefficiency from emission fee; light shaded area, inefficiency from quantity control. *Source: Kolstad (2000).*

abatement (Weitzman, 1974). Nonetheless, the uncertainty in the MD function for CO₂ is controversial, with possibilities ranging from constant, linear relationship, or exponential as seen with chemical toxins exhibiting a specific threshold. Therefore, policy would benefit from further advancements and research in this area. In addition, political choices will be reliant on the specific needs of the government and priorities of the public within each country.

4.2. The role and limitations of technology policy

Addressing technology is another important aspect to the economic analysis as well as policy. Much of the SR analysis is dependent on certain assumptions associated with the level of technology available in the future to mitigate global climate change. Thus, technology policy plays a significant role, which, as with all policy, is plagued by future uncertainty. With reference to the experience curves or learning rates and the high marginal cost for investment for new technologies, it is possible that society may be locked-in to today's emission intensive technologies if barriers to investment are not addressed through government policies.

Additionally, the difficulty to develop and create a market for innovative technologies may be augmented by market failures, specifically in the power generation sector (Stern, 2006b). The lack of certainty over the future price of carbon reduces the incentives for innovation. Thus far, even though climate change policies, such as the Kyoto Protocol, have been enacted by the majority of the countries in the world, carbon's environmental externality has yet to be incorporated into goods as a 'true' carbon price. This generates slower innovation in the future, and can have drastic effects on the scientific and economic analyses generated in the present (Anderson *et al.*, 2001; Jaffe, *et al.*, 2003, 2004). For investment in low emission-intensive technologies to occur, there needs to be a certainty for the rate of return on the investment. Since carbon pricing is a nascent concept, the uncertainties related to clear long-term price signals in the marketplace, which drives investment, will hamper innovation and deployment of new technologies – hence the lack of investment in low-carbon technologies (Stern, 2006b). Thus, in addition to incorporate a portfolio of low-emission technology options to avoid carbon lock-in, policy should integrate proper legislative framework with economic incentives for private firms to invest in these technologies.

4.3. Final words

The implementation of efficient policy is dependent on current and future understanding of the complex relationships linking economic growth, GHG emissions, the carbon cycle, the climate system, impacts and damages, and possible policies (Nordhaus, 2007). A major barrier to future understanding persists in the political

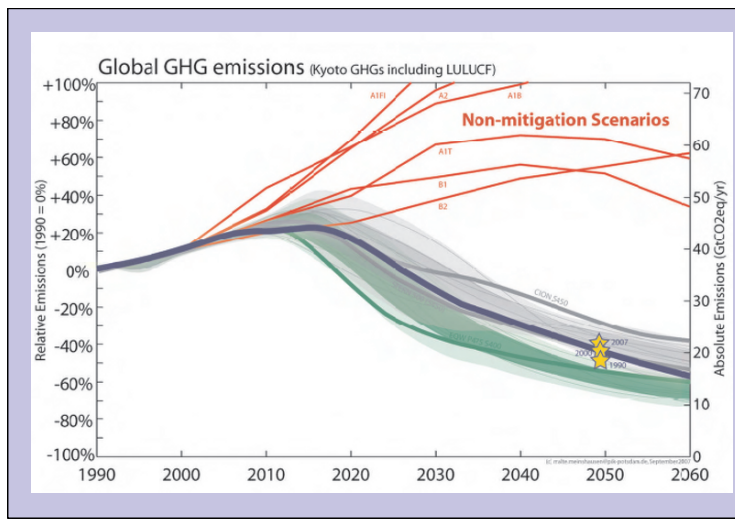


Fig. 18. Global GHG emissions indicating non-mitigation scenarios proposed by previous IPCC models (red trajectories), the Stern Review targets (green trajectory – with uncertainty in shaded green), and the goals set at the G8 Summit in Heiligendamm (trajectory), and targets shown by the yellow stars. The reference year from which global emissions shall be halved remains open, thus three options (1990, 2000, and 2007) are shown. *Source: Meinshausen (2007).*

environment, as political economies must consider the possible trade-offs between environmental conservation and economic growth. In the latest negotiations of the United Nations Framework on Climate Change held recently in Bali (in 2007), disagreements among nations led to a lack of consensus on a framework for the path of international climate policy. However, despite areas of delay for an international regime, the recent annual commitments from the Group of Eight (G8) in the Summit in Heiligendamm provides a great stride forward in terms of climate change energy efficiency, and energy security issues (G8, 2007), providing a reference target of halving global emissions by 2050 – as shown in Figure 18 (Meinshausen, 2007).

5. Conclusion

In brief, this paper attempts to synthesize an overall understanding of the scientific, economic, and political aspects analyzed in the Stern Review. Some of the principal uncertainties lie within the scientific advances of climate model predictions, the extent of reliance on the progress of technological change as a means to mitigate global climate change, the effect of bias and ethics in evaluating future damages, and the long-term political ambition and support to promote investment and creation of markets that internalize the previously ignored externalities. However, if the past is any indication for future actions, scientific uncertainties will

persist, short term policy will continue to contradict with long term goals, political and public perceptions will continue to clash, and there is no guarantee that the preferences of future generations will not change for the worst.

The range of uncertainties span throughout each chapter of the story, and it is important to remember that conclusions from any model can change alongside its assumptions. Nonetheless, in the future, further inclusion of sensitivity variables and the consequential factors affecting the climate system will only help in achieving greater understanding of steps necessary to achieve a climate change solution.⁸

Appendix: Definition of symbols in Figure 7

- A1FI: **Fossil-fuel Intensive**, coal, oil, and gas continue to dominate the energy supply for the foreseeable future.
- A1B: **Balance** between fossil fuels and other energy sources
- A1T: emphasis on new **Technology** using renewable energy rather than fossil fuel.
- A2: heterogeneous world, **self-reliance, increasing global population**, economic development is primarily regionally oriented and per capita economic growth and technological change are more **fragmented** and **slower** than in other storylines.
- B1: convergent world with the same global population that peaks in mid-century and declines thereafter, as in A1, but with rapid changes in economic structures toward a service and information economy, with reductions in material intensity, and the introduction of clean and resource-efficient technologies. The emphasis is on global solutions to economic, social, and environmental sustainability, including improved equity, but without additional climate initiatives.
- B2: family describes a world in which the emphasis is on local solutions to economic, social, and environmental sustainability. It is a world with continuously increasing global population at a rate lower than A2, intermediate levels of economic development, and less rapid and more diverse technological change than in the B1 and A1 storylines. While the scenario is also oriented toward environmental protection and social equity, it focuses on local and regional levels. *Source: IPCC (2000).*

⁸ For further discussions and comments on the Stern Report include: Tol and Yohe (2006) and Mendelsohn (2006). A particularly useful discussion of discounting issues is contained in Dasgupta (2006). An analysis which focuses on the extreme findings of the *Review* is Seo (2007). A discussion of ethics is in Beckerman and Hepburn (2007). A sensitivity analysis of the ethical parameters with much the same message as the present article is Mityakov and Ruehl (2007). A wide-ranging attack on various elements is contained in Carter *et al.* (2006) and Byatt *et al.* (2006). Insurance issues and discounting are discussed in Gollier (2006) and Weitzman (2006).

References

Anderson, D., C. Clark, and T. Foxon, *et al.* (2001). Innovation and the environment: challenges and policy options for the UK. A report for the UK Economic and Social Science Research Council. Imperial College London, Centre for Energy Policy and Technology (ICEPT) and the Fabian Society, London: Imperial College.

Barker, T., M.S. Qureshi, and J. Köhler. (2006). The costs of greenhouse-gas mitigation with induced technological change: a meta-analysis of estimates in the literature. 4CMR, Cambridge Centre for Climate Change Mitigation Research, Cambridge: University of Cambridge.

Beckerman, W. and C. Hepburn. (2007). Ethics of the discount rate in the Stern Review on the economics of climate change. *World Economics*, 8(1), 187–210.

Bradford, D.F. (1975). Constraints on government investment opportunities and the choice of discount rate. *American Economic Review*, 65(5), December: 887–899.

Brohan, P., J.J. Kennedy, I. Harris, *et al.* (2006). Uncertainty estimates in regional and global observed temperature changes: a new dataset from 1850. *Journal of Geophysical Research*, 111, D12106, doi: 10.1029/2005JD006548.

Broome, J. (1992). *Counting the Cost of Global Warming*. Cambridge: White Horse Press.

Butler, R. (2006). Record one-year increase in carbon dioxide levels. Last Updated March 14, 2006. Available at: <news.mongabay.com/2006/0313-co2.html>.

Byatt, I., I. Castles., I.M. Goklany, D. Henderson, N. Lawson, R. McKittrick, J. Morris, A. Peacock, C. Robinson, and R. Skidelsky. (2006). Economic aspects. *World Economics*, 7(4), October–December: 199–232.

Carter, R.M., C.R. de Freitas, I.M. Goklany, D. Holland, and R.S. Lindzen. (2006). Part I: The science. *World Economics*, 7(4), October–December: 167–198.

Cobb, J. and H. Daly. (1989). *For the Common Good*. Boston: Beacon Press.

Cropper, M.L., S.K. Ayded, and P.R. Portney. (1994). Preferences for life saving programs: how the public discounts time and age. *Journal of Risk and Uncertainty*, 8, 243–265.

Dasgupta, S.P. (2006). Comments on the stern review's economics of climate change. Prepared for a seminar on the Stern Review's economics of climate change, organised by the Foundation for Science and Technology at the Royal Society, London, on November 8, 2006. (Revised: December 12, 2006). Available at: <<http://www.econ.cam.ac.uk/faculty/dasgupta/STERN.pdf>>.

Frederick, S., G. Loewenstein, and T. O'Donoghue. (2002). Time discounting and time preference: a critical review. *Journal of Economic Literature*, XL, 351–401.

Giorgi, F. and Francisco, R. (2000) Evaluating uncertainties in the prediction of regional climate change. *Geophysical Research Letters*, 27(9), 1295–1298.

Gollier, C. (2002). Discounting an uncertain future. *Journal of Public Economics*, 85, 149–166.

Gollier, C. (2006). *Climate Change And Insurance: An Evaluation Of The Stern Report On The Economics Of Climate Change*. Barbon Institute: December.

Group of Eight (G8). (2007). G8 Summit documents – New: Chair's summary. Available at: <<http://www.g-8.de/Webs/G8/EN/G8Summit/SummitDocuments/summit-documents.html>>.

Grubb, M. (2004). Technology innovation and climate change policy: an overview of issues and options. *Keio Economic Studies*. XLI(2). Available at: <<http://www.econ.cam.ac.uk/faculty/grubb/publications/J38.pdf>>.

Hadley Centre. (2005). Stabilising climate to avoid dangerous climate change – a summary of relevant research at the Hadley Centre. United Kingdom. Available at: <http://www.metoffice.gov.uk/research/hadleycentre/pubs/brochures/2005/CLIMATE_CHANGE_JOURNAL_150.pdf>.

Hope, C. (2003). The marginal impacts of CO₂, CH₄ and SF₆ emissions. Judge Institute of Management Research Paper No. 2003/10, Cambridge, UK, University of Cambridge, Judge Institute of Management.

Intergovernmental Panel on Climate Change. (2000). Special Report Emission Scenarios. [Nakicenovic, N. and R Swart (Eds.)], Cambridge: Cambridge University Press, UK. pp. 570. Cambridge University Press, The Edinburgh Building Shaftesbury Road, Cambridge CB2 2RU, England.

Intergovernmental Panel on Climate Change. (2001). Climate Change 2001: The Scientific Basis. Contribution of Working Group I to the Third Assessment Report of the Intergovernmental Panel on Climate Change. [Houghton, J.T., Y. Ding, D.J. Griggs, *et al.* (Eds.)], Cambridge: Cambridge University Press.

Intergovernmental Panel on Climate Change. (2007). Climate Change 2007: The Physical Science Basis. Contribution of Working Group I to the Fourth Assessment Report of the Intergovernmental Panel on Climate Change [Solomon, S., D. Qin, M. Manning, Z. Chen, M. Marquis, K.B. Averyt, M. Tignor, and H.L. Miller (Eds.)], Cambridge University Press, Cambridge, United Kingdom and New York, NY, pp. 996.

International Energy Agency. (2000). Experience Curves for Energy Technology Policy. Paris: OECD/IEA.

Jaffe, A., R. Newell, and R. Stavins. (2003). Technological change and the environment. Handbook of Environmental Economics, [Mäler, K. and J. Vincent, J. (Eds.)], Amsterdam: North-Holland/Elsevier Science, pp. 461–516.

Jaffe, A., R. Newell, and R. Stavins. (2004). A tale of two market failures. RFF discussion paper. Available at: <<http://www.rff.org/Documents/RFF-DP-04-38.pdf>>.

Jain, A.K., H.S. Kheshgi, and D.J. Wuebbles. (1996). A Globally Aggregated Reconstruction of Cycles of Carbon and its Isotopes, *Tellus*, 48B, 583–600.

Joos, F., M. Bruno, R. Fink, U. Siegenthaler, T.F. Stocker, and C. LeQuere. (1996). *Tellus* 48B, 397.

Kahneman, D. and A. Tversky. (1979). Prospect theory: an analysis of decisions under risk. *Econometrica*, 47, 313–327.

Kolstad, C. (2000). Environmental Economics. New York, NY: Oxford University Press. 1st edition.

Koopmans, T.C. (1965). On the concept of optimal economic growth. *Pontificiae Academiae Scientiarum Scripta Varia*, 28, 225–300.

Lind, R.C. (1982). Introduction. Discounting for Time and Risk. *Energy Policy*. [Lind, R.C., K. Arrow, G. Corey, P. Dasgupta, A. Sen, T. Stauffer, J. Stiglitz, J. Stockfisch, and R. Wilson (Eds.)], Baltimore: Johns Hopkins University Press, pp. 1–20.

Lydon, P. (2002). Greenhouse warming and efficient climate protection policy, with discussion of regulation by “price” or by “quantity”. Working Paper 2002–5, Berkeley, CA: Institute of Governmental Studies.

Marshall, A. (1890). Principles of Economics. London: Macmillan and Co., Ltd., 1920. 8th edition.

Meinshausen, M. (2006). What does a 2°C target mean for greenhouse gas concentrations? A brief analysis based on multi-gas emission pathways and several climate sensitivity uncertainty estimates. *Avoiding Dangerous Climate Change*, [H.J. Schellnhuber, *et al.* (Eds.)], Cambridge: Cambridge University Press, pp. 265–280.

Meinshausen, M. (2007). Emission pathways and concentration levels under a 2°C climate target. Presentation for the EU Parliament, Temporary Committee on Climate Change. 10 September 2007, Bruxelles. Available at: <http://www.europarl.europa.eu/comparl/tempcom/clim/sessions/20070910/meinshausen_en.pdf>.

Mill, J.S. (1848). *Principles of Political Economy with some of their Applications to Social Philosophy*. Longmans, Green and Co., London, UK.

Mityakov, S. and C. Ruehl. (2007). Small Numbers, Large Meaning: A Sensitivity Analysis of the Stern Review on Climate Change. February 2.

Murphy, J.M., D.M.H. Sexton D.N. Barnett, *et al.* (2004). Quantification of modelling uncertainties in a large ensemble of climate change simulations. *Nature*, 430, 768–772.

Nordhaus, W. (2007). The challenge of global warming: economic models and environmental policy. Yale University, New Haven, CT. Available at: <http://nordhaus.econ.yale.edu/dice_mss_072407_all.pdf>.

Pearce, D.W., G. Atkinson, and S. Mourato. (2006). *Cost–Benefit Analysis and the Environment: Recent Developments*. OECD, Paris.

Pigou, A.C. (1920). *The Economics of Welfare*. MacMillan and Co., London, UK.

Pizer, W.A. (2002). Combining price and quantity controls to mitigate global climate change. *Journal of Public Economics*, 85, 409–534.

Portney, P. and J. Weyant (eds.) (1999). *Discounting and Intergenerational Equity, Resources for the Future*, Washington, DC.

Project Syndicate. (2007). The economists' voice commentary by Kenneth Arrow: the case for mitigating greenhouse gas emissions. Available at: <www.project-syndicate.org>.

Quiggin, J. (2006a). Stern and the critics on discounting. University of Queensland. Available at: <<http://johnquiggin.com/wp-content/uploads/2006/12/sternreviewed06121.pdf>>.

Quiggin, J. (2006b). Stern on the costs of climate change Part 1. November 17, 2006. Available at: <<http://johnquiggin.com/index.php/archives/2006/11/17/stern-on-the-costs-of-climate-change-part-1/>>.

Ramsey, F. (1928). A Mathematical Theory of Saving. *The Economic Journal*, 38, 543–559.

Rawls, J. (1971). *A Theory of Justice*. Oxford: Oxford University Press.

Seo, S.N. (2007). Is stern review on climate change alarmist? *Energy and Environment*, 18(5), 521–532.

Simon, H.A. (1957). *Models of Man*. New York, NY: Wiley.

Simon, H.A. (1991). *Models of My Life*. New York, NY: Basic Books.

Solow, R. (1994). An almost practical step toward sustainability. *Assigning Economic Value to Natural Resources*. National Academy Press, Washington, DC.

Stern, L.N. (2006a). Launch Presentation. London, UK: HM Treasury. Available at: <http://hm-treasury.gov.uk/independent_reviews/stern_review_economics_climate_change/sternreview_index.cfm>.

Stern, L.N. (2006b). The Stern Review: The Economics of Climate Change. London, UK: HM Treasury. Available at: <http://hm-treasury.gov.uk/independent_reviews/stern_review_economics_climate_change/sternreview_index.cfm>.

Stern, L.N. (2006c). What is the Economics of Climate Change? London, UK: HM Treasury. Discussion Paper. Available at: <http://hm-treasury.gov.uk/independent_reviews/stern_review_economics_climate_change/sternreview_backgroundtoreview.cfm#oxford>.

Tol, R.S.J. (2003). Is the uncertainty about climate change too large for expected cost–benefit analysis? *Climatic Change*, 56(3), 265–289.

Tol, R.S.J. and G.W. Yohe. (2006). A Review of the Stern Review. *World Economics, World Economics*, NTC Economic & Financial Publishing.

Weitzman, M.L. (1974). Prices versus quantities. *Review of Economic Studies*, 41(4), 477–491.

Weitzman, M.L. (1998). Why the far distant future should be discounted at its lowest possible rate. *Journal of Environmental Economics and Management*, 36, 201–208.

Weitzman, M.L. (1999). Just keep on discounting, but...[Portney, P. and J. Weyant (Eds.)], *Discounting and Intergenerational Equity*, Washington DC, Resources for the Future, pp. 23–30.

Weitzman, M.L. (2006). A Review of the Stern Review on the economics of climate change. *Journal of Economic Literature*, 45(3), 703–724.

Wigley, T.M.L. and S.C.M. Raper. (2001). Interpretation of high projections for global-mean warming. *Science*, 293, 451.

World Climate Research Programme (WCRP). (2007). Date of Access: 25 January 2008. *Regional Analysis of Climate Change Projections*. Presentation given by Carolina Vera, CIMA/FNA University of Buenos Aires, Argentina, Member of the Joint Science Committee at the UN Climate Change Conference 2007 in Bali, Indonesia. Available at: <http://regserver.unfccc.int/seors/file_storage/z68q7iqr11oeds.pdf>.

**CASE STUDY III. NATURAL
ATTENUATION
OF CONTAMINANTS
AND RISK ASSESSMENT**

Phytotechnologies: how plants and bacteria work together

Stefan Shilev¹, Iordanka Kuzmanova¹, Enrique Sancho²

¹ Department of Microbiology and Environmental Biotechnologies,
Agricultural University – Plovdiv, 12 Mendeleev Str., 4000 Plovdiv, Bulgaria.

² Dpto. Microbiología, Edif. Severo Ochoa, Campus Rabanales, Universidad de Córdoba,
14071, Córdoba, Spain.

Abstract

Decision on the type of remediation technology to adopt in any particular situation is a difficult issue. Biotechnologies are beginning to offer efficient tools and environmental solutions for the cleanup of contaminated sites. An environmentally friendly *in-situ* technology is phytoremediation. This term covers different processes applicable to heavy metal-contaminated soils: phytostabilisation, phytoimmobilization, phytodegradation, rhizofiltration, phytoextraction. The interactions in soil between plant and microbes are one of the most important factors that influence the technology. The capacity of soil bacteria to utilize 1-aminocyclo-propane-1-carboxylate (ACC) and thus increase root elongation is reviewed. A mathematical model of arsenic accumulation in sunflower plant treated with a plant growth-promoting rhizobacteria (PGPR) *Pseudomonas fluorescens* biotype F and the possibilities of utilization of biomass from phytoremediation are presented. Further perspectives in that direction are related to the use of natural or introduced PGPR.

Keywords: phytoremediation, PGPR, ACC, arsenic accumulation, model.

1. Introduction

Many soils around the world are contaminated with a variety of organic and inorganic compounds. Often, several different contaminants occur in the same soil, for example in case of proximity to different industrial activities. Removal from the environment of many contaminants is rendered difficult by their chemical nature and the often tight interaction between them and soil constituents. Consequently, existing remediation technologies that are suitable to clean up contaminated soils are generally expensive and occasionally lead to damages to the natural environment (e.g., in the case of technologies involving the incineration of polluted soils). As an alternative, in the last decade, a new technology was introduced that uses plants to remove contaminants from the soil.

Contamination of soils is widespread not just with inorganic, but also with organic contaminants such as chlorinated solvents, like trichloroethylene; explosives, like trinitrotoluene (TNT); petroleum hydrocarbons, like benzene, toluene and xylene (BTX), polyaromatic hydrocarbons (PAHs), and pesticides such as atrazine. While many of these compounds can be degraded partially or completely by some soil bacteria, this process when it occurs naturally, is slow and has insufficient efficiency, because of the relatively low numbers of microorganisms in soils and because of nutrient limitations. However, evidence exists that the biodegradation of organic compounds in soil is enhanced in the rhizosphere.

2. Phytoremediation technologies

Depending on the extension, depth and type of contamination, different remediation approaches have been proposed (Mulligan *et al.*, 2001). Generally, three strategies are possible: containment of the contaminants, their removal or their *in situ* (on the site, where the contamination occurs) stabilisation. Physical containment is the least expensive approach but it leaves the contaminant in the site of contamination without treatment. The *ex situ* techniques (contaminated soil is removed from the site and treated or just stored to another place) are expensive, environmentally invasive and labor intensive. The *in situ* approaches are preferred, because they are environmental friendly and protect the ecosystem stability causing minimum damages. As *in situ* technique, the phytoremediation uses plants to remove pollutants from the environment or to render them harmless (Salt *et al.*, 1995). It can be applied to both organic and inorganic pollutants present in soil or water and is quite competitive as it costs only \$10–40 per ton of soil (Mulligan *et al.*, 2001). The phytoremediation processes applicable for heavy metal-contaminated soils are described below and illustrated in Figure 1:

- *Phytostabilisation*: a containment technology that uses plants tolerant to the contaminants with the purpose to stabilise polluted soils by plant roots, to prevent erosion and leaching. This process requires adaptation of plants species to the contaminant concentrations in the soil and good developed roots.
- *Phytoimmobilisation*: the plants are able to decrease bioavailability and mobility of metals and metalloids in root zone preventing plant uptake. Two plant-based mechanisms have been described – root adsorption/absorption and plant-assisted formation of insoluble compounds (Wenzel *et al.*, 1999). On the other hand, rhizosphere microorganisms may participate in the immobilisation through fixation (adsorption and uptake) or synthesis of less mobile compounds. The phytoimmobilisation is a very important process because the reduction of pollutant plant uptake to shoots avoids transfer into the food chain. In this sense, screening of food cultivars is necessary to select species which accumulate metals at the lowest possible amounts.

- *Phytodegradation*: aimed the alternative of conventional microbial biodegradation or plant use to stimulate the microbial decontamination. The process is applicable mainly for organic pollutants, while metals and metalloids can not be destroyed. Normally, the plants participate in the mobilisation of contaminant into the rhizosphere and this fact helps to microorganisms in the biodegradation process.
- *Rhizofiltration*: it refers to the use of plants to absorb contaminants from solutions, accumulating them into the plant roots. This process is not directly related to soil bioremediation. It is based on the ability of plants to absorb into the roots organic or inorganic contaminants.
- *Phytoextraction*: plants have developed the ability to acquire nutrient ions and organic compounds at low concentrations from the environment and accumulate them into roots and shoots. This technology is known as *phytoextraction*. Nowadays, the accumulation of mineral elements by plants represents a big interest due to the possibility of utilization as a decontamination technology of toxic metals and metalloids. The phytoextraction is one of the most efficient, secure and low-cost alternatives for remediation of contaminated soils with presence of common metals (Ag, Al, Cd, Cr, Pb, Hg, Sn, Zn, Cu, etc.) and metalloids (As, Se).

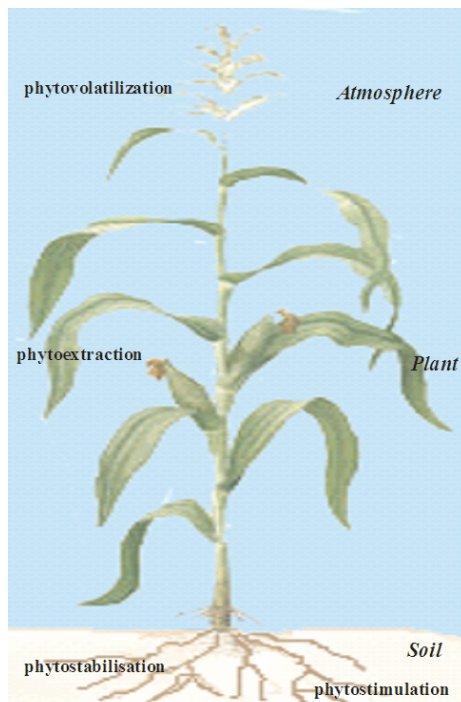


Fig. 1. Schematic diagram of the mechanisms of phytoremediation processes.

When we talk about phytoextraction, it is necessary to mention three main factors from which this process depends: the degree of metal contamination, its availability in soil, and the ability of plant to absorb metals, translocate and store them into the shoots (mainly in leaves). Many plants possess ability to grow in soils with high concentration of metals, but unfortunately their shoot biomass is very low. This conducts to necessity of decades to extract sufficient quantity to reduce the contamination in reasonable (legislation permitted for food plants growth) ranges. However, the vegetation in those highly contaminated regions contributes in prevent the soil wind erosion, leaching into the groundwater and support the ecosystem rehabilitation (phytostabilisation).

The metal availability is a very important factor that often limits the phytotechnologies. It means that when the metal (for example Pb) is presented in bound to the soil properties form, it could not be taken by the plant roots. In contaminated site in the south of the city of Plovdiv (South Bulgaria), the soil is carbonate-rich and the CaCl_2 -extractable Pb was found to be only 0.58 % of the total soil Pb content (Shilev *et al.*, 2007). In that situation, the soluble fraction that theoretically could be taken into the plant roots is quite limited. The use of synthetic chelators (chelate-assisted phytoextraction) permits to increase significantly metal ion concentration in soil solution when is introduced in the rhizosphere (Blaylock *et al.*, 1997). These compounds prevent the precipitation of Pb and maintain the metal as soluble chelate-Pb complex available to the plant-roots. Some of the chelating agents [ethylene-diamine-tetraacetate (EDTA), *N*-hydroxy-ethylene-diamine-tetraacetate (HEDTA), etc.] used in high concentrations mobilize huge amount of metals, that could be leached in the groundwaters. By other hand, they are less biodegradable in soil, which could pose an environmental risk by uncontrolled metal solubilization. However, a suitable alternative is the use of easily biodegradable chelating agents such as nitrilotriacetate (NTA), ethylene-diamine-disuccinate (EDDS) (Quartacci *et al.*, 2007) or elemental sulfur (Kayser *et al.*, 2000).

Two general categories of phytoextraction exist, based on utilization of different types of plants: continued and induced phytoextraction. The first one is based on the hyperaccumulation (e.g., *Thlaspi caerulescens*), usually small, with high foliar metal concentration and with slow growth rates that do not provide a high biomass. The second category includes high biomass crops (e.g., *Brassica juncea*, *Helianthus annuus*, *Zea mays*) that have a large biomass production but accumulates lower metal concentrations.

To overcome the limitations due to plant characteristics, different strategies have been suggested to improve the phytoextraction process. Brown *et al.* (1995) proposed to transfer the metal-removal properties of hyperaccumulator plants to high-biomass producing species. They are often tolerant to the metals (particularly Pb and Zn), because of the huge biomass the total extracted quantity is enhanced comparing with the hyperaccumulators. Thus, the time for site remediation is reduced when the territory management is correct. In most of the cases, the high-biomass-producing plants are crops for which agronomic practices are developed

Table 1. Phytoextraction potential of selected plant species.

Metal	Plant	Metal Concentration (mg kg ⁻¹)		DM Yield (t ha ⁻¹)	HM Removal (kg ha ⁻¹ year ⁻¹)	References
		Soil	Leaves			
Cd	<i>T. cearulescens</i>	10	1 600	1.6–5.2	4.2–8.3	Robinson et al. (1998)
	Poplar, willow	5	53	20	1	Robinson et al. (2000) Kayser et al.
Pb	<i>Brassica juncea</i>	–	280	4	1.12	(2000)
	<i>Zea mays</i>	2 500	225	10	2.2	Huang et al. (1997)
Zn	<i>T. cearulescens</i>	500	10 200	5.2	61	Robinson et al. (1998)
	<i>Helianthus annuus</i>	360–670	150	20	3	Kayser et al. (2000)
As	<i>Pteris vitata</i>	400	6 805	5	34	Ma et al. (2001)
	Asparagus fern	1 230	1 130	5	5.66	Bagga and Peterson (2001)

and used during their vegetation (Lasat, 2000). This makes the growth easier, reduces costs and contributes to avoid diseases.

An important factor that describes the time needed to remediate a heavy-metal-contaminated soil is the bioconcentration factor (BCF). It provides an index of the ability of the plant to accumulate a specific metal with respect to its concentration in soil (Zayed *et al.*, 1998a,b). BCF was calculated as a ratio between heavy metal concentration in the plant tissue and heavy metal concentration in the soil. On Table 1 are presented the accumulated values of some heavy metals and arsenic in different plants, the dry matter yield and the total heavy metal removal.

3. Plant microbe-interactions in rhizosphere

The rhizosphere is the narrow region of soil that is directly influenced by root secretions and associated soil microorganisms. It is teeming with bacteria that feed on sloughed-off plant cells, termed rhizodeposition, and the proteins and sugars released by roots. The protozoa and nematodes that graze on bacteria are also concentrated near roots. Thus, much of the nutrient cycling and disease suppression needed by plants occurs immediately adjacent to roots. In this environment the heavy metals are very important factor which influences and changes all other. Thereby, they suppressed the plant and the microorganism's growth and development through diverse toxic effects. In a lot of regions this is a serious problem due to the small yield production and high metal concentration into the food. It is known, that one of the phytoremediation goals is to recover the soil, obtaining safety food and decreasing the level of contamination. In this strategy plant biomass

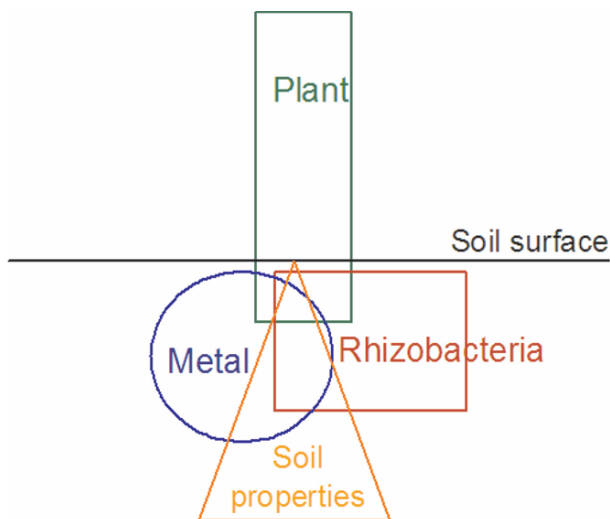


Fig. 2. Schematic description of rhizosphere factors.

is the basic factor together with plant tolerance to the contaminants. The interactions are represented schematically of Figure 2.

3.1. Ecology of rhizobacteria

The term rhizobacteria often refers to plant root associate bacteria which leave in close interactions with the roots, receiving plant metabolites and nutrients and secreting different enzymes, growth factors and compounds. They are important piece of the puzzle of plant–soil-contaminant interactions, managing plant water and nutrients supply, soil formation and conditioning, organic matter turnover and suppressing pathogens.

The microbes and their capacity to utilize 1-aminocyclo-propane-1-carboxylate (ACC) have been studied extensively. However, this characteristic is most common among plant growth-promoting rhizobacteria (Glick, 2003). Moreover, there is a great variation in ACC deaminase activity among them. They might facilitate phytoremediation directly and indirectly. The direct mechanisms by which rhizobacteria enhance phytoremediation include rhizodegradation supported by root exudates and biotransformation of toxic elements. Indirect mechanisms are optimizing bioavailability of toxic metals and other contaminants to accumulating-plants for their detoxification and storage (Khan, 2005). Interestingly, there is substantial evidence suggesting that rhizobacteria containing ACC deaminase activity protect plants from both biotic and abiotic stresses and dramatically increase plant biomass; an important factor for plants used in phytoremediation (Burd *et al.*, 1998; Glick, 2005). Many strains of genus *Pseudomonas* possess ACC deaminase activity.

P. fluorescens biotype F, isolated from heavy-metal-contaminated soil had been found to promote plant growth and tolerance to heavy metal and arsenic (Shilev *et al.*, 2001).

3.2. Biochemical aspects of ACC deaminase

ACC deaminase is a pyridoxal 5-phosphate (PLP)-dependent enzyme that degrades a cyclopropanoid amino acid, ACC, to α -ketobutyrate and ammonia (Honma and Shimomura, 1978). Molecular mapping of ACC deaminase revealed that there might be similar types of deaminase genes in different microbes. ACC deaminase demonstrates a vast array of biochemical and physical characteristics depending on the microbial species. The molecular mass of ACC deaminase is 105 000 Da and its subunit molecular mass ranges from 35 000 to 41 700 Da (Glick, 2005). Generally, ACC deaminase exhibits optimum activity at a pH 8, although it could vary depending on the species.

3.3. Mechanisms of enhanced plant-root-growth with associate PGPR

The soil bacteria that contain ACC deaminase stimulate plant-root-growth through decreasing the level of ethylene production into the roots (Glick, 2003). When the plant is submitted to heavy metal stress it starts to produce higher amount of ethylene as stress response. A significant amount of the ACC, intermediate metabolite in that process, is exuded out of the plant-roots in the rhizosphere. It is a unique source of carbon and nitrogen for the bacteria containing ACC deaminase and posses capacity to utilize it. Thus, the bacteria decrease the concentration of ACC in immediate vicinity of the roots increasing the number of it population. As a consequence, decreases internal concentration and the amount of last product in the chain, the ethylene.

4. Case study

We investigated the accumulation in sunflower of arsenic added as sodium arsenite in no-contaminated soil in a pot experiment. The experiment was carried out during 35 days in greenhouse using control (without arsenic) and two concentration of arsenic – 5 mg L⁻¹ and 20 mg L⁻¹ of soil, each one with or without addition of rhizobacteria *Pseudomonas fluorescens* biotype F, tolerant to heavy metals and arsenic (Shilev *et al.*, 2001). After the harvest of plant biomass (shoots and roots) it was washed with tap-water and deionized water, dried in oven at 80 °C and portion of it was submitted to wet digestion in autoclave (Shilev *et al.*, 2008).

Finally, the solution was filtered and analyzed by atomic absorption spectroscopy for arsenic. In this investigation, a regression mathematical model was made with the purpose of predicting the arsenic accumulation in shoots of sunflower in phyto-extraction and bioaugmentation assays. In this model the values of statistical *t* of Student with *g.l.d.*, were used.

(A) Effect of arsenic in soil and bacteria *Pseudomonas fluorescens* on arsenic concentration in the leaves. The As concentration in leaves was between four and five times higher than in the stems (Figure 3) and can be described by the mathematical model $\text{As}(\text{leaves}) = 1.099 + 0.629 * \text{arsenic} + 5.141 * \text{bacteria}$. Both explanatory variables results significantly distinct from zero with signification value of 1 %, where the value of R^2 was 0.626 and the F of ANOVA's demonstration model was significant at a level inferior to 1%. This means that the inoculation of the bacterial population supports the increment of As with $5.141 \mu\text{g g}^{-1}$ DW of leaves and 1 mg As L^{-1} of soil induces an increment of the leaf concentration of $0.629 \mu\text{g As g}^{-1}$ DW.

(B) Effect of arsenic in soil and bacteria *Pseudomonas fluorescens* on arsenic concentration in the roots.

In all treatments was observed that increasing soil As concentration the roots one increases too. On the other hand, the inoculation of bacteria provokes a major accumulation in the roots (four times when the soil concentration was 5 mg As L^{-1} , and more than eight times in the treatment with 20 mg As L^{-1}) (Figure 4).

In this sense the regression model is the following: $\text{As}(\text{root}) = -46.830 + 7.002 * \text{arsenic} + 80.163 * \text{bacteria}$, where $R^2 = 0.626$, and F of ANOVA, less of 1%, indicates that the presence of tolerant bacteria promotes the As accumulation in the roots with $80.163 \mu\text{g g}^{-1}$ DW, while every milligram of As per litre of soil contribute to 7.002 μg of As per gram DW.

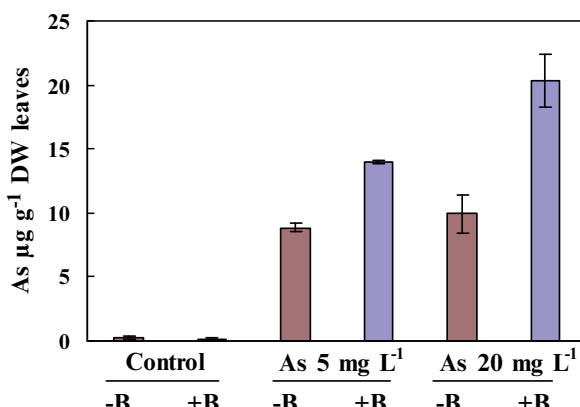


Fig. 3. Effect of arsenic in soil and bacteria *Pseudomonas fluorescens*, tolerant to metals and metalloids, on the arsenic concentration in the leaves (DW: dry weight).

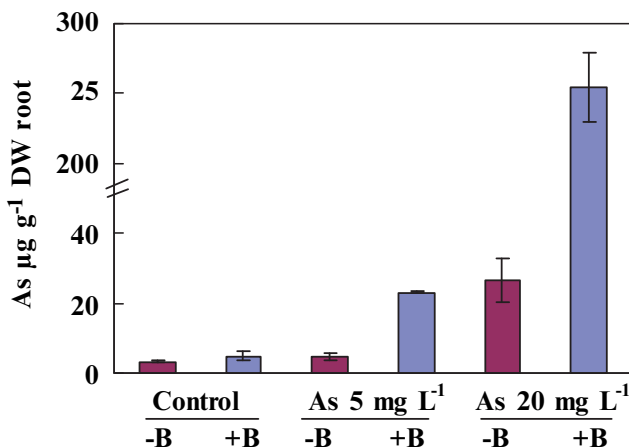


Fig. 4. Effect of arsenic in soil and bacteria *Pseudomonas fluorescens*, tolerant to metals and metalloids, on the arsenic concentration in the roots (DW: dry weight).

Finally, the presence of rhizobacteria *Ps. fluorescens* clearly promoted the arsenic accumulation in stems, leaves and roots. The fact, that the plant biomass was enhanced following to the inoculation of rhizobacteria tolerant to metals (results not shown) could be considered as PGPR-effect. These observations convert the bacteria in a suitable tool in the phytoextraction protocols.

5. Possibilities for biomass utilization

Ways to reuse plant biomass with high concentration of metals (Vassilev *et al.*, 2004):

1. Biomass direct combustion.

Biomass can be burned in small-scale modern boilers for heating purposes or in larger boilers for the generation of electricity or combined heat and power. Most electricity generation is based on the steam turbine cycle. Biomass combustion systems are in commercial use around the world, using disparate technology. Dedicated combustion plants can burn a wide range of fuel, including wastes.

2. Biomass gasification.

Biomass gasification converts biomass to a low to medium calorific value gaseous fuel. The fuel can be used to generate heat and electricity by direct firing in engines, turbines, and boilers after suitable clean up. Alternatively, the product gas can be reformed to produce fuels such as methanol and hydrogen, which could then be used in fuel cells or micro turbines, for example.

3. Biomass pyrolysis.

Biomass pyrolysis produces a liquid fuel that can be transported and stored, and allows for decoupling of the fuel production and energy generation stages. The fuel can be used to generate heat and electricity by combustion in boilers, engines, and turbines. The liquid can also be used to produce a range of specialty and commodity chemicals.

4. Physical-chemical conversion.

The physical-chemical conversion route applies to biomass from which vegetable oil can be obtained, and consists of pressing and extracting oil from the biomass. Vegetable oils can be used in special engines or in diesel engines after an esterification step to produce oil methyl ester. Biofuel from oilseed rape is produced in several European countries. Also, it could be used as lubricant for engines.

Fly ash generated from the biomass-ash-melting and gasification-melting plants, known as Melting Furnace Fly Ash, contains considerable amounts of heavy metals such as Pb and Zn. These metals can be recovered using a smelting furnace after “pre-treatment” for removal of unnecessary elements such as Cl, Sn and Si. Chemical methods have been studied for pretreatment in the past. However, they have been discussed only with regard to treatment cost and the concentration of Pb and Zn recovered (Okada *et al.*, 2007).

5. Composting.

Another possibility for reduction of the plant biomass resulted after the remediation is to compost it. It could be done in a small scale or in a large scale – cold (slow) composting, hot (fast) composting, etc.

Composting has been proposed as a post-harvest biomass treatment by some authors (Salt *et al.*, 1998). Hetland *et al.*, 2001, carried out laboratory experiments with lead-contaminated plant material (small sunflowers, grasses) obtained after induced phytoextraction. The disintegrated biomass (particles less than 0.16 cm in diameter) was composted in 125-mL borosilicate bottles with constant aeration for 2 months. Total dry weight loss was about 25%. Leaching tests of the composted material showed, however, that the composting process formed soluble organic compounds that enhanced lead solubility. These results documented that composting can significantly reduce the volume of harvested biomass; however, lead-contaminated plant biomass would still require treatment prior to disposal. Plant biomass harvested after induced phytoextraction can contain very mobile and leachable metal-chelate complexes. Moreover, Zhao *et al.* (2000), also showed that most of zinc within the leaves of hyperaccumulators is present also in water-soluble forms. It is necessary to emphasize that the purpose of composting is to reduce the volume and weight of plant material, with no consideration to the agricultural properties of the final product. Total dry weight loss of contaminated plant biomass is an advantage of composting as pretreatment step. It will lower costs of transportation to a hazardous waste disposal facility and costs of deposition or costs of transportation

to other facilities, where final crop disposal will take place. However, the duration of composting process is from 2 to 3 months, extending time from harvesting to a final disposal. Furthermore, contaminated decomposed biomass should be treated as hazardous material, while the resulted liquid from the composting process could be submitted to biosorption by immobilized yeast cells in biofilm (Marinkova *et al.*, 2007).

6. Further perspectives

Although phytoremediation has received great attention in the last decade, and a considerable number of reports exist suggesting that it should become the technology of choice for the clean up of various types of environmental contamination, this technology still does not work. Nevertheless, it is forecasted to account for about 10–15% of the environmental remediation market by the year 2010. On the other hand, to realize the potential of this technology, it is necessary for plants to grow as large as possible in the presence of various environmental contaminants. One way to achieve this goal is to utilize plant growth-promoting bacteria to facilitate the growth of the plants used for phytoremediation.

References

Bagga, D. and Peterson, S., 2001, Phytoremediation of arsenic-contaminated soil as affected by the chelating agent EDTA and different levels of soil pH, *Remediation Winter*, 77–85.

Blaylock, M.J., Salt, D.E., Dushenkov, S., Zakharova, O., Gussman, C., Kapulnik, Y., Ensley, B.D., and Raskin I., 1997, Enhanced accumulation of Pb by Indian mustard by soil-applied chelating agents, *Environmental Science Technology*, 31: 860–886.

Brown, S.L., Chaney, R.L., Angle, J.S., and Baker, A.J.M., 1995, Zinc and cadmium uptake by hyperaccumulator *Thlaspi caerulescens* and metal tolerant *Silene vulgaris* grown on sludgeamended soils, *Environmental Science and Technology*, 29: 1581–1585.

Burd, G.I., Dixon, D.G., and Glick, B.R., 2000, Plant growth-promoting bacteria that decrease heavy metal toxicity in plants. *Canadian Journal of Microbiology* 46(3): 237–245.

Glick, B.R., 2003, Phytoremediation: synergistic use of plants and bacteria to clean up the environment, *Biotechnology advances*, 21: 383–393.

Glick, B.R., 2005, Modulation of plant ethylene levels by the bacterial enzyme ACC deaminase, *FEMS Microbiological Letters*, 251: 1–7.

Hetland, M.D., Gallagher, J.R., Daly, D.J., Hassett, D.J., and Heebink, L.V., 2001, Processing of plants used to phytoremediate lead-contaminated sites. pp. 129–136. *In: Phytoremediation, Wetlands, and Sediments, The Sixth International in situ and on-site Bioremediation Symposium*, Leeson, A. Foote, E.A., Banks, M.K., Magar, V.S., (eds.), Battelle Press, Columbus, Richland.

Honma, M. and Shimomura, T., 1978, Metabolism of 1-aminocyclopropane-1-carboxylic acid, *Agricultural Biology Chemistry*, 42: 1825–1831.

Huang, J., Chen, J., Berti, W., and Cunningham, S., 1997, Phytoremediation of lead-contaminated soils: role of synthetic chelates in lead phytoextraction, *Environmental Science Technology*, 31: 800–805.

Kayser, A., Wenger, K., Keller, A., Attinger, W., Felix, H.R., Gupta, S.K., and Schulin, R., 2000, Enhancement of phytoextraction of Zn, Cd, and Cu from calcareous soil: the use of NTA and sulfur amendments, *Environmental Science and Technology*, 34: 1778–1783.

Khan, A.G., 2005, Role of soil microbes in the rhizospheres of plants growing on trace metal contaminated soils in phytoremediation, *Journal Trace Elements Medical Biology*, 18: 355–364.

Lasat, M.M., 2000, Phytoextraction of metals from contaminated soil: a review of plant/soil/metal interaction and assessment of pertinent agronomic issues, *Journal Hazardous Substance Research*, 2: 1–25.

Ma, L., Komar, K., Tu, C., Zhang, W., Cai, Y., and Kennelley, E., 2001, A fern that hyper-accumulates arsenic, *Nature*, 409: 579.

Marinkova, D., Tsibranska, I., Yotova, L. and Georgieva, N., 2007, An evaluation of kinetic parameters of cadmium and copper biosorption by immobilized cells, *Bio-automation*, 7: 46–56.

Mulligan, C.N., Yong, R.N., and Gibbs, B.F., 2001, Remediation technologies for metal-contaminated soils and groundwater: an evaluation, *Engineering Geology*, 60: 193–207.

Okada, T., Tojo, Y., Tanaka, N., and Matsuto, T., 2007, Recovery of zinc and lead from fly ash from ash-melting and gasification-melting processes of MSW – comparison and applicability of chemical leaching methods, *Waste management*, 27: 69–80.

Quartacci, M.F., Irtelli, B., Baker, A.J.M., and Navari-Izzo, F., 2007, The use of NTA and EDDS for enhanced phytoextraction of metals from a multiply contaminated soil by *Brassica carinata*. *Chemosphere*, 68(10): 1920–1928.

Robinson, B.H., Leblanc, M., Petit, D., Brooks, R.R., Kirkman, J.H., and Gregg, P.E.H., 1998, The potential of *Thlaspi caerulescens* for phytoremediation of contaminated soils, *Plant and Soil*, 203: 47–56.

Robinson, B.H., Mills, T.M., Petit, D., Fung, L.E., Green, S.R., and Clothier, B.E., 2009, Natural induced Cadmium-accumulation in poplar and willow: Implications for phytoremediation. *Plant and Soil*, 227(1-2): 301–306.

Salt, D.E., Blaylock, M., Kumar, N.P.B.A., Dushenkov, V., Ensley, B.D., Chet, I., and Raskin, I., 1995, Phytoremediation: a novel strategy for the removal of toxic metals from the environment using plants. *Biotechnology*, 13: 468–474.

Salt, D.E., Smith, R.D., and Raskin, I., 1998, Phytoremediation, *Annual Review Plant Physiology Plant Molecular Biology*, 49: 643–668.

Shilev, S., Benlloch, M., Dios-Palomares, E., and Sancho, E.D., 2008, Phytoremediation of metal contaminated soils for improving food safety. pp. 225–242. In: *Predictive Modelling and Risk Assessment*, Costa R. and Kristbergsson, K. (eds.), ISBN-10: 0387335129, Springer, Berlin, Germany.

Shilev, S., Naydenov, M., Tahsin, N., Sancho, E.D., Benlloch, M., Vancheva, V., Sapundjieva, K., and Kuzmanova, J., 2007, Effect of easily biodegradable amendments on heavy metals accumulation in technical crops – a field trial. *Journal of Environmental Engineering and Landscape Management*, 15(4), 237–242.

Shilev, S., Russo, J., Puig, A., Benlloch, M., Jorrin, J., and Sancho, E.D., 2001, Rhizospheric bacteria promote sunflower (*Helianthus annuus* L.) plant growth and tolerance to heavy metals, *Minerva Biotechnologica*, 13: 37–39.

Vassilev, A., Schwitzguébel, J.-P., Thewys, T., van der Lelie, D., and Vangrosveld, J., 2004, The use of plants for remediation of metal-contaminated soils, *The Scientific World Journal*, 4: 9–34.

Wenzel, W.W., Adriano D.C., Salt D., and Smith R., 1999, Phytoremediation: a plant-microbe-based remediation system, pp. 457–508. In: *Bioremediation of Contaminated Soils*, Adriano D.C., Bollang J.-M., Frankenberger W.T., Jr, and Slims R.C. (eds.), American Society of Agronomy, Madison, WI.

Zayed, A., Gowthaman, S., and Terry, N., 1998a, Phytoaccumulation of trace elements by wetland plants: I. Duckweed, *Journal of Environmental Quality*, 27: 715–721.

Zayed, A.M., Lytle, C.M., and Terry, N., 1998b, Accumulation and volatilization of different chemical species of selenium by plants, *Planta*, 206: 284–292.

Zhao, F.J., Lombi, E., Breedon, T., and McGrath, S.P., 2000, Zinc hyperaccumulation and cellular distribution in *Arabidopsis halleri*, *Plant Cell Environmental*, 23: 507.

Subject Index

A

Agent-based modeling 62
Algorithms 82
Anthropogenic 339
Approximation methods 119, 121
Aquifer 34
Arsenic accumulation 385
Artificial intelligence 69, 70
Artificial Neural Networks 225

B

Bayesian Model Averaging 191, 219, 221, 222, 228, 267, 278
Bayesian statistics 206
Benchmark 44–47, 267–276
Benchmark dose 269, 280
Bias 19
BMD (Benchmark dose) 269
BMDL 270
Bootstrapping 190
Boundary Element method 30

C

C4MIP (Coupled Climate Carbon Cycle Model Intercomparison Project) 284
CADNA library 108, 124
Calibration 3, 5, 15, 20, 129, 131, 137, 145
Per-datum calibration 146
CAMELOT 29, 41
Carbon capture 253, 257
Carbon dioxide emission 324
Carbon dioxide injection 253
Carbon dioxide sequestration 258
Carbon storage 253, 255, 258
Carbon tax 257
Catchment 3, 11
Cellular automata 27
CENTURY 327
CESTAC method 103, 107
Chaotic behaviour 93, 96
Checking 87
Climate change 238, 285, 292, 319, 339, 351, 353
Communicatio 68, 227, 233, 235
Companion modelling 72

Complex systems 58, 66, 249
Computational zero 105
Conceptual error 129
Confirmation 186
Constructivist 72
Contaminants 387
Convergence 87
Corroboration 186

D

Darcy's law 31
Decision-making 72, 180, 231, 240, 244
Decision-support systems 231
Delusion of uncertainty 185, 186
Discretization 30, 39, 102, 116
Differential equations 93
Discount rate 351, 367
Discourse 339
Discrete Stochastic Arithmetic 107, 124
DOC (Dissolved organic carbon) 319, 323, 324
Dynamical control 116, 123
DGVM (Dynamic Global Vegetation Model) 293
Dynamic properties 28, 93

E

Earth System model 283, 284
Economic framework 351
Enchytraeid worm 320
Energy 255
Environmental change 4, 346
Environmental economics 351
Epidemiology 270
Equifinality 215
Evapotranspiration 8
Exact arithmetic 89
Expected Utility Theory 233
Extent 5

F

Feedbacks 287
Finite Difference method 30
Finite Element method 30, 54

Finite Volume method 30
 Flow model 27
 Forecasting 205, 227
 Fossil fuels 255
 Framing 339, 340

G

Gauss-Legendre method 123
 Global carbon cycle 283
 GLUE (Generalized Likelihood
 Uncertainty Estimation) 214
 Greenhouse gas emissions 341, 348,
 351
 Groundwater 8, 186

H

Heterogeneity 34, 65, 160
 Hydrological catchment 16
 Hydrological processes 6, 27, 153
 Hydrological Response Unit 4
 (HUP) Hydrological Uncertainty
 processor 219

I

Impactassessmen 183
 Input Forecasting uncertainty 225
 Integral response 5
 Interval method 79
 Inverse method 138, 153
 IPCC (Intergovernmental Panel on
 Climate Change) 232, 256, 262,
 290, 341, 360

K

KIDS 65

L

Latin Hypercube sampling 179
 Lattice gas models 29
Lamp-posting 185
 Land use change 17, 68, 69

M

MACRO159
 Macroscopic cellular automata 29, 36
 Measurement error 134, 267, 271
 Media coverage 339, 341

Model comparison 4
 Model efficiency 9, 18
 Model
 Averaging 191
 Conceptual models 4, 12
 Conditional Processor 213, 219, 224,
 228
 Critique 187
 Distributed models 3, 19
 Economic models 233, 236, 239, 361
 Error 129, 134
 Lumped models 3, 7, 13
 Physically-based models 17
 Political models 237
 Psychological models 236
 Socioeconomic models 16
 Spatially explicit models 3, 6
 Multi-model ensemble 21
 Monte-Carlo approach 155, 161, 184
 Monte-Carlo filtering 198
 Multiple endpoints 267
 Multiplicity 271

N

Neoclassical economics 63
 NOAEL (No Observed Adverse Effect
 Level) 267, 268, 279
 NPP (Net Primary Production) 291–293

O

OAMBC 70
 Oceans 255
 Optimization 82
 ORCHIDEE model 286

P

Parameterization 4, 129, 161, 167, 173
 Parametric bootstrap 190
 PEC (Predicted Environmental
 Concentration) 158
 PELMO 159, 162, 176
 PRZM2 159
 PEARL 159
 Peatland 323, 330
 Permafrost 330
 Pesticide leaching 155
 Pesticide registration 158
 PGPR (Plant Growth-Promoting
 Rhizobacteria) 385
 Phytodegradation 385, 387

Phytoextraction 385, 387
 Phytoimmobilization 385
 Phytoremediation 385
 Phytostabilisation 385, 388
 Phytotoxicity 385
 Plausibility 22
 Policy-making 70, 73, 185, 231, 342, 352
 Positivist 72
 Post-normal science 188
 Precautionary principle 259
 Prediction reliability 131
 Predictive uncertainty 205, 206
 Prior belief 206
 Purpose (of modelling) 23

Q

Q_{10} 317, 330
 Quadrature method 120
 Qualitative-quantitative debate 61
 Quantization techniques 30
 QUMP (Quantifying Uncertainty in Model Predictions) 290, 293

R

Regulatory framework 200, 269
 Reliable computing 79
 Representations 339
 Respiration 317
 Rhizobacteria 385, 390
 Rhizofiltration 385, 387
 Risk assessment 155, 161, 267, 383
 Romberg's method 124
 RothC model 297, 303
 Rounding errors 79, 104, 105

S

Sampling 8, 179
 Scale 4, 23
 Scaling 5
 Scientific assessment 231
 Sensitivity analysis 185, 191, 201, 359, 371
 Scatterplots 194
 Variance-based method 196

Significant digits 105
 SIMULAT 8, 12
 Simpson's ruleSimulation 101
 SOC (Soil Organic Carbon) 286
 SOM (Soil Organic Matter) 318
 Soil 4, 7, 27, 37, 157
 Soil biology 317
 Soil carbon 285, 286
 Soil carbon pools 298, 299
 Soil moisture 9, 10, 304, 326
 Spatial resolution 14
 Spatial variability 8
 Spatially explicit models – see Models
 Standardization 67
 Stern review 343, 351
 Stream flow 8, 9
 Stochastic analysis 105
 Structural equations 267, 280
 Subcatchment 4
 Subjectivity 155
 Subsurface flow 37
 Support 5

T

Technological diffusion 351
 Temperature 300, 319, 329
 Testing 89
 TOPLATS 8–14
 TOPMODEL 8, 13
 TSPA (Total System Performance Assessment) 186
 Transdisciplinarity 72
 Transport model 138

U

UHP 8, 9
 UMD model 286
 Uncertainty 5, 13, 15, 21, 130, 134, 161, 183, 205, 216, 268, 270, 278, 300, 304, 307, 351, 355

V

Validation 3, 10, 15, 67, 186
 Verification 67, 79, 186